LITHOPROBE

Slave-***NOR***thern **C**ordillera ***L***ithospheric ***E***volution (***SNORCLE***)

and

CORDILLERAN TECTONICS WORKSHOP

Report of the 1998 Combined Meeting
March 6-8, 1998
Simon Fraser University

LITHOPROBE Report No. 64

Recommended Citation:

Cook, F. and P. Erdmer (compilers), 1998, Slave-Northern Cordillera Lithospheric Evolution (SNORCLE) Transect and Cordilleran Tectonics Workshop Meeting (March 6-8), Simon Fraser University, Lithoprobe Report No. 64, 331 pp.

LITHOPROBE SLAVE/NORTHERN CORDILLERA LITHOSPHERIC EVOLUTION WORKSHOP

and

CORDILLERAN TECTONICS WORKSHOP

Simon Fraser University, March 6-8, 1998

FRIDAY, March 6, 1998

0830-1010 SESSION 1 - INTRODUCTION AND RESULTS FROM THE SLAVE PROVINCE

Chairmen: F. A. Cook and P. Erdmer

PAGE

0830-0850 Introduction and Welcome
F. A. Cook and P. Erdmer

0850-0910 1) LITHOPROBE: Status, future and implications for SNORCLE
R. M. Clowes (Project Director)

0910-0930 2) Geochemical and isotopic constraints for tectonic evolution of the Slave province
K. Yamashita, R. Creaser, and L. Heaman..... 11

0930-0950 3) Unconformities, major faults, and the evolution of volcano-sedimentary basins of the Slave craton
W. Mueller, S. Bowring, P. Corcoran, and C. Picket..... 15

0950-1010 4) Metamorphism along the Slave portion of the SNORCLE transect
K. Bethune and D. Carmichael 17

1010-1040 COFFEE

1040-1240 SESSION 2 - SLAVE PROVINCE STRUCTURE AND TECTONICS

Chairmen: P. Erdmer and F. A. Cook

1040-1100 5) U-Pb geochronology of the Sleepy Dragon complex in the Morose-Patterson Lakes area, southwestern Slave province, with tectonic implications
J. Ketchum and W. Bleeker..... 25

1100-1120 6) The central Slave basement complex, it autochthonous cover, decollement, and structural topology: towards a new terrane model for the Slave province
W. Bleeker and J. Ketchum..... 31

PAGE

1120-1140 7) The Late Archean Prosperous granite suite: Syn-D2 laccoliths in the Yellowknife domain, Slave province
N. Ham, K. Benn, and W. Bleeker 36

1140-1200 8) Composition and thermal evolution of the upper mantle beneath the Archean Slave province: Evidence from xenolith studies
J. Mackenzie and D. Canil 37

1200-1220 9) Paleogeotherms, lower crustal metamorphism and heat generation in the Archean Slave province: Insights from xenoliths
D. Canil and J. Mackenzie 39

1220-1240 10) Upper mantle stratigraphy of the north-central Slave craton, Canada
M. Kopylova, J. K. Russell, and H. Cookenboo 41

1240-1340 LUNCH

1340-1520 SESSION 3 - DEEP STRUCTURE OF THE SLAVE PROVINCE

Chairmen: F. A. Cook and P. Erdmer

1340-1400 11) A steady-state conductive geotherm for the northern central Slave: Inversion of petrological data from the Jericho kimberlite pipe
J. K. Russell and M. Kopylova 45

1400-1420 12) Crustal structure of the Archean Slave craton from receiver function studies
J. Cassidy, M. Bostock, and C-G. Bank 49

1420-1440 13) Tectonic delamination of the Precambrian lithosphere in northwestern Canada mapped by LITHOPROBE
F. Cook, A. van der Velden, K. Hall and B. Roberts 54

1440-1500 14) Mantle stratigraphy and evolution of the Slave province
M. Bostock 70

1500-1520 15) The SNORE97 seismic refraction experiment: Preliminary results
G. Fernandez Viejo, R. Clowes, R. Ellis, I. Asudeh, and the SNORE 97 field crew 72

1520-1540 16) Elastic and seismic properties of forsterite-enstatite composites up to 3.0 GPa: Implications for compositional models of the upper mantle
S. Ji and Z. Wang 79

1540-1610 COFFEE

1610-1730 SESSION 4 - DEEP STRUCTURE OF THE SLAVE PROVINCE (continued)

Chairmen: P. Erdmer and F. A. Cook

PAGE

1610-1630 17) Plasticity of eclogite: Implications for rheology and seismic reflectivity of the subducting slab
S. Ji, Z. Wang, and K. Saruwatari 86

1630-1650 18) Heat flow transitions along the SNORCLE transect: Asthenospheric flow
T. Lewis and R. Hyndman..... 92

1650-1710 19) Electrical Resistivity structure between the Nahanni terrane and Slave province
X. Wu, I. Ferguson, and A. Jones..... 93

1710-1730 20) Source field contamination of SNORCLE magnetotelluric data
J. Cassels and A. Jones 103

SATURDAY, March 7, 1998

0830-1020 SESSION 5 - WESTERN SLAVE PROVINCE TO CORDILLERA

Chairmen: F. A. Cook and P. Erdmer

0830-0850 21) Early post-rift evolution of the northern Cordilleran margin: lithostratigraphic and conodont biostratigraphic framework along a platform-miogeocline-basin transect
L. Pyle and C. Barnes..... 104

0850-0910 22) Developing a sequence-stratigraphic framework for the Neoproterozoic-Cambrian evolution of the northwestern margin of North America
R. MacNaughton, G. Narbonne, and R. Dalrymple..... 109

0910-0940 23) Proterozoic sedimentation, magmatism, metasomatism and deformation in the Wernecke and Ogilvie Mountains, Yukon
D. Thorkelson, J. G. Abbott, J. Mortensen, R. Creaser, and M. Villeneuve..... 110

0940-1000 24) Mafic and ultramafic plutonic rocks south of Finlayson Lake, Yukon: Setting and implications for the early geological and metallogenic evolution of the Yukon-Tanana terrane
D. Murphy 120

PAGE

1000-1020 25) Kilometre-scale folding in the Teslin zone, northern Canadian Cordillera, and its tectonic implications for the accretion of the Yukon-Tanana terrane to North America
M. de Keijzer and P. Williams 130

1020-1050 COFFEE

1050-1230 SESSION 6 - NORTHERN CORDILLERA (continued)

Chairmen: P. Erdmer and F. A. Cook

1050-1110 26) The St. Cyr klippe, south-central Yukon: An outlier of the Teslin tectonic zone?
K. Fallas, P. Erdmer, D. Archibald, L. Heaman, and R. Creaser 131

1110-1130 27) Structural geometry of the Cassiar Platform and Teslin zone, Dycer Creek area, Yukon
C. Gallagher, R. L. Brown and S. Carr 139

1130-1150 28) Structure of the Teslin zone, Yukon, Canada
R. L. Brown M. de Keijzer, S. Carr, P. Williams, and C. Gallagher 152

1150-1210 29) Petrogenesis of the Cretaceous Cassiar batholith, Yukon-B. C. Canada
L. Driver, R. Creaser, T. Chacko, and P. Erdmer 158

1210-1230 30) The petrogenesis of the Mount Skukum/Bennett Lake igneous complex, Yukon Territory, and reflections on the Eocene tectonics of the Canadian Cordillera
G. Morris and R. Creaser 165

1230-1330 LUNCH

1330-1430 SESSION 7 - NORTHERN CORDILLERA (continued)

Chairmen: P. Erdmer and F. A. Cook

1330-1350 31) Geotectonics in the northern Cordillera from paleomagnetism and geobarometry: Progress report and recent results from the Eocene White Pass dikes and Jurassic Fourth of July batholith
D. Symons, M. Harris, C.Hart, and W. Blackburn 171

1350-1410 32) Contractional structures in the western Skeena fold belt: An indication of Cretaceous sinistral convergence within the Coast Belt
C. Evenchick 181

1410-1430 33) High temperature orogen-parallel extension during arc construction and exhumation
M. L. Crawford and K. Klepeis..... 182

1430-1700 - POSTER SESSION

SUNDAY, March 8, 1998

0830-1000 SESSION 8 - SOUTHERN CORDILLERA

Chairmen: F. A. Cook and P. Erdmer

0830-0850 34) Regional disharmonic structural evolution of the western Rocky Mountains, McBride, British Columbia
L. Reid and G. Ross..... 184

0850-0910 35) Provenance of the Belt-Purcell Supergroup, southern British Columbia: a SHRIMP study of detrital zircons
G. Ross and M. Villeneuve..... 186

0910-0930 36) The Christina Lake area in southeastern British Columbia: Upper Paleozoic Harper Ranch Subterrane of Quesnellia or pericratonic Kootenay terrane?
S. Acton and P. Simony..... 191

0930-0950 37) New metamorphic and geochronologic constraints on the tectonic evolution of the norther Selkirk Mountains, SE BC
N. Marchildon, G. Dipple, and J. Mortensen 192

0950-1010 38) Deformation induced inverted metamorphic field gradients, an example from southeastern Canadian Cordillera
H. D. Gibson and R. L. Brown..... 193

1010-1040 COFFEE

1040-1230 SESSION 7 - SOUTHERN CORDILLERA (continued)

Chairmen: P. Erdmer and F. Cook

1040-1100 39) Westward underthrusting, extrusion and exhumation of crystalline rocks of the Monashee complex, southeast B. C.
D. Johnston and P. Williams..... 194

1100-1120 40) Re-evaluation of the geology adjacent to Shuswap Lake, Vernon map area, British Columbia
N. Slemko, P. Erdmer, and R. Thompson..... 196

PAGE

1120-1140 41) NATMAP project proposed to study the Phanerozoic plate margin: Highlights from the Vernon map area (82L)
R. Thompson..... 201

1140-1200 42) Preliminary report on significant thrusting and extension of the Early Tertiary Chuckanut formation, NW Washington
R. Haugerud..... 203

1200-1220 43) Archean zircons in Upper Cretaceous sediments of the western Canadian Cordillera - Does the "Baja B. C." hypothesis fail a "crucial test"?
P. Mustard, J. Mahoney, J. Haggart, R. Friedman, M. Fanning, and V. McNicholl..... 204

1220-1330 LUNCH

1330-1500 - DISCUSSION

POSTERS
(Listed Alphabetically)

PAGE

44) Mesozoic to Eocene composite Endako batholith redefined
R. Anderson, J. Whalen, L.C. Struik, and M. Villeneuve..... 206

45) Geology of NE Nechako River map area, central B.C.: Evolution from composite Mesozoic arc to Eocene extensional magmatic complex
R. Anderson, L. Snyder, S. Wetherup, L. C. Struik, M. Villeneuve, and M. Haskin..... 210

46) Geochemical and isotopic constraints on ancient (700 Ma) seawater chemistry, western Canada
C. Augereau, R. Spencer, and G. Ross..... 213

47) Investigation of a displacement-transfer zone by 3-d seismic interpretation and physical modelling: Progress report on computer-graphics visualization and strain analysis
E. Aydemir and J. Dixon..... 215

48) Nature of movement across the Purcell thrust, Rocky Mountain Trench: Metamorphic transects
K. Boggs, E. Ghent, and P. Simony..... 217

49) The Acasta gneisses: Further evidence for a complex polymetamorphic history
W. Bleeker and R. Stern..... 220

PAGE

50) New U-Pb date for part of the Purcell supergroup, SE B.C. (title only)
D. Brown

51) U-Pb geochronology studies - Teslin zone and eastern Cassiar terrane, Yukon: Timing constraints on deformation and thermal history
S. Carr, and M. de Keijzer 223

52) Valhalla: A Cordilleran metamorphic core complex with origin, geometry and evolution controlled by plutonism
S. Carr, P. Simony, and P. Schaubs..... 228

53) Initial results from the Ravens Throat Project- Geology of Mount Kraft and part of the Dal Lake map areas, Mackenzie Mountains, Northwest Territories
M. Colpron..... 229

54) Volcanology and geochemical signature of correlative volcanic sequences in the Archean Slave province: A possible magmatic arc system
P. Corcoran and J. Dostal..... 237

55) Lithological, geochemical and isotopic characterization of clastic units in the Klinkit and Swift River assemblages, northern British Columbia
R. Creaser and T. Harms..... 239

56) U-Pb geochronological evidence for late Jurassic and late Cretaceous thermal events in the northern Monashee and Selkirk Mountains, Mica Creek area, B.C.
J. Crowley, E. Ghent, S. Carr, and P. Simony..... 243

57) Geochemistry and tectonic setting of the Powell Creek Group, southwestern British Columbia
T. Danielson, J. Mahoney, J. Riesterer, and C. Hickson..... 245

58) Physical modelling of fault propagation in roll-over structures associated with extensional (growth) faults
J. Dixon, S. Garneau, and J. Blackburn..... 247

59) The big flush- Paleomagnetic signature of a 70 Ma regional hydrothermal event in displaced rocks of the northern Canadian cordillera
R. Enkin, P.J. Wynne, J. Baker, S. Johnston, and C.J.R. Hart..... 249

PAGE

60) Middle and late Triassic arc volcanic rocks and associated intrusions in southern and central British Columbia: Evidence for correlation of Stikine, Cadwallader and Methow terranes
R. Friedman, P. Schiarizza, P. Mustard, P. van der Heyden, J. Mortensen, J. Thompson, and C. Deyell..... 250

61) Digital geology map of Yukon
S. Gordey, A. Makepeace, and S. Talwar..... 251

62) Preliminary Interpretations of Wavenumber Filtered Potential Field Data from Northwestern Canada
Kevin W. Hall, Frederick A. Cook, Elissa Lynn 252

63) ACCRETE crustal velocity structure across the Coast plutonic complex/Stikinia transition
P. Hammer, R. Clowes, and R. Ellis..... 258

64) Geophysical data analysis and regional gravity modelling in the southern Slave province
K.A.B. Hendry, W. Roest, W. Bleeker, and K. Benn..... 260

65) A regional seismic line across the Liard depression: Possible indications of Proterozoic strata involvement in Mackenzie Mountain foreland deformation
D. Hodder and L. Currie..... 264

66) Crustal structure along the ACCRETE corridor
L. Hollister, I. Morozov, S. Smithson, T. Das, J. Diebold, C. Andronicos, and D. Chardon..... 266

67) Blueschist metmorphism within the Bridge River complex, Goldbridge, B.C.
D. Hozjan and E. Ghent..... 268

68) U-Pb geochronological data from the west flank of Thor-Odin dome, Monashee complex, B.C.
D. Johnston, J. Crowley, P. Williams, S. Carr, and R. Brown..... 269

69) Microstructural, petrological and geochronological studies on the Thor-Odin dome, Monashee cmplex, southern Canadian Cordillera
Kuyper, Y..... 272

70) Magnetic constraints on Tertiary deformation in central British Columbia
C. Lowe, R. Enkin, J. Dubois, L. Struik, J. Baker, and R. Anderson..... 274

PAGE

71) Late Cretaceous and early Tertiary tectonics, magmatism and mineral deposits, central British Columbia
D. MacIntyre and L. Diakow 276

72) Geochronology studies in the Nass River area, British Columbia (title only)
V. McNicoll and C. Evenchick

73) Geochronological and geochemical studies of the Coates Lake diatreme, southern Mackenzie Mountains, western N.W.T.
J. Mortensen and M. Colpron 278

74) The southeastern Dorsey terrane: Characteristics and correlations
J. Nelson, T. Harms, and J. Mortensen 279

75) Volcanic studies in northern British Columbia
J. Nicholls and M. Stout 289

76) System of transfer fault zones across the Pacific continental margin of western Canada
M. Posavec 305

77) An improved seismic image below Yellowknife? Reprocessing results from line 1
B. Roberts 306

78) Seismic properties of the upper mantle beneath the Canadian cordillera- A study of mantle xenoliths
K. Saruwatari, S. Ji, and M. Salisbury 307

79) Tertiary crustal extension in central British Columbia
L.C. Struik, D.G. MacIntyre, R.G. Anderson, S. Wetherup, M. Villeneuve, R. Enkin, M. Haskin, L. Snyder, and N. Grainger 312

80) Comparative images of Proterozoic and Cenozoic subduction complexes
A. van der Velden and F. Cook 315

81) Hydrogen-enhanced electric conductivity of diopside crystals: Implications for conducting behavior of the upper mantle wedge above the subducting slab
Z. Wang, S. Ji, G. Dresen, and Q. Bai 319

82) Kinematics and fault zone processes, Denali fault system, SW Yukon
J. White 327

ABSTRACTS of ORAL PRESENTATIONS

Preface

This volume includes the abstracts and short articles submitted for the 1998 LITHOPROBE Slave - Northern Cordillera Lithospheric Evolution (SNORCLE) transect meeting and Cordilleran Tectonics Workshop. These meetings were held concurrently at Simon Fraser University on March 6-8. Accordingly, this volume includes several contributions related to both the southern and northern Cordillera. We sincerely thank Derek Thorkelson for his assistance in organizing the meeting.

Frederick A. Cook and Philippe Erdmer

Geochemical and isotopic constraints for tectonic evolution of the Slave province.

Katsuyuki Yamashita, Robert A. Creaser and Larry M. Heaman.
Department of Earth & Atmospheric Sciences, University of Alberta, Room 1-26 ESB, Edmonton Alberta, Canada T6G 2E3

Models for the tectonic development of the Slave province for the period ~2.7 to 2.6 Ga are diverse, spanning intracontinenal rift models (e.g. Henderson 1981, MacLachlan and Helmstaedt 1995), arc-continent collision models (Kusky 1989) and those emphasizing active continental margin processes (Davis et al. 1994) and combinations of these processes (Bleeker et al. 1997). Over the past four years, our research has focused on a detailed isotopic and geochemical study of the main lithotectonic units in the Slave province in order to provide a firm basis for establishing a refined tectonic model. We have examined [1] selected exposures of pre-2.8 basement granitoids and gneisses, [2] volcanic and sedimentary rocks of the ~2.72 - 2.65 Ga Yellowknife Supergroup (YKSG), and [3] ~2.6 Ga syn- to post-deformation granitoids from the western Slave province. A summary of significant conclusions are as follows.

- The U-Pb zircon age of pre-2.8 Ga basement in the Hanikahimajuk Lake area, northern Slave province is 3378 Ma. This age is very similar to that of the Kangguyak gneisses to the N, and that of a major metamorphic overprint in the Acasta gneisses to the SW (Bleeker and Stern 1997, and references therein). This clear temporal connection provides evidence that these basement fragments are part of a single crustal block, rather than, for example, fragments of material with diverse crustal histories juxtaposed at a later time.
- In the Hanikahimajuk Lake and Yellowknife areas, low εNd_T values of YKSG mafic-intermediate volcanic rocks and correlated trace element ratio variations document crustal contamination by pre-2.8 Ga basement. This is a clear indication that the volcanic package was built, at least in part, on the basement.
- Mafic-intermediate YKSG volcanic rocks in the Hanikahimajuk Lake study area can be classified into two associations based on trace element characteristics: [1] depleted, tholeiitic type and [2] calc alkaline type. These two groupings are also found in the Yellowknife and Indin Lake areas of the SW Slave province (e.g. Isachsen and Bowring 1994, MacLachlan and Helmstaedt 1995, Pehrrson; pers. comm.). Given the geochemical evidence for basement contamination of [1], we do not envisage an origin in a typical modern mid-oceanic ridge setting.
- The low εNd_T (-5.3) of one YKSG sedimentary rock from the Hanikahimajuk Lake area shows that part of the basement was exposed at the time of ~2.66 Ga YKSG sediment deposition.

- The εNd_T values of Burwash Formation turbidites in the Yellowknife area range from -1.8 to +3.1 (n=38) with the upper shale units of the Bouma sequence typically showing lower εNd_T than the lower sand units. Careful analysis of trace element abundances within the turbidite sequence indicates that the εNd_T profile is not an artifact of heavy mineral concentration , but is the result of "unmixing" of isotopically diverse detritus derived from at least two sources: [1] YKSG volcanic rocks variably contaminated by pre-YKSG basement and [2] little-contaminated granitic rocks. The westerly derivation of these turbidites (Henderson, 1975), implies the existence of little-contaminated, pre-2.66 Ga granitic rocks west of Yellowknife and, therefore, provenance regions not underlain or weakly influenced by pre-2.8 Ga basement.
- A regional study of 2.62~2.58 Ga syn- to post-deformation granitoids indicates that ~2.61 Ga syn-deformation granitoids are derived mainly through partial melting of mafic crustal protoliths (i.e. altered basalt), with local mantle input, whereas ~2.59 Ga post-deformation granitoids derive from partial melting of metasedimentary rocks (Yamashita et al. 1998). Pb isotopic modeling indicates that all granitoids from the western Slave province require input from a crustal source older than 3.2 Ga, but in variable amounts, and these new results do not support east-west trending isotopic boundaries within the western Slave province (Davis et al., 1996).
- The strongest geochronological and isotopic signature of the pre-2.8 Ga basement in the Slave province seems to be restricted to two areas; [1] the Acasta River area and [2] along the volcanic belt which runs from Arcadia Bay - Hanikahimajuk Lake - Point Lake - Winter Lake - Sleepy Dragon Complex/Yellowknife, approximately coincident with the "isotopic boundary" previously proposed (Thorpe et al. 1992, Davis and Hegner 1992). Interestingly, the known U-Pb ages of basement along this zone appears to young southward, possibly providing important clues as to the tectonic origin of the pre-YKSG basement.

In addition to these conclusions from our data, the following summarizes salient points made by previous researchers that must also be taken into consideration.

- Volcanic belts in the west-central Slave province are typically mafic dominated (i.e. Yellowknife-type) whereas volcanic belts in the east-northeastern Slave province are felsic dominated (i.e. Hackett River-type; Padgham 1985).
- Known pre-2.8 Ga basement is restricted to the western Slave province (Bleeker and Stern 1997 and references therein).
- Clear Nd and Pb isotopic signature of pre-2.8 Ga basement in younger rocks is restricted to the western Slave province (Thorpe et al. 1992, Davis and Hegner 1992, Davis et al. 1996).
- 2625-2640 Ma igneous rocks have not yet been documented from the east or west Slave province (Villeneuve et al. 1997).

We integrate these observations into a revised tectonic model which attempts to explain most field, isotopic and geochemical features of the Slave province. We contend that the mafic-intermediate volcanic rocks of the western Slave province can be generated in a single back-arc system, initially developed as an ensialic back-arc. In modern-day analogs, such as the Japan arc, depleted tholeiitic and calc-alkaline volcanic rocks (as well as felsic volcanic rocks) are both generated in the same back-arc system (e.g. Miyake 1994). We also note that YKSG mafic volcanic rocks near Point Lake, overlying the 3.15 Ga Augustus granite, are also interpreted to have formed in a back-arc setting (Corcoran and Dostal 1997). The basement blocks of the western Slave are interpreted to be the remnants of this rifted continental block. In this model, the two mafic dominated volcanic belts in the western Slave province (i.e. [1] Grenville Lake - Indin Lake - Ghost/MacNaughton Lake and [2] Arcadia Bay - Hanikahimajuk Lake - Point Lake - Winter Lake - Sleepy Dragon Complex/Yellowknife) may represent the margin of a (now collapsed and shortened) ensialic back-arc. Further, we propose that the felsic-dominated volcanic belt (Hackett River-type) in the eastern Slave province represents a fore-arc volcanic system(s). This could also be directly analogous to the modern Japan tectonic setting where a felsic dominated (easterly) fore-arc volcanic system, without significant ancient basement influence, developing adjacent to a mafic-dominated back-arc containing numerous fragmented blocks of the former continent (Sino-Korean Craton; e.g. Kimura et al. 1991). The size of the Slave craton is also compatible with the proposed model if the late-Archean regional compressional deformation is taken into account, as the width of the craton (~450 km) is approximately half of the combined Japan arc - back arc (i.e. sea of Japan) system (~1000 km). This tectonic setting is also characterized also by significant accumulations of turbidite, both fore-arc and back-arc. In our model, we propose west-facing subduction ultimately collapses this fore-arc back-arc system, possibly accounting for the 2640-2625 Ma cessation of magmatism, followed by crustal thickening and production of ~2.61 Ga metaluminous granitoids and ~2.59 Ga peraluminous granitoids. Notably, mafic igneous rocks and immature sedimentary rocks, which typically fill back-arc basins, are ideal sources for these granitoids (Yamashita et al. 1998). This model also accounts for the regional Nd-Pb isotopic variations in the crustally-derived ~2.61-2.59 Ga granitoids of the SW Slave province, as the more juvenile signatures found west of the 111°W "isotopic boundary" may reflect an origin for the granitoid protoliths in a mature back-arc with little basement influence.

References

Bleeker, W. and Stern, R.A. 1997. Lithoprobe Report, **56**: 32-35.

Bleeker, W., Davis, W.J., and Villeneuve, M.E. 1997. Lithoprobe Report, **56**: 36-37.

Corcoran P.L. and Dostal J. 1997. Lithoprobe Report, **56**: 205.

Davis, W. J., and Hegner, E. 1992. Contributions to Mineralogy and Petrology, **111**: 493-504.

Davis, W. J., Fryer, B. J., and King, J. E. 1994. Precambrian Research, **67**: 207-241.

Davis, W. J., Gariépy, C., and van Breemen, O. 1996. Chemical Geology, **130**: 255-269.

Henderson, J. B. 1975. Geological Survey of Canada, Bulletin, 246: 62 pp.

Henderson, J. B. 1981. *In* Plate tectonics in the Precambrian. Elsevier, Amsterdam, pp. 213-235.

Isachsen, C. E., and Bowring, S. A. 1994. Geology, **22**: 917-920.

Kimura, T., Hayami, I, and Yoshida, S. 1991. Geology of Japan. University of Tokyo Press. 287 pp.

Kusky., T. M. 1989. Geology, **17**: 63-67.

MacLachlan, K., and Helmstaedt, H. 1995. Canadian Journal of Earth Sciences, **32**: 614-630.

Miyake, Y. 1994. Geochemical Journal, **28**: 431-472.

Padgham, W.A. 1985. Geological Association of Canada Special Paper **28**: 133-151.

Villeneuve, M. E., Henderson, J. R., Hrabi, R. B. Jackson, V. A., and Relf, C. 1997. *In* Radiogenic age and isotopic studies: report 10: Geological Survey of Canada, Current Research 1997-F: 37-60.

Yamashita, K. and Creaser, R. A. 1996. Geological Society of America, Abstract with Programs, **28**: A-229.

Yamashita, K., Creaser, R. A., and Villeneuve, M. E. 1996. American Geophysical Union, Abstracts with programs, **77**: F-821.

Yamashita, K., Jensen, J. E., Creaser, R. A., and Gebert, J. S. 1995. Geological Association of Canada/ Mineralogical Association of Canada, Abstracts with programs, **20**: A-112.

Yamashita, K., Creaser, R. A. and Heaman, L. M. 1997. Lithoprobe Report, **56**: 18-19.

Yamashita, K., Creaser, R.A., Stemler, J.U., and Zimaro, T.W. 1998. Canadian Journal of Earth Sciences, submitted.

UNCONFORMITIES, MAJOR FAULTS AND THE EVOLUTION OF VOLCANO-SEDIMENTARY BASINS ON THE SLAVE CRATON

Mueller, W.U, Sciences de la Terre, Unversité du Québec à Chicoutimi, Québec, Canada, G7H 2B1; **Bowring, S.A.** Dept. Earth, Atmospheric, and Planetary Sciences, Massachusetts Institute of Technology, Cambridge, Ma. USA, 02139; **Corcoran, P. L.** Department of Earth Sciences, Dalhousie University, Halifax, Nova Scotia, B3H 3J5; **Pickett, C.** Sciences de la Terre, Unversité du Québec à Chicoutimi, Québec, Canada, G7H 2B1

The evolution of Archean supracrustal sequences is difficult to assess because they are preserved as deformed structural remnants and often poorly exposed. Correlation of individual volcano-sedimentary belts can be therefore problematic. Recognition of major stratigraphic markers or unconformities help constrain the evolution of supracrustal sequences and are important time-lines that can be used to link individual belts. The 4.03-2.5 Ga Slave craton is a complex association of (i) sialic (gneissic) basement complexes, (ii) oceanic and continental volcano-plutonic arcs, and (iii) platformal-, flysch- and molasse-type sedimentary basins. The accumulation of volcanic and sedimentary rocks from 2.7 Ga to 2.6 Ga reflects different tectonic environments and our knowledge of these successions outside the Yellowknife area is limited. Major unconformities represent first-order time-lines that in conjunction with precise U-Pb age determinations may help define the regional stratigraphy, determine the tectonic history, facilitate the interpretation of sedimentary facies successions, and subsequently enable reconstruction of the paleogeography. Their identification can be useful in creating pan-Slave tie lines so that various sectors of the Slave craton can be correlated.

During the latter stages of Slave craton evolution, late-orogenic, clastic basins developed at ca. 2.6Ga. These basins, now preserved as isolated sedimentary and structural entities, often occur adjacent to major faults and older basement. Their sedimentary characteristics such as large-scale, coarse clastic, fining-upward sequences, rapid lateral facies changes or cyclic repetition of lithofacies are consistent with tectonic control on sedimentation. The Jackson Lake and Beaulieu Formations are adjacent to the Jackson and Beniah Lake faults, respectively, and are convincing examples of tectonically influenced sedimentary basins. In both cases, a pronounced unconformity occurs with the mafic-dominated hinterland (subaqueous volcanic rocks) on the western margin, whereas a fault delineates the sedimentary rocks to the east. The 2.6 Ga molasse-type, Keskarrah Formation at Point Lake, the northern extension of this late sedimentary phase is significant because of unconformable contacts with (i) the 3.22 Ga Augustus granite, (ii) the ca. 2660-2670 Ma mafic-felsic volcanic Peltier Formation, and (iii) the time-equivalent, arc-related, flysch-type Contwoyto Formation. In addition, an important unconformity within the Beniah Lake fault zone (long. 112°29´ / lat. 63°27´) has been recently identified. The ca. 2.9 Ga, platformal-type, quartz-arenites of the Beniah Formation are unconformably overlain by conglomerates of inferred 2.6 Ga molasse-type affinity.

The interpretation of the clastic sedimentary rocks of the Beaulieu Formation has been problematic. However, the identification of elongate, quartz-feldspar- and feldspar-hornblende-phyric porphyry stocks within the Beniah Lake fault zone and clasts derived from the stock observed in the conglomerate beds, attests to contemporaneity of magmatism and basin subsidence. The similarity to classic Timikaming-type basins of the Superior Province is striking. U-Pb age determinations of the stocks has proven difficult. The porphyritic rocks have yielded zircons which define extremely discordant arrays on concordia diagrams. One sample has a well defined lower intercept of 370 Ma (anchored by nearly concordant points) and an upper intercept of ca. 2.6 Ga which we interpret to be the approximate age of crystallization. Another sample has zircons which have $^{207}Pb/^{206}Pb$ dates as young as 110 Ma! The extreme Pb-loss is puzzling and may point to as yet unrecognized thermal event in this part of the Slave craton.

Another important, but not well constrained unconformity which has been observed locally, is associated with 2700-2660 Ma, arc-related, volcanic sequences and related turbiditic flysch deposits. At Point Lake the Contwoyto turbiditic deposits and the Peltier Formation volcanics

overlie the Augustus granite unconformably. Two samples from subaqueous felsic to intermediate volcaniclastic rocks of probable pyroclastic origin from the Peltier Formation yield approximate upper intercept ages of 2.66-2.67 Ga. Similarly, an unconformity is observed between the Raquette Lake Formation of the Cameron River volcanic belt and the plutonic 2.8-2.9 Ga Sleepy Dragon complex. A preliminary age of 2.69 Ga for a quartz-feldspar-phyric, massive to brecciated, subaerial, rhyolite flow just above this unconformity is a maximum age for the unconformity. The abundance of ca. 3.0 Ga inherited zircons in this rhyolite indicates a contribution from underlying, older sialic crust. The continued recognition of unconformities coupled with radiometric age determinations will help link individual supracrustal sequences and constrain models for the evolution of Slave craton.

METAMORPHISM ALONG THE SLAVE PORTION OF THE SNORCLE TRANSECT

Kathryn M. Bethune & Dugald M. Carmichael
Dept. Geological Sciences Queen's University, Kingston, Ontario
K7L 3N6

Introduction

The Slave Province is well known for its regional low- to moderate-pressure metamorphism. Despite several decades of investigation, the tectonic setting of this metamorphism (ensialic rift *vs.* subduction environments) remains controversial. The present study, undertaken along the easternmost part of the SNORCLE Transect in Yellowknife domain (Fig. 1), aims to resolve some first-order questions regarding the tectonic and magmatic processes controlling this metamorphic style.

Tectono-metamorphic Framework

Figure 2 outlines the sequence of late Archean tectono-metamorphic events in Yellowknife domain. Following deposition of the Burwash formation at ≤2660 Ma (Bleeker & Villeneuve, 1995), turbidites and underlying rocks underwent polyphase deformation accompanied by regional low-pressure metamorphism and intrusion of granite. Metamorphism occurred in two principal stages (Bleeker & Beaumont-Smith, 1995). An earlier metamorphism (M_1) accompanied development of the F_1 foldbelt (Fig. 1). It is preserved only in areas remote from plutonic rocks where it is expressed by alignment of chlorite, biotite and muscovite that define an axial planar slaty cleavage to northeast-striking folds. M_1 was succeeded by higher-grade, pluton-enhanced metamorphism (M_2) which was broadly synchronous with D_2 deformation; the area contains a number of granite suites, whose timing varies from pre- to late-D_2. At map scale, the main expression of metamorphism is a set of regional isograds whose topology (Fig. 1) closely follows the outlines of gneissic and plutonic domains. From low to high metamorphic grade two index mineral isograds (biotite, cordierite or 'knotted schist') separate three metamorphic zones; only the 'knotted schist' isograd has been mapped at regional scale. The metamorphic pattern is thus one of thermal highs, around granitoid rocks, coupled with intervening lows. At amphibolite grade, pelitic rocks typically contain combinations of cordierite, andalusite, staurolite and/or garnet. Close to granite contacts, andalusite is commonly replaced by sillimanite. Collectively, the assemblage data define a Buchan-type (andalusite–sillimanite) facies series, characterized by low to intermediate pressure and high geothermal gradients (40-50°C/km; Thompson, 1978, 1989), a metamorphic style which is typical across the Slave Province.

It is notable that, although now preserved as dominantly greenschist facies, the maximum grade attained during M_1 is uncertain. However, mineral textural relationships support the interpretation that the transition between M_1 and M_2 was more-or-less a continuous progression punctuated only by a change in deformation regime. For example, at the biotite isograd, mm-scale biotite porphyroblasts contain S_1 inclusion trails, and are wrapped by S_2. In contrast, timing of porphyroblast growth at and above the cordierite isograd generally varies from syn- to post-S_2.

Dynamics of metamorphism

The strong zonal arrangement of isograds around granitic plutons implies a genetic link between magmatism and metamorphism. However, as pointed out by Thompson (1978), smaller plutons have locally intruded low-grade zones where they show narrow contact aureoles that transect regional isograds (cf. Bleeker & Beaumont-Smith, 1995; Davidson, 1967). This suggests that metamorphism proceeded by establishment of a set of regional isotherms (M_1) that were subsequently modified during continued burial and by thermal spikes associated with plutons (M_2) (e.g. Williams & Karlstrom, 1996). Thermal modelling of this style of low-pressure metamorphism (e.g. Barton & Hanson, 1989) suggests that the thermal anomalies related to individual intrusions are generally built upon the decaying temperature profiles of earlier events. Depending apon: (1) the regional distribution of heat (isotherms) within the crust, presumed to be constantly changing, and, (2) the location, volume and time interval between intrusions, the resultant map pattern reflects a complex interplay between regional and superimposed contact effects, variable in both space and time.

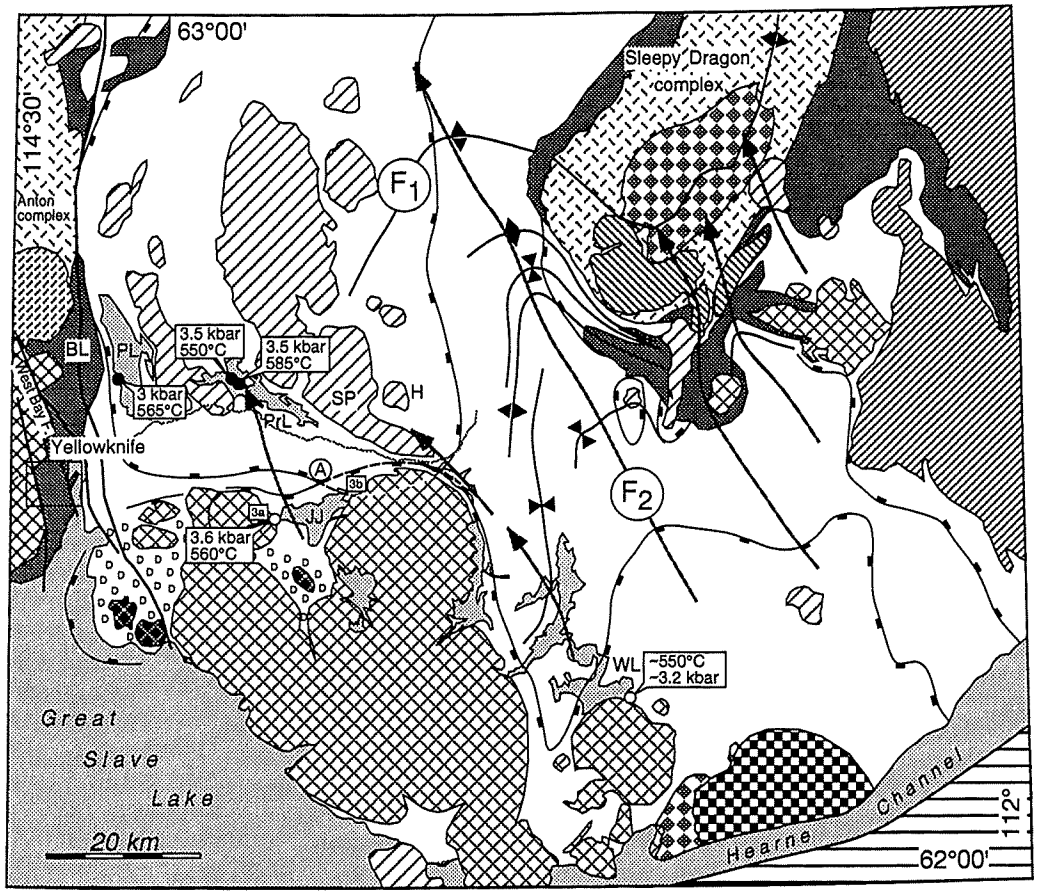

Paleoproterozoic

- Great Slave Supergroup (<1.93 Ga)
  Compton laccoliths (1.87 Ga)
- Dyke swarms
  Dogrib (2.19 Ga), Indin, Milt, Hearne (2.04 Ga)
- Blatchford intrusive suite (2.18 Ga)

Archean

Granitic rocks

- Morose granite (~2.58 Ga)
- Redout suite
- Prosperous suite (~2.61–2.6 Ga)
- Duckfish granite (~2.61 Ga)
- Meander Lake suite (granite-granodiorite)

Cordierite isograd (ornament on high-grade side) — mapped / inferred

Defeat suite (~2.64–2.6 Ga)

- Tonalite-granite with supracrustal inclusions
- Tonalite-granite
- Quartz diorite

Greenstone belt supracrustal rocks

- Burwash Formation (turbidites, ≤2.66 Ga)
- Metavolcanic rocks (~2.72–2.66 Ga)

Pre-Greenstone belt

- Gneissic granitoid rocks (~3.2–2.9 Ga)

Figure 1. Generalized geological map of Yellowknife domain, modified from Henderson (1985) and Bleeker (1996). Abbreviations: Bl = Banting Lake, PL = Prosperous Lake, PrL = Prelude Lake, JJ = Jennejohn Lake, WL = Watta Lake, SP = Sparrow pluton, H = Hidden Lake pluton. The Jackson Lake formation (not shown) is a narrow north-northeast-trending deposit occupying the core of the Yellowknife greenstone belt.

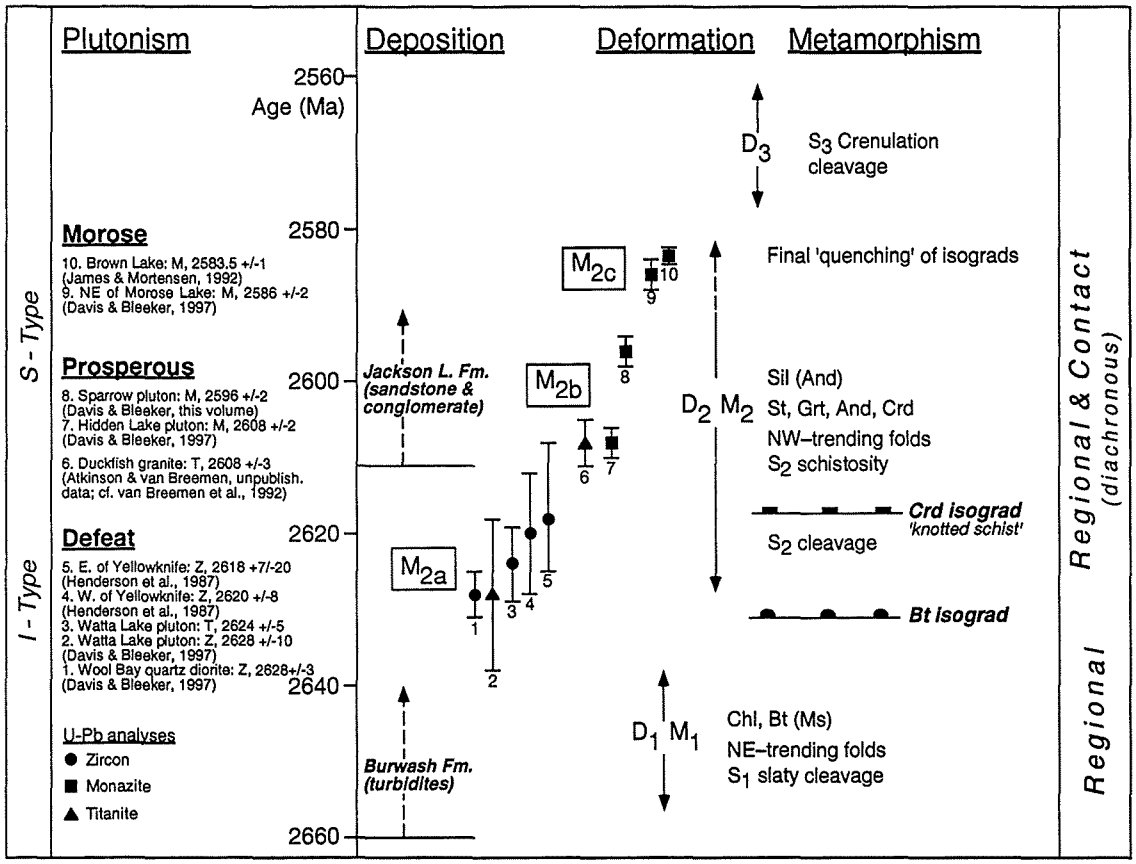

Figure 2. Metamorphism in Yellowknife domain in relation to depositional, intrusive and deformational events. U–Pb ages from van Breemen et al., 1992; Henderson et al., 1987; James & Mortensen, 1992; Davis & Bleeker, 1997, Isachsen & Bowring, 1997.

The U-Pb data for plutonic suites in Yellowknife domain, compiled in Figure 2, indicate that M_2 spanned a period of as much as 50 m.y., peaking at different times in the different thermal culminations within the map area. The main stage of Defeat plutonism occurred at ~2630–2620 Ma, whereas Prosperous plutonism occurred in the interval ~2610–2595 Ma; the Morose granite was emplaced ~10 m.y. later (~2585 Ma). The error limits of the data allow that, rather than occurring as discrete pulses, there could have been considerable overlap between the Defeat and Prosperous suites. Some plutons, for example the Duckfish granite north of Yellowknife (Fig. 1) and a small stock at Hidden Lake, may in fact be transitional between the two suites (W. Bleeker, pers. comm., 1997).

Defeat vs. Prosperous aureole

East of Yellowknife there is map-scale evidence for overprinting of thermal aureoles of different age. For instance, Henderson (1985) proposed that, in accord with their relative ages as determined from field relationships and imprecise Rb–Sr ages (e.g. Green and Baadsgaard, 1971; Green et al., 1968), the contact aureole around the Defeat batholith (M_{2a}) pre-dates the broader aureole around the Prosperous batholith to the north (M_{2b}). The closure of the cordierite isograd between the two batholiths (Locality A, Fig. 2) was therefore inferred to represent a point of intersection between their respective aureoles. Given its proximity to the SNORCLE line, the nature of this overprinting relationship has been one of the primary focuses of this study.

Field and petrographic work indicates that there are no significant differences in the mineral assemblages of the two aureoles. At higher grade than the 'knotted schist' isograd, both contain assemblages and sub-assemblages diagnostic of bathozone 2 (Carmichael, 1978), indicating emplacement within a *P-T* range of 2.5–3.7 kbar (8–12 km) and 500–600°C. However, whereas in the Prosperous aureole cordierite is the most abundant species of porphyroblast, in the Defeat aureole

staurolite predominates, and cordierite is comparatively rare. The prevalence of staurolite within the Defeat aureole may be an effect of bulk composition (e.g. Thompson, 1978); however, its regional extent suggests that, alternatively, it could be a function of a slightly greater emplacement depth, although this has yet to be substantiated quantitatively (see below).

Mineral textural relationships also support the overprinting relationship. For example, where the low grade part of the Prosperous aureole overlaps the Defeat aureole on the west side of Jennejohn Lake (Fig. 2), Defeat staurolite, andalusite and garnet are variably retrograded (Fig. 3a). At higher grade, coincident with the eastward extension of the Prosperous cordierite isograd on the northest arm of Jennejohn Lake (Fig. 2), there is evidence that staurolite, inferred to be of Defeat age, is completely replaced by cordierite, likely of Prosperous age (Fig. 3b). As a general rule, assemblages in the Defeat aureole show a greater degree of retrogression than Prosperous assemblages, suggesting they are indeed older. The implication is that the Defeat aureole had already cooled significantly before the Properous aureole reached its maximum temperature, and that the latter provided the H_2O flux responsible for retrogression.

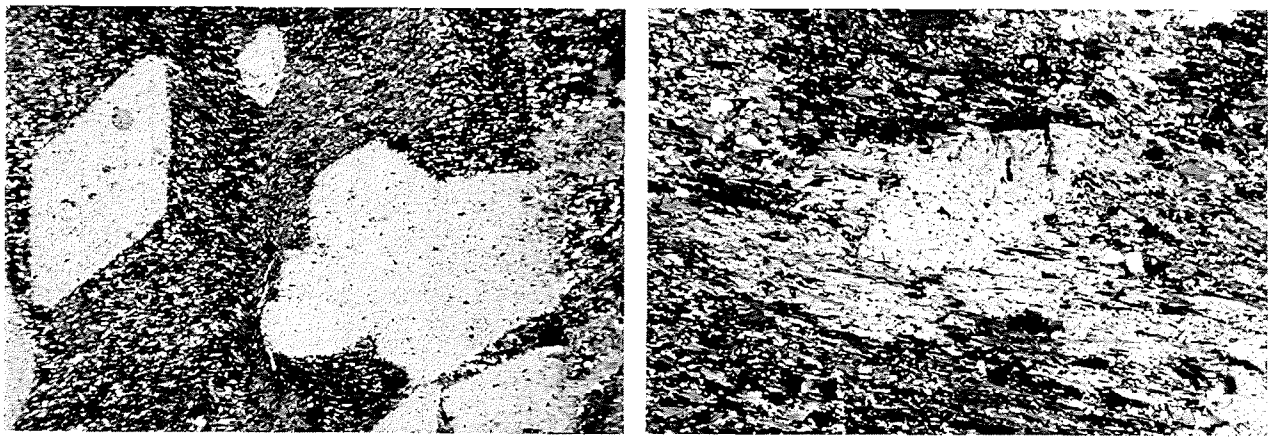

(a) *(b)*

Figure 3. *(a) Staurolite–garnet schist in Defeat contact aureole, west arm of Jennejohn Lake; staurolite is replaced by a fine intergrowth of chlorite and muscovite; late cleavage (upright; S_3?) crenulates earlier cleavage (S_2?) and deflects around porphyroblasts (width of photo ~1 cm); (b) Defeat staurolite completely pseudomorphed by Prosperous cordierite, northeast arm of Jennejohn Lake (width of photo ~0.7 cm).*

Textural observations, Prosperous aureole

In the Prosperous aureole there are several occurrences of the invariant assemblage And–Crd–St–Grt–Ms–Bt–Pl–Qtz, corresponding to a *P* and *T* of ~2.4 kbar and 540°C (Fig. 4). In these samples, staurolite commonly occurs as relict grains enclosed by andalusite or, more commonly, cordierite. In some cases, both andalusite and staurolite are rimmed by cordierite, the latter being spatially associated with garnet. These textural relations support a prograde reaction history whereby staurolite formed earlier than both cordierite and andalusite (Thompson, 1978). This temporal sequence is supported by porphyroblast-cleavage relationships. For example, where it is preserved as larger grains, staurolite is commonly seen to contain cleavage traces oriented at a high angle to the enveloping S_2 foliation. It is not clear whether these traces represent S_1 or possibly an early stage of development of S_2. In contrast to staurolite, andalusite porphyroblasts in the same rocks are generally characterized by curvilinear cleavage traces, suggesting growth more-or-less synchronous with development of S_2. Cordierite, on the other hand, tends to statically overgrow S_2, especially in cases where it occurs as distinct rims on pre-existing staurolite and andalusite.

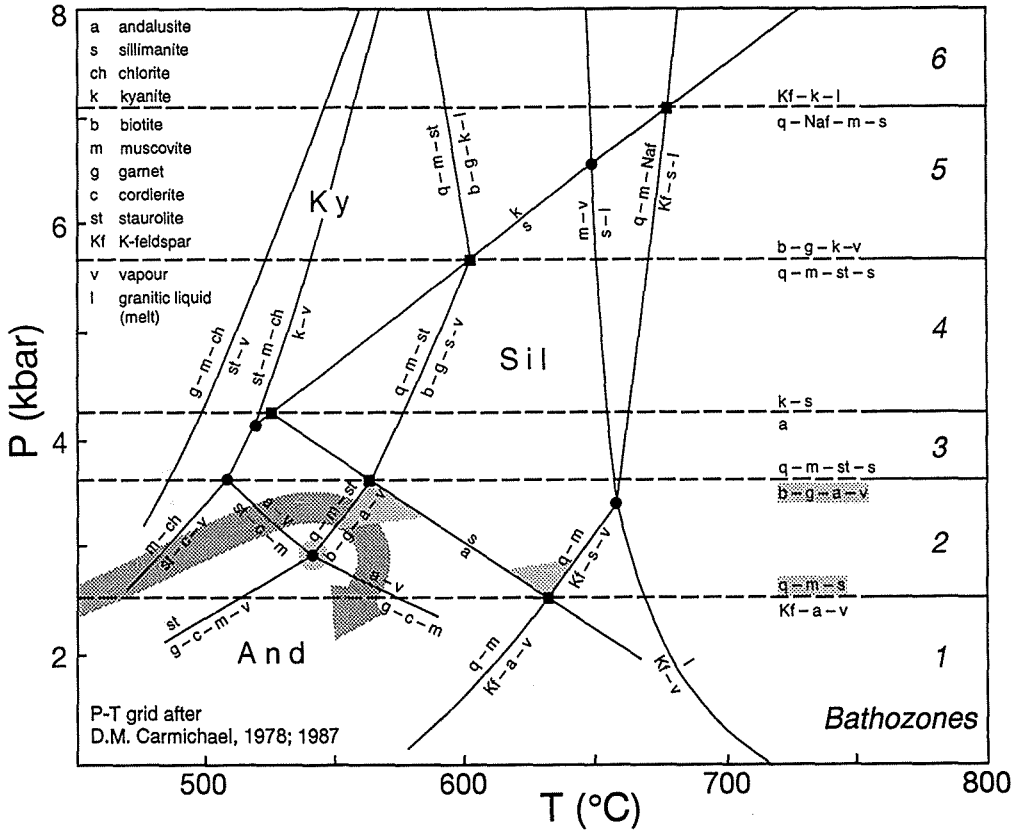

Figure 4. P–T grid modified from Carmichael (1987) showing petrogenetic relations for metapelites; bathozones are from Carmichael (1978). Textural and mineral compositional relations (see text) allow the possibility that staurolite formation occurred before andalusite and cordierite along a clockwise path, as depicted by the shaded curve.

On the basis of petrogenetic relations, Thompson argued that the staurolite in the Slave Province probably represents a lower grade (*e.g.* both lower *P* and *T*) of the same low-pressure metamorphism that produced cordierite and andalusite. However, based on the textural evidence cited above, especially the late-stage 'static' growth of cordierite, it is conceivable that the staurolite in the Prosperous aureole fomed earlier and at higher pressure (and lower *T*) along a clockwise *P-T* path, as illustrated schematically in Figure 3, warranting that cordierite rims on andalusite and staurolite reflect late decompression. Garnet–plagioclase compositional relationships, described below, support such a clockwise path.

Thermobarometry

Figure 5 presents a compilation of *P–T* results obtained to date. Two samples with low-variance assemblages in the amphibolite-facies zone of the Prosperous aureole at Prelude Lake (Fig. 2) yielded tight multi-equilibrium TWEEQU intersections at 3.5 kbar, 585°C and 3.5 kbar, 550°C, respectively. Another higher-variance sample from Prosperous Lake yielded a comparable, but less thermodynamically robust result of ~3 kbar, 565°C. The determinations straddle the andalusite–sillimanite reaction equilibria, or lie just within the sillimanite field, consistent with the fact that andalusite is locally replaced by sillimanite in the immediate vicinity. The results also show reasonable agreement with the published petrogenetic grid (Fig. 4).

Attempts to calibrate *P* and *T* in contact aureoles around Defeat plutons have been frustrated by both by lack of appropriate mineral assemblages, and the high degree of alteration. The best sign of equilibration in a partly retrograded And–St–Grt schist from the west arm of Jennejohn Lake (*see* Fig. 3a) was given by a garnet rim composition; the result (3.6 kbar, 560°C) is thus unlikely to reflect

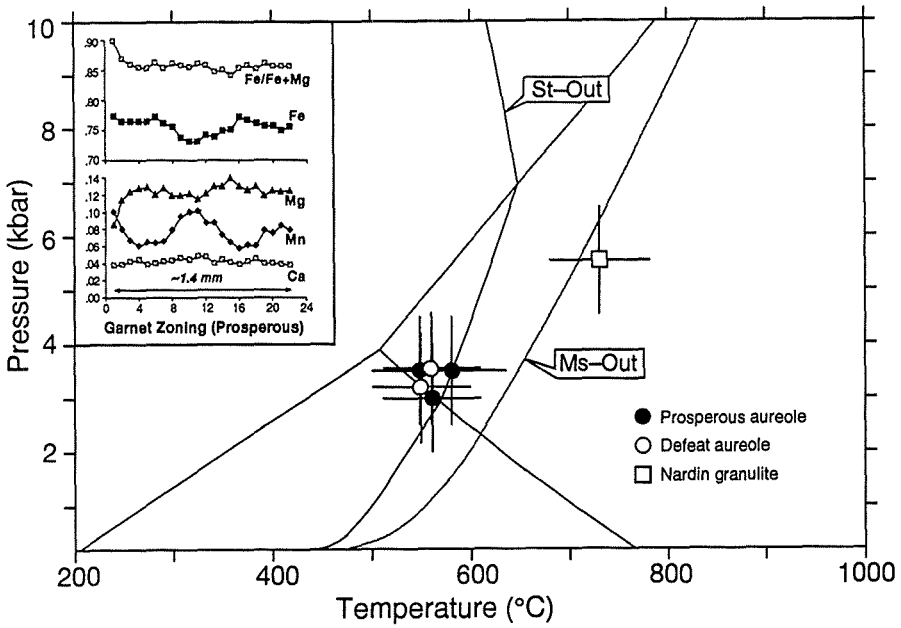

Figure 5. P–T estimates for rocks in Yellowknife domain and at Nardin Lake. Individual points are the representative P and T given by several intersecting equilibria calculated by the program TWEEQU (Berman, 1991, 1996). Error bars are +/- 1 kbar and +/- 50°C. Inset shows zoning typical in fine mm-scale garnets in the amphibolite-facies zone of the Prosperous aureole.

peak Defeat conditions. Assuming a temperature of 550°C, a maximum pressure of ~3.2 kbar is suggested for a Grt–And–Ms–Pl–Qtz–bearing vein intrusive into hornfelsed metapelitic rocks next to a Defeat stock south of Watta Lake (Fig. 2).

Part of this study has also been devoted to determining *P-T* conditions in an upper-amphibolite to granulite-facies domain in the vicinity of Nardin Lake (Stubley, 1995), located ~50 km north of the map area. The high-grade rocks include metabasic, semi-pelitic and pelitic bulk compositions, and are inferred to represent the deeper crustal equivalents of greenschist–amphibolite facies supracrustal rocks exposed in Yellowknife domain. A *P–T* result of 5–6 kbar and 700–750°C was obtained from a Sil–Crd–Kfs metapelite from the highest-grade part of this domain (Fig. 5).

Garnet Zoning

Garnet in the amphibolite-facies pelites of the Prosperous aureole varies from subhedral to highly embayed, and characteristically shows a small bell in Mn in the core, bounded by inflection points marking an increase in Mn and Fe toward the rim (Fig. 5, inset). These features are consistent with modification of earlier, prograde growth-zoning (Spear, 1993). In *P–T* calculations, garnet rim compositions give the best indication of equilibration, as opposed to either cores or inflection points. In one of the two Prelude Lake samples there is compositional evidence for late-stage consumption of the grossular component of garnet, coupled with increase in the anorthite content of plagioclase, indicating that reaction took place while pressure was decreasing.

Metamorphism – Jackson Lake Formation

An outstanding question in Slave geology concerns the timing of deposition and subsequent deformation and metamorphism of the youngest 'Timiskaming-type' fluviatile sandstone and polymictic conglomerate deposits, of which the Jackson Lake Formation in the Yellowknife greenstone belt represents an example. This formation is metamorphosed to greenschist facies; its metamorphic minerals define a strong subvertical cleavage which strikes north-northeast parallel to faulted contacts. Deposition is constrained to have occurred after 2605 +/-6 Ma, the U-Pb zircon age of a granitic clast in the conglomeratic facies near Yellowknife (Isachsen, 1992; Isachsen & Bowring 1997) (Fig. 2). Bleeker & Villeneuve (1995) proposed that deposition may have been controlled by major N–S corridors of faulting developed during the later stages of D_2, which would imply that heat for metamorphism must have been provided at least in part by neighbouring intrusions of the Prosperous batholith.

Based on a traverse conducted from the Jackson Lake Formation at Banting Lake westward across the cordierite isograd near Prosperous Lake (Fig. 1), we see no reason to dispute this interpretation. The metamorphic transition is in fact relatively continuous, leading to the conclusion that the Jackson Lake Formation and underlying units to the east experienced the same metamorphism, whose gradient has not been appreciably disrupted (at least in the vertical sense) by faulting. There is also little difference in structural style in all units across this transect.

Discussion

The accumulation of sandstone and conglomerate deposits containing clasts of diverse lithology (volcanic, siliciclastic, gneissic and granitic rocks) provides evidence for syn-tectonic exhumation and erosion of the suprastructure above Yellowknife domain, starting by as early as ~2.61 Ga. The *P–T* estimates from the Defeat aureole are not reliable enough to be sure of the precise difference in emplacement depth between the Defeat and Prosperous aureoles. However, petrogenetic data (Fig. 4) provide the constraint that it cannot be more than 1.2 kbar, corresponding to ~4 km. The U-Pb data furthermore indicate that the time-range between these suites varied between 30 and 10 m.y. This implies an erosion rate of 0.1–0.4 mm/yr, which is an order of magnitude lower than in most modern collisional orogens (e.g. 1–5 mm/yr), and seems incongruous with such high-energy deposits. However, given that the Defeat suite intruded during the early stages of D2 (Fig. 2), it is possible that rocks within the aureole underwent an initial phase of burial before onset of exhumation and later intrusion of the Prosperous suite; this could account for a higher (but unconstrained) erosion rate. Alternatively, one might appeal to localized topographic control (e.g. incised valleys) for conglomerate deposition, not out of line with the interpretation (e.g. Bleeker & Villeneuve, 1995) reported above. A further possibility is that exhumation was delayed, and occurred mainly within the time interval of Prosperous plutonism (e.g. 2610–2595 Ma); the petrological evidence in the Properous aureole for late-stage reaction under conditons of decreasing pressure would appear to support this.

Summary

1. Late Archean metamorphism in Yellowknife domain occurred in two stages; an earlier greenschist-facies metamorphism (M_1) accompanied development of the F_1 foldbelt. It was superseded by higher-grade metamorphsim related to regional D_2 deformation and intrusion of syn- to late-tectonic granite (M_2). Rather than discrete events, M_1 and M_2 probably represent a continuum separated only by a change in deformation regime.

2. U-Pb geochronology indicates that M_2 was diachronous over a time period of ~50 m.y. The pattern of metamorphism suggests a complex interplay between regional and contact effects.

3. The diachroneity of M_2 is illustrated east of Yellowknife where the thermal aureole around the Prosperous batholith (M_{2b}) overprints the aureole around the Defeat batholith (M_{2a}).

4. *P–T* estimates for the Prosperous aureole are 3–3.5 kbar (9–11 km), 550–600°C. Reliable estimates could not be obtained from the Defeat aureole due to retrogression. However, prolific staurolite within the Defeat aureole is a qualitative indicator of somewhat higher pressure.

5. The tectonic processes controlling deposition of Timiskaming-style conglomerate are not completely understood. Petrogenetic data provide the constraint that no more than ~4 km of exhumation could have occurred in the Defeat–Prosperous interval, implying an erosion rate of fractions of a mm per year, which seems low for such high-energy deposits. However, this assumes a single cycle of tectonic burial and exhumation, which may be an over-simplification.

6. In the Prosperous aureole, samples with the 'full-house' assemblage And–Crd–St–Grt–Ms–Bt–Pl–Qtz contain textural and chemical compositional evidence for late-stage static growth of cordierite while pressure was decreasing, consistent with evidence for contemporaneous exhumation and erosion.

References

Barton, M.D. & Hanson, B. H., 1989. Magmatism and the development of low-pressure metamorphic belts: Implications from the western United States and thermal modeling. Geological Society of America, **101**, 1051–1065.

Bleeker, W. Thematic Structural Studies in the Slave Province, Northwest Territories: the Sleepy Dragon complex. *In* Current Research, Geological Survey of Canada, Paper 1996–C, 37–48.

Bleeker, W. & Beaumont-Smith, C. Thematic structural studies in the Slave Province: preliminary results and implications for Yellowknife Domain. *In* Current Research, Geological Survey of Canada, Paper 1995–C, 87–96.

Bleeker, W. & Villeneuve, M.E., 1995. Structural studies along the Slave portion of the SNORCLE Transect. Lithoprobe report No. 44, 8–13.

Carmichael, D.M., 1978. Metamorphic bathozones and bathograds: a measure of the depth of post-metamorphic uplift and erosion on the regional scale. American Journal of Science, **278**, 769–797.

Carmichael, D.M., Helmstaedt, H.H., and Thomas, N., 1987. A field trip in the Frontenac Arch with emphasis on stratigraphy., structure and metamorphism. Friends of the Grenville, Field Trip Guidebook.

Berman, R.G. 1991. Thermobarometry with estimation of equilibrium state: a new technique with petrological applications. Canadian Mineralogist, **29**, 833–855.

Berman, R.G. & Aranovich, L. Ya. 1996. Optimized standard state and solution properies of minerals. I. Model calibration for olivine, orthopyroxene, cordierite, garnet and ilmenite in the system FeO–MgO–CaO–Al_2O_3–TiO_2–SiO_2. Contributions to Mineralogy and Petrology, **126**, 1–24.

Davidson, A., 1967. Metamorphism and intrusion in the Benjamin Lake map-area, Northwest Territories, Ph.D. Thesis, University of British Columbia, Vancouver, B.C., 204 p.

Davis W.J. & Bleeker, W. 1997. Timing of plutonism and regional deformation in the Yellowknife–Sleepy Dragon area, southern Slave Province. *In* Yellowknife Geoscience Forum (1997), Program with Abstracts, 34–36.

Green, D.C. & Baadsgaard, H., 1971. Temporal evolution and petrogenesis of an Archean crustal segment at Yellowknife, N.W.T., Canada. Journal of Petrology, **12**, 177–217.

Green, D.C., Baadsgaard, H., & Cumming, G.L., 1968. Geochronology of the Yellowknife area, Northwest Territories, Canada. Canadian Journal of Earth Sciences, **5**, 725–735.

Henderson, J. B., 1985. Geology of the Yellowknife–Hearne Lake area, District of MacKenzie: a segment across an Archean basin. Geological Survey of Canada, Memoir 414, 135 p.

Henderson, J.B., van Breemen, O., & Loveridge, W.D., 1987. Some U-Pb zircon ages from Archean basement, supracrustal and intrusive rocks, Yellowknife–Hearne Lake area, District of MacKenzie. In Radiogenic and Isotope Studies: Report 1, Geological Survey of Canada, Paper 87–2, 111–121.

Isachsen, C.E., 1992. U-Pb zircon geochronology of the Yellowknife volcanic belt and subjacent rocks: constraints on timing, duration and mechanics of greenstone belt formation. Ph.D. Thesis, Washington University, St. Louis, Missouri, 164 p.

Isachsen, C.E. & Bowring, S.A., 1997. The Bell Lake Group and Anton Complex: a basement – cover sequence beneath the Archean Yellowknife greenstone belt revealed and implicated in greenstone belt formation, Canadian Journal of Earth Sciences, **34**, 169–189.

James D.T. & Mortensen, J.K., 1992. An Archean metamorphic core complex in the southern Slave Province: basement-cover structural relationships between the Sleepy Dragon Complex and the Yellowknife Supergroup. Canadian Journal of Earth Sciences, **29**, 2133–2145.

Spear, F.S., 1993. Metamorphic Phase Equilibria and Pressure–Temperature–Time Paths. Mineralogical Society of America, Monograph, Washington, D.C., 799 p.

Thompson, P.H., 1978. Archean regional metamorphism in the Slave structural province – a new perspective on some old rocks. *In* Metamorphism in the Canadian Shield, Geological Survey of Canada, Paper 78–10, 85–102.

Thompson, P. H., 1989. An empirical model for metamorphic evolution of the Archaean Slave Province and adjacent Thelon Tectonic Zone, north-western Canadian Shield. Geological Society of London, Special Publication No. 43, 245–263.

van Breemen, O., Davis, W.J., and King, J.E., 1992. Temporal distribution of granitoid plutonic rocks in the Archean Slave Province, northwest Canadian Shield. Canadian Journal of Earth Sciences, **29**, 2186–2199.

Williams, M.L. & Karlstrom, K. E., 1996. Looping P–T paths and high-*T*, low-*P* middle crustal metamorphism: Proterozoic evolution of the southwestern United States. Geology, **24**, 1119–1122.

U-Pb Geochronology of the Sleepy Dragon Complex in the Morose-Patterson Lakes area, southwestern Slave Province, with tectonic implications

John Ketchum
Department of Earth Sciences, Memorial University, St. John's, Newfoundland A1B 3X5

Wouter Bleeker
Geological Survey of Canada, 601 Booth St., Ottawa, Ontario K1A 0E8

INTRODUCTION

A current goal of geological research in the Archean Slave Province, Northwest Territories, Canada, is to shed light on a long-standing debate over models of its lithotectonic evolution. Central to this debate is the tectonic and depositional setting of regionally extensive volcano-sedimentary sequences of the ~2720-2650 Ma Yellowknife Supergroup. In general terms, some workers favour deposition of these rocks within ensialic rift basins developed on an older, largely plutonic basement, whereas other workers favour accretionary models where supracrustal assemblages have more varied (and in some cases exotic) origins and form lithotectonic units in structural contact with older basement blocks. Much of the work around this issue has centred on the supracrustal rocks and their mutual contact with underlying basement. We have taken a somewhat different approach by focusing on the geological history of basement exposures throughout the southwestern Slave Province in order to place meaningful constraints on basement-cover relationships. An important additional goal of this work is to document the pre-2.7 Ga evolution of the Slave Province, which remains poorly understood.

Below we report both preliminary and final U-Pb data from a detailed structural, lithologic, and geochronologic study of the Sleepy Dragon "Basement" Complex (SDC) and its volcano-sedimentary cover in the Morose-Patterson Lakes area (Fig. 1). This segment of the SDC is a "type area" for documenting basement lithologies and basement-cover relationships, and is imaged at depth in the SNORCLE seismic reflection profile. Our goal is to outline a detailed chronology of events in this region which will hopefully serve as a benchmark for basement-cover transitions elsewhere in the western Slave Province. Although generally well exposed, key lithologic units and field relationships are modified by structural overprinting, and have only recently been the subject of detailed, integrated studies and U-Pb age dating (e.g., Bleeker and Beaumont-Smith 1995; Bleeker 1996; Bleeker et al. 1997a). Age information presented below provides several important constraints on the lithotectonic evolution of this region.

THE SLEEPY DRAGON COMPLEX

The SDC is located ~100 km northeast of Yellowknife within a large, north-trending granite-gneiss domain mantled by the Cameron and Beaulieu River mafic volcanic belts. The complex comprises a heterogeneous assemblage of foliated to gneissic, granodioritic to gabbroic rocks and mafic dykes that pre-date deposition of the Yellowknife Supergroup (Henderson 1985). The remainder of the granite-gneiss domain consists of foliated to massive granitoid plutons that intrude the SDC. Contact relationships between the SDC and overlying supracrustal rocks are varied. In some places, a structurally modified unconformity is documented (e.g., Henderson 1985; Bleeker et al. 1997a) whereas in others, the contact is entirely tectonic, with no evidence of a former stratigraphic relationship (e.g., Lambert 1988; James and Mortensen 1992). Davidson (1972), Lambert (1988), James and Mortensen (1992) and Bleeker et al. (1997a) have all demonstrated that the SDC has a pre-Yellowknife Supergroup history of high-grade metamorphism and deformation, although the details of these events are poorly known.

Younger fabrics and structures in cover rocks are also documented in the SDC. At its southern end, Bleeker and Beaumont-Smith (1995) and Bleeker (1996) have shown that the complex

represents a large-scale fold interference structure analogous to similar structures in the adjacent Yellowknife Supergroup. Fifty kilometres to the north, high-strain zones along the SDC margin and in the Cameron River volcanic belt are attributed both to early thrusting and later extensional shearing (James and Mortensen 1992). A high-strain zone along strike to the south with normal-sense kinematic indicators represents an older structure (Bleeker et al. 1997a).

Previous geochronological data from the SDC and younger plutons are limited. Preliminary U-Pb data from the northern part of the complex indicate that tonalite gneiss may be older than 3.0 Ga, and perhaps as old as 3.14 Ga ($^{207}Pb/^{206}Pb$ age of the oldest zircon fraction; James and Mortensen 1992). On the eastern margin, Lambert and van Breeman (1991) report an igneous crystallization age of 2936 +17/-14 Ma for gneissic granodiorite, and a minimum age of ~2750 Ma for granodiorite gneiss in the Meander Lake plutonic complex (east of the SDC). In the southwestern SDC, Henderson et al. (1987) obtained ages of 2819 +40/-31 Ma and 2683.5 ± 2 Ma for cataclastic granite gneiss and cross-cutting, weakly-foliated granodiorite, respectively. North of this location, James and Mortensen (1992) dated the foliated Suse Lake granite at 2641 ± 4 Ma, and the unmetamorphosed Morose granite at 2584 ± 1 Ma; both units are intrusive into the SDC. Nd isotopic data are limited to that of Dudás et al. (1988) who obtained depleted mantle model ages of ~3.3 Ga from migmatitic gneiss in the southern SDC.

U-PB RESULTS AND IMPLICATIONS

Figure 1 shows the location and preliminary age (italicized text) or final age (bold text) of seven samples from the SDC and one sample from a structurally higher unit with an inferred supracrustal origin. Additional data, mainly zircon and titanite analyses, will be presented at the meeting. The samples are discussed below in chronological order from oldest to youngest.

BNB95-050 - tonalite gneiss, Webb Lake

A sample of grey tonalite gneiss, representative of "typical" basement, was collected from the western margin of the SDC at Webb Lake (Fig. 1). This unit is protomylonitic at the sample site and is cut by three temporally distinct mafic dyke swarms (Bleeker et al. 1997a). Zircons separated from the tonalite gneiss consist of small brown prismatic grains. Five analyses of this material yield a roughly linear array of discordant data points on a conventional U-Pb concordia diagram, with a best fit regression line yielding an upper intercept age of ca. 2935 Ma. Two of the zircon fractions have elevated U concentrations (>1000 ppm) and plot farthest to the left of this line. Excluding these fractions, the remaining three colinear analyses give an upper intercept age of 2935 +9/-8 Ma, which we interpret as the primary crystallization age of the tonalite. Zircons making up the excluded fractions appear to have suffered initial Pb loss at an earlier time than those in the remaining fractions, consistent with their relatively high U content and probable greater degree of radiation-induced lattice damage. This relationship appears to be relatively common in zircons analysed for this study.

The tonalite gneiss is identical in age to a biotite granodiorite gneiss dated at 2936 +17/-14 Ma from the southeast margin of the SDC (Lambert and van Breemen 1991). Zircons of this age are also present in the overlying Raquette Lake (Bleeker et al. 1997a) and Patterson Lake Formations (Bleeker and Villeneuve, unpublished), indicating that both formations contain basement detritus. Although James and Mortensen (1992) present evidence for >3.0 Ga basement gneiss, the 2.93 Ga units are the oldest Sleepy Dragon lithologies to be successfully dated thus far.

97JKS-51b - fine-grained tonalite layer, Patterson Lake

The tonalite described above hosts numerous, thin (<0.2 m wide) layers of fine-grained tonalite to quartz diorite on an island at the north end of Patterson Lake. These layers are completely transposed in the gneissic foliation, and although they appear to be younger than their host, unambiguous field evidence of relative age is lacking. A fine-grained tonalite layer sampled from this island contains numerous small brown prismatic zircons, and a preliminary upper intercept age of 2910 +17/-12 Ma is obtained from three strongly discordant fractions. We interpret this as the primary crystallization age of the

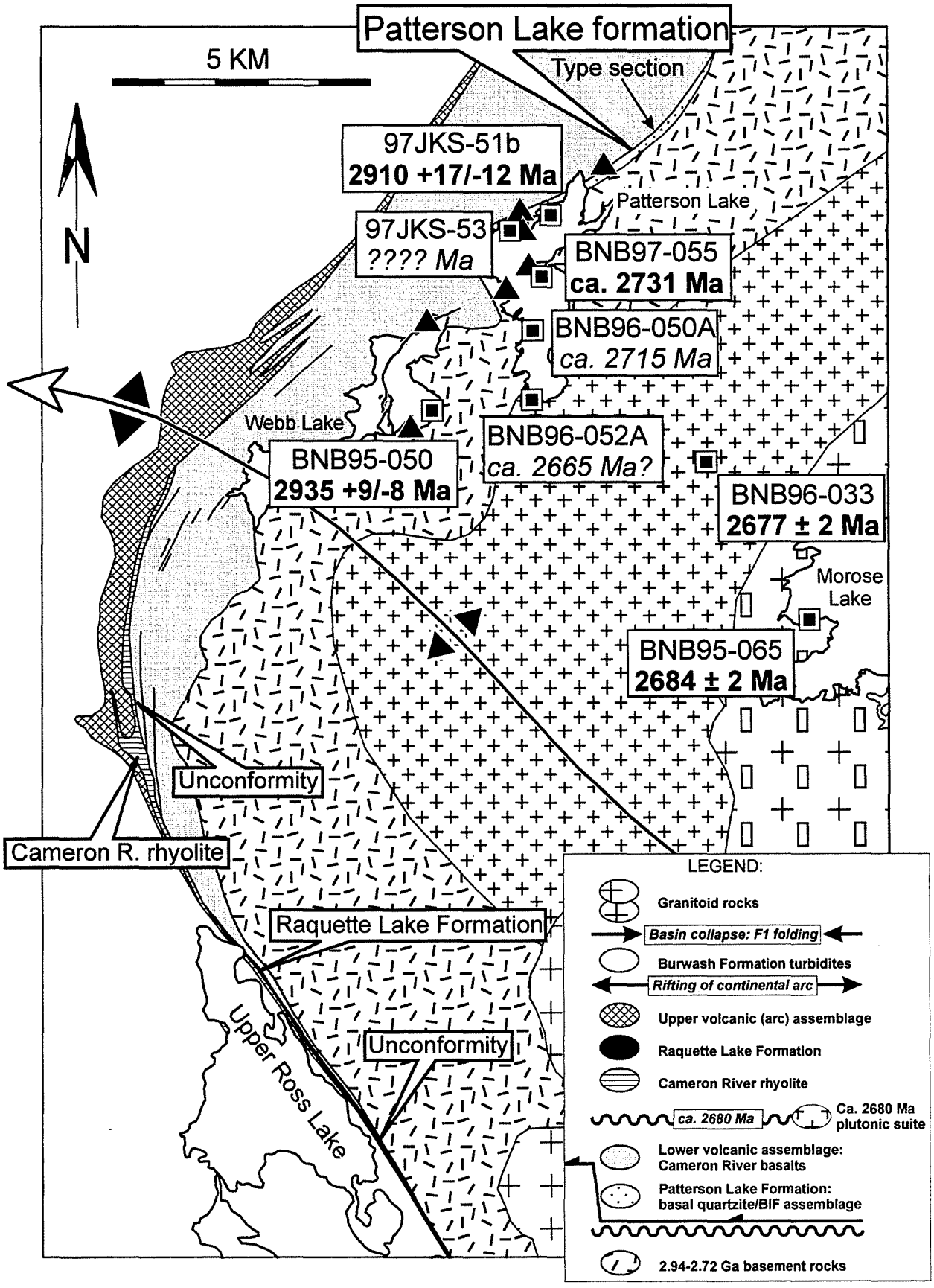

Figure 1. *Geology of the southwestern Sleepy Dragon Complex and adjacent units of the Cameron River Belt, Slave Province, N.W.T. (after Bleeker et al. 1997a). All ages are based on U-Pb zircon analyses. Ages shown in italics are preliminary. Triangles show location of swarm 2 mafic dykes (2686 ± 2 Ma; Bleeker et al. 1997b).*

fine-grained tonalite layer, which may have initially intruded the coarser-grained, 2935 Ma tonalite as veins prior to structural transposition.

The 2910 Ma tonalite dated for this study, and a ca. 2819 Ma granite gneiss from north of the present study area (Henderson et al. 1987) potentially mark younger phases of a major ca. 2.9 Ga plutonic suite that underlies a significant portion of the SDC.

97JKS-53 - mafic volcanic schist at base of Patterson Lake Formation, Patterson Lake

Bleeker et al. (1997a) present lithologic and stratigraphic details for the Patterson Lake Formation, a well-preserved but laterally discontinuous package lying between the SDC and the Cameron River volcanic belt. This assemblage mainly consists of conglomerate, quartz arenite, quartzite, and banded iron formation, and is potentially correlative with similar assemblages elsewhere in the western Slave Province (e.g., Bell Lake group north of Yellowknife; Bleeker and Ketchum 1998). Detailed age information for these rocks, which predate deposition of the Yellowknife Supergroup, is critical to understanding the early tectonic evolution of the western Slave Province.

The base of the Patterson Lake Formation is marked by a 10-30 m-wide unit of mafic schist that appears to be largely derived from pillow basalt (Bleeker et al. 1997a). This unit is well exposed on a small island at the north end of Patterson Lake where thin, alternating bands of mafic and intermediate composition material give the impression of highly stretched pillows and interpillow material, respectively. On the chance that the latter may be of volcanic origin (tuffaceous horizons within the volcanic pile?) and potentially zircon-bearing, we collected a sample containing both mafic and intermediate components. It yielded numerous small, euhedral to subhedral colourless zircon prisms with square cross-sections and double terminations. The three analyses obtained at the time of writing do not yield a consistent age, but one fraction of these low-U (~15 ppm) zircons is concordant at 2900 Ma. The significance of this result is not immediately apparent. It may provide a minimum age for the mafic volcanic unit, or alternatively, the zircons may be inherited from another source, providing a maximum age.

BNB97-55 - transposed amphibolite dyke (swarm 1), Patterson Lake

The three temporally distinct mafic dyke swarms that cut 2935 Ma basement tonalite at Webb Lake are readily observed at Patterson Lake. The oldest dykes (swarm 1 of Bleeker et al. 1997a) are completely transposed within the gneissic foliation and do not cut an older fabric, although field relationships are equivocal due to the high superimposed strain. A large swarm 1 dyke underlying a small island in Patterson Lake was sampled in the hope of obtaining zircons formed during amphibolite-facies metamorphism of the dyke. It instead yielded a single population of colourless, bladed, skeletal zircons of evident igneous origin. Three multigrain fractions of this population are variably discordant but yield a upper intercept age of ca. 2731 Ma, providing a preliminary emplacement age for the dyke. This result is important because swarm 1 dykes predate high-strain deformation associated with oblique normal movement along the basement-cover contact (Bleeker et al. 1997a). A younger age limit on this deformation is provided by discordant swarm 2 dykes which have been dated at 2686±2 Ma (Bleeker et al. 1997b). Swarm 1 dykes are present in the Patterson Lake Formation, providing a ca. 2731 Ma minimum age for deposition of this assemblage.

BNB96-50a - K-feldspar megacrystic granodiorite, Patterson Lake

Much of Patterson Lake is underlain by a distinctive unit of foliated, K-feldspar megacrystic granodiorite that becomes progressively more deformed toward the basement-cover contact (Bleeker et al. 1997a). This particular basement lithology does not contain mafic dykes of swarm 1 but is cut by swarms 2 and 3, providing an age bracket of 2731-2686 Ma for primary crystallization (see above). The granodiorite was sampled at a low strain locality on the west shore of Patterson Lake. It yielded a variety of zircon types including yellow prismatic grains with and without visible cores, large brown prisms with cores, and smaller brown and colourless needles. Composite grains were avoided during fraction selection due to the likelihood that cores represent inherited older zircon. The nine U-Pb results obtained thus far yield a pattern of complex,

multistage Pb loss, particularly for yellow grains which have U contents ranging from 1100-2500 ppm. However, three discordant fractions of lower U (500-900 ppm) brown zircon needles give an upper intercept age of ca. 2715 Ma, providing a preliminary age estimate for the granodiorite that falls within the above-mentioned age bracket. This result may constrain displacement along the basement-cover contact to the period 2715-2686 Ma as the granodiorite is overprinted by normal-sense shear fabrics, but given the preliminary nature of the age, we stress that this constraint is currently speculative. Evidence for inherited older basement material in the granodiorite is given by a single brown zircon prism with a $^{207}Pb/^{206}Pb$ age of 2930 Ma (3.7% discordant).

BNB95-065 - tonalite gneiss enclave in Morose Lake granite, Morose Lake

The ca. 2.58 Ga Morose Lake granite forms a prominent body in the core of the southern SDC (Fig. 1). This syn- to post-tectonic pluton contains large screens of older, foliated leucocratic tonalite (Davidson 1972; not shown in Fig. 1) that themselves contain foliated swarm 3 mafic dykes. A sample of this tonalite from Morose Lake contains numerous brown zircon prisms, some which exhibit core-overgrowth relationships. Four zircon fractions lacking visible cores provide a precise crystallization age of 2684±2 Ma. This age is identical to that for a foliated granodiorite at Sleepy Dragon Lake for which Henderson et al. (1987) obtained an age of 2683.5±2 Ma, and which also contains swarm 3 dykes. Ca. 2684 Ma granitoid plutonism in the SDC appears to be coeval with emplacement of swarm 2 mafic dykes (2686 Ma; Bleeker et al. 1997b) and with felsic volcanism at higher stratigraphic levels in the Yellowknife basin (e.g., 2684 Ma felsic flow in the Townsite Formation, Yellowknife; Henderson et al. 1987).

BNB96-033 and BNB96-052a - foliated tonalite and granodiorite between Patterson and Morose Lakes

A large map unit of foliated tonalite and granodiorite separates the Morose Lake granite from 2.9-2.7 Ga gneissic tonalite and megacrystic granodiorite at the western margin of the SDC. This unit appears to lack the three mafic dykes swarms observed in basement units to the west (Bleeker et al. 1997a), suggesting that it is younger than 2684 Ma plutons that host swarm 3 dykes. Samples of melanocratic tonalite (BNB96-033) from midway between Patterson and Morose Lakes, and biotite granodiorite (BNB96-052a) from the south end of Patterson Lake both contain abundant zircon. Five of seven single-grain analyses of brown prisms from the tonalite yield an upper intercept age of 2677±2 Ma, with one of these analysis overlapping concordia. The remaining two analyses, which are relatively high-U, are the most discordant and plot to to the left of the regression line. We interpret the 2677 Ma upper intercept age to date primary crystallization of the tonalite.

The granodiorite sample from Patterson Lake contains both yellow and brown prismatic zircons, many which contain obvious cores. Small, light brown zircon needles without visible cores provide the least discordant data and suggest an upper intercept age (based on 3 analyses) of 2665 Ma, although an alternative regression yielding a 2695 Ma upper intercept is also possible. However, the absence of mafic dykes in this unit suggests that the 2665 Ma result is the better preliminary age estimate for igneous crystallization of the granodiorite. A single brown prism with a $^{207}Pb/^{206}Pb$ age of 2990 Ma (3.5% discordant) demostrates the presence of an inherited basement component in this sample. Yellow zircon prisms and overgrowths, which have roughly two to seven times more U than their brown counterparts, are highly discordant and plot well to the left of the discordia lines for brown zircon. No meaningful age information was obtained from the yellow grains.

DISCUSSION

A detailed understanding of the geological history of the Sleepy Dragon Complex and its supracrustal carapace is slowly emerging from integrated studies in the Morose-Patterson Lake area and elsewhere. Results obtained here indicate that 2.9-2.71 Ga basement rocks form a significant part of the SDC, particularly along its margins, with younger 2.68 and 2.58 Ga plutons underlying much of the core region. At least one unit of the

Patterson Lake Formation may be as old as 2.9 Ga, although data collection is at a very preliminary stage. Temporally distinct mafic dyke swarms constrain the Patterson Lake Formation to be older than 2731 Ma, and stitch the Cameron River volcanic belt to both the Patterson Lake Formation and the SDC by 2686 Ma (Bleeker et al. 1997b). A normal-sense shear zone along the basement-cover contact appears to be younger than 2731 Ma swarm 1 dykes and older than 2686 Ma swarm 2 dykes, with an even narrower age constraint of 2715-2686 Ma indicated but not yet adequately demonstrated. Swarm 3 mafic dykes cut 2684 Ma plutons but appear to be absent from a 2677 Ma tonalite, suggesting a possible age bracket for their emplacement. These and other data indicated a protracted history for the SDC and overlying supracrustal units, all which predates extensive deposition of turbidite sequences in the adjacent Yellowknife basin. Simplistic lithological groupings and tectonic models are clearly not adequate to explain the tectonic evolution of the western Slave Province, with the extant data instead favouring a complex, multistage evolution involving a variety of tectonic settings (e.g., Bleeker et al. 1997b).

REFERENCES

Bleeker, W. 1996. Thematic structural studies in the Slave Province, Northwest Territories: the Sleepy Dragon Complex. In Current Research 1996-C; Geological Survey of Canada, p. 37-48.

Bleeker, W., and Beaumont-Smith, C. 1995. Thematic structural studies in the Slave Province: preliminary results and implications for the Yellowknife Domain, Northwest Territories. In Current Research 1995-C; Geological Survey of Canada, p. 87-96.

Bleeker, W., Villeneuve, M. , and Bethune, K. 1997a. Thematic structural studies in the Slave Province, Northwest Territories: contrasting basement/cover relationships on western and southwestern flanks of the Sleepy Dragon Complex. In Current Research 1997-C, Geological Survey of Canada, p. 27-37.

Bleeker, W., Davis, B., and Villeneuve, M. 1997b. The Slave Province: Evidence for contrasting crustal domains and a complex, multistage tectonic evolution. In Slave-Northern Cordillera Lithospheric Experiment (SNORCLE), Transect Meeting (March 7-9, 1997), University of Calgary, compiled by Cook, F.,and Erdmer, P., LITHOPROBE Report No. 56, p. 36-37.

Bleeker, W., and Ketchum, J.W.F. 1998. The Central Slave Basement Complex: its autochthonous cover, decollement, and structural topology. In Current Research, Geological Survey of Canada, in press.

Davidson, A. 1972. Granite studies in the Slave province. In Report of Activities, Part A, Geological Survey of Canada, Paper 72-1A, p. 109-115.

Dudas, F.O., Sullivan, R.W., Henderson, J.B., and van Breeman, O. 1988. Nd isotopic reconnaissance of Archean granitoids from the southern Slave Province. Geological Association of Canada, Program with Abstracts, v. 13, p. A34.

Henderson, J.B. 1985. Geology of the Yellowknife-Hearne Lake area, District of MacKenzie: a segment across an Archean basin. Geological Survey of Canada, Memoir 414, 135 p., 1:250,000 map.

Henderson, J.B., van Breemen, O., and Loveridge, W.D. 1987. Some U-Pb zircon ages from Archean basement, supracrustal and intrusive rocks, Yellowknife-Hearne Lake area, District of MacKenzie. In Radiogenic Age and Isotopic Studies: Report 1, Geological Survey of Canada, Paper 87-2, p. 111-121.

James, D.T., and Mortensen, J.K. 1992. An Archean metamorphic core complex in the southern Slave Province: basement-cover structural relationships between the Sleepy Dragon Complex and the Yellowknife Supergroup; Canadian Journal of Earth Sciences, v. 29, p. 2133-2145.

Lambert, M.B. 1988. The Cameron River and Beaulieu River volcanic belts, District of MacKenzie, Northwest Territories. Geological Survey of Canada of Canada, Bulletin 382, 145 p., 1:50,000 map.

Lambert, M.B., and van Breemen, O. 1991. U-Pb zircon ages from the Sleepy Dragon Complex and new occurrence of basement rocks within the Meander Lake Plutonic Suite, Slave Province, N.W.T. In Radiogenic and Isotopic Studies: Report 4, Geological Survey of Canada, Paper 90-2, p. 79-84.

THE CENTRAL SLAVE BASEMENT COMPLEX, ITS AUTOCHTHONOUS COVER, DÉCOLLEMENT, AND STRUCTURAL TOPOLOGY: TOWARDS A NEW TERRANE MODEL FOR THE SLAVE PROVINCE

Wouter Bleeker[1] and John Ketchum[2]

[1]Geological Survey of Canada, 601 Booth Street, Ottawa, ON, K1A 0E8,
Tel: (613) 995-7277, Email: wbleeker@gsc.NRCAN.gc.ca
[2]Department of Earth Sciences, Memorial University, St. John's, NF, A1B 3X5,
Tel: (709) 737-3713, Email: ketch@sparky2.esd.mun.ca

Introduction

A comprehensive and testable model is presented for basement/cover relationships in the south-central Slave Province (see also Bleeker and Ketchum, 1998). Pre-Yellowknife Supergroup basement rocks throughout the south-central Slave can be combined into a single basement block, which we propose to call the **Central Slave Basement Complex** or **CSBC** (Figure 1). The CSBC is characterized by a unique cover stratigraphy and, for a significant part of the tectonic history of the Slave Province, the CSBC acted as a distinct tectonic terrane, which we propose to call the **Central Slave Basement Terrane**. This terminology and the underlying concept of a better defined basement block, its distinctive cover, and its associated tectonic boundaries, should replace and supersede the "Anton Terrane" as proposed by Kusky (1990).

Central Slave Basement Complex

The CSBC encompasses the previously named Sleepy Dragon, Jolly Lake and Anton basement complexes, which merely represent different parts of the multiply folded CSBC (Figure 1). Furthermore, the CSBC reappears to the east of Sleepy Dragon Complex as basement below the southeastern flank of the Beaulieu River greenstone belt, the southern flank of the Beniah Lake greenstone belt, and the Camsell Lake greenstone belt. It is proposed that this complex be named the Step'nduck Complex after a dyke complex described by Lambert et al. (1992). Although this basement complex locally includes migmatitic diorite-tonalite gneisses, the full extent of old basement rocks in this complex, relative to younger intrusive granitoid intrusions, is poorly known. The eastern and southern limits of this complex are poorly constrained. In general, at least 50 percent of the CSBC appears to be intruded or reworked by younger granitoids.

Figure 1 (next page). Topological map of the Central Slave Basement Complex (CSBC). The CSBC includes the previously defined Anton Basement Complex (ABC), the Sleepy Dragon Complex (SDC), the Jolly Lake Complex (JLC), and the newly defined Beniah Basement Complex (BBC), Step'nduck Basement Complex (SBC), and tentatively, the Big Lake Complex (BLC) of Thompson and Kerswill (1994). Inclusion of the latter in the CSBC is contingent on a synclinal fold relationship across the Winter Lake greenstone belt, as is strongly suggested by the overall topology. Note also that the topology requires basement rocks to be present west of the northern extent of the Yellowknife supracrustal domain. However, we currently do not complete this part of the topology due to poor definition of the geology in this area. All known occurrences of the quartzite/BIF assemblage are indicated and are confined to the immediate cover of the CSBC. Note also the geochronology sample site discussed in this paper, on the west shore of MacKay Lake.

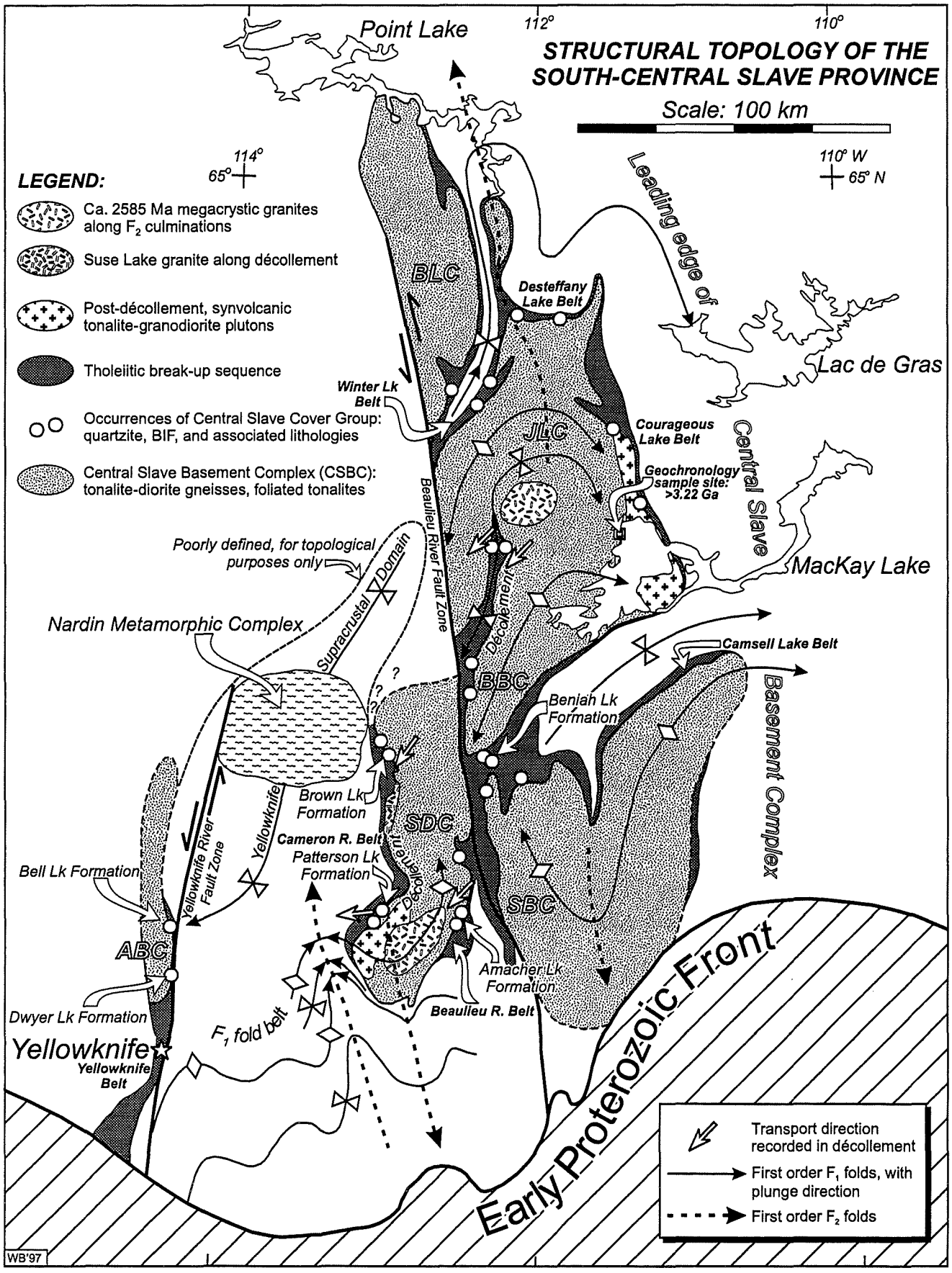

Wouter Bleeker and John Ketchum, SNORCLE March 1998

Basement rock types consisting of foliated tonalites and heterogeneous diorite-tonalite gneisses can be followed discontinuously from the southern end of the Sleepy Dragon Complex, to below the northern end of the Beaulieu River greenstone belt, into the Jolly Lake Complex, and further northeast into the footwall of the Courageous Lake greenstone belt (Figure 1).

U-Pb zircon data from a first sample of a regional sample suite, which was collected to test the proposed CSBC topology, confirm a ca. 3.2-3.4 Ga basement age for a diorite-tonalite migmatitic gneisses (Figure 2). The dated sample was collected along the western shore of MacKay Lake within eyesight of the overlying Courageous Lake greenstone belt. Although we stress the preliminary nature of the U-Pb results, they define a minimum age of 3218 Ma. The gneiss could be as old as ca. 3325 Ma, an upper intercept age defined by a discordia line through several colinear data points. Morphologically distinct, equant, colourless zircon grains of low U content define a zircon growth event at ca. 2723 Ma that is attributed to a cryptic metamorphic event.

Supporting evidence for the new CSBC topology is also provided by the Bouguer gravity field of the Slave Province, which shows a broad negative anomaly over much of the CSBC. It is suggested that the broad negative Bouguer anomaly tracks the older sialic crust. The proposed outline of the CSBC is also in agreement with the regional variation in Pb-isotopic data for syngenetic ore leads (Thorpe et al., 1992; and R. Thorpe, unpubl. data).

Central Slave Cover Group

All presently known and some new occurrences of a distinctive quartzite and banded iron formation assemblage occur in the immediate hanging wall of the CSBC (Figure 1) and are included in a new stratigraphic entity, the **Central Slave Cover Group** or **CSCG**, which represents the autochthonous cover of the CSBC (Figures 1 and 3). Evidence for a metamorphosed weathering mantle below the CSCG and a basal quartz cobble conglomerate have been found at Brown Lake (Bleeker and Ketchum, 1998). Elsewhere, the CSCG includes ultramafic flows and sills, detritus of which is represented as detrital chromite in the overlying quartzites.

Décollement

A regional décollement marks the contact between CSBC basement and its autochthonous cover on the one hand and the overlying parautochthonous to allochthonous tholeiitic break-up sequence on the other hand. Mutually consistent lineation data and kinematic indicators, at five widely spaced localities, suggest significant northeast-to-southwest transport of the tholeiitic sequence. General arguments suggest a displacement of >>10 km over a basal décollement with a preserved width of at least 300 km (i.e., from Courageous Lake to Yellowknife). The age of mylonitization in the décollement has now been bracketed to 2733-2686 Ma. Numerous mafic dykes that cut the basement rocks and are transposed in the décollement, and probably heralded the final break up of the CSBC, have now been dated at ca. 2733 Ma (see Ketchum and Bleeker, this volume).

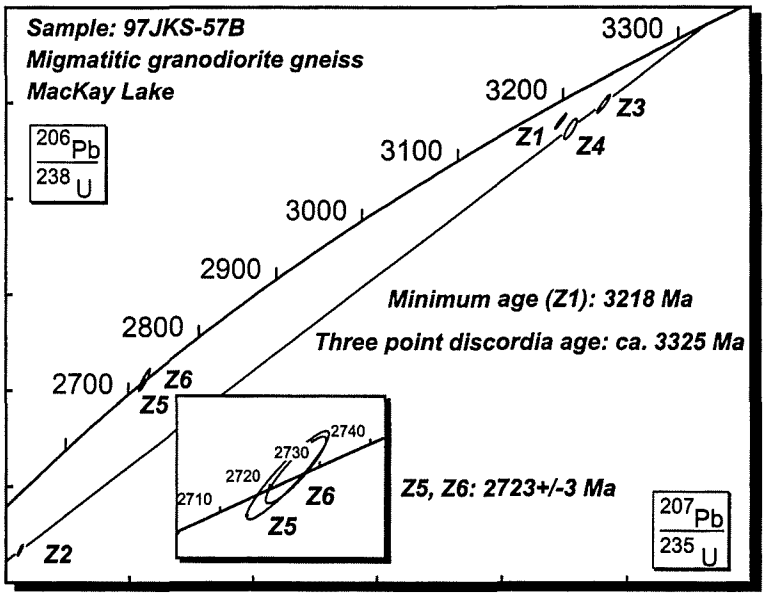

Figure 2. U-Pb concordia diagram showing preliminary results of six zircon fractions of a gneiss sample on the western shore of MacKay Lake. Brown prismatic grains (fractions Z1 to 4) define the crystallization age of the gneiss. The $^{207}Pb/^{206}Pb$ age of fraction Z1 provides a minimum age of ca. 3218 Ma. Three of the fraction are colinear and possibly indicate an upper intercept age of ca. 3325 Ma. An even older age is also possible on the basis of these preliminary results. Colourless, equant, low U grains record a younger zircon growth event at ca. 2722 Ma.

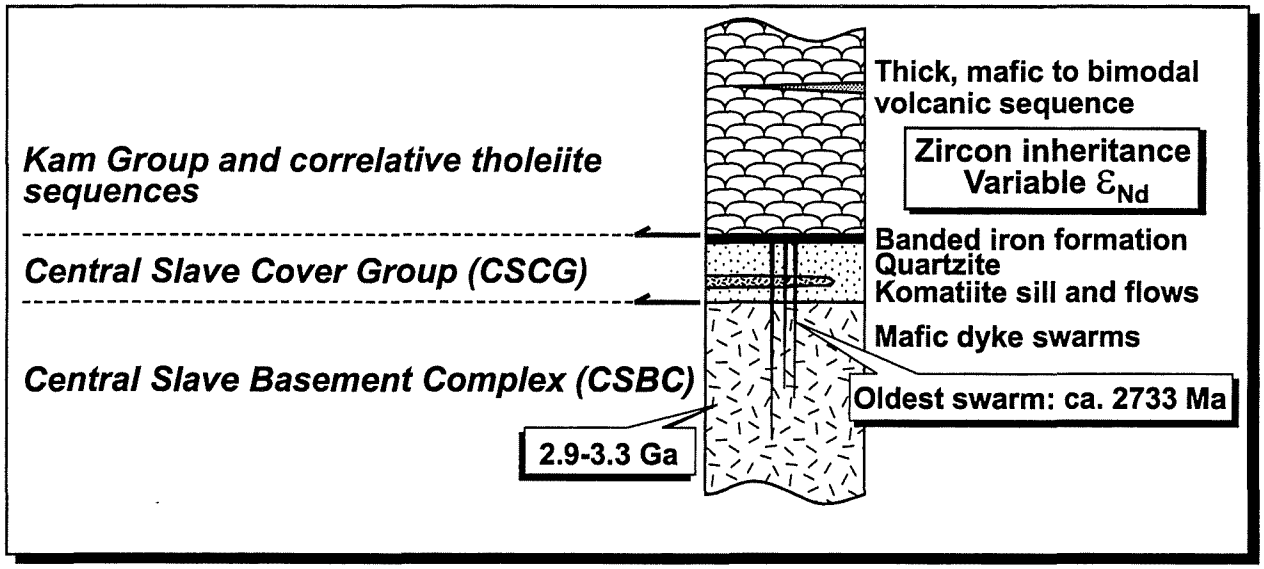

Figure 3. Schematic relationships between basement of the Central Slave Basement Complex and its autochthonous cover, the Central Slave Cover Group. Note that the oldest mafic dyke swarm heralding the break up of the CSBC has now been dated at ca. 2733 Ma (see Ketchum and Bleeker, this volume).

Conclusions

The new structural-stratigraphic model allows a number of important predictions. If the Winter Lake greenstone belt represent a syncline of the tectonostratigraphy, as is strongly suggested by the overall topology, then the Point Lake basement complex will likely be part of the CSBC. The high strain zone at Point Lake could then prove to be just another segment of the same regional décollement as at Sleepy Dragon. The present topology of the CSBC is greatly simplified by restoring a significant sinistral strike-slip displacement on the Beaulieu River Fault Zone.

Unfolding of the large-scale fold patterns that affected the final shape of the CSBC Terrane, in conjunction with consideration of the differences between different lithotectonic domains of the province, leads to a new terrane model for the Slave Province in which the CSBC Terrane can be viewed as the central core of a polyphase tectonic collage.

References

Bleeker, W., and Ketchum, J., 1998. The Central Slave Basement Complex: its autochthonous cover, décollement, and structural topology; in Current Research, Geological Survey of Canada, in press.

Kusky, T.M., 1990. Evidence for Archean ocean opening and closing in the southern Slave province; Tectonics, v. 9, no.6, p. 1533-1563.

Lambert, M.B., Ernst, R.E., and Dudás, F.Ö.,1992. Archean mafic dyke swarms near the Cameron River and Beaulieu River volcanic belts and their implications for tectonic modelling of the Slave Province, Northwest Territories; Canadian Journal of Earth Sciences, v. 29, p. 2226-2248.

Thompson, P.H., and Kerswill, J.A., 1994. Preliminary geology of the Winter Lake - Lac de Gras area, District of MacKenzie, Northwest Territories; Geological Survey of Canada, Open File 2740, scale 1:250,000.

Thorpe, R.I., Cumming, G.L., and Mortensen, J.K., 1992. A significant Pbisotope boundary in the Slave province and its probable relation to ancient basement in the western Slave province; in Project Summaries, CanadaNorthwest Territories Mineral Development Subsidiary Agreement 19871991, edited by Richardson, D.G., and Irving, M., Geological Survey of Canada, Open File 2484, p. 179184.

THE LATE-ARCHEAN PROSPEROUS GRANITE SUITE: SYN-D2 LACCOLITHS IN THE YELLOWKNIFE DOMAIN, SLAVE PROVINCE

Ham, N.M. and Benn, K., Ottawa-Carleton Geoscience Centre and Department of Geology, University of Ottawa, Ottawa, Canada K1N 6N5
Bleeker, W., Geological Survey of Canada, 601 Booth Street, Ottawa, Canada K1A 0E8

The Prosperous Suite of granites is a regionally extensive plutonic assemblage outcropping within cordierite- and andalusite-bearing meta-greywackes of the southern Yellowknife Domain, in the Slave Province of the Canadian Shield. The pervasive structural patterns in the Sparrow and Prosperous plutons (ca. 2596 Ma; U-Pb zircon, Davis and Bleeker, submitted) were mapped using measurements of the low-field magnetic susceptibility (K) and the anisotropy of magnetic susceptibility (AMS) in order to establish the relationships between plutonism and tectonics in the Yellowknife Domain.

Both plutons have NNW elongate rectangular shapes, with the southern portion of the Sparrow pluton having the form a narrow tail that trends NW. Microstructural study shows that the fabrics in the granites record magmatic deformation that continued during the early stages of cooling of the solidified granites. Paramagnetic Fe-phyllosilicates (biotite and chlorite) and very fine grained magnetite contribute to the magnetic susceptibility and its anisotropy. Both plutons have magnetic foliations striking predominantly parallel to their elongate dimensions (NNW to NW). The magnetic foliations are parallel to the regional (D2) fabric trajectories in the country rocks of the Burwash Formation. Shallowly dipping E-W striking foliations are commonly preserved in the Prosperous pluton, suggesting D2 deformation may have reworked an initially horizontal magmatic foliation into steeper orientations. In the Sparrow pluton, the distribution of K values suggests a pattern of NNW to NW trending, shallowly plunging folds of a shallowly dipping zonation. The zonation may be of magmatic or deuteric origin. Magnetic lineations in both plutons are horizontal and trend NNW-SSE to NW-SE. Exposed floor and roof contacts of the Prosperous pluton dip shallowly to the east, suggesting the pluton is tabular in shape and is approximately 2 km thick.

The magmatic to HT solid-state structural patterns in the Sparrow and Prosperous plutons are part of the regional D2 strain field and demonstrate syn-D2 emplacement. A horizontal maximum principal stretch of the plutons is inferred from the magnetic lineations. The magnetic fabrics are compatible with transpressional syn-emplacement tectonics, with a horizontal Z axis of the bulk regional D2 strain ellipsoid and an important component of horizontal stretching. Based on field observations and the magnetic fabrics a laccolithic emplacement model is proposed.

Composition and thermal evolution of the upper mantle beneath the Archean Slave Province: Evidence from xenolith studies

J.M. MacKenzie and D. Canil, School of Earth and Ocean Sciences, University of Victoria, PO Box 3500, Victoria, B.C., V8W 3P6, email: jasonmac@uvic.ca

A suite of peridotitic xenoliths entrained in the Torrie kimberlite, located in Canada's Northwest Territories, directly constrain the composition and thermal state of lithospheric mantle beneath the Archean Slave Province. The composition and thermal state of the upper mantle has been estimated by combining mineral chemical and petrographic data from mantle xenoliths as well as the application of various thermobarometers.

Coarse-, granuloblastic-, and porphyroclastic- textured harzburgite, lherzolite, and pyroxenite xenoliths yield equilibration temperatures ranging between 850-1350°C. Additionally, two samples show a more complex thermal evolution reflecting both a thermal perturbation and Ca-metasomatism. Thermobarometry requires a minimum lithospheric thickness of approximately 200 km at the time of kimberlite magmatism, similar to estimates from other geophysical and petrological studies in the region [1,2,3]. The distribution of pressures and temperatures (P-T's) of equilibration for the xenoliths lie on a calculated paleogeotherm with a corresponding surface heat flow of 42 mWm^{-2}. Paleogeotherms, calculated using P-T arrays for xenoliths from the Jericho and Grizzly kimberlites yield a slightly lower surface heat flow (Figure 1). These palaeogeotherms are ~9 mWm^{-2} higher than the present heat flow measured at Yellowknife [4](Figure 1). Combined with our estimate of lithospheric thickness, the varying surface heat flow are possibly due to regional variations in the vertical distribution of heat generating elements in the crust.

The Mg# [Mg/(Mg+Fe)] of olivine in peridotites varies from 0.906-0.938 with an average of 0.920. The Torrie xenolith suite shows variable degrees of serpentinization and/or carbonation with the rim compositions of many clinopyroxene grains showing Ca enrichment although overall, the xenoliths are homogeneous at all scales. The Torrie xenoliths are rich in orthopyroxene (~30 wt %) similar to other low temperature (<1100°C) peridotites from southern Africa, and Siberia. Estimates of bulk rock composition based on mineral chemical and modal data reveal a negative correlation between Si and Fe (Figure 2), similar to peridotite xenoliths from Udachnaya [5]. Boyd et.al [5] have suggested that this trend may reflect the physical segregation of olivine and orthopyroxene by either cumulate sorting, metamorphic differentiation, or metasomatic replacement of olivine by orthopyroxene. The similarity of olivine Mg#'s with other cratons combined with the negative correlation of Fe and Si suggest that the mantle lithosphere beneath the Slave craton has experienced an evolution similar to other cratons globally.

[1] Jones AG, Ferguson IJ (1997) LITHOPROBE Report No. 56: 42-47
[2] Bostock MG (1997) Nature 390: 392-395
[3] Kopylova MG, Russell JK, Cookenboo H (1997) In: Abstracts, Workshop on Continental Roots (Harvard/MIT 1997)
[4] Lewis TJ, Wang K (1992) Palaeogeography, Palaeoclimatology, Palaeoecology 98: 87-100
[5] Boyd FR, Pokhilenko NP, Pearson DG, Mertzman SA, Sobolev NV, Finger LW (1997) Contrib Mineral Petrol 128: 228-246
[6] Boyd FR, Canil D (1997) In: Abstracts, Seventh annual V.M. Goldschmidt Conference, LPI contribution No. 921, Lunar and Planetary Institute, Houston: 34-35
[7] Kennedy SC, Kennedy GC (1976) J Geophysical Res. 81: 2467-2470

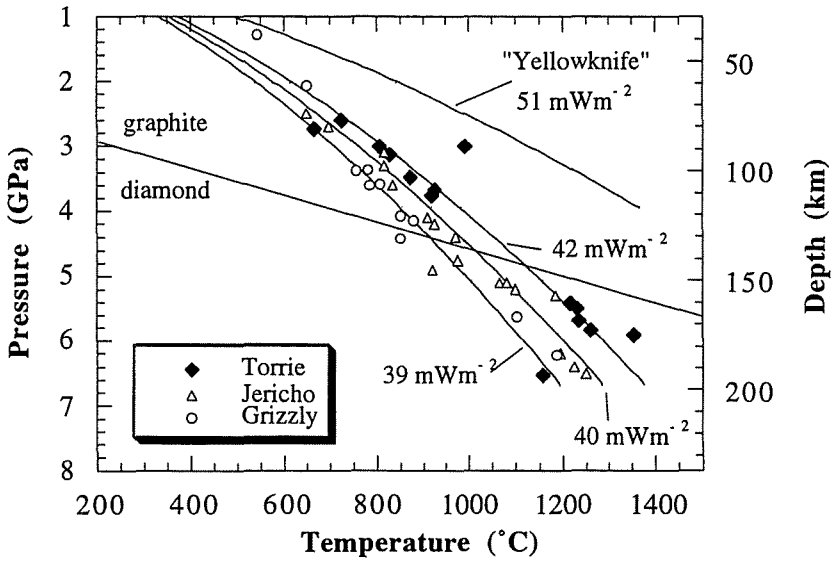

Figure 1: Calculated geotherms for locations across the Slave Province using kimberlite-hosted peridotite, pyroxenite and macrocryst xenoliths from the Torrie, Jericho and Grizzly pipes. P-T combinations include: T_{BKN}-P_{BKN} for samples from the Torrie (this study) and Jericho pipes [3] and T_{ONEILL}-P_{MC74} for samples from the Grizzly pipe [6]. Diamond-graphite transition after [7]. Yellowknife surface heat flow from [4]

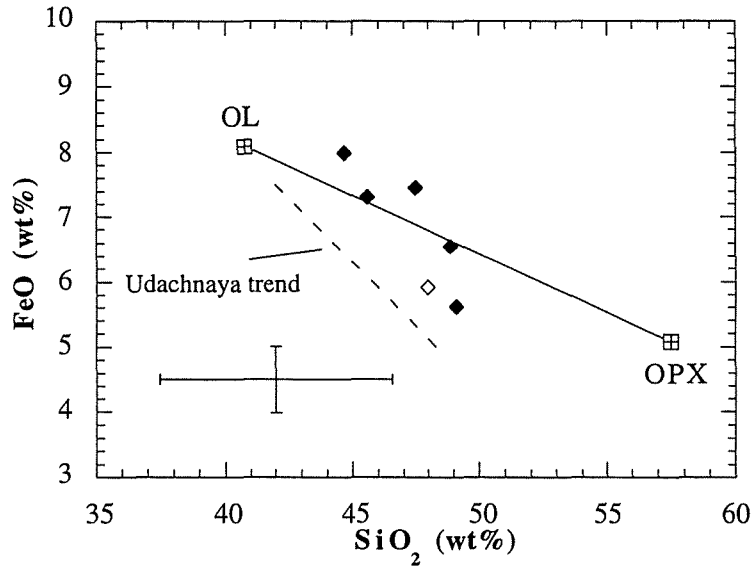

Figure 2: Bulk FeO vs. SiO_2 for Torrie Gt (solid diamonds) and Sp (open diamond) peridotites calculated using individual modal and mineral chemical data. OL= average olivine composition, OPX= average orthopyroxene composition. Negative trend suggests the physical segregation of olivine and orthopyroxene or Si enrichment. Dashed line from [5]. Error bars calculated at 2σ.

Paleogeotherms, Lower Crustal Metamorphism and Heat Generation in the Archean Slave Province: Insights from Xenoliths

D. Canil, J.M. MacKenzie (School of Earth and Ocean Sciences, University of Victoria, Victoria, BC, V8W 3P6) and W. Davis (Geological Survey of Canada, Ottawa)

The Archean Slave craton is unique in being a small craton with a greater component of metasedimentary rocks, highly radiogenic late stage K-rich plutonic rocks, and a paucity of mafic and ultramafic greenstone belts, relative to other Archean cratons [1]. These differences in surface geology might suggest that processes leading to formation and stabilization of the craton are also unique. The processes of craton formation and stabilization themselves are the subject of much debate.

Much information on craton amalgamation can be derived from surface geology, relating to crustal formation processes in the Archean. The third dimension for the surface geology can be provided by the geophysical investigations in LITHOPROBE. One possible link between surface geology and processes and structure at depth are samples of the lithosphere represented as xenoliths sampled in the numerous kimberlite pipes which have intruded the craton over a significant area. These samples provide a view of metamorphism deeper in the crust, and P-T conditions in the lithosphere. Furthermore, surface heat flow is a signal of the strength and stability of cratons, which depends on the distribution of heat generating elements in the craton, yet little information on this latter constraint is available for the deeper crust in the Slave Province.

Lower crustal xenoliths have been sampled in over five kimberlite pipes from the central, southeast and southwest Slave. The xenoliths have experienced varying degrees of alteration from their host kimberlite. Most of the lower crustal xenoliths are mafic granulites, recording peak metamorphic pressures up to 1.2 GPa. Peak temperatures from net transfer equilibria in some assemblages are as high 900°C and cooling temperatures of 800 - 650°C are recorded by Fe-Mg exchange thermometry. These metamorphic conditions are 300 to 400°C above the ambient geotherm suggesting either thinner lithosphere beneath the craton at that time of metamorphism, or possibly significant thermal input from basaltic underplating, as has been suggested for other Slave craton granulite xenoliths [2].

Geochronological studies of the lower crustal granulites are currently in progress. One unique sample, a felsic gneiss (gt+opx+pl+rt+ilm), records fairly old ages for metamorphism (~2550 Ma) which post-dates latest stage of plutonism in the surface rocks by only 30 to 50 Ma. Further geochronological information on xenoliths from other localities is forthcoming in order to gain an understanding of the spatial and temporal distribution of metamorphism in the lower crust for a larger region of the Slave.

A data base of P-T estimates for mantle xenoliths hosted in Slave kimberlites is now available for at least three localities in the central part of the craton [3,4,5]. These samples lie along paleogeotherms with slight but notable differences in their P-T distributions, suggesting either slight spatial variation in heat generation and/or crustal thickness. The P-T data for mantle xenoliths , as well as providing the minimum thickness

of mantle lithosphere, can be inverted to derive the distribution of heat generating elements in the crust if the surface heat flow is known (or assumed). If typical values for lower and upper crustal heat generation from Archean cratons elsewhere are assumed, a heat flow of about 38 to 42 mWm^{-2} is consistent with the mantle xenolith data. By comparison, if the highly radiogenic character of Slave upper crust is used , a much higher heat flow can be supported (> 50 mWm^{-2}) consistent with the only measurement of heat flow for the Slave craton near Yellowknife (~ 51 mWm^{-2} - [6]). These two end-member solutions are non-unique because the vertical distribution of heat generating elements is not well constrained.

Information on the depth extent of surface crustal rocks (especially the voluminous radiogenic plutons) and the thickness and heat generation of lower crustal granulite, can help further constrain models for geotherms and heat generation in the Slave Province. Such information is potentially gotten with geophysical information, and measuring the concentration of heat generating elements (K, U, Th) in lower crustal granulites from the Slave Province. One locality that is particularly well suited to this exercise is the Drybones Bay kimberlite, approximately 50 km south of Yellowknife. This kimberlite is located near the only heat flow measurement in the Slave Province, and contains mantle and lower crustal xenoliths from which P-T and heat generation data can be obtained. Most importantly, the Drybones Bay kimberlite is located immediately along Corridor 1, where magnetotelluric, seismic reflection and teleseismic studies will provide a reasonably constrained estimate of the vertical extent of various crustal rocks and mantle lithosphere, to be combined with the xenolith data for thermal modelling.

[1] Padgham and Fyson (1992) Can J Earth Sci, 29, 2072-2086.
[2] Davis WJ (1997) Geology, 25, 343-346.
[3] Boyd and Canil (1997) 7th VM Goldschmidt Abs Prog, LPI Contrib 921, Houston, 34-35.
[4] Kopylova et al (in press) Geology
[5] MacKenzie and Canil (submitted) Contrib Mineral Petrol
[6] Lewis and Wang (1992) Paleo, Paleo, Paleo, 98, 87-100.

Upper mantle stratigraphy of the north-central Slave Craton, Canada.

Kopylova, M. G.[1], Russell, J. K.[1], Cookenboo, H.[2]

1. Geological Sciences Division, Department of Earth and Ocean Science, The University of British Columbia, Vancouver, Canada, V6T 1Z4

2. Canamera Geological Ltd., 399 Mountain Highway, North Vancouver, Canada, V7J 2K9

Mantle xenoliths carried by kimberlite magma provide the only hard evidence of cratonic roots against which the inferences of geophysisists can be calibrated. We have studied peridotitic, pyroxenitic, and eclogitic xenoliths from the Jericho kimberlite in northern Canada to determine their equilibrium pressures and temperatures of formation and to constrain the upper mantle stratigraphy of the north-central Slave craton.

Five groups of texturally and mineralogically different rocks comprise the Jericho mantle. They are: i) coarse peridotite, ii) porphyroclastic peridotite, iii) eclogite, iv) megacrystalline pyroxenite, and v) ilmenite-garnet wehrlite and clinopyroxenite (Kopylova et al., in press). A P-T array (Fig. 1) reflecting the ambient paleo-geothermal regime was derived from compositions of coexisting garnet-clinopyroxene-orthopyroxene (Finnerty and Boyd, 1987; MacGregor, 1974). Cores of mineral grains were used in order to circumvent the effects of compositional zoning observed in some garnet and clinopyroxene grains. For the deep lithosphere (110-190 km) the P-T array can be approximated by a model conductive paleo-geotherm. For depths greater than 190 km the P-T array established from Jericho xenoliths deviates from a model conductive geotherm towards higher temperatures and shows substantially higher geothermal gradients. This thermal disturbance in the geotherm is commonly thought to be a transient, kimberlite-related phenomena ascribed to convection processes in the magma-bearing zone at the lithosphere/asthenosphere transition (Boyd, 1987; Griffin et al., 1996).

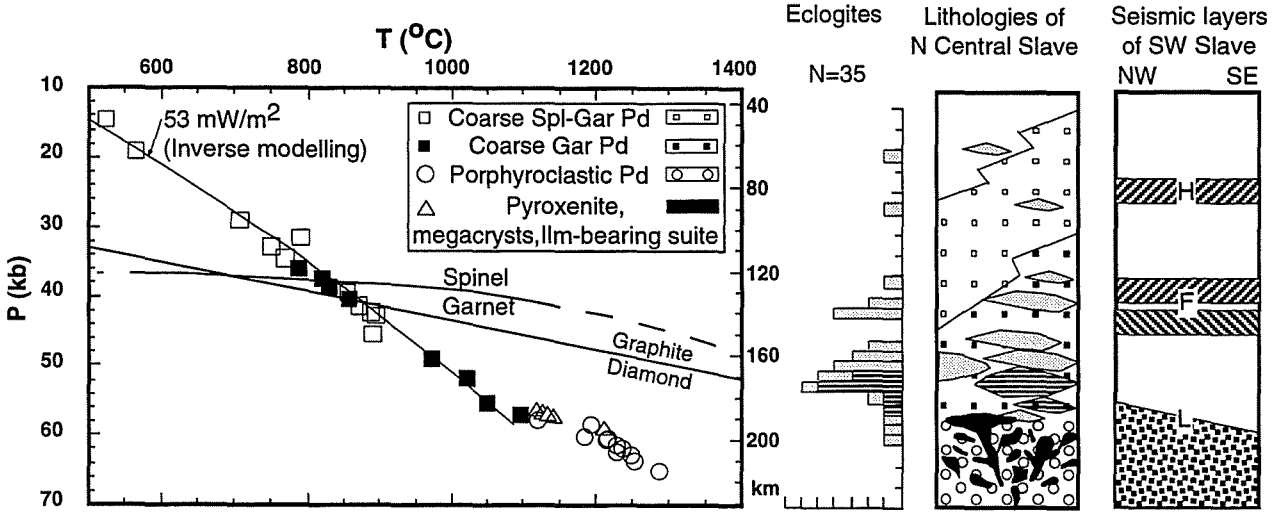

Fig. Summary of geothermobarometric results (see text). Schematic lithological column is based on peridotitic P-T array and on the depth distribution of eclogite (left panels). Solid curve denotes conductive geotherm with 53 mW/m^2 surface heat flux (Russell and Kopylova., this volume). Spinel-garnet transition was calculated accoding to O'Neill (1981) for mineral chemistry of an average Jericho peridotite. Eclogite of mantle origin (see text) are denoted by stripped bars. Schematic lithological column includes spinel peridotite (blank), coarse spinel-garnet peridotite (open squares); coarse garnet peridotite (black squares); porphyroclastic peridotite (open circles); pyroxenite, ilmenite-bearing suite and megacrysts (black); eclogite with possible mantle origin (striped), and subducted-related eclogite (grey). Seismic stratigraphic column is based on Bostock (1997 a,b) and shows highly anisotropic layers (hatched patterns) and isotropic mantle (dotted).

Univariant P-T lines for eclogite and orthopyroxene-free pyroxenite were calculated by garnet-clinopyroxene geothermometry (Ellis and Green, 1979). At any assumed pressure, eclogite samples recorded lower temperatures than pyroxenitic xenoliths (megacrystalline pyroxenite, and ilmenite-garnet wehrlite-clinopyroxenite). Estimates of equilibrium P (and corresponding T) were computed by finding the point of intersection between the calculated garnet-clinopyroxene univariant P-T line for each sample and a best-fit curve to the "peridotite P-T array". Bimodal distribution of clinopyroxene-garnet rocks over the range of equilibrium temperature translates into their bimodal depth distribution. Eclogite formed between 90 and 195 km (Fig.1, left panel), whereas magmatic rocks of megacrystalline pyroxenite, megacrysts, and ilmenite-garnet wehrilte and clinopyroxenite had apparent source regions below 190 km. For the latter groups of rocks, depth histograms cannot be produced. P-T lines for the pyroxenites intersect a deep, disturbed part of the "peridotite P-T array", where dynamic thermal conditions preclude exact estimate of equilibrium pressure.

Our results demonstrate that, at the time of kimberlite emplacement, there was a major petrological/geochemical boundary at 190 km in the mantle beneath this part of the Slave craton. This petrological boundary is manifest by the juxtaposition of porphyroclastic peridotite with magmatic rocks, and a coincident and pronounced disturbance in the calculated P-T array. If we employ the Brey and Kohler (1990) method for the thermal constaints, the boundary would lie at 160 km (Kopylova et al., in press).

In contrast to the recrystallized and texturally equilibrated rocks (coarse peridotite with eclogite lenses and layers) in the shallow mantle, most rocks from below the transition zone feature unequilibrated textures. Magmatic textures preserved in pyroxenite and the ilmenite-bearing suite must also be relatively young features as they have not equilibrated to ambient deep-mantle conditions. Furthermore, the textures found in samples of porphyroclastic peridotite attest to deformational events that must be essentially contemporaneous with the intrusion of the kimberlite magma.

Processes that deformed and magmatically and metasomatically reworked the horizon below the boundary may be related to mafic magmatism that preceded kimberlitic events. Mafic asthenospheric magmas may have metasomatized and deformed pre-existing coarse peridotite to form porphyroclastic rocks (Hops et al., 1989 and references therein). The magmas then crystallized in situ to produce pyroxenite, Cr-poor-megacrysts (Harte and Hawkesworth, 1989), and the ilmenite-bearing suite. These magmas were intrinsically related to the later kimberlitic magma (Schulze, 1987), hence, the Jericho kimberlite may well have been derived from this short-lived thermal and magmatic event.

The pervasive influence of asthenospheric magmas seen below 160-190 km can be interpreted in, at least, two ways.

Firstly, the deeper horizon characterized by fertile porphyroclastic peridotite may represent the "petrological asthenosphere", in contrast to the cratonic lithosphere made of coarse depleted peridotite (Boyd, 1987). The petrologically-defined lithosphere, however, does not necessarily correspond to the mechanically, thermally, or seismically-defined lithosphere. A base of the thermal lithosphere, or thermal boundary layer (TBL) characterized by the conductive heat transfer, was predicted to be at a 250-350 km depth and at a temperature of about 1350 °C below the Canadian Shield (Mareschal et al., 1997). The mechanical lithosphere, or a rigid plate, is commonly two times thinner than TBL (Polet and Anderson, 1995). Lithosphere mapped by magnetotelluric signals, is 200-250 km thick below the SW Slave and underlain by more electically conductive asthenosphere (Jones and Ferguson, 1997). Seismically detected lithosphere, (i.e. continental roots with high seismic velocities), extends down to 350 km beneath the southern Slave Craton (Bostock, 1997a). There is a striking similarity between the Slave and Kaapvaal cratons in the relative positions of the seismically fast continental root and the chemically defined lithosphere - asthenosphere boundary. In the Kaapvaal craton, porphyroclastic peridotite with asthenospheric affinity occurs at 140-180 km (Boyd and Gurney, 1986), within the 350 km seismic lithosphere (Vinnik et al., 1996), and may correspond to a within-lithosphere low-velocity zone (de Wit and Hart, 1993). Similarly, the chemically defined asthenosphere beneath the north-central Slave occurs at 190 km, well within mantle showing higher-than-average seismic velocity.

A second explanation is that the mantle below 160-190 km represents lithosphere which has been re-worked and overprinted by asthenospheric magmas. The localization of this overprinting may reflect a fundamental change in mantle rheological properties.

Layering in the upper mantle beneath the SW Slave was inferred from the analysis of teleseismic P-waves (Bostock, 1997b). A strongly anisotropic layer H at 75 km (10 kms thick) occurs within the coarse spinel-garnet peridotite layer with possible sparce spinel peridotite and eclogite (Fig. 1). An F layer (130 km ±15; possibly also anisotropic) (Bostock, 1997a) occurs near the base of the spinel-garnet

peridotite and near the top of the majority of eclogites. The 160-190 km petrological boundary, separating the long-stabilized mantle segment from the recently deformed and re-worked mantle, could account for the major discontinuity observed seismically at 195 km (Bostock, 1997b) and in magnetotelluric data at 200-250 km (Jones and Ferguson, 1997) for the SW Slave craton.

In conclusion, we would like to list several petrological observations, which can be helpful in constraining ideas concerning past subduction events and the assembly of the Slave craton:

1. Jericho eclogite samples have two distinct protoliths. A small proportion of samples, based on mineral chemistry, are similar to Group A Southern-African eclogite which is attributed to a mantle origin (Shervais et al., 1988). The Jericho eclogite is chemically close to undifferentiated Archean basalts and komatiites (Ireland et al., 1994). This eclogite may have formed as a high-pressure cumulate from basaltic magmas (Shervais et al., 1988) and does not derive from ocean-floor basalts (Snyder et al., 1997). P-T calculations imply a highly-restricted depth of origin for these eclogite samples (Fig).

2. The more common eclogite from Jericho is comparable, in terms of mineral chemistry, to Southern African Group B and C eclogites (Shervais et al., 1988) that are attributed to an oceanic crustal origin (Snyder et al., 1997). They may have formed as ocean-floor basalts and comprise a subducted slab which has been mapped seismically and associated with development of the 1.9-1.86 Ga Great Bear magmatic arc (Cook et al., 1997; Bostock, 1997a).

3. Although the second group of eclogites may be oceanic in origin, the surrounding low-temperature coarse cratonic peridotite may not have oceanic affinity (Boyd, 1989). In contrast, porphyroclastic high-temperature peridotite might be similar to residues of oceanic magmatism, and their protoliths may have a history of subduction (Boyd and Mertzman, 1987). Nevertheless, the chemical compositions of oceanic peridotite and high-temperature porphyroclastic peridotite are distinct: the latter is enriched in Ti and Fe, but otherwise depleted (Boyd et al., in press).

Acknowledgements

This research was made possible by an NSERC-Industry Collaborative Research and Development grant (94-0972) sponsored by Canamera Geological Ltd and Lytton Minerals Ltd. We thank Lytton Minerals Ltd for the opportunity to work with samples from Jericho and for permission to publish the results.

References:

Bostock, M. G., 1997a. Upper mantle stratigraphy and architecture of the Slave craton. Abstract, Continental Root Workshop, Harvard-MIT, 10-13 Oct 1997

Bostock, M. G., 1997b, Anisotropic upper mantle stratigraphy and architecture of the Slave craton: Nature, 390, 392-395

Boyd, F.R. & Gurney, J.J., 1986. Diamonds and the African Lithosphere. *Science*, **232:** 472-476

Boyd, F.R., and Mertzman, S.A., 1987. Composition and structure of the Kaapvaal lithosphere, southern Africa. In: Mysen BO (ed) Magmatic processes: physicochemical principles, Geochemical Society Special Publication, No 1, p. 13-24

Boyd, F.R., 1987, High- and low-temperature garnet peridotite xenoliths and their possible relation to the lithosphere-asthenosphere boundary beneath southern Africa, *In:* Nixon P. H., ed., Mantle xenoliths: New York, John Wiley and Sons, p. 403-412.

Boyd, F.R., Pokhilenko, N.P., Pearson D.G., Mertzman S.A., Sobolev N.V., and Finger L.W., in press. Composition of the Siberian cratonic mantle: Evidence fron Udachnaya peridotite xenoliths. Contrib. Mineral. Petrol.

Brey G. P., and Köhler T, 1990, Geothermobarometry in four-phase lherzolites. II. New thermobarometers, and practical assessment of existing thermobarometers. Journal of Petrology, 31, 6: 1353-1378.

Cook, F.A., Van der Velden, A.J., and Hall, K.W., 1997. Upper mantle reflectors beneath the SNORCLE transect - images of the base of the lithosphere? In: Cook F. and Erdmer (compilers) *Slave-Northern Cordillera Lithospheric Evolution (SNORCLE) transect and Cordilleran Tectonics Workshop Meeting* (March 7-9), Univ. of Calgary, LITHOPROBE Report No. 56, 58-62

de Wit MJ and Hart RA (1993) Earth's earliest continental lithosphere, hydrothermal flux and crustal recycling. Lithos 30: 309-335

Ellis, D.J. and Green, D.H., 1979, An experimental study of the effect of Ca upon garnet-clinopyroxene Fe-Mg exchange equilibria: Contributions to Mineralogy Petrology, v. 71, p. 13-33

Finnerty, A.A. and Boyd, J.J., 1987, Thermobarometry for garnet peridotites: basis for the determination of thermal and compositional structure of the upper mantle, *In:* P.H.Nixon, ed., Mantle Xenoliths: John Wiley and Sons, p 381-402

Griffin, W.L., Kaminsky, F.V., Ryan, C.G., O'Reilly, S.Y., Win, T.T., and Ilupin, I.P., 1996. Thermal state and composition of the lithospheric mantle beneath the Daldyn kimberlite field, Yakutia: Tectonophysics, v. 262, p. 19-33.

Harte, B., and Hawkesworth, C.J., 1989, Mantle domains and mantle xenoliths, *in* Ross, J., et al., eds., Kimberlites and related rocks: Geological Society of Australia Special Publication, 14, p. 649-686.

Hops, J. J., Gurney, J. J., Harte, B., and Winterburn, P., 1989, Megacrysts and high temperature nodules from the Jagersfontein kimberlite pipe, *in:* Ross, J., et al., eds., Kimberlites and related rocks: Geological Society of Australia Special Publications, 14, p. 760-770.

Ireland, T.A., Rudnick, R.L., Spetsius, Z., 1994. Trace elements in diamond inclusions from eclogites reveal link to Archean granites. Earth and Planetary Sci. Lett., 128, 199 -213.

Jones, A.G., and Ferguson, I.J., 1997. Results from 1996 MT studies along SNORCLE profiles 1 and 1A. *In:* Cook F. and Erdmer (compilers), 1997, Slave-Northern Cordillera Lithospheric Evolution (SNORCLE) transect and Cordilleran Tectonics Workshop Meeting (March 7-9), Univ. of Calgary, LITHOPROBE Report No. 56, p. 42-47

Kopylova, M.G., Russell, J.K., Cookenboo H., in press. Upper mantle stratigraphy of the Slave Craton, Canada: Insights into a new kimberlite province. Geology.

MacGregor, I.D., 1974, The system MgO-Al_2O_3-SiO_2: solubility of Al_2O_3 in enstatite for spinel and garnet peridotite compositions, American Mineralogist, v. 59, p. 110-119

Mareschal, J.-C., Jaupart, C., & Davaille, A., Guillou-Frottier, L., 1997. Heat Flow and Thickness of the Lithosphere in the Canadian Shield. *EOS Trans.*, AGU, **78** (46),Fall Meet. Suppl., F698

O'Neill, H. St. C., 1981, The transition between spinel lherzolite and garnet lherzolite, and its use as a geobarometer, Contributions to Mineralogy Petrology, v. 77, p. 185-194

Polet, J. & Anderson, D.L., 1995. Depth extent of cratons as inferred from tomographic studies. *Geology,* **23:** 3, 205-208

Schulze, D. J., 1987, Megacrysts from alkalic volcanic rocks. , *in:* Nixon P. H., ed., Mantle xenoliths: New York, John Wiley and Sons, p 433-451.

Shervais, J.W., Taylor, L.A., Lugmair, G.W., Clayton, R.N., Mayeda, T.K., and Korotev, R.L., 1988. Early Proterozoic oceanic crust and the evolution of subcontinental mantle: eclogites and related rocks from southern Africa. Geol. Soc. of Amer. Bull., 100, 411-423

Snyder, G.A., Taylor, L.A., Crozaz, G., Halliday, A.H., Beard, B.L., Sobolev, V.N., and Sobolev, N.V., 1997. The origins of Yakutian eclogite xenoliths. J. of Petrol., 38, 1, 85-113.

Vinnik, L.P., Green, E.W.E., Nicolaysen, L.O., Kosarev, G.L., Petersen, N.V., 1996. Deep seismic structure of the Kaapvaal craton. Tectonophysics, 262: 67-75

A Steady-State Conductive Geotherm for the Northern Central Slave: Inversion of Petrological Data From the Jericho Kimberlite Pipe

James K. Russell

and

Maya G. Kopylova

Igneous Petrology Laboratory

Geological Sciences, EOS

The University of British Columbia

Vancouver, B.C., V6T 1Z4

Mantle xenoliths sampled and entrained by the Jericho kimberlite (Kopylova et al. 1998, Kopylova et al., *This Volume*) have been analysed and used to construct P-T arrays that elucidate the paleogeotherm for the north-central Slave craton 172 Ma (Heaman et al. 1997). In this paper we derive a steady-state conductive geotherm for the region surrounding the Jericho pipe using these P-T data. The model geotherm assumes an exponential decrease in radiogenic heat sources with depth and has the form (e.g., Lachenbruch, 1968; Crowley, 1987):

$$T(z) = T_s + \frac{q_o}{K} \cdot z + \frac{A_o \cdot D^2}{K} \cdot \left[1 - \frac{z}{D} - e^{\frac{-z}{D}}\right]$$

Specifically, we have inverted the thermobarometric data available for mantle-derived peridotitic xenoliths to obtain model estimates of surface heat flow (**qo**) and the apparent depth-scale parameter **D** (representing the thickness of crust that contributes most of the radiogenic heat). We have used geologically-constrained values of thermal conductivity (**K** = 2.5 $Wm^{-1}K^{-1}$) and surface heat production (**Ao**). The value of **Ao** is assigned a fixed, calculated value of 2.16 μWm^{-3} based on the bedrock geology (King

et al. 1989) of a 14,000 km^2 area surrounding the Jericho kimberlite and chemical compositions of the corresponding rock types (Davis, 1991). Our best fit estimates of **qo** and **D** are 52.9 mWm^{-2} and 19.52 km, respectively (Figure 1).

These parameters show the north-central Slave craton to be characterized by high surface heat flow, relative to other Archean cratons. Our estimate of **qo** agrees well with the single heat flow measurement reported by Lewis and Wang (1992) and is considerably higher than values previously estimated for the Slave craton (e.g., 35-42 mWm^{-2}) via the approach of Pollack & Chapman (1977). The magnitude of the **D**-parameter is approximately equal to or slightly greater than the thickness of upper crust imaged by seismic studies in the southern Slave (e.g., Clowes 1997). The model geotherm predicts a value for conventional "*reduced heat flow*" of 26.3 mWm^{-2} (Figure 2) and a thermal gradient in the mantle of 4.3 °C/km. The latter parameter implies a mantle heat flow of 10.7 - 12.9 mWm^{-2}, depending on the assumed value of **K**. Despite the relatively high surface heat flow, the upper mantle beneath the north-central Slave appears to be relatively cold, as is typical of cratonic environments.

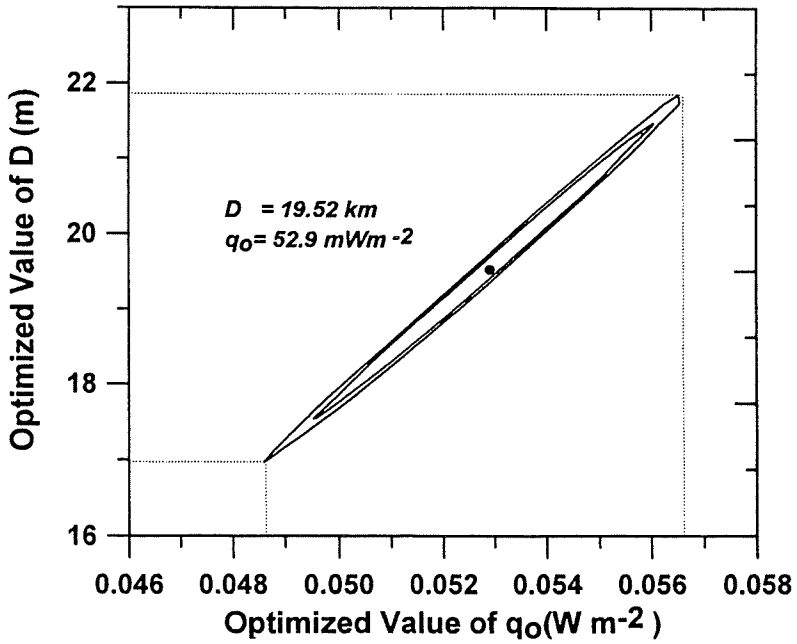

Figure 1. Confidence limits (1s and 3s) on the optimal fit parameters **D** and **qo**, showing the degree of correlation between the two model parameters and the maximum range of permissible values (dotted lines) given the observed distribution of P-T data.

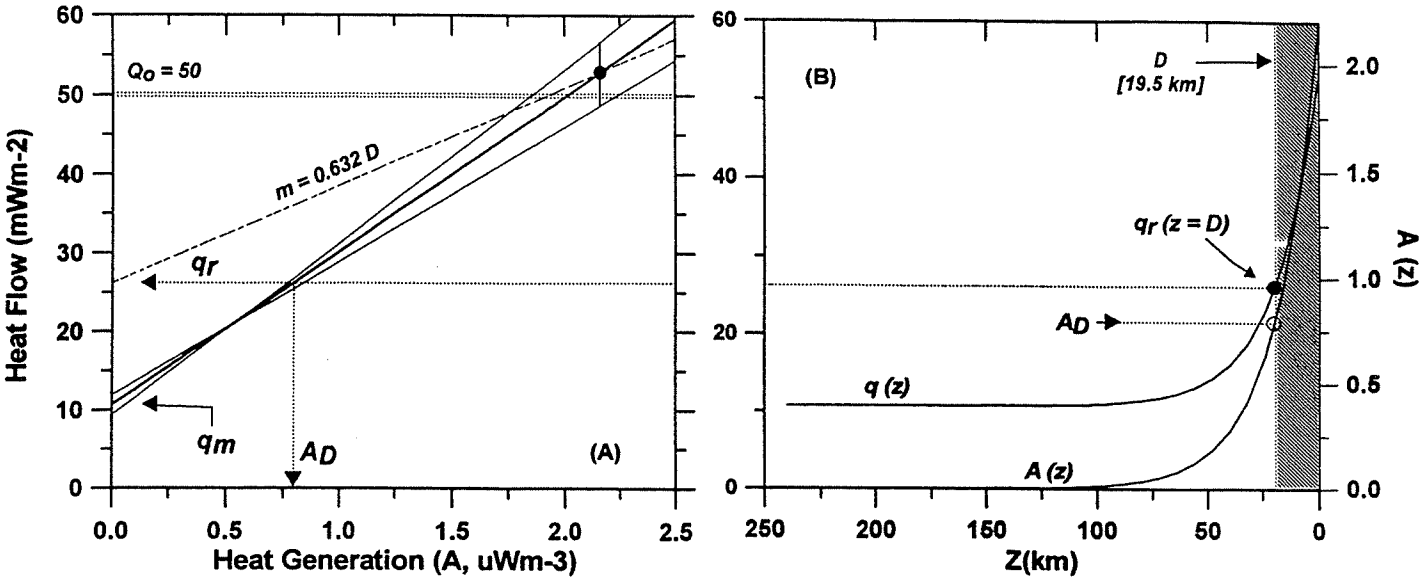

Figure 2. Implications of model parameters for heat flow in Slave lithosphere are plotted in (A) as heat flow vs. heat generation. Optimal solution is shown as solid dot **(qo, Ao)** and heavy line of slope (**D**). Also shown is the value of a single surface heat flow measurement reported for the Slave craton (**qo** = 50 mWm-2; Lewis & Wang, 1992). Light solid lines correspond to model curves for extreme range (e.g., 3s confidence limits) of permissible values of **qo** and **D** (Fig. 1). Linear relationships extrapolate to values of mantle heat flow. Dashed line denotes expected linear relationship if Ao were constant. Fig. (B) shows the corresponding values of heat flow and heat generation as a function of depth (z). The intersection of these curves with a depth z=**D** (19.5 km) defines the value of the "reduced heat flow" and the heat production at the base of the D-layer ($\mathbf{A_D}$=0.795).

Acknowledgments

This research was supported financially by Canamera Geological Ltd. And by NSERC through an IOR grant (Mineralogical and Petrological Studies in Diamondiferous Kimberlite from the Slave Structural Province). We thank Lytton Minerals Ltd. for generous access to samples.

References

Clowes, R.M. (Editor) 1997. LITHOPROBE Phase V Proposal - Evolution of a Continent Revealed. Published by the LITHOPROBE Secretariat, The University of British Columbia, Vancouver, B.C., 292 pgs.

Crowley, K.D. 1987. Distribution of radioelements and heat production in continental crust, testing hypotheses witht he drill. *EOS Transactions of American Geophysical Union*, 68, 553-558.

Davis, W. 1991. Granitoid geochemistry and Late Archean crustal evolution in the Central Slave Province, Unpublished PHD Thesis, Memorial University of Newfoundland, St. John's, Newfoundland.

Heaman, L.M. Kjarsgaard, B., Creaser, R.A., Cookenboo, H.O. & Kretschmar 1997. Multiple episodes of kimberlite magmatism in the slave Province, North America. *In. Cook, F. and Erdmer P. (Compilers) Slave-Northern Cordillera Lithospheric Evolution (SNORCLE) transect and Cordilleran Tectonics Workshop Meeting (March7-9)*, University of Calgary, LITHOPROBE Report No. 56, 14-17.

King, J.E., Davis, W. Relf, C. and Van Nostrand, T. 1990. Geology of the Contwoyto-Nose Lakes map area, central Slave Province, District of MacKenzie, N.W.T., in Current Research, Part C, Geological Survey of Canada, Paper 90-1c, 177-187.

Kopylova, M.G., Russell, J.K. & Cookenboo, H.O. 1998. Upper mantle stratigraphy of the Slave craton, Canada: Insights into a new kimberlite province. *Geology*, In Press 01/98.

Lachenbruch, A.H. 1968. Preliminary geothermal model of the Sierra Nevada. Journal of Geophysical research, 73, 6977-6989.

Lewis, T.J. & Wang, K. 1992. Influence of terrain on bedrock temperatures. *Global and Planetary Change*, 98, 87-100.

Pollack, H.N. & Chapman, D.S. 1977. On the regional variation of heat flow, geotherms and lithospheric thickness. *Tectonophysics*, 38, 279-296.

Crustal Structure of the Archean Slave Craton from Receiver Function Studies

John F. Cassidy[1], Michael G. Bostock[2], and Carl-Georg Bank[2]

[1]*Geological Survey of Canada, P.O. Box 6000, Sidney, B.C. V8L 4B2*
cassidy@pgc.nrcan.gc.ca
[2]*Department of Earth and Ocean Sciences, University of British Columbia, 2219 Main Mall, Vancouver, B.C., V6T 1Z4*

The Archean Slave craton is exposed over 210,000 km^2 in the western Northwest Territories. It is home to the oldest known terrestrial rocks (3.96 Ma), and recently, to unprecedented claim staking for diamond interests. In the autumn of 1996, an array of portable three-component broadband seismographs were deployed over the craton (Figure 1). Recordings of distant earthquakes made at these sites, and at the permanent Yellowknife array, are being used to image the crustal and upper mantle structure beneath the Slave craton. Here, we present progress to date on waveform modelling to examine the variation in crustal structure across the Slave craton.

We use the method of receiver function analysis to constrain the crustal shear-wave velocity structure. This technique utilises the P-waves of distant earthquakes, travelling at a steep angle of incidence through the crust and upper mantle. P-to-S converted phases are generated at significant S-velocity discontinuities beneath the recording site. These converted phases can be readily identified as they are found almost exclusively on the radial (horizontal) component of the waveform, whereas the direct P-wave dominates the vertical component. The amplitude of the Ps phase is determined by the S-velocity contrast across the interface; the arrival time of the phase is dependant on the depth of the interface and the average velocity between the surface and the interface.

In Figure 2a we present stacked receiver functions for stations on the Slave craton and the bordering Proterozoic orogenic belts. Each of these traces is a 'stack' of receiver functions formed from individual earthquakes (within a narrow range of azimuth and distance). The stacks contain between 2 events (KENN) and 9 events (LKSN). The traces are ordered from north (top) to south (bottom). In each of the traces, the largest arrival (at 0 seconds) represents the direct P-wave; locally generated Ps phases, and free-surface multiples follow. Note that there is a well-defined arrival near 5 seconds at the stations ULUN, KARN, COLN, KOAN, and LOCN. The timing and amplitude of this phase indicate that it was generated at the continental Moho beneath these sites - each of which is in the central portion of the Slave craton. A close-up of the waveforms for these stations is shown in Figure 2b. Note the consistency in both the amplitude and arrival time of the interpreted Moho phase. This indicates a homogeneous crust through the central Slave. The slight variation in the arrival time of the phase between the stations (e.g., ULUN and KARN) corresponds to a depth variation in the Moho of about 2 km, or a

change in the average crustal velocity of less than 5%. It is noteworthy that this phase is either absent, or has a significantly different character at each of the seismic stations close to the edge of the craton, or on the adjacent Proterozoic belts - suggesting that the Slave crust has been altered through collision, down to the Moho.

In Figure 3a we present data for the station KARN from the SE and NW azimuths, a stacked waveform (including data from all azimuths), and a synthetic waveform derived from preliminary forward modelling of these data. A simple crustal structure (Figure 3c) with a Moho depth of 37 km provides a good fit to the Moho phase near 5 seconds. Note that stations on the adjoining Churchill province (FCC, FFC, and FRB) show a Moho arrival that arrives later than that at KARN, suggesting that the Slave crust is slightly thinner than that of the Churchill province. These waveforms also show a smaller amplitude arrival near 3 seconds (arrowhead in Figure 3b) - that suggests a velocity discontinuity in the lower crust near 25-27 km.

In summary, preliminary modelling of receiver functions indicates that the crust is relatively simple and homogeneous beneath the central portion of the Slave craton. At the edges of the craton, the Moho is not readily apparent, suggesting that the Slave crust has been modified through collision down to the Moho. In the central Slave, the crustal thickness is 36-38 km.

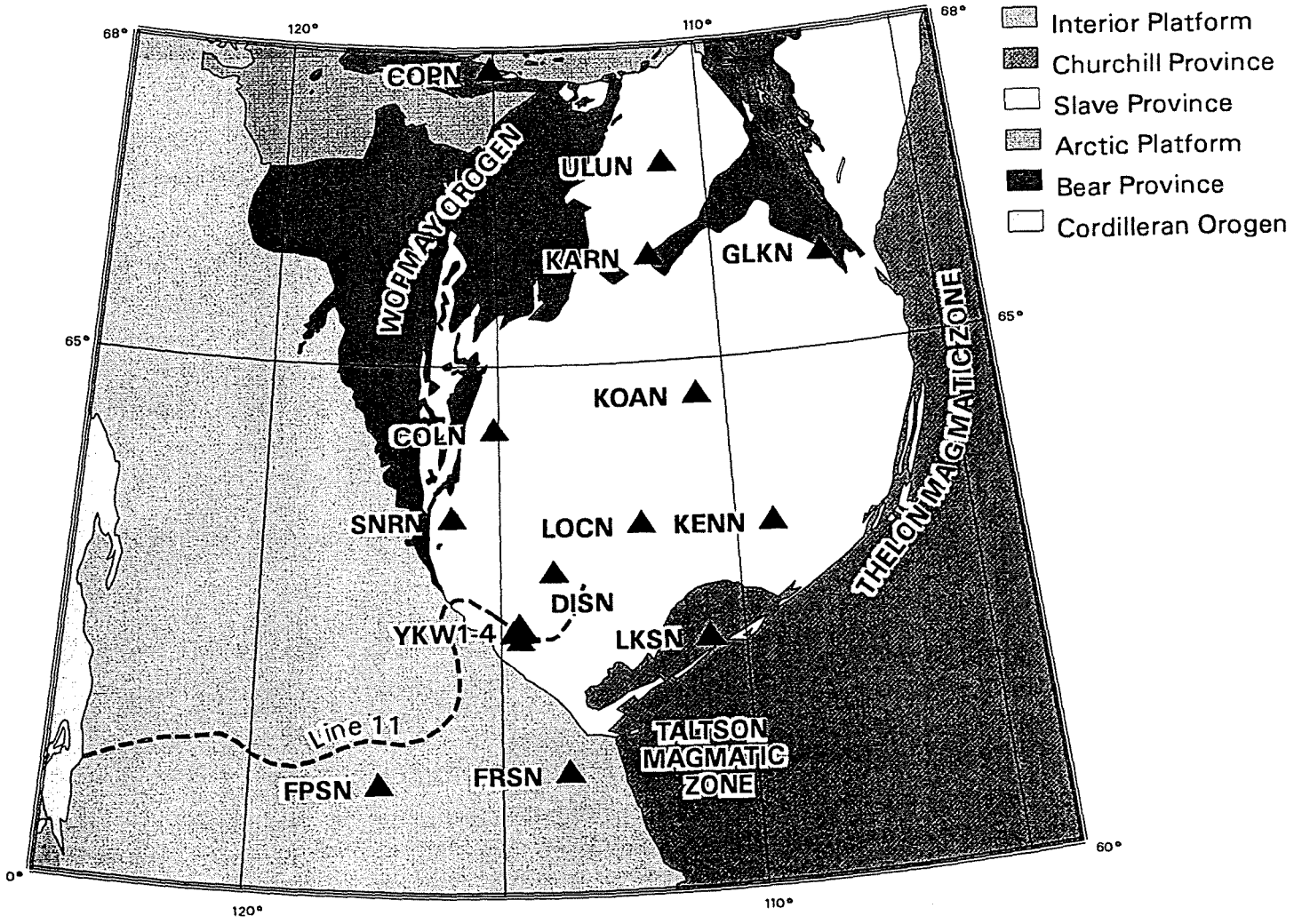

Figure 1. Location of portable broadband seismograph stations (triangles) used in this study. The dashed line denote SNORCLE seismic refraction line 11.

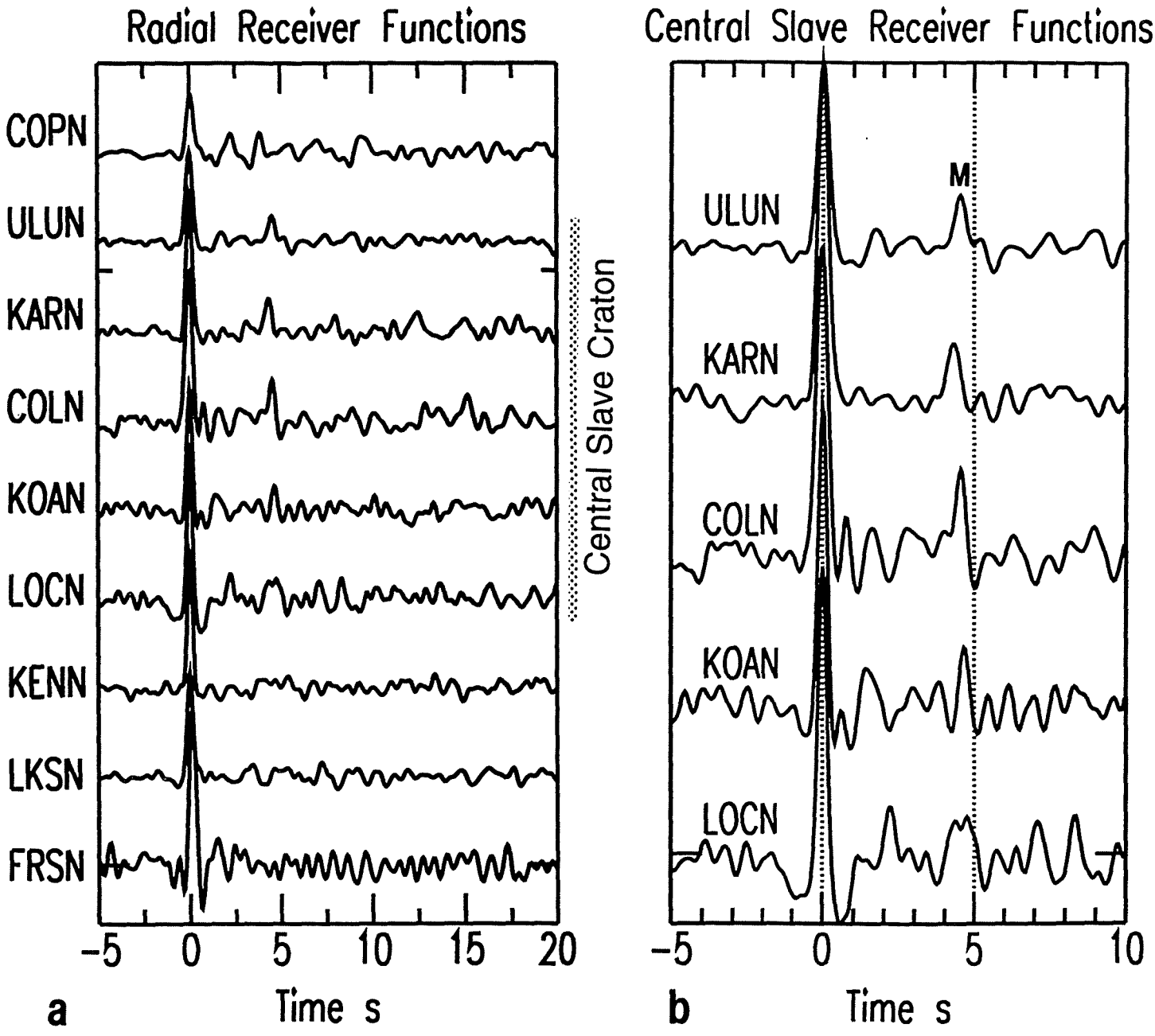

Figure 2. a) Stacked receiver functions arranged from north to south over the Slave craton and adjacent areas (stations locations are given in Figure 1). b) Close up of 5 stations on the Slave craton showing the well-defined Moho arrival.

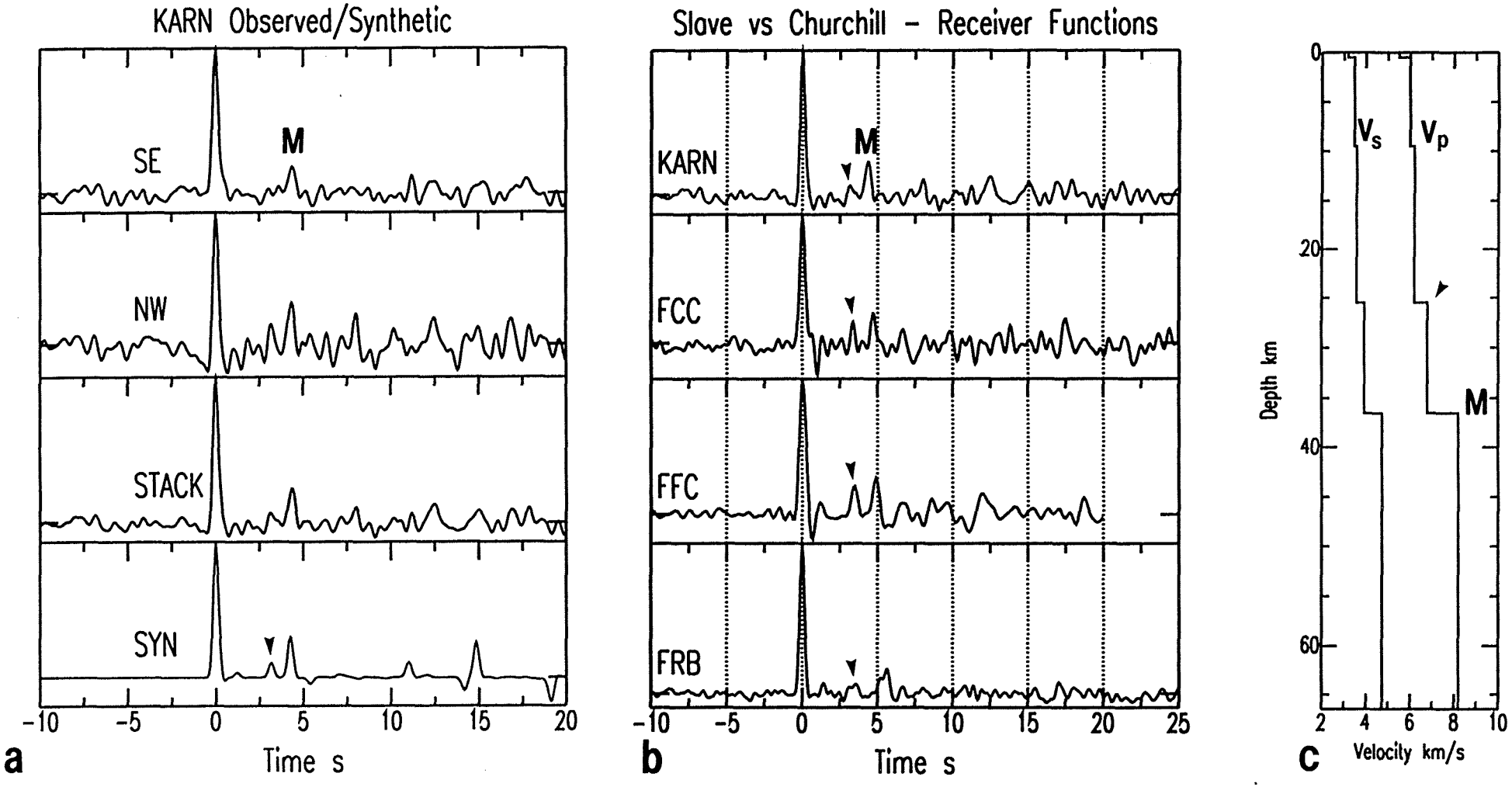

Figure 3. a) KARN stacked receiver functions at two quadrants, and stacked over all azimuths, compared to a synthetic waveform derived from forward modelling (SYN). 'M' indicates the interpreted Ps conversion from the Moho. b) A comparison of receiver functions from KARN with those from stations on the Churchill province (FCC - Churchill; FCC - Flin Flon; FRB - Frobisher Bay). Arrowhead denotes the small arrival that suggests a velocity discontinuity in the lower crust. c) Velocity model used to generate the synthetic trace shown in a).

Tectonic Delamination of the Precambrian Lithosphere in Northwestern Canada Mapped by LITHOPROBE

F. A. Cook, A. J. van der Velden, and K. W. Hall
Department of Geology and Geophysics
University of Calgary
Calgary, AB T2N1N4

and
B. J. Roberts
Geological Survey of Canada
1 Observatory Crescent
Ottawa, ON K1A0Y3

ABSTRACT

Seismic reflection profiling of the lithosphere in northwestern Canada has produced images of delamination structures (tectonic wedges) at crustal scale (to about 30 km depth) and, for the first time, lithospheric scale (to about 100 km depth). Coupled with observations of similar structures in thrust and fold belts, tectonic delamination is a persistent feature of deformation at many scales of observation.

Introduction

Tectonic delamination (wedging) occurs at many scales in deformed belts. Near the leading edges of thrust and fold belts, oppositely verging thrust faults delineate wedges of sedimentary rocks that were tectonically inserted into relatively undeformed foreland strata (e.g., "triangle zones"; Jones, 1983; Price, 1986; Lawton et al., 1995), and may even stack to produce "zig-zag" structures (Harrison and Bally, 1988; Cook and Varsek, 1994). At a larger scale, delamination structures have been interpreted on deep crustal seismic reflection data where reflections dip in opposite directions between upper and lower crust (Cook et al., 1992;Cook and Varsek, 1994) whose geometry is replicated by numerical simulations (Willet et al., 1994).

Delamination of the entire lithosphere has been proposed for various tectonic regimes, including contractional orogens (Oxburgh, 1972; Bird, 1978, Nicolas et al., 1990; Cook and

Varsek, 1994) and extensional regions (Bird, 1979; Nelson, 1992). In general, these structures were proposed based on projections of geological structures from the surface (Oxburgh, 1972) and have recently been supported by numerical models (Bird, 1978, 1979; Willet et al., 1994), often coupled with interpretations of crustal geological and geophysical data, for Phanerozoic orogens. Until now, however, no detailed images of delaminated *lithosphere* had been available. In this article, we describe results from the ca. 725 km long deep seismic reflection profile recorded by LITHOPROBE in the northwestern Canadian shield in which such images outline tectonic wedges at both crustal (ca. 30 km) and lithospheric (ca. 100 km) scales.

Regional Geology

The tectonic history of northwestern Canada spans most of the Earth's history, from ca. 4.0 Ga rocks in the Slave province (Bowring et al., 1986) to the Mesozoic/Tertiary Cordillera (Fig. 1). Westward growth of the continent took place as cratonic assembly of the Slave province was completed by about 2.6 Ga when volcanic arcs and microcontinents amalgamated, probably as a result of lithospheric subduction (Kusky, 1990; MacLachlan and Helmstaedt, 1995). Little activity occurred in this portion of the Slave craton until about 1.9-2.0 Ga when a westward facing passive margin developed as a result of lithospheric extension (Coronation margin). Rapid margin formation and associated supracrustal sedimentation was followed by contraction and eastward structural translation of detached strata and associated metamorphic and intrusive rocks (ca. 1.90-1.88 Ga. Calderian Orogeny) of the Wopmay orogen. This deformation was likely caused by the approach and accretion of a terrane (Hottah terrane) to the western margin of the Slave craton (Hildebrand et al., 1983; Hoffman and Bowring, 1984). Subsequent to this accretion event, between about 1.88 Ga and 1.84 Ga, magmatic rocks of the Great Bear magmatic arc were deposit onto deformed rocks of the both Wopmay orogen and parautochthonous rocks of the western Slave Province. Rocks of the Great Bear arc were themselves deformed by dextral oblique shearing, perhaps as another exotic terrane (Fort Simpson terrane) approached from the west

(Hildebrand et al., 1987). Lithospheric extension between about 1.8 Ga and 1.2 Ga formed a deep basin on the west side of the Fort Simpson terrane that received up to 20 km of sedimentary rocks.

In the vicinity of the LITHOPROBE seismic profile, rocks of the Wopmay orogen are covered by undeformed Phanerozoic sedimentary rocks of the Western Canada Sedimentary Basin (Figs. 1 and 2). Hence, the orientations and relative positions of the different linear belts of the Wopmay orogen in the vicinity of the seismic profile are determined by tracking regional magnetic and gravity anomalies southward from exposures (Fig. 2). In general, the regional belts trend north-south, and the seismic profile crosses them at high angle (Fig. 2).

Reflection Data

Seismic reflection profiling has been used for more than 20 years to map the fine structure (to ca. 100 m resolution) of the continental crust. In general, however, reflections from the sub-crustal mantle are rare, and where present, are discontinuous. Further, the ability to relate reflections from below the crust to known features at or near the surface is difficult because crustal structures that are younger than the mantle structures often mask the significance of older and deeper surfaces. For example, a prominent mantle reflector observed to about 80 km depth north of Scotland and has been variously interpreted as a thrust fault, an extensional fault, or a relict subduction zone (Brewer and Smythe, 1984; McGeary and Warner, 1985; Reston, 1990; Warner et al., 1996), and a similar reflector that could be followed to about 60-65 km depth beneath Archean (ca. 2.7 Ga) rocks of the Precambrian Abitibi subprovince in eastern Canada has been interpreted as an ancient subduction zone (Calvert et al., 1995).

The profile presented here is part of the LITHOPROBE SNORCLE (Slave NORthern Cordillera Lithospheric Evolution) transect that extends westward from the Slave Province, across the Western Canada Sedimentary Basin, the Northern Cordillera, and terminates near the Pacific Ocean. In total, the transect addresses the evolution of the North American craton from the Archean to present along a single corridor; the data presented here are from the deep reflection

profile in the eastern half of the transect where Precambrian rocks are at the surface (Slave Province), or are buried by Phanerozoic strata of the Western Canada Sedimentary Basin (Fig. 1).

Results

The crust is highly reflective along the entire profile, and the Moho is well defined at about 30-35 km. Although the mantle is less reflective than the crust, important correlatable reflections are visible from as deep as 100 km and can be followed to the crust where they are related directly to tectonic transitions interpreted from surface relationships. Detailed descriptions of data acquisition, processing and crustal structure are presented elsewhere (Cook et al., submitted); here we focus on two features related to tectonic wedging (Figs. 2-4).

Mantle reflections M1 dip eastward from beneath the crust of the Fort Simpson area to about 100 km depth beneath the Great Bear arc (Figs. 2 and 3). East of there, arcuate reflections (M1a) can be interpreted as uplifted (thrust?) layers that were detached from M1 (Fig. 2). Accordingly, M1 and M1a together form a correlatable pattern of mantle reflectivity over a distance of about 400 km. These reflections project into the lower crust of the Fort Simpson area thus providing definitive evidence that they represent lower crustal rocks that were carried into the mantle (subducted). Further, the position of the reflections at about 100 km depth beneath the Great Bear magmatic arc is evidence that the subducted rocks were responsible for formation of the arc at the surface, just as young magmatic arcs are situated above lithosphere subducted to ca. 100 km depth today. The Great Bear arc and Fort Simpson terrane have previously been linked geologically as the ca. 1.845 Ga Fort Simpson terrane was juxtaposed with the western margin of the Wopmay orogen when magmatic activity in the arc ceased (Hildebrand et al., 1987).

Reflection M1 thus delineates the lower surface of a geometric wedge whose apex is in the lower crust of the Fort Simpson terrane. The upper surface of this wedge is a set of west-dipping reflections that project from the wedge apex to near the surface beneath the thin Phanerozoic sediment cover (Figs. 2 and 3). Although the exact nature of the rocks within the wedge is

uncertain, they are part of the Wopmay orogen crust, and they have the geometry of an accretionary complex commonly seen in modern convergent zones.

Mantle reflection M2 dips eastward from the base of the crust beneath the Great Bear arc to about 85 km depth beneath the western Slave Province, and remains subhorizontal east of there. This reflection is not as layered as M1-M1a, but rather is a single simple reflection, and projects to the base of the crust where reflections above it are subhorizontal. Apparently, either the crustal reflections are structurally discordant with M2, or they are layered magmatic rocks above M2.

The presence of M2 beneath the Slave Province leads to two possible interpretations: (1) It may be an Archean (>2.5 Ga) boundary. In this case the mantle beneath it and to the west as far as M1 would also be Archean; (2) It may be a boundary between Proterozoic (Wopmay, ca. 2.1-1.84 Ga) mantle below and Archean (Slave) mantle above (Fig. 2). In this case, M2 would be either a detachment surface, or a magmatic layer.

The crust above M2 is highly deformed by low-angle faults that were active during formation of the Wopmay orogen (ca. 2.1-1.84 Ga, probably between 1.9-1.8 Ga; Figs. 2 and 4; Cook et al., submitted). Deformed structures are visible up to 125 km east of the B-41 well location. Thus, if M2 is Archean, Proterozoic structures were detached from Archean mantle from the position of the P-56 well to the Slave Province, a distance of about 300 km. Alternatively, if M2 is a Proterozoic detachment, the crustal structures were detached from the mantle east of the position of the B-41 well. In either case, the crustal structures were detached from the mantle. Near the transition from the Slave Province to the Wopmay orogen, the crustal geometry outlines a westward tapering wedge whose apex is at about 25 km (8.0 s; Figs. 2 and 4). As the crust west of this location was detached and carried eastward, some layers were inserted beneath the lower Slave crust, and others were carried above it.

The Slave-Wopmay crustal wedge situated near the east side of the Great Bear arc is delineated by east-dipping reflections in the lower crust, west-dipping reflections in the upper crust, and an apex near 25 km depth. This wedge probably formed above a detachment at or near the Moho that connected this deformation with Wopmay orogen structures farther west. Reflection

M2 may be from a surface within the mantle that accommodated the intracrustal deformation as the collision between accreted rocks (Hottah terrane) and Slave craton terminated at about 1.9 Ga.

Conclusions

The LITHOPROBE transect in northwestern Canada provides the first demonstrable image of tectonic wedging ("flaking") of the lithosphere (Fig. 5), in addition to crustal wedging similar to that seen on deep reflection profiles elsewhere. Tectonic delamination thus occurs at many scales in the crust and lithosphere and is analogous to triangle zone and passive-roof duplex geometry observed in foreland thrust and fold belts. The results affirm that deformation of the crust and lithosphere at about 2.0 Ga was similar to today as horizontal motion of the lithosphere is manifested as orogenic belts on the continents.

References

Bird, P. Initiation of intracontinental subduction in the Himalaya. *J. Geophys. Res.* **83**, 4975-4987 (1978).

Bird, P. Continental delamination and the Colorado Plateau. *J. Geophys. Res.* **84**, 7561-7571 (1979).

Brewer, J. A., & Smythe, D. K. MOIST and the continuity of reflector geometry along the Caledonian-Appalachian orogen. *J. Geol. Soc. Lond.* **141**, 105-120 (1984).

Bowring, S. A., Williams, I. S., & Compston, W. 3.96 Ga gneisses from the Slave province, Northwest Territories. *Geology* **17**, 971-975 (1986).

Calvert, A. J., Sawyer, E. W., Davis, W. J., & Ludden, J. N. Archean subduction inferred from seismic images of a mantle suture in the Superior Province. *Nature* **375**, 670-674 (1995).

Cook, F. A., Varsek, J. L., Clowes, R. M., Kanasewich, E. R., Spencer, C., Parrish, R. R., Carr, S. D., Johnson, B. J., & Price, R. A. LITHOPROBE crustal reflection cross-section of the southern Canadian Cordillera: foreland thrust and fold belt to Fraser river fault. *Tectonics* **11**, 12-35 (1992).

Cook, F. A., & Varsek, J. L. Orogen-scale decollements. *Rev. Geophys.* **32**, 37-60 (1994).

Cook, F. A., van der Velden, A. J., Hall, K. W., & Roberts, B. J., Frozen subduction in Canada's Northwest Territories, LITHOPROBE deep lithospheric reflection profiling of the western Canadian Shield, *Tectonics* (submitted).

Harrison, C. & Bally, A. W. Cross sections of the Parry Islands fold belt on Melville Island, Canadian Arctic islands: Implications for the timing and kinematic history of some thin-skin decollement systems. *Bull. Can. Petr. Geol.* **36**, 311-332 (1988).

Hildebrand, R. S., Bowring, S. A., Steer, M. E., &Van Schmus, W. R. Geology and U-Pb geochronology of parts of the Leith Peninsula And Riviere Grandin map areas, District of Mackenzie, *Geol. Surv. Canada Curr. Res.* **83-1A,** 329-342 (1983).

Hildebrand, R. S., Hoffman, P. F., & Bowring, S. A. Tectonomagmatic development of the Great Bear magmatic arc, northwestern Canadian Shield. *J. Volc. and Geotherm. Res.* **32**, 99-118 (1987).

Hoffman, P. F., & S. A. Bowring, Short-lived 1.9 Ga continental margin and its destruction, Wopmay orogen, northwest Canada. *Geology* **12**, 68-72 (1984).

Jones, P. B. Oil and gas beneath east-dipping underthrust faults in the Alberta foothills, Canada. in *Geologic Studies of the Cordilleran Thrust Belt, Vol. 1* (ed Powers, R. B.), Rocky Mountain Assoc. Geol., Denver, 61-74 (1983).

Kusky, T. M., Evidence for Archean ocean opening and closing in the southern Slave Province, *Tectonics, 9,* 1533-1563, 1990.

Lawton, D. C. Spratt, D. A., & Hopkins, J. C. Tectonic wedging beneath the Rocky Mountain foreland basin, Alberta, Canada. Geology 22, 519-522 (1994).

MacLachlan, K., & Helmstaedt, H. Geology and geochemistry of an Archean dike complex in the Chan Formation: Basis for a revised plate-tectonic model of the Yellowknife greenstone belt: *Can. J. Earth Sci.* **32**, 614-630 (1995).

McGeary, S. E. & Warner, M.R. Seismic profiling of the continental lithosphere. *Nature* **317**, 795-797 (1985).

Nelson, K. D., Are crustal thickness variations in old mountain belts like the Appalachians a consequence of lithospheric delamination? *Geology* **20**, 498-502 (1992).

Nicolas, A., Hirn, A., R. Nicolich, R. Polino & ECORS-CROP Working Group, Lithospheric wedging in the western Alps inferred from the ECORS-CROP traverse. Geology **18**, 587-590 (1990).

Oxburgh, E. R., Flake tectonics and continental collision. *Nature* **239**, 202-204 (1972)

Price, R. A. The southeastern Canadian Cordillera: thrust faulting, tectonic wedging and delamination of the lithosphere. *J. Struct. Geol.* **8**, 239-244 (1986).

Reston, T. J. Mantle shear zones and the evolution of the North Sea basin. *Geology* **18**, 272-275 (1990).

Villeneuve, M. E., G. M. Ross, R. R. Parrish, R. J. Theriault, W. Miles, and J. Broome, Geophysical subdivision, U-Pb geochronology and Sm-Nd isotope geochemistry of the crystalline basement of the Western Canada Sedimentary Basin, *Geol. Surv. Canada Bulletin* **447**, 86 pp., 1993.

Warner, M. R., J. Morgan, P. Barton, P. Morgan, C. Price, & K. Jones, Seismic reflections from the mantle represent relict subduction zones within the continental lithosphere, *Geology* **24,** 39-42 (1996).

Willet, S. D., & Beaumont, C. Subduction of Asiatic lithospheric mantle beneath Tibet inferred from models of continental collision. *Nature* **369**, 642-645 (1994).

Acknowledgments. This research was supported by the Natural Sciences and Engineering Research Council of Canada and the Geological Survey of Canada. The seismic data were recorded by JRS Exploration of Calgary and were processed at the LITHOPROBE Seismic Processing Facility at the University of Calgary. We are grateful to Dr. Kris Vasudevan and Dr. Rolf Maier for their assistance in the processing and Elissa Lynn for assistance with the graphics.

Figure Captions

Figure 1. Map of northwestern Canada with location of SNORCLE reflection line heavy line) east of the Cordillera (bold line with teeth). The Slave Province represents ancient (>2.5 Ga) craton, and the north-south oriented zones between the Slave Province and the Cordillera are domains of the 2.1-1.84 Ga Wopmay orogen that were accreted to the western Slave. Along the profile, these are all buried beneath thin sedimentary rocks of the Western Canada Sedimentary basin, the eastern edge of which is the bold line WCSB. The domains of the Wopmay orogen are patterned to the northeast-southwest Great Slave Lake shear zone; south of there domains are labeled but not shaded. Abbreviations (Villeneuve et al. 1993) are: BH = Buffalo Head domain; CH = Chinchaga domain; FS = Fort Simpson terrane; GB = Great Bear arc; HO = Hottah terrane; KS = Ksituan domain; KW = Kiskatinaw domain; NH = Nahanni domain; RA = Rae Province; TA = Taltson arc; TT = Tintina fault. P-56 and B-41 are locations of two wells that penetrate into Proterozoic rocks beneath the sedimentary cover.

Figure 2. Migrated and coherency-filtered seismic reflection profile from the Slave province on the east almost to the front of the Cordillera on the west, a distance of about 725 km. The two bold arrows indicate the positions of intra-crustal (east) and lithospheric (west) wedges. It is not know at this time if the reflections at about 70-80 km beneath the Great Bear arc are from subducted and then uplifted Fort Simpson crust as shown here. Locations of Figures 3 and 4 are indicated.

Figure 3. Enlargement of the reflection data in the vicinity of the Fort Simpson lithospheric wedge (M1). Large arrow indicates centre of wedge. Note the reflections that dip into the mantle from the crust.

Figure 4. Enlargement of the reflection data in the vicinity of the Slave - Wopmay crustal wedge. Note that the structures above the Moho all flatten into or above it and that layers in the upper crust dip west while those of the lower crust dip east, thus outlining the crustal wedge.

Figure 5. Flake tectonics as illustrated by Oxburgh (1972). The model was drawn to explain geology of the Alps and has been reversed for simple comparison to Figure 2. B = Bohemian massif; M= Moho; L = base of lithosphere.

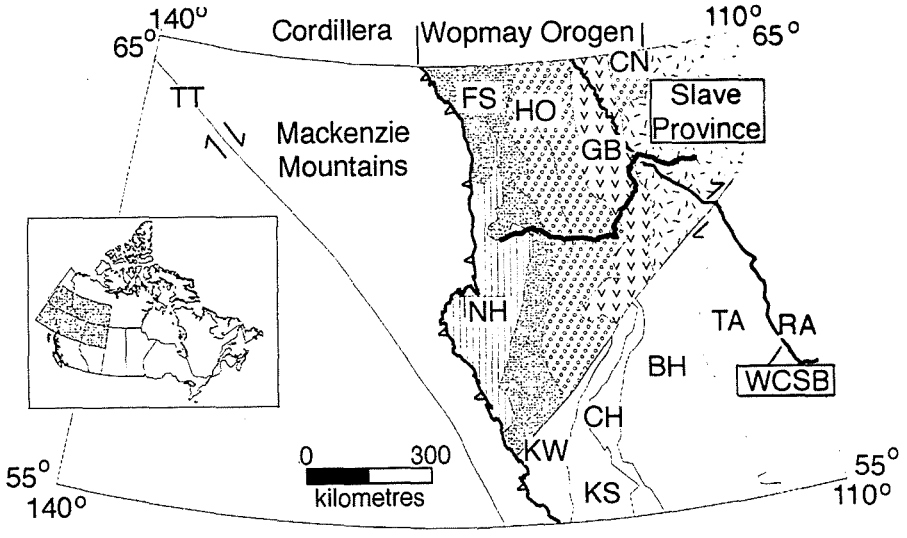
140°
65°
Cordillera
Wopmay Orogen
110°
65°
CN
TT
FS
HO
Slave
Province
Mackenzie
Mountains
GB
NH
TA
RA
BH
WCSB
CH
KW
KS
0
300
kilometres
55°
140°
55°
110°

Figure 1.

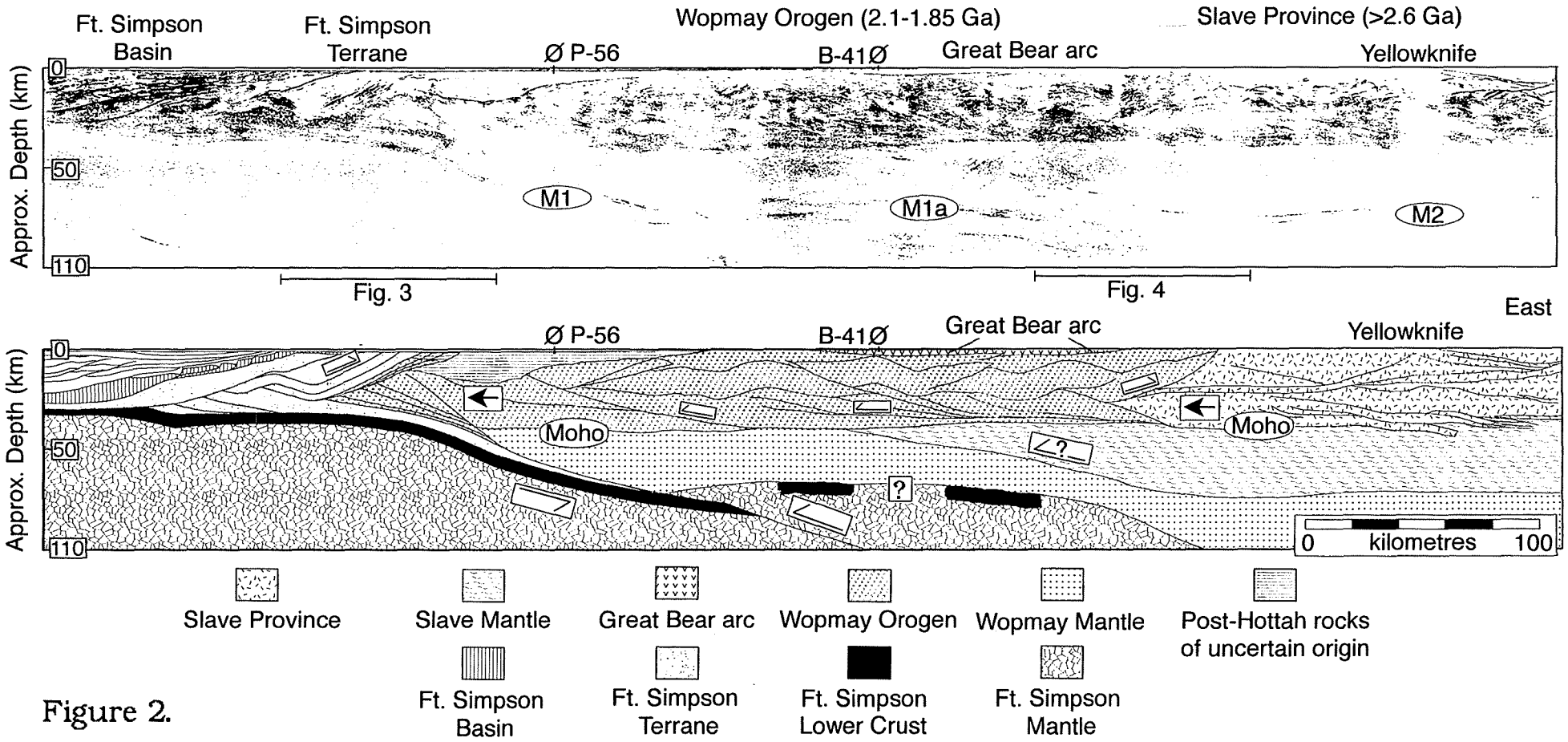
Ft. Simpson Basin
Ft. Simpson Terrane
Wopmay Orogen (2.1-1.85 Ga)
Slave Province (>2.6 Ga)
Ø P-56
B-41Ø
Great Bear arc
Yellowknife
Approx. Depth (km)
0
50
110
M1
M1a
M2
Fig. 3
Fig. 4
East
Moho
?
0 kilometres 100
Slave Province
Slave Mantle
Great Bear arc
Wopmay Orogen
Wopmay Mantle
Post-Hottah rocks of uncertain origin
Ft. Simpson Basin
Ft. Simpson Terrane
Ft. Simpson Lower Crust
Ft. Simpson Mantle

Figure 2.

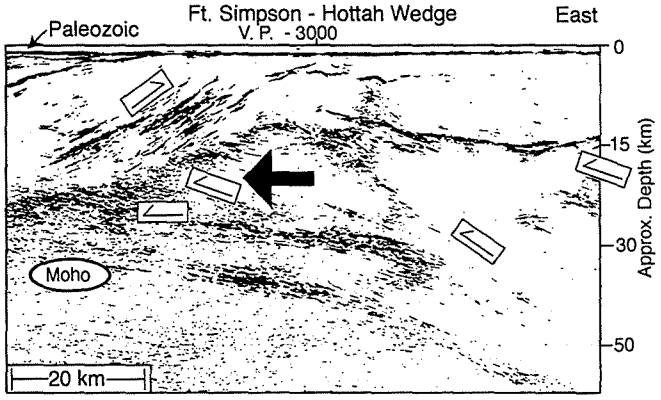

Figure 3.

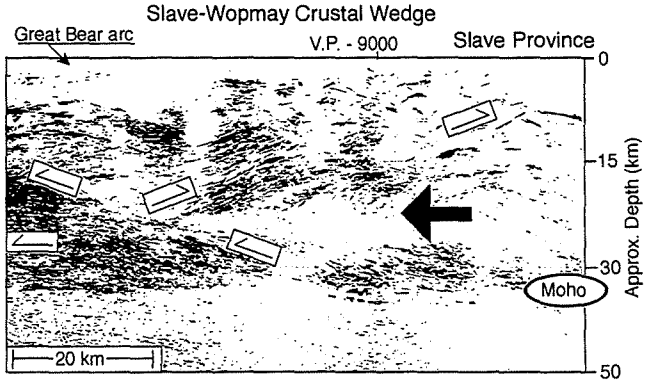

Figure 4.

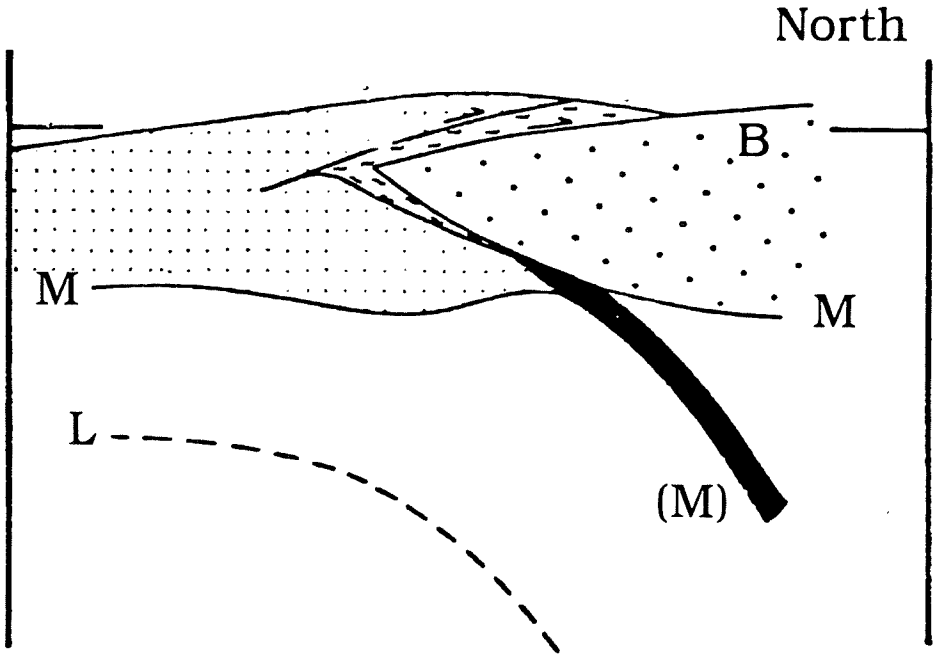

Figure 5.

Mantle stratigraphy and evolution of the Slave province

M. G. Bostock, (Department of Earth and Ocean Sciences, University of British Columbia, Vancouver, Canada),

Archean cratons have played an important role in the origin and stabilization of continents as revealed by long-period seismology and the geochemistry of mantle xenoliths erupted in kimberlites. Further progress in deciphering the processes effecting continental evolution requires an interrogation of the cratonic lithosphere at scales intermediate to these two approaches. A data set of 1033 three-component P-wave seismograms from 5 broadband stations at the Yellowknife Array is assembled to investigate mantle structure below the southern Slave province in Canada's Northwest Territories. Following wavefield decomposition, seismograms are source-normalized through simultaneous deconvolution of multiple seismograms to estimate the near-receiver impulse response as a function of epicentral distance and back azimuth. Images of impulse response reveal a well developed mantle stratigraphy, anisotropic in part, extending from the Mohorovicic discontinuity to the transition zone. A layer of depth localized anisotropy ($\pm 5\%$), termed H, is situated between $\sim$ 70-80 km depth with an average shear velocity comparable to that of the ambient mantle and a sharp upper boundary less than 100 m in transition width. The absence of free surface crustal reverberations on the transverse component affords a window into the upper mantle between 100-200 km depth. A sequence of at least 2 layers between 120-150 km depth, collectively termed X, is most clearly evident to the north and is underlain by a second structure, L, which dips from 170 km in the west to 230 km into the center of the Slave province. The deepest interface above the transition zone, W, marks a shear velocity inversion near 350 km depth whose signature is restricted to the SV component signalling a dominantly isotropic response. Consideration of these observations in light of data acquired in a recent *LITHOPROBE* seismic reflection traverse and in petrological studies of kimberlite xenoliths prompts speculation into the role of subduction in craton construction. It is suggested that the proto-Slave craton was assembled through processes of shallow subduction resulting in a near-horizontal mantle stratigraphy (i.e. H, X) both compositional and rheological in nature. Interpretation of L as the continuation of dipping reflectors on the seismic reflection profile argues for a final phase of craton assembly involving oblique underplating of subducted lithosphere in the Proterozoic. Subsequent modification of the lithosphere, as manifest by Phanerozoic kimberlite volcanism, may be related to W if an interpretation as the top of a layer containing a dense silicate melt fraction is invoked

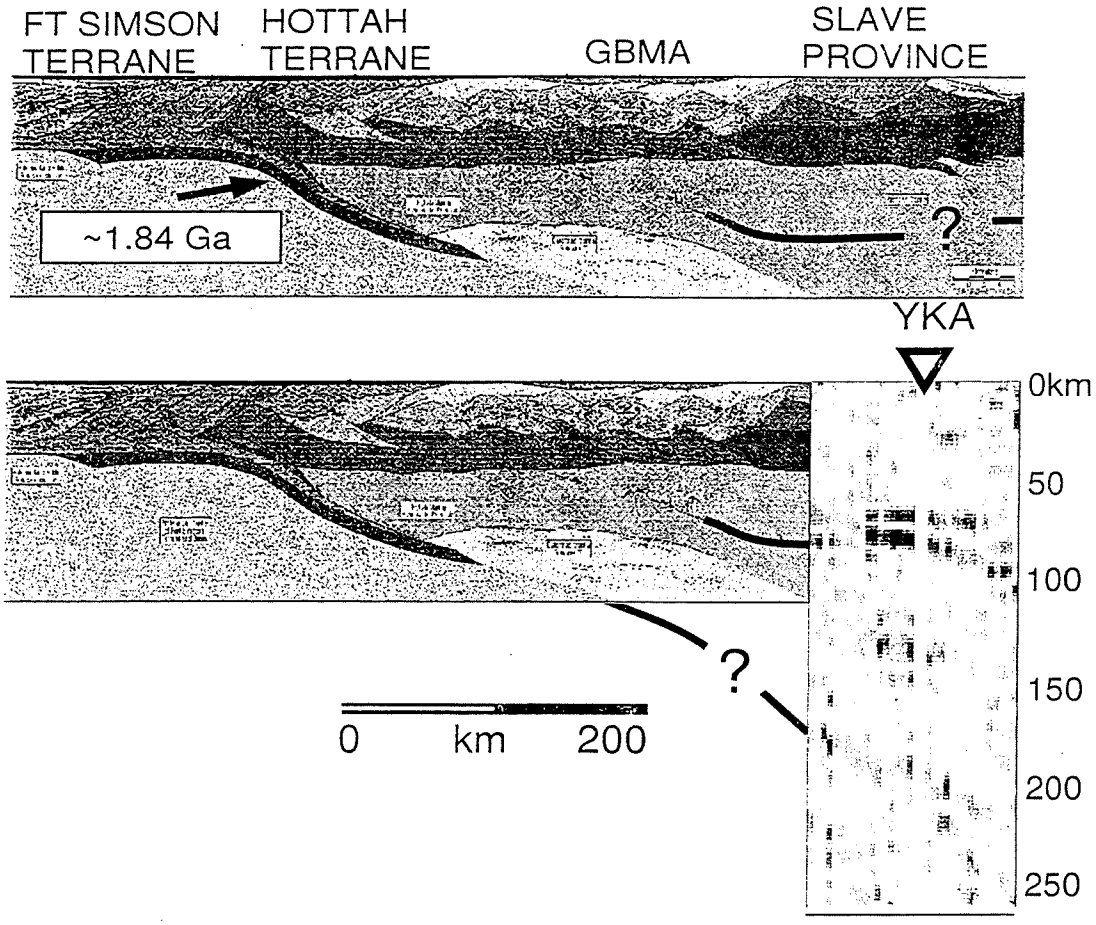

Figure: Integration of reflection seismic and $P_{D}s$ profiles. Top panel shows interpreted reflection seismic section, courtesy of Fred Cook, wth prominent mantle reflections indicated. Bottom panel shows juxtaposition with northern section of transverse (SH) impulse response mapped to depth.

THE SNORE 97 SEISMIC REFRACTION EXPERIMENT: PRELIMINARY RESULTS.

G. Fernández Viejo, R.M. Clowes*, R.M. Ellis*, G. Spence**, I. Asudeh*** and the SNORE 97 Field Crew*

* Dept. of Earth and Ocean Sciences. University of British Columbia, Vancouver, B.C., Canada

** University of Victoria, B.C., Canada

*** Geological Survey of Canada, Ottawa

ABSTRACT

During August-September 1997, LITHOPROBE conducted a seismic refraction/wide-angle reflection (R/WAR) survey (SNORE 97) in northwestern Canada. This experiment is one component of the Slave-Northern Cordillera Lithospheric Evolution (SNORCLE) Transect, a multidisciplinary study of the structure and evolution of the continental lithosphere in a region where the rock record spans 90% of Earth's history.

The seismic experiment is designed to determine the velocity structure of the crust and sub-crustal lithospheric mantle from Great Slave Lake in the NorthWest Territories to the coast of the Alaska "Panhandle". The relationships of the velocity structural models with coincident geophysical and geological data will improve our knowledge of the tectonic structure of these domains and elucidate their past history. Four R/WAR profiles were collected over the transect area. For each line, 594 portable seismographs were deployed at a station spacing of 0.5 to 1.2 km. A total of 36 explosive shots were detonated at intervals of about 60 km along the profiles, and also at distant offsets from both ends of line 11 to provide additional upper mantle information. All profiles display good signal-to-noise ratio out to about 600 km offset. Strong shear-wave arrivals are observed along most of the profiles, including prominent upper mantle arrivals.

GEOTECTONIC SETTING

SNORE 97 is one component of the scientific program of the SNORCLE Transect, which addresses structure and evolution of the continental lithosphere in a region of NW North America where the rock record spans 90% of Earth's history. The principal transect objectives include:

1) Structure and formation of Early Archean crust and evolution of cratons. 2) Archean to Proterozoic transitional collisional suturing associated with Proterozoic orogens. 3) Processes of ocean opening and the Proterozoic-Paleozoic rifted margin and miogeocline. 4) Growth of continents by terrane accretion. 5) Deep architecture and Phanerozoic evolution of the Cordilleran orogen.

From East to West, SNORCLE Transect crosses a series of orogens:

The **Archean** (4.0-2.5 Ga) **Slave Province**, comprising geological elements representrative of Archean cratons worldwide, including the granite-greenstone Contwoyto terrane, gneissic basement of the Sleepy Dragon Complex, the Yellowknife greenstone belt, the metamorphosed supracrustal basin of the Yellowknife domain and the oldest known sialic crust of the Anton terrane.

The Paleoproterozoic (2.1-1.9 Ga) **Wopmay Orogen**, comprising from east to west the Great Bear calc-alkaline magmatic arc, the Hottah accreted arc terrane, the Fort Simpson magmatic arc and the enigmatic Nahanni terrane (buried beneath Phanerozoic cover) and the Mesoproterozoic (1.3-1.1 Ga)**Racklan Orogen**, a contractional feature buried beneath Phanerozoic cover throughout NW Canada (Cook, 1988, 1992).

The Neoproterozoic to Mesozoic (0.9-0.06 Ga) **Eastern (Miogeoclinal) Cordillera.** Cordilleran orogeny overprinted the passive margin history that followed the rifting and breakup of the Neoproterozoic continent. During the long passive margin history, at least 3 phases of crustal extension are recorded (Thompson, 1987). Structures in the Northern Cordillera are different from the southern Cordillera, like postorogenic extension which is not so well developed in the north.

The **Tintina Fault Zone**, a Late Cretaceous to Oligocene brittle structure, almost 2000 km long, with dextral strike-slip of several 100s of km (Gabrielse 1985; Price & Carmichael 1986). The Pre-Cretaceous history of this structure is unclear. If interpretation as an intracontinental transform is correct, the fault may penetrate the lithosphere.

The Mesozoic-Cenozoic (0.3-0.0 Ga)**Western Accreted Cordillera.** Comprises terranes of distal North American affinity and entirely exotic terranes: from east to west, the Kootenay terrane, derived from contiguous Precambrian N.A. basement, and Slide Mountain Terrane, with oceanic or marginal basin floor and sediments; Cassiar terrane, which is a displaced continental margin sequence, bounded on the east by Tintina fault; Cache Creek Terrane, an extensive accreted terrane interpreted as oceanic crust plus overlying strata, also small flakes of the Quesnellia terrane, a magmatic arc assemblage; Stikinia, the largest accreted terrane in the Cordillera, comprising platform carbonate, island arc and related strata; and the Nissling Terrane, another continental margin succession whose origin is uncertain.

EXPERIMENT DESCRIPTION AND DATA ACQUISITION

SNORCLE Transect includes three main corridors and SNORE 97 crosses all the three corridors. The primary purpose of the R/WAR experiment is the determination of the velocity structure of the crust and sub-crustal lithospheric mantle of the tectonic elements crossed by the profiles, and the relationship of the results to the coincident seismic reflection, magnetotelluric and other geophysical and geological data, to better define the current tectonic structure of these domains and their past history.

SNORE 97 will enable:

1) a near-continuous velocity structural cross-section of the lithosphere from the Archean Slave Craton to the young accreted crust of the Cenozoic western Cordillera; 2) indication of the lateral variability of crustal

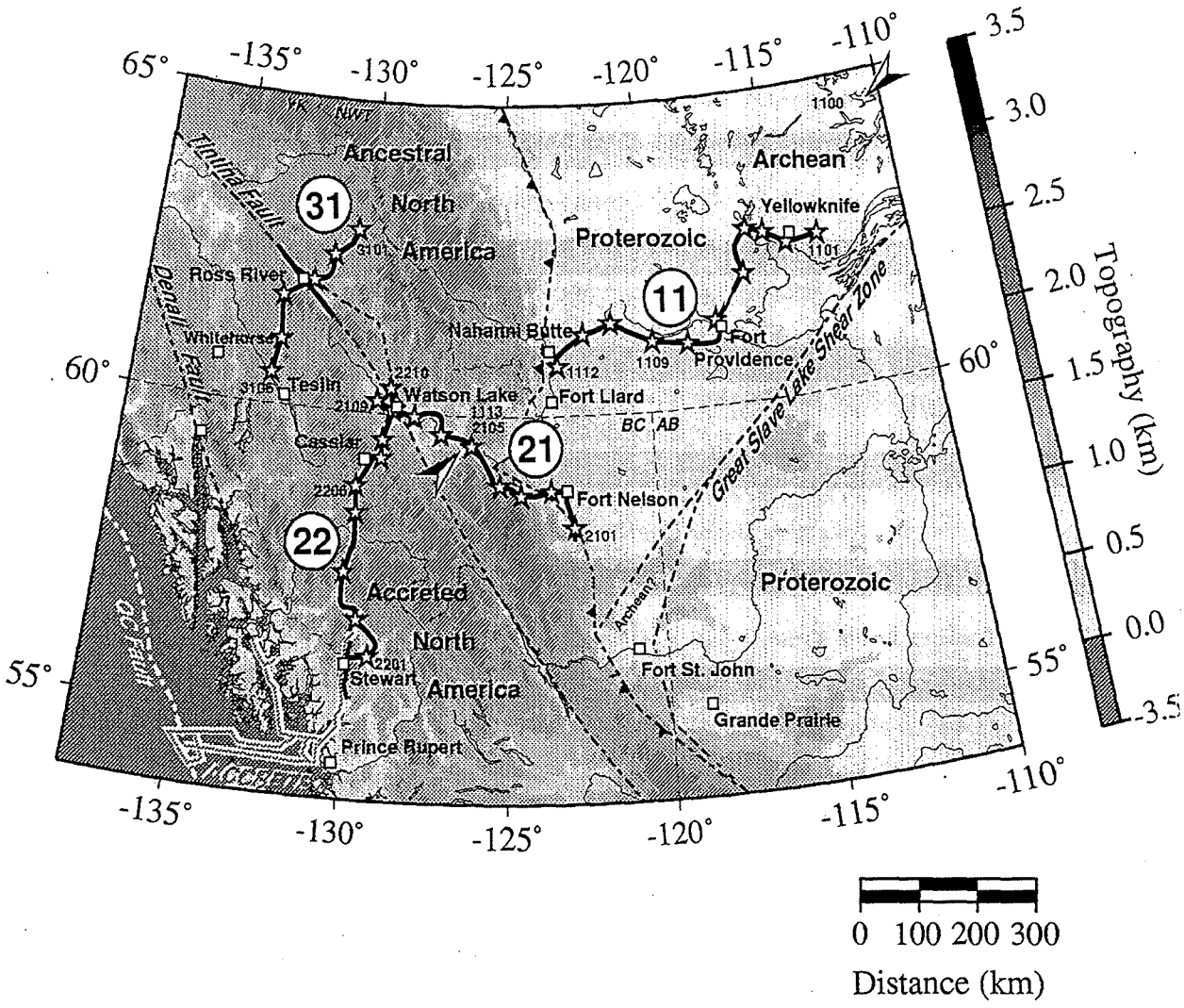

Figure 1: Topographic map of the study area showing the three corridors of SNORE 97. Stars show the location of the shots. Also indicated with arrows, the sites of the big shots off Line 11.

structure along strike in the northern Cordillera; 3) a direct tie with ACCRETE, an NSF-funded seismic experiment located in the southern Alaska Panhandle; 4) comparison with the velocity structure of the Southern Canadian Cordillera (Clowes et al, 1995); and 5) comparison with seismic cross-section across a similar region of Alaska (Beaudoin et al, 1994).

The field experiment took place during 4 weeks in August-September 1997 with 87 people from 15 different institutions participating in the acquisition. During the experiment, 28 vans, 6 trucks, 1 car and 1 boat took part; 594 seismographs (179 PRS1s, 20 PRS4s, 212 REFTEKs and 182 SGRs) were deployed and 36 shots, totaling 90000 kg of Hydromex T3 explosive, were detonated. Shot sizes were typically between 1000 and 3000 kg but two big shots (5000 and 10000 kg) were placed off end of Line 11. *BHP Diamonds* provided the 10000 kg shot point to the NE of the line, and all of the logistical support associated with its

detonation by LITHOPROBE personnel.

The four SNORE 97 refraction lines recorded in the three SNORCLE corridors are (figure 1):

Line 11, Corridor 1 extends WSW for more than 600 km from east of Yellowknife to west of Nahanni Butte in NWT; 13 shot points were detonated with an average station spacing of 1.2 km; two long offset shots were placed to determine velocity structure in sub-crustal lithosphere; this line coincides with a lithospheric reflection and magnetotelluric profile recorded in 1996.

Line 21 in Corridor 2 extends 450 km from Fort Nelson west to Watson Lake; this line has 8 shot points and station spacing of 1.0 km. Stations were also deployed at 2.0 km spacing halfway down Line 22 to provide broadside coverage across the Tintina Fault.

Line 22 in Corridor 2 extends 550 km from Watson Lake south to Stewart where it ties with ACCRETE. 9 shots with station spacing of 1.0 km and also stations deployed at 2.0 km spacing halfway along Line 21 were used for broadside coverage across the Tintina fault.

Line 31, Corridor 3, extends 300 km NE to SW from the miogeocline across the Tintina Fault into the accreted terranes; 6 shot points with station spacing of 0.8 km; some stations were also deployed at 2.0 km spacing for about 120 km in a perpendicular direction either side of the main line for broadside recording.

DATA AND PRELIMINARY INTERPRETATION.

Data were band-pass filtered (1-10 or 2-12 Hz) and are shown with trace-normalized amplitudes at reduced velocity of 8 km/s (figure2); the sections do not include data from the SGR seismographs as the data have not yet been merged with those from the PRS and Reftek instruments.

The principal phases identified in the preliminary interpretation are: **Pg**, refracted phase through upper and middle crust; **PmP**, reflected phase from crust-mantle boundary; **Pn**, refracted phase in uppermost mantle; **PN** only seen on Line 11, interpreted as a reflected phase from within the mantle (about 60-65 km depth) (figure 3).

To provide a preliminary interpretation, it has been applied to the data a τ-p analysis based on an algorithm developed by A. Gorman at UBC, following the theory by Clayton and Mc Mechan (1981). This method provides a quick way to obtain a one-dimensional velocity model, avoiding the task of picking arrivals in the seismic section.

The τ-p processing involves two main steps. First, the uninterpreted data are transformed into the τ-p domain through a τ-p transform. Second, the data are downward continued into z-p space using an arbitrary input velocity function. This velocity function can be modified as needed to produce a good fit of the data. The velocity functions can be tested afterwards with a ray-tracing algorithm to get a better fit. In this manner, 1-D velocity functions have been obtained for all the shot points from Line 11 and some shots for Lines 21 and 22, and they will be used for the starting velocity model in the 2D interpretation of the data.

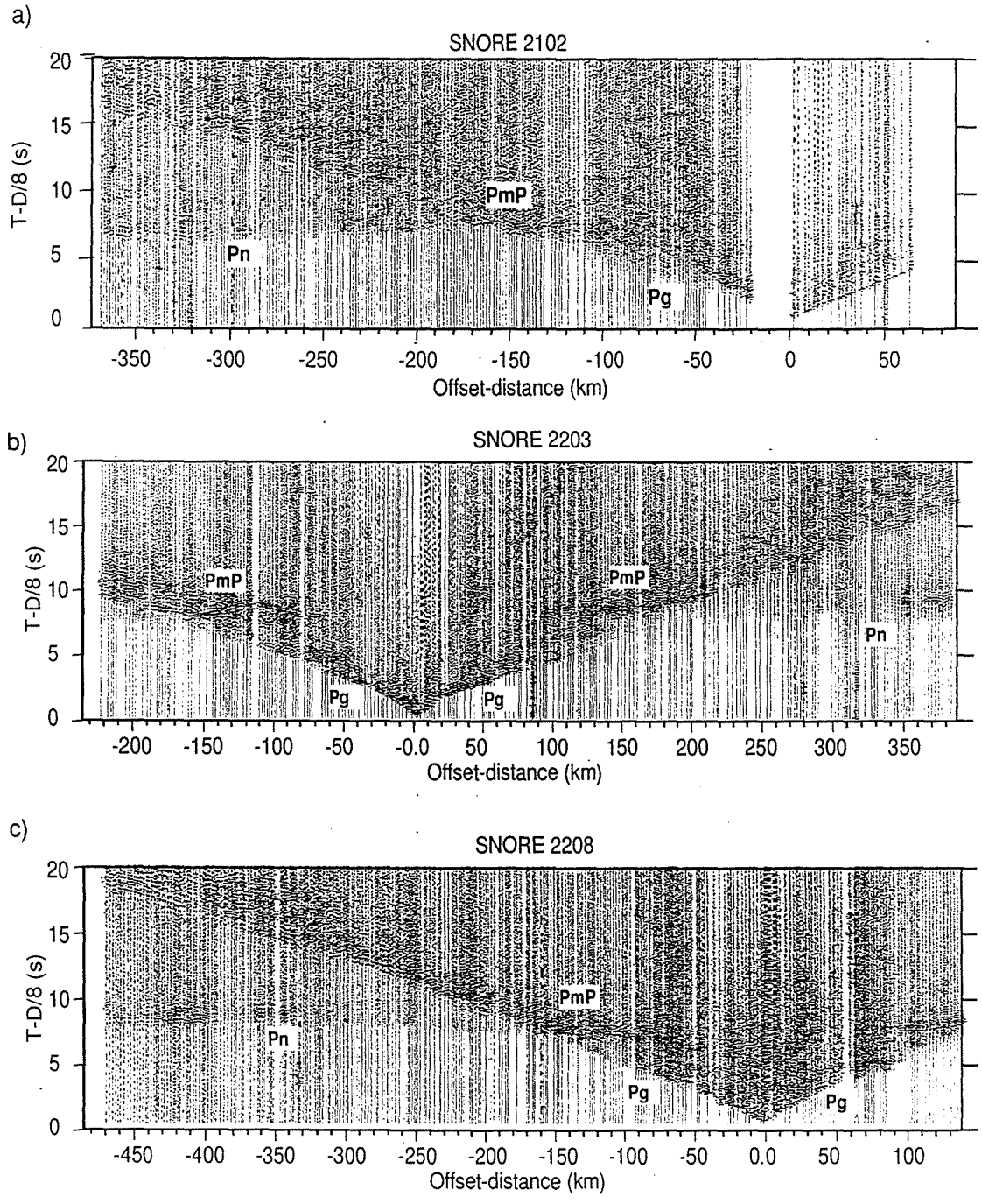

Figure 2: Some examples of SNORE 97 data. a) Shot point 2102 in Line 21 b) Shot point 2203 in Line 22 c) Shot point 2208 in Line 22

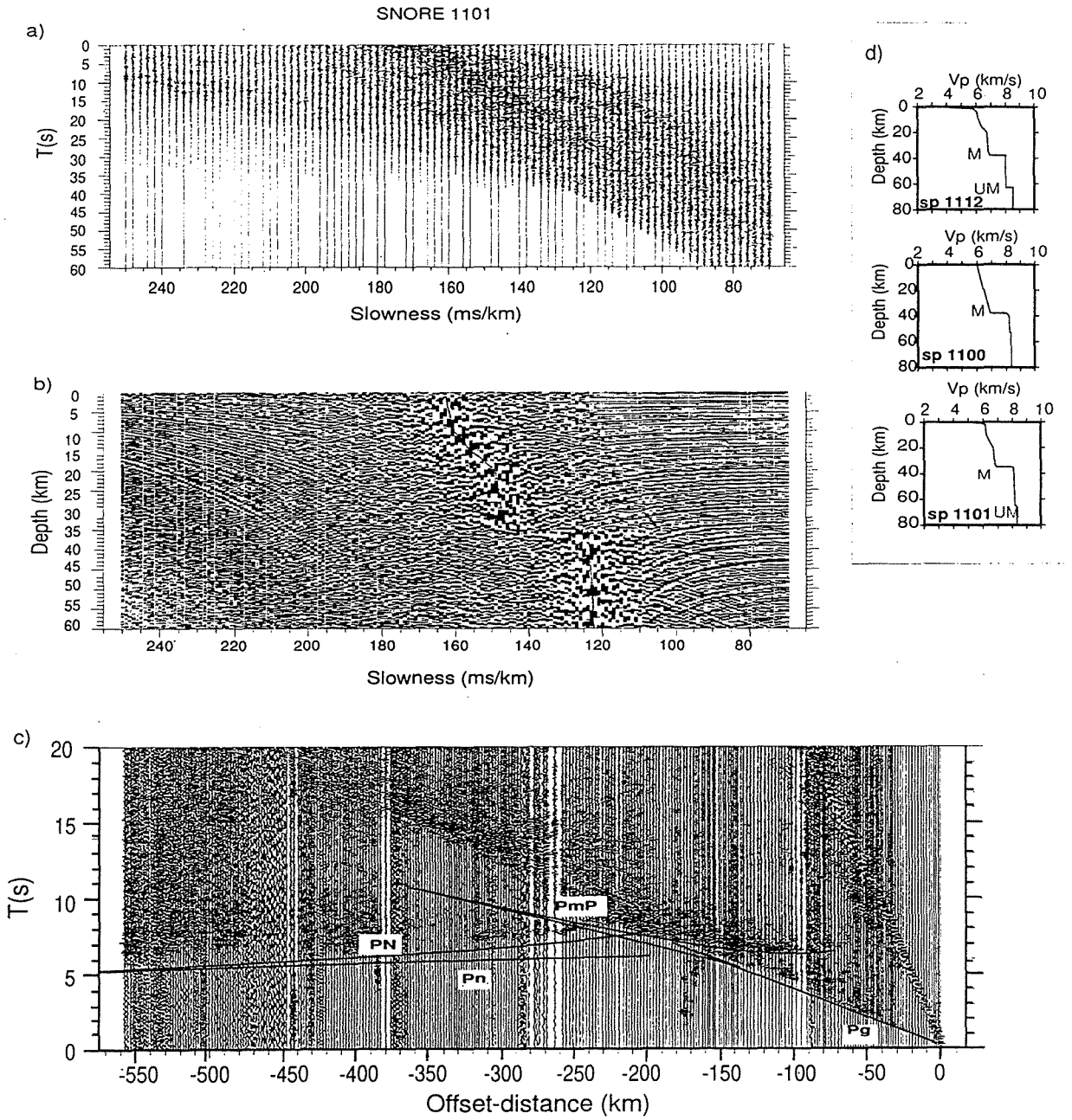

Figure 3: τ-p analysis for shotpoint 1101. a) τ-p transform; b) downward continuation to z-p space, veloc function overprinted; c) data with the calculated phases overprinted; d) velocity functions obtained by τ analysis for some shots of Line 11. M:Moho, UP: Upper Mantle discontinuity

Future work will include the modeling of Line 11 with consideration of the crooked geometry (2.5 D modeling); determining v-z models for the rest of the lines and their comparison with future reflection and MT profiles; and also comparison with results from Alaska and Southern Cordillera.

ACKNOWLEDGEMENTS

SNORE 97 data and results have been possible thanks to: IRIS-PASSCAL for Reftek instruments and technical/scientific personnel; USGS/Stanford University for SGR instruments and technical personnel; GSC for PRS instruments and technical-scientific personnel; field participants from the Universities of British Columbia, Victoria, Calgary, Saskatchewan, Manitoba, Laurentian, Western Ontario and Wisconsin (Eau Claire), who carried out a successful program in spite of some very difficult developments. BHP Diamonds, Kelowna and Lac de Gras, for providing shot point 1100 and logistic support to detonate it. First nations personnel from Lower Post BC, Watson Lake YT, Teslin YT, and Fort Providence NWT who contributed to the success of the experiment. Funding for SNORE 97 was provided by the NSERC Collaborative Special Proyects grant to LITHOPROBE, the Geological Survey of Canada, and NSERC Research Grants to R. M. Clowes, R. M. Ellis and G. Spence. G. Fernandez held a postdoctoral fellowship funded by the Ministry of Education of Spain.

REFERENCES

Bowring, S.A., I.S. Williams and W.Compston, 1989. 3.96 Ga gneisses from the Slave Province, NWT, Canada. *Geology*, **17**: 971-975.

Beaudoin, B.C., G.S. Fuis, W.J. Lutter, W.D. Mooney and T.E. Moore, 1994. Crustal velocity structure of the northern Yukon Tanana upland, central Alaska:results from TACT, refraction/wide angle reflection data. *Geological Society of America Bulletin*, **106**: 981-1001.

Clayton, R.W., and G.A. MacMehan, 1981. Inversion of refraction data by wavefield continuation. *Geophysics*, **46**(6):860-868.

Clowes, R.M., C.A. Zelt, J.R. Amor and R.M. Ellis, 1995. Lithospheric structure in the southern Canadian Cordillera from a network of seismic refraction lines. *Canadian Journal of Earth Sciences*, **29**: 142-157.

Cook, F.A., 1988. Middle Proterozoic compressional orogen in Northwest Canada. *Journal of Geophysical Research*, **93**: 8985-9005.

Cook, F.A., 1992. Racklan Orogen. *Canadian Journal of Earth Sciences*, **19**: 2490-2496.

Gabrielse, H. 1985. Major dextral transcurrent displacements along the Northern Rocky Mountain trench and related lineaments in north-central British Columbia. *Geological Society of America Bulletin*, **96**: 1-14.

Hoffman, P.F. 1987. Continental transform tectonics: Great Slave Shear zone (ca 1.9 Ga), Northwest Canada. *Geology*, **15**: 785-788.

Thompson, R.I. E. Mercier, and C.F. Roots, 1987. Extension and its influence on Canadian Cordillera passive margin evolution . In: *Continental Extensional Tectonics*. M.P. Coward JF. Dewey and P.L. Hancock (eds). Geological Society of London Special Publication **28**:409-417.

Elastic and Seismic Properties of Forsterite-Enstatite Composites up to 3.0 GPa: Implications for Compositional Models of the Upper Mantle

Shaocheng Ji and Zichao Wang

Département de Géologie, Université de Montréal, Montréal, Québec, H3C 3J7.

Introduction

Our knowledge of the lithological composition of deep interior of the Earth is largely constrained by comparing in-situ observed seismic velocities with those of relevant mineral assemblages thought to exist in the range of temperature and pressure of the interest. Seismic velocities of proposed mineral assemblages are generally calculated from laboratory measured elasticity and density of constituent minerals and appropriate rules of mixtures. The rules of mixtures describe variations of elastic moduli of polymineralic composites as a function of their end-member elastic moduli and volume fractions. The success of such modeling depends on not only an accurate knowledge of the elastic properties of the proposed minerals but also the relevance of the rule of mixtures used. It is commonly accepted that the upper mantle above the 400-km discontinuity consists of essentially olivine, orthopyroxene and clinopyroxene with garnet as minor component. The elastic properties and densities of these minerals have been extensively studied by experiments over the last two decades. However, the applicability of different rules of mixtures, which were initially developed in material science, to mantle mineral assemblages have not yet been systematically examined. It is thus especially important to test the existing rules of mixtures using carefully designed experiments on synthetic polyphase composites of controlled modal composition and microstructures.

In this paper, we report the elastic properties of two-phase composites with varying volume fractions of forsterite (olivine) and enstatite (orthopyroxene) as determined by ultrasonic interferometric measurements at pressures up to 3.0 GPa. Our results strongly suggest that the variation of the composite elasticity with olivine content cannot be precisely described by Voigt-Reuss-Hill averages, Hashin-Shtrikman bounds, Ravichandran (1994) bounds, Halpin-Tsai model (Halpin and Tsai, 1967), and Paul model (1960). In contrast, the shear lag model (Taya and Arsenault, 1989; Ji and Zhao, 1994; Hull and Clyne, 1996) yields remarkably good agreement between the observed and calculated elastic moduli for the studied composites. This is thought to be due to neglecting the mechanical interaction and stress transfer between different phases in the models except of the shear lag model.

Experimental technique and procedure

Description of Fo-En composite specimen

Polycrystalline aggregates with forsterite volume fraction (V_f) of 0(En), 0.2(Fo_{20}), 0.4(Fo_{40}), 0.5(Fo_{50}), 0.6(Fo_{60}), 0.8(Fo_{80}), and 1.0(Fo) were prepared through a

two-step sintering - hot pressing procedure. We first synthesized Fo and En separately at the temperatures of 0.8-0.9 T_m (T_m-melting temperature) using chemical compounds MgO and SiO_2 (both were commercially purchased with better than 99.99% purity) as starting materials. Synthetic Fo and En powders were mixed mechanically with desired volume fractions, then cold-pressed into pellet with dimension of $\phi 12 \times 6$ mm, which was finally hydro -statically hot-pressed at the conditions of 1.0 GPa and 1000 °C for 4-5 hours.

Examination on synthetic aggregates through SEM showed, in general, a granular texture with equilibrium grain boundary. Mean grain size ranges from 10 to 15 μm and the mean grain aspect ratio from 1.3 to 1.6. The specimen densities were consistent to within 0.038 g/cm^3 of the theoretical densities. The theoretical densities of composites were calculated from the densities of single crystal Fo and En and their volume fractions. The initial porosity of specimen were estimated between 0.5%-1.2%, which were largely attributed to pore space presented at grain boundary and triple junctions. Samples, for velocity measurement, were core-drilled from center part of the synthesized bulk samples and right-cylindrical in shape with typical dimension of 6.0 mm in diameter and 4.5 mm in length.

Velocity measurements

A combination of piston-cylinder high pressure apparatus (liquid pressure medium with an internal pressure gauge) and high precision ultrasonic interferometer (ANU-TECH), which technically is identical to that described by Fischer et al. (1993), was employed in this study to improve both precision and accuracy in velocity measurements. We obtained a resolution 1 ns of traveltime, giving the accuracy of measured velocity about 10^{-4} km/s with sample length of 6 mm. With an internal installed pressure gauge, the pressure can be controlled within 0.1 MPa. The maximum pressure reached in this study was 3.0 GPa. All experiment were performed at a constant temperature of T=27 °C.

Experimental results

Both compressional and shear wave velocities were measured up to 3.0 GPa. Travel time data for both P- and S-waves were converted to velocities after correction for the length change. The results show significant non-linear increase of velocities with pressure below 1.0 GPa, but became insensitive to pressure above ~1.0 GPa for both P- and S-wave. Therefore the data obtained at pressure higher than 1.0 GPa should be intrinsic, which are used in calculation moduli (K and G). Table 1 summarized room pressure velocities, moduli and pressure derivatives for the Fo-En composites. Both the K and G values of the composite increase with the volume fraction of forsterite (V_f) that is the strong phase (fiber) in the composite. However the dependence on V_f is non-linear. A substantial increase in moduli occurs when V_f approaches about 0.4-0.5.

Comparisons between experimental data and theoretical models

Numerous approaches have been proposed for homogeneous and isotropic composites, and several involving only the elastic moduli and the volume fractions of the two phases are considered below.

Voigt-Reuss-Hill average and Hashin-Shtrikman bounds

Voigt-Reuss-Hill (VRH) average is the arithmetic mean of the upper and lower bounds based on the assumptions of uniform strain and stress, respectively. Hashin and Shtrikman (1963) derived two bounds on the elastic properties of composite by employing the variation principle that considers the change in strain energy in a load homogeneous body due to the insertion of inhomogeneity. In Fig. 1, the VRH and Hashin and Shtrikman (HS) predictions for the relative Young's and shear moduli are plotted in conjunction with experimental data for the olivine-pyroxene composites. The relative Young's and shear moduli are defined as $(E_c - E_m)/(E_f - E_m)$ and $(G_c - G_m)/(G_f - G_m)$, respectively. The VRH and HS bounds are very close each other and vary almost linearly with the volume fraction of olivine (V_f). The measured values actually lie below these predicted values.

Table 1. Elasticities of Fo-En composites

Sample	Vp (km/s)	Vs (km/s)	V_p' (km/s. GPa)	V_s' (km/s. GPa)	μ (GPa)	K (GPa)	μ'	K'	sources
Fo	8.534	4.998	1.037	0.041	79.8	126.3	1.65	5.01	1
	(0.013)	(0.003)			(3.2)	(3.9)			
Fo80	8.372	4.938	1.007	0.042	77.5	119.4	1.73	4.93	1
	(0.011)	(0.007)			(2.7)	(4.5)			
Fo60	8.229	4.890	1.007	0.044	76.1	114.1	1.86	5.15	1
	(0.009)	(0.005)			(3.0)	(3.1)			
Fo50	8.170	4.857	0.096	0.045	75.0	112.2	1.84	4.84	1
	(0.007)	(0.007)			(3.7)	(1.7)			
Fo40	8.095	4.838	0.094	0.047	74.7	109.5	1.82	4.78	1
	(0.010)	(0.006)			(3.4)	(2.7)			
Fo20	8.040	4.842	0.091	0.043	74.6	106.2	1.81	4.83	1
	(0.006)	(0.005)			(1.5)	(1.9)			
En	8.008	4.835	0.097	0.043	74.2	104.6	1.84	4.16	1
	(0.005)	(0.003)			(2.8)	(1.7)			
Fo					81.6	128.8	1.4	4.2	4
Fo					81.1	128.6	1.80	5.37	3
Fo	8.593	5.034	0.098	0.036	81.6	129.0	1.81	4.88	2
En	8.078	4.864			75.7	107.8			2

1. From this study (polycrystal); 2. From Sumino and Anderson (1984); 3. Kumazawa and Anderson (1969); 4. Zha et al. (1996). All referred data are for single crystals using VRH average method. Numbers in bracket show the error range.

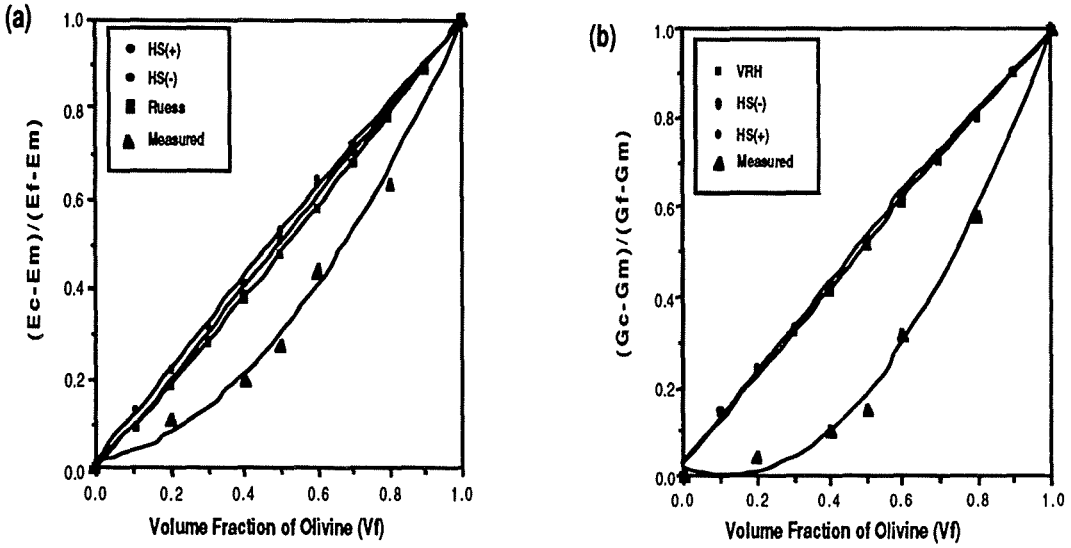

Fig. 1. Comparison between experimental data and predications by Voigt-Ruess-Hill average and Hashin-Shtrikman (HS). (a) Young's modulus; (b) Shear Modulus

Ravichandran, Halpin-Tsai and Paul models

Recently, a number models have been proposed by taking geometric configuration of two phase aggregates into consideration. Ravichandran (1994) derived expressions for elastic properties of two-phase composites on the basis of approximation of two-phase composite microstructure to a unit cell incorporating isostrain and isostress type elements, arranged in two different ways. Halpin and Tsai (1967) developed semi-empirical equations designed to give accurate estimates for the overall elastic constants of two phase composites. They introduced a parameter, ξ, as an adjustable parameter, which may depends on the packing geometry, grain shape, and loading conditions. Utilizing the energy theorems of elasticity theory, Paul (1960) derived an approximate formula for the elastic modulus of particulate composite in which the strong phase inclusion is of a cubic shape. Comparisons show that the relative moduli predicted by these models are higher than the measured data.

Shear-lag model

Shear-lag model (SLM) was originally proposed by Cox (1952) and subsequently refined by others (e.g., Outwater, 1956; Zhao and Ji, 1997). Its mechanical analysis centers on the transfer of tensile stress from matrix (weak phase) to fiber (strong phase) by means of interfacial shear stresses. Based on an assumption that no slip on the phase interfaces occurs, the SLM derives that the presence of the fiber redistributes the stresses and strains within the composite material and has an effect of transferring load from the matrix to the fiber. Consequently, a shear stress occurs at the fiber-matrix interface, and the harder phase carries a comparatively greater part of the stress while the soft phase tends to take the greater part of the strain (with reference to the volume fraction ratio). Unlike the other models considered in this paper, the SLM takes into

account the effects of elastic interaction and stress transfer between the phases. The calculated moduli from SLM were present in Fig. 2 together with the experimental data. It can be seen that the shear-lag model represents a fairly good approximation to the measured moduli.

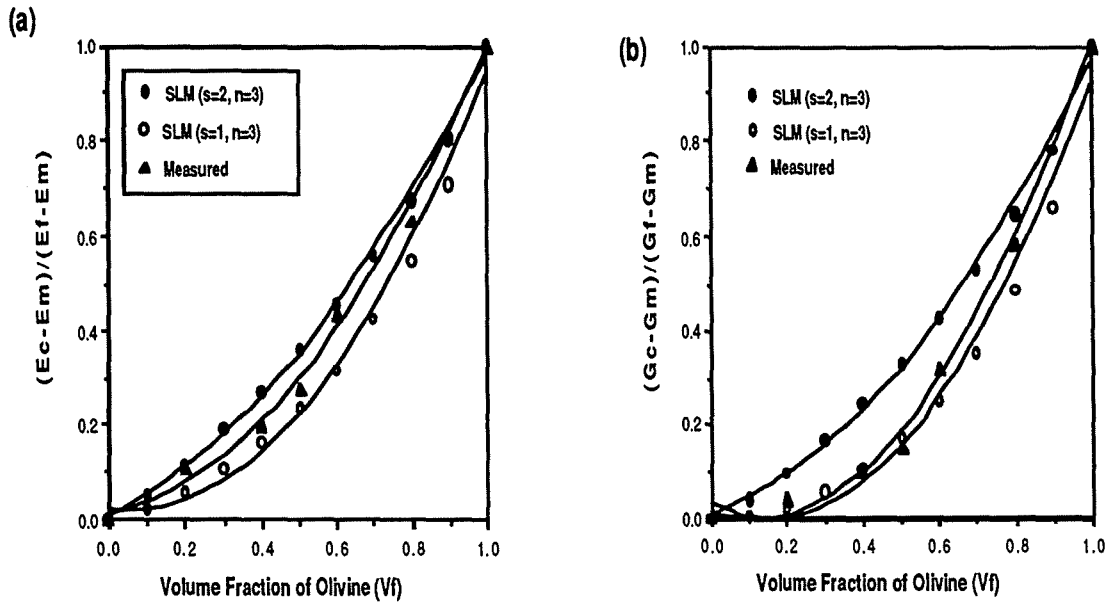

Fig. 2. Comparison of the predictions from the shear-lag model (SLM) using s=1 and s=2 with the experimental data on relative Young's modulus (a) and shear modulus (b) of the Fo-En composites. s is the average aspect ratio of the strong phase. n is a constant which describes the geometrical configuration of the strong phase in the matrix of weak phase.

Implications for the compositional models of the upper mantle

For the olivine-orthopyroxene system, all the models except the shear-lag model give almost the same values for the overall Young's and shear moduli which vary linearly with the volume fraction of olivine. These theoretical values are significantly higher than the measured values. However, the shear-lag model can mimic the composite properties in the range of experimental errors. The likely reason for this discrepancy is that the effects of elastic interactions between phases are taken into account in the shear-lag model, but neglected in the other models. The elastic interactions cause redistribution of the stress and strain between phases: the stronger phase carries the relatively greater proportion of the stress while the weaker phase takes the relatively greater proportion of the strain (with reference to the volume fraction ratio). The models that neglect the elastic interactions between phases lead to an overestimation on the overall moduli of the composite. The present experiments show that the shear-lag model is a favored model for the olivine-pyroxene composite rocks.

It is a common practice to constrain mantle chemical composition by comparing calculated overall elastic properties of mantle mineral composites with seismic Earth

model velocities. In the previous studies, the HS bounds are generally used for estimating elastic properties of monomineralic aggregates while the VRH average is used for those of polyphase rocks. For example, by matching the measured seismic profile with that calculated using the VRH procedure, Duffy and Anderson (1989) suggested that the mantle consists of 40% olivine, 37% clinopyroxene, 13% garnet, and 10% orthopyroxene. However, based on high temperature and high pressure petrological experiments, Ringwood (1975) suggested that the mantle consists of 61% olivine, 15% orthopyroxene, 14% garnet, and 10% clinopyroxene.

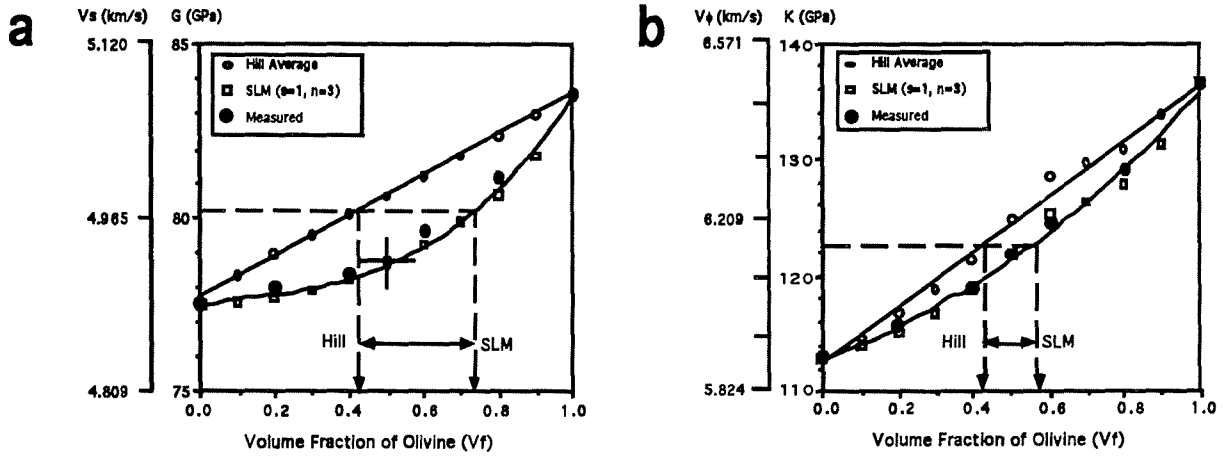

Fig. 3. Estimation of modal composition in the Fo-En composites based on the Hill average (open circles) and SLM (open square) at a given shear (a), and bulk (b) properties. The experimental data, shown as solid circle, are best fitted by SLM. "+" in (a) shows the uncertainty in measured shear properties. The uncertainty in bulk properties is smaller than the size of the symbols anywhere in (b). A large discrepancy in olivine contents predicted by the two models is showed as double arrows. The content of the strong phase (Fo) is underestimated by the Hill average up to ~30% using bulk properties, and ~15% using shear properties.

The present study shows that either the HS bounds or the VRH average overestimate the elastic moduli (E, G, and K) and thus seismic velocities (V_P and V_S) of the olivine-orthopyroxene composites. Consequently, the volume fraction of olivine in the composites is underestimated for a given value of P- or S-wave velocity. This idea is conveyed in Fig. 3. The underestimated volume fraction of olivine can be as high as 15% using the bulk velocity or 30% using the shear velocity in the investigated system. On this basis, we infer that the difference in olivine content in the upper mantle between the piclogite and pyrolite models may significantly reduced by using shear-lag model rather than the VRH average in the calculations of seismic velocities in the mantle rocks.

Acknowledgments. We are grateful to Drs. G. Fischer and H. Niesler for their extraordinary effort and skill to have developed and maintained the equipment for the velocity measurements. We thank the LITHOPROBE (SNORCLE) for research grants.

References

Cox, H.L. 1952. The elasticity and strength of paper and other fibrous materials. British Journal of Applied Physics, **3**: 72-79.

Duffy, T.S. and Anderson, D.L. 1989. Seismic velocities in mantle minerals and the mineralogy of the upper mantle. Journal of Geophysical Research, **B94**: 1895 - 1912.

Fischer G.J, Wang Z.C. and Karato S.I. 1993. Elasticity of $CaTiO_3$, $SrTiO_3$ and $BaTiO_3$ perovskite up to 3.0 GPa: the effect of crystallographic structure. Physics and Chemistry of Minerals, **20**: 97-103.

Halpin, J.C. and Tsai, S.W. 1967. Environmental factors in composite design. Air Force Materials Laboratory Technical Report, AFML-TR-67-423.

Hashin, Z. and Shtrikman, S. 1963. A variation approach to the theory of the elastic behavior of multiphase materials. Journal of Mechanics and Physics of Solids, **11**: 127-140.

Hull, D. and Clyne, T.W. 1996. An Introduction to Composite Materials, Cambridge University Press.

Ji, S. and Zhao, P. 1994. Strength of two-phase rocks: a model based on fiber-loading theory. Journal of Structural Geology, **16**: 253-262.

Kumazawa, M. and Anderson. O.L. 1969. Elastic moduli, pressure derivatives and temperature derivatives of single-crystal olivine and single crystal forsterite. Journal of Geophysical Research, **74**: 5961 - 5972.

Outwater, J.O., 1956. The mechanics of plastics reinforced in tension. Modern Plastics, **33**: 56-65.

Paul, B. 1960. Prediction of elastic constants of multiphase materials. Transactions of the Metallurgical Society of AIME, **218**: 36-41.

Ravichandran, K.S. 1994. Elastic properties of two-phase composites. Journal of American Ceramic Society, **77**: 1178-1184.

Ringwood, A.E., 1975. Composition and Petrology of the Earth's mantle. McGraw-Hill Book Company.

Sumino, Y. and O.L. Anderson 1984. Elastic constants of minerals. In Handbook of Physical Properties of Rocks, v. 3 (R.S. Caqrmichael, ed.), 39-138, CRC Press, Boca Raton, Florida.

Taya, M. and Arsenault, R.J. 1989. Metal Matrix Composites. Pergamon Press, Oxford.

Zha, C.S., Duffy, T.S., Downs, R.T. and Mao, H.K. 1996. Sound velocity and elasticity of single-crystal forsterite to 16 GPa. Journal Geophysical Research. **101**(B8): 17,535-17545.

Zhao, P. and Ji, S. 1997. Refinement of shear-lag model and its applications. Tectonophysics, **279**: 23 - 36.

Plasticity of Eclogite: Implications for Rheology and Seismic Reflectivity of the Subducting Slab

Shaocheng Ji, Zichao Wang and Kazuko Saruwatari

Départément de Géologie, Université de Montréal, Montréal, Québec, H3C 3J7

The continental lithospheric upper mantle beneath SNORCLE Corridor 1 contains strong, gently-dipping, continuous, regionally extensive, seismic reflectors (Cook et al., 1997; Bostock, 1997)). This 725 km Lithoprobe reflection profile crosses the major Proterozoic terranes east of the Cordillera, the Anton Terrane of the Slave craton, and the Yellowknife Supergroup in the Slave. Similar mantle reflectors have also been observed in other regions of the world, for example, the western margin of Canada (Clowes et al., 1987), the Superior province (Calvert et al., 1995), the Skagerrak area, south of Norway (Larsson and Husebye, 1991), the Baltic sea (Abramovitz et al., 1997), the Eromanga bassin in eastern Australia (Finlayson et al., 1993), and the north coast of Scotland (Warner and McGeary, 1987; Warner et al., 1996). The purpose of this study is to evaluate the possible origins of seismic reflections in the upper mantle. Specially, we have investigated the seismic reflectivity and anisotropy of plastically deformed eclogite layers which represent relict oceanic crust in ancient subduction zones.

Previous studies on the mantle reflection along the Flannan thrust beneath the north coast of Scotland (Warner and McGeary, 1987) suggests that reflection coefficients around 0.1 are needed to cause such reflections within the upper mantle. The boundary between sheared (anisotropic) peridotites and their undeformed (isotropic) protoliths cannot be a candidate for the observed mantle reflection because the reflection coefficient related to lattice-preferred-orientation (LPO)-induced anisotropy is generally smaller than 0.03. Therefore, ductile shear zones are not the cause for the strong reflectors in lithologically monotonous peridotites. Moreover, dunite, spinel lherzolite, garnet lherzolite and harzburgite have almost similar seismic velocities and densities. The first-

order boundaries between these rocks and the compositional layering in peridotites are unlikely to originate strong seismic reflections in the upper mantle.

Investigations of Morgan et al. (1994), Warner et al. (1996), and Bostock (1997) show that the mantle reflectors represent apparently high velocity (Vp>8.4 km/s) and high density (>3500 kg/m^3) layers. This excludes metasomatized shear zones which contain slower, less dense hydrated minerals such as amphibole or phlogopite from the candidates for the origin of mantle reflectors. Although the boundary between metasomatized shear zones and their wallrock has impedance contrasts large enough to produce a strong reflection, the metasomatized shear zones should be the low velocity zones.

The transition zone between the dislocation creep and diffusion creep regimes does not likely originate the strong reflection for the following reasons: (1) Typical maximum seismic anisotropies formed by dislocation creep in the mantle xenoliths are about 4-6%. Even though the assumption that no LPO is formed in the diffusion regime is correct (see Rutter et al., 1994 for discussion), the boundary between the two regimes has a reflection coefficient smaller than 0.03. (2) As shown by Ji et al. (1994) and Saruwatari and Ji (1997), the average grain size of olivine in upper mantle xenoliths from the Canadian Cordillera and Alaska is commonly larger than 0.5 mm, dislocation creep prevails over a thickness of at least 250 km. The transition zone between dislocation and diffusion creep regimes cannot appear in the depth range of mantle reflectors. (3) As pointed out by Bostock (1997), the transition zone between dislocation and diffusion creep regimes may not be sharp enough to produce the interface transition widths smaller than 200 m required by the seismic reflection data (Cook et al., 1997).

Calvert et al. (1995), Warner et al. (1996), and Bostock (1997) proposed that the mantle reflectors represent eclogitic layers within normal peridotites. The eclogitic layer can be formed by crystallization of a mafic magma due to partial melting of the peridotitic upper mantle or by phase transformation from the original basaltic layer of subducting oceanic

crust. However, the above proposition has not been supported by existing petrophysical data in the literature (Database of rock petrophysical properties, Ji and Canavà, 1998). First, laboratory measurements of 67 eclogite samples showed that at 1.0 GPa, the eclogite has an average density of 3408 kg/m^3 and an average P-wave velocity of 8.18 km/s, while measurements of 64 peridotite samples under the same conditions gave an average density of 3.278 and an average Vp of 8.268 km/s. This gives a very small reflection coefficient (0.014) for the boundary between the eclogite and peridotite layers and renders it impossible as likely candidate for the mantle reflectors. Second, the eclogites are generally considered in the literature to be rheologically too strong to be deformed plastically and thus no tectonically transposed compositional layering is developed in these rocks. This renders it difficult to explain the multilayer origin of the mantle reflectors inferred for the reverberatory $P_{135}s$ phase (Bostock, 1997). Third, the mean velocity anisotropy in the 64 eclogite samples is only 2.8%, which is much lower than that value (10%) required by the reflectivity modeling of Bostok (1997). The above controversy has not been resolved until recently we studied lithology, deformation and microstructures of eclogites from the Su-Lu ultrahigh pressure metamorphic (UHPM) terrane, northern Jiangsu and eastern Shandong provinces of China.

The eclogites occur as pods, layers and blocks, ranging in size from tens of centimeters to hundreds of meters, within ultramafic blocks, metapelites (garnet-quartz-jadeite gneisses), kyanite quartzite and marble. Ultramafic rocks, which are mainly garnet lherzolite, garnet wehrlite, garnet pyroxenite and hornblende peridotite, generally show a well-developed foliation. P-T estimates (Zhang et al. 1994) indicate that the ultrahigh metamorphism of ultramafic rocks occurred at 820-900 °C and 36-41 kbar. Most eclogites enclosed within ultramafic rocks are garnet-omphacite-rutile±quartz rocks. Coesite and quartz pseudomorphs after coesite are ubiquitous as minor fine-grained inclusions in garnet and omphacite in the eclogites in metapelites and marble, and occasional in the eclogites in ultramafic rocks. These eclogites developed pronounced foliation, stretching lineation and compositional (garnet-rich and omphacite-rich) layering. In garnet-rich layers, garnet content varies from

70-95%. Garnet, rutile and particularly omphacite are strongly elongated and flattened. No omphacites are observed to be curved around the garnet, indicating that there is no marked rheological contrast between these two minerals. In some eclogite samples, coarse-grained garnets have been granulated to fine-grained aggregates, indicating appearance of dynamic recrystallization during ductile deformation. TEM observations show that the elongated and flattened garnets contain dynamic recovery substructures such as subgrain boundaries. Omphacite crystals shows strong LPO. Peak metamorphism of the eclogites occurred at 730-900 °C and >28 kbar (Zhang et al., 1994 and 1995). In addition, foliations of ultramafic rocks, eclogite layers and country rocks (gneisses, quartzite and marble) are generally subparallel, suggesting that in-situ contact relations between these rocks were not considerably disturbed during tectonic emplacement. These UHPM rocks were materials of subducted oceanic lithosphere and then tectonically emplaced into continental crust during the Triassic collision between the Sino-Korean and Yangtze cratons.

To understand the deformation behavior of garnets in the eclogites, we performed deformation experiments on six representative silicate garnets at temperatures (T) of 900-1400 °C and strain-rates ($\dot{\varepsilon}$) of 10^{-7}-10^{-4} /s and well-controlled thermodynamic conditions. By acquiring high quality mechanical data, examining microstructures and comparing experimental results with naturally-deformed garnets, this study yields three new insights into deformation behavior of silicate garnets: (1) The critical temperature (T_C) for the brittle-ductile transition of garnet deformation, in terms of melting temperature (T_m) and strain-rate ($\dot{\varepsilon}$), can be described by the following empirical equation: $T_c = T_m\left[(1.043 \pm 0.032) + (0.030 \pm 0.001)\log\left(\dot{\varepsilon}\right)\right]$. In the ductile regime, where $T > T_c = T_m\left[1.075 + 0.029\log\left(\dot{\varepsilon}\right)\right]$, steady-state creep of garnets follows a power-law: $\dot{\varepsilon} = A\left(\frac{\sigma}{\mu}\right)^n \exp\left(-g\frac{T_m}{T}\right)$, where n=3.0±0.5, $\log_e$A(/s)=40.1±5.6, g=32±2, σ is the flow stress at steady-state creep, and μ is shear modulus of garnet. (2) Microstructural investigation suggests that crystal plasticity, which is enhanced by the activation of dislocation glide (slip systems $1/2<111>\{110\}$),

is the dominant physical mechanism responsible for the brittle-ductile transition. (3) Extrapolation of the experimental results to geological strain rates (10^{-16}-10^{-14} /s) suggests that the brittle-ductile transition of silicate garnets in nature occurs at $T>0.65T_m$ without considering effects of confining pressure and water. This indicates that garnets such as almandine, rhodolite and grossular can be deformed ductilely under extremely high temperature (T>800 °C). The extrapolation also shows that garnet is much stronger than clinopyroxene at temperature lower than 800 °C, but the rheological contrast of garnet with clinopyroxene is minimal at temperature higher than 800-900 °C. If the effects of confining pressure and the presence of water are taken into consideration, the brittle/ductile transition of garnet can even occur at lower temperatures.

The major conclusions of this study are listed below:

(1) The mantle reflectors are most likely originated from garnet-rich and omphacite-rich layering within eclogites and the boundaries between eclogite and peridotite layers.

(2) The eclogites can be plastically deformed and are not rheologically rigid as thought previously. Strong seismic anisotropy of eclogites is induced from strong LPO of omphacite and particularly to compositional layering with varying relative contents of garnet and omphacite. Moreover, plastic flow of eclogites under UHPM conditions may preclude effective shear heating, rendering the cool thermal structures within the subducting slab. This makes it possible to preserve the relict subducted oceanic crust within the upper mantle for long geological time.

(3) Previous petrophysical measurements were performed mostly on eclogites from the base of the continental crust rather than on UHPM eclogites from the upper mantle. The formers are less deformed and less anisotropic and contain less garnet than the latters. The presence of alteration and microcracks leads to an underestimation of density and seismic velocities for the eclogites. Further petrophysical work is needed to be carried out on UHPM eclogites and associated peridotites.

References

Abramovitz, A., A. Berthelsen, H. Thybo (1997) Tectonophysics, 270, 259-277.

Bostock, M. (1997) Nature, 390, 392-395.

Calvert, A.J., Sawyer, E.W., Davies, W.J. & Ludden, J.N. (1995) Nature, 670-674.

Clowes, R.M., Yorath, C.J. & Hyndman, R.D. (1987) Roy. astro. Soc. Geophys. J., 89, 79-84.

Cook, F.A., van der Velden, A.J., Hall, K.W. & Roberts, B.R. (1997) Transact and Cordilleran Tectonics Workshop Meeting, 58-62 (Lithprobe Report No. 56, 1997).

Finlayson, D.M., A. Owen, D. Johnstone, K.D. Wake-Dyster (1993) Geology, 21, 707-710.

Ji, S., Zhao, X. & Francis, D. (1994) Tectonophysics, 239, 1-27.

Larsson, F.R. and Husebye, E.S. (1991) Tectonophysics, 189, 35-148.

Morgan, J.V., Hadwin, M., Warner, M.R., Barton, P.J. & Morgan, R.P. (1994) Tectonophysics, 232, 319-328.

Rutter, E.H., Casey, M. & Burlini, L., 1994. J. Struct. Geol., 16, 1431-1447.

Saruwatari, K. & Ji, S. (1997) Workshop on Continental Roots, Harvard University and Massachusetts Institute of Technology, Oct. 10th-13th, 1997. Abstract.

Warner, M. & McGeary, S. (1987) Geophys. J. R. astro. Soc., 89. 223-230.

Warner, M., Morgan, J., Barton, P., Morgan, P., Price, C. & Jones, K. (1996) Geology, 24, 39-42.

Zhang, R.-Y., Liou, J.G. & Cong, B. (1994) J. metamorphic. Geol., 12, 169-186.

Zhang, R.-Y., Hirajima, T., Banno, S., Cong, B. & Liou, J.G. (1995) J. metamorphic. Geol., 13, 659-675.

Heat Flow Transitions along the SNORCLE Transect: Asthenospheric Flow

Trevor Lewis and Roy Hyndman
Pacific Geoscience Centre
Box 6000
Sidney, B.C. V8L 4B2
lewis@pgc.emr.ca

The heat flow is expected to increase along the SNORCLE transect, going from the Archean Slave province to the Cordillera, similar to that now documented for the southern Cordillera. Over the past few field seasons geothermal data have been acquired in northern B.C. and the southern Yukon, to define this transition. Most of the 30 heat flow sites now available in this region are in crystalline rocks, and are of good quality. The average measured heat flow in this region of the Cordillera is 88 mW/m^2. The transition to lower, craton-like values lies east of the mountains, but is not yet well defined. However, in the Cordillera there is considerable variation along strike: south of 59° N the average heat flow is 78.5 +/- 14.2 mW/m^2, and north of 59° N, it is 103.3 +/- 21.0 mW/m^2. The high, northern values are similar to those further to the south near 51° N. The two regions of highest heat flow are inland of recent subduction and/or terrane collision. Between the two, inland of the Queen Charlotte transform fault, is a region of reduced heat flow, although still above the world average. The high heat flows indicate a larger amount of heat is flowing into these two areas, from beneath the lithosphere, probably due to asthenospheric motion. Majorowicz (1996), using heat flows calculated from bottom hole temperatures and lithologic logs of hydrocarbon wells, has found within the Western Canada Basin a transition to much higher heat flow to the north of about 59-60° N, indicating this heating effect extends out under the northern Western Canada Basin.

East of the mountain belts, the well defined heat flow at Yellowknife is 53 mW/m^2, and near Ft. Providence it is approximately 100 mW/m^2. This latter value is based on accurate temperature measurements and measurements of thermal conductivity on cuttings from an abandoned well. We have collected cuttings from several other wells near this part of the SNORCLE transect on which to measure thermal conductivities, and further define this transition. Based on the bottom hole temperatures and lithology, the thermal transition appears to lie just east of Ft. Providence. This position is in contrast to near the Southern Canadian Cordillera Transect, where such a transition is west of the foreland belt, close to the Rocky Mountain Trench.

Majorowicz, J.A. Anomalous heat flow regime in the western margin of the North American craton, Canada, J. Geodynamics, *21*, 123-140 (1996).

Electrical resistivity structure between the Nahanni terrane and Slave Province

Xianghong Wu[1], Ian Ferguson[1] and Alan Jones[2]

1. Department of Geological Sciences, University of Manitoba, Winnipeg, MB, R3T 2N2

2. Natural Resources Canada, 1 Observatory Crescent, Ottawa, ON, K1A 0Y3

Introduction

MT data were collected at 58 sites on LITHOPROBE SNORCLE Corridors in Summer 1996. On Corridor 1 there were 12 sites on the exposed Slave craton, 8 sites on Great Bear magmatic arc, and 25 sites on the Proterozoic section (including the Hottah, Fort Simpson and Nahanni terranes); on Corridor 1A there were 13 sites crossing the Taltson, Buffalo Head and Great Bear magmatic arc and the Great Slave Lake shear zone. At each site recordings included Phoenix V5 data (10 kHz - 0.01 Hz) and Geological Survey of Canada LIMS data (20 - 30,000 s). In this study, 36 sites from the centre and west of the corridors are used to examine the transition between the Slave craton and the Proterozoic terranes, and the geoelectric structure of the Proterozoic crust and overlying Phanerozoic sediments (Fig.1).

Data processing and analysis

The MT response from high geomagnetic latitudes as in the SNORCLE area may be contaminated by signals associated with auroral geomagnetic activity. It may be further complicated by galvanic distortion from local, near-surface resistivity structures. Methods applied here to extract the regional earth response from the recorded time-series include:

1. *Least-squares and robust, remote-reference impedance estimation* removes the effects of artificial noise-sources and reduce the bias from non-uniform geomagnetic source-fields.
2. *Groom-Bailey decomposition and static shift removal* remove the galvanic distortion from near-surface inhomogeneities (*eg.* Groom & Bailey 1989).

The regional geoelectric response is characterized using several parameters:

1. *The MT impedance*, defining the transfer function between horizontal components of the recorded electric and magnetic fields, is examined in terms of apparent resistivity and phase. Apparent resistivity at increasing period corresponds to average resistivity over increasing depth and the phase provides an independent estimate of the resistivity variation with depth.
2. *The geoelectric strike* of 2-D structures can be determined (to $\pm$ 90°) from the four impedance tensor components. The strike can be determined from either full tensor decomposition or from

simple rotation to maximize the phase-difference between off-diagonal impedance terms. Optimal statistical estimation is obtained by recalculation of the impedance after rotation of time-series into axes parallel and perpendicular to the geoelectric strike.

3. *The induction vector* represents graphically the transfer function between the vertical component of magnetic field and the inducing horizontal components. For simple 2-D structures consisting of a good conductor embedded in a poorly conducting half-space, the real induction vector will point to the conductor. The length of the vector is proportional to the conductivity contrast but decreases with distance from the conductor.

Results

Geoelectric Strike Directions. The geoelectric strike response (Fig. 2) reveals significant differences exist between the near-surface and deeper resistivity structures, and between the east and west ends of the profile. At short-periods (near-surface response) the strike direction is $\sim$N30°W in the west and $\sim$N30°E in the east. The scatter in the angle indicates the resistivity structure of the Phanerozoic sedimentary rocks is almost 1-D. The general coincidence of the strike direction and the trend of gravity and magnetic anomalies does indicate a contribution to the response from the underlying Precambrian rocks.

At periods of 100 s, corresponding to signal penetration into the crust, the geoelectric strike is close to N30°E across the whole transect except several sites in the east (Slave craton). This direction is adopted as the strike for modelling the resistivity structure of the crust. At periods of $> 10^3$ s, corresponding to signal penetration into the deep crust and lithospheric mantle, the strike is $\sim$N30°E in the west and east but changes to $\sim$N30° W in the area of Great Bear magmatic arc. This result indicates significant differences in the deep resistivity structure and thus crustal structure across the study area.

Induction Vector Response. Figure 3 shows the induction vectors along the profile. The vectors indicate the presence of a strong conductor in the southwest of the profile. The conductor is striking NNE. At longer periods the apparent strike of the conductor changes to ENE. At these periods it is possible that the response is sensing the large-scale variations in the thickness of the Phanerozoic rocks.

MT Apparent Resistivity and Phase Response. Figure 4 shows apparent resistivity and phase sections for electric currents parallel and perpendicular to the geoelectric strike. Data have been corrected for weak tensor distortion and static shift effects. The conductive response observed at short periods (< 1 s) can be attributed to the low resistivity of the Phanerozoic sedimentary rocks. The apparent

resistivity and phase sections indicate both lateral and vertical variations in the resistivity of these rocks. The most conductive Phanerozoic section is near site 131, the least conductive section is near site 142, and conductive rocks appear to extend to the surface near site 136. The similarity of the short-period response for both polarization modes indicates the shallow geoelectric structure is locally close to 1-D.

The longer-period (> 1 s) apparent resistivity and phase sections are related to resistivity structure in the Proterozoic rocks. The differences between the two polarization modes indicates that this structure has a strong 2-D component. Although the lateral changes in the response are relatively small they indicate the presence of significant resistivity structures since the conductive Phanerozoic rocks will have the effect of masking the response from underlying structure. Features observed in the longer-period response include a spatial variation in apparent resistivity and phase at site 131, near the boundary of the Fort Simpson terrane and the Hottah terrane and a variation near site 142, at the boundary of Nahanni terrane and Fort Simpson terrane.

Preliminary Modelling and Inversion Preliminary inversions have been completed using the Occam modelling method of Constable *et al.* (1987) to determine the geoelectric models with the minimum amount of structure that can acceptably fit the data. 1-D modelling was completed with an emphasis on examining the Phanerozoic structure. Major features of the resulting models (Fig. 5) are:

1. A general three-layer resistivity structure at most sites that includes a conductive surface layer which is thicker in the Proterozoic than in the Archean. The thickness of the layer increases from 0 m in the east to 1000 m in the west. The models show that there are significant resistivity variations within the layer with the most conductive rocks occurring at several hundred metres depth.

2. The models include a resistive upper crust. The H-polarization results suggest the upper-crustal resistivity is highest at the east end of the profile. Full 2D modelling is presently underway to provide more accurate images of the upper and mid-crustal structure.

3. The resistivity models resolve a conductor region at depth. Work by Jones & Ferguson (1997) has shown that beneath the lithosphere thins from around 200 km in the Slave province to 100 km west of the Great Bear magmatic arc.

Future Modelling and Inversion

Improved resolution of the resistivity structure of the Phanerozoic section will be obtained using 1D and 2D inversions constrained by borehole information. In addition to increasing the information available on the sedimentary rocks, this work should improve the resolution on the upper crustal resistivity structure. Modelling of the upper crustal structure will proceed through 2D

inversion and modelling, using several different algorithms to assess model resolution. A subsequent stage of modelling will incorporate constraints from seismic and other geophysical responses.

References

Constable, S.C., Parker, R.L., & Constable, C.G., 1987. "Occam's inversion: a practical algorithm for generating smooth models from electromagnetic sounding data", Geophys., **52,** 289-300.

Groom R.W. and Bailey, R.C., 1989, Decomposition of magnetotelluric impedance tensors in the presence of local three-dimensional galvanic distortion. *J. Geophy. Res.*, **94**, p. 1913-1925.

Jones A.G. and Ferguson, I.J. 1997, Results from 1996 MT studies along SNORCLE profiles 1 and 1A. *In Lithoprobe Slave-Northern Cordillera Lithospheric Evolution and Cordillera Tectonics Workshop Meeting, Lithoprobe Report* No. **56,** Ed. Cook, F.A. and Erdmer, P., p. 42-47.

Figure Caption

Figure 1. Location of the MT sites (dots) along SNORCLE transect Corridor 1. Background is the Bouguer gravity map marking the terranes.

Figure 2. The geoelectric strike directions along Corridor 1 as determined from the tensor decomposition orientation for periods of (a) 1.3×10^{-3} s, (b) 85.3 s, (c) 853 s.

Figure 3. The real induction vector response along the Corridor 1. (a) 85.3 s; (b) 853 s.

Figure 4. Apparent resistivity (a) and phase (b) sections after Groom-Bailey decomposition. The E-polarization mode corresponds to electric currents parallel to geoelectric strike (N30°E) and the H-polarization mode to currents perpendicular to strike.

Figure 5. Stitched 1-D Occam inversion models for the Proterozoic segment of Corridor 1.

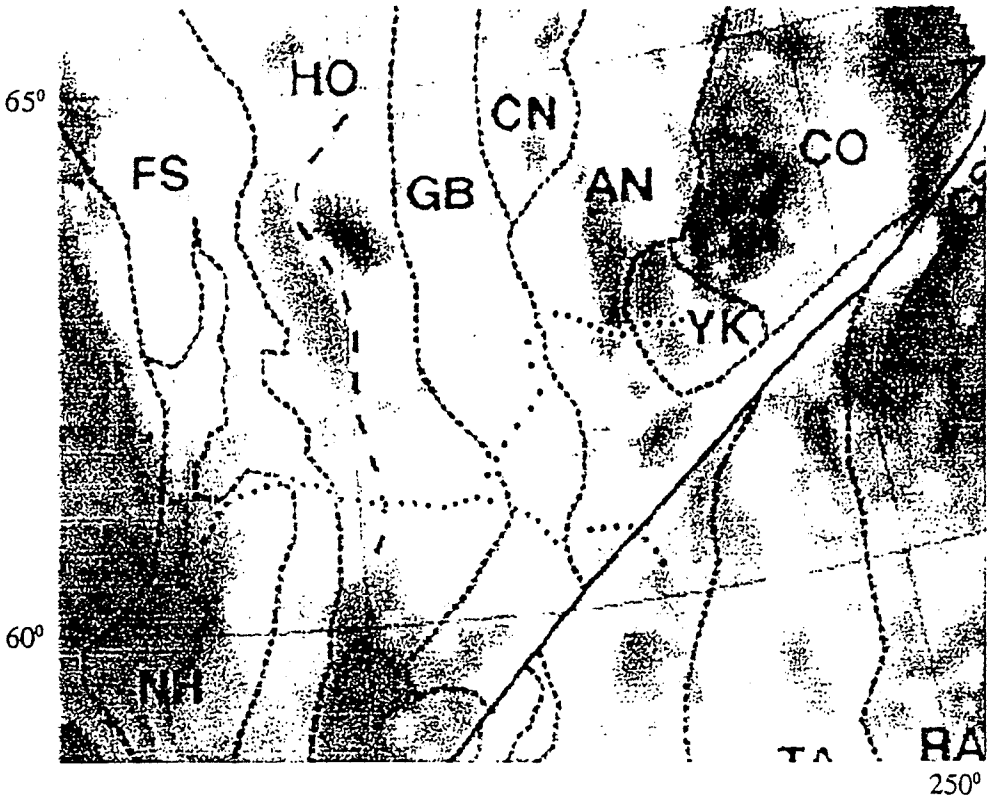

Figure 1. Location of the MT sites (dots) along SNORCLE transect Corridor 1. Background is the Bouguer gravity map marking the terranes.

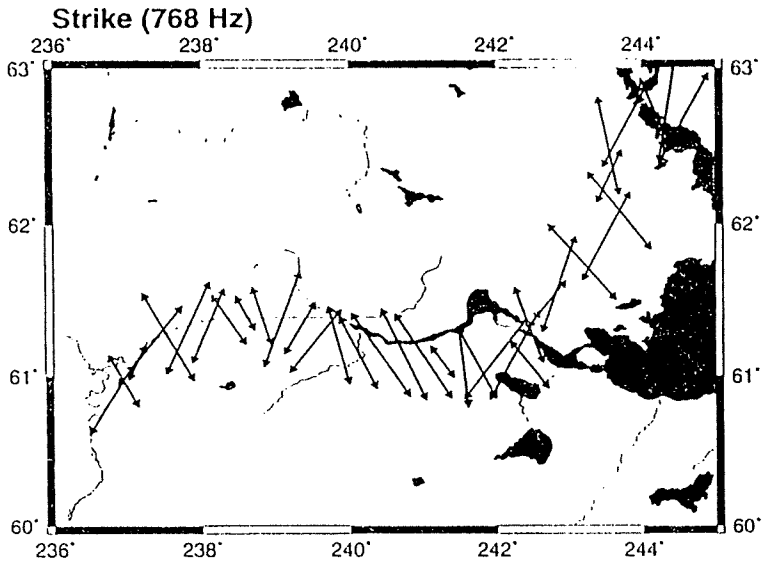

(a)

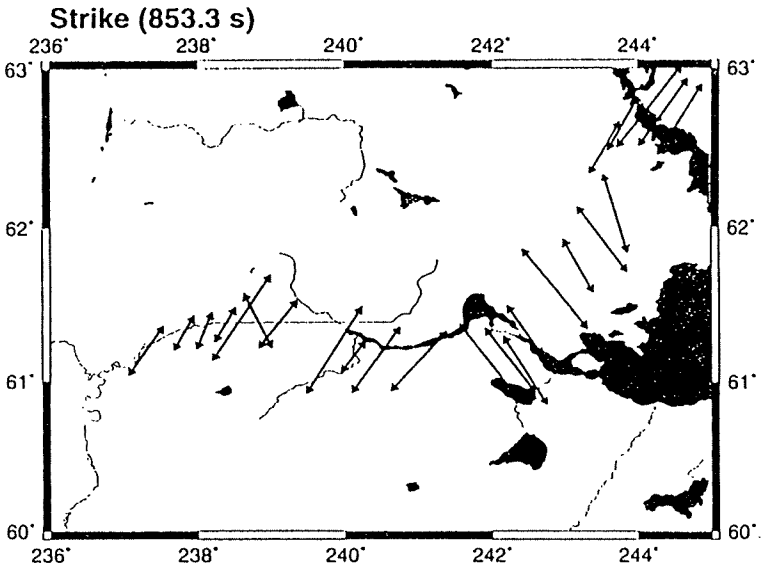

(c)

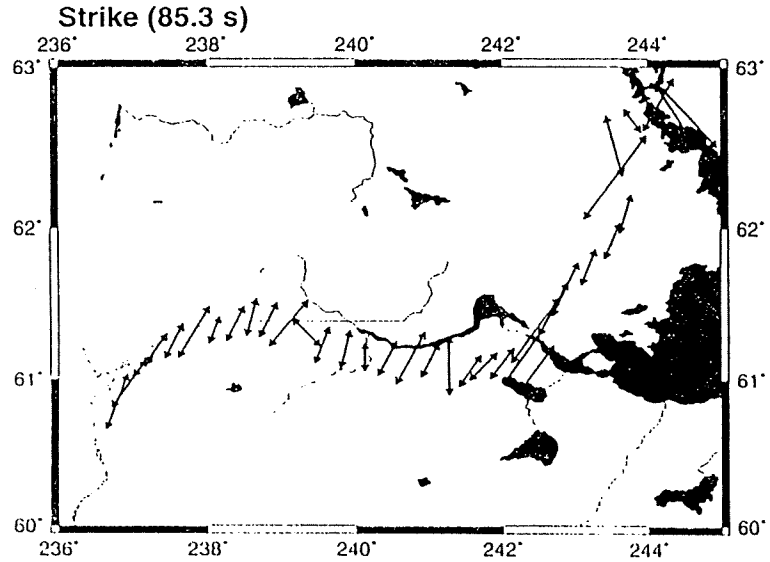

(b)

Figure 2. The geoelectric strike directions along Corridor 1 as determined from the tensor decomposition orientation for periods of (a) 1.3×10^{-3} s, (b) 85.3 s, (c) 853 s.

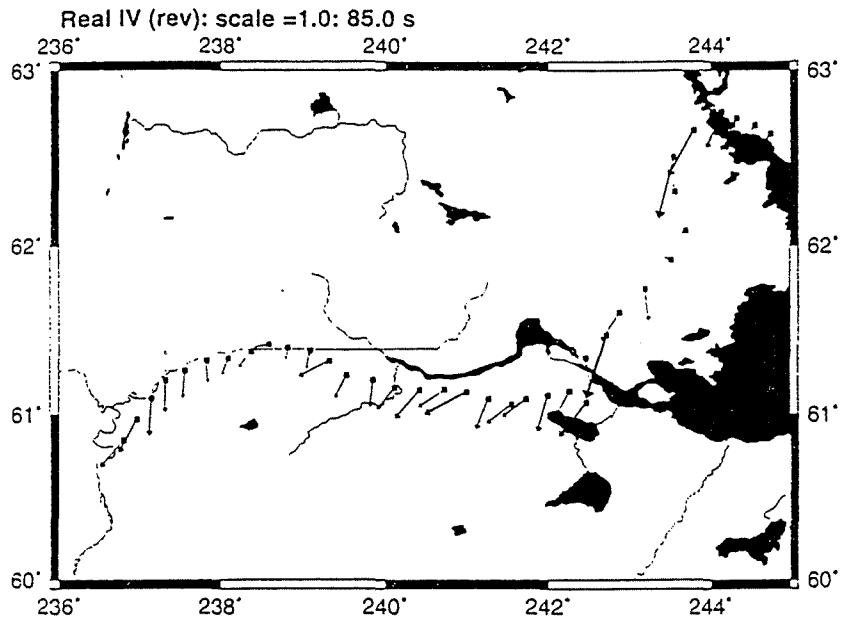

(a)

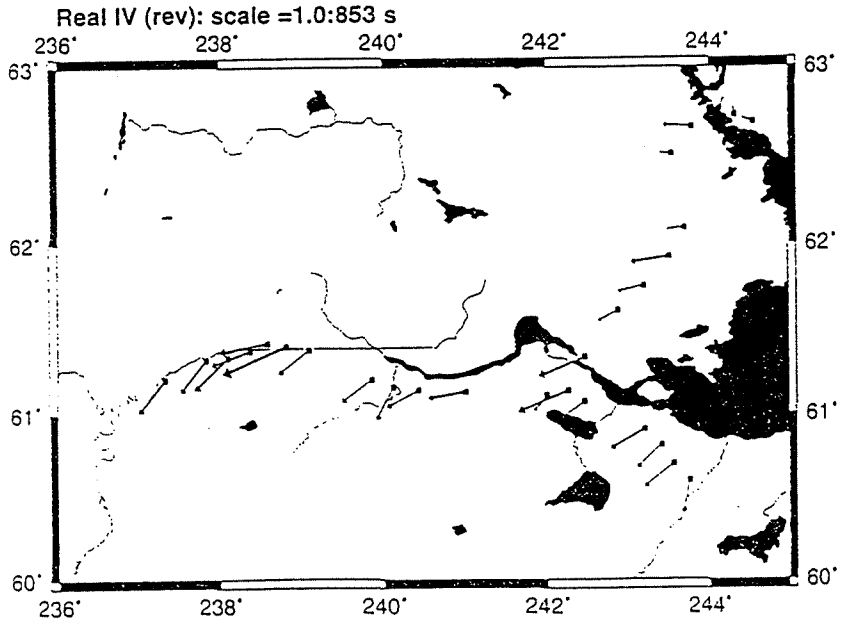

(b)

Figure 3. The real induction vector response along the Corridor 1. (a) 85.3 s; (b) 853 s.

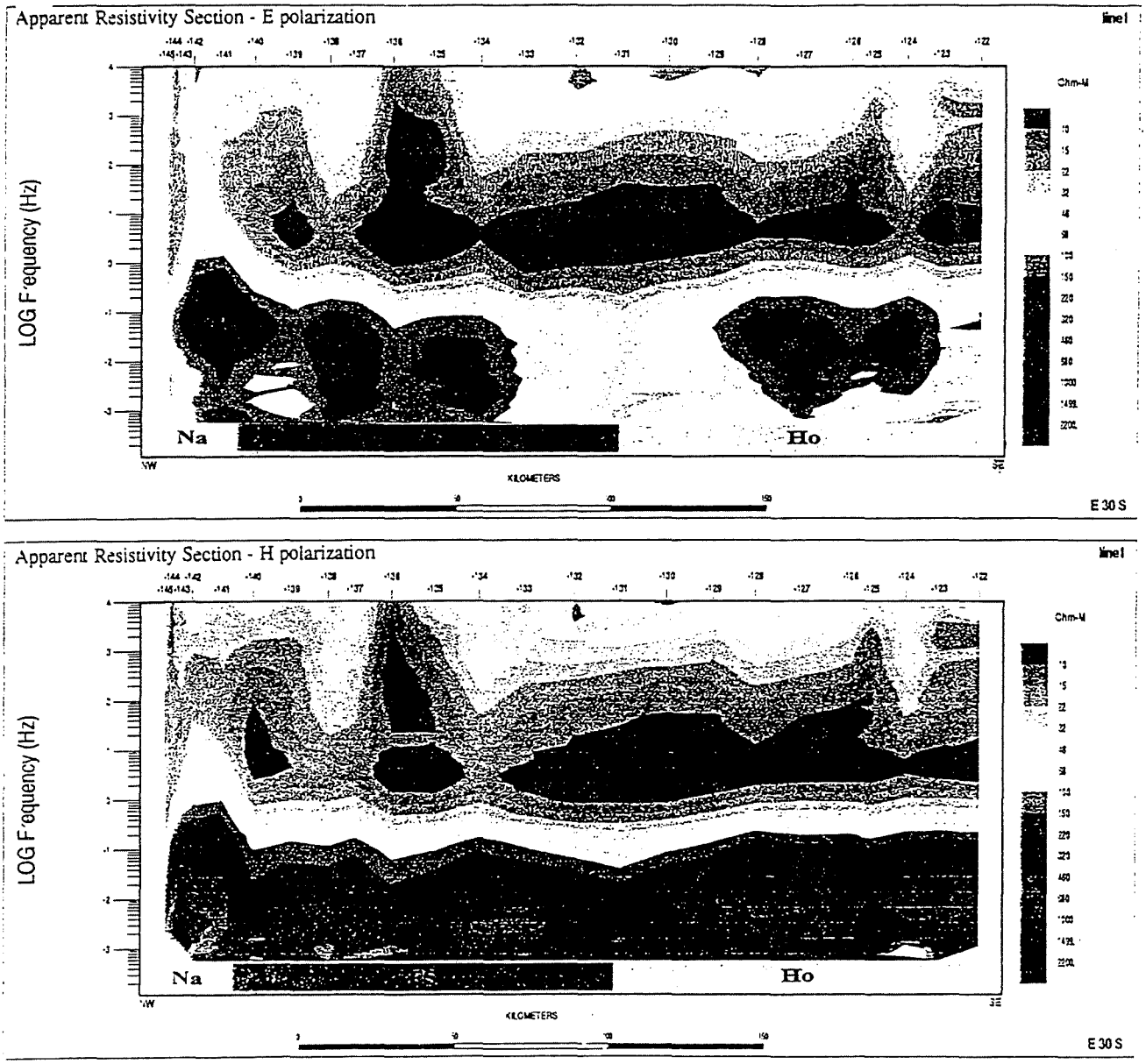
Apparent Resistivity Section - E polarization
LOG Frequency (Hz)
Na
Ho
KILOMETERS
E 30 S
Apparent Resistivity Section - H polarization
LOG Frequency (Hz)
Na
Ho
KILOMETERS
E 30 S

(a)

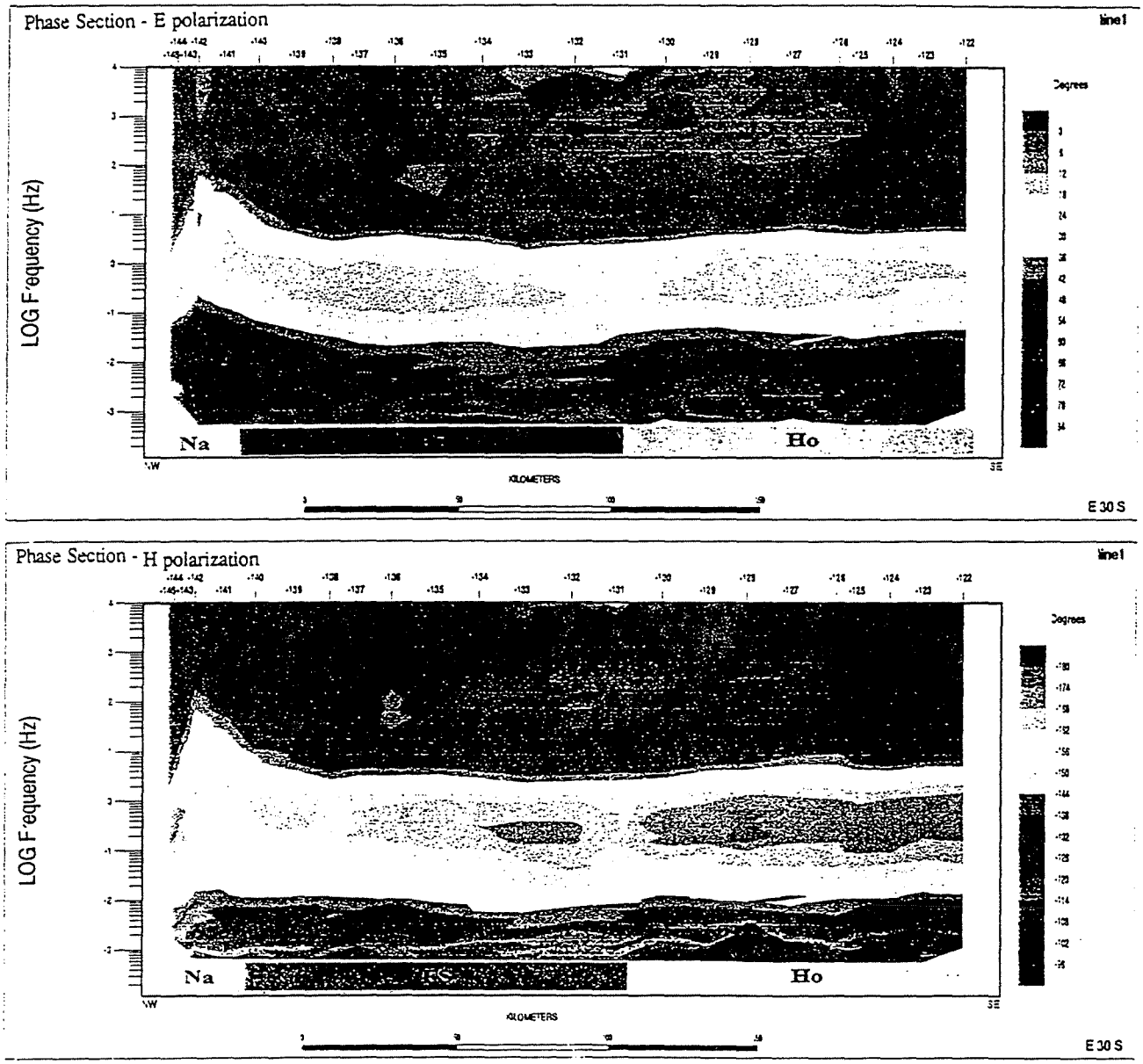

(b)

Figure 4. Apparent resistivity (a) and phase (b) sections after Groom-Bailey decomposition. The E-polarization mode corresponds to electric currents parallel to geoelectric strike (N30°E) and the H-polarization mode to currents perpendicular to strike.

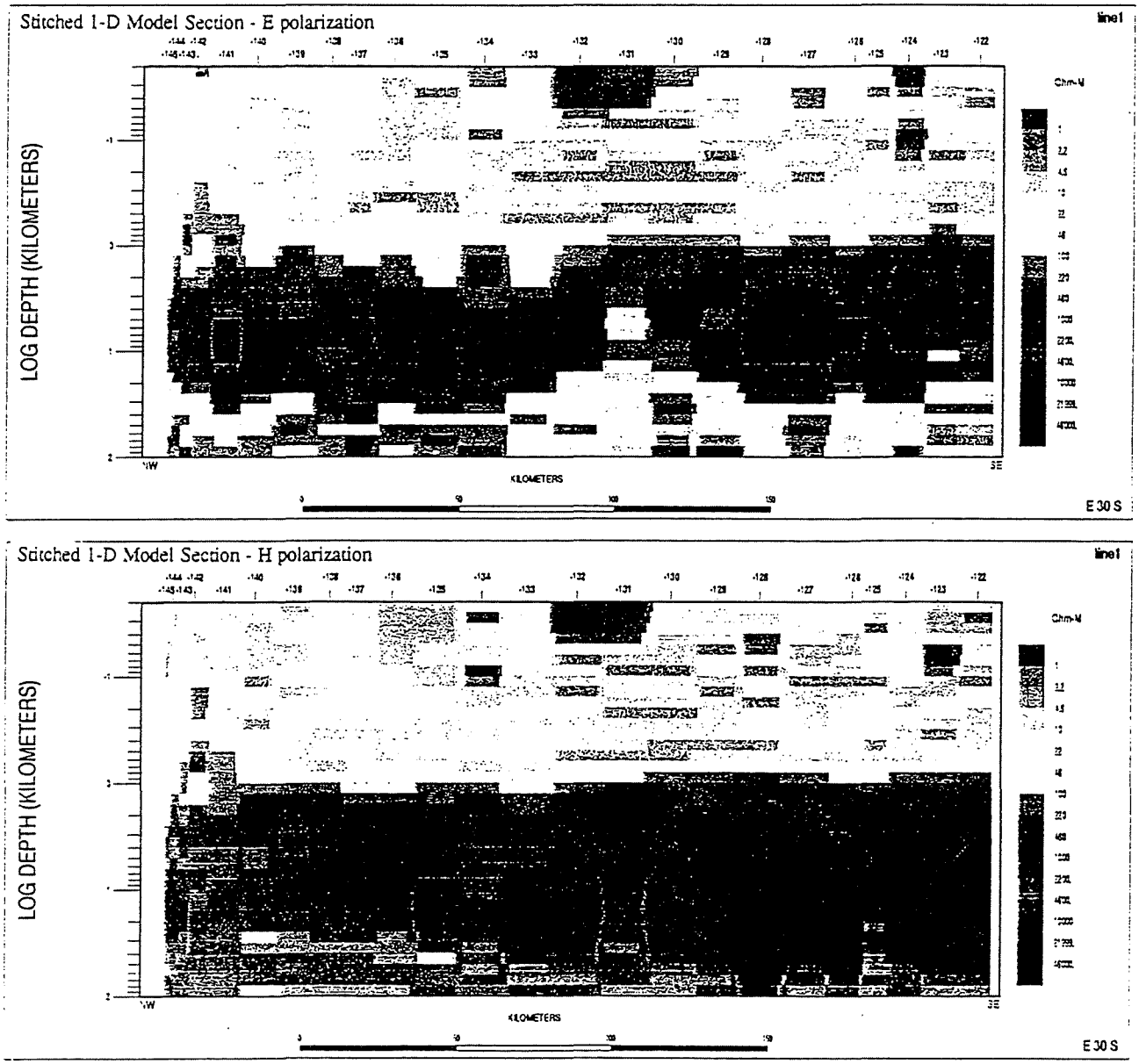

Figure 5. Stitched 1-D Occam inversion models for the Proterozoic segment of Corridor 1.

Source-field contamination of SNORCLE magnetotelluric data

James Cassels, Queen's University
Alan G. Jones, Geological Survey of Canada

Long period magnetotelluric (MT) data collected in northern Canada have to be inspected for contamination caused by the spatially non-uniform and temporally non-stationary external source fields. These effects result in MT response functions that contain both information about the Earth below, and also about the source fields above. Incorrect assumptions about the nature of the source fields can lead to erroneous Earth structure models.

An example of the problems encountered is shown in the figure to the right. The MT response, expressed as apparent resistivities and phases, for an Earth representative of northern Scandinavia (3 layers of resistivity 10,000 Ω.m, 360 Ω.m and 77 Ω.m, bases at 7 km, 46 km and 173 km over a 5 Ω.m half-space) for an uniform source-field is shown by the lines with a wavelength $\lambda = \infty$. The other responses are for the same Earth, but for non-uniform sources characterized by wavelengths of 1,000 km, 500 km and 200 km. A source field of 1000 km leads to an underestimate in the depth to resistive "lithosphere"/conductive "asthenosphere" boundary of almost 50 km (128 km instead of 173 km). Smaller wavelength fields give even more significant errors.

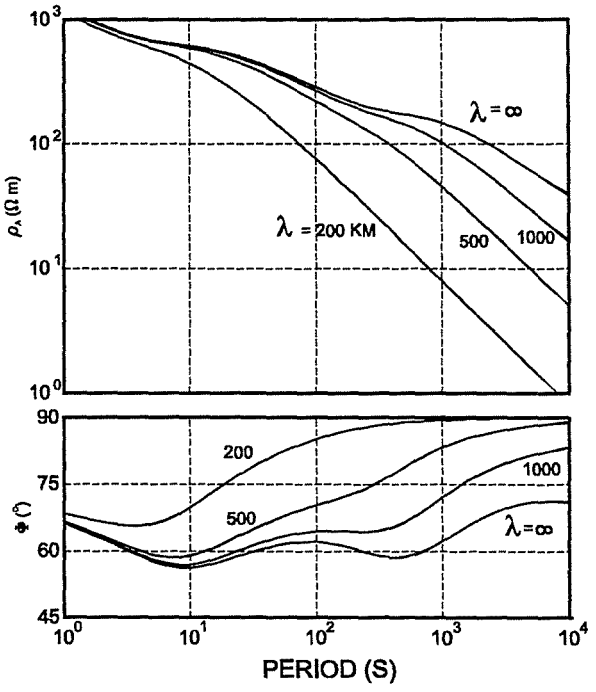

This paper will show the results of analysing almost a year of MT data recorded at Yellowknife during 1996. Approaches discussed in Garcia *et al.* (1997) have been tried, as well as others. The goal is to determine appropriate methods for selecting objectively data segments lease contaminated by source field problems, and to apply those methods to both the existing SNORCLE 1996 dataset, and to the forthcoming 1998/99 SNORCLE Winter Road dataset.

Garcia, X., A.D. Chave and A.G. Jones, 1997. Robust processing of magnetotelluric data from the auroral zone. *J. Geomagn. Geoelectr.*, **49**, 1451-1468.

Early Paleozoic post-rift evolution of the northern Cordilleran margin: lithostratigraphic and conodont biostratigraphic framework along a platform-miogeocline-basin transect

Leanne J. Pyle and Christopher R. Barnes
School of Earth and Ocean Sciences, University of Victoria, P. O. Box 3055, Victoria, BC, V8W 3P6; e-mail: leanne@uvic.ca; crbarnes@uvic.ca

Introduction

Lower Paleozoic strata of the Canadian Cordilleran miogeocline accumulated in the Southern Cordilleran Upper Plate Zone south of Liard Line which includes the Kechika Trough and the Macdonald Platform (Fig. 1; Cecile et al., 1997). The stratigraphy documents the early tectonic evolution and syn- to post-rift phases of the ancestral northern margin of Laurentia. Stratigraphic and conodont biostratigraphic studies using 12 principal sections provide an east-west platform-miogeocline-basin transect across the margin. The line of transect approximates to part of Line 2 of the LITHOPROBE/SNORCLE transect and complements similar studies in the southern Cordillera and across the ancient southern Laurentian margin of the Newfoundland Appalachians.

Lithostratigraphy and Sequence Stratigraphy

The main stratigraphic units are the platform to basin facies of the Kechika Group (upper Cambrian to lower Ordovician), the shallow water platform facies of the Skoki Formation (lower to upper Ordovician), and the slope to basin facies of the Road River Group (lower Ordovician to Silurian) which were deposited along the rifted northern margin of Laurentia. Over three field seasons, sections have been described, measured and sampled for conodonts. Successions of shallow-water shelf carbonates of the Kechika Group and overlying Skoki Formation which accumulated on the Macdonald Platform occur in the easternmost part of the study area. The 380m thick section contains subunits which are not as clearly defined as in the expanded sections further west.

An expanded, nearly complete section of Kechika limestone and shale overlain by Skoki dolostone and limestone was described and collected south of Mount Sheffield. It will form the template to which data from other sections are compared.

Successions of shelf to outer miogeocline and upper slope facies along the western edge of Macdonald Platform were examined at several sections. A thick, spectacular section is preserved at Grey Peak in Kwadacha Wilderness Park which includes the platform to deeper shelf (shelfbreak) transition. Thin bedded carbonate and deeper basinal shale of the Kechika Group (1400m) abruptly overlie Cambrian shallow-water sandstone, carbonate and breccia and

indicate the initiation of thick packages of Kechika Group sediments developed as the Kechika Trough subsided rapidly. The Road River Group (500m) conformably overlies the Kechika Group and comprises breccia debris flows which contain clasts of Skoki lithologies interbedded with Road River black, anoxic shale indicating further extensional phases and a steepening of the platform edge.

In addition to these key sections, a complete exposure of Road River Group has been sampled north of the Akie River where it is underlain by the Kechika Group and overlain by higher Silurian clastics. A nearly complete succession of Skoki Formation has also been collected west of the Prophet River. Over 300m of calcareous Road River Group were sampled in a core from the Akie prospect of Inmet Mining Corporation.

Basinal facies within the Kechika Trough were examined in condensed sequences of Kechika and Road River groups such as at Driftpile Creek (400m thick) and Bluff Creek (700m thick) in the Kechika map-area. The distinction of lithologic units is difficult at Bluff Creek and requires further investigation. In other regions of the Kechika Trough, sequences of the Kechika Group thicken to over 1000 m at Gataga Mountain and suggest a positive tectonic element west of the trough (Ferri et al., 1994, 1995).

The Kechika Trough is bounded on the west by the Northern Rocky Mountain Trench, beyond which lies the parautochthonous Cassiar Terrane that has been displaced at least 450 km from the south (Gabrielse, 1985), possibly representing a segment of the Kakwa Platform. The inital site of the Cassiar Terrane has also been suggested to be from a miogeoclinal gap in southern Idaho (Pope and Sears, 1997). An east-west transect across the Cassiar Terrane has been accomplished by sampling Kechika and Road River facies from three sections at Moodie Creek, Deadwood Lake and Cassiar to examine changes from shallow-water to deeper-water facies.

The stratigraphic record is complex as local rifting events are overprinted by eustatic events. Each unit contains regionally distinct subunits as defined provisionally by Cecile and Norford (1979). The age of stratigraphic events represented by flooding surfaces which mask formational bases can be determined by condont biostratigraphy. Sequence stratigraphic analysis and the dating of stratigraphic, eustatic and tectonic events reflected in the stratigraphy are principal objectives of this project.

Preliminary Conodont Biostratigraphy

Over 400 4kg conodont samples provide the basis for constrained regional correlations and interpretations of tectonic and eustatic events, particularly the timing of syn- and post-rift events. The samples have yielded many tens of thousands of conodont specimens in which diversity, abundance and preservation increases eastwards from the basin to the platform. The

conodont faunas include many key biozonal species and two parallel biozonations are being established for both the basin-shelfbreak and the miogeocline/platform. Conodont biostratigraphy has established that deepening phases marking the onset of Kechika and Road River groups occurred in the latest Cambrian and latest Tremadoc, respectively. A sequence of zonal faunas occurs in Tremadoc units of the Kechika including zonal indicators such as *Cordylodus, Iapetognathus, Rossodus, Scolopodus* and *Paracordylodus.* Within units of the Skoki Fm., zonal faunas span upper Arenig to Caradoc and include genera such as *Pygodus*. In the lower Road River Group, *Paracordylodus, Periodon* and *Protopanderodus* species provide zonal indices for the Arenig through Caradoc interval. The upper Road River Group contains Llandovery (lower Silurian) species such as *Distomodus* and *Pseudoneotodus*. Taxonomic work is in progress as the basis for refining the biozonations.

Conodont paleoecologic patterns (i.e., provinces and communities) across the platform-shelfbreak-slope-basin transect will be documented by studying biofacies relationships. Subtle changes in faunal patterns through time caused by tectonic and eustatic events will help interpret the details of regional sequence stratigraphy and tectonic evolution. Lateral ecological differentiation is evident, especially with the onset of a pronounced shelfbreak separating anoxic Road River basinal facies from equivalent shallow platform carbonates of the Skoki Formation. The transition between the two main biofacies realms (North Atlantic; Midcontinent) clearly occurs near the shelfbreak, being more sharply discriminated during periods of margin steepening and/or regression. Work on establishing spatial and temporal patterns of conodont biofacies within each faunal realm is ongoing. Conodont colour alteration index (CAI) values across the transect are also being assessed and lie mainly in the 4-5 range indicating a burial temperature range of 190-400°C, above the oil window.

The rifted upper-plate segment of the continental margin of ancestral North America, although characterized as Atlantic-type, has undergone several phases of rifting and extensional phases in the Early Paleozoic. The conodont biostratigraphy, integrated with lithostratigraphic and paleoecologic data, will constrain regional interpretations of tectonic and eustatic events, particularly the timing of syn- and post-rift events along the margin of Laurentia.

References

Cecile, M. P., Morrow, D. W., and Williams, G. K., 1997, Early Paleozoic (Cambrian to Early Devonian) tectonic framework, Canadian Cordillera, Bulletin of Canadian Petroleum Geology, 45, p. 54-74.

Cecile, M. P., and Norford, B. S., 1979, Basin to platform transition, Lower Paleozoic strata of Ware and Trutch map areas, northeastern British Columbia, *in* Current Research, Part A. Geological Survey of Canada, Paper 79-1A, p. 219-226.

Ferri, F., Nelson, J., and Rees, C., 1994, Geology and mineralization of the Gataga River Area, northern Rocky Mountains (94l/7,8,9 and 10): British Columbia Ministry of Energy, Mines and Petroleum Resources, Geological Fieldwork 1995, Paper 1995-1, p. 277-295.

Ferri, F., Nelson, J., and Rees, C., 1995, Geology and mineralization of the Gataga River Area, northern Rocky Mountains (94L/10, 11, 14 and 15): British Columbia Ministry of Energy, Mines and Petroleum Resources, Geological Fieldwork 1996, Paper 1996-1, p. 137-154.

Gabrielse, H., 1985, Major dextral transcurrent displacements along the Northern Rocky Mountain Trench and related lineaments in north-central British Columbia: Geological Society of America Bulletin, v. 96, p. 1-14.

Pope, M. C., and Sears, J. W., 1997, Cassiar platform, north-central British Columbia: A miogeoclinal fragment from Idaho, Geology, 25, 515-518.

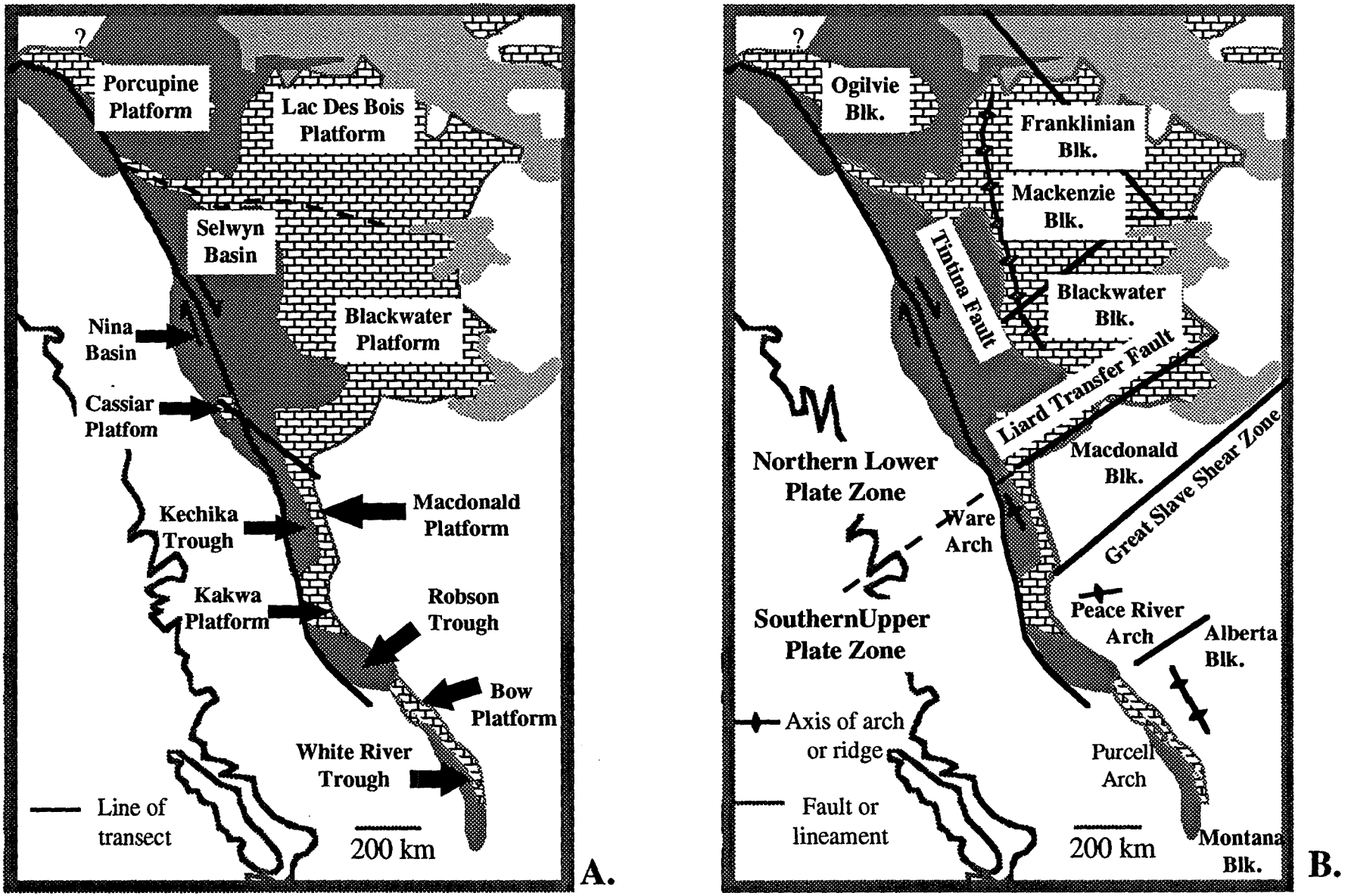

Figure 1. Maps showing Lower Paleozoic paleogeography (A) and blocks and upper and lower plate divisions (B) (after Cecile et al., 1997).

Developing a Sequence-Stratigraphic Framework for the Neoproterozoic-Cambrian Evolution of the Northwestern Margin of North America

Robert B. MacNaughton, Guy M. Narbonne, and Robert W. Dalrymple
Department of Geological Sciences, Queen's University
Kingston, Ontario, Canada, K7L 3N6

The Neoproterozoic to subtrilobite Cambrian succession of northwestern Canada consists of a continental shelf to slope succession that is widely regarded as representing part of the initial western margin of Laurentia. The precise sequence and timing of events during the formation of this margin is a subject of debate. Some workers correlate the onset of rifting with the base of the Windermere Supergroup, while others favour a major thermal and/or rifting event near the Precambrian-Cambrian boundary. Sequence stratigraphy, with its emphasis on the recognition and correlation of interregional unconformities (sequence boundaries), is an ideal technique for interpreting the margin's evolving tectono-stratigraphic history.

The Mackenzie Mountains contain one of the thickest, most complete depositional records for the Neoproterozoic and earliest Cambrian yet described. Superb exposure and a generally straightforward stratigraphic succession allow us to explore the early history of the margin, and potentially to produce a "type section" for its evolution. The potential of the Mackenzie Mountains succession in this regard is greatly enhanced by the variety of analytical techniques to which it is amenable, including process sedimentology, trace-fossil and Ediacaran body-fossil biostratigraphy, and carbon-isotope chemostratigraphy.

Field studies conducted during the summer of 1997 on the upper Windermere Supergroup (Gametrail, Blueflower, and Risky Formations) fill the gap between underlying, lower Windermere Supergroup (Ice Brook and Sheepbed Formations) and overlying, subtrilobite Cambrian units (Ingta, Backbone Ranges, and Vampire Formations) previously described by our group. As a result, complete lithostratigraphic, sequence-stratigraphic, chemostratigraphic, and biostratigraphic documentation now exists for the terminal Neoproterozoic and subtrilobite Cambrian succession in the Mackenzie Mountains. This provides a template for tectono-stratigraphic comparison with regions where the succession is less complete or more tectonically complex.

At least seven major sequence boundaries that delineate large-scale (hundreds of metres thick) sequences can be recognized in the Windermere Supergroup and subtrilobite Cambrian units. One occurs at the base of the Ice Brook Formation, one within the Sheepbed Formation, at least two in the Blueflower Formation, one at the base of the Inga Formation, and a further two within the Backbone Ranges Formation; minor sequence boundaries can also been recognized. The major sequence boundaries show good potential for correlation into other regions. For example, the sequence boundary within the Sheepbed Formation is represented by tens to hundreds of metres of downcutting in shelf facies. This sequence boundary apparently correlates with Varanger glacial deposits exposed in North Atlantic sections, a correlation supported by paleontologic and chemostratigraphic data. The sequence-stratigraphic framework developed in the Mackenzie Mountains thus has great potential for tectono-stratigraphic correlation not only within the North American Cordillera, but also with coeval successions worldwide.

Proterozoic sedimentation, magmatism, metasomatism and deformation in the Wernecke and Ogilvie Mountains, Yukon

Derek J. Thorkelson
Department of Earth Sciences, Simon Fraser University
Burnaby, British Columbia V5A 1S6

J. Grant Abbott
Yukon Geology Program
Box 2703, Whitehorse Yukon Y1A 2C6

James K. Mortensen
Department of Earth and Ocean Sciences, University of British Columbia
Vancouver, B.C. V6T 2B4

Robert A. Creaser
Department of Earth and Atmospheric Sciences, University of Alberta
Edmonton, Alberta T6G 2E3

Michael E. Villeneuve
Geological Survey of Canada
601 Booth St., Ottawa, ON K1A 0E8

Abstract

Five main sedimentary successions were deposited in the Wernecke and Ogilvie mountains of Yukon in Proterozoic time. From oldest to youngest these are: (1) the Wernecke Supergroup (>1.72 Ga); (2) the lower Pinguicula Group (units A-C) and units R1-R4 of the lower Fifteenmile Group (~1.38-1.27? Ga); (3) the upper Pinguicula Group (units D-F) and unit R5 of the lower Fifteenmile Group (~1.0-0.9 Ga); (4) the upper Fifteenmile group and the Callison Lake dolostone (~1.0-0.8 Ga); and (5) the Mount Harper Group and the Windermere Supergroup (~750-550 Ma). Five magmatic events are also recorded: the Bonnet Plume River intrusions (1.72-1.71 Ga), the Slab volcanics (possibly ~1.6 Ga), the Hart River sills and volcanics (~1.38 Ga), the Bear River dykes (~1.27 Ga), and the Mount Harper volcanics (~750 Ma). The four oldest magmatic events generated hydrothermal activity, particularly at ~1.59 Ga, when metasomatism and phreatic brecciation produced the Wernecke breccias and related mineral occurrences. All of the igneous events may correlate with crustal extension, but the evidence is most clear for the 1.38 Ga (Hart River-Pinguicula) and 750 Ma (Mount Harper-Windermere) events. Two periods of contractional deformation are also recorded. The Racklan orogeny (east to southeasterly directed) probably occurred after the ~1.7 Ga igneous event, and definitely before Wernecke brecciation at 1.59 Ga. The Corn Creek orogeny (westerly directed) occurred between upper Pinguicula and Windermere deposition. The geological history delineated in this report indicates that Yukon and the western Northwest Territories shared major events of sedimentation, magmatism and deformation throughout much of Proterozoic time.

Introduction

Our program of regional mapping and geochronology in the Wernecke and Ogilvie mountains of Yukon (Fig. 1) has clarified the Lower and Middle Proterozoic geological evolution of northwestern Canada. The chronology of events and the correlation of units described in this report differ significantly from depictions presented a few years earlier (e.g., Aitken and McMechan, 1992; McMechan and Price, 1982; Young et al., 1979). Many of the new findings have been described by Thorkelson and Wallace (1994; 1995), Rainbird et al. (1997), Abbott et al. (1997), and Abbott (1997), but this report is the first to summarize all the salient data – both old and new – in a succinct geological history.

The chronology of events given below shows how the geological processes which shaped the Yukon are reflected in equivalent events in the Mackenzie Mountains and proximal parts of the Northwest Territories. The geological events are presented numerically, from first to last, and are grouped into specific intervals of time bounded by important igneous or metasomatic events. The timing of these events is shown on an accompanying stratigraphic diagram (Fig.2).

Geological History

>1.71 Ga

1. Formation of continental basement. The cratonic basement of Yukon is not exposed, and its age and nature are unkown. It may consist of rocks of Archean to Early Proterozoic age. The nearest cratonic constituent is the Nahanni domain which extends from the western Northwest Territories to southeastern Yukon and northeastern British Columbia. Hoffman (1989) distinguished the Nahanni domain from the Fort Simpson domain to the east on the basis of aeromagnetic character. Whether the Nahanni domain extends westward beneath the Ogilvie and Wernecke Mountains is unknown. The Fort Simpson domain contains granitic rocks as young as 1.845 Ga, and may be a subduction-generated magmatic arc or collisional welt built on the eastern edge of the Nahanni domain (Villeneuve et al., 1991).

2. Rifting and formation of the Wernecke basin, probably after ca 1.84 Ga Fort Simpson magmatism. Attenuation of the basement is implied by the 14 km thickness of the overlying Wernecke Supergroup (Delaney, 1981). Rifting may have separated or partially separated North America from another continent, perhaps Australia. Syn-rift igneous rocks are not exposed, inferring that the main axis of extension lay to the west of the present Wernecke basin.

3. Wernecke Supergroup sedimentation from (?)1.84 Ga-1.72 Ga. Three regionally extensive groups were deposited, forming two clastic-to-carbonate grand cycles (Delaney, 1981). An event of syndepositional rifting is likely to have initiated the second grand cycle, as indicated by an abrupt transition from dolostone to pyritic shale at the top of the Fairchild Lake Group. Minor Pb-Zn sedimentary exhalations occurred toward the top of the Wernecke Supergroup. Deposition of the Supergroup was probably concurrent with accumulation of thinner, more platformal sedimentary strata of the lower Hornby Bay Group (East River and Lady Nye formations; Kerans et al., 1981; Cook and Maclean, 1995).

4. Intrusion of mainly mafic igneous magmas from 1.72-1.71 Ga (Bonnet Plume River intrusions; Thorkelson and Mortensen, unpublished), probably accompanied by volcanism. Magmatism was probably related to mantle plume activity and/or extensional tectonism. Local

Cu-Au-Co enrichments at the SLAB and possibly other mineral occurrences may have been generated during emplacement of local intrusions.

1.71-1.59 Ga

5. Racklan orogeny: east- to southeast-directed deformation producing folds, schistosity and kink bands in the Wernecke Supergroup. Deformation occurred probably after 1.71 Ga dyking, and definitely before eruption of the Slab volcanics and 1.59 Ga development of Wernecke breccia (Thorkelson and Wallace, 1994; Abbott et al., 1997). Erosion of the inferred 1.71 Ga volcanics also occurred during this interval. Racklan deformation is probably equivalent to the Forward orogeny (ca. 1.66 Ga) in the Northwest Territories (Bowring and Ross, 1985; Cook and Maclean, 1995). It is older than deformation described from the subsurface and the Coppermine Homocline by Cook (1992). Concurrent deformation in West and South Australia may be represented by the Isan or Kimban orogenies.

6. Plutonism and probable volcanism at about 1.6 Ga. Plutonic activity in the region is inferred from a ca. 1.6 Ga inherited zircon component in a granitic diatreme clast from the Mackenzie Mountains (Jefferson and Parrish, 1989). Concurrent volcanism may be represented by the Slab volcanics, a remnant of an undated shield volcano in the Wernecke Mountains that is engulfed by 1.59 Ga Wernecke breccia. The Slab volcanics are considered to be younger than 1.71 Ga because they are undeformed and less altered than dykes and stocks of the Bonnet Plume River intrusions. Undated biotite lamprophyre dykes crosscut by hematite veinlets may belong to the suggested 1.6 Ga magmatism. Possible correlatives in South Australia include the Gawler Range volcanics and the Hiltaba plutonic suite, both of which are about 1.6 Ga.

7. Surges of hydrothermal activity and phreatic explosions at about 1.59 Ga, producing zones of hematitic breccia (Wernecke breccia) and enrichments of Cu, Au, Co, and U (Thorkelson and Wallace, 1994; Abbott et al., 1997). Brecciation was probably accompanied by explosive venting and maar formation above the Slab volcanics, and by normal faulting. The mega-clast of the Slab volcanics was incorporated in the breccia, apparently during clastic fall-back after diatreme-like venting. The hydrothermal activity may have been generated during emplacement and cooling of the 1.6 Ga intrusions. Time-equivalent breccias of similar lithology and mineralogy were generated at the Olympic Dam mine in South Australia (Bell and Jefferson, 1987; Hitzman et al., 1992; Creaser and Cooper, 1993).

1.59-1.27 Ga

8. Faulting in the Wernecke Mountains producing shear fabrics in Wernecke breccia that are truncated by the Pinguicula Group.

9. Deep weathering of the Wernecke Supergroup and Wernecke breccia during the interval 1.59-1.38 Ga. Local supergene enrichment of mineralized rock (Thorkelson and Wallace, 1994).

10. Rifting, mafic magmatism, and deposition of the basal Pinguicula and Fifteenmile groups at ca. 1.38 Ga. Rifting is implied by development of the Pinguicula basin, which accommodated >3 km of basinal clastic to platformal carbonate deposits (Eisbacher, 1981). The time of rifting is known from the ca. 1.38 Ga Hart River sills. One of the sills lies unconformably beneath the Pinguicula Group, and another intrudes the base of the Pinguicula Group (Abbott, 1997; Thorkelson and Mortensen, unpublished). The undated Hart River volcanics, which sit below

the Pinguicula Group, are considered co-magmatic with the Hart River sills. Listric normal faulting and rifting accompanied depositon of the basal lower Fifteenmile Group in the western Ogilvie Mountains (Thompson, 1995; Abbott, 1997). Hydrothermal activity during rifting is indicated by (1) rutile dated at ca. 1.38 Ga from the Slab volcanics (Thorkelson and Mortensen, unpublished); and (2) the HART RIVER polymetallic massive sulphide deposit which crosscuts the Hart River volcanics but not the overlying Pinguicula Group (Abbott, 1997). The lower Pinguicula Group (units A-C) and units R1-4 of the Lower Fifteenmile Group are correlated with the Dismal Lakes Group of the Northwest Territories. The 1.38 Ga rift event is approximately time equivalent to the East Kootenay orogeny in southern British Columbia (McMechan and Price, 1982; Doughty and Chamberlin, 1996).

11. Emplacement of the Bear River dykes, and probable eruption of mafic lavas, at ca. 1.27 Ga (Thorkelson and Mortensen, unpublished). Igneous intrusions of this age probably extend northward into the Richardson Mountains where hydrothermal alteration is recorded by 1.27 Ga monazite (Parrish and Bell, 1987). Hematitic alteration of a Bear River dyke in the Wernecke Mountains was probably part of this magma-fluid event. Bear River magmatism is considered part of the huge Mackenzie igneous event in the Canadian Shield, including emplacement of the Mackenzie dyke swarm and the Muskox intrusion, and eruption of the Coppermine Lavas (LeCheminant and Heaman, 1989).

1.27-0.8 Ga

12. Minor plutonism in the crust beneath the Mackenzie Mountains at approximately 1.15 Ga as indicated by the age of a granite clast in a diatreme (Jefferson and Parrish, 1989). This igneous event may be tied to weak Grenville-age orogenesis which extended through Australia and into western Canada (Ross et al., 1992).

13. From 1.27-1.1 Ga, complete erosion of all volcanic strata inferred to have been deposited during the 1.27 and (?)1.15 igneous events.

14. Deposition of the upper Pinguicula Group (units D-F) and the lower upper part of the Fifteenmile Group (unit R5) as epicontinental clastic and carbonate deposits. (The upper Pinguicula Group may be formally removed from the Pinguicula Group and re-named by Thorkelson (in prep.)). Deposition, which was probably restricted to the interval 1.1-0.9 Ga, occurred on a terrain of locally karsted and tilted carbonate strata of the lower Pinguicula Group in the Wernecke Mountains, and with angular unconformatity on rocks as old as the Wernecke Supergroup and Wernecke breccia in the western Ogilvie Mountains. Sandstone beds contain Grenville-age zircon and muscovite grains (Rainbird et al.,1997; Thorkelson and Villeneuve, unpublished). Apparently, sediment was shed from the Grenville orogen and transported northwestward across the continent by major river systems (Rainbird et al., 1997). The upper Pinguicula and middle Fifteenmile groups are two of several successions that formed during widespread subsidence of western and northern Canada in response to Grenville orogenesis along the eastern and southern parts of Laurentia. Other successions include the Katherine Group and possibly other parts of the Mackenzie Mountains Supergroup, and the Shaler Supergroup in the western Canadian arctic. The unconformity separating the upper and lower parts of the Pinguicula Group and the lower and upper parts of the Lower Fifteenmile Group may reflect wholly or in part, the 1.27 Ga igneous event and associated uplift and rifting documented in the Coppermine homocline (reviewed in Cook, 1992).

15. Corn Creek orogeny: west-directed folding and thrust-faulting of the Pinguicula Group (Eisbacher, 1981) and, locally, of the Wernecke Supergroup (Thorkelson and Wallace, 1995). The timing and regional extent of this orogenic event (named herein) are not well understood. The orogeny is best displayed in the Wernecke Mountains where overturned folds and thrust faults in the upper Pinguicula Group are truncated by the Sayunei Formation of the Windermere Supergroup (Eisbacher, 1981). This relationship constrains the timing of Corn Creek deformation to the interval between the end of upper Pinguicula Group deposition (<1.0 Ga) and the onset of Sayunei deposition (<0.75 Ga). If the Corn Creek orogeny occurred early in this interval, it could be regarded as a "late Grenville" event. Despite unequivocal evidence for deformation in the Wernecke Mountains, the expression of orogenesis in other areas is unclear, and the timing of contraction is problematic.

16. Deposition of Callison Lake dolostone and units F1-F3 (mainly carbonate) of the upper Fifteenmile Group. Sedimentation occurred before Windermere Supergroup deposition, probably in the interval 900-800 Ma. The Callison Lake-upper Fifteenmile strata are bounded by unconformities, one of which may correspond to the Corn Creek orogeny. The Little Dal Group, and possibly only the upper Little Dal carbonate, are probable correlative units in the Mackenzie Mountains (Abbott, 1997).

800-550 Ma

17. Rifting, and deposition of the Mount Harper Group in the western Ogilvie Mountains. Deposition began with coarse clastics, and continued with mainly mafic volcanism at ca. 750 Ma (Mustard and Roots, 1997). The rifting may be considered the first part of the Hayhook tectonic event during which the crust in the Mackenzie Mountains and adjacent areas was extended (Young et al., 1979; Jefferson and Parrish, 1989; Norris and Dyke, 1997), and the basal Windermere Supergroup was deposited (Mustard and Roots, 1997). In the Mackenzie Mountains, magmatism broadly coevel with Mount Harper volcanism occurred as a quartz diorite stock (ca. 778 Ma; Jefferson and Parrish, 1989) and the Tsezotene sills (ca. 779 Ma; Heaman et al., 1992). The nearby and chemically similar Little Dal basalts probably erupted at this time (Dudas and Lustwerk, 1997; Mustard and Roots, 1997). Consequently, the Coates Lake Group should also be considered part of the basal Windermere Supergroup (Aitken, 1981).

18. Deposition of the Rapitan Group and higher parts of the Windermere Supergroup. Sedimentation began sometime after ca. 755 Ma, which is the age of a granite clast in basal Windermere conglomerate (Ross and Villeneuve, 1997). Deposition involved a wide range of sediment types, with conglomerate and glacial diamictite dominant near the bottom, and sandstone, shale, and carbonate dominant toward the top (Eisbacher, 1981; Jefferson and Parrish, 1989). Banded iron formation of the CREST mineral occurrence was deposited early in Windermere time (Yeo, 1981). Ediacaran fauna are recorded in the top half up the Windermere succession (Narbonne and Hoffman, 1987). Synsedimentary block faulting occurred during protracted extension of the Hayhook event. This event and subsequent Early Paleozoic rifting and subsidence may record complete, oceanic separation of Australia from western North America (Ross, 1991).

References Cited

Abbott, J.G., 1997. Geology of the upper Hart River Area, Eastern Ogilvie Mountains, Yukon Territory (116A/10. 116A/11); Exploration and Geological Services Division, Yukon, Indian and Northern Affairs Canada, Bulletin 9, 76 p.

Abbott, G., Thorkelson, D., Creaser, R., Bevier, M.L., and Mortensen, J., 1997. New correlations among Proterozoic successions and intrusive breccias in the Ogilvie and Wernecke Mountains, Yukon. In Lithoprobe Report No. 56, p.188-197

Aitken, J.D., 1981. Stratigraphy and sedimentology of the Upper Proterozoic Little Dal Group, Mackenzie Mountains, Northwest Territories. In: Proterozoic Basins of Canada, F.H.A. Campbell, (ed.). Geological Survey of Canada Paper 81-10, p. 47-72.

Aitken, J.D. and McMechan, M.E., 1992. Middle Proterozoic assemblages, Chapter 5. In: H. Gabrielse and C.J. Yorath (eds.), Geological Survey of Canada, Geology of the Cordilleran Orogen in Canada, no. 4, p. 97-124.

Bell, R.T. and Jefferson, C.W., 1987. An hypothesis for an Australian-Canadian connection in the late Proterozoic and the birth of the Pacific Ocean. In: Pacific Rim Congress '87, Parkville, Victoria, p. 39-50.

Bowring, S.A., and Ross, G.M., 1985. Geochronology of the Narakay Volcanic Complex: implications for the age of the Coppermine Homocline and Mackenzie igneous events. Canadian Journal of Earth Sciences, Vol. 22, p. 774-781.

Cook, D. G., and MacLean, B.C., 1995. The intracratonic Forward orogeny, and implications for regional correlations, Northwest Territories, Canada. Canadian Journal of Earth Sciences, Vol. 32, p. 1991-2008.

Cook, F.A., 1992. Racklan Orogen. Canadian Journal of Earth Sciences, Vol. 29, p. 2490-2496.

Creaser, R.A. and Cooper, J.A., 1993. U-Pb geochronology of Middle Proterozoic felsic magmatism surrounding the Olympic Dam Cu-U-Au-Ag and Moonta Cu-Au-Ag deposits, South Australia. Economic Geology, v. 88, p. 186-197.

Delaney, G.D., 1981. The mid-Proterozoic Wernecke Supergroup, Wernecke Mountains, Yukon Territory. In: Proterozoic Basins of Canada, F.H.A. Campbell, (ed.). Geological Survey of Canada Paper 81-10, p. 1-23.

Doughty, P.T. and Chamberlin, K.R., 1996. Salmon River Arch: new evidence for rifting near the end of deposition in the Middle Proterozoic Belt basin; Canadian Journal of Earth Sciences, v. 33, p.1037-1052.

Dudas, F.O., and Lustwerk, R.L. 1997. Geochemistry of the Little Dal basalts: continental tholeiites from the Mackenzie Mountains, Northwest Territories, Canada. Canadian Journal of Earth Sciences, V. 34, p. 50-58.

Eisbacher, G.H., 1981. Sedimentary tectonics and glacial record in the Windermere Supergroup, Mackenzie Mountains, northwestern Canada. Geological Survey of Canada, Paper 80-27, 40 p.

Hitzman, M.W., Oreskes, N., and Einaudi, M.T., 1992. Geological characteristics and tectonic setting of Proterozoic iron oxide (Cu-U-Au-REE) deposits. In: G. Gall and K. Schulz (Eds.): Precambrian Metallogeny Related to Plate Tectonics. Precambrian Research. vol. 58.

Hoffman, P., 1989. Precambrian geology and tectonic history of North America. In: A.W. Bally and A.R. Palmer (eds.), The Geology of North America – an overview, Geological Society of America, Geology of North America v. A., p. 447-512.

Jefferson, C.W., and Parrish, R.R., 1989. Late Proterozoic stratigraphy, U-Pb zircon ages, and rift tectonics, Mackenzie Mountains, northwestern Canada. Canadian Journal of Earth Sciences, Vol. 26, p. 1784-1801.

Kerans, C., Ross, G.M., Donaldson, J.A., and Geldsetzer, H.J., 1981. Tectonism and depositional history of the Helikian Hornby Bay and Dismal Lakes groups, Distrcit of Mackenzie. In: Proterozoic Basins of Canada, F.H.A. Campbell, (ed.). Geological Survey of Canada Paper 81-10, p.157-182.

LeCheminant, A.N., and Heaman, L.M., 1989. Mackenzie igneous events, Canada: Middle Proterozoic hotspot magmatism associated with ocean opening. Earth and Planetary Science Letters, Vol. 96, p. 38-48.

Heaman, L.M, LeCheminant, A.N., and Rainbird, R.H., 1992. Nature and timing of Franklin igneous events, Canada: Implications for a Late Proterozoid mantle plume and the break-up of Laurentia. Earth and Planetary Science Letters, v. 109, p. 117-131.

McMechan, M.E. and Price, R.A., 1982. Superimposed low-grade metamorphism in the Mount Fisher area, southeastern British Columbia – implications for the east Kootenay Orogeny. Canadian Journal of Earth Sciences, v. 19, p. 476-489.

Mustard, P.S. and Roots, C.F., 1997. Rift-related volcanism, sedimentation, and tectonic setting of the Mount Harper Group, Ogilvie Mountains, Yukon Territory. Geological Survey of Canada, Bulletin 492, 92 p.

Narbonne, G.M. and Hofmann, H.J., 1987. Ediacaran biota of the Wernecke Mountains, Yukon, Canada. Paleontology, v. 30, p. 647-676.

Norris, D.K, and Dyke, L.D., 1997. Chapter 4: Proterozoic. In: Norris, D.K., Geology and mineral and hydrocarbon potential of northern Yukon Territory and Northwestern District of Mackenzie. Geological Survey of Canada, Bulletin 422, p. 65-83.

Parrish, R. R. and Bell, R.T., 1987. Age of the NOR breccia pipe, Wernecke Supergroup, Yukon Territory. In Radiogenic and Isotopic Studies: Report 1, Geological Survey of Canada, Paper 87-2, p. 39-42.

Rainbird, R.H., McNicoll V.J., Theriault, R. J, Heaman, L.M., Abbott, J.G., Long, D.G.F., and Thorkelson, D. J., 1997. Pan-continental river system draining Grenville orogen recorded by U-Pb and Sm-Nd geochronology of Neoproterozoic quartzites and mudrocks, northwestern Canada. Journal of Geology.

Ross, G.M., Parrish, R.R., and Winston, D., 1992. Provenance and U-Pb geochronology of the Mesoproterozoic Belt Supergroup (northwestern United States): implications for age of deposition and pre-Panthalassa plate reconstructions. Earth and Planetary Science Letters, vol. 113, p. 57-76.

Ross, G.M. and Villeneuve, M.E., 1997. U-Pb geochronology of stranger stones in Neoproterozoic diamictites, Canadian Cordillera: implications for provenance and ages of deposition; in: Radiogenic Age and Isotopic Studies: Report 10, Geological Survey of Canada, Current Research 1997-F, p. 141-155.

Thompson, R. I., 1995. Geological compilation (1:250 000) of Dawson map area (northeast of Tintina Trench). Geological Survey of Canada, Open File 3223.

Thorkelson, D. J. and Wallace, C.A., 1994. Geological setting of mineral occurrences in Fairchild Lake map area (106C/13), Wernecke Mountains, Yukon. In Yukon Exploration and Geology 1993. Exploration and Geological Services Division, Yukon, Indian and Northern Affairs Canada, p. 79-92.

Thorkelson, D.J. and Wallace, C.A., 1995. Geology and mineral occurrences of the "Dolores Creek" map area (106C/14), Wernecke Mountains, Northeastern Yukon. In: Yukon Exploration and Geology, 1994. Exploration and Geological Services Division, Yukon, Indian and Northern Affairs Canada, p. 19-30.

Villeneuve, M.E., Theriault, R.J. and Ross, G.M., 1991. U-Pb ages and Sm-Nd signature of two subsurface granites from the Fort Simpson magnetic high, northwest Canada. Canadian Journal of Earth Sciences, v. 28, p. 1003-1008.

Yeo, G., 1981. The late Proterozoic Rapitan glaciation in the northern Cordillera. In: Proterozoic Basins of Canada, F.H.A. Campbell, (ed.). Geological Survey of Canada Paper 81-10, p. 25-46.

Young, G. M., Jefferson, C.W., Long, D.G.F., Delaney, G.D., and Yeo, G.M., 1979. Middle and Late Proterozoic evolution of the northern Canadian Cordillera and Shield. Geology, Vol. 7, p.125-128.

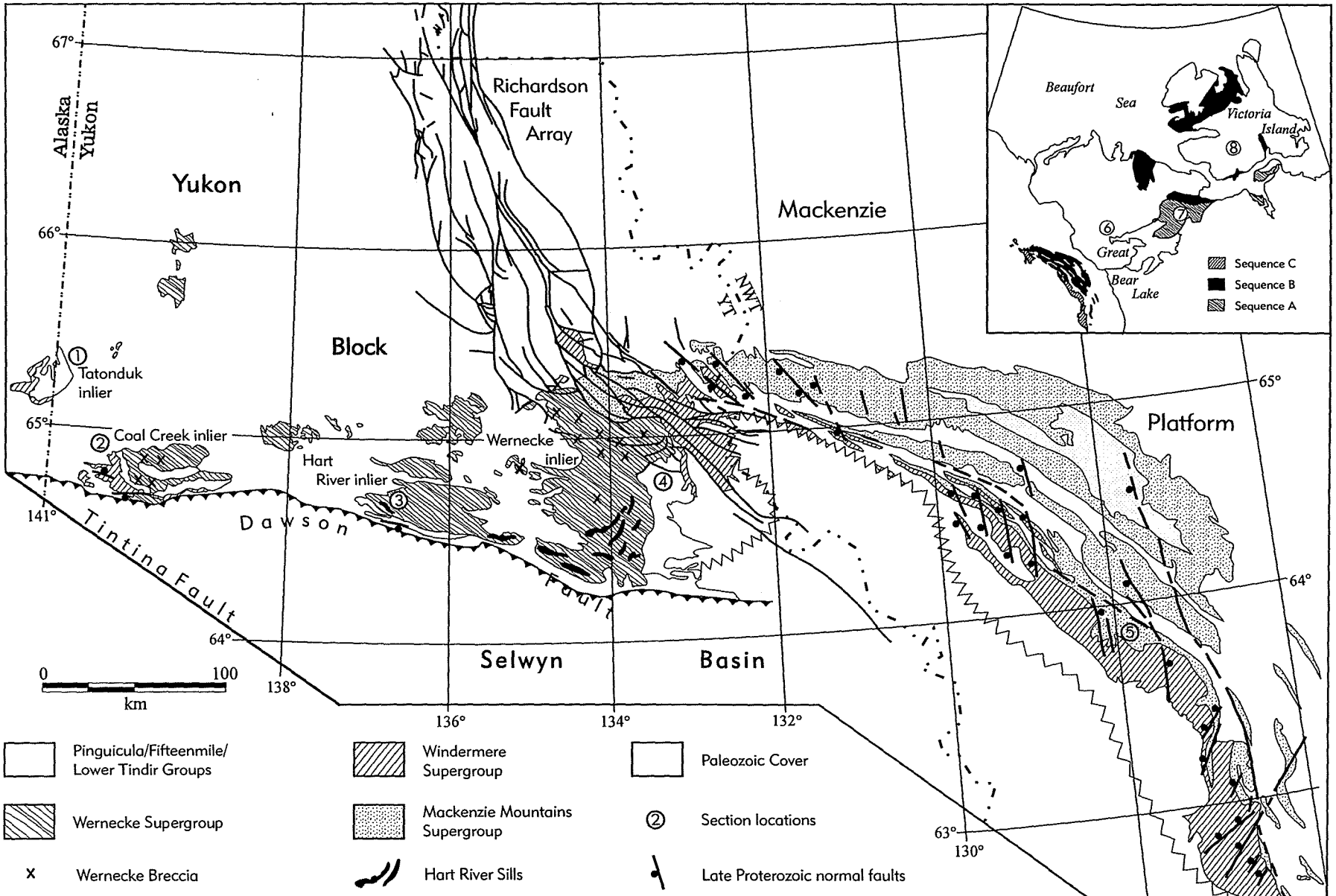

Fig. 1 Regional map of principal Proterozoic sequences and Proterozoic structures in the Ogilvie, Wernecke and Mackenzie mountains, and location of sections in Fig. 2. Inset shows relevant geological features of the western Arctic.

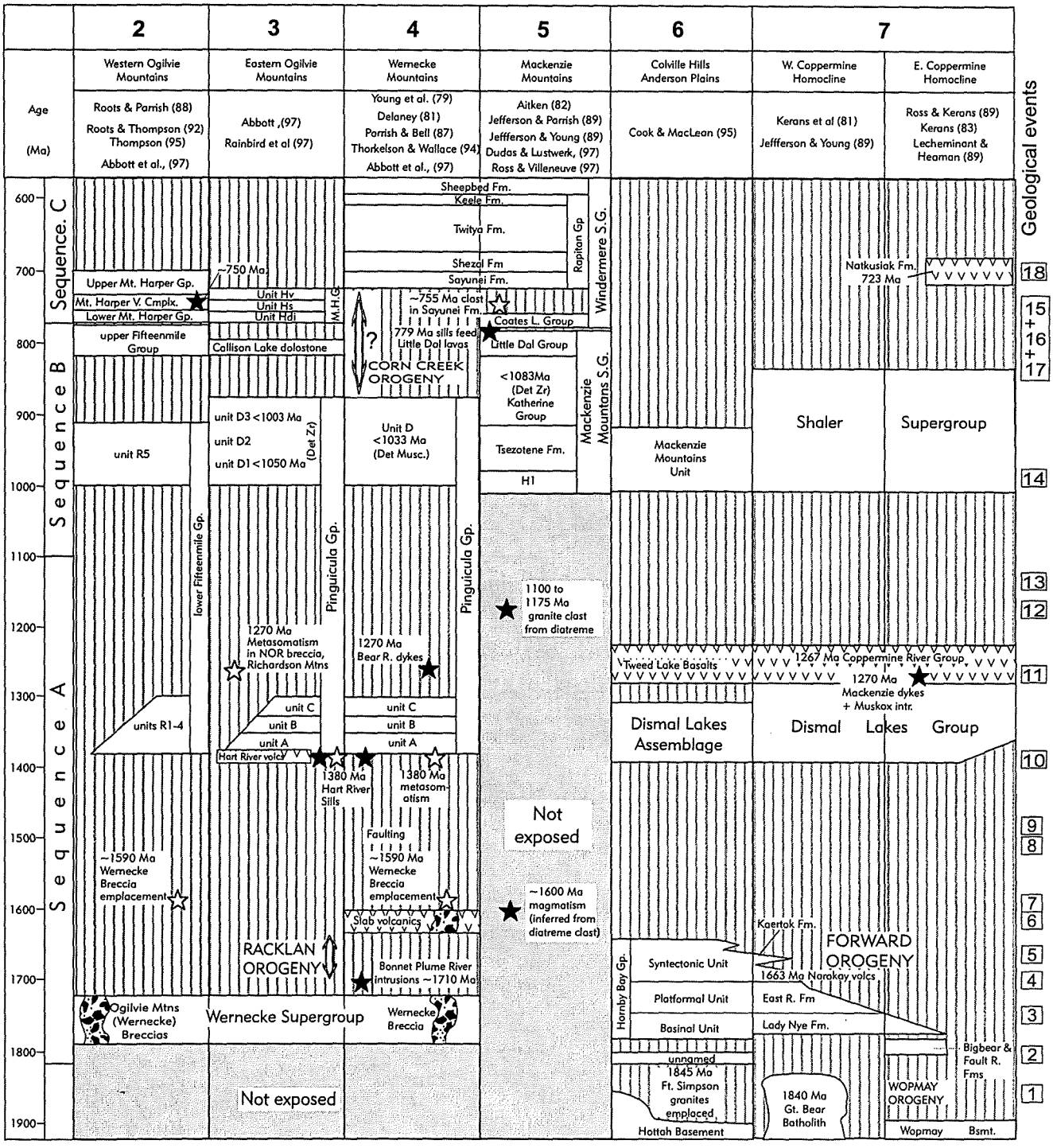

Fig. 2. Correlation of Proterozoic sequences in the Ogilvie, Wernecke, and Mackenzie mountains, and the western Arctic (modified from Cook and MacLean, 1995). Sections are located in Fig. 1. Approximate positions of the geological events discussed in text are indicated along right margin.

Mafic and Ultramafic Meta-Plutonic Rocks South of Finlayson Lake, Yukon: Setting and Implications for the Early Geological and Metallogenic Evolution of Yukon-Tanana Terrane

DONALD C. MURPHY

Yukon Geology Program, Government of the Yukon, Whitehorse, Yukon Y1A 2C6 Canada

Introduction

Mafic meta-volcanic and mafic and ultramafic meta-plutonic rocks locally occur with Upper Paleozoic meta-sedimentary and meta-volcanic rocks of Yukon-Tanana Terrane (YTT, Fig. 1) northeast of the Tintina Fault, southeastern Yukon (Wheeler et al. 1960; Tempelman-Kluit 1977, 1979; Mortensen and Jilson 1985; Mortensen 1992a,b). These bodies range from relatively small outliers of meta-basite and meta-ultramafic rocks with or without accompanying meta-volcanic rocks, to large regions of weakly deformed pillowed and massive flows interbedded with chert and argillite and lesser mafic and ultramafic plutonic rocks such as in the Campbell Range Belt (Fig. 1). These rocks have been interpreted as allochthonous slices of ocean floor that were juxtaposed against YTT during Jurassic thrust imbrication (see Mortensen 1992b for a recent summary).

Mafic and ultramafic meta-plutonic rocks are spatially associated with mafic meta-volcanic rocks in southern Grass Lakes map area south of Finlayson Lake (Fig. 2). As with similar rocks elsewhere, these rocks have been interpreted as allochthonous slices. These exposures were examined during the course of 1:50 000-scale regional mapping and the nature of these rocks and their relationship to the meta-sedimentary and meta-volcanic rocks of YTT has been re-evaluated. In contrast to previous interpretations, these rocks are not the structurally highest rocks in the area nor are they in structural contact with YTT rocks. Instead they are stratabound within a regionally persistent mafic meta-volcanic unit of YTT and show many features that are

compatible with the interpretation that they are an *in situ* sill(s). Furthermore, there is evidence that the sill(s) was fed by dyke(s) that intruded along a syn-volcanic, basin-bounding fault that may have controlled massive sulphide deposition at the Fyre Lake Cu-Co-Au deposit.

Setting of Mafic and Ultramafic Meta-Plutonic Rocks in Grass Lakes Map Area

Most of Grass Lakes map area is underlain by intensely foliated and lineated layered meta-sedimentary and meta-volcanic rocks and granitic orthogneiss of the Mississippian and older part of YTT, and two large stocks of peraluminous Cretaceous granite (Fig. 2). Mafic and ultramafic meta-plutonic rocks occur in the south-central and southeastern parts of the map area (Fig. 2, units 2mum and 2um). These include coarse-grained whitish-green leucoamphibolite (meta-gabbro), medium to dark green amphibolite (meta-pyroxenite, both shown together as unit 2mum in Fig. 2) and aeromagnetically prominent, dun-coloured meta-ultramafic rocks made up of talc, magnetite, serpentine, tremolite, phlogopite, and relict olivine, orthopyroxene and possibly chromite (unit 2um). West of the North River, four domains of meta-ultramafic rock are shown; these actually belong to one near-continuous sheet that is dissected by topography in such a way as to appear fragmented. Although offset by a fault in the North River valley, the sheet continues east of the North River where it is thicker, comprising two levels of meta-ultramafic rock overlain by a thick unit of leuco-amphibolite and amphibolite (Fig. 3).

Mapping around the meta-plutonic sheet shows that it is not on top of all the surrounding rocks but stratabound within one unit (Fig. 2 and 3). The sheet occurs for the most part within a regionally persistent biotite-actinolite-epidote-chlorite schist unit (unit 2m in Fig. 2) that is part of the YTT stratigraphic sequence defined for the area (Murphy 1997, 1998). The sheet is discontinuous, terminating to the west in unit 2m schist (Fig. 4). It increases in thickness from zero at its westward lateral termination to over 500 meters east of the North River. In the

southeasternmost corner of the map area, the base of the sheet cuts down through unit 2m to the extent where it lies directly on top of quartz-rich schist of the underlying stratigraphic unit, unit 1qsu. Uniquely to this area, meta-ultramafic rocks also appear at different levels in unit 1, occurring in unit 1qsu west of the Cretaceous granite and in stratigraphically deeper unit 1qsl at the same structural level east of the granite (Fig. 2). Southeast of the map area, the combined thickness of units 2m, 2mum and 2um decreases to less than 100m. Where observed, the contacts between the sheet and units 1 and 2 are sharp and show no evidence for being faulted or inordinately sheared. Locally the contact zone is characterized by the development of cm- to decimetre-scale crystals of epidote.

It is difficult to reconcile these observations with the interpretation that the mafic meta-volcanic and mafic and ultramafic meta-plutonic rocks are allochthonous. There is no evidence to suggest that the contacts with unit 2m are faults or shear zones. There is also no evidence that the contact between unit 2m and the underlying unit 1 is a fault or shear zone. Unit 2m chlorite schist is regionally extensive, and if its lower contact is a major thrust fault where associated with mafic and ultramafic meta-intrusive rocks, it would have to be a major thrust fault in other places; there is no evidence in support of this interpretation.

In contrast, the characteristics of the sheet of mafic and ultramafic meta-plutonic rocks are compatible with it being an *in situ* intrusion. The stratabound character of much of the sheet is reminiscent of a sill. The relationship of the sheet to units 1 and 2 in the southeastern corner of the map area and the occurrence of ultramafic rocks in unit 1 below the sheet in this area suggest a discordant character, possibly marking the locus of a transition from a sill to a feeder dyke. Furthermore, as this zone of apparent discordance is marked by the juxtaposition of different stratigraphic levels of unit 1 and a dramatic drop in the combined thickness of units 2m, 2mum

and 2um, the dyke may have intruded along a syn-volcanic fault. It should be noted that the **Fyre Lake** Cu-Co-Au massive sulphide deposit (Foreman, 1998; Hunt and Murphy, 1998) occurs in the upper part of unit 2m along strike from this area of discordance, stratigraphic juxtaposition and thickness change, suggesting a possible common genesis. Synvolcanic faults, thickness changes of volcanic rocks and increases in abundance of comagmatic intrusions are all considered to be pathfinders to the proximal portions of volcanic systems where volcanic-hosted massive sulphide deposits typically reside (e.g. Gibson et al. 1997).

Other smaller bodies of mafic and ultramafic meta-plutonic rocks occur in Grass Lakes map area. Where observed in detail, these are spatially associated with unit 2m. No mafic and ultramafic meta-plutonic rocks that could reasonably be interpreted as *in situ* intrusions occur above unit 2m, and only in the southeastern corner of the map area are ultramafic rocks associated with unit 1. This spatial association suggests that the mafic and ultramafic meta-plutonic rocks intruded into their possibly comagmatic unit 2m volcanic cover.

Discussion

One implication of this study is that other occurrences of mafic meta-volcanic and mafic and ultramafic meta-plutonic rocks associated with YTT should be re-evaluated. Obviously the large tracts of basalt, chert, gabbro and ultramafic rock such as in the Campbell Range Belt are best interpreted as ocean floor deposits that may be allochthonous with respect to YTT. However, there are several occurrences of rocks similar to those studied here that bear further investigation, especially in light of the proposed genetic association with the Fyre Lake deposit.

When combined with other stratigraphic information from Grass Lakes map area, the (Devono-?) Mississippian meta-volcanic rocks of YTT evolved from mafic to felsic and were succeeded by voluminous peraluminous granitic orthogneiss. Unit 2m mafic schist is the lowest

stratigraphic unit of Mortensen's (1992a) middle meta-volcanic-bearing unit of Yukon-Tanana Terrane. In Grass Lakes map area, unit 2m passes upward into carbonaceous schist with laterally variable and upwardly increasing amounts of Early Mississippian (Mortensen, 1992a) felsic meta-volcanic rock. Although mafic meta-volcanic rocks and carbonaceous phyllite also overlie the felsic rocks, the contact may be a significant regional unconformity which post-dated the intrusion of the voluminous peraluminous granitic orthogneisses (Murphy 1998). If so the overlying sequence is a significantly younger volcanic episode.

If applicable regionally, this locally defined evolution from mafic to felsic compositions is a feature that any tectonic model for YTT would need to address. If the (Devono-?) Mississippian meta-igneous rocks of Yukon-Tanana Terrane represent a continental magmatic arc (Mortensen and Jilson 1985, Rubin et al. 1990, Mortensen 1992b), perhaps the initial mafic meta-volcanic and mafic and ultramafic meta-plutonic rocks formed during the initial extensional cracking of the mechanical lithosphere at the onset of subduction and arc initiation similar to what has been proposed for supra-subduction zone ophiolites (e.g. Stern and Bloomer 1992). More detailed stratigraphic information from YTT is necessary before the full implications of these data for the evolution of the terrane can be appreciated.

References

Foreman, I.,1998, The Fyre Lake project 1997: geology and mineralization of the Kona massive sulphide deposit, *in* Yukon Exploration and Geology 1997, Exploration and Geological Services, Yukon Region, Indian and Northern Affairs Canada, p.99-109.

Gibson, H., Morton, R., and Hudak, G., 1997, Subaqueous volcanism: environments and controls on VMS mineralization. *in* Barrie, C.T. and Hannington, M.D. eds., Volcanic-associated massive sulfide deposits: processes and examples in modern and ancient settings, a short course

sponsored by the Geological Association of Canada and Society of Economic Geologists, Ottawa, May, 1997. Unpublished notes, p. 13-52.

Hunt, J.A. and Murphy, D.C., 1998, A note on preliminary bedrock mapping in the Fire Lake area, *in* Yukon Exploration and Geology 1997, Exploration and Geological Services, Yukon Region, Indian and Northern Affairs Canada, p. 79-90.

Mortensen, J.K., 1983, Age and evolution of the Yukon-Tanana terrane, southeastern Yukon Territory. Unpublished Ph.D thesis, University of California, Santa Barbara, 155p.

Mortensen, J.K., 1992a, New U-Pb ages for the Slide Mountain Terrane in southeastern Yukon Territory, *in* Radiogenic Age and Isotopic Studies: Report 5, Geological Survey of Canada, Paper 91-2, p. 167-173.

Mortensen, J.K., 1992b, Pre-mid-Mesozoic tectonic evolution of the Yukon-Tanana Terrane, Yukon and Alaska: Tectonics, v. 11, p. 836-853.

Mortensen, J.K. and Jilson, G.A., 1985, Evolution of the Yukon-Tanana terrane: evidence from southeastern Yukon Territory: Geology, v. 13, p. 806-810.

Murphy, D.C., 1997, Preliminary geological map of Grass Lakes area, Pelly Mountains, southeastern Yukon (105G/7), Exploration and Geological Services Division, Yukon, Indian and Northern Affairs Canada, Open File 1997-3, scale 1:50 000.

Murphy, D.C., 1998, Stratigraphic framework for syngenetic mineral occurrences, Yukon-Tanana Terrane south of Finlayson Lake: A Progress Report, *in* Yukon Exploration and Geology 1997, Exploration and Geological Services, Yukon Region, Indian and Northern Affairs Canada, p. 43-50.

Stern, R.J. and Bloomer, S.H.,1992, Subduction zone infancy: Examples from the Eocene Izu-Bonin-Mariana and Jurassic California arcs: Geological Society of America Bulletin, v. 104, p. 1621-1636.

Tempelman-Kluit, D.J., 1977, Quiet Lake (105F) and Finlayson Lake (105G) map areas, Yukon Territory: Geological Survey of Canada, Open File 486.

Tempelman-Kluit, D.J., 1979, Transported cataclasite, ophiolite and granodiorite in Yukon Territory: evidence of arc-continent collision: Geological Survey of Canada, Paper 79-14.

Wheeler, J.O.; Green, L.H. and Roddick, J.A., 1960, Finlayson Lake map area, Yukon Territory: Geological Survey of Canada, Map 8-1960.

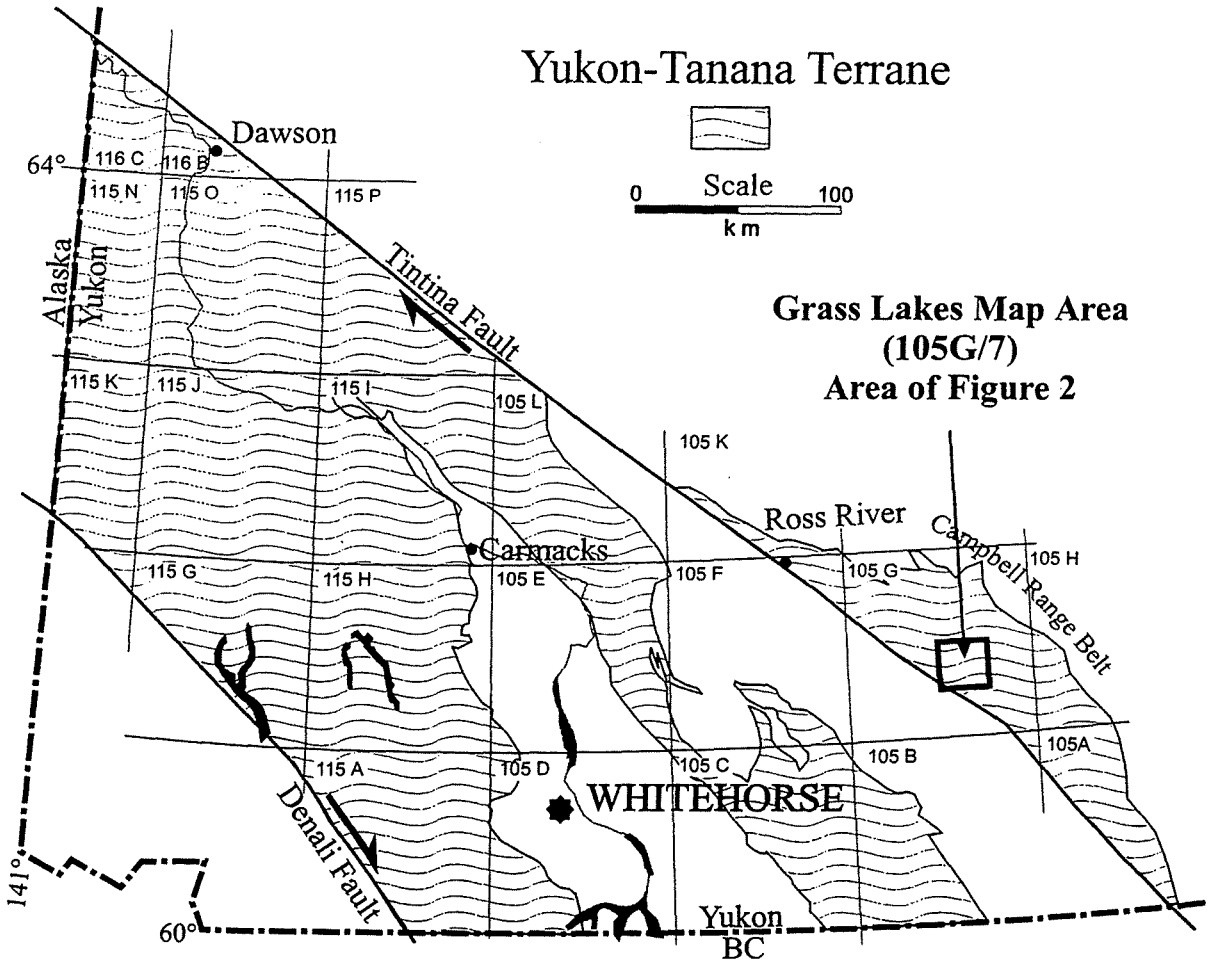

Fig. 1. Grass Lakes map area (105G/7) with respect to the distribution of Yukon-Tanana Terrane in Yukon. Bodies of mafic and ultramafic meta-plutonic rocks described in this report are generally too small to be shown at this scale.

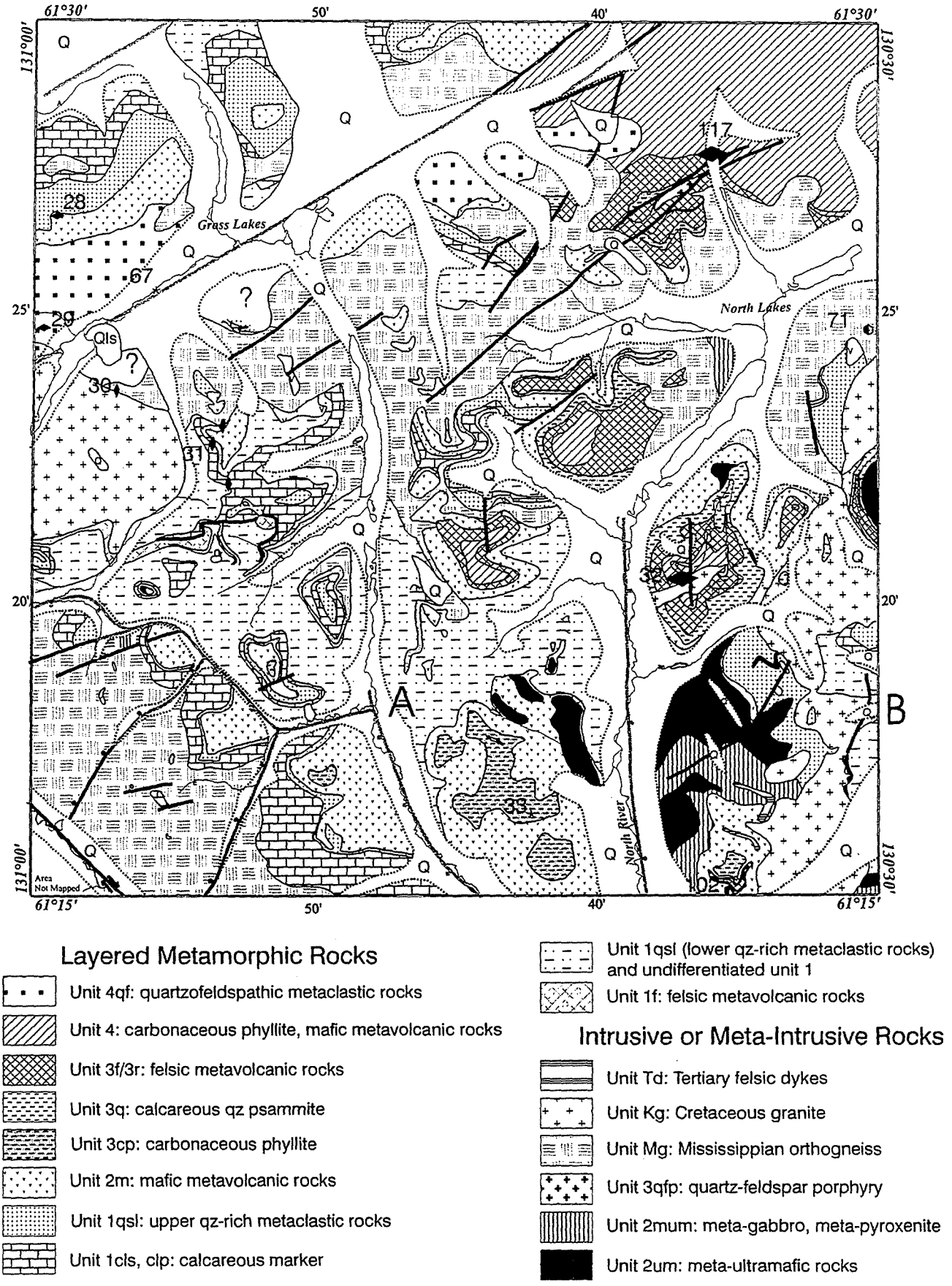

Fig. 2. Bedrock geological map of Grass Lakes map area (from Murphy 1997). Heavy dark and shaded lines are defined and inferred faults respectively. Section A-B shown in Figure 3.

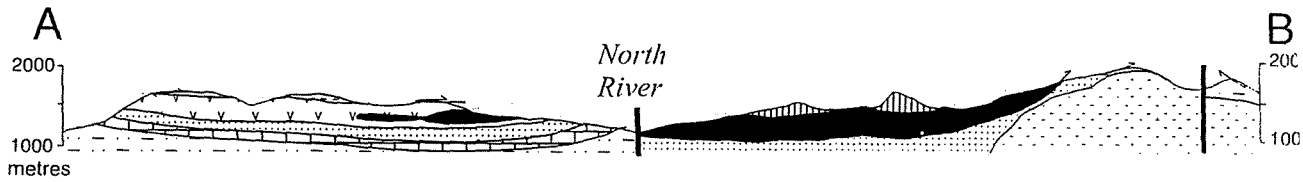

Fig. 3. Cross section through sheet of mafic and ultramafic meta-plutonic rocks discussed in text. Symbols are the same as in Figure 2.

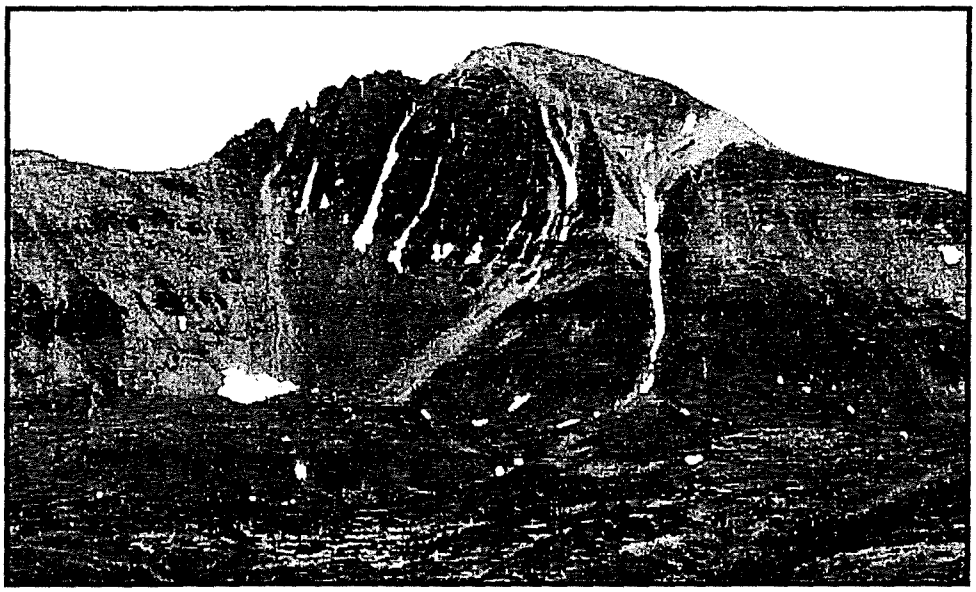

Fig. 4. View to south of lateral termination of meta-ultramafic body. The top of the peak is made up of chloritic schist of unit 2m which continues to the west (right) behind ridge. The massive meta-ultramafic body overlies a few metres of chloritic schist of unit 2m and the notably layered rocks of unit 1qsu. Note how deformation has wrapped the underlying unit 1 and 2m rocks around its westward termination

Kilometre-scale folding in the Teslin zone, northern Canadian Cordillera, and its tectonic implications for the accretion of the Yukon-Tanana terrane to North America

Martin de Keijzer and Paul F. Williams

Department of Geology, University of New Brunswick, P.O. Box 4400, Fredericton, N.B., E3B 5A3 , n29r@unb.ca

Abstract

Kilometre-scale folds (F_1 - F_4) mapped in rocks of the Anvil and Yukon-Tanana Nisutlin assemblages in the Teslin zone, northern Canadian Cordillera, place new constraints on the accretion of these rocks to the continental margin of ancestral North America. The folds have been established by mapping enveloping surfaces, overprinting relationships, and fold vergence. They largely explain the distribution of lithologies in the Teslin zone. At least three generations of regionally penetrative foliations (S_1 - S_3) associated with folding and transposition have previously been grouped into a single "steeply dipping" transposition foliation. The steep attitude, relative to surrounding rocks, of this transposition foliation was considered an important argument in modelling the Teslin zone as a steeply dipping crustal suture. Importantly, however, a regional-scale northwest-plunging F_3 synform partially explains the steep attitude of the Teslin zone rocks, in the area studied, since most of the zone coincides with the steep limb of this previously unrecognized synform. In addition, dips are steep on the shallow limb due to later localised F_4 folding. Hence the Teslin zone is not a 'simple' steeply dipping crustal suture. We suggest that the Teslin zone may incorporate part of a deformed and folded suture, most probably the contact between the Nisutlin and (eclogite-bearing) Anvil assemblages (comprising the hanging wall rocks) and North America (comprising the footwall rocks), but it is not a suture in the sense of previous interpretations.

The established geometry allows North American rocks (the Cassiar terrane) to be present at deeper crustal levels in the Teslin zone and to outcrop west and south of the Nisutlin and Anvil assemblages. Further, the northwest-plunging F_3 synform, truncated to the east by the d'Abbadie fault system, provides a possible explanation for the marked narrowness of the Teslin zone relative to the Yukon-Tanana terrane to the north. If the F_3 fold is one of a train of similar folds then the structure should open to the north (widening of the Yukon-Tanana terrane) as successive hinges cut the surface.

THE ST. CYR KLIPPE, SOUTH-CENTRAL YUKON: AN OUTLIER OF THE TESLIN TECTONIC ZONE?

[1]**Karen M. Fallas** (e-mail: karen.fallas@ualberta.ca)
[1]**Philippe Erdmer** (e-mail: p.erdmer@ualberta.ca)
[2]**Douglas A. Archibald** (e-mail: archiba@geol.queensu.ca)
[1]**Larry M. Heaman** (e-mail: larry.heaman@ualberta.ca)
[1]**Robert A. Creaser** (e-mail: robert.creaser@ualberta.ca)

[1] Dept. of Earth and Atmospheric Sciences, University of Alberta, Edmonton, AB, T6G 2E3.
[2] Dept. of Geological Sciences, Queen's University, Kingston, ON, K7L 3N6.

Studies of the Yukon-Tanana and Slide Mountain terranes in south-central Yukon have in the past focused on the Teslin Tectonic Zone (TTZ - Hansen et al., 1989, Hansen, 1992, Stevens et al.,1996). Very little work has been done in the klippen which lie to the NE of the TTZ on the Cassiar terrane, even though it has long been inferred that the klippen record the same structural and metamorphic history as the TTZ (Tempelman-Kluit, 1979). The St. Cyr klippe (SCK) is one of these klippen (Fig. 1). It preserves mafic and ultramafic metaigneous rocks of the Anvil allochthonous assemblage (ANV - correlated with the Slide Mountain terrane), as well as metasedimentary rocks of the Nisutlin allochthonous assemblage (NIS - correlated with Yukon-Tanana terrane, Wheeler and McFeely, 1991). Current work on the St. Cyr klippe demonstrates that there are both similarities and differences between the timing of deformation and metamorphism in the TTZ and the klippen to the NE.

Structural relationships:

Original reconnaissance-scale mapping by Tempelman-Kluit (1977) identified allochthonous klippen preserved in broad regional synformal warps. The klippen interpretation is based on the contrast in the amount of ductile strain and metamorphic grade between ANV and NIS vs. platformal rocks of the Cassiar terrane. The high-angle relationships between footwall and hangingwall fabrics and the trace of the inferred thrust further support this interpretation. The similarity in rock type, mylonitic fabrics and metamorphic grade between the TTZ and the SCK led to the interpretation of the TTZ as the root zone from which the ANV and NIS were thrust to the NE to form the SCK in the late Jurassic or early Cretaceous (Tempelman-Kluit, 1979).

Recent work by Hansen (1989) and Stevens and Erdmer (1996) documented dip-slip extension lineations in mylonitic rocks of the TTZ, which have been interpreted either as recording dip-slip shear in a subduction zone (Hansen, 1992), or a zone of transpression (Stevens and Erdmer, 1996). After thrusting to the NE, these lineations should be sub-horizontal and trending NE-SW. Extension lineations in the SCK are sub-horizontal to moderately plunging and trend NW or SE (Fallas, 1997), which clearly conflicts with the kinematics of fabrics in the TTZ and is not related to thrusting. Interestingly, NW-SE trending fold axes have been documented in the Last Peak area of the TTZ (de Keijzer, 1997), but their relationship to the extension lineations is unclear. One explanation for the difference in extension lineation orientation is the possibility that the lineations in the SCK are older, and the TTZ has since been overprinted by younger deformation.

Within the TTZ, coherent domains of consistent lineation orientation and shear sense have been identified (Hansen, 1992, Stevens and Erdmer, 1996). Domains of consistent fabric orientation are rare in the SCK, and shear-sense indicators from one outcrop to another are in

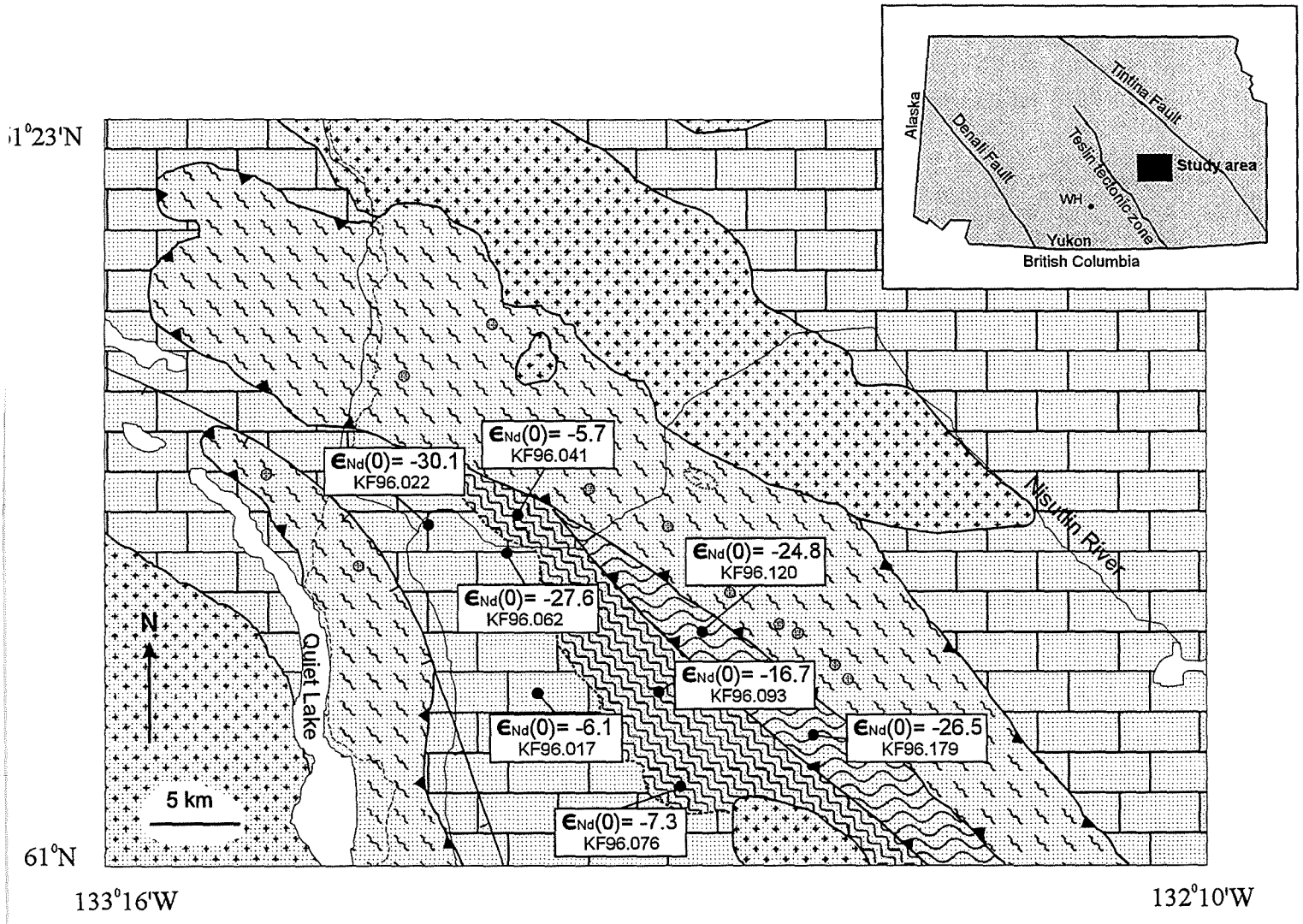

Figure 1. Simplified geology of the St. Cyr and Quiet Lake klippen showing the results of Sm-Nd geochemistry on metasedimentary rocks of the Cassiar and Nisutlin terranes (white boxes).

many cases opposing or non-systematic. The possibility remains that opposing senses of shear are the result of more than one phase of ductile simple shear. Again, the SCK appears to record a different phase(s) of ductile deformation which may be related to overprinting in the TTZ.

Nisutlin geochemical signature:

In an effort to further distinguish between allochthonous and autochthonous rocks in the SCK area, Sm-Nd isotopic analyses were obtained for metasedimentary rocks of the NIS and the Cassiar terrane. Sample locations and ϵNd(0) values are shown in Figure 1. Rocks of the Cassiar terrane have ϵNd(0) values ranging from -6.1 to -30.1, rocks from the upper panel of NIS have ϵNd(0) values of -24.8 and -26.5, and rocks from the lower panel of NIS have ϵNd(0) values ranging from -5.7 to -16.7. The distinction between the upper and lower panels of NIS is made from differences in the amount of strain and metamorphic grade. This distinction can also be made based on the ϵNd (0) values, which do not overlap for these two units. However, the overlap of ϵNd(0) values for both panels of the NIS with those of the Cassiar terrane leaves the allochthonous vs. autochthonous relationship unclear. This is not helped by the lack of Sm-Nd data for the North American platform of the Northern Cordillera. To further confuse matters, ϵNd(0) values reported for the NIS in the TTZ range from +0.5 to -28.4 (Creaser et al., 1997) which covers the range of values determined for both the NIS and the Cassiar terrane in the SCK. Overlap in t_{DM} values also occurs between the NIS of the TTZ (t_{DM}= 0.9-2.8 Ga) and both the NIS and Cassiar terrane of the SCK (t_{DM}=1.2-2.4 Ga). This can be interpreted to support the correlation of NIS in the SCK with NIS in the TTZ. What this technique cannot yet do, is distinguish between allochthonous and autochthonous rocks for the Northern Cordillera.

Geochronology:

Another test of the link between the SCK and the TTZ has been done using U-Pb and $^{40}Ar/^{39}Ar$ geochronological techniques to date both primary igneous activity and metamorphic events (summarized in Fig. 2). Igneous activity for the ANV within the SCK is constrained by one new U-Pb zircon age for a sheared hb tonalite (concordia plot shown in Figure 3b). Foliation within the tonalite body is parallel to foliations in neighboring amphibolite indicating the structurally conformable nature of the contacts. Zircon fractions A and C were clear, colourless prisms with no cores and good prism faces. Fraction B had small inclusions of hornblende, which explains the greater discordance of this fraction. The correspondence of the $^{207}Pb/^{206}Pb$ ages for fractions A and C suggests that their discordance is the result of modern lead loss. The simplest interpretation of this data is to average the $^{207}Pb/^{206}Pb$ ages for fractions A and C and infer a primary crystallization age of 373 +/- 1 Ma. This age is similar to Devonian igneous activity for the Slide Mountain terrane elsewhere in the Cordillera (Mortensen, 1992), and is marginally older than a tonalite body in the TTZ (Stevens et al., 1993).

The timing of metamorphism in the SCK is constrained by U-Pb and Ar-Ar results. Low Th/U ratios in zircon fractions from the Deer Creek eclogite (KF95-10) indicate metamorphic growth in otherwise zircon-barren basalt (see Heaman and Parrish, 1991). Garnet-pyroxene thermometry on this sample yielded peak metamorphic temperatures of 450 - 525°C (Erdmer et al., in press), which is below the closure temperature for the U-Pb system in zircon (>800°C, Heaman and Parrish, 1991). Thus the age of 266 +/- 1 Ma likely dates either prograde or peak metamorphism (Fig. 3a). The slight discordance and tight cluster of fractions A, B, D, and E did not yield a meaningful discordia line, so the age was calculated by averaging the $^{206}Pb/^{238}U$ and $^{207}Pb/^{235}U$ ages of the four fractions. This age matches within error the age of the Last Peak eclogite from the TTZ (269 +/- 2 Ma, Creaser et al., 1996), providing another strong link between the SCK and the TTZ.

A more widely applicable method for

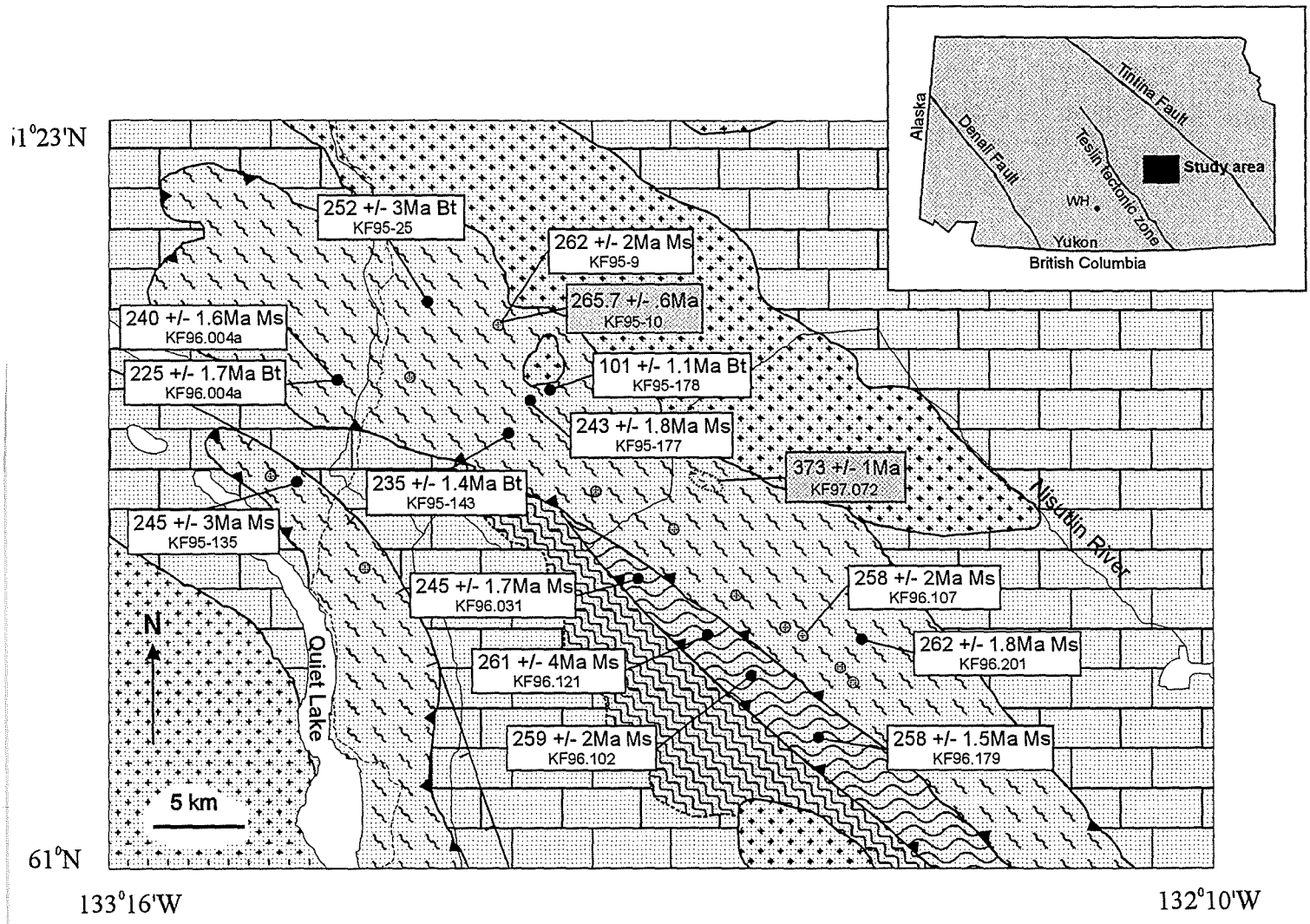

Figure 2. Results of ^{40}Ar-^{39}Ar geochronology on muscovite and biotite separates from mica schists and eclogites of the Anvil and Nisutlin allochthonous assemblages (white boxes), and U-Pb (zircon) geochronology from an eclogite and a sheared hb tonalite of the Anvil allochthonous assemblage (grey boxes). All errors are 2σ.

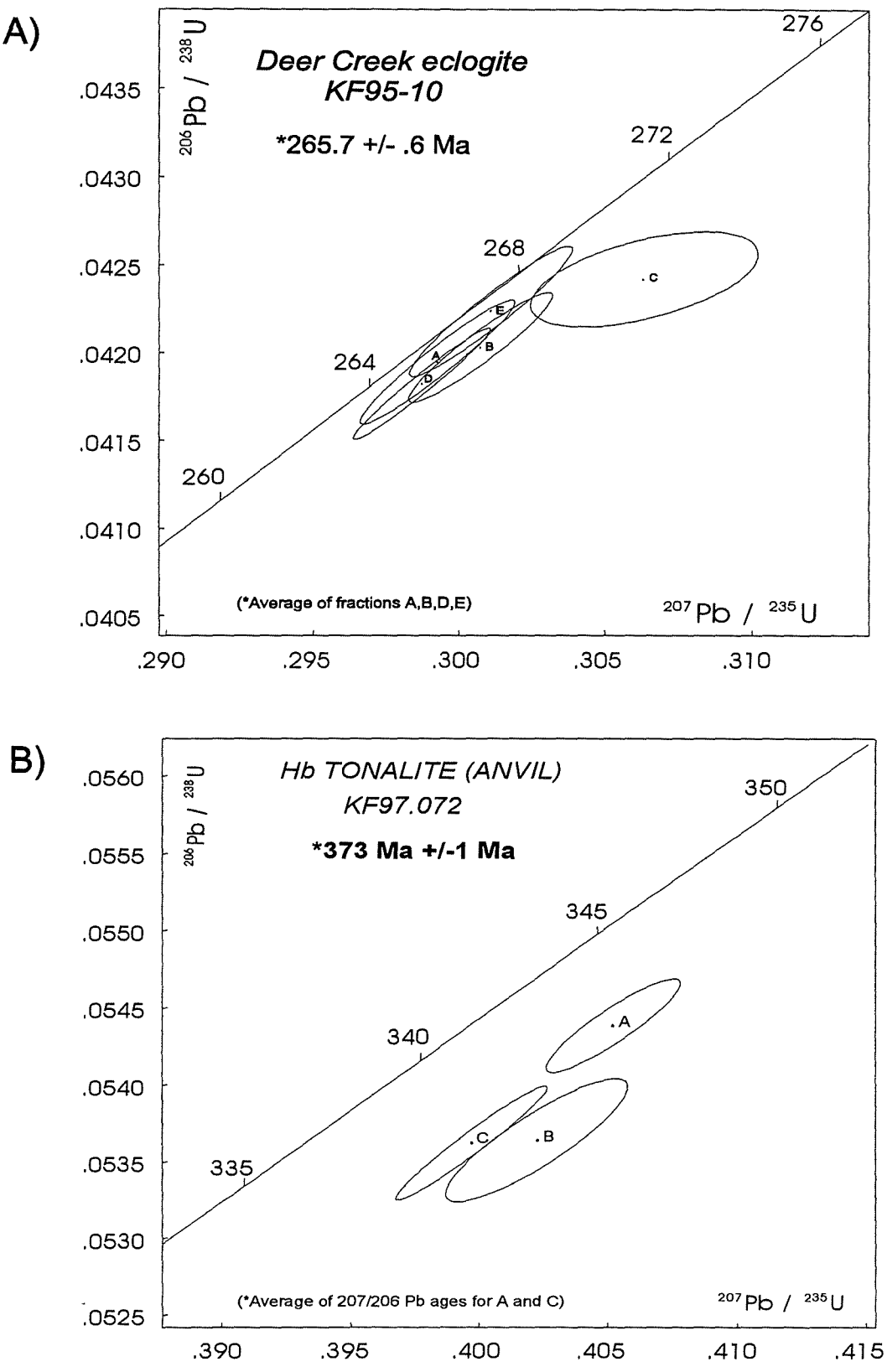

Figure 3. U-Pb concordia diagrams for zircon analyses from the Anvil allochthonous assemblage. Error ellipses for each fraction are 2σ. Plot A) constrains the timing of eclogite facies metamorphism to mid-Permian, and plot B) constrains primary igneous activity to late Devonian (or possibly as young as Mississippian).

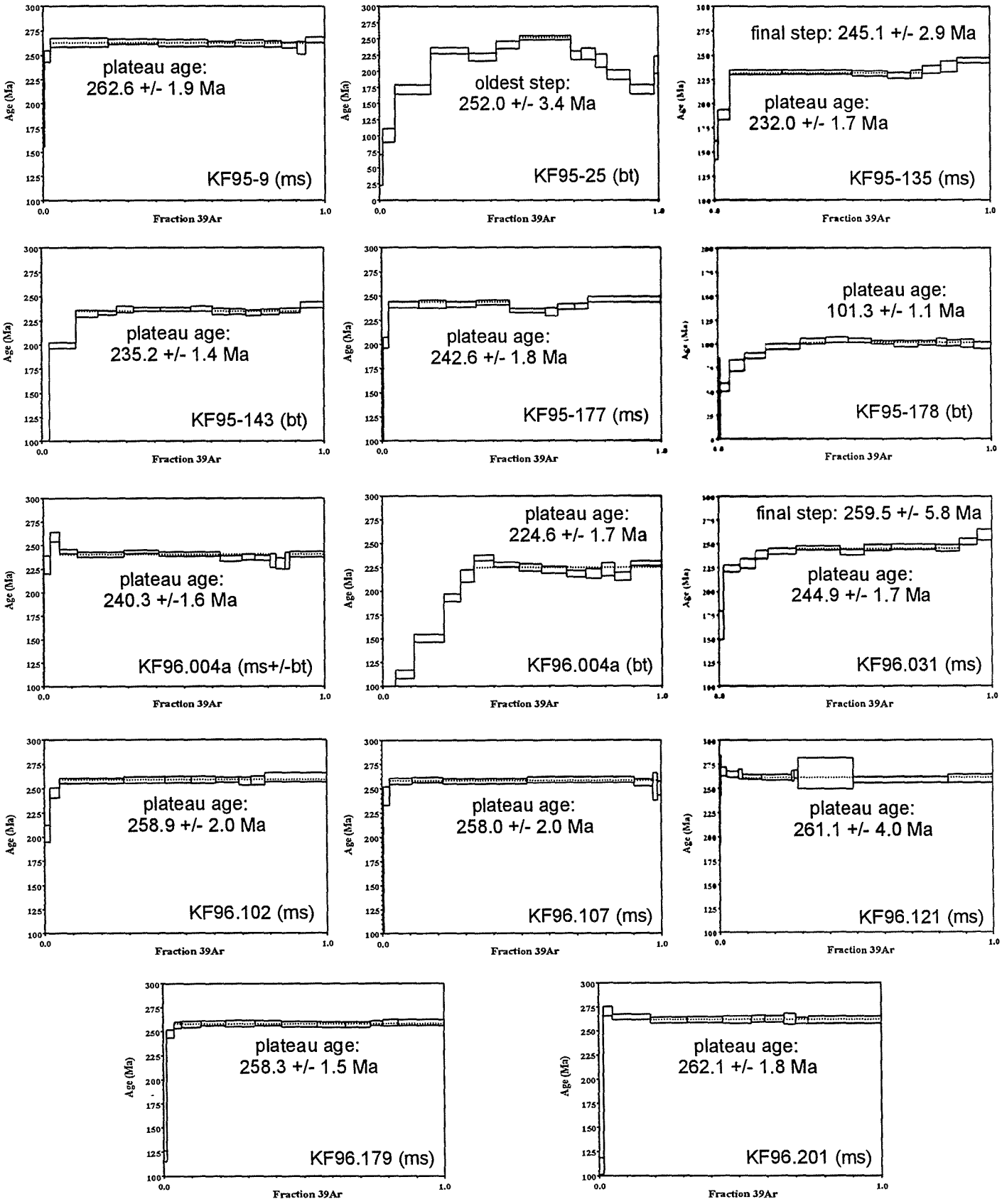

Figure 4. Ar release spectra for step heating of mica separates from eclogite and siliceous mylonite of the Anvil allochthonous assemblage, and gt-ms schist of the Nisutlin allochthonous assemblage. The dashed line indicates which steps are included in the plateau age calculation. Errors are at the 2σ level.

dating metamorphism in the SCK is $^{40}Ar/^{39}Ar$ dating of micas found in schists, micaceous mylonites, and eclogite in both the ANV and NIS. Ages and sample locations are shown in fig.2 and Ar release spectra are shown in fig.4. The first point of note in this data is a Ms cooling age of 262 +/- 2 Ma (undisturbed plateau) for sample KF95-9, which was taken from the same outcrop as sample KF95-10 for which the metamorphic zircon age is 266 +/- 1 Ma. The short time between the two dates is consistent with cooling after one metamorphic event since muscovite has a lower closure temperature for Ar (350°C, Heaman and Parrish, 1991) than Pb in zircon. Both systems must therefore be recording the same metamorphic event. Secondly, ages ~260 Ma with undisturbed plateaus (see Fig.4) also occur in micaceous mylonites of the ANV and schists of the NIS indicating that this metamorphic event was widespread and not limited to the eclogites of the SCK. This in turn emphasizes the common metamorphic history of the ANV and NIS. Thirdly, the micas in these samples are fabric-defining (syn-kinematic), so these cooling ages also date the ductile fabrics as mid-Permian in age.

In cases where the Ar release spectra are disturbed (eg. KF96.031, Fig.4), final steps are significantly older, and some approach 260 Ma suggesting that these samples originally experienced the Permian metamorphic event and were subsequently overprinted in the Triassic. Ar release spectra for biotite samples are less systematic (eg. KF95-25, Fig.4) but are consistently younger than muscovite cooling ages, which is consistent with its lower closure temperature (~280°C, Heaman and Parrish, 1991). It is worth noting that the only sample overprinted by the mid-Cretaceous intrusions in the area is a sample of biotite collected within 200 m of a mid-Cretaceous stock (KF95-178, Fig.4).

Regionally, rocks which record Permian metamorphic events are so far limited to a few blueschists and eclogites scattered throughout the Cordillera (Erdmer et al., in press). Significantly, there are no documented Permian mica cooling ages within the TTZ - the only Permian age in the TTZ is the zircon age of the Last Peak eclogite. In general, mica cooling ages in the TTZ record Jurassic cooling (Hansen et al., 1989). Two Triassic cooling ages of 213 Ma and 233 Ma on the east side of the TTZ at Little Salmon Lake (D. Oliver, pers. comm., 1997) may record the same Triassic event which overprints some of the SCK samples.

Summary:

Rocks of the Teslin Tectonic Zone and the St. Cyr klippe share numerous features which support their correlation and the interpretation of the TTZ as the root zone of the SCK. These features include: rocks types, amount of strain, metamorphic grade, $\epsilon Nd(0)$ values, t_{DM} values and timing of eclogite facies metamorphism. Important differences between the TTZ and the SCK are in the orientation of extension lineations, kinematics inferred from sense of shear, metamorphic cooling ages, and possibly the timing of primary igneous activity. Most of these differences may be explained by younger (Jurassic) shearing and metamorphism which would overprint older (Permian) shearing and metamorphism within the TTZ and does not affect the SCK.

References

Creaser, R.A., P. Erdmer, R.A. Stevens, and S.L. Grant (1997) Tectonic affinity of Nisutlin and Anvil assemblage strata from the Teslin Tectonic Zone, Northern Canadian Cordillera: constraints from neodymium isotope and geochemical evidence. *Tectonics,* vol.16, pp.107-121.

Creaser, R.A., L.M. Heaman, and P. Erdmer (1996) U-Pb zircon dating of eclogite from the Teslin tectonic zone: Constraints for the age of high-pressure metamorphism in the Yukon-Tanana terrane. in F. Cook and P. Erdmer (compilers), *Slave-Northern Cordilleran Lithospheric Evolution (SNORCLE) and Cordilleran Tectonics Workshop Meeting (March 1-3), University*

of Calgary, Lithoprobe Report No. 50, pp.58-60.

de Keijzer, M., and P.F. Williams (1997) A new view on the structural framework of the Teslin zone, south-central Yukon. in F. Cook and P. Erdmer (compilers), *Slave-Northern Cordilleran Lithospheric Evolution (SNORCLE) and Cordilleran Tectonics Workshop Meeting (March 7-9), University of Calgary, Lithoprobe Report No. 56,* pp.96-102.

Erdmer, P., E.D. Ghent, D.A. Archibald, M.Z. Stout (in press) Paleozoic and Mesozoic high-pressure metamorphism at the margin of ancestral North America in central Yukon. *GSA Bulletin,* May 1998 issue.

Fallas, K.M. (1997) Preliminary constraints on the structural and metamorphic evolution of the St. Cyr klippe, south-central Yukon. in F. Cook and P. Erdmer (compilers), *Slave-Northern Cordilleran Lithospheric Evolution (SNORCLE) and Cordilleran Tectonics Workshop Meeting (March 7-9), University of Calgary, Lithoprobe Report No. 56,* pp.90-95.

Hansen, V.L. (1989) Structural and kinematic evolution of the Teslin suture zone, Yukon: record of an ancient transpressional margin. *Journal of Structural Geology,* vol.11 (6), pp.717-733.

Hansen, V.L. (1992) Backflow and margin-parallel shear within an ancient subduction complex. *Geology,* vol.20, pp.71-74.

Hansen, V.L., J.K. Mortensen, and R.L. Armstrong (1989) U-Pb, Rb-Sr, and K-Ar isotopic constraints for ductile deformation and related metamorphism in the Teslin suture zone, Yukon-Tanana terrane, south-central Yukon. *Canadian Journal of Earth Sciences*, vol.26, pp.2224-2235.

Heaman, L.M., and R. Parrish (1991) U-Pb geochronology of accessory minerals. in L. Heaman and J.N. Ludden (eds.), *MAC Short Course on Radiogenic Isotope systems,* vol.19, pp.59-102.

Mortensen, J.K. (1992) New U-Pb ages for the Slide Mountain Terrane in southeastern Yukon Territory. in *Radiogenic age and isotopic studies: Report 5; Geological Survey of Canada,* Paper 91-2, pp.167-173.

Stevens, R.A., and P. Erdmer (1996) Structural divergence and transpression in the Teslin tectonic zone, southern Yukon Territory. *Tectonics,* vol.15 (6), pp.1342-1363.

Stevens, R.A., J.K. Mortensen, and P.A. Hunt (1993) U-Pb and 40Ar-39Ar geochronology of plutonic rocks from the Teslin suture zone, Yukon Territory. in *Radiogenic age and isotopic studies, report 7; Geological Survey of Canada,* Paper 93-2, pp.83-90.

Tempelman-Kluit, D.J., (1977) Quiet Lake (105F) and Finlayson Lake (105G) map areas, Yukon. *Geological Survey of Canada,* Open File 486.

Tempelman-Kluit, D.J. (1979) Transported cataclasite, ophiolite and granodiorite in Yukon: evidence of arc-continent collision. *Geological Survey of Canada,* Paper 79-14.

Wheeler, J.O., and P. McFeely (1991) Tectonic Assemblage Map of the Canadian Cordillera and adjacent parts of the United States of America. *Geological Survey of Canada Map* 1712A.

STRUCTURAL GEOMETRY OF THE CASSIAR PLATFORM AND TESLIN ZONE, DYCER CREEK AREA, YUKON

Chris S. Gallagher, Richard L. Brown and Sharon D. Carr
Ottawa-Carleton Geoscience Centre and Department of Earth Sciences, Carleton University, Ottawa, Ontario, K1S 5B6

INTRODUCTION

The Teslin Zone (TZ) is the narrowest portion of the Yukon Tanana Terrane (YTT), measuring 15-20 km wide by 200 km long, and is distinguished from the rest of the YTT by a generally NW striking, steeply dipping fabric. In the central Yukon, (inset, Figure 1) it is bounded to the west by the Big Salmon Fault and to the east by the north-south trending d'Abbadie Fault Zone (DFZ). To the west of the TZ lie oceanic and island arc rocks of Quesnellia (Gabrielse and Yorath, 1991). The Teslin Zone consists mainly of greenschist-facies metasedimentary rocks interpreted to be part of the Nisutlin Assemblage (Kooteny terrane) and greenschist-facies mafic volcanic rocks of the Anvil Assemblage (Slide Mountain terrane; Tempelman-Kluit, 1979; Hansen, 1989, 1991a, 1992b; Mortensen, 1992; Harvey et al. 1997a, de Keijzer and Williams 1997). To the east of the TZ lie autochthonous rocks of the Cassiar Platform (CP) that consist mainly of Proterozoic Windermere Supergroup rocks (Gabrielse and Yorath, 1991).

Previous workers have interpreted the TZ as a trench melange situated above a west-dipping subduction zone that separates autochthonous North American strata to the east from allochthonous strata to the west (Tempelman-Kluit, 1979; Hansen, 1989, 1991a, 1991b). These interpretations were made on the basis of eclogite and blueschist facies rocks within Anvil rocks (Tempelmen-Kluit, 1979; Erdmer and Helmstaedt, 1983; Erdmer, 1985; Creaser et al., 1997), the presence of 'cataclastic' or mylonitic fabrics consisting of two generations of stretching lineations and asymmetric S-C fabrics (Tempelmen-Kluit, 1979; Hansen, 1989), and a lack of stratigraphic continuity within the zone (Hansen, 1989; Erdmer, 1989; Tempelmen-Kluit, 1979).

As part of a joint Lithoprobe project with R. L. Brown and, S. D. Carr of Carleton University, and P. F. Williams of the University of New Brunswick, 1:5000 and 1:25000 scale geologic mapping of the Teslin Zone, Cassiar Platform and associated klippen has been conducted by de Keijzer and, Harvey and Gallagher in 1995, 1996 and 1997 (Figure 1). Their results indicate that map units in the Teslin Zone occur as km-scale lenses and layers that may be continuous for up to 20 km in length. This map pattern is not consistent with chaotic trench melange geometry; rather it results from at least two phases of transposition within the Teslin Zone (Harvey *et al.*, 1997a; de Keijzer and Williams, 1997). de Keijzer and Williams (1997) show that the steep orientation of fabrics within the Teslin Zone resulted from a km-scale east verging fold that rotated flat lying transposed stratigraphy into a steep orientation. Panels of flat-lying and steeply west-dipping fabrics represent the shallow and steep limbs of the km-scale F_3 Grizzly synform mapped at Last Peak (Figure 1; de Keijzer and Williams, 1997). This geometry is not consistent with that of a suture zone situated above a west dipping subduction zone; rather the Teslin Zone and adjacent rocks have been reinterpreted as a fold thrust belt (Brown *et al.*, 1995, 1998).

This paper contains some of the results from 1:25,000 scale geologic mapping of

the Dycer Creek Area (Figure 1), and constitutes the M. Sc. Project of C. S. Gallagher. Research was conducted during the summer of 1997 in order to determine the structural style and geometry of the Dycer Creek area to see if it is representative of a fold belt, and to determine the timing and style of deformation of the d'Abbadie Fault Zone to evaluate whether or not it is a terrane boundary as suggested by Tempelman-Kluit (1979) and Hansen (1989, 1992a,b).

GEOLOGY OF THE DYCER CREEK AREA

The 9 km by 14 km Dycer Creek area straddles the d'Abbadie Fault Zone (DFZ), a steep ductile-brittle fault which separates the Teslin Zone from the Cassiar Platform (Figure 1). The map area will be described in terms of two structural domains, the Western Domain and the Eastern Domain, which lie to the west and east of the d'Abbadie Fault Zone, respectively.

Western Domain

The Western Domain consists of polyfolded greenschist to lower amphibolite facies metasedimentary and metavolcanic rocks of the Last Peak Assemblage and the Mendocina Assemblage (Harvey *et al.*, 1997a). The Last Peak Assemblage, consisting of calcareous schists, quartzites, marbles, and chlorite psammites, comprises most of the map area (Figures 1 & 2). The Mendocina Assemblage consists of fine grained chlorite schists, and is poorly exposed along the western margin of the map area. The dominant fabric in the metasediments is a steeply east-dipping $S_{0\text{-}2}$ transposition fabric. The Last Peak Assemblage was intruded by two variably deformed granites, the Mendocina Orthogneiss and the Last Peak Granite (Harvey *et al.* 1997a,b).

The Last Peak Granite is a NNW trending leucogranite which extends along strike for 14 km (Figure 2). A U-Pb igneous monazite age of 98±1 Ma is interpreted to represent the igneous crystallization age (Harvey *et al.*, 1997a,b). Cross cutting relationships indicate that the granite intruded the metasedimentary rocks of the Last Peak assemblage after regional ductile deformation in the adjacent country rock had ceased (Harvey *et al.*, 1997a). A chilled margin at the western contact, along with a thin metamorphic aureole, is consistent with intrusion into a cool upper-crustal environment (Harvey *et al.*, 1997a,b). Fabrics within the Last Peak Granite display ductilely deformed K-feldspar and quartz grains, indicative of high temperature deformation, and occur throughout the granite. Protomylonitic and mylonitic fabrics within the granite are sub-parallel to the NW trending regional transposition fabric ($S_{0\text{-}2}$) of the Western Domain. The granite displays well developed S-C fabrics and sigma and gamma K-feldspar and plagioclase porphyroclasts, all of which indicate a dextral sense of shear (Harvey *et al.*, 1997a,b). These field relationships indicate that the Last Peak Granite intruded into the upper crust immediately prior to or during motion along the DFZ (Harvey *et al.* 1997a,b).

The Mendocina Orthogneiss is a NNW trending two mica granite that outcrops along the western margin of the Last Peak Granite. Its age is not well constrained and a U-Pb study is underway by Carr and Gallagher to refine the age. Hansen *et al.* (1989, 1991) obtained a strongly discordant U-Pb igneous zircon age of 355.5+49/-50 Ma and Rb-Sr, K-Ar and ^{40}Ar - ^{39}Ar ages of 102-97 Ma. Contacts between the Mendocina Orthogneiss and the metasedimentary rocks of the Last Peak assemblage are concordant (Figure 2) and there is no apparent chilled margins or contact metamorphism (Harvey *et al.*, 1997a). The fabric of the orthogneiss is more complex than that of the Last Peak

Granite, suggesting a protracted deformation history. In hand specimens a foliation is observed that has been crenulated and transposed into the dominant shear foliation. This early fabric may record a deformation associated with regional shortening that pre-dates dextral shear along the DFZ.

d'Abbadie Fault Zone (DFZ)

The DFZ is a north-south trending sub-vertical structure which extends from Last Peak (de Keijzer and Williams, 1996) to the South Big Salmon River (Figure 1). To the south, it is crosscut by the Quiet Lake Batholith (Stevens, 1996; 83 Ma K-Ar age; Tempelman-Kluit, 1984). The DFZ generally occurs within a siliceous graphitic phyllite unit which appears to have acted as a weak zone within the TZ (de Keijzer and Williams, 1997). Brittle deformation is concentrated within vertical, roughly N-S trending micro faults separating 5 - 15 cm thick zones of very fine grained cataclasite. Although no consistent sense of displacement could be determined from these brittle fabrics, fourth order drag folds suggest a component of dextral strike-slip shear within the brittle fault zone. No piercing points could be determined and the constraints on the magnitude of displacement are uncertain. At the latitude of the Dycer Creek area, there is a similarity in structural style on both sides of the fault, and there is no apparent metamorphic offset associated with motion along the DFZ.

Eastern Domain

Greenschist-facies metasedimentary rocks of the Cassiar Platform have been intruded by two variably deformed igneous bodies, the Dycer Creek Stock and the Little Lake Granite. Metasedimentary rocks consist mainly of light grey marble and graphitic phyllite with minor siliceous mica schist, quartzite and minor slate (Figure 2). Contacts between units vary from sharp to gradational. The dominant fabric is a variably dipping NW trending transposition fabric ($S_{0\text{-}2}$).

The Little Lake Granite is a fine grained muscovite - biotite granite which has a light grey fresh surface and weathers dark grey to brown. It is a 100 - 150 metre thick NW trending sheet (Figure 2), with contacts parallel to the regional transposition foliation. The western contact of the granite with adjacent marbles is well exposed. The eastern margin of the granite, which is in contact with both marble country rock and the Dycer Creek Stock, is not as well exposed.

The Dycer Creek Stock is a coarse grained biotite granite with a weak foliation defined by ~1 cm diameter biotite crystals. The intrusive contact of the stock varies from highly-discordant to concordant with the transposition foliation in the country rock. Locally there is a distinct contact aureole consisting of a 10 metre wide calc-silicate skarn composed of coarse grained calcite, diopside, biotite and garnet.

STRUCTURE OF THE WESTERN DOMAIN

Three generations of structures were identified and each is characterized by a penetrative foliation ($S_{0\text{-}1}$, $S_{0\text{-}2}$, S_3) and fold generation (F_1, F_2, F_3).

Fabrics

The earliest transposition fabric, $S_{0\text{-}1}$, is locally preserved within F_2 hinges where it is at an angle to $S_{0\text{-}2}$. Compositional layering on the centimetre scale as well as the preferred orientation of metamorphic chlorite, biotite and muscovite defines $S_{0\text{-}1}$. The

dominant transposition fabric, S_{0-2}, is consistently NW striking and displays a steep eastward dip. It is defined by transposed compositional layering on the centimetre to decimeter scale and boudinaged quartz veins concordant with a metamorphic mineral foliation composed of graphite, chlorite, muscovite and biotite. S_3 is a penetrative cleavage that is axial planar to F_3 folds with a typical spacing of 1 - 3 cm. S_3 is consistently east dipping at ~45 ° and is best preserved within the calcareous graphitic schist of the Last Peak Assemblage. S_3 axial planar cleavage is defined by both graphite and muscovite and becomes more prominent to the north at Last Peak (de Keijzer and Williams, 1996).

Minor Fold Geometry

F_1 isoclinal folds are preserved as hooks and sheared hinges within S_{0-1} and S_{0-2} and are axial planar to the S_{0-1} transposition fabric. It is unclear whether primary layering or an unidentified older transposition fabric is being folded by F_1 folds. There are no mineral lineations associated with the F_1 folds. F_2 folds are tight to isoclinal, upright to slightly overturned folds with typically steeply east-dipping axial planes parallel to S_{0-2} (Figure 3a). They are shallowly plunging to the NW at approximately 20 °-30 °, but some plunge shallowly to the SE. An L_2 actinolite mineral lineation lies parallel to F_2 fold axes. F_2 folds, with a wavelength of 500 m, are east-verging with east-dipping axial planes and shallowly NW-plunging fold axes.

Minor F_3 folds are open to close and plunge shallowly to the NW, typically at 15° with axial planes that typically dip at 45 ° to the east. F_3 folds have a consistent vergence to the east throughout the western domain. They also form rare doubly verging box folds in the western portion of the map area within the calcareous graphitic schist. There is a strong crenulation lineation associated with F_3 on the S_{0-2} surface and there are no mineral lineations associated with F_3 folds.

Western Domain Geometry

The S_{0-2} transposition fabric is east-dipping throughout the southern part of the domain, but changes to a near vertical orientation to the north (Figure 2). The scarcity and highly deformed nature of the preserved F_1 hinges does not allow inference of large scale F_1 closures on the basis of minor structures; however, there is one potential F_1 fold closure which is refolded by the F_2 Panda Antiform (Figure 3a). This closure has been interpreted on the basis of lithologic asymmetry and the fact that it is on strike with a well mapped F_1 closure further to the north at Last Peak (de Keijzer and Williams, 1996; Harvey *et al.*, 1996). There is an increasing wavelength of F_2 major folds from east to west. Minor scale F_2 folds, with wavelengths of 250 m to 500m, in the eastern portion of the domain reveal two tight antiforms and one synform that fold a marble marker unit (Figure 3a). Further to the west, a reversal in F_2 minor fold vergence identifies the Panda Antiform with a wavelength of 2 km (Figure 3a). The easterly vergence of the F_3 folds throughout the Western Domain indicates that these rocks are situated on the shortened, overturned limb of a large scale NW-plunging F_3 fold (Figure 4).

STRUCTURE OF THE EASTERN DOMAIN

There are three generations of structures identified within the Eastern Domain; each characterized by a foliation (S_{0-1}, S_{0-2}, S_3) and a fold generation (F_1, F_2, F_3).

Planar Fabrics

S_{0-1} fabrics are rare but do occur as cm-spaced compositional layering in the

marble and a cm-spaced cleavage in the phyllites. The dominant fabric is the S_{0-2} transposition fabric and is defined by 1-3 cm thick compositional layering, boudinaged quartz veins and foliated graphite and muscovite. In the western portion of the Eastern domain, S_{0-2} is steeply dipping at 80° to 90° to the west. There is a gradual transition in dip from west to east; in the eastern part of the map area S_{0-2} dips at ~20° to the west. S_3 axial cleavages are developed locally within the phyllites and typically dip moderately at approximately 45° to the east.

Minor Fold Geometry

F_1 fold hinges are rare, but cm-scale isoclinal sheared fold hinges have been identified. S_{0-1} transposition fabric is axial planar to F_1 folds, although it is unclear whether an earlier, unidentified transposition fabric or primary layering is being folded. F_2 folds are the dominant minor structures. They are tight to isoclinal, and S_{0-2} is axial planar to F_2 folds (Figure 3b). They most commonly plunge at ~20° to the NW, although they sometimes plunge shallowly to the SE.

F_3 folds are open, have interlimb angles of 60° to 120° and plunge moderately NW. Where S_{0-2} is steeply dipping, F_3 folds are observed; however, they were not observed within the shallow lying rocks in the eastern part of the domain (Figure 2). Commonly F_3 folds form doubly verging box folds and kink bands within the graphitic phyllite. Where F_3 folds do not form box folds and are asymmetric, they consistently verge to the east.

Structure of Granitoids

The Little Lake Granite has a strong foliation defined by muscovite, biotite and flattened quartz and a down-dip stretching lineation defined by quartz rods. The foliation is parallel to the regional transposition foliation S_{0-2}. Asymmetric fabrics such as S-C fabrics or pressure shadows were not observed. The granite is intruded by both undeformed discordant as well as boudinaged concordant dykes of granite pegmatite similar in composition to the Dycer Creek Stock.

There is a weak fabric, defined by 1 cm diameter biotite crystals, in the Dycer Creek Stock which is parallel to S_{0-2} within the metacarbonates. The fabric within the stock varies from a steep west dipping orientation along the western margin to a shallow west-dipping orientation along the eastern margin (Figure 2). Shallowly west-dipping shear bands indicate top-to-the-east sense of shear. Metamorphic garnet, diopside and carbonates within the 10 meter wide contact aureole define a foliation which is parallel to S_{0-2} in the country rocks. For example, S_{0-2} wraps around garnet pressure shadows.

Eastern Domain Geometry

F_1 minor folds are rare and it has not been possible to establish whether or not the stratigraphy has been deformed by major F_1 structures. The distribution and vergence of F_2 minor structures define several 250m-scale tight to isoclinal F_2 folds in the western portion of the domain (Figure 2). Map scale F_2 folds have steeply west-dipping axial planes parallel to the regional transposition fabric (Figure 3b). The central portion of the eastern domain is dominated by the Dycer Creek Stock. With the exception of a weak foliation, the stock, does not display minor folds and no inference of large scale structures could be made. Near the eastern margin of the map area there are consistently west-verging F_2 minor folds that indicate the presence of the overturned limb of a map-scale F_2 fold.

The east vergence of F_3 folds along the western margin of the domain (Figure 2)

suggests that the steeply west-dipping S_{0-2} fabric represents the short limb of a km-scale west-verging F_3 fold (Figure 3b). Although there is a lack of F_3 minor structures within the eastern portion of the domain, the observed transition of the S_{0-2} fabric from shallow to steep, indicates the presence of a large-scale NW-plunging F_3 antiform; herein named the Two Cub Antiform (Figure 2).

The contacts and internal fabric of the Little Lake Granite, as well as the foliation in the contact aureole, are concordant with the regional transposition foliation (S_{0-2}) in the country rocks. The Little Lake granite is interpreted to have intruded prior to or during D_2 deformation. U-Pb geochronology studies will be undertaken to determine the crystallization age of the granite.

GEOMETRY OF THE DYCER CREEK AREA

There are insufficient data to confidently correlate S_{0-1} fabrics in the Western and Eastern Domains; however, S_{0-2} on both sides of the DFZ is defined by transposed compositional layering concordant with a chlorite-muscovite-biotite foliation. S_{0-2} is indistinguishable in nature throughout the map area although there is a variation in orientation from steep to shallow as a result of F_3 folding. S_3 dips eastward at ~45° throughout both the western and eastern domains. Similarly, F_1, F_2 and F_3 fold styles and orientation are similar throughout the Dycer Creek area.

The similarity in fabrics and folds on both sides of the d'Abbadie Fault Zone is consistent with interpretation that the entire Dycer Creek area underwent a common deformation history. The east-verging F_3 minor folds, both east and west of the d'Abbadie Fault Zone, are consistent with the interpretation that the F_3 Two Cub Antiform rotated originally gently dipping S_{0-2} of the Western Domain and part of the Eastern domain into a steep east-dipping orientation on the short limb of the fold (Figure 4a,4b).

Dextral strike-slip motion along the DFZ at ca. 98 Ma, resulted in an apparent reverse displacement of structures across the fault, and juxtaposed steeply east-dipping greenschist to lower amphibolite facies rocks of the Western domain against variably west-dipping greenschist facies rocks of the Eastern domain (Figure 4c). It is proposed that the geometry of the Dycer Creek area can be explained by the presence of a km-scale west verging F_3 fold whose steep limb has been bisected and subsequently offset by dextral motion on the late fault.

INTERPRETATION

The relationship of dextral-sense ductile shear fabrics, observed within the Last Peak Granite and Mendocina Orthogneiss, to the DFZ remains unresolved. Nor is it clear whether or not these sheared intrusions are coeval with emplacement and deformation of the Little Lake Granite and Dycer Creek Stock. It is hopeful that geochronologic studies in progress will resolve these issues.

Figure 4 illustrates a scenario for the structural evolution of the Dycer Creek Area that is compatible with data presented in this paper. During D_2 transposition, tight to isoclinal folding resulted in the prominent S_{0-2} fabric recognized today in the Dycer Creek area (Figure 4a). During D_3, F_3 Two Cub Antiform rotated generally flat lying rocks into a steep orientation (Figure 4b). F_3 minor folds are concentrated on the short, overturned limb of the back fold, where the majority of shortening occurred.

The d'Abbadie Fault Zone post dates D_3 deformation (Figure 4b). Dextral strike-slip displacement was ongoing at 98±1 Ma, the age of the syntectonic Last Peak granite. An upper age bracket is provided by the 83 Ma K-Ar age from the Quiet Lake batholith which intrudes the southern end of the fault (Stevens and Erdmer, 1993). The DFZ displaced the F_3 hinge and overturned limb of the F_3 back fold, resulting in the juxtaposition of generally flat lying rocks of the eastern Cassiar Platform against the overturned rocks of the Teslin Zone (Figure 4c).

Third generation km-scale folds at both Last Peak (de Keijzer and Williams, 1997) and in the Dycer Creek area have the opposite vergence from one another. In both areas F_3 folds plunge moderately to the NW, have similar geometry and style, and commonly form box folds. One model to explain the opposing vergence is that they are both part of a large scale F_3 box fold. Another interpretation is that the folds are of different generations and that there are one or more generations of deformation that were not recorded in the Dycer Creek area.

CONCLUSIONS

1) The Dycer Creek Area consists of greenschist facies metasedimentary rocks of the Cassiar Platform and greenschist to lower amphibolite facies metasedimentary and metavolcanic rocks of the Teslin Zone. Last Peak Assemblage rocks have been correlated with Nisutlin assemblage of the Yukon-Tanana Terrane (Harvey *et al.*; 1996, 1997a) and Mendocina assemblage rocks have been correlated with Anvil assemblage (Harvey *et al.*; 1996,1997a).

2) Regional transposition fabrics $S_{0\text{-}1}$ and $S_{0\text{-}2}$ are defined by compositional layering and foliated metamorphic minerals, and S_3 is a moderately dipping penetrative axial planar cleavage. F_1 and F_2 folds occur as NW-plunging tight to isoclinal folds, and NW-plunging F_3 minor folds verge to the east. Structures are identical on both sides of the d'Abbadie Fault Zone and are consistent with the argument that rocks of the Cassiar Platform and Teslin Zone underwent a common deformation history.

3) Prior to D_3, regional attitudes are interpreted to have been shallowly westward dipping and major D_2 folds verged to the east. The development of steep attitudes within the Dycer Creek Area is interpreted to be in large part a result of late folding.

4) Although the magnitude and direction of displacement of the d'Abbadie fault zone are uncertain, the Late Cretaceous age brackets, ductile and brittle dextral structures and cross-cutting nature indicate that it a late structure in the evolution of the Teslin Zone, and does not represent a fundamental terrane boundary.

REFERENCES

Brown, R. L., Carr, S. D., Harvey, J. L., Williams, P. F and de Keijzer, M. 1995. Structure and tectonic significance of the Teslin suture zone. LITHOPROBE Report No. 44, 1995 SNORCLE Transect Meeting, Calgary, AB, 56-62.

de Keijzer, M. and Williams P.F. 1997b. Fabric Development in the Cassiar Terrane, Yukon Territory: A response to terrane accretion or subsequent extension? GAC-MAC Abstracts: 22: A36.

de Keijzer, M. and Williams, P. F. 1996. Structural analysis in the Teslin Tectonic zone, south-central Yukon. LITHOPROBE Report No. 50, 1996 SNORCLE and Cordilleran Tectonics Workshop, Calgary, AB, 45-53.

de Keijzer, M and Williams, P .F. 1997. A new view on the structural framework of the Teslin Zone, south-central Yukon. LITHOPROBE Report No. 56, 1997 SNORCLE and Cordilleran Tectonics Workshop, Calgary, AB., 96-102.

Creaser, R.A., Heaman, L. M. and Erdmer, P. 1997. Timing of high-pressure metamorphism in the Yukon - Tanana terrane, Canadian Cordillera: constraints from U - Pb zircon dating of eclogite from the Teslin tectonic zone. Canadian Journal of Earth Sciences: 34: 709-715.

Erdmer, P. 1985. An examination of the cataclastic fabrics and structures of parts of Nisutlin, Anvil and Simpson Allochthons, central Yukon: test of the arc-continent collision model. Journal of Structural Geology, 7: 57-72.

Erdmer, P. and Helmsteadt, H. 1983. Eclogite from central Yukon: a record of subduction at the western margin of ancient North America. Canadian Journal of Earth Sciences, 20, 1389-1408.

Hansen, V. L. 1989. Structural and kinematic evolution of the Teslin suture zone, Yukon: record of an ancient transpressional margin. Journal of Structural Geology, 11: 717-733.

Hansen, V. L. 1992a. Backflow and margin-parallel shear within an ancient subduction complex. Geology, 20: 717-733.

Hansen, V. L. 1992b. P-T evolution of the Teslin suture zone and Cassiar tectonites, Yukon, Canada: evidence of A- and B-type subduction. Journal of Metamorphic Geology, 10: 239-263.

Hansen, V. L., Mortensen, J. K. and Armstrong, R. L. 1989. U-Pb, Rb-Sr, K-Ar isotopic constraints for ductile deformation and related metamorphism in the Teslin suture zone, Yukon-Tanana terrane, south-central Yukon. Canadian Journal of Earth Sciences, 26: 2224-2235.

Harvey, J. L., Brown, R. L., and Carr, S. D. 1996. Progress in structural mapping in the Teslin Suture Zone, Big Salmon Range, Central Yukon Territory. LITHOPROBE report No. 50, 1996 SNORCLE and Cordilleran Tectonics Workshop, Calgary, AB, 33-41.

Harvey, J. L., Carr, S. D., Brown, R. L., and Gallagher, C. 1997a. Deformation history and geochronology of plutonic rocks near the D'Abbadie fault, Big Salmon Range, Yukon. LITHOPROBE report No. 56. 1997 SNORCLE and Cordilleran Tectonics Workshop, 103-114.

Harvey, J. L., Carr, S. D., and Brown, R. L. 1997b. Ages of deformed plutonic rocks along the D'Abbadie fault, Teslin zone, Big Salmon Range, Yukon: Implications for timing of strike-slip deformation. GAC-MAC Abstracts: 22: A65.

Gabrielse, H. and Yorath, C.J. Geology of the Cordilleran Orogen in Canada. 1991

Mortensen, J. K. 1992. Pre-mid Mesozoic tectonic evolution of the Yukon-Tanana Terrane, Yukon and Alaska. Tectonics, 11: 836-853.

Mortensen, J. K. and Jilson, G. A. 1985. Evolution of the Yukon-Tanana terrane: Evidence from the southeastern Yukon Territory, Geology, 13, 806-810.

Stevens, R. A. and Erdmer, P. 1993. Geology and structure of the Teslin suture zone and related rocks in parts of the Laberge, Quiet Lake, and Teslin map areas, Yukon Territory.

Geological Survey of Canada, Paper, 93-1A: 11-20.

Stevens, R.A., and Erdmer, P. 1996. Structural divergence and transpression in the Teslin Tectonic zone, southern Yukon Territory. Tectonics, 15: 1342-1363.

Tempelman-Kluit, D.J. 1979. Transported cataclasite, ophiolite, and granodiorite in Yukon: Evidence of arc-continent collision. Geological Survey of Canada, Paper 79-14, 27p.

Figure 1- Regional geology of the Teslin Zone from South Big Salmon to Last Peak (Modified after Harvey et al., 1997)

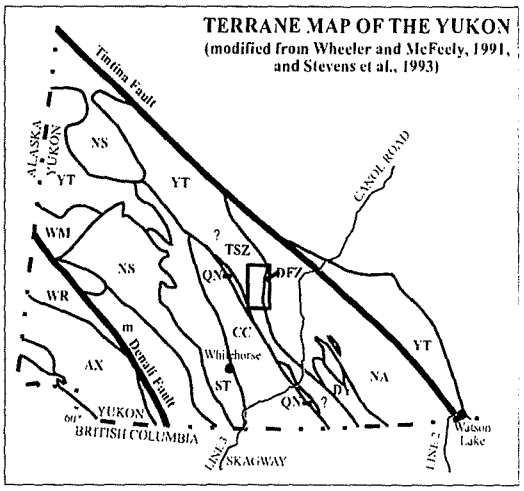

Terranes:
NA = North America
YT = Yukon Tanana
TSZ = Teslin suture zone
NS = Nisling
DY = Dorsey
QN = Quesnellia
CC = Cache Creek
ST = Stikinia
WM = Windy McKinley
AX = Alexander
WR = Wrangellia

m = undivided metamorphic rocks
DFZ = D'Abbadie fault

LEGEND

Teslin Zone
- Last Peak Assemblage (LPA)
- Mendocina Assemblage (MA)

Cassiar Platform
- Eastern Domain

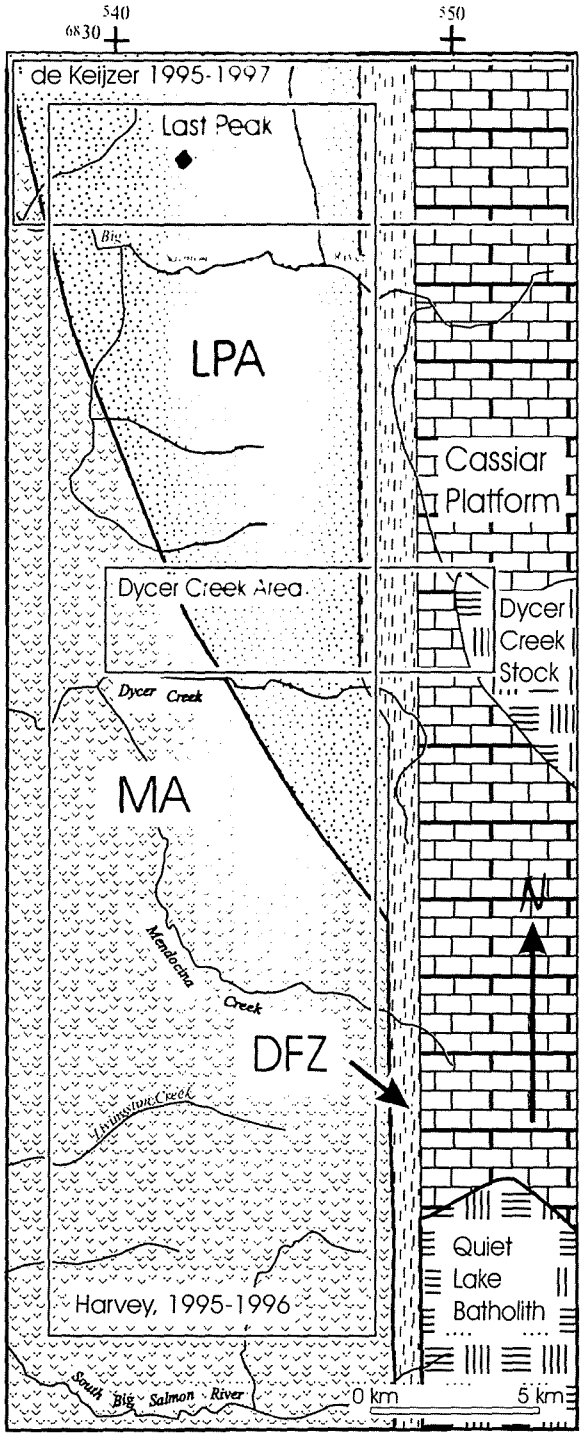

Figure 2 - Regional geology of the Dycer Creek Area showing geologic relationships of the Western Domain, d'Abbadie Fault Zone and Eastern Domain. Structural data is a compilation of Gallagher (1997) and Harvey (1995)

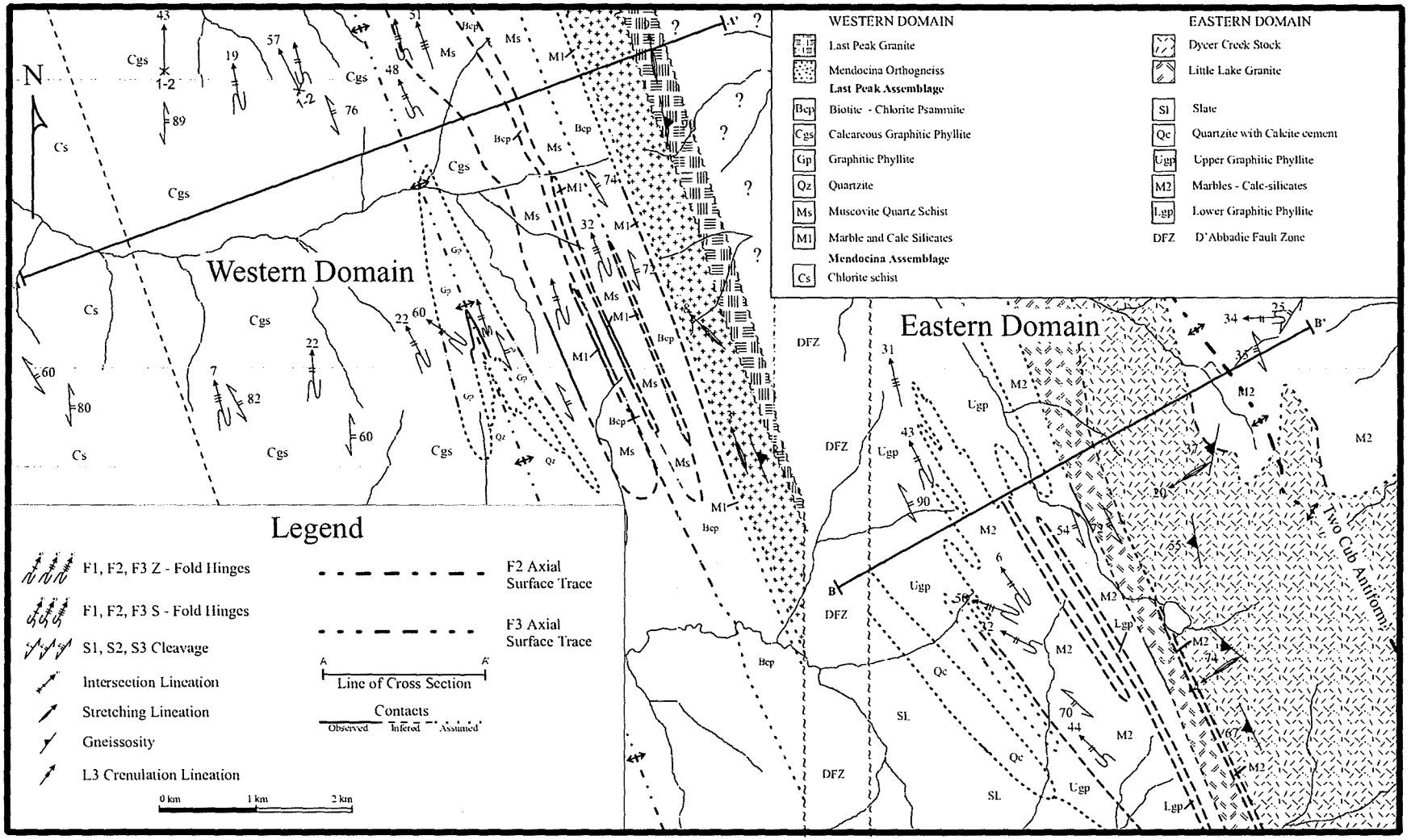

Figure 3a - Structural Cross Section of the Western Domain displaying a multiply refolded lithologic sequence

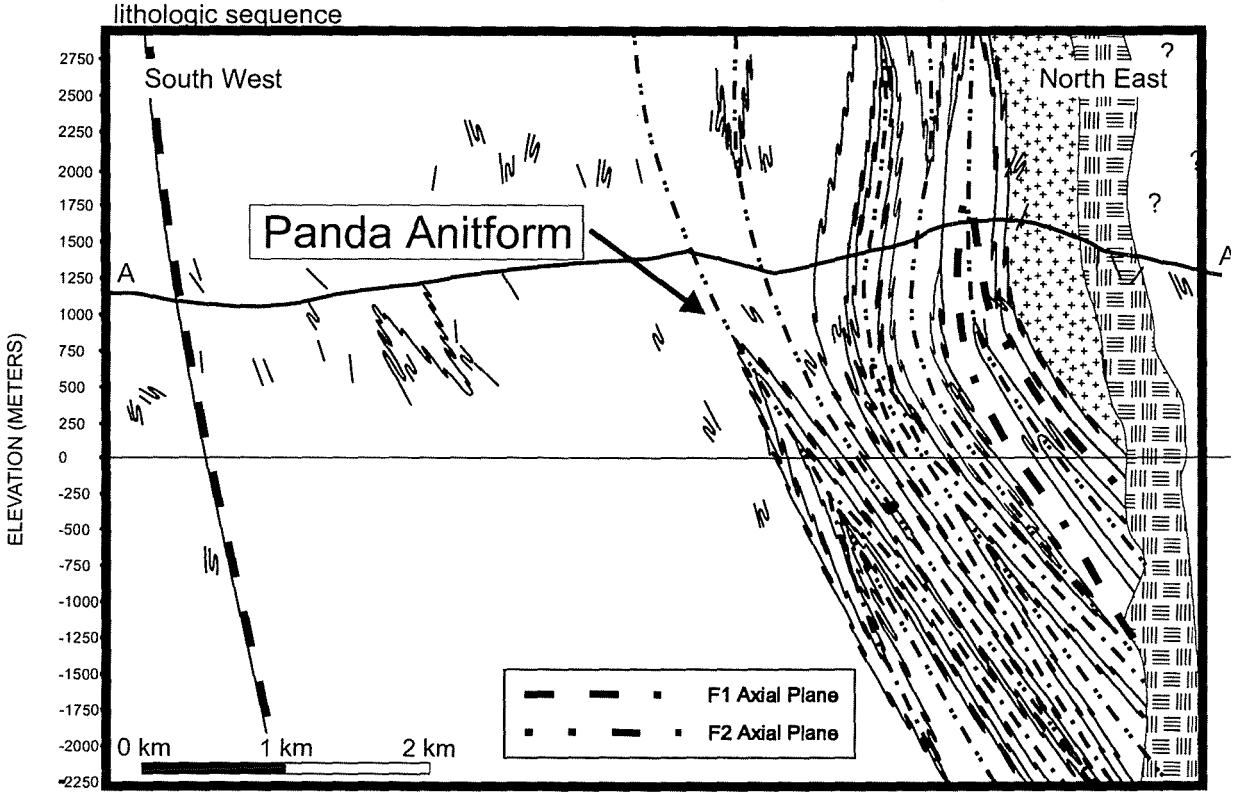

Figure 3b - Structural Cross Section of Eastern Domain showing it's relationship to the DFZ and the Dycer Creek Stock

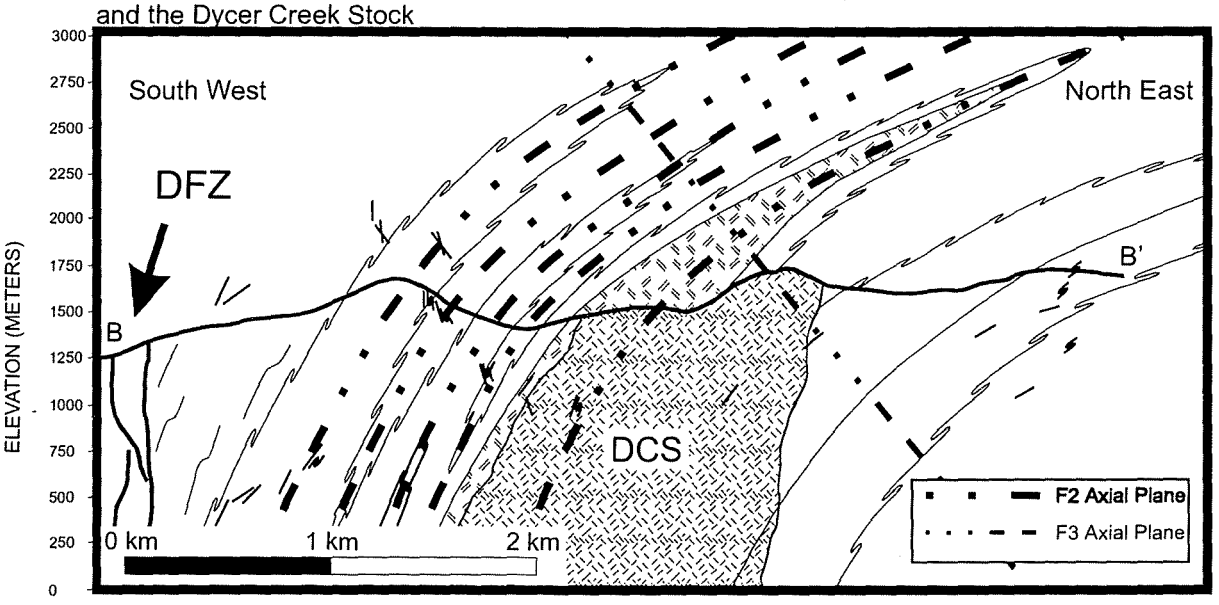

Figure 4a - D1 and D2 post 283 Ma transposition resulted in flat lying transposed contacts and variably deformed granites.

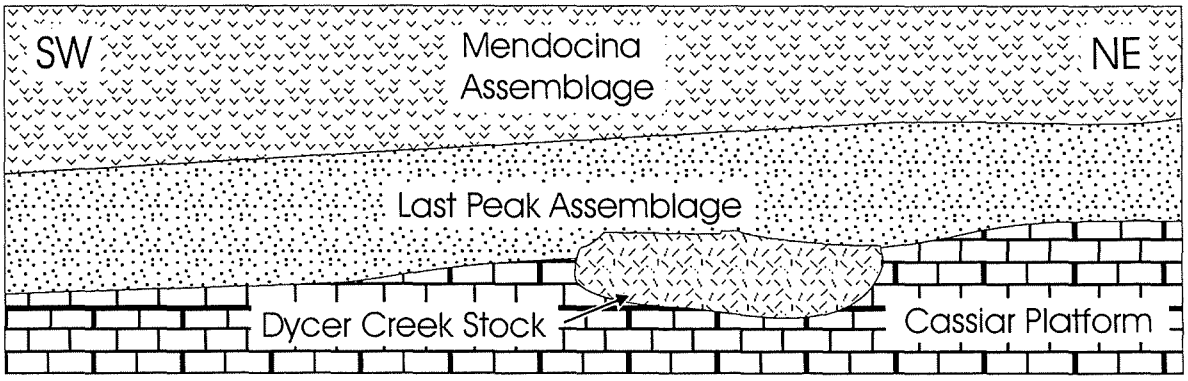

Figure 4b - Formation of the F3 Two Cub Antiform prior to Cretaceous time, folding transposed stratigraphy and syn-D2 Dycer Creek Stock. The d'Abbadie Fault Zone was active, in part, at 98 Ma.

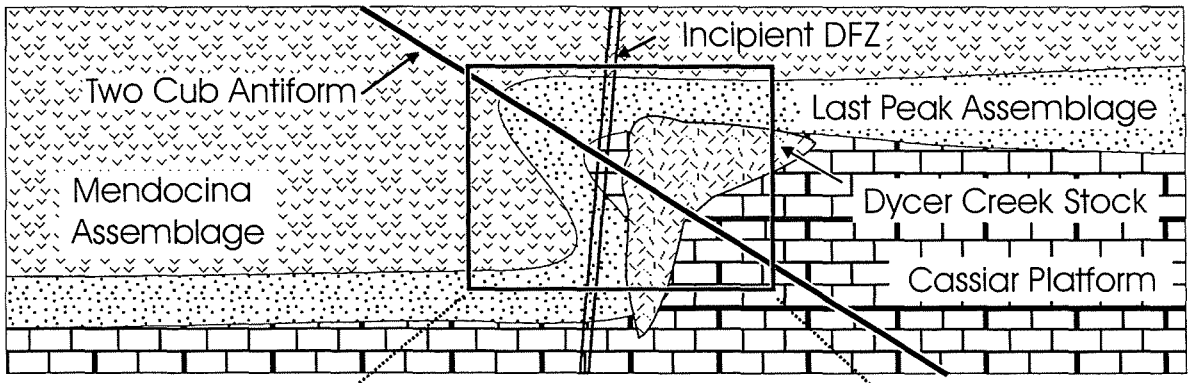

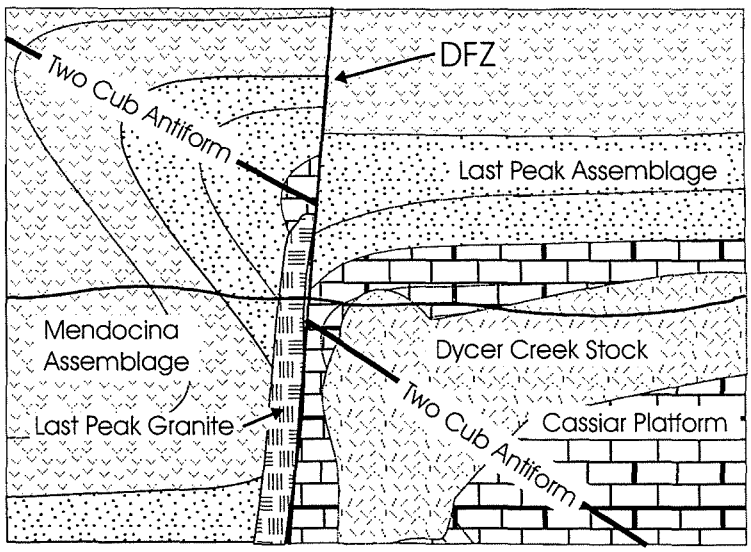

Figure 4c - Present day geometry resuting from dextral strike-slip displacement along DFZ during intrusion of the Last Peak Granite (98 Ma)

STRUCTURE OF THE TESLIN ZONE, YUKON, CANADA

Richard L. Brown[1], Martin de Keijzer[2], Sharon D. Carr[1], Paul F. Williams[2], and Christopher S. Gallagher[1]

[1]Ottawa-Carleton Geoscience Centre and Department of Earth Sciences, Carleton University, Ottawa, Ontario, K1S 5B6. [2]Department of Geology, University of New Brunswick, Fredericton, N.B. E3B 5A3

INTRODUCTION

The Teslin suture zone was first described in 1979 by Tempelman-Kluit. According to his model the Teslin suture zone is a westerly dipping subduction zone with North American rocks in its footwall and accreted arc terrane and oceanic rocks in its hanging wall. He envisaged an arc-continent collision that occurred in the Middle Jurassic with significant obduction of the arc and related oceanic rocks taking place in the Late Jurassic and the Early Cretaceous. In central Yukon, penetratively deformed klippen that lie on comparatively undeformed North American strata have been interpreted as being obducted rocks of the hanging wall of the subduction zone, and rocks within the Teslin zone have been described as a cataclastic melange (Erdmer, 1985). This subduction model has enjoyed wide acceptance with detailed modifications proposed by several authors (e.g. Erdmer, 1985; Hansen, 1989, 1992a, 1992b). Hansen (1989) recognized the importance of strike slip faulting along the eastern boundary of the zone and modified the model to include the role of transpression. Brown et al. (1995) questioned the subduction zone model and suggested that North American rocks may extend westward well beyond the Teslin suture zone. Stevens and Erdmer (1996) have also questioned the importance of subduction at the Teslin suture zone, and they consider the structures of the zone to be primarily related to strike slip faulting; they renamed the Teslin suture zone the "Teslin Tectonic Zone ".

Some of the rocks within the Teslin zone are correlated with Yukon-Tanana Terrane, which exhibits evidence of Middle Permian to Early Triassic deformation and metamorphism (Mortensen and Jilson, 1985: Mortensen 1991; Stevens and Erdmer 1993); locally these generally low-grade metamorphic rocks include lenses bearing eclogite and blueschist assemblages. These observations have generally been reconciled with the subduction model by suggesting that deep burial of some of the Yukon-Tanana rocks occurred in a Permian subduction zone prior to accretion in the Jurassic (e.g. Stevens and Erdmer, 1993; Creaser et al. 1997).

The purpose of this communication is to discuss new and recently published data, which are not compatible with the subduction zone model of earlier authors. Based on mapping of a 50 x 20 km area in the Big Salmon Range in the Teslin zone and adjacent rocks to the east (Brown et al. 1995, de Keijzer and Williams, 1996, 1997, 1998; Harvey et al. 1996, 1997a, b; Gallagher et al. 1998), the Teslin zone is reinterpreted as a zone of ductile thrusting, which includes thrust sheets of North American affinity and accreted rocks that have

been complexly folded and displaced northeastward and then folded again. Rather than marking the western limit of rocks of North American origin, the zone is most likely underlain by North American basement that extends westward beneath the Intermontane Belt. An interpretive crustal section indicates that deep structures beneath the Teslin zone have shallow to horizontal dips rather than a steeply dipping fabric with roots in the upper mantle. The eclogite and blueschist assemblages are explained as structurally included slices within the thrust sheets, which reflect a Permian subduction history that was exotic with respect to North America and unrelated to the Teslin zone.

STRUCTURE

D'Abbadie fault zone: The steep N-S D'Abbadie fault has been generally taken to represent the eastern margin of the Teslin zone. Dextral shearing is clearly evident with mylonitic fabrics most readily observed in elongate granitic plutons that have intruded this part of the orogen (Hansen, 1989; Hansen, et al. 1989: Harvey et al. 1997a, b; Gallagher et al. 1998). Superimposed on the ductile deformation is a narrow zone of brittle deformation that is of uncertain significance but may reflect a period of upper crustal normal faulting (cf. de Keijzer and Williams, 1997). The mylonitic fabrics, which record dextral shearing cut across regionally developed generations of folding on both sides of the fault, and are younger (Harvey et al. 1996, 1997a, b). The ca. 98 Ma Last Peak granite, on the basis of contact and structural relationships, is interpreted to have intruded while the D'Abbadie fault zone was active, thus placing a time constraint on part of the displacement history (Harvey et al. 1997a, b).

Structure of the Teslin zone and adjacent rocks to the east: The structure of the region is typified by multiple generations of meso- and macroscopic folding (de Keijzer and Williams, 1997, 1998; Gallagher et al. 1998). The first two generations each resulted in transposition of stratigraphic units, so that the original stratigraphic order has not been preserved. In the eastern part of the region, east of the D'Abaddie fault zone, folds are generally recumbent with a clear easterly vergence. Second generation folds dominate the map pattern and these structures change from nearly recumbent in the east to nearly upright near the eastern boundary of the Teslin zone. Moderately westerly dips of the enveloping surface of compositional layering prevail.

In the Dycer Creek area (Gallagher et al. 1998) east of the D'Abaddie fault zone, post transposition minor folds (third generation folds in this map area) have been recognized and correlated with a km-scale westerly verging antiform, the Two Cub antiform. To the east of the axial surface trace, limbs of second generation isoclinal folds dip gently to the west. Westward across the axial surface trace, these structures have been rotated into steep to nearly vertical attitudes.

In the northern part of the area near Mt. D'Abbadie (de Keijzer and Williams 1997) this transition is not observed to the east of the D'Abbadie fault. Instead a panel of gently dipping structures extends across the area and is

truncated at the western margin by the D'Abbadie fault. However to the west of the fault, the enveloping surface dips gently on the flat limb of a major third generation northeasterly verging synform, the Grizzly synform. Further to the west the enveloping surface passes around the hinge of the synform into a steep westerly dipping overturned limb (de Keijzer and Williams, 1997). Fourth generation folds are weakly developed, and are open easterly verging structures with steeply dipping short limbs.

The important point is that the change from gentle westerly dips of transposition foliation to steep dips is associated with post transposition deformation, and this transition has been mapped on both the east and west sides of the D'Abbadie fault zone. Perhaps because the folds are upright and tight to isoclinal the Teslin zone has previously been described as a nearly vertical panel of highly sheared rocks. What is apparent from the fold geometry is that prior to the third generation of folding the transposed and isoclinally folded and faulted stratigraphy was horizontal to moderately dipping. In this interpretation, the gently dipping second generation structures in the eastern part of the region reflect regional attitudes prior to superposition of post transposition structures. If this geometry is extrapolated into the subsurface one would expect to see zones of steeply dipping transposed layering on the overturned limbs of the late folds and moderate dips on the upright limbs. On the scale of a seismic reflection profile, moderate dips of reflections should be the dominant attitudes.

Mylonitic fabrics: Following Tempelman-Kluit (1979), the rocks within the Teslin zone have been variously described as having cataclastic or mylonitic fabrics. Our observations do not support this interpretation. As a result of progressive folding, the original bedding has been thickened in the hinges and attenuated in the limbs. Axial plane cleavage was well developed during the first and second generation of folding, and in general the compositional layering has been transposed such that it is now parallel to the dominant second generation cleavage. Intersection of first and second generation cleavages with the compositional layering resulted in a lineation that is parallel to the fold hinges. Locally third and fourth generation folds have been superimposed on these fabrics giving rise to additional intersection lineations and crenulation cleavages. There are local shear zones that contain an extension lineation and have undergone a reduction in grain size, but these features are a minor part of the regional fabric. Mylonites occur in the granitic rocks that were caught up in the dextral shearing of the D'Abbadie fault zone and along the western margin of the Teslin zone west of Last Peak.

Tectonic melange(?): Individual marker units and coherent lithologic packages have been mapped along strike for up to 20 km in the Teslin zone (de Keijzer and Williams, 1997; Harvey et al. 1997a, b). During transposition progressive thinning of fold limbs ultimately results in boudinage of the competent layers. It is clear at the outcrop scale and where marker units have

been mapped in sufficient detail, that this process accounts for the discontinuous nature of the lithologies within the Teslin zone. There is no indication of chaotic disruption such as would occur in a tectonic melange.

METAMORPHISM

Within the map area (Harvey et. al. 1996, 1997a; de Keijzer and Williams 1996, 1997, 1998), all the metasedimentary rocks are metamorphosed under greenschist to lower amphibolite facies conditions, and there is no evidence of significant retrogression. Past workers have suggested that these rocks reflect high pressure and high temperature conditions based primarily on the rare occurrences of lenses of eclogite and blueschist (see Erdmer et al. 1997 for a recent review). One such body within our map area is located 8 km west of Last Peak. This eclogitic body, which contains brown hornblende, late stage oligoclase and biotite yielded P-T estimates up to 625°C at a minimum pressure of 14 kbar; a U-Pb age of 269 Ma and white mica from the body yielded an apparently undisturbed age of 236 ± 2 Ma (Erdmer et al., 1997; Creaser et al. 1997). Other Teslin zone rocks cooled between 195-179 Ma (Hansen et al. 1991; Stevens et al. 1993). These relationships require two distinct metamorphic environments and imply that the eclogitic lens was exhumed to middle or upper crustal levels in Triassic time, and then tectonically incorporated into its present tectonic setting. The age of the greenschist metamorphism within the Teslin zone is not well constrained, but must be older than emplacement of the ca. 98±1 Ma Last Peak granite that occurs along the eastern margin of the zone (Harvey et. al., 1997a, b). The transposition foliations in the country rock are truncated by the granite and a thermal aureole overprints these regional deformation fabrics. Regional studies of intrusive rocks and cooling ages suggest a complex history with important exhumation in Jurassic time (Hansen et al. 1991; Stevens et al. 1993).

DISCUSSION

The widely accepted idea that the Teslin zone is a suture marking the western limit of the North American plate is not compatible with structural data presented in this paper and recent publications by Brown et al. (1995), de Keijzer and Williams (1997, 1998) and Gallagher et al. (1998). Transition from shallow to steeply dipping strata occurs along the eastern boundary of the Teslin zone. This change is a result of post transposition folding and the steep attitudes characteristic of the Teslin zone are found on the overturned short limbs. Tectonic melange reported by previous authors (e.g. Tempelman-Kluit, 1979; Erdmer, 1985) to be present in the Teslin zone has not been observed. It appears that highly transposed stratigraphy that resulted from folding has been mistaken for trench melange. There is no petrologic evidence to support the contention of previous authors (e.g. Hansen, 1989) that the metasedimentary rocks of the Teslin zone evolved in the high pressure setting of a subduction zone; rather, the bulk of the rocks appear to have been metamorphosed at middle to upper crustal conditions as suggested by the regional metamorphic

grade of middle to upper greenschist (Harvey et al. 1997a, b). This result is reconciled with the local occurrences of eclogitic rocks, such as those near Last Peak (Creaser et al. 1997), by assuming that these assemblages, which developed in Permian times were later incorporated into the greenschist assemblages.

CONCLUSIONS

1) The Teslin Suture Zone does not exist and the name should be abandoned.

2) Steeply dipping transposition foliation in the map area is a result of rotation from shallowly dipping orientations during late stages of northeasterly verging folding. This rotation occurred after thrusting and the emplacement of ophiolite bearing thrust sheets.

3) Subduction related to the formation of Permian eclogites and blueschists is interpreted to have occurred well to the west of the Teslin region and its roots may well have been obliterated by younger convergence and strike slip faulting.

4) Seismic reflectors beneath the zone are predicted to be primarily gently dipping and to be a result of the anisotropy of moderately dipping enveloping surfaces of folded and transposed strata

REFERENCES

Brown, R. L., Carr, S. D., Harvey, J. L., Williams, P. F and de Keijzer, M. 1995. Structure and tectonic significance of the Teslin suture zone. LITHOPROBE Report No. 44, 1995 SNORCLE Transect Meeting, Calgary, AB, 56-62.

de Keijzer, M. and Williams, P. F. 1996. Structural analysis in the Teslin Tectonic zone, south-central Yukon. LITHOPROBE Report No. 50, 1996 SNORCLE and Cordilleran Tectonics Workshop, Calgary, AB, 45-53.

de Keijzer, M and Williams, P .F. 1997. A new view on the structural framework of the Teslin Zone, south-central Yukon. LITHOPROBE Report No. 56, 1997 SNORCLE and Cordilleran Tectonics Workshop, Calgary, AB., 96-102.

de Keijzer, M and Williams, P .F. 1998 (this volume). Kilometre-scale folding in the Teslin zone, northern Canadian Cordillera, and its tectonic implications for the accretion of the Yukon-Tanana terrane to North America. LITHOPROBE Report, 1998 SNORCLE and Cordilleran Tectonics Workshop, Vancouver, B.C.

Creaser, R.A., Heaman, L. M. and Erdmer, P. 1997. Timing of high-pressure metamorphism in the Yukon - Tanana terrane, Canadian Cordillera: constraints from U - Pb zircon dating of eclogite from the Teslin tectonic zone. Canadian Journal of Earth Sciences: **34**: 709-715.

Erdmer, P. 1985. An examination of the cataclastic fabrics and structures of parts of Nisutlin, Anvil and Simpson allochthons, central Yukon: test of the arc-continent collision model. Journal of Structural Geology, **7**: 57-72.

Gallagher, C., Brown, R. L. and Carr, S. D. 1998 (this volume). Geometry of the Dycer Creek map area, Teslin zone, Yukon. LITHOPROBE Report, 1998 SNORCLE and Cordilleran Tectonics Workshop, Vancouver, B.C.

Hansen, V. L. 1989. Structural and kinematic evolution of the Teslin suture zone, Yukon: record of an ancient transpressional margin. Journal of Structural Geology, **11**: 717-733.

Hansen, V. L. 1992a. Backflow and margin-parallel shear within an ancient subduction complex. Geology, **20**: 717-733.

Hansen, V. L. 1992b. P-T evolution of the Teslin suture zone and Cassiar tectonites, Yukon, Canada: evidence of A- and B-type subduction. Journal of Metamorphic Geology, **10**: 239-263.

Hansen, V. L., Mortenson, J. K. and Armstrong, R. L. 1989. U-Pb, Rb-Sr, K-Ar isotopic constraints for ductile deformation and related metamorphism in the Teslin suture zone, Yukon-Tanana terrane, south-central Yukon. Canadian Journal of Earth Sciences, **26**: 2224-2235.

Hansen, V. L., Heizler, M. T. and Harrison, T. M. 1991. Mesozoic thermal evolution of the Yukon-Tanana composite terrane: New evidence from $^{40}Ar/^{39}Ar$ data. Tectonics, **10**: 51-76.

Harvey, J. L., Brown, R. L., and Carr, S. D. 1996. Progress in structural mapping in the Teslin Suture Zone, Big Salmon Range, Central Yukon Territory. LITHOPROBE report No. 50, 1996 SNORCLE and Cordilleran Tectonics Workshop, Calgary, AB, 33-41.

Harvey, J. L., Carr, S. D., Brown, R. L., and Gallagher, C. 1997a. Deformation history and geochronology of plutonic rocks near the D'Abbadie fault, Big Salmon Range, Yukon. LITHOPROBE report No. 56. 1997 SNORCLE and Cordilleran Tectonics Workshop, 103-114.

Harvey, J. L., Carr, S. D., and Brown, R. L. 1997b. Ages of deformed plutonic rocks along the D'Abbadie fault, Teslin zone, Big Salmon Range, Yukon: Implications for timing of strike-slip deformation. GAC-MAC Abstracts: **22**, A23.

Mortenson, J. K. 1991. Pre-mid Mesozoic tectonic evolution of the Yukon-Tanana Terrane, Yukon and Alaska. Tectonics, **11**: 836-853.

Mortenson, J. K. and Jilson, G. A. 1985. Evolution of the Yukon-Tanana terrane: Evidence from the southeastern Yukon Territory, Geology, **13,** 806-810.

Stevens, R. A., Mortensen, J. K. and Hunt, P. A. 1993. U-Pb and $^{40}Ar/^{39}Ar$ geochronology of plutonic rocks from the Teslin suture zone, Yukon Territory, Radiogenic Age and Isotopic Studies, Report 7, GSC Paper, 93-2: 83-90.

Stevens, R. A., Erdmer, P., Creaser, R. A. and Grant, S. L. 1996. Mississippian assembly of the Nisutlin assemblage: evidence from primary contact relationships and Mississippian magmatism in the Teslin tectonic zone, part of the Yukon-Tanana terrane of south central Yukon. Canadian Journal of Earth Sciences, 33: 103-116.

Stevens, R. A. and Erdmer, P. 1993. Geology and structure of the Teslin suture zone and related rocks in parts of the Laberge, Quiet Lake, and Teslin map areas, Yukon Territory. Geological Survey of Canada, Paper, 93-1A: 11-20.

Stevens, R. A., and Erdmer, P. 1996. Structural divergence and transpression in the Teslin Tectonic zone, southern Yukon Territory. Tectonics, 15: 1342-1363.

Tempelman-Kluit, D. J. 1979. Transported cataclasite, ophiolite, and granodiorite in Yukon: Evidence of arc-continent collision. Geological Survey of Canada, Paper 79-14, 27p.

Petrogenesis of the Cretaceous Cassiar batholith, Yukon-B.C. Canada.

Leslie Ann Driver, leslie.driver@ualberta.ca
Rob Creaser, Tom Chacko, Philippe Erdmer

Department of Earth and Atmospheric Sciences
University of Alberta, Edmonton AB T6G 2E3

Introduction

The Cassiar batholith is the single largest plutonic body in the hinterland of the Canadian Cordillera. The batholith, which is part of widespread mid-Cretaceous magmatism, is located within the Omineca Crystalline Belt, and extends continuously for 350 km along strike from southern Yukon into northern British Columbia, with east-west dimensions ranging from 5-40 km (Figure 1) (Gabrielse, 1962a; 1962b; 1963; 1969). Lithologically similar granitoids outcrop sporadically along strike for another 300 km into northern Yukon. In addition to its large areal extent, the Cassiar batholith also occupies a key position in the overall tectonic framework of the North American Cordillera. To the east are rocks of cratonic North America, while the rocks to the west are believed to be accreted terranes of the Cordilleran margin. The presence of such an enormous volume of magmatic rock near this major geologic boundary, as well as its dimensions and orientation, strongly suggests that the generation and emplacement of the batholith played a fundamental role in the evolution of this part of the North American Cordillera.

Despite its importance, only limited work has been carried out on the Cassiar batholith. This paper reports new petrographic, geochemical, and isotope (Sr, Nd, O) data from the Cassiar batholith. These data provide important constraints on the origin of compositional variations within the batholith and on possible source materials for the Cassiar magmas. We also use the data to gain insight on the tectonic setting in which the Cassiar magmas were generated. In particular, we evaluate subduction-related versus collision-related settings for the generation of the magmas.

Geological Setting

The North American Cordillera experienced widespread magmatism during the Mesozoic and Cenozoic. This magmatism extended from Alaska to northern Mexico, and from the western coast of North America inland for up to 600 km. It can be divided into two chronological and spatial groups. A coastal group and a more easterly group. The coastal magmatism, represented by the Sierra Nevada batholith in California, and the Peninsular Ranges batholith in southern California and Mexico, generally occurred during Middle to Late Jurassic and represents typical arc-related (subduction) magmas, with low K contents (dominantly tonalite and granodiorite), and a notable mantle component to the magmas (Brandon and Lambert, 1994). These magmas, along with the Peruvian coastal batholith, are considered to be typical Andean-type subduction magmas located at continental margins (cf. Pitcher, 1983; Pitcher *et al.*, 1985; Gromet & Silver, 1987).

In contrast, the more easterly magmatism of batholiths such as the Idaho batholith, the Bugaboo, White Creek, and Horsethief Creek batholiths, of British Columbia, and smaller batholiths in B.C., Washington, Utah, eastern Nevada, southeastern California, Arizona, New Mexico, Montana, and

Colorado (Miller and Barton, 1990) occur inland from the continental margin. These plutons are distinct in composition and origin from the more westerly magmatism. This more easterly group of magmatism is bounded to the west in Canada by accreted terranes, and in the United States by the $^{87}Sr/^{86}Sr=0.706$ line. These magmas are generally younger than their coastal counterparts (Middle to Late Cretaceous), do not show arc-related signatures, and their compositions become notably more felsic and peraluminous with time (Miller and Barton, 1990). Dominant rock types are biotite or muscovite-biotite granodiorites and granites.

The exact origin of these magmas is still controversial, but the interior location and the association of magmatism with compressional tectonics on cratonic North America suggest that subduction may not have been a major factor in their genesis. Crustal anatexis, or at least the addition of major crustal components to a basaltic magma can account for the geochemistry and isotopic signatures found in these batholiths (Miller and Barton, 1990). Brandon and Lambert (1993; 1994) recently suggested that four batholiths in southeastern B.C., Canada, were specifically generated from crustal anatexis due to overthickening of the crust during the Mesozoic accretion of microcontinents along western North America. The present study is the first detailed evaluation of the petrogenesis of the Cassiar batholith, which is the largest example of this suite of magmas in the Canadian Cordillera.

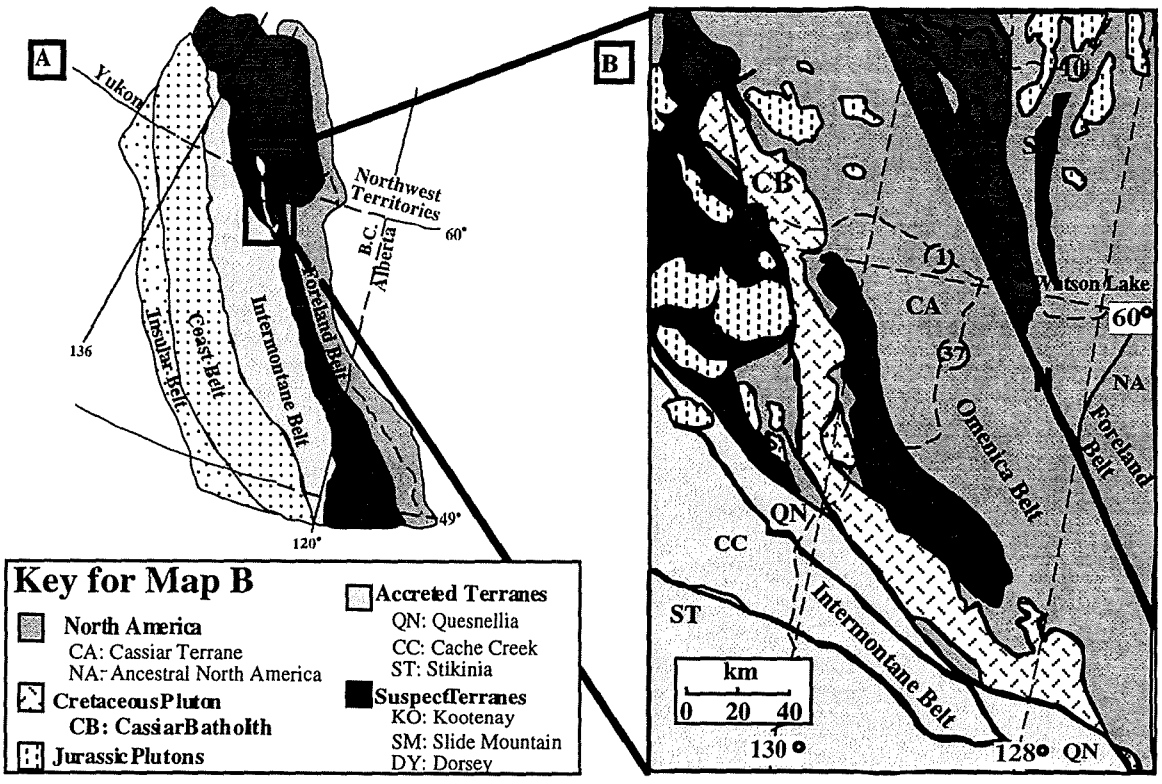

Figure 1: Map of Cassiar batholith: a) within the Canadian Cordillera and b) within a regional geological setting.

Petrology and Field Relations

The Cassiar batholith consists of medium- to coarse-grained equigranular granitoids, with occasional occurrences of K-spar porphyritic granitoid. All samples contain quartz, plagioclase, K-feldspar, and biotite. Primary muscovite is abundant in the granites and some of the granodiorites, whereas hornblende is much less abundant, and only occurs as small very small crystals in the granodiorites. Accessory minerals are apatite, and zircon, with localized occurrences of sphene, epidote, and allanite. Boundaries between different rock types within the batholith are gradational, and no distinct pulses of magmatism have been identified in the field. Rocks generally become more mafic and coarser-grained to the south. Rocks within 8 km of the western boundary become increasingly foliated, sheared and eventually mylonitized to the west. Rock textures along this boundary show both syn- and post-emplacement deformation.

Major- and Trace- Element Geochemistry

Within the Cassiar batholith, SiO_2 ranges from 57.36 to 76.66 wt. %, with the greatest majority of samples known containing >65% wt. % SiO_2. Harker diagrams (Figure 2) display typical granitic variations of oxides versus SiO_2 with decreasing trends in Al_2O_3, FeO*, CaO, MnO, Na_2O, TiO_2, MgO, and P_2O_5 and an increasing trend in K_2O. The alkali-lime index (Peacock, 1931) (55.5 wt. % SiO_2) classifies the batholith as calc-alkalic, and the alumina saturation index (0.937 to 1.334) indicates dominantly peraluminous magmas. IUGS classification from CIPW normative mineralogy (**Figure 3**) yielded a suite of granite, granodiorite, quartz monzodiorites and quartz monzonites, which accurately reflects the modal rock types observed within the Cassiar batholith.

The continuous variation of most oxides on Harker diagrams is suggestive of a single parent magma which was related to its more evolved derivatives through the process of magma differentiation. However, as discussed further below, such an interpretation is not compatible with the isotopic data, which require at least two different source rocks or parent magmas. the range of alumina saturation values may also reflect multiple source rocks, including a metaluminous igneous source and a strongly peraluminous sedimentary source.

Tectonic interpretations based solely on the geochemistry are equivocal. The calc-alkaline signature in the alkali-lime index classification suggest that the Cassiar batholith resulted from subductional tectonics. Pearce plots (Figure 4), however, suggest that the Cassiar batholith formed in either a volcanic arc setting, or a continent-continent syn-collisional setting.

Therefore, from the major, trace and rare earth element geochemistry alone, classification of the Cassiar batholith rocks is useful, but no clear interpretations about source material or tectonic setting can be made.

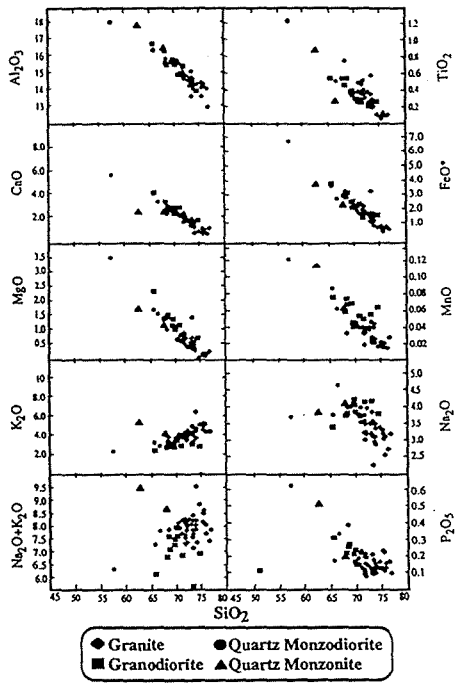

Figure 2: Harker Diagrams for the Cassiar batholith.

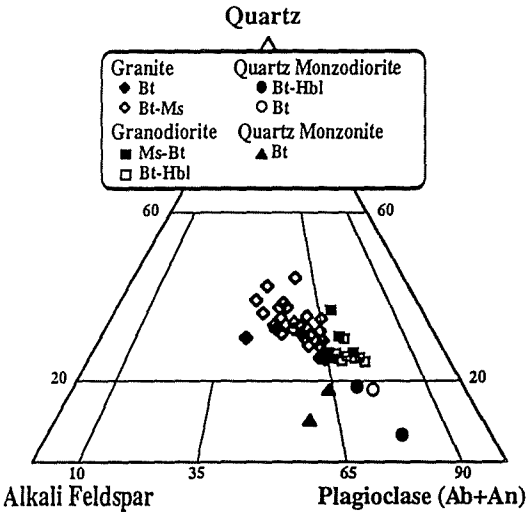

Figure 3: IUGS classification for the Cassiar batholith.

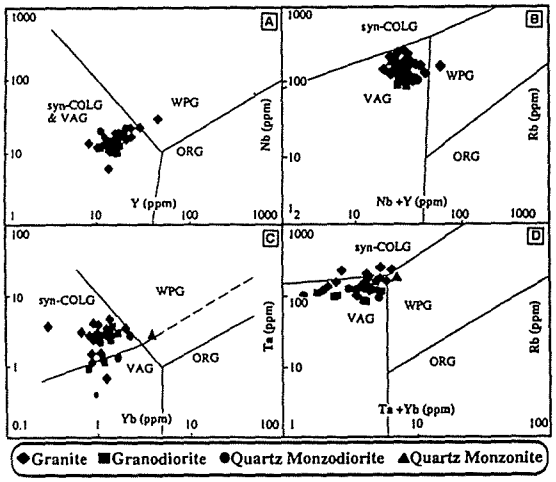

Figure 4: Pearce plots for the Cassiar batholith.

Isotope Geochemistry

In order to develop more comprehensive petrogenetic and tectonic models for the Cassiar granitoids, we carried out Sr, Nd and O isotope analyses of representative samples from the full north-south strike length of the batholith. This multiple isotope approach provides information on both the petrological character and the crustal residence time of the granitoid source materials. Initial $^{87}Sr/^{86}Sr$ ratios and ε_{Nd} values range from 0.706 to 0.734, and -3.5 to -17.9, respectively. $\delta^{18}O$ values range from 7.6 to 11.6‰. In general, the isotopically evolved samples (high $^{87}Sr/^{86}Sr$ and $\delta^{18}O$, negative ε_{Nd}) are granites whereas the granodiorites and quartz monzodiorite have somewhat less evolved isotopic signatures.

The wide ranges in isotopic compositions indicate that a single, homogeneous source rock could not have given rise to the full spectrum of Cassiar magmas. Rather, the data require multiple magma sources. This hypothesis is supported by the linear array of data on the $^{87}Sr/^{86}Sr$ versus Sr(ppm) plot (Figure 5) and the curved data array on the ε_{Nd} versus $^{87}Sr/^{86}Sr$ plot (Figure 6). Such data arrays are characteristic of magma suites that have formed either by mixing of magmas generated from two compositionally and isotopically distinct source rocks, or by mafic, mantle derived magmas, that have assimilated varying amounts of ancient crustal rocks (Taylor and Sheppard, 1986; DePaulo et al., 1992). In either case, the Cassiar magmas bear the imprint of both mafic and felsic sources. The felsic source, which was the primary contributor to the granites (senso stricto) of the Cassiar Suite, was peraluminous, had high initial $^{87}Sr/^{86}Sr$ ratios and $\delta^{18}O$ values, and strongly negative ε_{Nd} values. These geochemical and isotopic features are characteristic of Meso- to Neoproterozoic metasedimentary rocks that are present in many parts of the Omineca Crystalline Belt. The 1.0-2.0 Ga Nd model ages of the Cassiar granitoids also overlap those of the metasedimentary rocks. The nature of the mafic source is more problematic. This source was metaluminous rather than peraluminous, had less evolved isotopic signatures than the felsic source, but still possessed distinctly crustal isotopic ratios. One possibility is that this source was basaltic magma, generated in the mantle at ~105 Ma, that interacted extensively with Proterozoic age continental crust. Arguing against this possibility is general absence of reported mid-Cretaceous age basaltic magmatism,

either in the vicinity of the Cassiar batholith or throughout the Omineca Crystalline Belt. An alternate possibility is that this source represents ancient mafic material; that is, Proterozoic age basaltic composition rocks that were tectonically buried and then partially melted at ~105 Ma to give rise to the more mafic magmas in the Cassiar batholith (granodiorites and quartz monzodiorites). The lower Rb/Sr and higher Sm/Nd ratios of ancient, basaltic composition source rock would give rise to less evolved, though still distinctly crustal, isotopic ratios. It is interesting to note that basaltic lavas and sills are widespread in both the Meso- and Neoproterozoic supracrustal sequences in the Omineca Crystalline Belt.

Tectonic Setting

Data from known subduction-related magmatism in the Andes and the Himalayas were chosen for comparison with the Cassiar batholith. This magmatism is known to have a mantle component that is variably contaminated by intruding into and incorporating large amounts of overthickened continental crust. Although the Cassiar batholith's more mafic end-member (Figure 6) has ε_{Nd} values and $^{87}Sr/^{86}Sr$ ratios similar to those found in 1 to 2 Ma Andes volcanics (James, 1982), the Cassiar batholith overall has a much wider range in crustal values in both ε_{Nd} and $^{87}Sr/^{86}Sr$. This difference is even more noticeable in $\delta^{18}O$ (Figure 7). Although there is minor overlap in $^{87}Sr/^{86}Sr$ in the more mafic end-member of the Cassiar batholith, the $\delta^{18}O$ values from the Andes and the Himalayas (James, 1982; Longstaffe et al., 1983; Debon et al., 1986) are nearly 1‰ lower than all but one of the Cassiar batholith samples.

The important conclusion that can be drawn from this comparison is that the distribution of isotopic data for the Cassiar batholith is significantly different from that observed in known subduction-zone environments. A large mantle contribution to subduction-zone magmatism is easily recognized even when subduction takes place underneath thick continental crust. In contrast, the isotope data for the Cassiar batholith can be explained with little or no mantle contribution. This strongly suggests that the Cassiar magmas were not generated in a subduction setting. Rather, an intra-continental collisional setting seems more appropriate, with magma generation triggered by elevation of the geotherm caused by overthickening of continental crust.

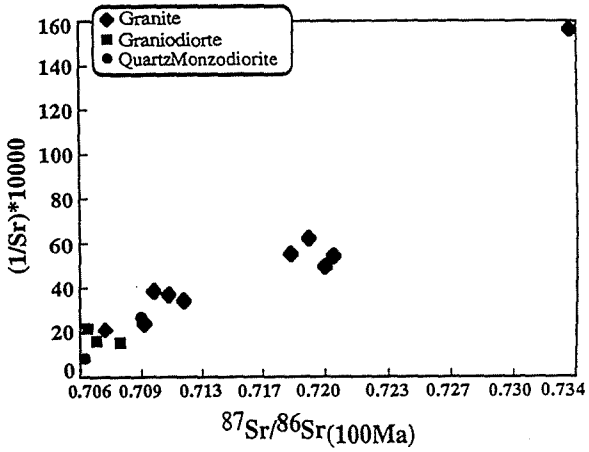

Figure 5: 1/Sr*10000 versus initial $^{87}Sr/^{86}Sr$ (100Ma) ratios for the Cassiar batholith.

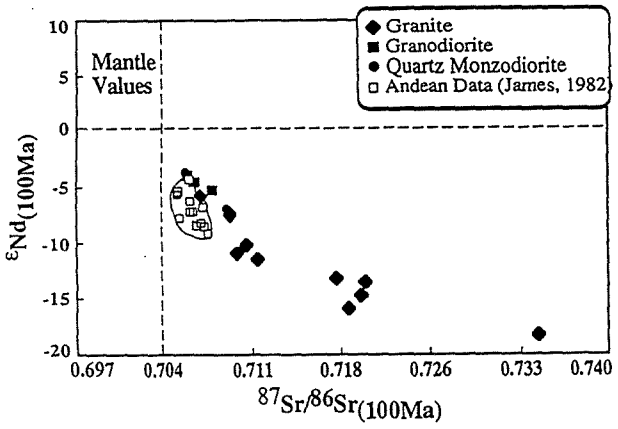

Figure 6: ε_{Nd} values versus initial $^{87}Sr/^{86}Sr$ (100Ma) ratios for the Cassiar batholith.

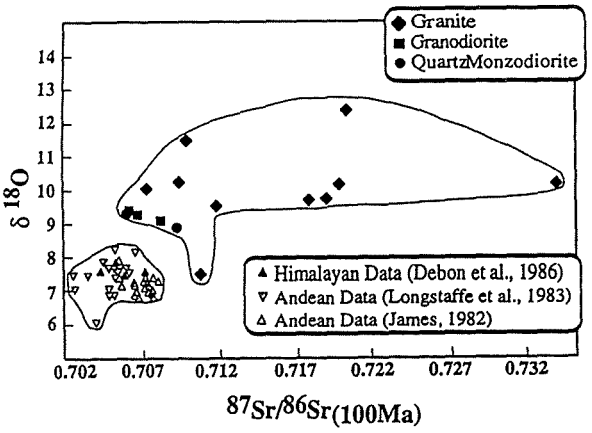

Figure 7: $\delta^{18}O$ versus initial $^{87}Sr/^{86}Sr$ (100Ma) for the Cassiar batholith.

Summary and Conclusions

We found that:

1) The rock types within the Cassiar batholith are high in K, and range from biotite-muscovite granite, biotite ± muscovite granodiorite, biotite ± hornblende granodiorite, quartz monzodiorite, and quartz monzonite. Most samples are equigranular, some contain K-spar phenocrysts, and rocks within 8 km of the western boundary become highly foliated, sheared, and mylonitized.

2) Major and trace element geochemistry is useful in classifying the rocks and the batholith itself, but petrologic interpretations from this data alone are equivocal.

3) The combination of stable and radiogenic isotopes provides the best determination into the source material of the Cassiar batholith magma, which appears to represent the mixing of 2 crustal sources: 1) a more juvenile, mafic crustal component, and 2) a more evolved, felsic crustal component.

4) The Cassiar batholith has strongly crustal radiogenic and stable isotope signatures, and is not comparable to known subduction-related magmas. Rather, magma generation triggered by elevation of the geotherm caused by overthickening of continental crust in an intra-continental collisional setting seems more appropriate.

References

Brandon, D. A. & Lambert, R. St.J., 1993. Geochemical characterization of mid-Cretaceous granitoids of the Kootenay Arc in the southern Canadian Cordillera. Canadian Journal of Earth Science 30, 1076-1090.

Brandon, D. A. & Lambert, R. St.J., 1994. Crustal melting in the Cordilleran interior: the mid-Cretaceous White Creek Batholith in the southern Canadian Cordillera. Journal of Petrology 53, 239-269.

Chappell, B.W. & White, A.J.R., 1992. I- and S-type granites in the Lachlan Fold Belt. Transactions of the Royal Society of Edinburgh: Earth Sciences, 83:1-26. In: Brown, P.E., & Chappell, B.W. (eds.) Second Hutton Symposium of the Origin of Granites and Related Rocks. Geological Society of America Special Paper 272. 507p.

Debon, F., LeFort, P., Sheppard, S.M.F. and Sonet, J. 1985. Transhimalaya-Himalaya: a chemical, mineralogical, isotopic, and chronological synthesis along a Tibet-Nepal section. Journal of Petrology 27, 219-250.

DePaolo, D.J., Perry, F.V. and Baldridge, W.S. 1992. Crustal versus mantle sources of granitic magmas: a two-parameter model based on Nd isotopic studies. Transactions of the Royal Society of Edinburgh: Earth Sciences, 83:4339-446 *in:* P.E. Brown, and B.W. Chappell, (eds.), Second Hutton Symposium of the Origin of Granites and Related

Rocks. Geological Society of America Special Paper 272. 507p.

Gabrielse, H. 1962a. Cry Lake Map No. 29-1962, 1:250,000, sheet 104I. Geological Survey of Canada.

Gabrielse, H. 1962b. Kechika Map No. 42-1962, 1:250,000, sheet 94L. Geological Survey of Canada.

Gabrielse, H. 1963. McDame Map No. 1110A, 1:250,000. Geological Survey of Canada Memoir 319.

Gabrielse, H. 1969. Jennings River Map No. 18-1968, 1:250,000, sheet 104O. Geological Survey of Canada.

Gromet, L. P. & Silver, L. T., 1987. REE variations across the Peninsular Ranges batholith; Implications for batholithic petrogenesis and crustal growth in magmatic arcs. Journal of Petrology 28, 171-210.

James, D.E. 1982. A combined O, Sr, Nd, and Pb isotopic and trace element study of crustal contamination in central Andean lavas, I; Local geochemical variations. Earth and Planetary Science Letters, 57,47-62.

Longstaffe, F.J., Clark, A.H., McNutt, R.H., and Zentilli, M. 1983. Oxygen isotopic compositions of Central Andean plutonic and volcanic rocks, latitudes 26°-29° south. Earth and Planetary Science Letters, 64, 9-18.

Miller, C. F. & Barton, M. D., 1990. Phanerozoic plutonism in the Cordilleran Interior, U.S.A. In: Kay, S. A. & Rapela, C. W. (Eds.) Plutonism from Antarctica to Alaska. Boulder, Colorado: Geological Society of America Special Paper 241, 213-231.

Peacock, M. A., 1931. Classification of igneous rocks. Journal of Geology 39, 54-67.

Pitcher, W. S., 1983. Granite type and tectonic environment. In: Hsü, K. J. (ed.) Mountain building processes. London: Academic Press, 18-40.

Pitcher, W. S., Atherton, M. P., Cobbing, E. J. & Beckinsale, R. D., eds., 1985. Magmatism at a plate margin: Glasgow, Scotland: Blackie & Sons, Ltd., 435 p.

Taylor, H.P. Jr., and Sheppard, S.M.F. 1986. Igneous Rocks: I. Processes of isotopic fractionation and isotope systematics (Chapter 8) in: Valley, J.W., Taylor, H.P., and O'Neil, J.R. (Eds.) Stable Isotopes in High Temperature Geological Processes: Reviews in Mineralogy, 16, Mineralogical Society of America, Washington D.C., 227-271, 570p.

The Petrogenesis of the Mount Skukum / Bennett Lake Igneous Complex, Yukon Territory, and reflections on the Eocene tectonics of the Canadian Cordillera.

George A. Morris, and Robert A. Creaser,
Department of Earth and Atmospheric Sciences, University of Alberta, Edmonton, Alberta, T6G 2E3, Canada. e-mail: george.morris@ualberta.ca, robert.creaser@ualberta.ca

INTRODUCTION

The Mount Skukum / Bennett Lake Igneous complex consists of two similar Eocene volcanic complexes that lie across, and just north of the Yukon / British Columbia border (59°55'N to 60°18'N) and unconformably overlie the boundry between Palaeozoic metamorphic rocks of the Stikinia Terrane and Cretaceous granites of the Coast Plutonic Complex (135°05'W to 135°35'W; Figure 1). These complexes form the northern-most expression of a belt of similar Eocene volcanics that lie along the northeastern margin of the Coast Plutonic Complex between 58°N and 60°N called the Sloko Volcanic Province (Souther, 1970). The basic mapping of the Bennett Lake Complex was carried out by Lambert (1974) who defined the caldera, bounded by two generations of ring dyke and filled with four volcanic, and three sedimentary formations. The basic mapping of the Mount Skukum complex was carried out by Pride (1985; 1986; nee Smith, 1982). Further work was carried out by McDonald (1987), Doherty and Hart, 1988 and Love (1989) leading to the present stratigraphy, as summerised in Hart and Radcliff (1990), which we follow. Readers are referred to these sources for details. A summary of the volcanic stratigraphy of both complexes is presented in Figure 2.

The Bennett Lake Complex is well constrained in age to between 54 Ma (U-Pb on early ring dyke intrusion; written comm R.L. Armstrong in Hart and Radloff, 1990) and 51 Ma (Rb-Sr on late caldera fill lavas; this study). The inception of the Mount Skukum Complex is a less clear but the later stages of activity appear to correlate with the Bennett Lake Complex. High level rhyolite intrusions on the border of the complex have been dated by Rb-Sr geochronology at 53 Ma (Pride and Clark, 1985) while late stage lava flows have returned a date of 51 Ma by the same method (this study).

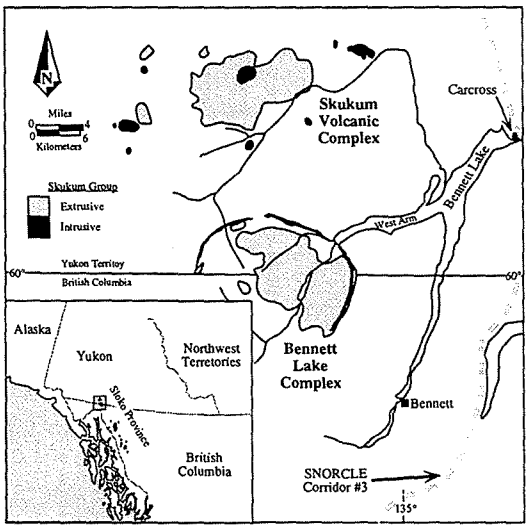

Figure 1. Location of the Skukum Volcanic and Bennett Lake complexes, Yukon and northern British Columbia. Also plotted is the location of SNORCLE Corridor #3. Insert shows location of complexes within the Sloko Province. Adapted from Smith (1982) and Lambert (1974).

GEOCHEMISTRY: Major and Trace Elements

All major and trace element geochemistry was analysed at Washington State University by X-ray fluorescence following standard proceedures reported in Johnson et al. (1997).

The Mount Skukum complex shows an almost perfect bi-modal

distribution of major element data (figure 3). The first group, largely corresponding to samples of welded and non-welded ignembrites, range from 74 to 82 wt% SiO_2 (rhyolite). The second group, consisting of lava flows and domes, range from 58 to 67 wt% SiO_2 (trachyandesites, andesites and dacites). Some formations (the *Butte Fm.*, the *lower Watson River Fm.* and late bi-modal dykes) return data in both groups while other formations are restricted to one or other group (the *Vesuvius Fm.* to the lower group and the *upper Watson River Fm.* to the upper group). While the eruptive sequence generally follows the sequence of high silica rhyolite ignimbrites followed by lower silica lava flows or domes, the intrusion of the late bi-modal dykes reverses this sequence.

Mount Skukum Volcanic Complex	Bennett Lake Volcanic Complex
Vesuvius Formation Felsic volcanics and volcanoclastics	**Boudette Creek Formation** Granite boulder conglomerate
Watson River Formation Intermediate volcanics and associated tuff	**Jones Creek Formation** Intermediate volcanics and felsic volcanoclastics
Butte Formation Intermediate and felsic volcanics and associated tuff	**Lemieux Creek Formation** Granite boulder conglomerate and reworked volcanoclastics
Mount Ried Formation Non-volcanic conglomerate, sandstone and siltstone	**MacAuley Creek Formation** Intermediate volcanics and ignembrites
	Gault Formation Granite boulder conglomerate and sandstone
	Cleft Mountain Formation Intermediate to silicic lavas and ignembrites
	Partridge Lake Formation Intermediate to silicic lavas and ignembrites

Figure 2. Stratigraphy of the Mount Skukum Volcanic Complex and the Bennett Lake Volcanic Complex. Formations in bold are dominantly volcanic and are discussed in this paper. Adapted from Hart and Radloff (1990) and Lambert (1974).

Trace element data for the Mount Skukum complex reflects the bi-modal distribution of the major elements. The high silica group shows a small to moderate enrichment in Rb, Th, Nb and Y coupled with a strong depletion in Sr, Ba, P and Ti compared to the lower silica group (figure 4). Such a distribution could be accounted for by the fractionation of plagioclase, along with ferromagnesium minerals and apatite from a common source magma to produce the high silica group, the low silica group representing non- or less-fractionated magma.

Rocks of the Bennett Lake complex show a similar bi-modal distribution to those from the Mount Skukum complex, with the exception of the *MacAuley Creek Fm.* (figure 5). The high silica group within the Bennett Lake complex range from 73 to 77 wt% SiO_2 (rhyolite) while the low silica group range from 61 to 65 wt% SiO_2 (andesite and dacite). Like the Mount Skukum complex, some formations fall with both groups (the *Cleft Mountain Fm.* and the *Jones Creek Fm.*) while the *Partridge Lake Fm.* falls exclusivly within the high silica group. The *MacAuley Creek Fm.* falls between the low and high silica groups may result from mixing of the two magma types.

The bi-modal nature of the Bennett Lake Complex is again reflected in the trace element data, with the *MacAuley Creek Fm.* falling between the two end members (figure 6.) A similar depleation in Sr, Ba, P and Ti again suggests that plagioclase, ferromagnesium minerals and apatite fractionation is an important factor in the differentiation of the complex.

GEOCHEMISTRY: Radiogenic Isotopes

Analysis of radiogenic isotopes of srontium and neodymium for both the Mount Skukum and the Bennett Lake complexes return a remarkably tight range of values (Sr_i 0.70498 to 0.70591; Nd_i 0.512598 to 0.512663) regardless of the silica content of the magma (figure 7). This data falls at the lower end of the mantle array, suggesting that the source of magmas for both complexes was primitive, probably directly from the mantle, with little or no contamination from ancient crustal sources.

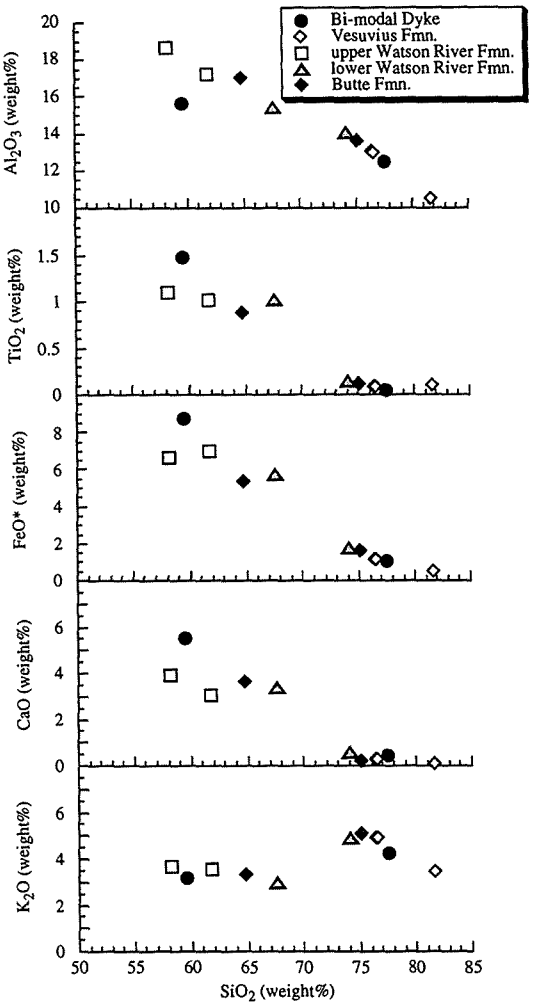

Figure 3. Selected Harker diagrams for the Mount Skukum Igneous Complex.

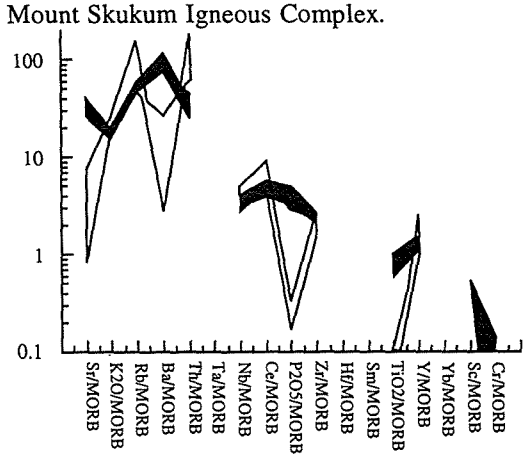

Figure 4. MORB normalised plot for the Mount Skukum Igneous Complex. Dark traces from the low silica group and white traces from the high silica group.

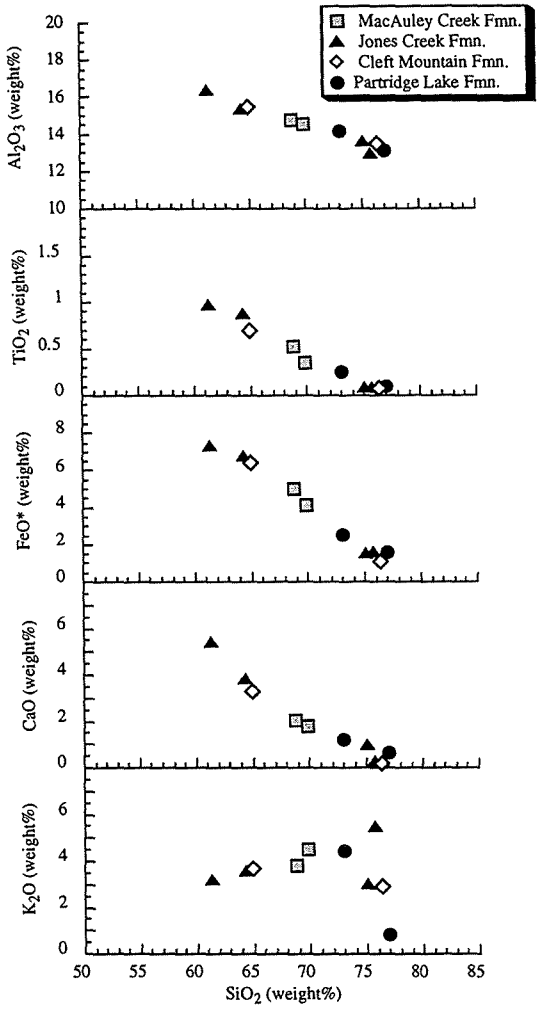

Figure 5. Selected Harker diagrams for the Bennett Lake Igneous Complex.

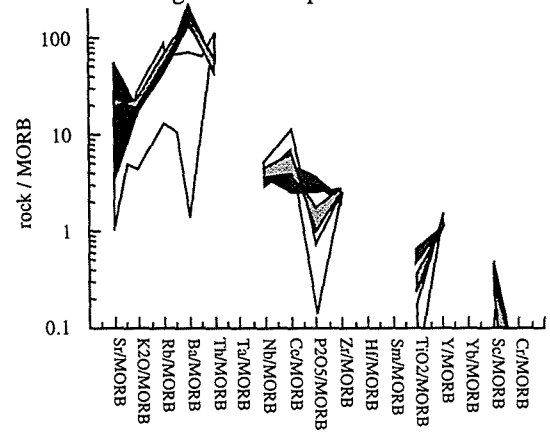

Figure 6. MORB normalised plot for the Bennett Lake Igneous Complex. Dark traces from the low silica group, intemediate traces from the intemediate silica group and white traces from the high silica group.

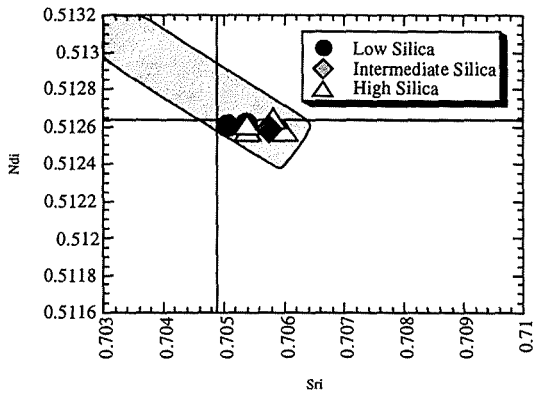

Figure 7. Sr_i v. Nd_i for the Mount Skukum / Bennett Lake Igneous Complex with samples divided based upon major element geochemistry. The Mantle Array (after Faure, 1986) is also plotted.

PETROGENESIS

We suggest that, based upon the tight array of isotopic data, grouped within the mantle array, that the main source of magma in both the Mount Skukum and the Bennett Lake complexes was directly from the mantle. The range of compositions present in both complexes can be accounted for by simple fractionation of phases such as plagioclase, ferromagnesium minerals and apatite. If crustal contamination was a factor in the development of these magmas, the crustal source must have been relatively primitive, leaving the isotopic ratios of the magmas virtually unaffected. The presence of a marked depletion in HFS elements such as Nb (and TiO_2 in higher silica members), coupled with a reletive enrichment of LIL elements (Sr, K_2O, Rb, Ba, Th) suggests a subduction origin. Unlike Eocene rocks of similar compositions further south in the Cordillera (Morris and Hooper, 1997) there is no evidence to dispute a contemporaneous subduction model for the formation of the Mount Skukum and Bennett Lake igneous complexes.

EOCENE TECTONICS OF THE CORDILLERA

Despite many apparent similarities in petrology and geochemistry between Eocene volcanics of the southern Canadian / northern US Cordillera, and those of the northern Canadian Cordillera, there appears to be a dramatic differences in the petrogenetic and tectonic origin of these two areas. Previous, and ongoing work in the Southern Canadian / northern US Cordillera (figure 8), in the Absoroka volcanics of NE Wyoming (M. Hiza, pers comm, 1997), the Colville Igneous Complex of NE Washington and S British Columbia (Morris and Hooper, 1997), and the Francis Lake Complex of central British Columbia (N. Grainger, op. cit., 1998), conclude that the large quantities of calc-alkaline magma that were erupted in the area were derived from mid to deep crustal melting during post Laramide orogenic collapse. The subduction signature that almost all of these rocks display was inherited from the Proterozoic subduction events that originally formed this crust. The only rocks that can clearly be tied to a contemporaneous mantle source (basalts in the Colville Igneous Complex) show no subduction enrichment.

The rocks of the Mount Skukum / Bennett Lake complex, despite being the same age and showing the same range in composition as those to the south, were clearly formed by a quite different process. The tight grouping of isotopic signatures suggest that these rocks came from the same source, and model age data is indicative of a contemporaneous, or near contemporaneous separation from the mantle. Trace element data can be reconciled with a simple fractionation, or a fractionation / assimilation process from a common magma. These data all suggest that the formation of the Mount Skukum / Bennett Lake complex was a result of contemporaneous subduction to the west of the northern Candian Cordillera during the Eocene.

We therefore propose that there were two distinct magmatic belts within the Cordillera during the Eocene. The first, forming within the Omineca Crytalline Belt, and into Cratonic North America to the south, was a result of post orogenic collapse of the overthickened Laramide orogenic belt. The second, forming in the northern Cordillera between (and into?) the Coast Plutonic Belt and the Intermontane Belt, was formed during continued eastward subduction of the Kula plate into the Eocene.

An important aspect of this study is that two superficially identical magmatic belts, erupted at the same time, are infact formed by distinctly different tectonic processes.

REFERENCES

Doherty, R.A., and Hart, C.J.R., 1988: Preliminary geology of Fenwick Creek (105D/3) and Alligator Lake (105D/6) map areas. *Indian and Northern Affairs Canada, Northern Affairs, Yukon Region Open File* **1988-2**, 65p.

Faure, G., 1986: Principles of Isotope Geochemistry (2nd Edition). *New York, Wiley*, 589p.

Hart, C.J.R., and Radcliff, J.K., 1990: Geology of Whitehorse, Alligator Lake, Fenwick Creek, Carcross and part of Robinson map areas (105D/11, 6, 3, 2, &7). *Indian and Northern Affairs Canada, Northern Affairs, Yukon Region Open File* **1990-4**, 113p.

Johnson, D.M., Hooper, P.R., and Conrey, R.M., 1997: XRF analysis of rocks and minerals for Mjor and Trace Elements on a Single Low Dilution Li-tetraborate Fused Bead. *Advances in X-ray Analysis*, **41**.

Lambert, M.B., 1974: The Bennett Lake Cauldron Susidence Complex, British Columbia and Yukon Territory. *Geological Survey of Canada, Bulletin* **277**, 213p.

Love, D.A., 1989: Geology of the epithermal Mount Skukum gold deposite, Yukon Territory. *Geological Survey of Canada, Open File* **2123**, 51p.

McDonald, B.W.R., and Godwin, C.I., 1987: Geology of Main Zone at Mt. Skukum, Wheaton River area, southern Yukon. *Yukon Geology* **1**, p6-11.

Morris, G.A., and Hooper, P.R., 1997: Petrogenesis of the Colville Igneous Complex, northeast Washington: Implications for Eocene tectonics in the northern U.S. Cordillera. *Geology*, **25**, p831-834.

Pride, M.J., 1985: Preliminary geological map of the Mount Skukum Volcanic Complex, 105D/3, 4, 5, 6. Exploration and Geological Services Division, Yukon, Indian and Northern Affairs Canada, Open File, 1:25,000 scale map.

Pride, M.J., 1986: Description of the Mt. Skukum volcanic complex in southern Yukon. *Yukon Geology*, **1**, p148-160.

Pride, M.J., and Clark, G.S., 1985: An Eocene Rb-Sr isochron for rhyolite plugs, Skukum area, Yukon Territory. *Canadian Journal of Earth Sciences*, **22**, p1747-1753.

Smith, M.J., 1982: Petrology and geology of high level rhyolite intrusives of the Skukum area, 105D SW, Yukon Territory. *Yukon Exploration and Geology 1981, Department of Indian and Northern Development*, p68-72.

Souther, J.G., 1970: Volcanism and its relationship to recent crustal movements in the Candian Cordillera. *Canadian Journal of Earth Sciences*, **7**, p553-568.

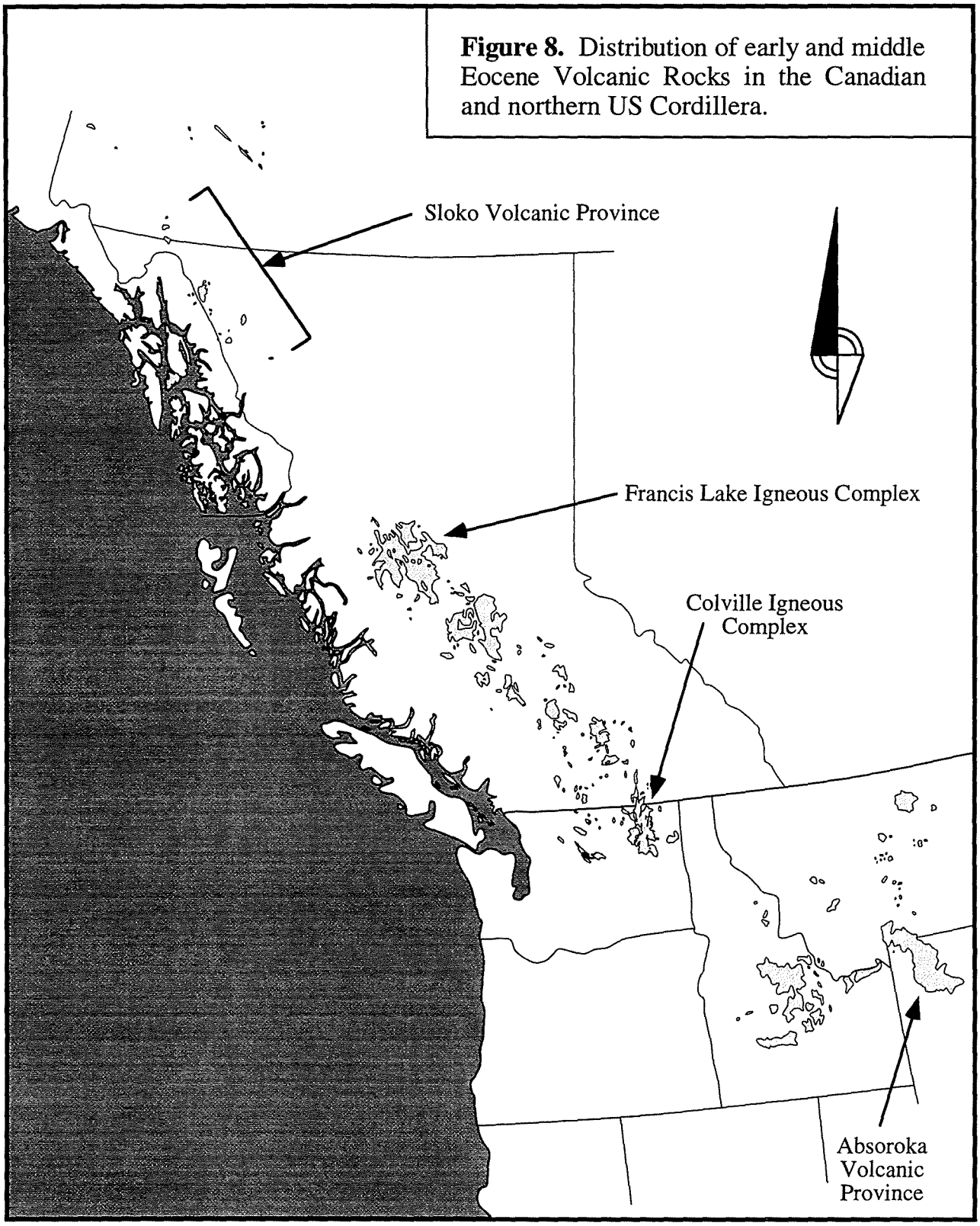

Figure 8. Distribution of early and middle Eocene Volcanic Rocks in the Canadian and northern US Cordillera.

GEOTECTONICS IN THE NORTHERN CORDILLERA FROM PALEOMAGNETISM AND GEOBAROMETRY: PROGRESS REPORT AND RECENT RESULTS FROM THE EOCENE WHITE PASS DIKES AND JURASSIC FOURTH OF JULY BATHOLITH

Symons, D.T.A.[1], Harris, M.J.[2], Hart, C.J.R.[3], Blackburn, W.H.[1]

(1) Dept. of Earth Sciences, Univ. of Windsor, Windsor, ON, N9B 3P4, dsymons@uwindsor.ca; (2) Dept. of Earth Sciences, Univ. of Western Ontario, London, ON, N6A 5B7; (3) Yukon Geology Program, Whitehorse, YT, Y1A 2C6

1) PROGRESS REPORT

Paleomagnetic studies at Windsor on rock units in the SNORCLE transect area are currently in their third year of funding by LITHOPROBE. Studies on the mid Cretaceous Whitehorse tonalite and the mid Cretaceous Mount McIntyre granodiorite (Fig. 1) have been completed, presented at three meetings, and since published (1,2). A study of clasts in the Early Jurassic Laberge conglomerate has been completed with the results given in abstract (3,4) and a final manuscript under revision. The paleomagnetic and geobarometric data have been analysed for the Middle Jurassic Fourth of July batholith and presented in abstract (5), however, we are waiting for some age dating results before an interpretation can be finalized. In the case of the Eocene White Pass mafic dikes, the paleomagnetic and age dating results are complete, however, we await completion of the geobarometry. Preliminary results from both the White Pass dikes and Fourth of July batholith are discussed in the following two sections. For both the Late Cretaceous Mount Lorne granodioritic pluton and the Early Jurassic Teslin Crossing syenitic pluton, the paleomagnetic and geothermobarometric results are now in hand, existing radiometric data is sufficient, and initial results have been reported for Teslin Crossing (6). Paleomagnetic analysis has been completed for the Cassiar batholith, but no hornblende has been found to do the geobarometry. We are testing other geothermobarometers in hope that they will provide reliable evidence for the degree of tilt, if any. All of the above studies are focused on terranes underlying the Intermontane Belt and constitute the Ph.D. thesis research of M.J. Harris. They should be completed in the next few months.

The focus of this research is now moving to examine the geotectonic motion of the Yukon-Tanana terrane where two collections were made this past summer from northwest of Carmacks, YT. One is from the Early Jurassic Big Creek batholith that is composed of

hornblende syenite and monzogabbro and the second is from the Late Cretaceous Seymour Creek syenite stock. The former collection has been measured and is being analysed paleomagnetically by Pat Williams for his B.Sc. thesis, and the latter collection has been measured and awaits analysis.

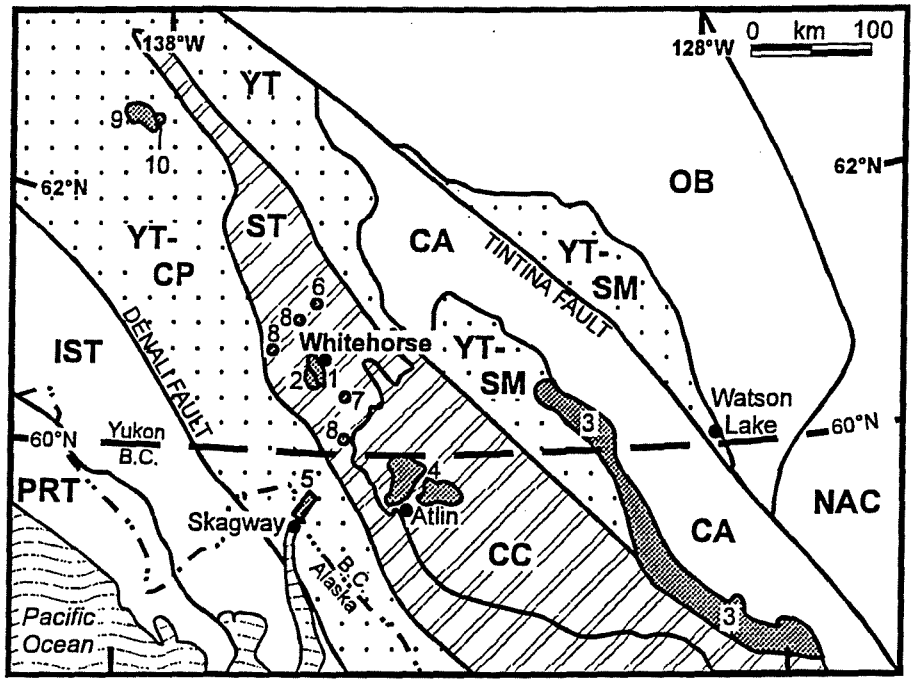

Figure 1 - Tectonic subdivisions of the northern Cordillera. Abbreviations: North American craton (NAC); Omineca fold belt (OB); Yukon-Tanana-Slide Mountain terrane (YT-SM); Cassiar terrane (CA), displaced craton; Yukon Tanana terrane (YT); Cache Creek terrane (CC); Stikine terrane (ST); Yukon Tanana-Coast plutonic terrane (YT-CP); Insular superterrane (IST); Pacific Rim terranes (PRT); Target units: 1) Whitehorse pluton; 2) Mount McIntyre pluton; 3) Cassiar batholith; 4) Fourth of July batholith; 5) Skagway dykes; 6) Teslin Crossing pluton; 7) Mount Lorne pluton; 8) Laberge conglomerate; 9) Big Creek pluton; and, 10) Seymour Creek pluton.

2. WHITE PASS DIKES

The White Pass dikes, an unofficial name for the swarm, are at the southwest end of SNORCLE transect #3. They are well exposed in rock cuts for ~35 km through White Pass summit astride the border between British Columbia and Alaska along the Klondike highway from Carcross, Yukon Territory, to Skagway, Alaska. The dikes are mafic in composition and range up to ~10 m in width. They strike north-northeast with vertical to near-vertical dips, indicating that they have not been subjected to significant post-intrusion tilt. Three K-Ar

age dates from sampled dikes along the highway give an average Eocene age of ~51 ± 3 Ma. The sampled dikes are emplaced into gneisses and migmatites of the Nisling Terrane and into Late Cretaceous to Eocene plutons i.e. the Log Cabin granite (72 ± 2 Ma), Skagway granodiorite (59 ± 1 Ma), Fraser tonalite (54 ± 2 Ma), Summit Lake granodiorite (53 ± 2 Ma), and Clifton granodiorite (48 ± 2 Ma) (7-10). These plutons are part of the Coast Plutonic Complex (Fig. 1). Paleomagnetic analysis included alternating field and/or thermal step demagnetization of ~400 specimens from 26 sites in dikes and 6 sites in adjacent felsic plutons. Most dike specimens have high unblocking temperatures for magnetite (540° - 585°C), indicating that they retain very stable characteristic remanent magnetization (ChRM) directions. Saturation isothermal remanent magnetization analyses confirm that the ChRM is retained mainly by single to pseudosingle domain magnetite. In a few dikes the ChRM direction is also found in pyrrhotite. The granites, on the other hand, have lower unblocking temperature spectra that are indicative of titano-magnetite, resulting in a lower stability ChRM. However, a hematite component was isolated in a few of these felsic specimens. As a result of the close similarity in age between the mafic dikes and host felsic plutons and of the generally low remanence stability of the plutons, the results of the six paleomagnetic contact tests that were attempted, are generally poor. Nevertheless, using endpoint analysis (11) for the majority of specimens and remagnetization circle analysis (12) for a few reversed-polarity specimens, we found 24 dikes that yield well-defined site mean directions — 16 with reversed polarity, 2 with mixed polarity, and 6 with normal polarity. When combined they give a primary ChRM direction of D = 196°, I = -81° (α_{95} = 2.3°, k = 173, N = 24) (13) that is clearly a thermoremanent magnetization in origin (Fig. 2).

The resulting preliminary pole position for the dikes is located at 113°W, 77°N (d_p = 4°, d_m = 4°) (Fig. 3). This can be compared in a preliminary fashion to the lower Tertiary (52 ± 12 Ma, N = 26) reference pole for the North American craton (14). It is located at 173°E, 77°N (α_{95} = 7°). The comparison indicates that the White Pass dikes' terrane has been rotated clockwise by about 41° ± 15° but not translated significantly with respect to the continent i.e. -5° ± 6°.

This result leads to three conclusions. First, the northern portion of the Coast Plutonic Complex has not been translated northward relative to the craton in the past ~51 Ma. Indeed,

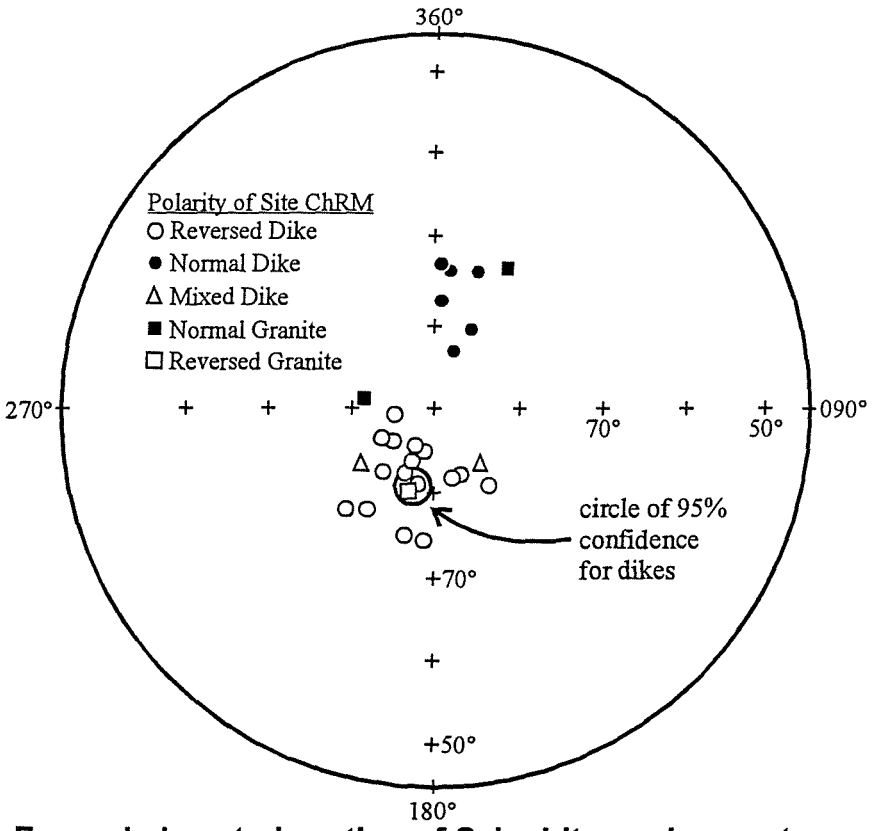

Figure 2 - Expanded central portion of Schmidt equal-area stereonet with site mean ChRM directions for the White Pass dikes' collection. Down (up) directions are shown by solid (open) symbols.

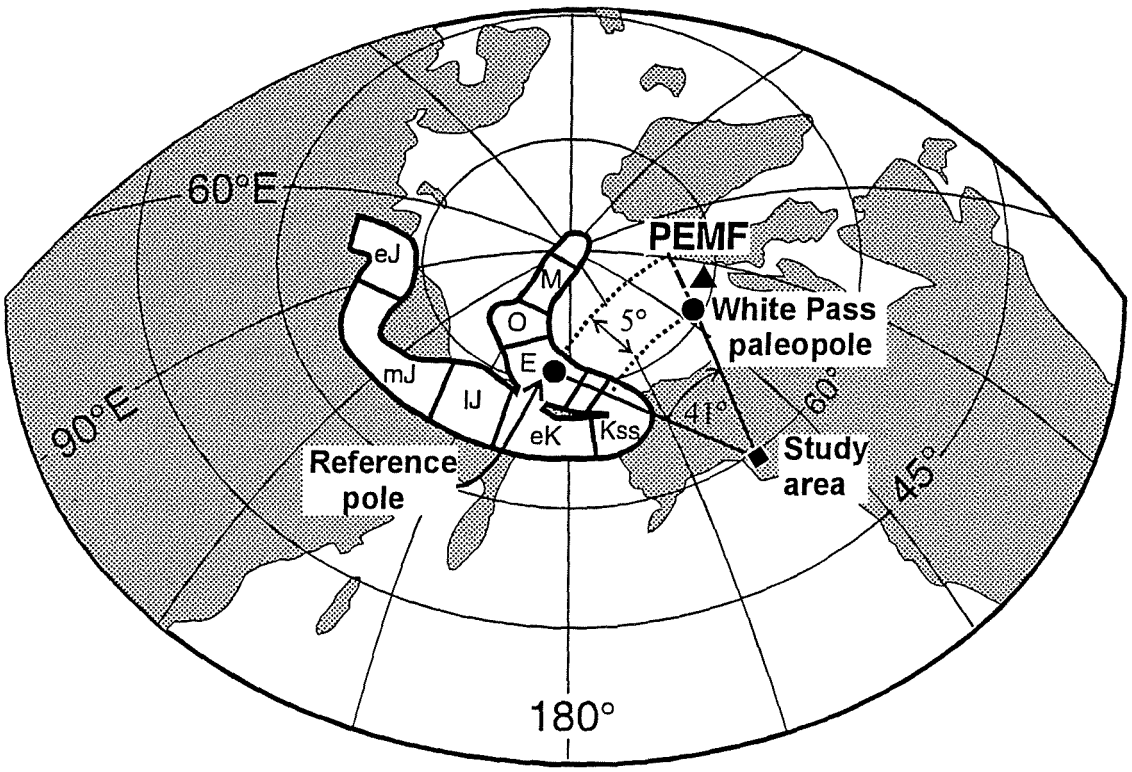

Figure 3 - Measured and reference pole positions for the White Pass dikes.

the result shows a minor southward translation of ~600 km that could speculatively be related to the counterclockwise rotation of Alaska in early Tertiary time. This result also provides further evidence that the terrane motion estimate from the Carmacks Volcanics (15) in the Yukon is flawed because the proposed translation rate must now be increased by ~50%, making it faster than the rate for the Kula Plate on which the volcanics were postulated to have been carried. Second, the indicated clockwise rotation for the White Pass terrane of $41° \pm 15°$ is substantial. Initially we attribute it to dextral shear on the Coast Shear Zone - Denali Fault system (16) that passes outboard of the study area about 25 km to the west. Third, substantial clockwise rotation has been observed in a number of paleomagnetic studies of plutonic rocks in the Coast Plutonic Complex. It has been attributed to southwest-side down tilt by some authors (e.g. 17) or to viscous remagnetization by the present Earth's magnetic field (e.g. 18). Certainly neither mechanism can be true for the White Pass dikes, indicating that these rotations are real and must be accounted for in tectonic terms.

Finally, the above translation and rotation values are regarded as preliminary. Minor changes, but not likely to be statistically significant ones, are possible from more precisely defining the cratonic reference pole to within a narrower age window and from a tilt adjustment based on the geothermobarometry analyses that are in progress.

3. FOURTH OF JULY BATHOLITH

The 172 Ma Fourth of July batholith is exposed ~130 km southeast of Whitehorse, YT, near the town of Atlin, BC (Fig. 1). The body intruded mainly oceanic rocks of the Cache Creek Terrane which underlies the Intermontane Belt. The batholith has an outcrop area of ~650 km^2 and is composed primarily of granite, granodiorite, tonalite and monzonite. It is crosscut by a series of mafic dikes that are thought to be late-stage intrusions because they have similar compositions to the more mafic phases of the batholith (19,20). The dikes are typically 0.3 to 5 metres thick and trend at ~300° with moderate to steep dips to the northeast. The Fourth of July batholith is also intruded on the southeast by the 72 Ma Surprise Lake batholith (Fig. 4).

Al-in-hornblende geobarometric analyses were done on 10 granitic samples from across the batholith, and crystallization depths were calculated from the pressures assuming a crustal

Figure 4 - Regional geology and site locations for the Fourth of July batholith study.

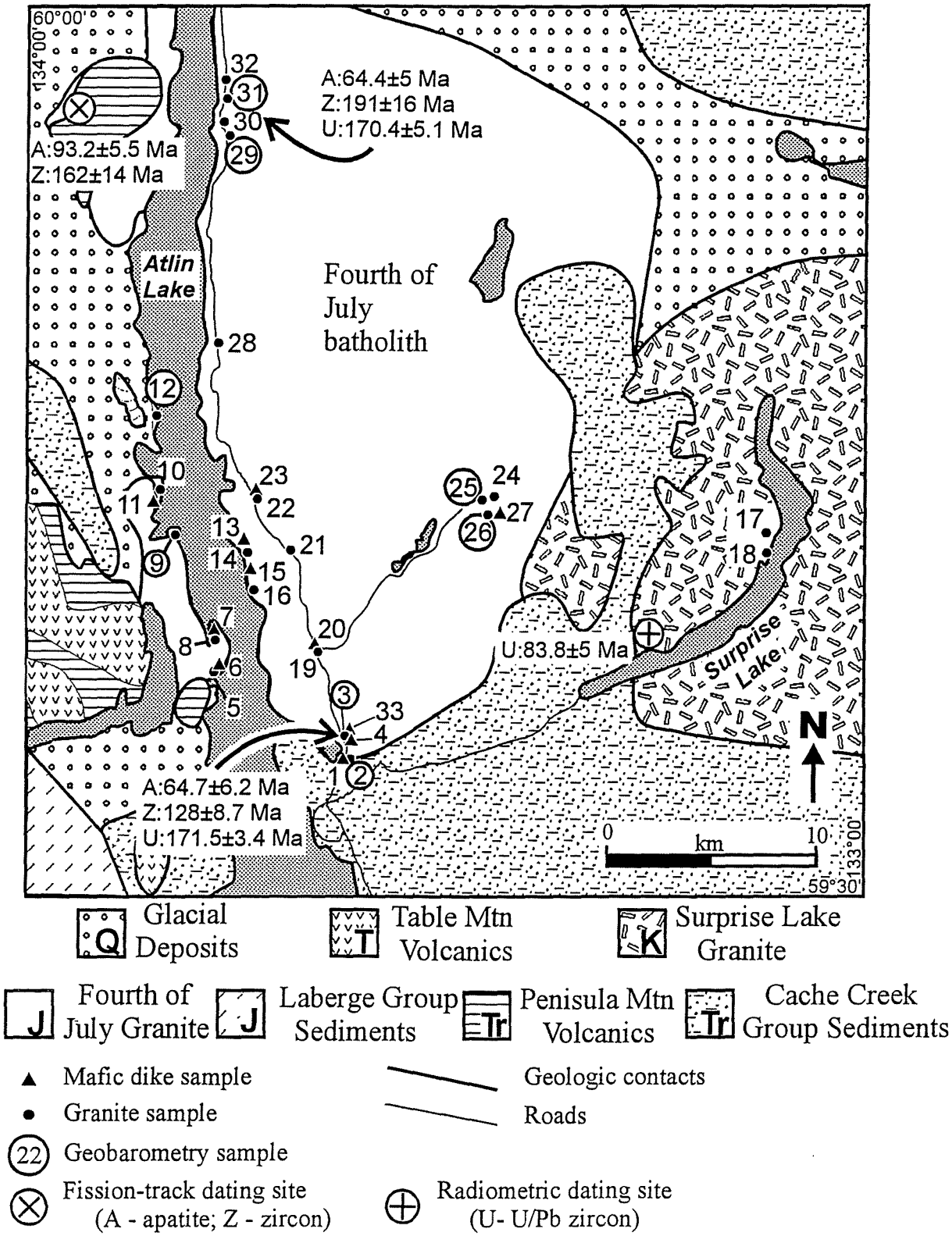

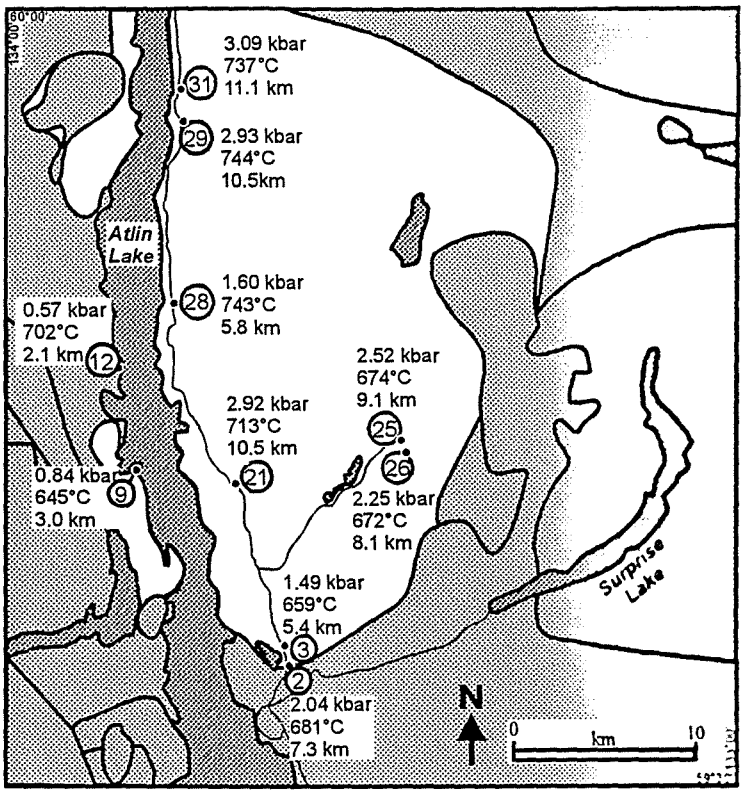

Figure 5 - Geothermobarometric results for the Fourth of July batholith.

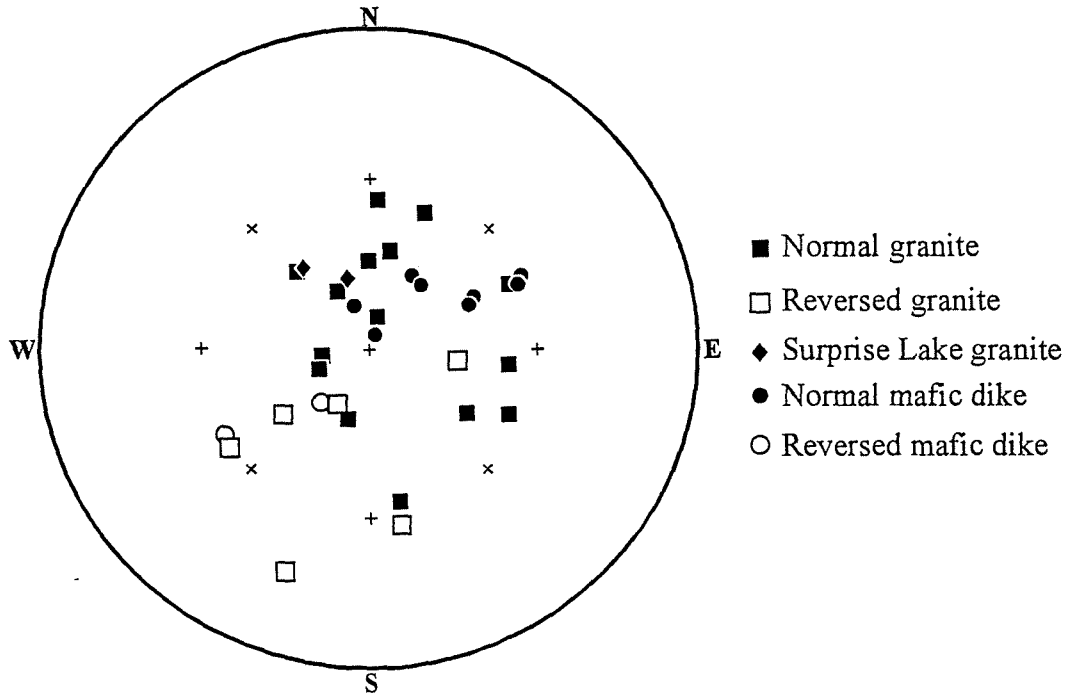

Figure 6 - Schmidt equal-area stereonet with site mean ChRM directions for the Fourth of July batholith collection. Down (up) directions are shown by solid (open) symbols.

density of 2.8 g/cm^3 and a gradient of 3.6 km/kbar (Fig. 5). The two sites on the west shore of Atlin Lake statistically show no evidence of tilting and minimal uplift/erosion (~2.5 km). In contrast, the northern, eastern and southern sites show up to 11 km of differential uplift and erosion. Average depths from the three locations indicate this part of the batholith is tilted to the south-southwest (~200°) at a 10° angle.

Paleomagnetic samples were taken from 33 sites (Fig. 4) of which 20 were sampled within granitoids of the Fourth of July batholith, 11 from mafic dikes, and two from the Surprise Lake batholith. The *in situ* mean characteristic remanence magnetization (ChRM) direction for the Fourth of July Batholith, excluding two sites, is D = 29.3°, I = 73.0° (α_{95} = 12.3°, k = 8) (Fig. 6). The corresponding paleopole is located at 52°W, 75°N (d_p = 19.6° d_m = 21.9°), while its 172 Ma reference pole for the North American craton is located at 110°E, 67.5°N, α_{95} = 3.5° (21) (Fig. 7). This suggests that the Fourth of July batholith has undergone southwards translation of 13° ± 10° (1450 ± 1100 km) and clockwise rotation of 59° ± 20°. If the paleomagnetic data were corrected for tilt, the southwards translation and clockwise rotation would increase by 11° and 6°, respectively.

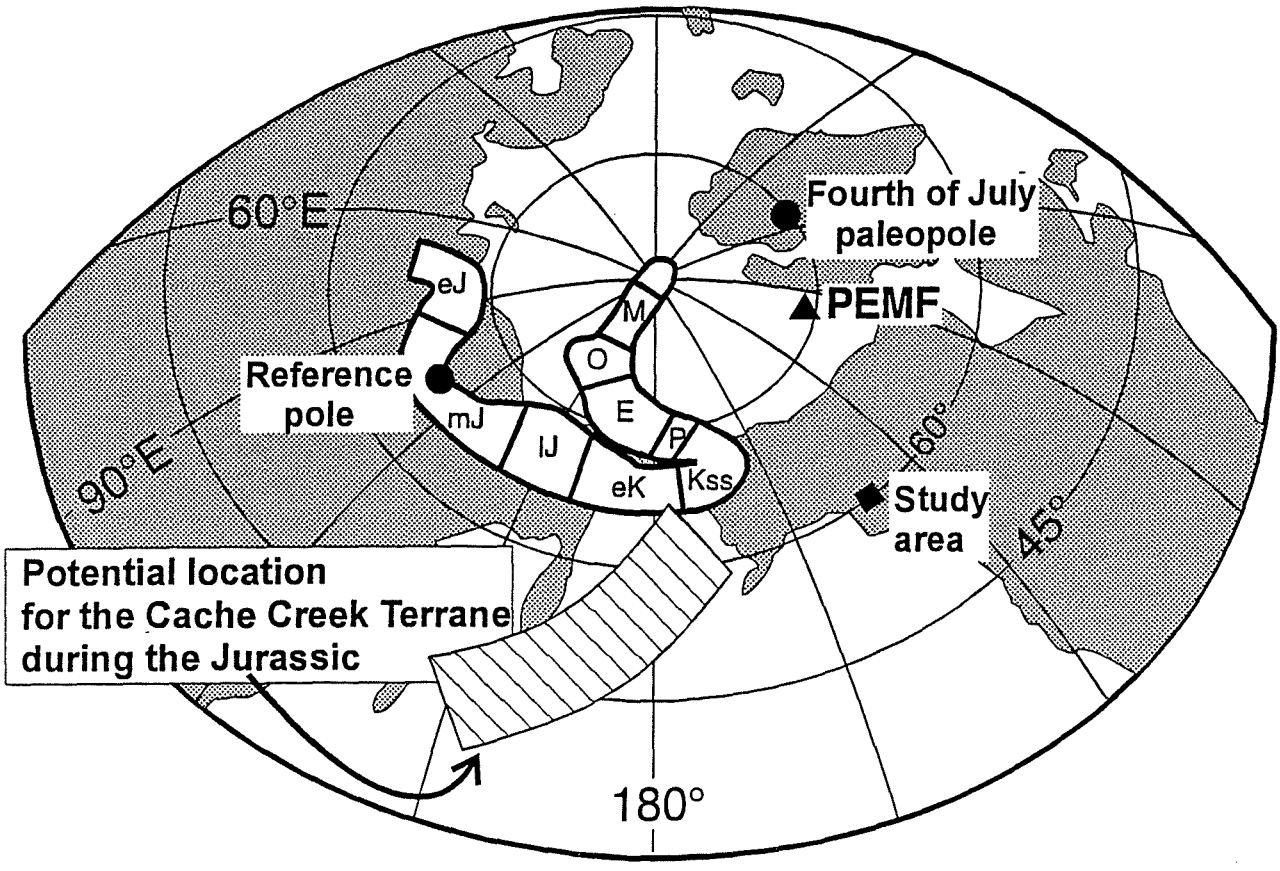

Figure 7 - Measured and reference pole positions for the Fourth of July batholith and potential location of the Cache Creek Terrane during Jurassic time.

The significance of these results is that the Intermontane Belt can now be traced along its path of motion for pre-Cretaceous time. This result now places the Intermontane Belt in the ancestral Pacific Ocean well away from the North American craton during the Middle Jurassic (Fig. 7). This position is supported by geological evidence, as the Cache Creek Terrane contains Permian Tethyan faunal assemblages that are similar to coeval assemblages in eastern Asia (22).

REFERENCES

1. Harris, M.J., Symons, D.T.A., Blackburn, W.H., and Hart, C.J.R., 1996. Paleomagnetic study of the mid-Cretaceous Mount McIntyre pluton, Whitehorse map area (105D), southern Yukon Territory. Yukon Exploration & Geology 1996, pp 122-130.
2. Harris, M.J., Symons, D.T.A., Blackburn, W.H., and Hart, C.J.R., 1997. Paleomagnetic and geobarometric study of the mid Cretaceous Whitehorse pluton, Yukon Territory. Canadian Journal of Earth Sciences, **34**, pp 1379-1391.
3. Harris, M.J., Symons, D.T.A., and Hart, C.J.R., 1997. A test for Laramide remagnetization in the Intermontane on the Yukon Territory. Geological Association of Canada, Abst. Vol. p. A65.
4. Harris, M.J., Symons, D.T.A., and Hart, C.J.R., 1997. Regional conglomerate test for orogenic remagnetization of plutons in the northern Cordillera of Canada. 8th Scientific Assembly, International Association of Geomagnetism and Aeronomy, p. 74.
5. Harris, M.J., Symons, D.T.A., Blackburn, W.H., and Hart, C.J.R., 1997. Tectonic motion of the Jurassic Fourth of July Batholith, northern British Columbia, from paleomagnetism. EOS, **78**, p. F189.
6. Symons, D.T.A., Blackburn, W.H., Harris, M.J., and Hart, C.J.R., 1997. Paleomagnetic and Geobarometric Study of the Teslin Crossing Stock, Stikine Terrane, Yukon, Canada. EOS, **78**, p. F189.
7. Barker, F., Arth, J.G., and Stern, T.W., 1986. Evolution of the Coast batholith along the Skagway traverse, Alaska and British Columbia. American Mineralogist, **71**, pp 632-643.
8. Gehrels, G.E., McClelland, W.C., Samson, S.D., Patchett, P.J., and Jackson, J.L., 1990. Ancient continental margin assemblage in the northern Coast Mountains, southeast Alaska and northwest Canada. Geology, **18**, pp 208-211.
9. Gehrels, G.E., McClelland, W.C., Samson, S.D., Patchett, P.J., and Brew, D.A., 1991. U-Pb geochronology and tectonic significance of Late Cretaceous-early Tertiary plutons in the northern Coast Mountains batholith. Canadian Journal of Earth Sciences, **28**, pp 899-911.
10. Johnston, S.T., Hart, C.J.R., Mihalynuk, M.G., Brew, D.A., and Ford, A.B., 1993. Field guide to accompany the 1993 Nuna conference on the northern Intermontane Superterrane, 19 pg.
11. Kirschvink, J.L. 1980. The least squares line and plane and the analysis of paleomagnetic data. Geophysical Journal of the Royal Astronomical Society, **62**, pp 699-718.

12. Halls, H.C., 1978. The use of converging remagnetization circles in palaeomagnetism. Physics of the Earth and Planetary Interiors, **16**, pp 1-11.
13. Fisher, R.A., 1953. Dispersion on a sphere. Proceedings of the Royal Society of London, **A217**, pp 295-305.
14. Van der Voo, R., 1993. Paleomagnetism of the Atlantic, Tethys and Iapetus oceans. Cambridge University Press, Cambridge.
15. Johnston, S.T., Wynne, P.J., Francis, D., Hart, C.J.R., Enkin, R.J., and Engebretson, D.C., 1996. Yellowstone in Yukon: The Late Cretaceous Carmacks Group. Geology, **24**, pp 997-1000.
16. Hollister, L.S., Andronicos, C., Crawford, M.L., Davidson, C.M., Klepeis, K.A., and Rusmore, M.E., 1997. Geological data cannot rule out large scale (< 1000 km) transcurrent motion across the Coast orogen. In F. Cook, and P. Erdmer (compilers), 1997 Slave-Northern Cordillera Lithospheric Evolution (SNORCLE) Transect and Cordilleran Tectonics Workshop Meeting, Lithoprobe Report No. 56, pp 155-159.
17. Butler, R.F., Gehrels, G.E., McClelland, W.C., May, S.R., and Klepacki, D., 1989. Discordant paleomagnetic poles from the Canadian Coast Plutonic Complex: Regional tilt rather than large-scale displacement? Geology, **17**, pp 691-694.
18. Butler, R.F., Gehrels, G.E., and Bazard, D.R., 1997. Paleomagnetism of Paleozoic strata of the Alexander terrane, southeastern Alaska. GSA Bulletin, **109**, pp 1372-1388.
19. Mihalynuk, M.G., Mountjoy, K.J., McMillan, W.J., Ash, C.H., and Hammack, J.L., 1991. Highlights of 1990 fieldwork in the Atlin area (104N/12W). *In* Geological Fieldwork 1990, British Columbia Geological Survey Branch, Paper 1991-1, pp 145-151.
20. Mihalynuk, M.G., and Smith, M.T., 1992. Highlights of 1991 mapping in the Atlin-west map area (104N/12). *In* Geological Fieldwork 1991, British Columbia Geological Survey Branch, Paper 1992-1, pp 221-227.
21. Besse, J., and Courtillot, V., 1991. Revised and synthetic apparent polar wander paths of the African, Eurasian, North American and Indian plates, and true polar wander since 200 Ma. Journal of Geophysical Research, **96**, B3, pp 4029-4050.
22. Monger, J.W.H. and Ross, C.A., 1971. Distribution of fusulinaceans in the western Canadian Cordillera. Canadian Journal of Earth Sciences, **8**, pp 259-278.

CONTRACTIONAL STRUCTURES IN THE WESTERN SKEENA FOLD BELT: AN INDICATION OF CRETACEOUS SINISTRAL CONVERGENCE WITHIN THE COAST BELT

EVENCHICK, Carol A., Geological Survey of Canada, 101-605 Robson Street, Vancouver, BC, V6B5J3, cevenchick@gsc.nrcan.gc.ca.

The Skeena Fold Belt is a thin-skinned fold and thrust belt which occupies much of the width of the northern Intermontane Belt of the Canadian Cordillera. It is composed largely of northwest trending contractional structures, but includes domains of northeast to north-northeast trending contractional structures along its western margin. The fold belt roots to the west in the Coast Belt and is Cretaceous and possibly earliest Tertiary in age. The north-northeast and northeast trending structures are enigmatic because they are orthogonal to the vast majority of contractional structures in the Cordillera. Similar orientations of structures occur sporadically for at least 900 km along the boundary of the Coast and Intermontane belts, from 350 km north-northwest of the Skeena Fold Belt to100 km south-southeast of it.

A speculative explanation for the origin of the north-northeast trending structures is that they are a result of southeast shortening along the Cordilleran margin during a period of sinistral convergence. Sparse cross-cutting relationships suggest that they are overprinted by north-trending contractional structures, which may record a transition to the dominant northwest trend of the Skeena Fold Belt. Because the rocks are as young as latest Jurassic or earliest Cretaceous in age, the sinistral convergence and transition to dextral convergence must also be Cretaceous. In the region northwest of the Skeena Fold Belt the age of north-northeast trending structures is limited to between 135 Ma and 106 Ma.

Plate motion studies by other workers, based on the hot spot reference frame, suggest a transition from sinistral to dextral oblique convergence along the northern Cordilleran margin in mid-Cretaceous time. The interpretation of structures in the western Skeena Fold Belt as resulting from sinistral convergence provides structural evidence on a large scale for the proposed Cretaceous relative plate motions. Possible candidates for the Early Cretaceous sinistral shear zone would be earlier structures along or near the present Denali Fault and Coast Shear Zone.

High-temperature orogen parallel extension during arc construction and exhumation

M.L. Crawford, Dept. of Geology, Bryn Mawr College, Bryn Mawr, PA 19010 and K.A. Klepeis, Dept. of Geology and Geophysics, University of Sydney, Sydney, NSW 2006, Australia

We present a model of arc emplacement and exhumation using new structural and kinematic data that emphasize the importance of horizontal arc-parallel extension, sinistral transtension, and arc-normal to oblique convergence in the Coast Mountains orogen, northern coastal British Columbia. The early phases of this ~65-51 Ma regional-scale orogen parallel intra-arc extension occurred in the deep crust concurrent with arc-normal convergent deformation. This extension accompanied and outlasted the emplacement of the northern Coast Mountains batholith and culminated in rapid uplift and exhumation of the deep roots of the batholith prior to 50 Ma by continued orogen-parallel extension, by near vertical displacements on shear zones on both the eastern and western side of the batholith, and by top-to-the-northeast extension at upper crustal levels on the eastern side of the batholith. These orogen-parallel and orogen-normal displacements accompanied the transition from late Mesozoic plate convergence to Recent right lateral transform displacement along the northwestern margin of North America.

Our study area lies in the central part of the Coast orogen, east of Prince Rupert (~54°N latitude), between the Skeena River and Portland Inlet. It is east of the Coast shear zone that marks the western side of the batholith complex and that records a complex history of dominantly orogen normal to high angle crustal-scale displacements (Klepeis et al., 1998). The area consists of upper amphibolite to granulite facies metamorphic rocks intruded by tabular gabbro, tonalite and granodiorite plutons that range from 100's of meters to 10 km in thickness, and are either (1) low angle generally north dipping bodies or (2) vertical.

In the southern part of the area a 7-8 km thick series of sheeted, tabular leucotonalite and granodiorite sills and gneiss dip gently to moderately northward in a direction oblique to the regional north-northwest trend of the Coast Plutonic belt. Screens of conformable migmatitic metasediment occur between the sills. In the migmatite and orthogneiss of the complex kinematic indicators (C′ shear bands, S-C fabric, asymmetric tails on feldspar porphyroclasts) show a top-to-the-north and northwest transport parallel to regional north and northwest-plunging stretching lineations. Some of the sills share the country rock fabric, in others the fabric is dominantly magmatic. The observed structural relations suggest that emplacement of the sills accompanied the deformation that generated the extensional planar fabric in the country rocks. The tonalite sills and the foliation are reoriented by upright folds with gently north-plunging axes that parallel the north-plunging stretching lineation. This suggests that the top-to-the-northwest extension that produced the pervasive lineation and the kinematic indicators was accompanied by east-west or northeast-southwest contraction.

Superimposed on these fabric elements are hundreds of minor, oblique-sinistral, north-side-down transtensional shear zones that truncate and transpose the regional N-dipping foliation as well as extensional (north-side down) shear zones that dip gently to the north and contain strong northwest-plunging down-dip mineral lineations,. These shear zones are identified as extensional by kinematic indicators including asymmetric boudinage, S-C fabrics, synthetic C′ shear bands and asymmetric tails on mafic clasts. Felsic dikes were emplaced within many of the steep shear zones. The mostly solid state fabric of the shear zones locally is transgressed by migmatitic melt patches and dikes that both crosscut the shear zone foliation and contain, albeit weakly, the regional north-dipping foliation. These relationships suggest that synkinematic magma emplacement continued during the top-to-the-northwest, arc-parallel extension recorded by these shear zones. A major subvertical, sinistral transtensional shear zone, oriented obliquely to the overall north-northwest trend of the orogen, cuts across the complex. This large shear zone displays the same geometry, steep orientation, oblique transport direction and oblique-sinistral (north-side-down) sense of motion as the majority of the minor shear zones. The trace of this shear

zone is at least 12 km long but may be much longer. The large shear zone merges with a detachment zone at the top of the complex. The detachment zone is characterized by tabular lithologic units with planar fabric that uniformly dips gently to the north. No fabrics older than those ascribed to the detachment, such as characterize the rocks north and south of the detachment, can be observed. The detachment separates the complex of sheeted intrusive rocks and migmatitic gneiss described above from overlying amphibolitic and metasedimentary rocks in the northern part of the study area. Rocks above the detachment zone experienced a minimum of intrusive activity, little to no melting, and display a strong structural discordance with the detachment zone and with the fabric of the underlying complex. A large, gently northwest-plunging synform deforms the foliation of the upper plate. The synform may have formed as a result of down-dip drag induced by top-to-the-northwest motion on the extensional detachment.

The Quottoon pluton, a long relatively narrow steeply dipping tabular body, lies along the western side of the sheeted complex and the overlying schist and gneiss of the northern part of the map area. It is one of a number of similar tabular plutons that lie between the high temperature metamorphic rocks of the Central Gneiss Complex and lower temperature but higher pressure rocks to the west. We interpret the shape of this pluton, its relations to the several generations of extensional shear zones, the steeply dipping magmatic fabrics, the remarkably concordant pluton margins, and the lack of evidence of tectonic strain until late in its crystallization history to suggest that space for the pluton was created during the orogen parallel extension recorded in the adjacent Central Gneiss Complex.

This documentation of arc-parallel extension and transtension yields new information on the way deformation was accommodated across the Central Gneiss Complex. Structural evidence from the western side of the orogen, west of the study area, documents dominantly contractional deformation in the mid-Cretaceous oriented approximately EW to NE-SW normal to the orogen. After ~65 Ma extension along the orogen became the dominant deformation mechanism and accommodated significant magma emplacement of the Paleogene arc. The later stages of arc-parallel extension and transtension in the Central Gneiss Complex on the eastern side of the Quottoon pluton occurred at the same time as near vertical displacement within the Coast shear zone on the western side of that pluton. We suggest that these vertical displacements on the Coast shear zone combined with the tectonic unroofing of the batholith via arc-parallel extensional displacements led to rapid exhumation of the batholith. The late stages of the deep crustal, arc-parallel extension we describe on the western side of the Coast Mountains batholith was also approximately simultaneous with near vertical displacements and top-to-the-northeast extension on upper crustal shear zones on the eastern side of the batholith. Together these processes facilitated the tectonic unroofing of the mid-crustal roots of the batholith prior to 50 Ma.

REGIONAL DISHARMONIC STRUCTURAL EVOLUTION OF THE WESTERN ROCKY MOUNTAINS, McBRIDE, BRITISH COLUMBIA

Leslie F. Reid, Department of Geology and Geophysics, University of Calgary, Calgary AB, T2N 1N4
Gerald M. Ross, Geological Survey of Canada – Calgary, 3033-33rd Street NW., Calgary, AB, T2L 2A7

Regional structural patterns in orogenic belts, determined by field-based mapping of vergence and structural geometries can be used as a means of structural correlation and establishment of regional deformation scenarios. We present the results of recent 1:50 000 scale mapping in the McBride area, British Columbia, which demonstrates the presence of regional-scale west-verging structural patterns in the western Rocky Mountains.

The Croyden 1:50 000 map area straddles the Southern Rocky Mountain Trench (SMRT) at the latitude of ca. 54°N in British Columbia and includes parts of the western Rocky Mountains of the Foreland Fold and Thrust Belt, and the Cariboo Mountains of the Omineca Crystalline Belt. The SMRT at this latitude is bound by a post-metamorphic northeast-verging thrust fault along its west wall, and a steep fault of uncertain movement history along its east wall. The Rocky Mountain portion of the Croyden map area comprises the western flank of the Mt. Ryder / Mt. Robson Synclinorium of the western Main Ranges, that occurs structurally east of the Porcupine Creek Anticlinorium. This part of the Croyden map area is underlain by sub-greenschist facies metasedimentary rocks of the Neoproterozoic Miette Group and early Cambrian quartz arenites of the McNaughton Formation (Gog Group). The structural evolution of this region is complex, but can be summarized as follows on the basis of detailed mapping:

1. Formation of a northeast-verging cleavage and locally developed fold closures (metre to decametre-scale).
2. Development of southwest-verging kilometre-scale fold structures and a variably developed axial planar crenulation cleavage. The folds outline a regional anticlinorium structure composed of tight to isoclinal folds outlined by grit bands within the Miette Group.
3. Northeast-dipping, high-angle faulting that places upright McNaughton Formation against overturned pelitic rocks of the Miette Group.
4. Development of a centimetre-scale transverse crenulation cleavage that is well-developed in phyllitic lithologies and increases in intensity towards the SMRT.

The intensity of the southwest-verging structures and their associated fabrics is an interesting aspect of this area, generally considered characteristic of deformation in the Cariboo Mountains at this latitude. In the Rocky Mountains, these structures die out to the northwest and southeast into areas mapped by Carey (1984) and McDonough (1989) respectively. In these latter areas, deformation can be related to northeast-verging folding and thrusting during imbrication of the continental margin wedge. The controlling factor on the localization of the southwest-verging structures in the Croydon map-area is uncertain. The southwest-verging folds may have developed in the hanging wall of a local intercutaneous wedge, analogous to the triangle zone of the Foothills of the western

Canadian Cordillera. Alternatively, these structures may have formed as a result of fold fanning in the relatively incompetent Miette Group below a large detachment surface at the base of the more competent, broadly folded McNaughton Formation. These structures may also represent the local preservation of west-verging structures associated with a regional-scale west-verging detachment. Whatever the mechanism, our map work demonstrates the presence of large-scale vergence reversals and overprinting relationships that cautions against regional fabric correlations at this latitude in the western Canadian Cordillera.

PROVENANCE OF THE BELT PURCELL SUPERGROUP, SOUTHERN BRITISH COLUMBIA: A SHRIMP STUDY OF DETRITAL ZIRCONS

Gerald M. Ross, G.S.C. Calgary, 3303 33rd Street N.W., Calgary, AB. T2L 2A7
(gerry@earth.geo.ucalgary.ca)

Michael E. Villeneuve, G.S.C. Ottawa, 601 Booth Street, Ottawa, Ont. K1A 0E8

The Belt-Purcell Supergroup is an immense thickness of predominantly siliciclastic strata, close to 16 km thick, that is widespread in southern British Columbia and the northwest United States. The tectonic setting of this Mesoproterozoic basin remains enigmatic and controversial with rift basin, intracratonic lake basin, continental margin delta and trapped ocean basin all appearing in the literature in the past 30 years. The sediment fill generally is characterized by fine grain size with only local occurrences of conglomerate or coarse sand-grade material. The main stratigraphic elements consist of the Lower Belt, Ravalli Group, Middle Belt Carbonate and Missoula Group. The Lower Belt consists largely of the Prichard-Aldridge turbidites, fine-grained sands and siltstones that flowed from south-southeast to north-northwest. The Ravalli Group contains sandstone intervals that are thickest in the southwest and pinch out to the northeast, which prompted Harrison (1972) to suggest a source area called the "Belt Island" in present day northeast Oregon. The overlying Middle Belt Carbonate also reflects this northeast-southwest asymmetry with very clean carbonate rocks in the northeast that become progressively sandier towards the southwest, closer to a clastic source area. The Missoula Group represents clastic strata derived almost exclusively from the south-southwest and again shows thinning to the northeast (Winston, 1986). The southwest provenance, from a mysterious "western craton", has also been recognized on the basis of Sm-Nd whole rock studies (Frost and Winston, 1987). These authors showed that over the entire geographic and stratigraphic range of the Belt-Purcell, that the Nd isotopes were inconsistent with sediment derivation from an eastern, predominantly Archean Laurentian source. Subsequent detrital zircon and monazite U-Pb and Sm-Nd studies by Ross et al. (1992) further substantiated this conclusion and on the basis of U-Pb crystallization ages suggested that the "western craton" was Paleoproterozoic crust of eastern Australia.

The SHRIMP II (Sensitive High Resolution Ion Microprobe) at the G.S.C. in Ottawa is an ideal tool for detrital zircon studies, particularly for sedimentary rocks of the Belt-Purcell that are characterized by fine grain size. In this study we report on the results of SHRIMP analyses of detrital zircons from the lowermost unit of the Belt-Purcell, the Fort Steele Formation, a sample from the

overlying Aldridge Formation as well as several units higher in the stratigraphy and on the eastern margin of the basin. All errors are reported at the 1 σ level unless otherwise noted.

The Fort Steele Formation is composed predominantly of mature quartz arenites, in excess of 2000 m in thickness. It represents deposition from a north-flowing braided fluvial system and is transitional upwards into the fine-grained turbidites of the overlying Aldridge Formation (Hoy, 1993). Detrital zircons separated from a coarse quartz arenite in the lower Fort Steele Formation are all very well-rounded with distinctive pitted surfaces, perhaps due to aeolian abrasion. Spot analyses of 22 randomly selected grains from the least magnetic fraction are all within 2% of concordia and hence measured ages are close to actual zircon crystallization ages. Three distinct groupings are apparent. $^{207}Pb/^{206}Pb$ ages between 2617-2726 Ma (n=12) predominate with a single poor quality analysis of 2794±38 Ma that may extend the range of this group to slightly older ages. Two analyses (3316±9; 3250±10 Ma) document the presence of a distinctly older Archean source. The third group consists of Paleoproterozoic grains with $^{207}Pb/^{206}Pb$ ages of 1804-1876 Ma (n=4). Grains that fall outside of these groups consist of a concordant analysis at 1639±2 Ma, a poor quality analysis of 2401±28 Ma and a third grain at 2517±7 Ma.

The predominance of Archean zircon ages, including grains in the range of ca. 3.2-3.3 Ga, is consistent with a Wyoming Craton provenance for the grains. The 1804-1876 Ma grains may have been derived from Paleoproterozoic crystalline rocks along the northwest edge of the Wyoming Craton known as the Great Falls Tectonic Zone.

The Aldridge Formation is a thick (>4200 m) succession of deep water turbiditic strata deposited along the floor of a north-northwest-flowing dispersal system (Hoy, 1993; Cressman, 1989). Most of the sediments are siltstones or fine grained quartz wackes except for local coarse, medium grained sandstones in the middle Aldridge Formation. Our sample came from this interval and yielded very well-rounded pitted and frosted zircon grains generally of small grain size (<70 μm). 18 analyses resulted in two distinct groupings of $^{207}Pb/^{206}Pb$ ages with several additional grains. Paleoproterozoic grains with $^{207}Pb/^{206}Pb$ ages between 1776-1876 Ma (n=9) predominate. Archean grains form a second group with $^{207}Pb/^{206}Pb$ ages of 2585-2607 Ma (n=4) and an additional grain with an age of 2654±9 Ma. Concordant Paleoproterozoic grains with $^{207}Pb/^{206}Pb$ ages 2037±22 Ma, 2060±10 Ma and 2204±24 Ma are also present.

The range of detrital zircon ages in the Aldridge Formation contrasts with those seen in the underlying Fort Steele Formation, even though both units are characterized by north-trending paleocurrent indicators. The predominance of Paleoproterozoic ages as well as the juvenile nature of whole rock Nd reported from this unit (Frost and Winston, 1987) suggest that the predominant source area was juvenile Paleoproterozoic crust with a subordinate contribution from

Archean sources. According to Cressman (1989) this source area would have lain within present day eastern Oregon.

The Revett Formation (Creston Formation in Canada) comprises one of several clastic wedges within the Ravalli Group. The facies geometry, thickness patterns and paleocurrent indicators from the Ravalli Group led to Harrison's (1972) suggestion of a "Belt Island" as a source area in what is now eastern Oregon. Previous analyses (TIMS) of the detrital zircons in the Revett Formation produced 4 concordant analyses of ca. 1590-1600 Ma and a discordant grain with a $^{207}Pb/^{206}Pb$ age of ca. 1780 Ma (Ross et al., 1992). We revisited the Revett sample in order to expand the data base for this important sandstone unit.

Two distinct morphologic populations of rounded and euhedral detrital zircons are present in the Revett Formation. Some euhedral grains showed cores with overgrowths in cathodoluminescence imaging. We thus chose a smaller spot size for the SHRIMP ion beam in an attempt to individually date these components. This resulted in larger errors associated with each analysis. For those grains with observed core-overgrowth relationships no age differences were discernible. $^{207}Pb/^{206}Pb$ ages (n=14 on 11 grains) for euhedral grains range from 1505-1893 Ma. The larger errors (±20 to ±50 Ma) associated with the smaller spot size prevent reliable assignment of individual ages within this range. The rounded population shows a similar range of $^{207}Pb/^{206}Pb$ ages although three distinct components can be resolved. A cluster of 5 concordant grains gives an average $^{207}Pb/^{206}Pb$ age of 1606±13 Ma (2 σ error), a concordant analysis resulted in a $^{207}Pb/^{206}Pb$ age of 1508±10 Ma and two discordant analyses gave ages of 1794±10 Ma (9% discordant) and 1802±10 Ma (4% discordant).

The range of ages from the Revett Formation is considered distinctive of a source area in the basement of eastern Australia, inboard from the Tasman orogen, which was accreted during the Paleozoic. These ages are in accord with the previously determined U-Pb TIMS ages that identified a ca. 1590 Ma source that was linked to the widespread Gawler volcanics.

The Sheppard Formation, a unit of dolomite, quartz arenite, siltstone and argillite occurs relatively high in Belt-Purcell stratigraphy and unconformably overlies the Purcell Lava and correlative Nicol Creek Formation. In southern British Columbia it is characterized by dramatic thickness changes and the presence of a local conglomerate at the base of the unit. The conglomerate is notable in that it contains clasts of crystalline material, mostly amygdaloidal basalt but also porphyritic dacite and granitic material. The dacite cobbles were unlike any lithology in the Belt Basin and this led Hoy (1993) to suggest an exotic extrabasinal origin. Previous large fraction multigrain TIMS analyses resulted in discordant $^{207}Pb/^{206}Pb$ ages of 1498 -1452 Ma with upper intercepts in excess of 1500 Ma. We re-examined two of the dacite cobbles with the hope of securing a more reliable age determination.

Zircons separated from the dacite cobbles were mostly well-formed euhedra but with local inclusions and dust-rich domains suggestive of inheritance; such grains were avoided during SHRIMP analysis. 7 spot analyses on clear euhedral crystals cluster near concordia with $^{207}Pb/^{206}Pb$ ages of 1426-1499 Ma and a weighted mean of 1452±18 Ma (2 σ error). 8 spot analyses of zircons from a second cobble resulted in a similar pattern of data but yielded a slightly more precise weighted mean of 1438±14 Ma (2 σ error). The ages of these two cobbles overlap and are similar to SHRIMP ages reported from felsic differentiates of the Purcell Lava from the Yaak River area (1443±5 Ma; Aleinikoff et al., 1996). This suggests that the cobbles have an intrabasinal source likely from felsic differentiates within the Purcell Lava and Nicol Creek Formation that are not widely preserved.

Summary: The new detrital zircon data, when used in combination with previously published isotopic data and geologic constraints provides a new view of the evolution of the Belt Basin and its source area. The stratigraphic units appear to represent predominant sediment derivation from source areas that lay to the west-southwest of the basin. The lower part of the Belt (Fort Steele Formation) contains a provenance signature from the adjacent Wyoming Craton. This signature is lost with the onset of Aldridge Formation deposition which appears to receive the bulk of its detritus from juvenile Proterozoic sources to the south or southwest. The change in source area corresponds with the onset of deep water deposition and rapid rates of subsidence, suggesting that the changes in provenance are controlled by tectonic modification of drainage systems. The Revett Formation contains grains of distinctive non-NorthAmerican affinity, a pattern that persists up through and including the Missoula Group. The lack of ca. 1500-1600 Ma grains in the Aldridge Formation suggest that it's river systems had not tapped into a Gawler-like Australian source. The pebbles in the basal Sheppard Formation are intrabasinal in origin and derived from the underlying Purcell Lava. We are presently dating detrital zircons populations within stratigraphically higher formations (Creston, Siyeh and Grinnell formations) in order to complete a provenance history of the Belt-Purcell Supergroup and to test for the presence of an eastern provenance, long suspected on the basis of facies patterns, but difficult to reconcile with the Nd data.

Acknowledgements: Trygve Höy is thanked for sending us the two igneous cobbles form the Sheppard Formation. Derek Brown collected the Creston and Aldridge samples and Dave Kisilewsky collected the Grinnell and Siyeh samples.

References Cited:

Aleinikoff, J.N., Evans, K.V., Fanning, C.M., Obradovich, J.D., Ruppel, E.T., Zieg, J.A., and Steinmetz, J.C., 1996, SHRIMP U-Pb ages of felsic igneous

rocks, Belt Supergroup, western Montana. Geological Society of America, Abstracts with programs, v. p. A-376.

Frost, C.D., and Winston, D., 1987, Nd isotope systematics from coarse- and fine-grained sediments: Examples from the Middle Proterozoic Belt Purcell Supergroup. Journal of Geology, c. 95, p. 309-327.

Harrison, J.E., 1972, Precambrian Belt basin of northwestern United States-its geometry, sedimentation, and copper occurrences. Geol. Soc. Amer. Bull., v. 83, p. 1215-1240.

Höy, T., 1992, Geology of the Purcell Supergroup in the Fernie West-half map area, southeastern British Columbia Mineral Resources Division, Geological Survey Branch, B.C. Ministry of Energy, <ines and petroleum Resources, Bulletin 84, 157 pp.

Ross, G.M., Parrish, R.R., and Winston, D., 1992, Provenance and U-Pb geochronology of the Mesoproterozoic Belt Supergroup (northwestern United States): implications for the age of deposition and pre-Panthalassa plate reconstructions. Earth and Planetary Science Letters, 113, 57-76.

Winston, D., 1986, Middle Proterozoic tectonics of the Belt Basin, western Montana and northern Idaho. In Belt Supergroup, a guide to Proterozoic rocks of western Montana and adjacent areas. S. Roberts, ed., Montana Bureau Mines, Spec. Publ. 94, p. 245-257.

The Christina Lake Area in Southeastern British Columbia: Upper Paleozoic Harper Ranch Subterrane of Quesnellia or Pericratonic Kootenay Terrane?

Acton, S.L., Simony, P.S. Department of Geology and Geophysics, University of Calgary, Calgary, AB, T2N 1N4

In the southwestern Omineca Crystalline Belt, the allochthonous accreted terranes comprising the Intermontane Superterrane occur as large thrust sheets upon pericratonic rocks along the ancestral margin of North America. Late Triassic to Mid-Jurassic volcanic island-arc assemblages of Quesnellia are observed locally to lie upon the Devonian to Triassic oceanic Slide Mountain Terrane, Paleozoic Quesnellia, and the Proterozoic to Upper Triassic pericratonic Kootenay Terrane. In many locations, the age and extent of strata underlying the Triassic-Jurassic assemblages of Quesnellia is unknown due to the presence of unmapped geology, complex stratigraphy, structure, and the superposition of Omineca Belt metamorphism and plutonism on the Intermontane Superterrane. The Christina Lake area, in southeastern British Columbia, is an area in which little detailed geologic work has been completed, hence, it is not known if the rocks in this area represent a continuation of the rocks of Quesnellia or strata of North American affinity.

Supracrustal rocks in the Christina Lake area have been interpreted as the westernmost continuation of the Permian to Lower Triassic Mount Roberts Formation defined in the Rossland area. East of Christina Lake, these strata consist of compositionally banded epidote-biotite siltstone with layers of coarse-crystalline marble and widely scattered, thin pelitic bands. These sedimentary rocks are extensively intruded by hornblende-biotite diorite. The supracrustal rocks and the diorite have been metamorphosed together and deformed into complex SW-verging folds as a result of at least two phases of deformation. A strong schistosity is preserved throughout the sedimentary and dioritic rocks; locally, the diorite is sheared to hornblende-biotite schist. The Mount Roberts formation is thought to comprise part of the volcanic-island arc related Harper Ranch Subterrane, which represents Upper Paleozoic "basement" rocks of Quesnellia. However, it has also been proposed that the supracrustal rocks in the Christina Lake area may be western equivalents of Ordovician to Devonian rocks of the pericratonic Kootenay Terrane. If this is the case, then the supracrustal rocks near Christina Lake may have been rifted from North America and were later incorporated into Quesnellia, or are of North American affinity and are in thrust contact with Quesnellia.

In order to determine if the metasiltstones in the Christina Lake area are the continuation of the arc related "basement" rocks of Quesnellia or the continuation of the pericratonic Kootenay Terrane, an approximate age for the metasiltstones is needed. Throughout the study area, both the metasiltstone and diorite-schist are intruded by granites and granodiorites of the Mid-Jurassic Nelson Suite. Based on this relationship, the diorites and metasiltstones are at least older than Mid-Jurassic. To further constrain the age of the supracrustal rocks in the Christina Lake area, U-Pb geochronology of the diorites is in progress.

NEW METAMORPHIC AND GEOCHRONOLOGICAL CONSTRAINTS ON THE TECTONIC EVOLUTION OF THE NORTHERN SELKIRK MOUNTAINS, SE B.C.

NATHALIE MARCHILDON, GREGORY M. DIPPLE, AND JAMES K. MORTENSEN, UBC Earth and Ocean Sc., 6339 Stores Rd., Vancouver, B.C., V6T 1Z4; nmarchil@eos.ubc.ca

An outstanding problem relating to the tectonic evolution of the southern Omineca Belt is the apparent discrepancy between the absolute and relative ages of deformation and metamorphism on either side of the Selkirk Fan Axis (SFA), in the Northern Selkirk and Monashee Mountains of British Columbia. While metamorphism is interpreted to be synchronous with development of D2 structures on both flanks of the SFA, the absolute timing of metamorphism is thought to be mid-Cretaceous (ca. 100 Ma), and mid-Jurassic (ca. 170 Ma) on the east and west flanks of the SFA, respectively.

The relationships of structure development and metamorphic mineral growth were described in detail for rocks of the western flank of the SFA north of Goldstream River. Three distinct metamorphic events were recognized: M1 is preserved as variably retrogressed garnet and staurolite; garnet, staurolite and kyanite developed during M2; M3 is recorded by large, post-D2 andalusite porphyroblasts commonly retrogressed to muscovite. M1 was synchronous with development of the dominant west-verging structures (S_2) in the area. Although M2-minerals generally overgrow S_2, local flattening of S_2 around, and gentle rotation of, M2 porphyroblasts is consistent with reactivation of deformation parallel to S_2 during M2. Boudinaged M3 andalusite porphyroblasts suggest that M3 pre-dated, or was synchronous with a late extensional event.

M1 in the study area is probably correlatable with mid-Jurassic (ca. 170 Ma) metamorphism described in other parts of the western flank of the SFA, and more generally, of the Selkirk Allochthon. Metamorphic assemblages assigned here to M2 have been interpreted by previous workers as contemporaneous with emplacement of the Bigmouth granodiorite exposed at the northeastern edge of the study area. Zircons and titanites from this intrusion yield U-Pb ages of 149 ± 11 Ma and 141 ± 7 Ma, respectively, indicating that M2 is late Jurassic to early Cretaceous in age. The absolute timing of M3 remains unclear, but can not be related to mid-Jurassic low-P metamorphism interpreted for rocks on the western flank of the SFA south of the study area. Further geochronological work is underway to better constrain the timing of the different metamorphic events.

Our results suggest that the western flank of the SFA underwent a protracted history of metamorphic pulses which extended over at least 30 Ma, attended by protracted, largely co-axial deformation. Comparison with other areas on the western flank of the SFA indicates that the relative preservation of different metamorphic pulses is spatially variable. This, and the strong co-axiality of deformation in the area over an extensive period of time (at least 30 Ma) may explain the apparent discrepancy in the relative timing of metamorphism and deformation on either side of the SFA.

DEFORMATION INDUCED INVERTED METAMORPHIC FIELD GRADIENTS, AN EXAMPLE FROM SOUTHEASTERN CANADIAN CORDILLERA

H. DANIEL GIBSON, AND RICHARD L. BROWN

Ottawa-Carleton Geoscience Centre and Department of Earth Sciences, Carleton University, Ottawa, ON, K1S 5B6, Canada. email: dhgibson@ccs.carleton.ca

and

RANDALL R. PARRISH

Department of Geology, University of Leicester and NERC Isotope Geosciences Centre, British Geological Survey, Keyworth, Notts., NG12 5GG, United Kingdom

Exhumed middle crustal rocks of the hinterland of the southeastern Canadian Cordillera were deformed and metamorphosed during Mesozoic and Tertiary progressive crustal thickening. High structural levels were transported northeasterly relative to lower levels through a combination of thrusting and ductile noncoaxial flow. Progressive growth of the orogen and advance of hinterland rocks toward the foreland is revealed through analysis of diachronous metamorphism and associated deformation. At the deepest exposed levels, allochthonous rocks of the orogen (Selkirk allochthon) structurally overlie early Proterozoic basement and younger cover rocks (Monashee complex) that are correlated with autochthonous North American crust underlying the eastern foreland (Rocky Mountain Belt). The crustal zone (Monashee décollement), which marks the boundary between the Selkirk allochthon and Monashee complex exhibits an inverted metamorphic field gradient. New data presented in this paper refute previous interpretations, which assert that the metamorphic inversion is a result of the downward transfer of heat from the allochthon to the underlying Monashee complex. Rather, the inversion is attributed to synmetamorphic noncoaxial progressive deformation. A coupled thermo-tectonic model is proposed in which substantial northeasterly directed shear strain and attendant attenuation led to lateral transfer of rocks preserving evidence of strongly diachronous deformation ($\geq$ 18.3 Ma) and an apparent inverted metamorphism.

WESTWARD UNDERTHRUSTING, EXTRUSION AND EXHUMATION OF CRYSTALLINE ROCKS OF THE MONASHEE COMPLEX, SOUTHEAST B.C.

Dennis H. Johnston and Paul F. Williams
University of New Brunswick, Fredericton, New Brunswick, Canada E3B 5A3

Two basement-cored antiformal culminations of high-grade metamorphic rock, Thor–Odin and Frenchman Cap, comprise the Monashee complex in the hinterland of the southern Canadian Cordillera. Rocks in the studied area along the west flank of the Thor–Odin dome are thoroughly transposed (into S_2). The extent of the transposition, and a well-developed northeasterly-trending L_2 lineation, indicate intense strain during F_1/F_2 throughout the culmination (4-5 kilometre thickness exposed). Penetrative northeastward ductile flow parallel to the transposition foliation continued, resulting in northeasterly-verging F_3 folds and related fabrics. West of Thor–Odin dome, in the Selkirk allochthon, F_3 folds verge west-southwest (e.g., Joss Mountain fold nappe). Along the west flank of the Thor-Odin dome, in the Greenbush Lake shear band zone (GLSBZ), the L_2 lineation was rotated to a west-southwest trend, folds were truncated and abundant mesoscopic W-SW-dipping top-to-W-SW shear bands formed as a result of D_5 extension and reactivated slip on S_2.

Northeasterly flow during F_1/F_2 developed in response to westward underthrusting of North American basement and its sedimentary cover beneath a burgeoning hinterland (Fig. 1a). With continued westward underthrusting during the Mesozoic, eventually a gravitationally unstable crustal edifice formed that may have been on the scale of the modern Himalayan front. Continued northeastward flow during F_3 resulted in extrusion of a westward-tapering crustal wedge towards the foreland (Fig. 1b). The most rapid rate of extrusion occurred in the middle portion of the wedge, resulting in opposing F_3 vergence above and below. Rapid extrusion of the wedge is indicated by the preservation of kyanite within a narrow zone along the west flank of the Thor–Odin dome; the well-preserved kyanite is bounded above and below by zones in which sillimanite has psuedomorphously replaced kyanite. The crystalline rocks of the Monashee complex were then exhumed along the D_5 GLSBZ and major Eocene normal faults (e.g., Columbia River fault; Fig. 1c).

References cited in Figure 1:

Grujic, D., Casey, M., Davidson, C., Hollister, L.S., Kündig, R., Pavlis, T. and Schmid, S. 1996. Ductile extrusion of the Higher Himalaya Crystalline in Bhutan: evidence from quartz microfabrics. Tectonophysics, **260:** 21–43.

Johnson, B.J., and Brown, R.L. 1996. Crustal structure and early Tertiary extensional tectonics of the Omineca belt at 51°N latitude, southern Canadian Cordillera. Canadian Journal of Earth Sciences, **33:** 1596–1611.

Read, P.B., and Klepacki, D.W. 1981. Stratigraphy and structure: northern half of Thor–Odin Nappe, Vernon east-half map area, southern British Columbia. *In* Current research, part A. Geological Survey of Canada, Paper 81-1A, pp. 169–173.

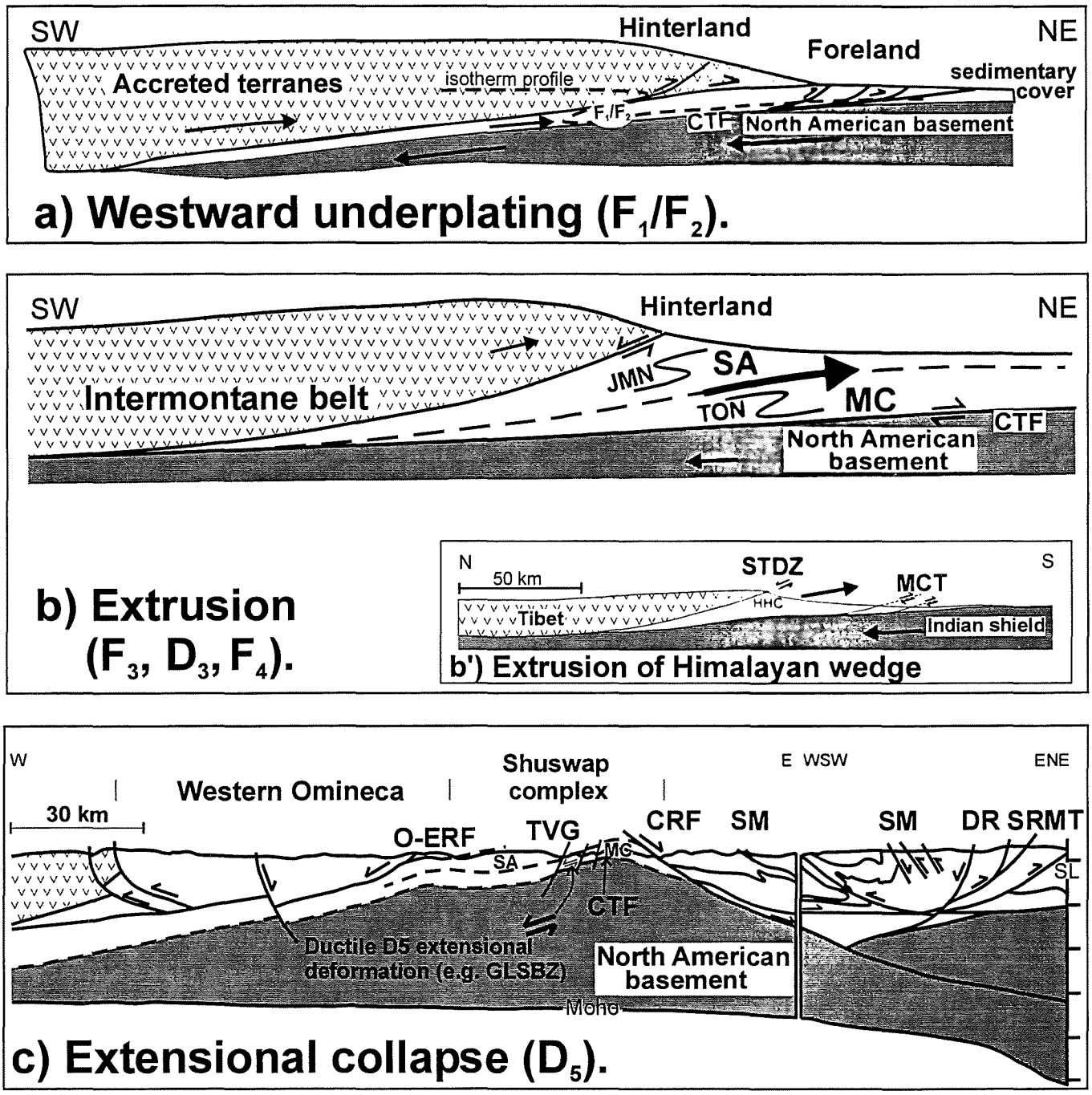

Figure 1. Proposed tectonic evolution of the study area. Horizontal and vertical scales equal in b' and c. (a) Schematic cross-section, not to scale, showing F_1/F_2 NE-directed flow of crystalline rocks of the Monashee complex above the Cordilleran tectonic front (CTF) during westward underthrusting of North American basement and its sedimentary cover beneath the hinterland. (b) Schematic cross-section, not to scale, relating major structures to extrusion of a crustal wedge between the Intermontane belt and North American cratonic basement; wedge is interpreted as having been extruded in a manner similar to the Himalayan wedge shown in b'. Length of arrows give relative rates of movement. JMN, Joss Mountain nappe; MC, Monashee complex; SA, Selkirk allochthon; TON, Thor–Odin nappe of Read and Klepacki (1981). (b') Schematic cross-section of the Himalayas showing extrusion of a crustal wedge between the STDZ (South Tibet detachment zone) and the MCT (Main Central Thrust) zone. HHC, High Himalaya Crystallines. From Grujic et al. 1996. (c) Extensional collapse of the southern Canadian Cordillera as shown in a crustal cross-section through the Omineca belt. Crystalline rocks of the Shuswap complex are shaded. The major faults interpreted from siesmic data and surface geology are: O–ERF, Okanagan–Eagle River fault; MD, Monashee décollement; TVG, Three Valley Gap; CRF, Columbia River fault. SM, Selkirk Mountains, DR, Dogtooth Range; SRMT, Southern Rocky Mountain Trench; SL, sea level. Simplified from Johnson and Brown 1996; modified for CTF and ductile D_5 deformation and for MC/SA contact since evidence of a MD was not observed in the study area.

A Reevaluation of the Geology adjacent to Shuswap Lake, Vernon map area, British Columbia

[1]Nadya M. Slemko (e-mail nslemko@gpu.srv.ualberta.ca)
[1]Philippe Erdmer (e-mail p.erdmer@ualberta.ca)
[2]Robert I. Thompson (e-mail rthompson@gsc.NRCan.gc.ca)

[1] Dept. of Earth and Atmospheric Sciences, University of Alberta, Edmonton, AB, T6G 2E3
[2] GSC Pacific - Sidney Subdivision, Pacific Geoscience Centre, Sidney, BC, V8L 4B2

INTRODUCTION

The Shuswap Lake area is part of the Omineca Belt, a morphogeological division of the Cordillera that includes both pericratonic and displaced terranes (Gabrielse et al., 1991). This study, located in northeastern Vernon map area (82L) (Figure 1), focuses on stratigraphic, structural, and metamorphic relations between Proterozoic schist and gneiss (Silver Creek Formation of Jones, 1959) of miogeoclinal affinity and Paleozoic carbonate and volcanic strata (Sicamous and Eagle Bay formations of Jones, 1959) of eugeoclinal affinity, exposed in the general area of the former continental margin.

Field work in the summer of 1997 extended from the town of Sicamous north to Cinnemousun Narrows, on Shuswap Lake (Figure 2), and focused on rocks in the hanging wall of the Eagle River Fault. The purpose of this study was to elucidate the relationship between miogeoclinal and eugeoclinal strata, to determine the relationship between rocks on the east and west sides of the lake, to investigate the internal stratigraphy of the Silver Creek, Sicamous, and Eagle Bay formations, and to establish the structural and metamorphic history of the region.

STRATIGRAPHY AND METAMORPHISM

Queest Mountain Assemblage

In the northeast part of the area mapped is an assemblage of high metamorphic grade schists. Feldspar-quartz-mica schist, which locally contains almandine and hornblende or sillimanite, and hosts partial melt in places, is most abundant. Carbonate or calcsilicate schist containing calcite, quartz, feldspar, diopside, grossular, amphibole, and epidote form a band approximately 1 km thick. The mineral assemblages are diagnostic of amphibolite facies metamorphism, higher grade than the greenschist-facies Eagle Bay Formation to the south. Previously (Johnson, 1990; Okulitch, 1974), these rocks had been mapped as part of the Eagle Bay Formation. However, on the

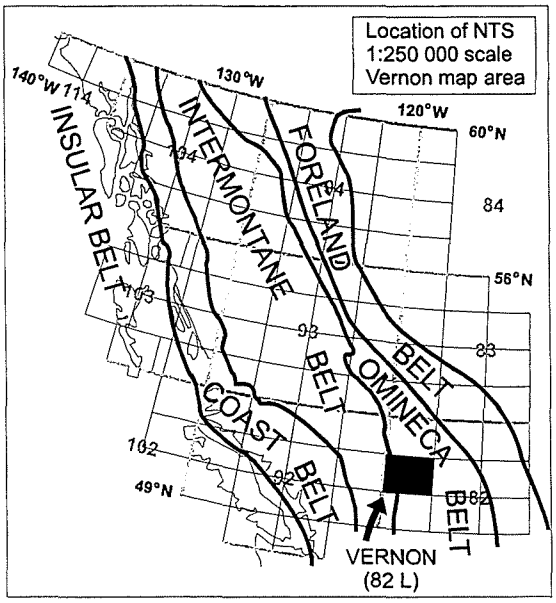

Figure 1. Location of the Vernon map area on the NTS 1:250 000 scale map grid and within the tectonic belts of the Canadian Cordillera.

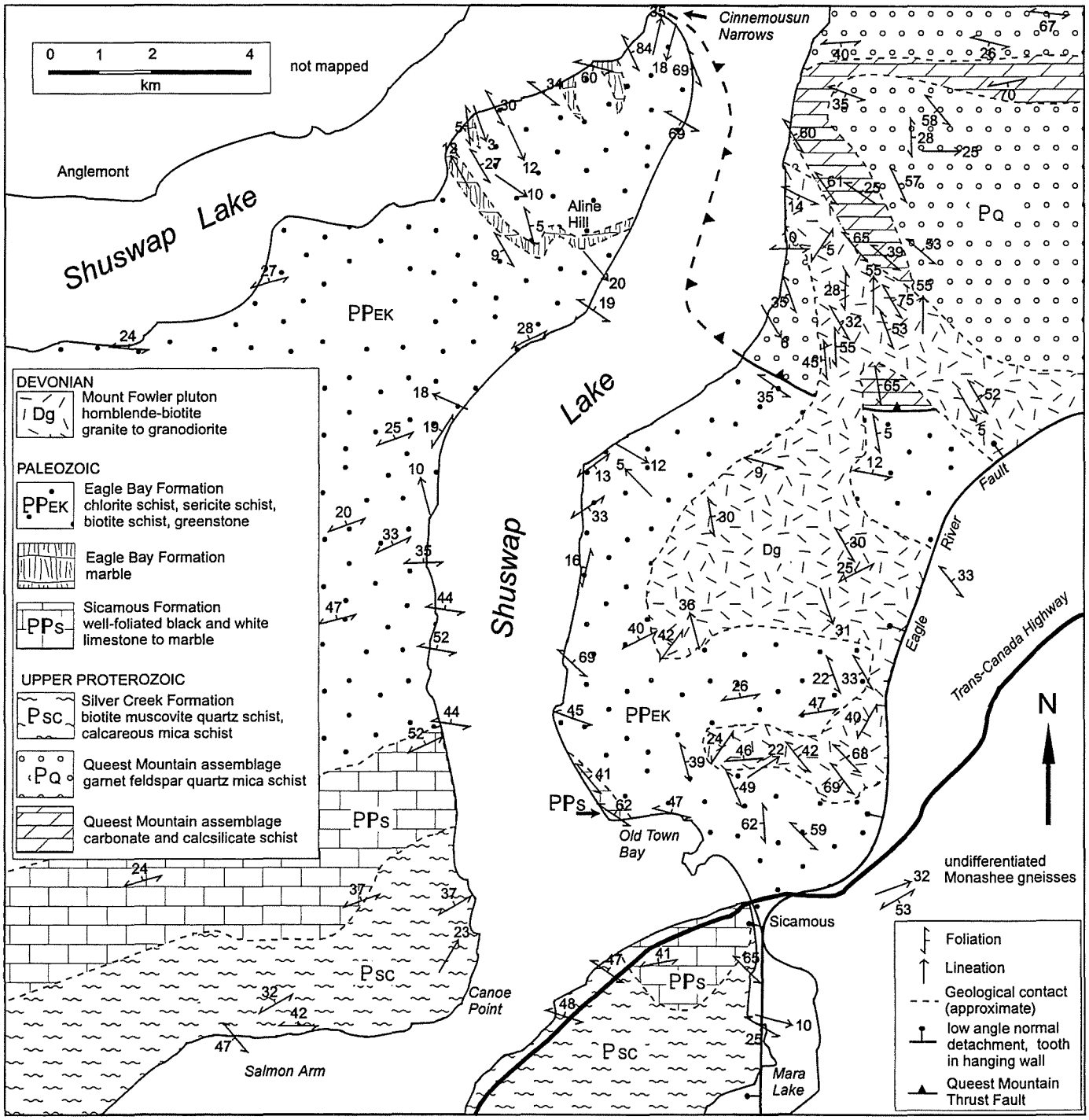

Figure 2. Geological map of the Shuswap Lake area north of Sicamous.

basis of protolith composition and metamorphic grade, they have much closer affinity with older (Neoproterozoic) quartz- and feldspar-rich assemblages such as the Silver Creek Formation. Although further work is required to determine the exact regional stratigraphic affinity of the high-grade rocks, for the purpose of this report they are termed the Queest Mountain assemblage.

Silver Creek Formation

The Neoproterozoic Silver Creek Formation is composed of biotite muscovite quartz schist, with minor calcareous layers. It is intruded by numerous pegmatite and aplite sills and dykes, which prompted Daly (1915) to term it the "sill-sediment complex." The Sicamous-Silver Creek contact exposed along the Trans-Canada Highway is inferred to be depositional. In the area mapped, the Silver Creek Formation is at greenschist grade, as are the overlying Sicamous and Eagle Bay formations. Regionally, rocks mapped as Silver Creek Formation (Okulitch, 1974; Thompson and Daughtry, 1997) are at garnet-sillimanite grade. Therefore, there must be a change in metamorphic grade within rocks mapped as Silver Creek; this could be a metamorphic gradient, an unconformity, or a fault. Additional investigation is required to determine the nature and location of this change in metamorphic grade, but if it is an unconformity or a fault, it is unlikely that both the low-grade and high-grade rocks are Silver Creek Formation.

Sicamous Formation

The Silver Creek Formation is overlain by the Lower? Paleozoic Sicamous Formation. This eugeoclinal succession is a fine- to medium-grained metamorphosed carbonaceous limestone, with a distinctive black and white layering in outcrop. It was likely deposited outboard from the North American miogeocline. The Sicamous-Eagle Bay contact is interfingered near Old Town Bay, and thus is inferred to be depositional.

Eagle Bay Formation

The Lower? Paleozoic Eagle Bay Formation contains fine-grained chlorite schist, chlorite sericite schist, biotite muscovite schist, and volcanic greenstone. One or more streaked white to black marble marker horizons, typically 100 m to 200 m thick, are present. Significant variations in apparent metamorphic grade, from lower-greenschist chlorite schist to upper-greenschist biotite muscovite schist, occur over horizontal distances of 1 to 2 km. The chlorite is mostly retrograde, suggesting that these variations in grade result from patchy retrogression.

Unit Dg

A large intrusion of biotite-hornblende, equigranular to megacrystic granite to granodiorite, correlated by Okulitch (1975) with the Devonian Mount Fowler Batholith, cuts the Eagle Bay Formation and the Queest Mountain assemblage north of Sicamous. Strain within the granodiorite is heterogeneous, varying from none to penetrative. Strain fabrics within the host rocks are cut by the granodiorite. Geochronological work is in progress to establish the crystallization and metamorphic ages of this unit.

STRUCTURE

Folding

The mica-rich metasedimentary rocks are well foliated. Mineral lineation, locally present in schist, has no apparent preferred orientation, based on a sample of 24 locations.

Only one foliation is observed, with one exception near Aline Hill, where two are present. The main foliation is a fine schistosity to phyllitic cleavage, S_1. Near Aline Hill, the S_1 foliation, parallel to transposed bedding, is folded into upright mesoscopic scale folds; a weak cleavage, S_2, is axial planar to these folds. The single foliation observed at other locations, S_1, is parallel or subparallel to major lithologic contacts.

From the strike variation and dip reversals seen on the map scale, the S_1 foliation is inferred to be folded into large (approximately 10 km wavelength) open upright folds. Fold axes trend broadly west-northwest, and appear to plunge shallowly. The folds may be contemporaneous with the S_2 foliation near Aline Hill, but did not give rise to a pervasive axial foliation. The folding event records shortening in a northeast-southwest orientation.

Queest Mountain Contraction Fault

The contact between the greenschist-grade Eagle Bay Formation and the amphibolite-grade Queest Mountain assemblage is sharp, planar, west-northwest striking, and north-northeast-dipping. The sharp change in metamorphic grade is likely caused by a pre-Devonian contraction fault, termed here the Queest Mountain contraction fault, which juxtaposed the higher-grade Queest Mountain assemblage and the lower-grade Eagle Bay Formation.

The Queest Mountain contraction fault resulted from northeast compression. Its strike is parallel to the axial traces of the large open folds on the east side of Shuswap Lake, suggesting that the fault and folds may be kinematically related.

Unit Dg

The schistosities in Unit Dg and the host rocks are locally discordant, showing that Dg has not undergone the same early deformation as the country rock. Dg foliation is variable in orientation and intensity. The schistosity may result from a weak deformation postdating the S_1 foliation in the host rocks.

Unit Dg is occupies both the hanging wall and footwall of the Queest Mountain contraction fault, and is mapped across the fault with no map-scale offset. The intrusion of Dg postdates metamorphic mineral growth and early fabric development in the Queest Mountain assemblage. If the pluton correlates with the Devonian Mount Fowler suite (Okulitch et al., 1975), a record of pre-Devonian deformation is preserved.

CONCLUSIONS

The miogeoclinal Neoproterozoic Silver Creek Formation appears, at least within the map area, to be in stratigraphic contact with eugeoclinal Lower? Paleozoic Sicamous and Eagle Bay formations; there is no change in metamorphic grade at the Silver Creek - Sicamous contact. However, the Silver Creek reaches much higher grade regionally, and there must be a change in metamorphic grade within the formation, a transition which remains enigmatic.

The Sicamous and Eagle Bay formations were deposited as limestone, volcanic rock, and fine clastic sediment derived from the nearby volcanic strata, in a distal continental margin setting.

Lithologic differences between rocks on the east and west sides of Shuswap Lake, as well as metamorphic contrasts north of the town of Sicamous, have led to the recognition of the Queest Mountain assemblage in rocks previously mapped as Eagle Bay Formation. The Queest Mountain contraction fault dips NNE, verges SSW, and juxtaposes the high grade Queest Mountain assemblage against the lower grade Eagle Bay Formation.

Unit Dg cuts the Queest Mountain contraction fault, and postdates metamorphism and early deformation. Thus, if Dg is Devonian, pre-Devonian metamorphism and deformation occurred in this area.

REFERENCES

Daly, R.A. (1915) A geological reconnaissance between Golden and Kamloops B.C., along the Canadian Pacific Railway; Geological Survey of Canada, Memoir 68, 260 p.

Gabrielse, H., Monger, J.W.H., Wheeler, J.O., and Yorath, C.J. (1991) Part A. Morphogeological belts, tectonic assemblages, and terranes; in Chapter 2 of Geology of the Cordilleran Orogen in Canada, H. Gabrielse and C.J. Yorath (ed.); Geological Survey of Canada, Geology of Canada, no. 4, p. 15-28.

Johnson, B.J. (1990) Geology adjacent to the western margin of the Shuswap Metamorphic Complex: Province of British Columbia Ministry of Energy, Mines and Petroleum Resources. Open File 1990-90. 15 p.

Jones, A.G. (1959) Vernon map-area, B.C.; Geological Survey of Canada, Memoir 296, 186 p.

Okulitch, A.V. (1974) Stratigraphy and structure of the Mount Ida Group, Vernon (82L), Seymour Arm (82M), Bonaparte Lake (92P) and Kettle River (82E) map-areas, British Columbia; in Report of Activities: Part A, April to October 1973, Geological Survey of Canada, Paper 74-1, Part A, p. 25-30.

Okulitch, A.V. (1975) Stratigraphy and structure of the western margin of the Shuswap Metamorphic Complex, Vernon (82L) and Seymour Arm (82M) map-areas, British Columbia; in Report of Activities: Part A, April to October 1974, Geological Survey of Canada, Paper 75-1, Part A, p. 27-30.

Okulitch, A.V., Wanless, R.K., and Loveridge, W.D. (1975) Devonian plutonism in south-central British Columbia; Canadian Journal of Earth Sciences, v.12, p. 1760-1769.

Thompson, R.I. and Daughtry, K.L. (1997) Anatomy of the Neoproterozoic - Palaeozoic continental margin, Vernon map area, British Columbia; in Current Research 1997-A; Geological Survey of Canada, p. 145-150.

NATMAP PROJECT PROPOSED TO STUDY THE PHANEROZOIC PLATE MARGIN: HIGHLIGHTS FROM VERNON MAP AREA (82L)

Thompson, Bob, Geological Survey of Canada, Sidney, B.C. V8L 4B2

A NATMAP project to address the stratigraphic history and tectonic evolution of rock assemblages deposited along the outer plate margin of ancestral North America during Paleozoic and early Mesozoic time has been proposed by GSC Pacific Division.

The target rock assemblages constitute a deformed, metamorphosed and intruded belt 50 to 200 kilometres wide that extends from south central British Columbia into west central Yukon and east central Alaska. It occupies a central position between strata on the east and north that formed the more proximal portions of overlapping continental terrace wedges, and rock assemblages to the west that evolved in and on fragments of crust derived from elsewhere in the Pacific ocean.

There are five primary scientific objectives:

1) To define the paleogeographic nature of the outermost ancestral plate margin, how it evolved, and what the stratigraphic linkages are between regions;

2) to establish the timing and nature of tectonic events that affected the margin;

3) to recognize pieces of the margin that may have been mobile with respect to the North American craton and establish the degree of mobility;

4) to better define the character of tectonic boundaries that separate plate margin rock assemblages from exotic terranes farther outboard;

5) To define the metallogeny of prospective units, particularly in the context of rifing events.

Geologic mapping is required in areas that provide access to the critical rock assemblages that are most likely to "bridge" existing knowledge gaps. From the mapping we anticipate learning more about arc setting and polarity; the locus and history of large, strike-slip faults; the character and extent of Late Paleozoic deformation; terrane accretion mechanism(s); and thermal regime and structure of the crust. Five 1:250,000 scale map areas require additional mapping and investigation to provide information critical to achieving the stated objectives, they are: Vernon (82L), Bonapart Lake (92P), Jennings River (104O), Wolf Lake (105B) and Stewart River (115NO). University parrticipation will be sought if funding for this project is approved.

Several of the sceintific aims noted above are being addressed in Vernon map area (82L) as part of a regional mapping program. The map area sits astride the stratigraphic and structural boundaries interpreted to separate miogeoclinal from eugeoclinal rocks, and eugeoclinal from rocks that are exotic with respect to the North American craton margin -- volcanic arc related clastic and volcanic assemblages such as Quesnel Terrane (and subterranes therein), and volcanic and clastic rocks of ocean floor affinity known collectively as Slide Mountain Terrane. Not surprisingly, the location and nature of the boundaries separating miogeoclinal from eugeoclinal from exotic rocks are less apparent and more open to reinterpretation as the scale of observation decreases from compilation scale to field mapping scale. We present evidence to suggest that eugeoclinal rocks stratigraphically overlie miogeoclinal strata, that they were deposited into one or more marginal basins superimposed on what had been a relatively stable Eocambrian shelf prior to "the bottom dropping out" from beneath the outer portion of the craton margin early in Cambrian time, and that they include strata previously interpreted as exotic.

A major tectonic (thrust) boundary separating exotic (Quesnel Terrane) from

"pericratonic" (eugeoclinal) North American rocks has been interpreted to cross Vernon map area. Our observations support two conclusions: 1) The interpreted thrust boundary is stratigraphic; and 2) the rocks ascribed to Quesnel Terrane are part of a stratigraphic overlap assemblage.

A late Jurassic age pluton has been mapped across the inferred locus of the Okanagan Valley detachment fault in the vicinity of Wood Lake, and marker units have been mapped acorss the North Okanagan Valley. A crustal scale detachment would have to occur at greater structural depth within the high metamorphic grade assemblage. It appears the Okanagan Valley, between Wood Lake and Mara Lake, is the locus of steep-dipping extension faults which do not necessarily flatten with depth into a master detachment.

Preliminary report on significant thrusting and extension of the early Tertiary Chuckanut Formation, NW Washington

Haugerud, R.A., U.S. Geological Survey at University of Washington, Seattle WA 98195, *rhaugerud@usgs.gov*

Micaceous arkosic sandstone, siltstone, conglomerate and coal of the Chuckanut Formation crop out in the western foothills of the North Cascade Range between 48°30′ and 49°N, at and east of the town of Bellingham. Following earlier work by S.Y. Johnson (*CJES*, 1984), I map two units within the Chuckanut. The lower Bellingham Bay unit is characterized by thin-bedded crevasse-splay sandstone, thick channel sandstone beds with trough cross-bedding and convolute bedding, rare conglomerates that contain rare chert, and palm fossils. Sandstones weather to cream and buff colors. The upper Padden unit is characterized by common pebbley sandstone and conglomerate (both with abundant chert pebbles), thick, relatively featureless channel sandstone beds amidst siltstone, and grayer colors. The Padden lacks palm fossils. These lithologic criteria are sufficient to assign about 2/3 of Chuckanut outcrops to one unit or the other.

All of the Chuckanut is younger than about 57 Ma (detrital fission track ages by Joseph A. Vance, oral communications 1997.) Mustoe and Gannaway (*Washington Geology*, 1997) interpret Padden leaf fossils to record a cooler, more seasonal climate than the sub-tropical Bellingham Bay flora, and suggest that the Padden may have been deposited after latest-Eocene global cooling. The top of the Chuckanut could be as young as Oligocene.

Limited outcrop, indistinct lithologies, and extensive landslides make it difficult to confidently interpret the structure of the Chuckanut Formation. Nonetheless, after one and one-half seasons of field work I see the following: 1) Folds S and SE of Bellingham overlie NE-verging thrusts. An imbricate fan on Chuckanut Mountain is truncated by the base of the Padden unit. Other parts of the thrust system involve the entire section. The base of the Bellingham Bay unit is a preferred decollement horizon and thrusts locally involve basement. Shortening appears to be on the order of 5–15 km. 2) On the west slope of American Sumas Mountain, NE of Bellingham, a gently west-dipping thrust places pre-Tertiary phyllite, semischist, and greenstone on top of Padden unit(?—previous workers have called this Huntingdon). Shortening here is at least 2 km. 3) Upright Bellingham Bay unit along the summit of Stewart Mtn, E of Bellingham, is on top of upright, shallowly-dipping Padden unit. I cannot tell where the intervening thrust roots. 4) Farther east, from the basal contact at Acme north to the northernmost and stratigraphically highest Chuckanut on eastern American Sumas Mountain, the Chuckanut consistently dips to the N and NW. The steepest dips (circa 70°) are at the north end of the section, adjacent to the Boulder Creek fault which juxtaposes Chuckanut with pre-Tertiary basement. This fault appears to be a listric, down-to-the-SE, low-angle normal fault with at least 5 km of slip. Similar faults may be present farther south, within the Chuckanut Fm. Extension may in part be younger than thrusting. 5) Undisturbed sections of the Bellingham Bay unit are 1–1.5 km thick. The top of the Padden is nowhere exposed, but the Padden could be no thicker than 2 km.

I see several implications for Cordilleran tectonics. First, when evaluating the structural framework of the Cascadia forearc we should look for structures adequate to transfer many kilometers of displacement from the plate boundary to the Bellingham area in proto- or early-Cascade arc time. Second, not all faults and fabrics in pre-Tertiary rocks of the western North Cascades and San Juan Islands date from mid-Cretaceous and older orogeny. Much strain is probably mid-Tertiary. Finally, although most deformation in the Chuckanut probably is mid-Tertiary, overall strain is consistent with the N-S contraction and dextral slip on NNW-striking zones that characterize modern deformation in this part of the Cascade forearc.

ARCHEAN ZIRCONS IN UPPER CRETACEOUS SEDIMENTS OF THE WESTERN CANADIAN CORDILLERA - DOES THE "BAJA B.C. " HYPOTHESIS FAIL A "CRUCIAL TEST"?

MUSTARD, P.S., Simon Fraser University; **MAHONEY, J.B.**, University of Wisconsin - Eau Claire; **HAGGART, J.W.** Geological Survey of Canada, Vancouver; **FRIEDMAN, R.M.,** University of British Columbia; **FANNING, M.** Australian National University; **McNICOLL, V.J.** Geological Survey of Canada, Ottawa.

The magnitude of late Mesozoic terrane translation along the western continental margin is a fundamental controversy in Cordilleran tectonics. Paleomagnetic data suggests ~3000 km of dextral displacement of the Insular superterrane (IS), the " Baja B.C. " hypothesis. Several lines of geologic evidence indicate considerably less offset (roughly <500km). The presence or absence of Archean zircon within easterly-derived sediments in Cretaceous basins associated with IS has been proposed as a crucial test of the "Baja B.C." hypothesis (Cowen et. al., 1997). Archean crust is restricted to northern latitudes (>40°N) in North America, therefore Archean detrital zircon provide a provenance tracer of sediments derived from northern latitudes.

Archean zircon has been identified in easterly-derived sediments in the Cretaceous Queen Charlotte (2.54-2.56 Ga; JWH), Nanaimo (2.51 Ga; PSM) and Methow (2.54-2.56 Ga; JBM) basins. In each case, the Archean component forms a small (<5%) but distinctive population. There is no plausible first or second cycle source of this Archean zircon except Archean crust of the Canadian Shield or closely associated Proterozoic strata. Both sources are restricted to a northern paleogeographic position now and during the Cretaceous.

Exceptional explanations, which permit both southern positions of the sedimentary basins and a northern source area, are rejected. A minimum of several hundred kilometers of river transport followed by extensive longshore transport of Archean zircon for >2000 km along the topographically complex Mesozoic continental margin is unlikely in general and not supported by the many detailed sedimentology/provenance studies from these basins. Third or fourth order derivation of the Archean zircons from recycling of Paleozoic strata is statistically improbable, given the <5% content of Archean zircon present to begin with in the Paleozoic strata (Gehrels et. al., 1995). The possibility of an unrecognized Archean source area in central or southern Mexico is an untestable hypothesis.

Cowen et al. (1995) specifically highlight the search for Archean zircons in late Cretaceous sediments of IS as a crucial test of the "Baja B.C." hypothesis. If this premise is accepted, our demonstration of Archean zircons from three of the major sedimentary basins of the IS provides a strong negative test of the hypothesis.

ABSTRACTS of POSTER PRESENTATIONS

Mesozoic to Eocene composite Endako Batholith redefined.

R.G. Anderson[1], J.B. Whalen[2], L.C. Struik[1], and M.E. Villeneuve[2]

1. Geological Survey of Canada, Vancouver, B.C. V6B 5J3 (email: banderson@gsc.nrcan.gc.ca / bstruik@airwolf.gsc.emr.ca)

2. Geological Survey of Canada, 601 Booth Street, Ottawa, Ont. K1A 0E8 (email: jwhalen@gsc.nrcan.gc.ca / mvillene@nrn1.nrcan.gc.ca)

ABSTRACT

The world-class Endako porphyry molybdenite (Mo) deposit occurs in the northwesterly-trending, Triassic to Eocene, composite Endako batholith. The intrusive rocks occur along the eastern margin of Stikinia within the Fort Fraser and Nechako River map areas (NTS 93F and K). The batholith has been variously considered part of the Jurassic Topley Intrusions, Endako Intrusions and Early Cretaceous Francois Lake Plutonic Suite. New mapping, geochronology, and chemical and isotopic analyses define at least 6 constituent suites:

* poorly-mineralized Late Triassic Boer suite (ca. 220-215? Ma);
* poorly-mineralized Middle Jurassic (176-165 Ma) Stag Lake suite;
* Late Jurassic (159-154 Ma), older part of the Francois Lake Plutonic Suite (partly hosts but is petrogenetically unrelated to Endako-style, low-fluorine, porphyry Mo deposits);
* Jura-Cretaceous (148-145 Ma), younger Francois Lake Plutonic Suite directly coeval and related to the Mo deposits;
* unmineralized, satellitic mid- to Late Cretaceous Fraser Lake suite, and,
* unmineralized Eocene(?) mafic and miarolitic felsic stocks and phases.

New Ar-Ar ages for hydrothermal biotite at 144-143 Ma clearly links Mo mineralization at the Endako Mine to terminal Jurassic magmatism and is cospatial with the younger Francois Lake Plutonic Suite.

A characteristic of the batholith's external intrusive relationships is that exposures of supracrustal wall rocks, either as screens, pendants or inclusions, are rare, with older plutonic suites within the batholith forming the wall rock for successively younger intrusions. Episodic but localized intrusion of plutonic pulses over an extended time frame, suggests a fundamental crustal structural control, probably as the result of crustal extension within an arc setting. These characteristics are typical of 'Andean-type' plutonic suite in continental margin arcs.

The suites include (oldest to youngest):

Late Triassic (220-215? Ma) Boer Plutonic Suite

These intrusions occur along the northern part of the batholith and include dark grey, hornblende (±biotite) diorite to quartz diorite. The suite is coeval with parts of the Topley intrusions (s.l.) and western Takla Group volcanic rocks recognized by D. MacIntyre to the north. In the Endako batholith, the Boer suite:

- is commonly mesocratic, equigranular, coarse- to medium-grained and generally weakly to strongly foliated.
- hornblende displays a distinctive stubby euhedral habit.
- includes the Stern Creek phase which consists of foliated biotite and hornblende diorite and granodiorite. Locally the rock has a gneissic texture, can have potassium feldspar phenocrysts and varies significantly in texture and composition on the outcrop scale.

Parts of the undated Mount Hobson pluton in northeastern Nechako River map area resemble members of the Boer Plutonic Suite. The suite is coeval with and resembles the Late Triassic Stikine Plutonic Suite in northeastern Stikinia north of the Stikine River.

Middle Jurassic (175-165 Ma) Stag Lake Suite:

These intrusions define the eastern and northeastern batholith margins and include sequentially-intruded biotite-hornblende diorite and gabbro, and hornblende-biotite quartz monzodiorite and granodiorite; biotite quartz monzonite to monzogranite may represent related felsic phases. The suite is coeval with Middle Jurassic mafic to felsic volcanic rocks (Naglico and Entiako formations) recognized to the south. The plutonic rocks are commonly:

- mesocratic, equigranular to megacrystic.
- xenolith-, clinopyroxene- and titanite-bearing.
- locally foliated: mineral and xenolith foliations are most common near contact zones between mafic and intermediate phases.
- compositionally heterogenous but are generally of calc-alkaline, metaluminous, moderate-potash and volcanic arc affinities.

The suite closely resembles the coeval Three Sisters Plutonic Suite in northeastern Stikinia north of the Stikine River and in the Iskut-Telegraph Creek map areas.

Late Jurassic (159-154 Ma) "Older" Francois Lake Plutonic Suite (Glennanan and Nithi phases):

This subsuite includes biotite monzogranite to hornblende-biotite granite to granodiorite plutons in the north-central and northwestern parts of the batholith as well as finer-grained equivalents to the north. The suite is coeval with Upper Jurassic mafic and felsic volcanic rocks to the north and south (Netalzul and Nechako volcanics). The plutonic rocks are:

- quartz-rich, leucocratic, massive, unaltered to altered, and compositionally uniform.
- further subdivided based on grain size, biotite abundance, degree of alteration, intergranular textures, and intrusive relationships.

- medium- to very coarse-grained, unfoliated, subporphyritic to megacrystic.
- seriate, miarolitic and grade to druzzy (highly miarolitic), patchy pegmatitic biotite aplite of the Tatin Lake subphase.
- both units contain disseminations and miarolitic fillings of sulphides.
- are more geochemically evolved than older plutons (higher SiO_2, K_2O, meta- to peraluminous, entirely calc-alkaline and alkali-rich, lower CaO, higher Rb, weaker Eu anomaly).

Jura-Cretaceous (148-145 Ma) "Younger" Francois Lake Plutonic Suite (Francois, Endako and Casey phases)

The younger subsuite of the Francois Lake intrusions includes biotite monzogranite plutons along the western and northwestern part of the Endako batholith. They are the most quartz-rich, leucocratic, and mineralized of all and are further subdivided based on grain size, biotite abundance, degree of alteration, intergranular textures, and intrusive relationships. The subsuite records a complex, protracted history that included: emplacement, solidification, locally intense veining, Mo and pyrite mineralization and alteration, and late dykes, fractures, and joints. The structural control on the co-spatial but younger (ca.144-143 Ma) mineralizing system suggests a possible dextral, trans-tensional tectonic environment for emplacement of the younger subsuite. The rocks are distinctly:

- medium- to fine-grained and subporphyritic to aplitic.
- the most geochemically evolved of all (high SiO_2, high K_2O, slightly peraluminous, entirely calc-alkaline and alkali-rich, low CaO, very high Rb relative to Ba and Sr, marked Eu anomaly and HREE depletion, and of volcanic arc affinity with a relatively primitive or juvenile radiogenic and stable isotopic character).

Their characteristic geochemical composition helps distinguish them from texturally similar but older members of the Francois Lake suite.

Mid-Cretaceous (ca. 115-90 Ma) Fraser Lake Plutonic Suite (Cabin Lake, Fraser Lake and Leg Lake? plutons):

These mottled pink and white, (hornblende-) biotite monzogranite, quartz monzonite or granodiorite plutons form small stocks along the northwestern, northeastern and northern margins of the Triassic-Jurassic phases. Only the Cabin and Fraser lakes plutons are dated. They are characterized by:

- medium- to fine-grained and texturally heterogeneous (subporphyritic to equigranular).
- graphic and granophyric textures common; less commonly miarolitic.
- resemble younger FLP and Eocene? suites modally but are less geochemically evolved.

Eocene? Copley Lake Plutonic Suite (Copley Lake and unnamed intrusions):

These undated, mottled pink and white, (hornblende-) biotite monzogranite, and melanocratic diabase to diorite and hornblende-plagioclase porphyry intrusions occur as small to large intrusions co-spatial with extensive Eocene (ca. 52-50 Ma), felsic Ootsa Lake Group volcanic rocks mainly south of the main batholith. Felsic phases have a variety of equigranular, porphyritic and intrusive breccia phases. The rocks are characterized by:

- finer grain size, paucity of associated alteration or molybdenite showings and miarolitic cavities distinguish phases from younger Francois Lake Plutonic Suite.
- common graphic and granophyric textures.
- modal and textural resemblance of porphyry phases to the Ootsa Lake Group rhyolitic biotite-quartz-alkali-feldspar porphyry flows which suggests a cogenetic relationship.

SEE ALSO:

Anderson, R.G., L'Heureux, R., Wetherup. S. and Letwin, L.
1997: Geology of the Hallett Lake map area, central British Columbia: Triassic, Jurassic, Cretaceous and Eocene? plutonic rocks; in Current Research 1997-A; Geological Survey of Canada, p. 107-116.

Anderson, R.G. and Snyder, L.D.
1998: Jurassic to Tertiary volcanic, sedimentary and intrusive rocks in the Hallett Lake area, central British Columbia; in Current Research 1998-A; Geological Survey of Canada, p. 135-144.

Anderson, R.G., Snyder, L.D., Resnick, J., and Barnes, E.
1998: Geology of the Big Bend Creek map area, central British Columbia; in Current Research 1998-A; Geological Survey of Canada, p. 145-154.

L'Heureux. R. and Anderson, R.G.
1997: Early Cretaceous plutonic rocks and molybdenite showings in the Nithi Mountain area, central British Columbia; in Current Research 1997-A; Geological Survey of Canada, p. 116-124.

Wetherup, S.
1997: Geology of the Nulki Hills and surrounding area, central British Columbia; in Current Research 1997-A; Geological Survey of Canada, p. 125-132.

Whalen, J.B. and Struik, L.C.
1997: Bedrock geology of southeast Fort Fraser map area, British Columbia: Part 2, plutonic rocks; in Current Research 1997-A; Geological Survey of Canada, p. 77-84.

Whalen, J.B., Struik, L.C., and Hrudey, M.G.
1998: Bedrock geology of the Endako map area, central British Columbia; in Current Research 1998-A; Geological Survey of Canada, p.113-123.

Geology of NE Nechako River map area, central B.C.: evolution from composite Mesozoic arc to Eocene extensional magmatic complex.

R.G. Anderson[1], L.D. Snyder[2], S. Wetherup[3], L.C. Struik[1], M.E. Villeneuve[4], and, M. Haskin[2]

1. Geological Survey of Canada, Vancouver, B.C. V6B 5J3 (email: banderson@gsc.nrcan.gc.ca / bstruik@airwolf.gsc.emr.ca)

2. University of Wisconsin-Eau Claire, Eau Claire, WI, U.S.A. 54702-4004 (email: snyderld@uwec.edu)

3. Department of Earth and Atmospheric Sciences, University of Alberta, Edmonton, Alta. T6G 2E5 (email: wetherup@gpu.srv.ualberta.ca)

4. Geological Survey of Canada, 601 Booth Street, Ottawa, Ont. K1A 0E8 (email: mvillene@nrn1.nrcan.gc.ca)

ABSTRACT

Five tectonostratigraphic assemblages exposed in the northeastern Nechako River map area (NTS 93F) record the evolution of eastern Stikinia from a Triassic-Middle Jurassic composite plutono-volcanic arc to a fault-bounded, Eocene bimodal volcano-plutonic complex. The latter is coeval with terminal cooling of the nearby, extensional Vanderhoof Metamorphic Complex (VMC). In the Eocene, brittle faulting and the magmatism occurred well inboard of the Eocene continental margin during an episode of trans-tensional tectonics.

The assemblages are:

Triassic arc assemblage: not as extensive as farther north (NTS 93F, L, and M) but may include the undated, foliated, and dioritic Mount Hobson pluton (similar to ca. 219 Ma Stern Creek phase of Late Triassic Boer Suite?)

Lower to Middle Jurassic Hazelton arc assemblage: a bipartite plutonic-volcanic assemblage including: a) Lower Jurassic, calc-alkaline, feldspar-rich volcaniclastic and epiclastic rocks, newly dated at ca. 195.2 +/- 1.1 Ma (U-Pb), and; b) a Middle Jurassic assemblage of Bajocian mafic clinopyroxene-bearing laharic volcaniclastic rocks and mafic to felsic(?), (biotite-) hornblende-bearing plutonic rocks dated at 171-169 Ma. The plutonic rocks form the main record of the Middle Jurassic component of the composite Endako Batholith. The strong correlation between timing of plutonism and arc volcanism supports the volcanic arc affinities of the calc-alkaline, moderate-K, metaluminous plutonic suite.

Middle to Upper Jurassic Bowser Lake overlap assemblage and Upper Jurassic arc: a two-part

assemblage of partly Callovian, poorly exposed, finer- and coarser-grained sedimentary facies of the Bowser Lake Group (BLG), and slightly younger (159-154 Ma), felsic plutons of the Late Jurassic, older members of the Francois Lake Suite (FLPS). The plutonic rocks are coeval with Oxfordian volcanic rocks which occur to the south and north of the Nechako River area. The BLG is locally deformed in a Late Jurassic to Cretaceous event. Compared to the Middle Jurassic plutons, the FLPS rocks are more evolved (higher SiO_2 and K_2O, meta- to peraluminous, entirely calc-alkaline and alkali-rich, lower CaO, higher Rb, weak to marked Eu anomaly, and HREE depletion).

Late Cretaceous arc assemblage: mainly ca. 70 Ma andesitic hornblende porphyry plutonic representative of Kasalka volcanics.

Eocene bimodal extensional magmatic assemblage: Distribution of ca. 52-50 Ma felsic Ootsa Lake Group and slightly younger (49-45 Ma), mafic Endako Group (EG) as well as coeval, compositionally similar, bimodal, high-level plutons was controlled by the development of small- and large-scale, NE- and NW-trending, synvolcanic fault systems. Post-Eocene tilting of the bimodal volcanic assemblage accounts for regional northeastward dips of about 20 degrees.

Stratigraphic, petrographic, geochronological, and geochemical characterizations of the Endako Group (EG) mafic flow rocks clearly distinguish them from the Miocene Chilcotin Group basaltic flows and show EG to be:

- amygdaloidal, clinopyroxene-plagioclase phyric andesite to basaltic andesite
- entirely Eocene in age and of short duration (regionally: ca. 4 Ma; locally < 1 m.y.)
- mildly alkaline transitional to calc-alkaline, with high-K, within plate, continental geochemical affinities

SEE ALSO:

Anderson, R.G., L'Heureux, R., Wetherup. S. and Letwin, L.
1997: Geology of the Hallett Lake map area, central British Columbia: Triassic, Jurassic, Cretaceous and Eocene? plutonic rocks; in Current Research 1997-A; Geological Survey of Canada, p. 107-116.

Anderson, R.G. and Snyder, L.D.
1998: Jurassic to Tertiary volcanic, sedimentary and intrusive rocks in the Hallett Lake area, central British Columbia; in Current Research 1998-A; Geological Survey of Canada, p. 135-144.

Anderson, R.G., Snyder, L.D., Resnick, J., and Barnes, E.,
1998: Geology of the Big Bend Creek map area, central British Columbia; in Current Research 1998A; Geological Survey of Canada, p. 145-154.

Haskin, M.L., Snyder, L.D., and Anderson, R.G.
1998: Tertiary Endako Group volcanic and sedimentary rocks at four sites in the Nechako River and Fort Fraser map areas, central British Columbia; in Current Research 1998-A; Geological Survey of Canada, p. 155-164.

L'Heureux. R. and Anderson, R.G.
1997: Early Cretaceous plutonic rocks and molybdenite showings in the Nithi Mountain area, central British Columbia; in Current Research 1997-A; Geological Survey of Canada, p. 116-124.

Wetherup, S.
1997: Geology of the Nulki Hills and surrounding area, central British Columbia; in Current Research 1997-A; Geological Survey of Canada, p. 125-132.

Geochemical and Isotopic Constraints on Ancient (700Ma) Seawater Chemistry, Western Canada

Augereau, Carole M., Spencer, Ronald J.
Department of geology and Geophysics, The University of Calgary
2500 University Drive NW, Calgary Alberta, Canada, T2N 1N4

Ross, Gerald M.
Geological Survey of Canada
3303 – 3rd Street NW, Calgary, Alberta, Canada, T2L 2A7

The Windermere Supergroup comprises a thick, regionally extensive succession of sedimentary strata deposited on the western margin of Canada during the Neoproterozoic (1000Ma to 540Ma). Near absence of fossils in these rocks makes global and regional biostratigraphic correlations extremely difficult, especially in southern Canada where the Windermere is altered to sub-green schist facies and has undergone complex structural deformation. This project employs a chemostratigraphic approach and attempts to use the stable carbon isotope ratio ($\delta^{13}C$) of these rocks to correlate them regionally and place them in the global picture of the Neoproterozoic Earth. This technique may be suited to the Windermere Supergroup, since results of previous studies indicate that near depositional (i.e. seawater) carbon isotopic compositions are commonly preserved, even in altered Precambrian whole-rock samples (Kaufman and Knoll, 1995). However, tests are needed to evaluate the degree of alteration of individual samples.

Two intervals of the Windermere Supergroup were chosen for this study: the Old Fort Point Formation and the lower to middle Isaac Formation and correlative East Twin Formation. The Old Fort Point Formation is a lithological distinctive interval of mudrocks and sandy carbonates interpreted as a deep water equivalent of a "cap carbonate" (Ross and Murphy, 1988; Ross et al., 1995). It is suited for this chemostratigraphic study since it records the youngest Neoproterozoic glacially influenced sea level rise (Ross and Murphy, 1988), and contains lithologies suitable for this technique. The Isaac Formation of the Cariboo Group (and the correlative East Twin Formation, Upper Miette Group) is a thick succession of intervals of graded silty shales, grits and two regionally extensive deep-water carbonate units. The prevalence of black (potentially organic rich) shale and the presence of deep water carbonates in the Isaac and East Twin formations makes them good candidates for isotopic studies. These units are interpreted as slope facies deposited on the flank of seaward prograding continental shelf assemblage (Ross, 1991). Trace element analysis are being used to determine if the deep water character of both intervals studied (Old Fort Point and Isaac formations) has spared them from the geochemically destructive effects of meteoric diagenesis.

Isotopic data ($\delta^{13}C$, $\delta^{18}O$) were collected from samples of carbonate and organic carbon from four sections of the Old Fort Point Formation, and five sections of the lower to middle Isaac Formation. Aliquots of powdered micro-samples were analyzed for their concentrations of Mn, Sr, Mg, and Ca which are important in evaluating the degree of alteration due to diagenesis and dolomitization (Kaufman and Knoll, 1995). No trend suggesting the presence of alteration products likely to have affected the original $\delta^{13}C$,

was found. Therefore, measured $\delta^{13}C$ values appear to be a valid proxy for seawater carbon for these intervals. Data are only completed for carbonate $\delta^{13}C$ and trace elements from the Old Fort Point Formation. The $\delta^{13}C$ of organic matter offers an additional means to evaluate the degree of post-depositional alteration of carbonate carbon isotopic composition (Kaufman et al., 1991). The laboratory work required to measure the $\delta^{13}C$ of the organic carbon from shales interbedded with the carbonates is in progress.

The $\delta^{13}C$ values for the carbonate carbon obtained from the Old Fort Point Formation vary from -1‰ to -11‰ with a strong concentration around -8‰. . The values obtained from the Old Fort Point Formation are more depleted in ^{13}C than other sections globally which typically range from –2 to –4.6‰ (Narbonne et al., 1994; Kaufman et al., 1991; and others). The cause of these differences may be related to the commonly invoked Neoproterozoic stagnant ocean model but this must await verification through results of isotopic studies of organic carbon from these sections. Nonetheless, preliminary results indicate that the geochemical data are a useful tool for local correlation.

Kaufman, A.J., Hayes, J.M., Knoll, A.H. and Germs, G.J.B., 1991. Isotopic compositions of carbonates and organic carbon from upper Proterozoic successions in Namibia: stratigraphic variation and effects of diagenesis and metamorphism. Precambrian Res., 49: 301-327.

Kaufman, A.J. and Knoll, A.H., 1995. Neoproterozoic variations in the C-isotopic composition of seawater: stratigraphic and biogeochemical implications. Precambrian Res., 73: 27-49.

Narbonne, G.M., Kaufman, A.J., and Knoll, A.H., 1994. Integrated chemostratigraphy and biostratigraphy of the Windermere Supergroup, northwestern Canada: Implications for Neoproterozoic correlations and the early evolution of animals. GSA Bull., 106: 1281-1292.

Ross, G.M., 1991. Tectonic setting of the windermere Supergroup revisited. Geology, 19: 1125-1128.

Ross, G.M., McMechan, M.E., and Hein, F.J., 1989. Proterozoic history: the birth of the miogeocline. In: Ricketts, B.D. (Ed.), Western Canaidan Sedimentary Basin: A case history, p.79-99. Canadian Society of Petroleum Geologists, Calgary.

Ross, G.M. and Murphy, D.C., 1988. Trangressive stratigraphy, anoxia, and regional correlations within the late Precambrian Windermere grit of the southern Canadian Cordillera. Geology, 16: 139-143.

Ross, G.M., BLoch, J.D., and Krouse, H.R., 1995. Neoproterozoic strata of the southern Canadian Cordillera and the evoultion of seawter sulfatte. Precambrian Research, 73:71-99.

Investigation of a displacement-transfer zone by 3-d seismic interpretation and physical modelling: progress report on computer-graphics visualization and strain analysis

Evsen O. Aydemir and John M. Dixon, Experimental Tectonics Laboratory, Department of Geological Sciences, Queen's University, Kingston, Ontario K7L 3N6

In the context of fold-thrust tectonics, a displacement-transfer zone is a three-dimensional region between the terminations of two *en echelon* thrust faults. As a case study of this phenomenon, interpretation has been done on a 3-D seismic data set from the Rocky Mountain Foothills of northeastern British Columbia (see Figure 1). The volume is interpreted to include three foreland- and three (possibly four) hinterland-vergent thrusts. The initiation of backthrusting appears to be related to the presence of pre-existing antiforms as faults cut up-section through the strained rocks in the back-limb. One backthrust cuts a detachment fold above an older forethrust and another cuts what may be a buckle or fault-bend fold. It may be important to recognize that complex zones of displacement transfer exist between foreland- and hinterland-vergent faults and that pop-up features and larger backthrusts may play an important role in the distribution of strain. The unit juxtaposition created by backthrusting through synchronous or older folds may be significant when targeting such features as structural hydrocarbon traps.

The interpreted seismic volume has been used to create a geological computer model representation (Fig. 2) of the study area using the GoCad7 three-dimensional visualization software package. GoCad is a powerful tool for visualizing details of a complex structural setting. This 3-D construction will be used as the basis for detailed comparison between the structures in the study area and those created in the analog physical models.

We have carried out exploratory scaled physical modelling using the centrifuge technique. A model design has been developed (Fig. 3) that produces structural features closely resembling those in the study area. The experimental procedure results in along-strike variations and displacement transfer between *en echelon* structures. The models have led to possible alternatives to the initial interpretation of the seismic data.

A method of model construction has been developed (see Fig. 4) that allows for detailed examination of strain inside the model, within the plane of a competent stratigraphic unit. It is possible to create a grid of markers within a layer of the model. The positions of these markers can be determined in plan view by x-ray imaging, before and after deformation. The points can also be located in the vertical dimension by interpolation between cut sections using marker strips that contain the x-ray markers. It is possible to quantify the strain within the physical model in three-dimensions by using this information about the displacements of the marker points to build a GoCad representation. This will be used to analyse the possible distribution of fracture porosity in displacement-transfer zones.

Acknowledgements: This work was carried out as part of the Foothills Research Project FRP), a collaboration between principal investigators D.C. Lawton and D.A. Spratt of the University of Calgary and J.M. Dixon of Queen's University. Financial support from FRP sponsor firms in the petroleum industry and NSERC is acknowledged with thanks. We are very grateful to Husky Oil for making available the 3-D seismic data.

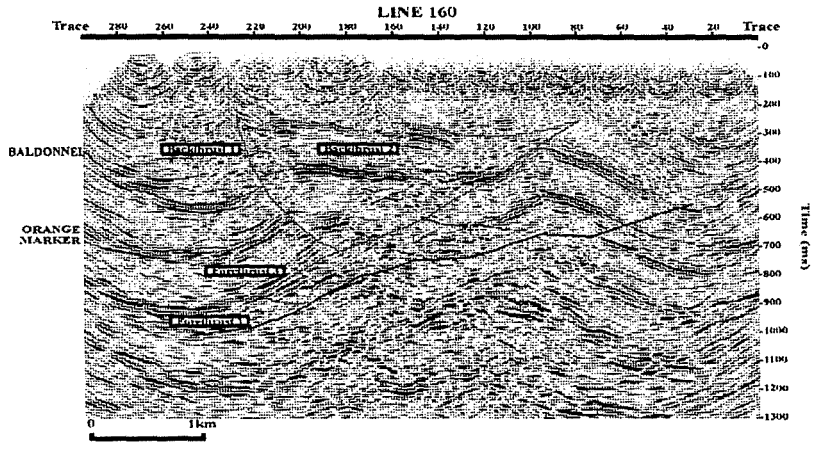

Figure 1. Seismic line 160 from the interpreted seismic volume in NE BC. Comparison with Figure 3 shows that the deformation style in the study area is similar to that produced in the physical models. Note that structures below Forethrust 1 have not been interpreted due to poor imaging. It is the interrelationships of structures in the shallower portion that are of interest in this study.

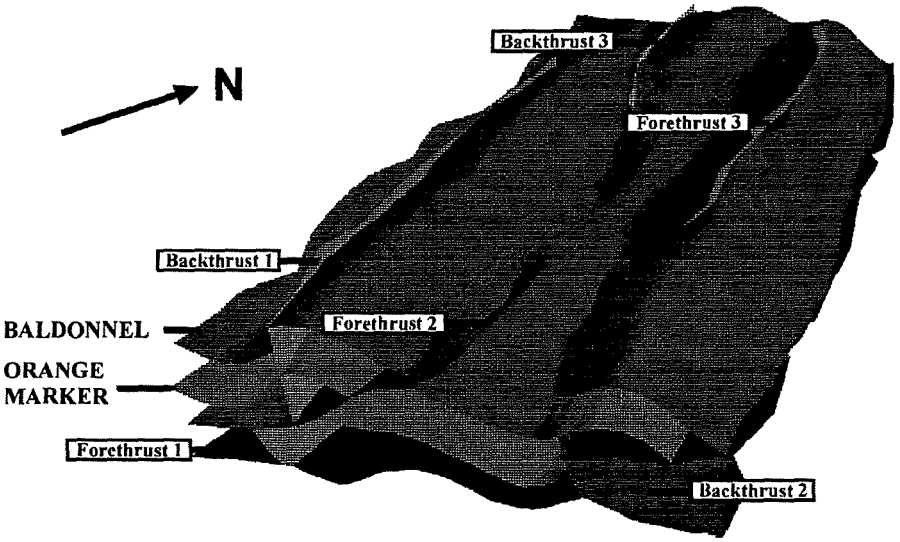

Figure 2. Geological model of the study area constructed with GoCad visualization software, based on the interpreted 3-D seismic volume (see Fig. 1).

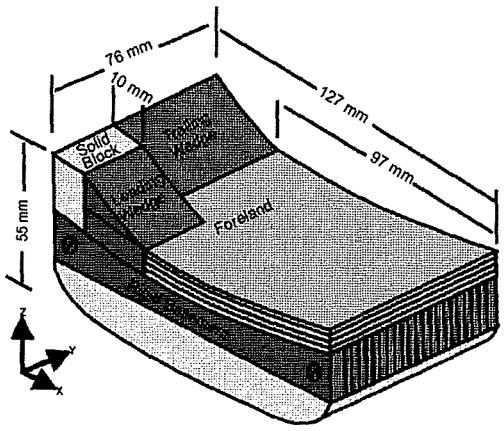

Figure 3. Dimensions and original configuration of model EA 22. The Foreland portion of the model is constructed of interlayered plasticine and silicone putty. The plasticine hinterland wedges are offset from each other but are of equal length. Both wedges have a surface slope of 1:3. The solid block behind the leading wedge does not deform during the evolution of the model. The rigid base-plate is made of aluminum plates, each 0.125 inches thick, which can be separated for serial-sectioning of the model.

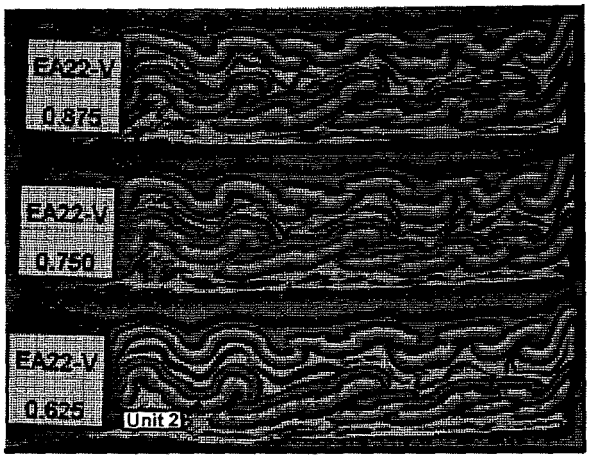

Figure 4. Transverse sections through model EA 22 after five stages of deformation. Unit 2 is made up of five stacked plasticine layers. The central white layer hosts a series of parallel, evenly spaced, coloured strips of plasticine that appear here in cross-section as small dots. During model construction, galena crystals are planted along the strips with a spacing of 2 mm. After rolling to final thickness, the galena crystals form an array 6 mm along strike and 2 mm across strike. Section positions are shown in inches from one edge of the model and the labels are 1 cm wide. Compare structural style with Figs. 1 and 2.

NATURE OF MOVEMENT ACROSS THE PURCELL THRUST, ROCKY MOUNTAIN TRENCH: METAMORPHIC TRANSECTS

Boggs, K.J.E., Ghent, E.D., and Simony, P.S. Department of Geology and Geophysics, University of Calgary, 2500 University Dr. NW, Calgary, Alberta, T2N 1N4.

The Purcell Thrust is a regional scale out-of-sequence thrust that obliquely transects the southern Rocky Mountain Trench and places more westerly structural elements against the western margin of the Rocky Mountains. Motion along the Purcell Thrust is proposed to be a result of the last phase of compressional deformation in the Dogtooth Range (before the mid-Cretaceous; Kubli and Simony 1994), but the exact timing, duration and nature of movement along the Purcell Thrust are unknown. The age relationship between thrust motion and metamorphism is also not clearly established.

Kubli and Simony (1994) suggested that the northeastward thrust motion on the Purcell Thrust was accompanied by a throw of ~ 6km near Golden, B.C. where the thrust places upper Proterozoic and Lower Cambrian strata over Upper Cambrian strata in the Trench. These relationships can be observed along strike for 65 km from Golden northwestward to Bush Arm (Figure 1). The Purcell Thrust is exposed in a new railroad cut west of Donald were Lower Cambrian Donald Formation *Archaeocyathus* -bearing limestones are placed on top of the grey-black slates of the Upper Cambrian Canyon Creek Formation. In a transect across the Trench and Purcell Thrust some 80 km northwest of Golden between the Adamant (Selkirk) and Solitude Ranges (Rockies), Meilliez (1973) and Gal and Ghent (1990) demonstrated that there is little strike separation of the garnet isograd. Gal and Ghent (1990) suggested the possiblity of similar metamorphic conditions (~ 6-7kbar) on either side of the Purcell Thrust. There the Purcell Thrust is cut by a west-side-down normal fault in the Trench. Gal and Ghent (1990) suggest two alternative models that can explain their observations. In a transect across the Trench between the northern Selkirks and the Park Ranges of the Western Rockies some 150km northwest of Golden Craw (1976) and Ghent et al. (1980) show that metamorphism in the northern Selkirks and adjacent Monashees took place at pressures ~ 2kbar higher than

metamorphism in the western Rockies corresponding to ~ 6-7km west-side-up throw on a post-metamorphic fault.

Metamorphism in the hanging wall and footwall of the Purcell Thrust is being re-examined in detail in the region northwestward from Bush Arm. This encompasses a range in metamorphic grade from chloritoid bearing slates in the southeast to amphibolite facies (staurolite-kyanite zone) migmatite in the northwest. Detailed mineralogical and geobarometric studies may reveal geobarometric breaks across the Purcell Thrust and imply post-metamorphic throw on this fault.

Craw, D. 1977. Metamorphism, structure and stratigraphy in the Southern Part Ranges, British Columbia. Canadian Journal of Earth Sciences, 15, 86-98.

Gal, L.P., and Ghent, E.D. 1990. Metamorphism in the Solitude Range, southwestern Rocky Mountains, British Columbia: comparison with adjacent Omineca Belt rocks and tectonometamorphic implications for the Purcell Thrust. Canadian Journal of Earth Sciences, 27, 1511-1520.

Ghent, E.D., Simony, P.S., and Knitter, C.C. 1980. Geometry and pressure-temperature significance of the kyanite-sillimanite isograd in the Mica Creek area, British Columbia. Contributions to Mineralogy and Petrology, 74, 67-73.

Kubli, A.M., and Simony, P.S. 1994. The Dogtooth Duplex, a model for the structural development of the northern Purcell Mountains. Canadian Journal of Earth Sciences, 31, 1672-1686.

Meilliez, F. 1973. Etude Géologique du Secteur Meridional de Solitude Range (Rocheuses), Columbie Britannique (Canada). Doctorate Thesis, Université des Sciences et Techniques de Lille, Lille, France, pp. 189.

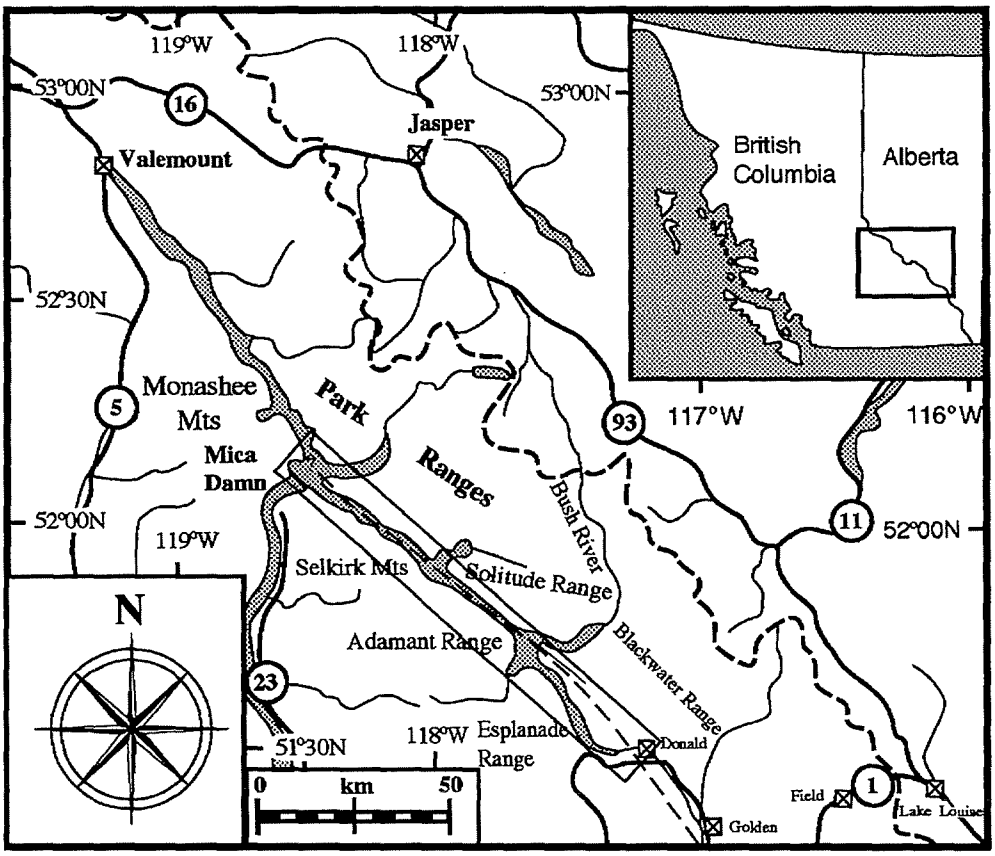

FIGURE 1: Location of geographical features in field area.

Study area

Purcell Thrust

Trench Normal Fault

THE ACASTA GNEISSES: FURTHER EVIDENCE FOR A COMPLEX POLYMETAMORPHIC HISTORY

Wouter Bleeker and Richard A. Stern

Geological Survey of Canada, 601 Booth St., Ottawa, ON, Canada K1A 0E8
(wbleeker@gsc.NRCAN.gc.ca or rstern@.NRCan.gc.ca)

Abstract

The Acasta Gneiss Complex (Figure 1), on the western edge of the Slave structural province, contains the oldest known rocks on Earth (Bowring et al., 1989). A systematic geological and geochronological study of these complex polymetamorphic gneisses has been initiated at the Geological Survey of Canada relying heavily on new, in-house SHRIMP II ionprobe analytical capabilities.

Preliminary results had pushed back the age of the "oldest rock": 4017±7 Ma for a grey tonalitic gneiss (sample BNB95-103; Stern et al., 1997; Bleeker and Stern, 1997). Further analysis of the age results on this tonalite gneiss sample yields a final age of 4025±15 Ma (Stern and Bleeker, 1998). Zircon rims on several prismatic grains yield an average age of 3356±14 Ma, indicating a significant metamorphic and zircon growth event. We correlate this age with high grade metamorphism and leucosome development in the tonalitic gneiss.

New results on a nearby garnet-bearing biotite gneiss sample (tonalite to granodiorite protolith, sample BNB95-123B) yields somewhat similar results although zircons in this sample are generally less well preserved. Nevertheless, many of the altered zircons show an "atoll texture" with preserved central domains in which concordant primary ages have been preserved (Figure 2a). Several of these intra-granular domains yield consistent ionprobe results with an average age of **4041±12 Ma** (Figure 2a,b). We interpret this as the crystallization age of the tonalitic to granodioritic protolith and this is currently the oldest age reported for Acasta and the terrestrial rock record.

Secondary alteration products in the altered zircons locally include small (1-10 μm) thorite grains that yield ca. 3.3 Ga $^{207}Pb/^{206}Pb$ ages (Stern and Bleeker, in preparation). As in many of our other samples, this result corroborates the importance of a ca. 3.3 Ga metamorphic overprint on the Acasta gneisses.

Foliated granitoid sheets in the gneisses have been dated at two different localities and yield ages of 3348+43/-34 Ma and 2875+39/-16 Ma, respectively. Preliminary Sm-Nd results on a garnet separate from sample BNB95-103 (zircon age: 4025±15 Ma) suggests an age of ca. 2.8 Ga for garnet growth.

Even ignoring significant tectonothermal events at ca. 2.6 Ga (Slave Province) and 1.8 Ga (Wopmay Orogen), it is becoming clear that the Acasta gneisses experienced a complex polymetamorphic history. Several of the high grade events occurred long after initial protolith generation with "delay times" of several 100s of million to more than a billion years. We thus sugges that initial Nd isotopic ratios calculated for even the best-preserved Acasta gneisses should be treated with extreme caution. Extrapolation of such ratios beyond the high grade 3.3 Ga event is likely to result in erroneous initial ε_{Nd} values. Where such values are derived from internal isochrons on slabbed samples with apparent ages of ca. 3.8-4.0 Ga ages (Bowring et al., 1995; Coleman and Bowring, 1997), overall uncertainties in the calculated initial ε_{Nd} values should be quoted and carefully evaluated.

References

Bleeker and Stern, 1997, *GAC Abstract Volume*, p. A13.
Bowring et al., 1989, *Geology*, v. 17, p. 971-975.
Bowring and Housh, 1995, *Science*, v. 269, p. 1535-1540.
Coleman and Bowring, 1997, *GAC Abstract Volume*, p. A40.
Stern et al., 1997, *GAC Abstract Volume*, p. A142.
Stern and Bleeker, 1998, *Geoscience Canada*, in press.

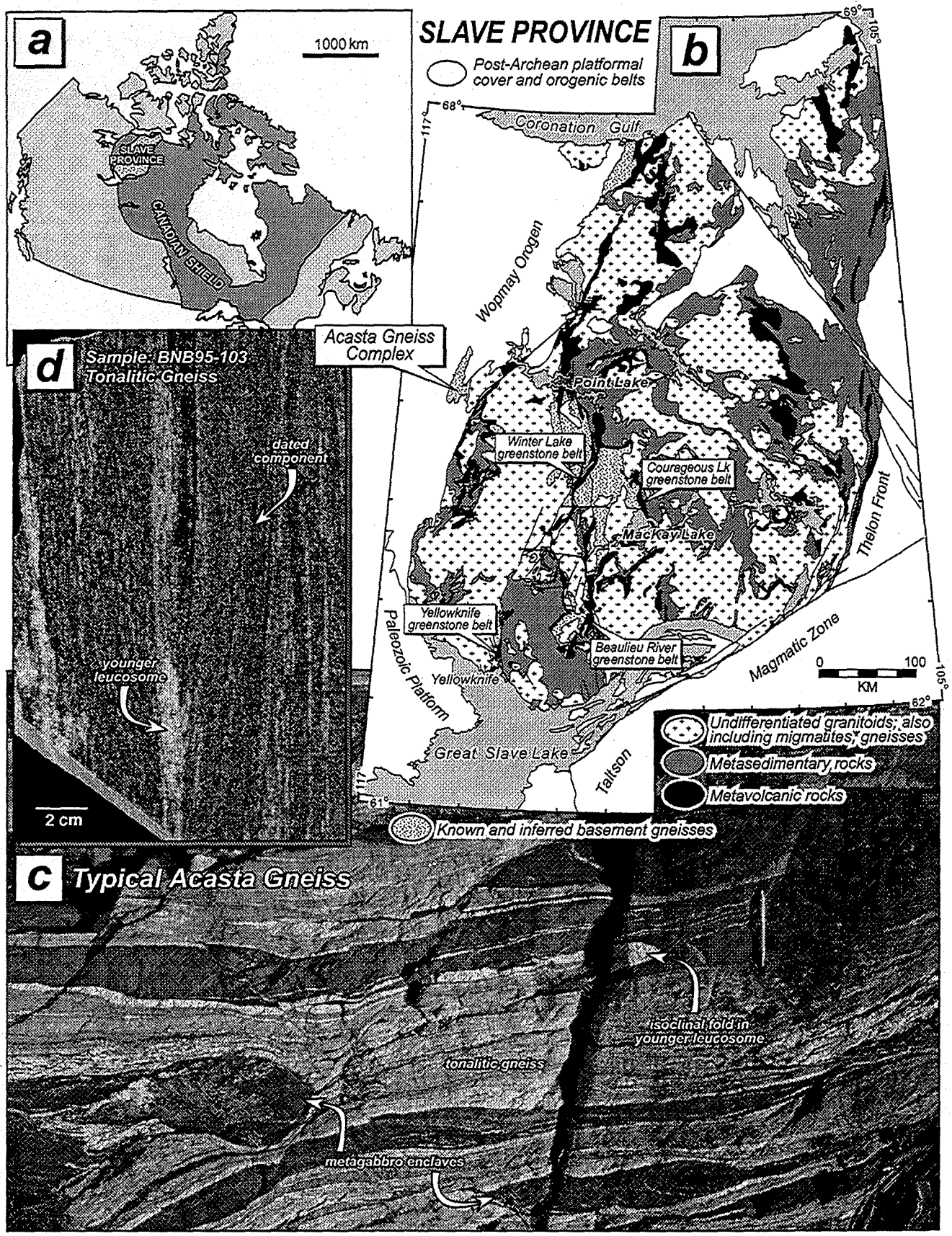

Figure 1: a) Location of the Slave structural province within the Canadian Shield. b) Simplified geological map of the Slave Province showing the Acasta Gneiss Complex in the core of antiformal fold culminations in the foreland of Wopmay orogen. c) Typical multicomponent Acasta gneiss showing metagabbro enclaves in metatonalite. d) Polished slab of tonalitic gneiss sample BNB95-103B dated at 4029±15 Ma (Stern and Bleeker, 1997 and in prep.).

Wouter Bleeker and Richard Stern, GSC, SNORCLE March 1998

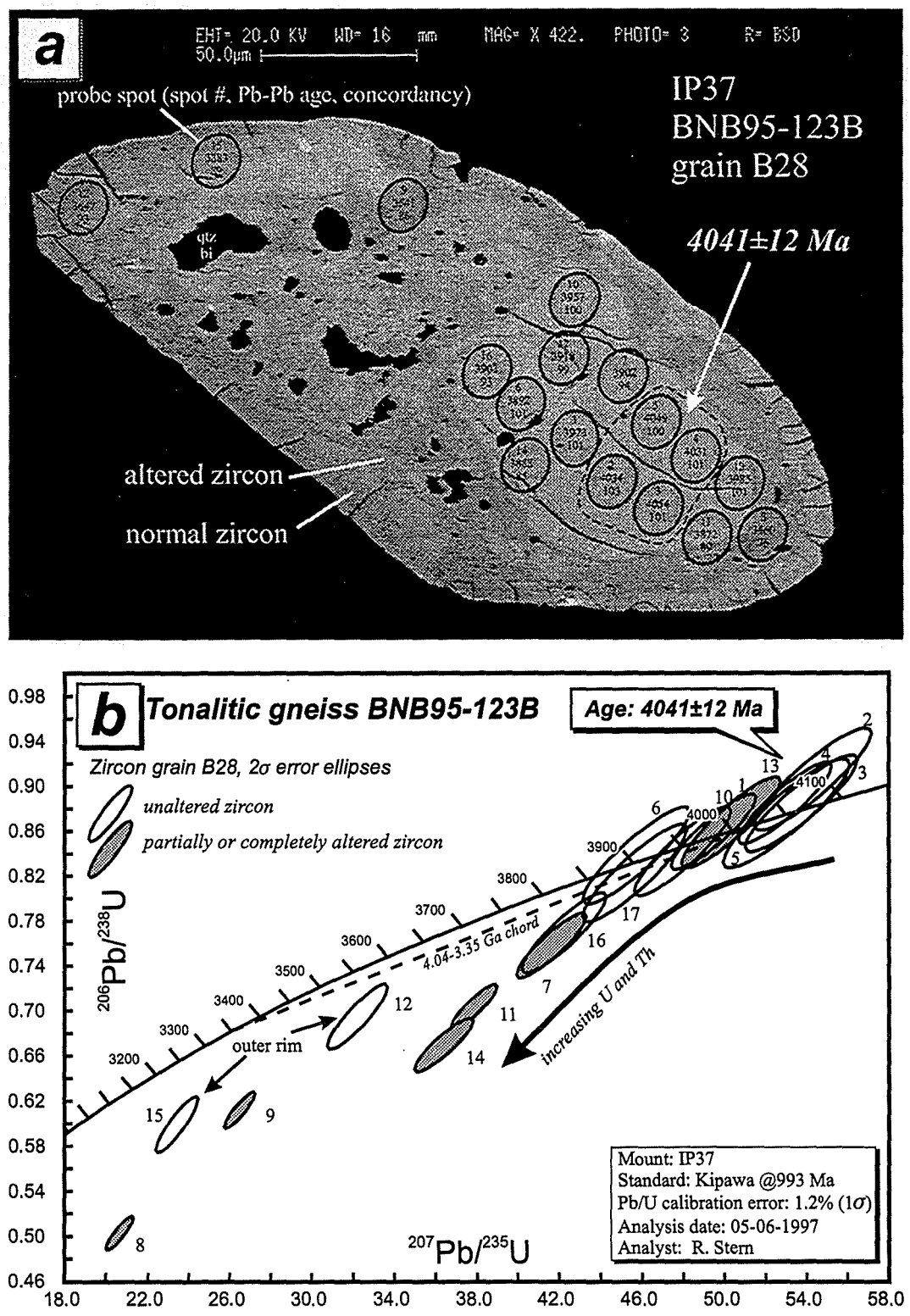

Figure 2: a) Back-scatter electron image of typical zircon grain in metatonalite sample BNB95-123B. Zircons in this sample typically show an "atol struture" consisting of a better preserved central domain, a strongly altered matrix, and commonly a less altered rim. Individual ion probe spots yield a wide range of Pb-Pb ages and discordancies, but in the central domain approach an age of 4041±12 Ma (average). In other grains, small secondary thorite grains that are part of the alteration have been dated at 3.3 Ga (Pb-Pb age; Stern and Bleeker, in prep). b) Concordia diagram of analytical results obtained on grain B28 shown in Figure a.

U-Pb GEOCHRONOLOGY STUDIES - TESLIN ZONE AND EASTERN CASSIAR TERRANE, YUKON; TIMING CONSTRAINTS ON DEFORMATION AND THERMAL HISTORY

S. D. Carr[1] and M. de Keijzer[2]

[1]Ottawa-Carleton Geoscience Centre and Department of Earth Sciences, Carleton University, Ottawa, ON, Canada K1S 5B6; [2]Department of Geology, University of New Brunswick, Fredericton, N.B. E3B 5A3

Based on mapping of a 50 x 20 km area in the Big Salmon Range in the Teslin zone and adjacent rocks to the east (Brown et al. 1995, 1998; de Keijzer and Williams, 1996, 1997a, b, 1988; Harvey et al. 1996, 1997a, b; Gallagher et al. 1988), the Teslin zone is reinterpreted as a zone of ductile thrusting, which includes thrust sheets of North American affinity and allochthonous rocks that have been complexly folded and displaced northeastward, and then refolded. Early gently-dipping regionally pervasive syn-metamorphic transposition fabrics (S_T) were rotated into steep orientations on the short limbs of km-scale post-transposition folds such as the east-verging F_3 Grizzly synform (Figure 1). The steep limb of this regional-scale structure, together with localized younger F_4 folding on the shallowly inclined lower limb, explains the steep attitude of most Teslin zone rocks. Later structures include ductile dextral as well as brittle offsets on the N-S D'Abbadie fault zone, which cuts off the shallowly inclined limb of the Grizzly synform.

U-Pb studies are designed to determine the timing of metamorphism, penetrative transposition and post-transposition folding within structural domains of the Teslin zone and adjacent rocks to the east. The domains are: the western and eastern Teslin zone, which broadly correspond to the Anvil and Nisutlin assemblages, respectively, the Cassiar terrane, and the ultramafic-bearing klippen (Figure 1; see also de Keijzer and Williams 1997a, 1988, Brown et al. 1988). We are testing the model that rocks in the Teslin zone and Cassiar terrane share a common transposition folding history. Accessory minerals have been separated from fifteen samples, and igneous zircons from five samples are currently being processed (Table 1).

Three zircon-bearing samples collected east of the D'Abbadie fault will bracket the age of regionally penetrative transposition fabrics in the Cassiar terrane. Samples 1 & 2 are the D'Abbadie pluton and a planar late andesitic dyke, respectively (Table 1). These igneous bodies cross-cut penetrative deformation fabrics in the surrounding amphibolite-facies metasedimentary rocks. Boudinaged andalusite in pelitic schist, interpreted to have grown in the contact aureole, indicates that intrusion of the D'Abbadie pluton may be synchronous with the later stages of NE-SW extension in the Cassiar terrane (de Keijzer and Williams 1997b). A penetratively deformed medium-grained leucocratic granitic orthogneiss (Sample 3) contains a mineral lineation (L_M) and foliation (S_T) that are concordant with that of the surrounding semipelitic schists. Thus it is older than at least part of the S_T deformation.

Sample four is a foliated and cataclastic chlorite-bearing granite from the klippe east of Mount Last Peak. It occurs as cm- to dm-scale sheets within metavolcanic and/or volcaniclastic schists beneath extensive exposures of serpentinite and metagabbro (Figure 1). At least part of the penetrative deformation and metamorphism in the klippe is younger than this sample.

Sample five was collected in the western Teslin zone , 1 km west of predominantly metavolcanic rocks that host the Permian eclogite pods of Creaser et al. (1997; Figure 1). It is a leucocratic foliated and lineated granite within a package of concordant garnet-bearing siliceous metasedimentary rocks. The crystallization age will constrain the timing of at least part of the early transposition event in this area and the protolith age will help characterize the host metasedimentary assemblage.

Laboratory work is currently underway, and includes analysis of zircon, monazite and titanite from samples representative of each structural domain. Results will provide direct constraints on the timing of deformation and thermal history of fault bounded structural domains: the western and eastern Teslin zone, the Cassiar terrane, and overlying klippen (Figure 1). Similar ages will support the interpretation that all domains have undergone a similar deformation history; different ages will reveal post S_T displacement on domain bounding structures.

REFERENCES

Brown, R. L., Carr, S. D., Harvey, J. L., Williams, P. F and de Keijzer, M. 1995. Structure and tectonic significance of the Teslin suture zone. LITHOPROBE Report No. 44, 1995 SNORCLE Transect Meeting, Calgary, AB, 56-62.

Brown, R. L., De Kiejzer, M, Carr, Williams, P. F. and Gallagher, C. S. 1988 (this volume). Structure of the Teslin Zone, Yukon, Canada. LITHOPROBE Report. 1998 SNORCLE and Cordilleran Tectonics Workshop, Vancouver, B. C.

Creaser, R. A., Heaman, L. M. and Erdmer, P. 1997. Timing of high-pressure metamorphism in the Yukon - Tanana terrane, Canadian Cordillera: constraints from U - Pb zircon dating of eclogite from the Teslin tectonic zone. Canadian Journal of Earth Sciences: **34**: 709-715.

de Keijzer, M. and Williams, P. F. 1996. Structural analysis in the Teslin Tectonic zone, south-central Yukon. LITHOPROBE Report No. 50, 1996 SNORCLE and Cordilleran Tectonics Workshop, Calgary, AB, 45-53.

de Keijzer, M and Williams, P .F. 1997a. A new view on the structural framework of the Teslin Zone, south-central Yukon. LITHOPROBE Report No. 56, 1997 SNORCLE and Cordilleran Tectonics Workshop, Calgary, AB., 96-102.

de Keijzer and Williams 1997b. Fabric development in the Cassiar terrane, Yukon Territory: A response to terrane accretion or subsequent extension? GAC-MAC Abstracts, 22: A36.

de Keijzer, M and Williams, P .F. 1998. Kilometre-scale folding in the Teslin zone, northern Canadian Cordillera, and its tectonic implications for the accretion of the Yukon-Tanana terrane to North America. In preparation.

Gallagher, C., Brown, R. L. and Carr, S. D. 1998 (this volume). Geometry of the Dycer Creek map area, Teslin zone, Yukon. LITHOPROBE REPORT. 1998 SNORCLE and Cordilleran Tectonics Workshop, Vancouver, B. C.

Harvey, J. L., Brown, R. L., and Carr, S. D. 1996. Progress in structural mapping in the Teslin Suture Zone, Big Salmon Range, Central Yukon Territory. LITHOPROBE report No. 50, 1996 SNORCLE and Cordilleran Tectonics Workshop, Calgary, AB, 33-41.

Harvey, J. L., Carr, S. D., Brown, R. L., and Gallagher, C. 1997a. Deformation history and geochronology of plutonic rocks near the D'Abbadie fault, Big Salmon Range, Yukon. LITHOPROBE report No. 56. 1997 SNORCLE and Cordilleran Tectonics Workshop, 103-114.

Harvey, J. L., Carr, S. D., and Brown, R. L. 1997b. Ages of deformed plutonic rocks along the D'Abbadie fault, Teslin zone, Big Salmon Range, Yukon: Implications for timing of strike-slip deformation. GAC-MAC Abstracts: **22**: A23.

Sample	UTM Coordinates	Rock type	Setting and Fabric Development	U-Pb zircon Geochronology Provides...
1. MK-96-26-2	**Cassiar Terrane** 549 850 m. E 6 840 850 m. N	D'Abbadie pluton; muscovite-bearing (1-2 %) granite	Cross-cutting undeformed pluton in transposed rocks of the CT, recording S_T and L_M	1) Minimum age of regionally pervasive deformation in the CT, (2) Microstructural evidence indicates that the d'Abbadie pluton is closely related (syn- to post-kinematic) to uplift of, and NE-SW extension in the CT
2. MK-96-29-8	**Cassiar Terrane** 546 700 m. E 6 840 150 m. N	Medium to fine-grained andesitic dyke with <2 % xenoliths of quartzitic material.	4 metre wide undeformed dyke (115/80); no chilled margin; cross-cuts both limbs of transposition fold (F_T), hinge near-parallel to L_M and S_T axial planar to F_T fold, in semi-pelitic and calc-silicate rocks and marble in the CT	Minimum age of regionally pervasive deformation (including transposition folding) in the CT (Rare slickenside surfaces in the dyke indicate minor deformation, probably during the later stages of NE-SW extension in the CT)
3. MK-96-31-7	**Cassiar Terrane** 548 350 m. E 6 840 000 m. N	Leucocratic biotite-muscovite orthogneiss with feldspar phenocrysts	3 metre wide concordant body (230/26) in the CT at the boundary of alternating pelitic schist and marble (above) and alternating semi-pelitic and siliceous schists (below); S_T and L_M in orthogneiss parallel to that in country rock	1) Constraints on the protolith age of the country rocks in the CT 2) Maximum age of pre-latest stage of formation of S_T and L_M in the CT 331.5 ± 2. 1 concordant fraction.
4. MK-97-kl-Gr-1	**Klippe** 550 100 m. E 6 828 600 m. N	Foliated and cataclastic chlorite muscovite bearing leucocratic granite	Deformed granite occcurs as Cm- to dm-lenses and layers in chlorite-rich intermediate schists that underly the serpentinite and metagabbro in the klippe; both the schist and leucocratic bodies have been affected by transposition folding (F_T hinges parallel to LM; 267/12) with formation of pervasive axial planar S_T cleavage	Maximum age of pre-latest stage of F_T transposition folding and formation of S_T and L_M in rocks of the Dunite klippen 2 concordant no overlap 267 ± 10
5. MK-97-32-4	**Western Teslin Zone** 530 625 m. E 6 830 850 m. N	Leucocratic biotite-muscovite-garnet (total <5 %) quartzofeldspathic schist (igneous zircons established)	M-scale 'monotonous' poorly layered quartzo-feldspathic schist in the western TZ, west of eclogite-bearing mafic schist. The country rocks and the igneous rock are invariably transposed (S_T in orthogneiss and country rock 077/78; L_M 152/36)	1) Constraints on the protolith age of meta-sedimentary country rocks (correlated with the CT by de Keijzer and Williams, in prep), 2) Maximum age of pre-latest stage of formation of S_T and L_M and F_T folds in the western Teslin zone

CT, Cassiar terrane ; S_T, regionally pervasive transposition foliation, formed syn- or post-accretion of, amongst others, the Anvil and Yukon-Tanana Nisutlin assemblages with the CT; L_M, mineral lineation

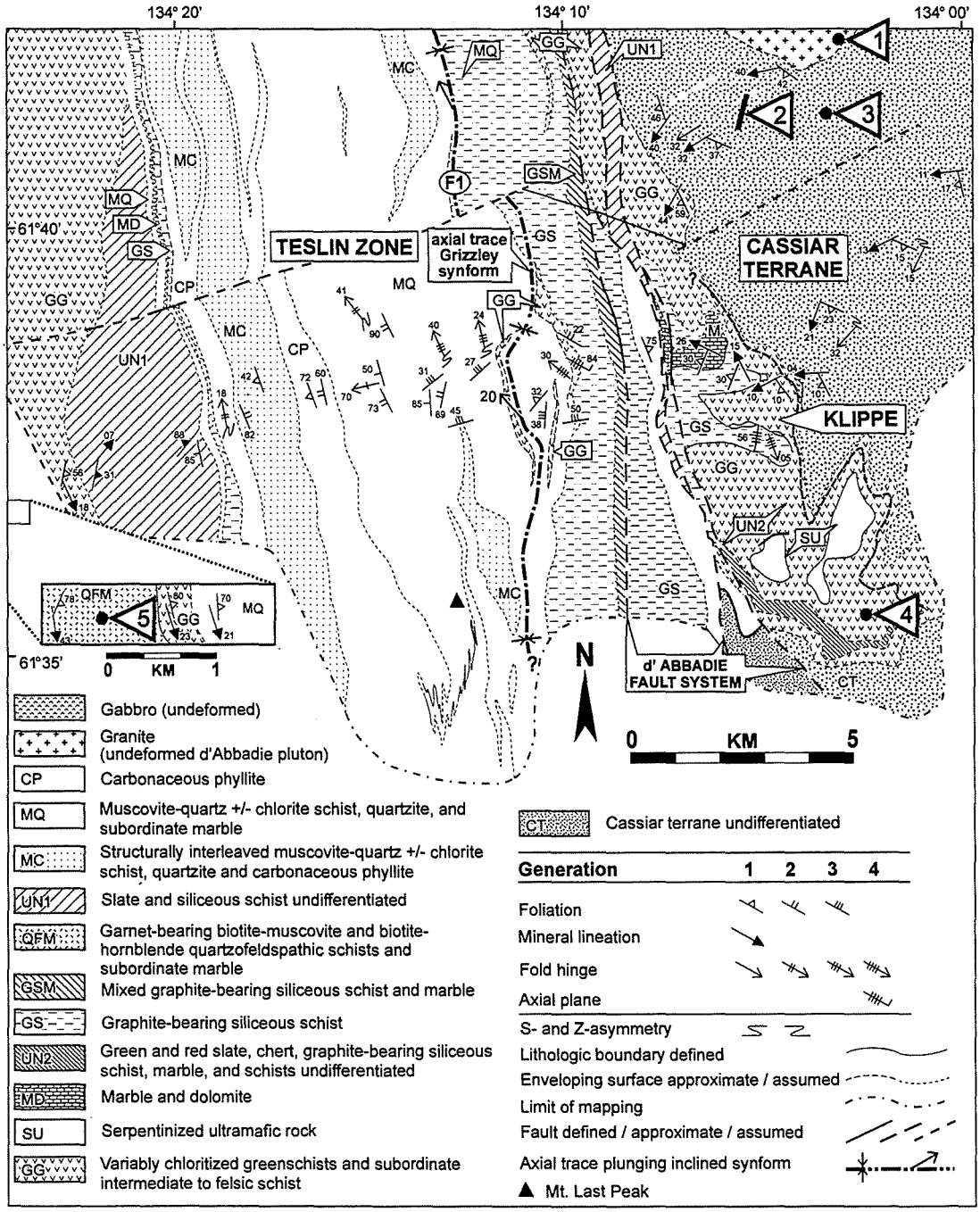

Figure 1. Geological map modified from de Keijzer and Williams (in prep) showing the distribution of rock types in the Teslin zone in the Last Peak area and in the Dunite klippen, and the locations of 5 samples (triangles 1 - 5) currently being processed for U-Pb zircon geochronoloy. See Table 1 for details about the samples.

VALHALLA: A CORDILLERAN METAMORPHIC CORE COMPLEX WITH ORIGIN, GEOMETRY AND EVOLUTION CONTROLLED BY PLUTONISM

S. D. CARR[1], P. S. SIMONY[2] and P. M. SCHAUBS[1&3]

[1]Ottawa-Carleton Geoscience Centre and Department of Earth Sciences, Carleton University, Ottawa, ON, Canada K1S 5B6; [2]Department of Geology and Geophysics, University of Calgary, Calgary, AB, Canada T2N 1N4; [3]School of Earth Sciences, University of Melbourne, Parkville 3052, Australia

The Valhalla complex occupies an area of 20 x 80 km in southern British Columbia, west of the Canadian Rocky Mountain thrust belt where allochthonous terranes overlap rocks of ancient North America and, with them, have undergone Mesozoic and Tertiary tectonism. The complex comprises Mesozoic and older paragneisses and orthogneisses that are disposed in gently arched sheets much injected by Paleocene-Eocene leucogranite, aplite and pegmatite of the Ladybird suite. They are metamorphosed to amphibolite facies. This constitutes a lower plate separated by the ductile Eocene extensional Valkyr shear zone (VSZ) from an upper plate characterized by Paleozoic, Triassic and Lower Jurassic assemblages at chlorite, biotite and garnet grade, injected by Jurassic, Cretaceous and Eocene plutons. Ladybird suite granitic rocks are absent from the upper plate.

The base of the upper plate, the trajectory of the Valkyr shear zone and the upper level to which sheets of Ladybird leucogranite were injected closely coincide everywhere with the base of interconnected, flat-bottomed Jurassic laccoliths. This indicates that; (1) tonalite laccoliths acted as a barrier to the rising leucogranite melt and, (2) the trajectory of the ductile extensional detachment (the Valkyr shear zone) was controlled by the rheological contrast between an upper plate stiffened by cool tonalite sheets and a lower plate rendered hot and ductile for about 4 Ma by the injection of 4500 km^3 of leucogranite and associated pegmatitic fluids under an area of 1600 km^2 (700m^3 km^{-2} a-1). At the northern and southern extremities of the complex, shear zone displacement is small enough for the original relationships to be preserved; the Valhalla "core" complex is primarily a leucogranitic intrusive complex and represents one end member type of the cordilleran core complexes.

Initial Results from the Ravens Throat Project – Geology of Mount Kraft and part of Dal Lake map areas, Mackenzie Mountains, Northwest Territories

Maurice Colpron
C.S. Lord Northern Geoscience Centre
Resources, Wildlife and Economic Development, Government of the Northwest Territories
P.O. Box 1320, Yellowknife, Northwest Territories X1A 2L9 (ColpronM@inac.gc.ca)

Abstract: *The Ravens Throat project area is underlain by strata of the Neoproterozoic Mackenzie Mountains and Windermere Supergroups, and by Lower Cambrian to Upper Devonian siliciclastic and carbonate rocks of the Mackenzie Platform. The basal Windermere strata were deposited during Neoproterozoic rifting, and numerous extension faults associated with this tectonic event cut older Neoproterozoic strata of the Mackenzie Mountains Supergroup. Mesozoic contractional deformation resulted in the development of broad folds and thrust faults, which were transected by younger right-lateral strike-slip faults. The development of both thrust faults and strike-slip faults was influenced by pre-existing, basin-bounding extension faults.*

INTRODUCTION

Regional (1:50,000-scale) mapping of the Ravens Throat area was initiated in 1997 as part of a three-year mapping project in the Mackenzie Mountains region of the western Northwest Territories. A primary objective of this project is to delineate the stratigraphy which hosts Cu and Zn-Pb concentrations. Numerous Cu and Zn-Pb showings are located within the map area, which lies to the immediate north of the Redstone Copper deposit at Coates Lake (37 million tonnes, averaging 3.9% Cu, 11.3 g/t Ag). Specific objectives for the 1997 field season included: 1) completing the detailed mapping of the Neoproterozoic stratigraphy in the Mount Kraft (95L/15) map area (initiated by C.W. Jefferson in 1976, 1977 and 1984) and extending this mapping into the Dal Lake (95M/2) map area to the north; 2) tracing the Paleozoic sequences; and 3) re-evaluating the nature of the faults in the area.

Regional geology

The Ravens Throat area lies within the Foreland belt of the northern Canadian Cordillera (Fig. 1). It is underlain by Neoproterozoic strata of the Mackenzie Mountains and Windermere Supergroups, and by Cambrian to Devonian strata of the lower to mid-Paleozoic Mackenzie platform (Table 1). The area lies along the west flank of the Redstone Arch (Fig. 1), a late Proterozoic - early Paleozoic culmination where terminal Neoproterozoic (Windermere) to Devonian strata overlie the Neoproterozoic Mackenzie Mountains Supergroup along a series of overstepping unconformities. The study area is located in the footwall of the Plateau Fault; a major east-verging thrust fault which extends some 350 km along strike to the northwest.

STRATIGRAPHY

Table 1 summarizes the lithostratigraphic units present in the Dal Lake and Mount Kraft map areas (Figs. 2 and 3, respectively). The lithostratigraphy of the area is best decribed in terms of three assemblages which reflect distinct tectonic/depositional settings. The oldest assemblage, the Mackenzie Mountains Supergroup (Sequence B of Young et al., 1979; 1.08-0.78 Ga), records stable platformal deposition, possibly in an intracratonic basin (Aitken and McMechan, 1991; Narbonne and Aitken, 1993; Rainbird et al., 1996). The overlying Windermere Supergroup (Sequence C of Young et al., 1979; 0.78-0.54 Ga) records the Neoproterozoic rifting of northwestern Laurentia and the subsequent development of a passive margin (Ross, 1991). The basal part of the Windermere Supergroup was deposited (in part) in restricted, fault-bounded basins developed upon a "basement" of Mackenzie Mountains Supergroup strata. The youngest assemblage comprises the Paleozoic rocks that define the Mackenzie Platform. Lower Cambrian to Devonian siliciclastic and carbonate rocks of the Mackenzie Platform overlie the Neoproterozoic sequences along a series of overstepping unconformities. Together, these lithostratigraphic assemblages comprise up to 28 distinct map units, a third of which were not identified during previous reconnaissance mapping of the area (Gabrielse et al., 1973).

It is not the purpose of this report to discuss each lithostratigraphic unit mapped in the Mount Kraft and Dal Lake areas. Instead, our discussion of the stratigraphy will focus on new contributions made by our mapping of the area. The reader is referred to Narbonne and Aitken (1993;

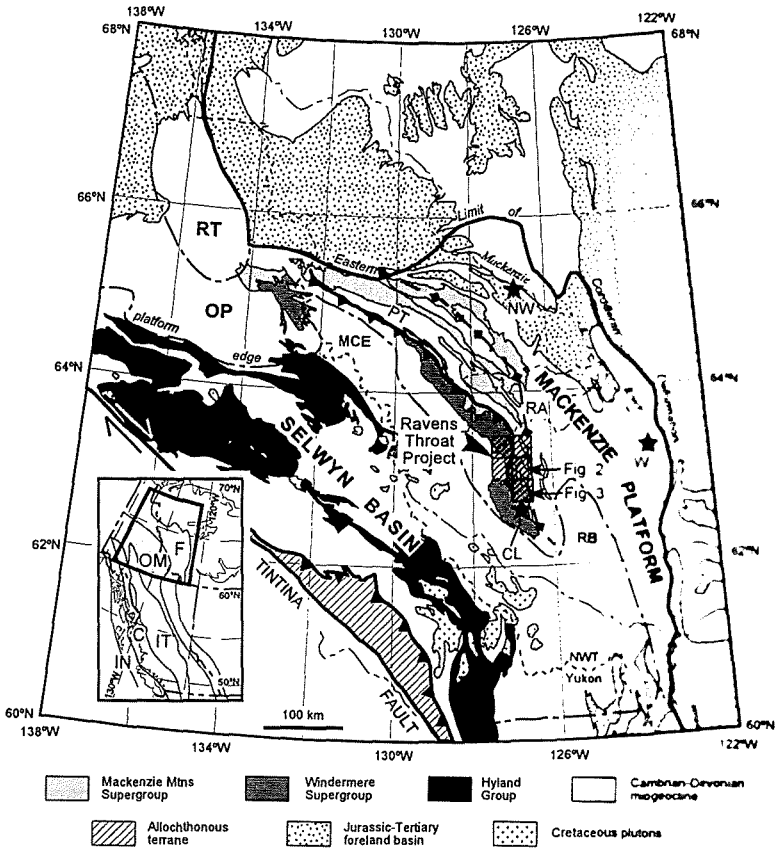

Figure 1. *Simplified geologic map of the northern Canadian Cordillera showing distribution of Neoproterozoic assemblages (after Wheeler and McFeely, 1991). The location of the Ravens Throat mapping project, in the Mackenzie Mountains, is indicated. This report present the results of regional mapping in the Dal Lake (95M/2; Fig. 2) and Mt. Kraft (95L/15; Fig. 3) map areas. Inset shows morphogeologic belts of the Canadian Cordillera: F = Foreland belt, OM = Omineca belt, IT = Intermontane belt, C = Coast belt, and IN = Insular belt. Stars indicate geographic locations: CL = Coates Lake, NW = Norman Wells, and W = Wrigley. Other abbreviations: RA = Redstone arch, PT = Plateau thrust, RT = Richardson through, OP = Ogilvie platform, MCE = Misty Creek embayment, and RB = Root basin.*

Table 1. Stratigraphic units present in the Mt. Kraft and Dal Lake map areas.

Era	Period	Super-group	GROUPS	FORMATIONS	*LITHOLOGIES*	*MAP UNIT*
Paleozoic	*Miss.*			Besa River (?)	*black shale, limestone, chert*	DMs
	Devonian			Nahanni	*fossiliferous limestone*	DN
				Headless	*very fossiliferous argillaceous limestone*	DH
				Landry	*limestone*	DL
				Amica	*thinly bedded dolostone*	DA
				Sombre	*dolostone*	DS
	Sil.			Delorme	*tan weathering dolostone*	SDD
	Ord.		*unconformity*	Whittaker	*dark grey, cherty dolostone*	OSW
	Cambrian		*unconformity*	Backbone Ranges	*sandstone*	€BR
Neoproterozoic		**Windermere**		Keele	*sandstone, minor dolostone*	PKe
				Twitya	*sandstone/shale*	PTw
			Rapitan	Shezal	*green diamictite*	PSh
				Sayunei	*maroon mudstone, rhythmites (dropstones)*	PSa
				Mt. Berg	*diamictite/conglomerate*	PMB
			Coates Lake	Coppercap	*limestone*	PCp
				Redstone River	*red mudstone/evaporites*	PRr
			unconformity	Thundercloud	*sandstone/mudstone*	PTh
		Mackenzie Mtns.	**Little Dal PLD**	Little Dal volc.	*basalt*	PLDv
				"upper" Upper carb. Rusty shale Gypsum	*dolostone, red weathering argillaceous limestone, evaporites*	PLDu
				"lower" Grainstone Platform Mudcracked	*oolitic limestone, packstone* PLDg; *micritic limestone, stromatolite bioherms* PLDp; *shale/sandstone*	PLDl
			Katherine PK	"upper" *(K7)*	*sandstone*	PKu
				"middle" *(K6)*	*black shale, brown weath. cherty dolostone*	PKm
				"lower" *(K1-K5)*	*sandstone*	PKl
				Tsezotene	*black shale, siltstone, sandstone (±dolostone)*	PTz

and references therein) for a concise summary of the Neoproterozoic stratigraphy of the Mackenzie Mountains (Mackenzie Mountains and Windermere Supergroups). The Paleozoic rocks of the Mackenzie Platform are described by Gabrielse et al. (1973), Fritz et al. (1991) and Morrow (1991).

Mackenzie Mountains Supergroup

The informally defined Mackenzie Mountains Supergroup comprises four main units: unit H_1, Tsezotene Formation, Katherine Group and Little Dal Group. Only the uppermost three units of the Mackenzie Mountains Supergroup are exposed in the Ravens Throat area (Table 1; Figs. 2-3).

Tsezotene Formation

The sequence of pyritic, dark grey and black shale, grey and green siltstone and sandstone, and minor orange weathering, cherty dolostone, that is exposed in stream sections in the south-central part of the Dal Lake area (Fig. 2), is herein assigned to the Tsezotene Formation of Gabrielse et al. (1973). These exposures of the Tsezotene Formation were previously unrecognized by Gabrielse et al. (1973) who mapped them as part of the Katherine Group (Tigonankweine Formation). The Tsezotene Formation is restricted to the hangingwall of the Mount Kraft thrust (new name; Fig. 2).

Katherine Group

Orthoquartzites of the Katherine Group (Aitken et al., 1978) gradationally overlie the Tsezotene Formation. Aitken et al. (1978) subdivided the Katherine Group (the Tigonankweine Formation of Gabrielse et al., 1973) into 3 units of formational rank which are readily mapped in the Dal Lake area (Fig. 2). The middle Katherine (unit K_6 of Aitken et al., 1978) is a particularly useful stratigraphic marker. It is composed of dark grey to black shales and orange to brown weathering cherty dolostone which stand in sharp contrast with the orthoquartzites of the Katherine Group.

Little Dal Group

Aitken (1981) subdivided the Little Dal Group into six informal units of formational rank (Table 1). Although all units are recognized in the Ravens Throat area, only a twofold subdivision of the Little Dal Group (following the criteria defined by Aitken, 1981; Table 1) can be mapped at a regional scale (Figs. 2 and 3).

Throughout much of the area, only the lower Little Dal Group is preserved beneath the sub-Rapitan or sub-Whittaker unconformities (Figs. 2 and 3). Strata of the upper Little Dal Group are only preserved in the west-central part of the Dal Lake map area (Fig. 2) and in the east-central part of the Mount Kraft map area (Fig. 3). In the Dal lake area, the base of the upper Little Dal Group is drawn at the base of the red weathering "Rusty Shale" formation. The underlying "Gypsum" formation (which defines the base of the upper Little Dal as defined by Aitkens, 1981; Table 1) is very recessive and only locally identified. The upper Little Dal is apparently bevelled beneath the sub-Rapitan unconformity in the southwest part of the Dal Lake area (Fig. 2).

Windermere Supergroup

The Windermere Supergroup of the Mackenzie Mountains, as defined by Narbonne and Aitken (1993), includes the Coates Lake Group (Jefferson, 1983; Jefferson and Ruelle, 1986), the glaciogenic Rapitan Group (Gabrielse et al., 1973; Eisbacher, 1978, 1981; Yeo, 1981) and six post-Rapitan formations (Narbonne and Aitken, 1993; see Table 1).

Coates Lake Group

The Coates Lake Group was originally included within the Mackenzie Mountains Supergroup (Young et al., 1979; Jefferson, 1983) because of the similarities in lithologies and environment of deposition (equatorial) between the two rock assemblages. However, Aitken (1981; 1991) proposed that the Coates Lake Group be considered as the basal part of the Windermere Supergroup because of its obvious relation to rift tectonism and the presence of a major unconformity at its base.

The Coates Lake Group includes three formations: the Thundercloud, Redstone River and Coppercap (Jefferson, 1983; Jefferson and Ruelle, 1986; Table 1). They record alluvial fan, sabkha and shallow platformal deposition in restricted basins in an extensional tectonic setting under arid to semi-arid conditions. Strata of the Coates Lake Group are only exposed in the east-central part of the Mount Kraft map area (Fig. 3) in the northern extension of the Coates Lake embayment (Jefferson and Ruelle, 1986).

Rapitan Group

Previous mapping of the Ravens Throat area by Gabrielse et al. (1973) only locally subdivided the Rapitan Group (which also included the shales and sandstones now attributed to the Twitya Formation). In the Mount Kraft area, the Rapitan Group locally includes a basal conglomerate/diamictite facies, in addition to the regionally extensive Sayunei and Shezal Formations (Table 1; Fig. 3). This conglomerate/diamictite unit is tentatively correlated with the Mount Berg Formation of Yeo (1981). Eisbacher (1981), Jefferson (1983), and Jefferson and Parrish (1989) have described carbonate orthoconglomerate and breccia deposited adjacent to paleo-fault scarps cutting the lower part of Little Dal Group (see Fig. 5 in Jefferson and Parrish, 1989, p. 1792). In most cases, the basal conglomerate unit overlies rocks of the Little Dal Group, with no intervening strata identified as Coates Lake Group (Jefferson, 1983; Jefferson and Parrish, 1989), and grades upward into the Sayunei Formation.

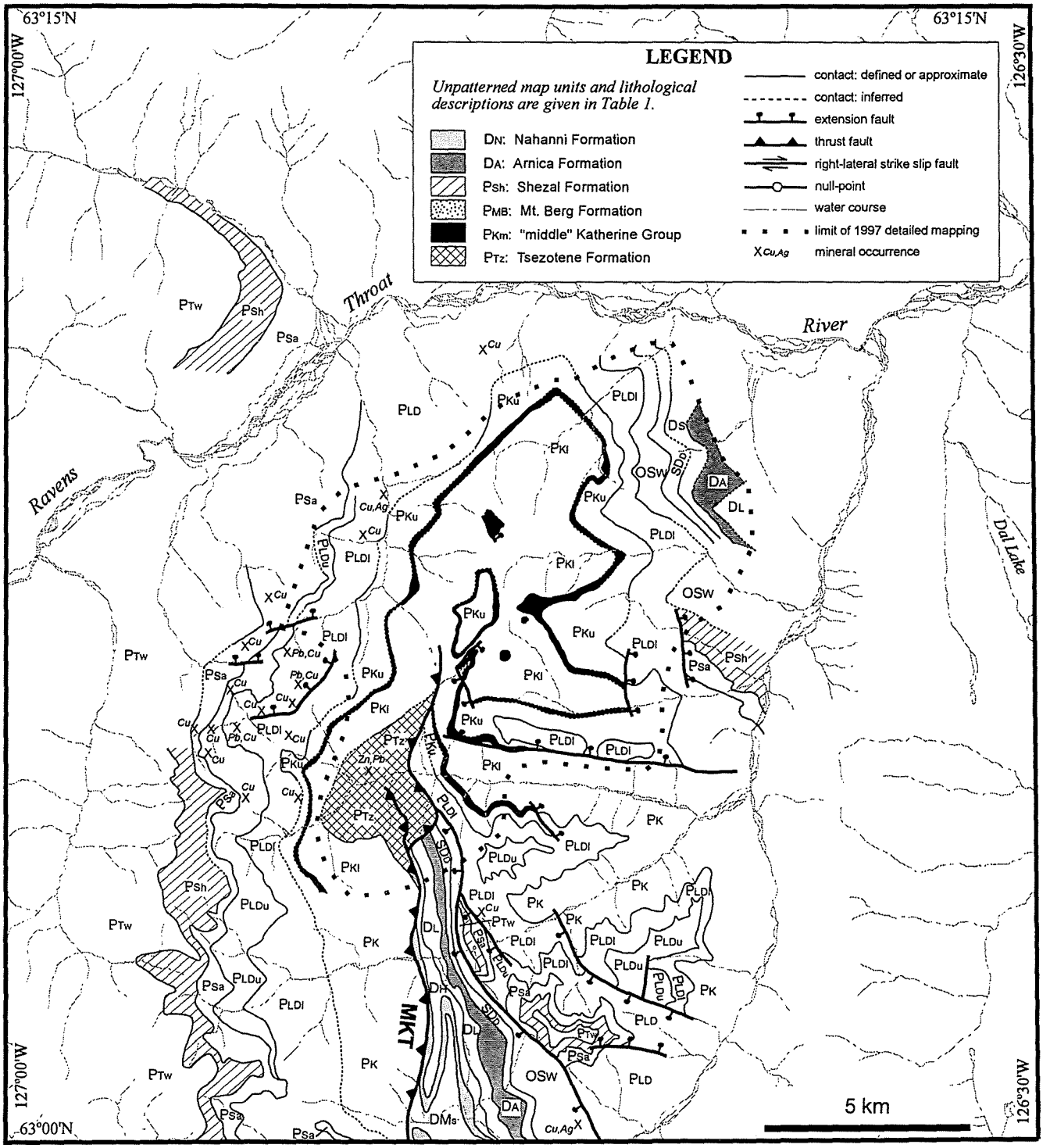

Figure 2. Preliminary geology of part of the Dal Lake (95M/2) map area. Compiled from mapping by M. Colpron and C. Augereau (1997), and Jory (1962) and Gabrielse et al. (1973). See Table 1 for description of all map units. Abbreviation: MKT = Mount Kraft thrust.

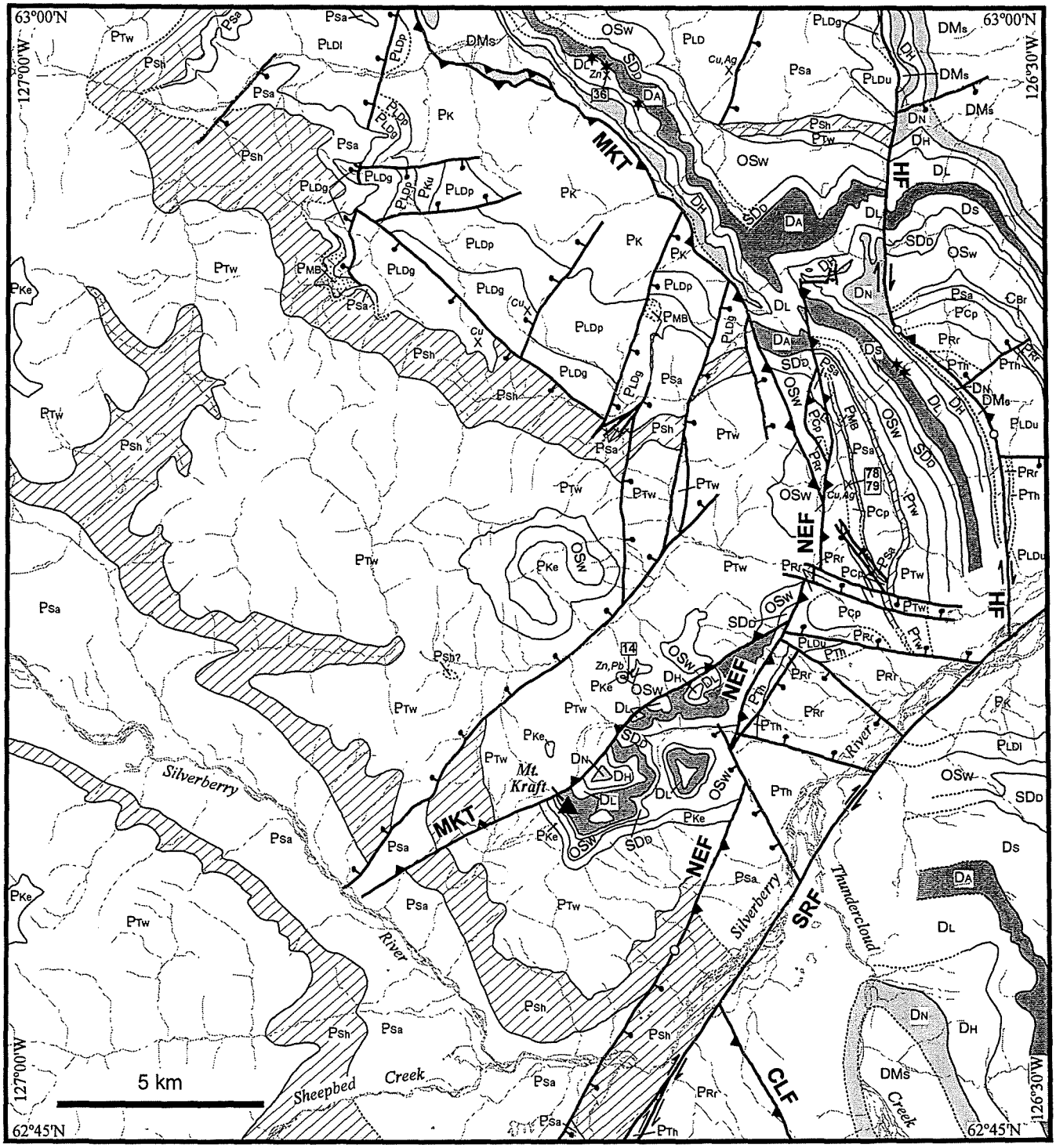

Figure 3. *Simplified geology of the Mount Kraft (95L/15) map area. Compiled from mapping by C.W. Jefferson (1976, 1977, 1984), M. Colpron and C. Augereau (1997), and Gabrielse et al. (1973) and Eisbacher (1981). Legend is given in Table 1 and Figure 2. Numbers in rectangles refer to assay samples. Stars (*) indicate occurrences of Manetoe dolomite facies at the base of the Landry Formation. Abbreviations: MKT = Mount Kraft thrust; NEF = North Extension fault; HF = Hayhook fault; SRF = South Redstone fault; CLF = Coates Lake fault.*

In the hangingwall of the North Extension fault (Fig. 3), the base of the Rapitan Group is marked by a 100 metres-thick section of sharpstone diamictite (also decribed by Eisbacher, 1981, p. 31). The first diamictite bed overlies highly weathered cherty dolostone of the Coppercap Formation with apparent disconformity. But, higher in the section, the diamictite is interbedded with black, cherty dolostone and pale green calcareous mudstone, similar to rocks of the underlying Coppercap Formation, and, therefore, at this locality the contact between the Coates Lake and Rapitan Groups appears to be conformable. This diamictite unit is gradationally overlain by red mudstone of the Sayunei Formation.

The Sayunei and Shezal Formations are predominantly mudstone (varves) and tillites of glacial origin. The abrupt transition from equatorial (Coates Lake Group) to glacial (Rapitan Group) environments is a conundrum. A detailed examination of the sedimentlogical and isotopic characters of the transition between Coppercap Formation and basal Rapitan units will provide additional information as to the nature of this transition.

Post-Rapitan formations

The Twitya and Keele Formations are the only two post-Rapitan, Windermere units exposed in the study area (Table 1; Figs. 2-3). The Twitya Formation consist of a coarsening-upward sequence of turbiditic shales and sandstones. At one locality, 4.2 km northwest of Mount Kraft, an outcrop of green diamictite similar to typical diamictite of the Shezal Formation occurs within the Twitya Formation (Fig. 3). This single occurrence of diamictite is interpreted as a mass flow deposit of recycled Shezal diamictite. Debris flow deposits of orange-weathering, stromatolitic dolostone are also present near the top of the Twitya Formation in the southwest corner of Mount Kraft map area (Fig. 3). These mass flow deposits are similar to breccias decribed in the Twitya Formation of the Wernecke Mountains (Gabrielse and Cambell, 1991).

The Keele Formation is exposed on high mountain peaks in the central part, and along the western edge of the Mount Kraft map area (Fig. 3). It consists predominantly of clean, cross-stratified orthoquartzite with only minor buff-weathering, oolitic dolostone at the base of the formation. The orthoquartzite commonly has a dolomitic cement, and locally contains ovoid-shaped, brown weathering dolomitic concretions. North of Mount Kraft, the Keele Formation locally contains a few thin (<1 m) horizons of coarse, graded arkosic grit and conglomerate which contain rounded pebbles of orthoquartzite. This suggests episodic deposition and erosion in a shallow marine to fluvial environment.

Paleozoic sequence of the Mackenzie Platform

Throughout much of the Mount Kraft and Dal Lake area, dolostones of the Upper Ordovician-Silurian Whittaker Formation overlie Neoproterozoic strata of the Mackenzie Mountains and Windermere Supergroups with angular unconformity. The Whittaker Formation marks the base of the conformable sequence of Upper Ordovician to Upper Devonian carbonate rocks that defines the Mackenzie platform (Table 1; Figs. 2-3). The basal Whittaker Formation typically is a dark grey weathering, fossiliferous dolostone with abundant chert nodules. It is a bioclastic dolostone in the northern part of the Dal Lake map area (Fig. 2), where it has a characteristic light and dark grey banding. In the central part of Mount Kraft map area (Fig. 3), the sub-Whittaker unconformity is marked by a gossaneous regolith.

A white orthoquartzite unconformably overlies the Coates Lake and Rapitan Groups along the east side of the Hayhook fault, in the Mount Kraft map area (Fig. 3). This orthoquartzite was interpreted by Eisbacher (1981, p. 11) as part of the Keele Formation, although he noted that its stratigraphic position is uncertain (*ibid.*, p. 31). We propose that this orthoquartzite be reassigned to the Lower Cambrian Backbone Ranges Formation, because its hematitic cement and its onlapping relationship above a Windermere-age fault are uncharacteristic of the Keele Formation in the area (Fig. 3). The orthoquartzite of the Backbone Ranges Formation is unconformably overlain by the Whittaker Formation.

STRUCTURAL RELATIONSHIPS

The structural style of the Ravens Throat area is the result of the interplay between Neoproterozoic – Early Paleozoic extension faulting and Mesozoic folding and thrust faulting. Neoproterozoic transtension faults developed during rift tectonism, accompanied by deposition of the Coates Lake and Rapitan Groups (Eisbacher, 1981; Park and Jefferson, 1991). The majority of extension faults in the study area cut older Neoproterozoic units of the Mackenzie Mountains Supergroup but are onlapped by the basal units of the Rapitan Group (Sayunei and Shezal Formations; Fig. 3). Fanglomerates assigned to the Mount Berg Formation were locally deposited adjacent to extension faults in the Mount Kraft area. A few extension faults offset the Twitya Formation and this may indicate that rifting continued during deposition of the Twitya Formation. Alternatively, these faults may have been reactivated during later Paleozoic and/or Mesozoic deformation.

The Mount Kraft Thrust is the most significant Mesozoic compressional structure in the study area (Figs. 2-3). The southern segment of this fault was previously interpreted by Eisbacher (1981, p. 11) as a southeast-dipping extension fault. Our mapping of the Mount Kraft area indicates that this fault is a shallow to moderately, westerly-dipping thrust fault, which juxtaposes Neoproterozoic rocks, in its hangingwall, over Paleozoic strata, in its footwall (Figs. 2 and 3). The Mount Kraft Thrust is arcuate and broadly follows the trend of Neoproterozoic extension faults preserved in its hangingwall, to the west (Fig. 3). It dies out to the north in

the core of a broad anticline which exposes strata of the Tsezotene Formation and Katherine Group (Fig. 2). To the south, the Mount Kraft Thrust and an extension fault preserved in its hangingwall both terminate abruptly in the Silverberry Valley (Fig. 3). This may indicate that the Plateau Thrust extends along Silverberry River from the west, where it was mapped by Gabrielse et al. (1973).

The Mount Kraft Thrust is truncated by the North Extension Fault in the east-central part of Mount Kraft map area (Fig. 3). The North Extension Fault is a moderately east-dipping, west-verging thrust fault which marks the western limit of exposure of the Coates Lake Group in the area. It is interpreted to follow the trace of an older southeast-dipping extension fault which delimited the western margin of the north extension of the Coates Lake Embayment (Jefferson, 1983).

Gabrielse et al. (1973) speculated that about 15 km of right-lateral transcurrent displacement occurred along the Hayhook Fault. Our examination of the fault in the eastern part of Mount Kraft map area (Fig. 3) supports the notion of strike-slip displacement along Hayhook Fault. The fault is steeply dipping and, in the northeast part of Mount Kraft map area, it juxtaposes a south-dipping sequence of Paleozoic rocks, on the west, and a north-dipping panel comprising the same stratigraphic interval, on the east (Fig. 3). Paleozoic rocks along the fault are locally silicified and commonly have a cataclastic structure. The fold pattern west of Hayhook Fault shows a complex interplay between folding associated with thrusting (along Mount Kraft and North Extension faults) and strike-slip displacement along Hayhook Fault. In the north-central part of Mount Kraft area (Fig. 3), Paleozoic strata are exposed along the lower limb of a northeast-verging syncline which developed in the footwall of the Mount Kraft Thrust. The axis of this syncline and a congruent anticline-syncline pair are rotated counterclockwise by as much as 90° near the northern termination of the North Extension Fault. In the immediate vicinity of Hayhook Fault, the folds are tight, upright and congruent with the trend of the fault. This pattern of folding suggests that transcurrent displacement along Hayhook Fault occurred, at least in part, during the Mesozoic. Another possible implication is that this fold pattern reflects the presence of a lateral ramp (possibly localized along an older extension fault) along the west side of Hayhook Fault. Distinct facies in the Neoproterozoic rocks on either side of Hayhook Fault suggest that it follows the locus of an older extension fault (Eisbacher, 1981).

The South Redstone Fault is another structure which is interpreted to follow an older basement discontinuity (Aitken and Pugh, 1984; Cecile et al., 1997). On a regional scale the South Redstone Fault shows as much as 10-12 km of right-lateral strike-slip displacement (Jefferson, 1983). The South Redstone Fault truncates Mesozoic thrust structures (e.g. Coates Lake Fault; Fig. 3) and, therefore, part of its displacement postdates the development of compressional structures in the area.

Our preliminary assessment of the Ravens Throat project area suggests the following sequence for the evolution of structures:

1- Development of transtension faults during Neoproterozoic rifting (some of these faults may have been reactivated during later Paleozoic and/or Mesozoic deformation).
2- Folding and east-verging thrust faulting (Mount Kraft Thrust).
3- West-verging thrust faulting along North Extension Fault.
4- Out-of-sequence thrust faulting along the east-verging Plateau Thrust (?; Gabrielse et al., 1973)
5- Right-lateral strike-slip faulting along Hayhook and South Redstone faults.

Absolute timing of the compressional structures cannot be determined directly in the study area. Folding and thrust faulting in the Selwyn Fold Belt, to the southwest, postdates deposition of Middle Jurassic rocks, but predates emplacement of Late Cretaceous (80-104 Ma) granitoid plutons (Gordey and Anderson, 1993). At the Mackenzie Mountain front, to the northeast, strata as young as Tertiary are deformed (Aitken and Cook, 1974). Therefore, structures in the Ravens Throat project area are broadly of Late Cretaceous - Tertiary age.

ACKNOWLEDGMENTS

Carole Augereau provided cheerful assistance during the soggy–foggy 1997 field season. Thanks to Charlie Jefferson for the wealth of data he has contibuted to this project and the stimulating discussions. Andrea Mills assisted with the preparation of the figures.

REFERENCES

Aitken, J. D., 1981: Stratigraphy and sedimentology of the Upper Proterozoic Little Dal Group, Mackenzie Mountains, Northwest Territories; *in* Campbell, F. H. A. (ed.), Proterozoic basins of Canada; Geological Survey of Canada, Paper 81-10, p. 47-71.

Aitken, J. D., 1991: The Ice Brook Formation and post-Rapitan, Late Proterozoic glaciation, Mackenzie Mountains, Northwest Territories; Geological Survey of Canada, Bulletin 404, 43 pages.

Aitken, J. D. and Cook, D. G., 1974: Carcajou Canyon map area (96D), District of Mackenzie; Geological Survey of Canada, Paper 74-13, 28 pages.

Aitken, J. D. and McMechan, M. E., 1991: Middle Proterozoic assemblages (Chapter 5); *in* Gabrielse, H. and Yorath, C. J. (ed.), Geology of the Cordilleran Orogen in Canada; Geological Survey of Canada, Geology of Canada, no. 4, p. 97-124.

Aitken, J. D. and Pugh, D. C., 1984: The Fort Norman and Leith Ridge structures: major, buried, Precambrian features underlying Franklin Mountains and Great Bear and Mackenzie plains; Bulletin of Canadian Petroleum Geology, v. 32, p. 139-146.

Aitken, J. D., Long, D. G. F. and Semikhatov, M. A., 1978: Progress in Helikian stratigraphy, Mackenzie Mountains; *in* Current Research, Part A; Geological Survey of Canada, Paper 78-1A, p. 481-484.

Cecile, M. P., Morrow, D. W. and Williams, G. K., 1997: Early Paleozoic (Cambrian to Early Devonian) tectonic framework, Canadian

Cordillera; Bulletin of Canadian Petroleum Geology, v. 45, p. 54-74.

Eisbacher, G. H., 1978: Re-definition and subdivision of the Rapitan Group, Mackenzie Mountains; Geological Survey of Canada, Paper 77-35, 21 pages.

Eisbacher, G. H., 1981: Sedimentary tectonics and glacial record in the Windermere Supergroup, Mackenzie Mountains, northwestern Canada; Geological Survey of Canada, Paper 80-27, 40 pages.

Fritz, W. H., Cecile, M. P., Norford, B. S., Morrow, D. and Geldsetzer, H. H. J., 1991: Cambrian to Middle Devonian assemblages, Chapter 7; *in* Gabrielse, H. and Yorath, C. J. (ed.), Geology of the Cordilleran Orogen in Canada; Geological Survey of Canada, Geology of Canada, no. 4, p. 151-218.

Gabrielse, H. and Campbell, R. B., 1991: Upper Proterozoic Assemblages, Chapter 6; *in* Gabrielse, H. and Yorath, C. J. (ed.), Geology of the Cordilleran Orogen in Canada; Geological Survey of Canada, Geology of Canada, no.4, p. 125-150.

Gabrielse, H., Blusson, S. L. and Roddick, J. A., 1973: Geology of Flat River, Glacier Lake and Wrigley Lake map-areas, District of Mackenzie and Yukon Territory; Geological Survey of Canada, Memoir 366 (Part I and II), 421 pages.

Gordey, S. P. and Anderson, R. G., 1993: Evolution of the northern Cordilleran miogeocline, Nahanni map area (105I), Yukon and Northwest Territories; Geological Survey of Canada, Memoir 428, 214 pages.

Jefferson, C. W., 1983: The Upper Proterozoic Redstone Copper Belt, Mackenzie Mountains, N.W.T.; Ph.D. thesis, University of Western Ontario, 445 pages.

Jefferson, C. W. and Parrish, R. R., 1989: Late Proterozoic stratigraphy, U-Pb zircon ages, and rift tectonics, Mackenzie Mountains, northwestern Canada; Canadian Journal of Earth Sciences, v. 26, p. 1784-1801.

Jefferson, C. W. and Ruelle, J. C. L., 1986: Late Proterozoic Redstone Copper Belt, Mackenzie Mountains, N.W.T.; *in* Morin, J. A. (ed.), Mineral deposits of the northern Cordillera; Canadian Institute of Mining and Metallurgy, Special Volume 37, p. 154-168.

Jory, L. T., 1962: Geological mapping and trenching, North Redstone claim group, Dal Lake, N.W.T.; Department of Indian Affairs and Northern Development, Assessment Report 017596.

Morrow, D. W., 1991: The Silurian-Devonian sequence in the northern part of the Mackenzie shelf, Northwest Territories; Geological Survey of Canada, Bulletin 413, 121 pages.

Narbonne, G. M. and Aitken, J. D., 1993: Neoproterozoic of the Mackenzie Mountains, northwestern Canada; Precambrian Research, v. 73, p. 101-121.

Park, J. K. and Jefferson, C. W., 1991: Magnetic and tectonic history of the Late Proterozoic upper Little Dal and Coates Lake Groups of northwestern Canada; Precambrian Research, v. 52, p. 1-35.

Rainbird, R. H., Jefferson, C. W. and Young, G. M., 1996: The early Neoproterozoic sedimentary Succession B of northwestern Laurentia: Correlations and paleogeographic significance; Geological Society of America Bulletin, v. 108, p. 454-470.

Ross, G. M., 1991: Tectonic setting of the Windermere Supergroup revisited; Geology, v. 19, p. 1125-1128.

Wheeler, J. O. and McFeely, P., 1991: Tectonic assemblage map of the Canadian Cordillera and adjacent parts of the United States of America; Geological Survey of Canada, Map 1712A.

Yeo, G. M., 1981: The Late Proterozoic Rapitan glaciation in the northern Cordillera; *in* Campbell, F. H. A. (ed.), Proterozoic basins of Canada; Geological Survey of Canada, Paper 81-10, p. 25-46.

Young, G. M., Jefferson, C. W., Delaney, G. D. and Yeo, G. M., 1979: Middle and late Proterozoic evolution of the northern Canadian Cordillera and Shield; Geology, v. 7, p. 125-128.

VOLCANOLOGY AND GEOCHEMICAL SIGNATURE OF CORRELATIVE VOLCANIC SEQUENCES IN THE ARCHEAN SLAVE PROVINCE: A POSSIBLE MAGMATIC ARC SYSTEM

CORCORAN, P.L., Department of Earth Sciences, Dalhousie University, Nova Scotia, Canada B3H 3J5, corcoran@is2.dal.ca; DOSTAL, J., Geology Department, Saint Mary's University, Nova Scotia, Canada B3H 3C3

North-trending volcanic belts adjacent to the Beniah Lake Fault are similar in composition and volcanic facies and may represent one coherent arc sequence. Three study areas include the 2.69 Ga Peltier Formation (lat. 65° 12'-65°21'/long. 112°53'-113°10') and the northern (lat. 63°17'-63°27'/long. 112° 05'-112° 30') and southern (lat. 63°00'-63°05'/long. 112°23'-112°26') segments of the Beaulieu River volcanic belt. The mafic-dominated Peltier Formation contains massive and pillowed flows, pillow breccia, and mafic sills and dykes that locally intrude the 3.15 Ga basement of the Augustus Granite. Massive and pillowed flow units are 2-100 m thick and 2-220 m thick, respectively, and pillow breccia ranges from 10-40 m thick. Flows are intruded by 20-45 m thick mafic sills and 2-15 m thick mafic dykes. Dykes are characterized by multiple intrusions that exhibit mm-thick chilled margins. Local 10 m thick massive felsic/intermediate units appear to overlie basalts. The mafic to felsic northern segment of the Beaulieu River volcanic belt unconformably overlies older quartz arenites and a tonalitic basement. Massive flow units are 12-100 m thick and pillowed units range from 1-60 m thick. Dykes of unknown age commonly intrude the sequence which also contains 4-30 m thick felsic flow units and 10-200 cm thick tuffaceous layers. The southern segment of the Beaulieu River volcanic belt, unconformably overlying the Sleepy Dragon Complex, is composed of mafic massive and pillowed flows and pillow breccia and is associated with local felsic units. Massive flow units, 2-20 m thick, underlie 5-50 m thick pillowed units and 20 m thick pillow breccia. Mafic centres with abundant sills and dykes associated with local subaqueous felsic/ intermediate edifices are indirect indicators of extension, commonly found in arc-backarc settings. These successions may be interpreted as a laterally extensive magmatic arc system which unconformably overlie older granitic crust that has been intruded by numerous syn-volcanic plutons.

Geochemical results from the Peltier Formation indicate that the volcanic rocks are predominantly tholeiitic basalts which can be subdivided into two distinct groups. Group 1 volcanic rocks display flat REE patterns with $(La/Yb)_n \sim 1$ and positive ε_{Nd} values. In contrast, Group 2 volcanic rocks have slightly enriched REE patterns with $(La/Yb)_n \sim 2$, negative ε_{Nd} values, higher Zr/Y and Ti/V ratios and an elevated abundance of incompatible trace elements. Group 2 rocks are more Nb depleted and regional mapping shows that they are stratigraphically lower than those of Group 1. The correlation of Mg# with ε_{Nd} values suggests that crustal contamination in conjunction with fractional crystallization affected the evolution of the tholeiitic rocks. Initially the tholeiitic basalts were affected by crustal contamination but, with time, crustal influence was diminished. Additionally, the Peltier Formation contains subordinate calc-alkaline basalts and andesites which are distinctly enriched in incompatible trace elements and display positive ε_{Nd} values. REE patterns are fractionated with $(La/Yb)_n \sim 22\text{-}26$ and $(La/Yb)_n \sim 3.5\text{-}5$ whereas the mantle normalized patterns are depleted with respect to Nb and Ti. The study suggests that the rocks of the Peltier Formation probably formed on continental crust in a

magmatic arc environment. Preliminary geochemical results from the northern Beaulieu River volcanic belt demonstrate similar trends to Group 1 tholeiitic basalts. The evidence is suggestive of the development and unroofing of a N-S aligned magmatic arc.

LITHOLOGICAL, GEOCHEMICAL AND ISOTOPIC CHARACTERIZATION OF CLASTIC UNITS IN THE KLINKIT AND SWIFT RIVER ASSEMBLAGES, NORTHERN BRITISH COLUMBIA

Robert A. Creaser, Dept. of Earth & Atmospheric Sciences, Univ. Alberta, Edmonton, Alberta T6G 2E3
Tekla A. Harms, Dept. of Geology, Amherst College, Amherst, MA 01002

INTRODUCTION

The Klinkit and Swift River assemblages are distinctive Late Paleozoic sequences of deformed clastic and biogenic sedimentary strata and extrusive mafic igneous rocks that occur in a NW-trending belt between North American miogeoclinal strata of the Cassiar terrane to the east and arc-related Mesozoic rocks of Quesnellia to the west (Harms et al, 1997). Areas of both the Klinkit and Swift River assemblages have previously been assigned to the Slide Mountain and Dorsey terranes (Wheeler and McFeely, 1991) but are unlike the Slide Mountain terrane as it is characterized in the Sylvester allochthon immediately to the east (Harms, 1986; Nelson, 1993) and do not correspond to two other assemblages within the Dorsey terrane as defined in the Dorsey Range (Stevens, 1996; Harms and Stevens, 1996a). The Klinkit assemblage characteristically consists of: (i) thick, massive, clean quartz sandstone, commonly black or purply-grey, or interbedded quartz sandstone, shale, chert, and minor conglomerate that may or may not be a facies equivalent of the quartz sandstone. The latter has yielded Triassic conodonts (M. Orchard, personal communication); (ii) an equally thick or thicker heterogeneous volcanic unit that includes both fine and very coarse volcaniclastic accumulations and mafic flows, and (iii) one or more Pennsylvanian (Gabrielse, 1970; Abbott, 1981; M. Orchard, GSC report no. MJO-1997-7) carbonate horizons. The Swift River assemblage occurs everywhere immediately adjacent to the Klinkit assemblage - but appears to be structurally juxtaposed with, and possibly thrust beneath, the Klinkit assemblage. The Swift River assemblage is a monotonous sequence of folded, interbedded phyllite, slate, greywacke and chert, with minor carbonate and tuff horizons. The lithologies of the Klinkit and Swift River assemblages suggest mafic volcanism in a marine setting with continental influence. This is similar to the nature of late Paleozoic rocks that form the basement to Quesnellia in southern British Columbia (Harms et al, 1997; Harms and Stevens, 1996b, and references therein). Geochemical and isotopic analyses have been conducted on clastic sedimentary rocks from the Klinkit and Swift River assemblages to better characterize these tectonostratigraphic entities.

KLINKIT ASSEMBLAGE

Few locales within the Klinkit assemblage have yielded datable fossils, and the assemblage is deformed by folding, probably including map-scale overturned limbs and layer-parallel faults. As a consequence, a consistent, uniform, detailed stratigraphy of the assemblage has been elusive. Clastic rocks occur as interlayered sequences of variable proportions of sandstone, shale, carbonate, chert and pebble

conglomerate, in total thicknesses ranging from < 100 m to > 500 m. Clastic sequences are bounded above or below by massive mafic volcanic rocks and appear to represent related facies at equivalent structural horizons on that basis. All share very pure quartz sandstone, with well-rounded, glassy sand grains as a common component.

Three such clastic sequences were sampled and analyzed in this program:
SAMPLES 52a-z: This sequence consists of interlayered black slate, rusty-weathering black argillite, grey siliceous siltstone and fine sandstone, recrystallized black carbonate, and rare 5-10 m thick beds of pebble to cobble conglomerate in which the clasts are uniformly well rounded, resistant, siliceous sedimentary and metasedimentary rock types. The unit is dominated by slate and argillite by volume. Triassic conodonts (M. Orchard, GSC report no. MJO-1997-7) were recovered from carbonates within this sequence. Nd isotopic data for most of these samples show T_{DM} model ages of ~2.2Ga, with εNd_T values of ~ -9 to -11.
SAMPLES 69a-z: This sequence includes black argillite, black porcellanite, bedded black to grey chert, siltstone, and both white and black quartz sandstone with glassy grains. Sandstone forms a greater percentage, although still less than finer sediments, in this sequence than the previous one. No datable fossils have been recovered from this sequence. The T_{DM} model ages are ~1.8-2.0Ga, with εNd_T values of ~ -9 to -11, broadly similar to *52a-z*. This similarity is also shared by key trace element ratios such as Th/Sc (mostly ~ 0.4).
SAMPLE 70c: This sequence is almost entirely massive quartz sandstone with negligible interbedded olive grey siliceous argillite. Both white, framework-supported, pure quartz sandstone with quartz cement, and black, siltstone-matrix-supported quartz sandstone occur. Carbonate cemented quartz sandstone is present but rare. Two 10-20 m thick, thin-bedded carbonate horizons are interlayered within the sequence, but have yielded no datable material. The Nd isotopic data show a T_{DM} model age of 2.6Ga, and the Th/Sc ratio is high (1.65), quite different to *52a-z* and *69a-z*.

SWIFT RIVER ASSEMBLAGE

The Swift River assemblage is a dominantly clastic or clastic and chert unit (minor tuff horizons occur in some places, and one carbonate horizon has been observed). The unit includes greywacke, phyllite, slate and chert; in some areas the assemblage is predominately finer grained and dominated by phyllite - in other places the assemblage is dominated by greywacke. Regardless of lithology, the Swift River assemblage is typified by a pervasive phyllitic grade of fabric development and recrystallization, accompanied by a spaced cleavage that is axial planar to ubiquitous outcrop-scale, open to close, concentric folds.
Samples 62-67: Geochemical samples were collected from a greywacke-dominated area of the Swift River assemblage that had previously been mapped as "unit 18" by Gabrielse (1970). On the basis of lithologic similarity, Gabrielse (1970) tentatively correlated his unit 18 to the Jurassic Inklin Formation, a unit that occurs within Mesozoic arc terranes to the west of the Klinkit assemblage. The Nd isotopic data, however, show T_{DM} model ages of ~2.6-2.7Ga, and the rocks have high Th/Sc (1.5-1.6).

CONCLUSIONS

The similarity of geochemical and isotopic characteristics between Samples *52a-z* and *69a-z* is consistent with field evidence that indicates a facies relationship between the two clastic sequences from which the sample sets were obtained. On the basis of conodonts recovered from one of these sequences, both may be considered Triassic. Preliminary interpretations suggest that the Klinkit assemblage may have been in close proximity to the North American continent at that time, as there are some similarities with Nd isotopic character of Triassic clastic strata of the miogeocline (e.g., Boghossian et al., 1996).

On the other hand, Sample 70z is very different from these Triassic Klinkit clastics. Lithologically, it has a much higher proportion of quartz sandstone than the other two sequences. It may represent a very different stratigraphic horizon within the Klinkit assemblage rather than a facies difference, or may be a here-to-fore unrecognized occurrence of Swift River assemblage rocks, to which is has isotopic and geochemical similarity.

The isotopic character of the Swift River assemblage makes correlation with the arc-related Inklin formation unlikely, and consequently leaves the age of the assemblage again unconstrained. The Swift River assemblage is also geochemically and isotopically distinct from Klinkit assemblage clastics. Because it is undated, it cannot be known whether the Swift River is genetically linked to the Klinkit but the geochemical difference results from displacement or change in provenance for the two over time, or if the two are genetically unrelated and came together after clastic deposition. The general Nd isotopic and geochemical characteristics of the Swift River material are very similar both to pre-Ordovician miogeoclinal clastic strata and some lithologies of the Nisutlin assemblage of the Yukon-Tanana terrane (Creaser et al., 1997).

REFERENCES

Abbott, J.G., 1981, Geology of the Seagull tin district: in Yukon Geology and Exploration 1979 1980, Indian and Northern Affairs Canada, p. 32-44.

Boghossian, N.D., et al., 1996, Nd isotopes and the source of sediments in the miogeocline of the Canadian Cordillera. Journal of Geology, v. 104, p. 259-277.

Creaser, R.A., et al., 1997, Tectonic affinity of Nisutlin and Anvil assemblage strata from the Teslin tectonic zone, northern Canadian Cordillera: Constraints from neodymium isotope and geochemical evidence. Tectonics, v. 16, 107-121.

Gabrielse, H., 1970, Geology of Jennings River map-area, British Columbia (104-O); Geological Survey of Canada, Paper 68-55.

Harms, T.A., 1986, Structural and tectonic analysis of the Sylvester Allochthon, northern British Columbia: Implications for paleogeography and accretion: Unpublished PhD dissertation, University of Arizona, Tucson, AZ, 81 pp.

Harms, T.A., and Stevens, R.A., 1996a, Assemblage analysis of the Dorsey Terrane, in, Cook, F. and Erdmer, P. (compilers), Slave-Northern Cordillera Lithospheric Evolution (SNORCLE) Transect and Cordilleran Tectonics Workshop Meeting, Lithoprobe Report No. 50, p. 199-201.

Harms, T.A. and Stevens, R.A., 1996b, A Working hypothesis for the tectonostratigraphic affinity of the Stikine Ranges and a portion of the Dorsey terrane, in, Cook, F. and Erdmer, P. (compilers), Slave-Northern Cordillera Lithospheric Evolution (SNORCLE) Transect and Cordilleran Tectonics Workshop Meeting, Lithoprobe Report No. 50, p. 93-95.

Harms, T.A., Stevens, R.A., and Creaser, R.A., 1997, Assemblage analysis and tectonostratigraphic affinity of Dorsey terrane and adjacent areas - northeastern BC and southern Yukon; Geological Association of Canada-Mineralogical Association of Canada Annual Meeting Abstracts, v. 22, p. A 64.

Nelson, J.L., 1993, The Sylvester Allochthon: upper Paleozoic marginal-basin and island-arc terranes in northern British Columbia: Canadian Journal of Earth Sciences, v. 30, p. 631-643.

Stevens, R.A., 1996, Dorsey assemblage: Pre-mid-Permian high temperature and pressure metamorphic rocks in the Dorsey Range, southern Yukon, in, Cook, F. and Erdmer, P. (compilers), Slave-Northern Cordillera Lithospheric Evolution (SNORCLE) Transect and Cordilleran Tectonics Workshop Meeting, Lithoprobe Report No. 50, p. 70-75.

Wheeler, J.O., and McFeeley, P., 1991, Tectonic assemblage map of the Canadian Cordillera and adjacent parts of the United States of America: Geological Survey of Canada Map 1712A, scale 1:2 000 000.

U-PB GEOCHRONOLOGIC EVIDENCE FOR LATE JURASSIC AND LATE CRETACEOUS THERMAL EVENTS IN THE NORTHERN MONASHEE AND SELKIRK MOUNTAINS, MICA CREEK AREA, B.C.

Crowley, J.L.[1], Ghent, E.D.[1], Carr, S.D.[2], Simony, P.S.[1]

[1]Department of Geology and Geophysics, University of Calgary, Calgary, AB T2N 1N4;

[2]Ottawa-Carleton Geoscience Centre and Department of Earth Sciences, Carleton University, Ottawa, ON K1S 5B6

The Mica Creek area is an ideal place to compare the geologic histories of the northern Monashee and Selkirk mountains because it straddles the only part of their boundary that does not coincide with a major fault. The only known displacement on the boundary in the Mica Creek area occurred on a minor brittle normal fault, and thus it has been possible to correlate structures, stratigraphic units, and isograds between the Selkirk and Monashee mountains. Monazite, zircon, and xenotime U-Pb isotopic data collected from pelitic schist, pegmatite, and leucosome indicate that rocks in both mountain ranges were affected by Late Jurassic and Late Cretaceous thermal events.

The lowest grade rocks in the Mica Creek area lie in a synformal metamorphic low in the Monashee Mountains. Pelitic schist typically contains garnet and there are local occurrences of staurolite and kyanite. Single-grain monazite and xenotime U-Pb analyses from two schists from the centre of the metamorphic low form a discordant linear array between ~160 and ~70 Ma. The analyses lie closer to the upper intercept of the discordia than the lower intercept, with five of the eight analyses being less than 15% discordant. We interpret most of the discordance as being a result of diffusional Pb loss at ~70 Ma rather than mineral overgrowth because (i) larger grains typically plot closer to the upper intercept than smaller grains and (ii) Th zoning patterns in polished grains that were imaged with backscattered electrons (BSE) suggest a single phase of monazite growth. Electron microprobe analysis indicates that there was a single phase of garnet growth and peak temperatures were not high enough to modify the garnet growth zoning (in Fe, Mg, Ca, and Mn) profiles. Given that there was a single phase of garnet and monazite growth and petrographic observations suggest a simple metamorphic growth history, we propose that monazite growth at ~160 Ma was coeval with garnet growth during the metamorphic peak. Single monazite grains from a strongly deformed pegmatite layer in the metamorphic low were also dated. One analysis is concordant at 70 Ma and two other analyses lie on the ~160-70 Ma discordia. The 70 Ma monazite is thought to be a metamorphic grain because its U concentration (2000-3000 ppm) is characteristic of metamorphic monazite grains in the region and much lower than those of igneous grains from pegmatites. A schist collected from higher grade rocks on the flank of the metamorphic low contains a monazite analysis that is concordant at ~160 Ma and two other analyses that are concordant at ~90 Ma. The thermal significance of the ~90 Ma grains is uncertain. Deformation on the flank of the metamorphic low ceased prior to the intrusion of a cross-cutting pegmatite at 70 Ma, an age based on monazite that is interpreted as igneous based on its high U concentration (13000-30000 ppm).

The highest grade rocks in the Mica Creek area lie in the Selkirk Mountains. Pelitic schist are migmatitic and typically contain kyanite and muscovite. One schist contains two monazite U-Pb analyses that are ~70 Ma and three other analyses that define a linear array that suggests older monazites (perhaps Jurassic) in this schist were severely overprinted at ~70 Ma. It is likely that the monazites that define the discordia were overgrown by ~70 Ma monazite and suffered substantial Pb loss at ~70 Ma. BSE imaging of a thin section reveals that monazite occurs as

inclusions in kyanite, garnet, and biotite, and lies within the dominant regional foliation (S_2). Another schist from this level contains a monazite analysis that plots adjacent to the ~160-70 Ma discordia defined by the analyses from the Monashee Mountains. This analysis plots slightly farther from the upper intercept than the Monashee analyses, probably due to a greater amount of Pb loss at ~70 Ma. Three other monazite analyses from this schist also define a discordant array that is consistent with a Cretaceous overprint of Jurassic grains. We infer from the significant amount of Pb loss and (or) mineral growth at ~70 Ma that there was a substantial thermal event at ~70 Ma. However, we are uncertain whether kyanite growth, migmatization, and attainment of temperatures that were high enough to cause diffusional homogenization of garnet zoning profiles occurred at ~70 Ma or at an older time, perhaps Jurassic. Some of the deformation responsible for S_2 occurred after intrusion of a boudinaged leucosome pod at 61 Ma, an age based on monazite and zircon with igneous characteristics (e.g., high U concentration and euhedral shape). Deformation ceased before intrusion of a cross-cutting pegmatite at 58 Ma.

These data demonstrate that rocks in the Mica Creek area were affected by thermal events in the Late Jurassic and Late Cretaceous. Although there are parts of the southern Omineca belt that were intruded by Jurassic and Cretaceous plutonic rocks, the Mica Creek area is the first to be identified as having undergone regional thermal events at these times.

Geochemistry and Tectonic Setting of the Powell Creek Group, Southwestern British Columbia

T.J. Danielson, J. Brian Mahoney, *Department of Geology, University of Wisconsin-Eau Claire, Eau Claire, Wisconsin 54702*; J. Riesterer, *Department of Geology, Idaho State University, Pocatello, Idaho 83209*; C.J. Hickson, *Geological Survey of Canada, Vancouver, British Columbia V6B 1R8*

The Powell Creek Group, of southwestern British Columbia, is a thick succession (~4000 m) of Albian to Cenomanian volcanic and volcaniclastic rocks, exposed along the eastern edge of the Insular superterrane, west of the Intermontane superterrane. Paleomagnetic data require ~2000 km of relative displacement between the Insular and Intermontane superterranes. The main outcrop belt of the Powell Creek Group lies immediately adjacent to the boundary between the two superterranes. Thick successions of Albian-Cenomanian volcanogenic conglomerate containing volcanic clasts lithologically similar to the Powell Creek Group occur east of the Group's main outcrop belt, along the western margin of the Intermontane superterrane. The Powell Creek Group and subjacent Silverquick Conglomerate overlie rocks of the Tyaughton Basin, which form an overlap assemblage linking the Bridge River and Methow terranes. The coeval volcanogenic conglomerates to the east overlie rocks assigned to the Spences Bridge Group of Quesnellia. The purpose of this investigation is to analyze the geochemical characteristics of the volcanic rocks of the Powell Creek Group, and compare those characteristics with the geochemical signature of coeval volcanogenic conglomerates to the east. If the Powell Creek Group can be shown to be the source of the coeval volcanogenic conglomerates, then the superterrane boundary and any proposed translational structure cannot occur between these units.

The Powell Creek Group is dominated by volcaniclastic rocks, with ash to lapilli tuff, feldspar and hornblende-feldspar phyric volcanic breccia, and intermediate to felsic volcanic cobble to boulder conglomerate constituting the majority of the succession. Lesser sandstone, siltstone, and intermediate volcanic flows are also present. Major, minor, and trace element geochemical analyses were conducted by X-ray fluorescence (XRF) spectrometry, on ~60 samples of Powell Creek Group volcanic flows and breccias and clasts of coeval volcanogenic conglomerates. Major and trace element ratios, trace element abundances, and rare earth element patterns were used to characterize the suite. Major element ratios indicate that samples are basaltic-andesite to dacite in composition and are sub-alkaline and calc-alkaline in nature. The sub-alkaline and calc-alkaline nature is consistent with magmas generated in modern destructive plate margin settings. Trace element ratios (Hf/3-Th-Nb/16, Zr/117-Th-Nb/16, Ti/100-Zr-Sr/2, La-Ba) also support a destructive plate margin setting. On spider diagrams, the niobium trough and barium and strontium spikes are consistent with subduction related magmatism. Trace element abundances of the Powell Creek Group and clasts within coeval conglomerates closely correspond to those of subduction

related continental arc volcanic suites (e.g. Aleutian Islands). Slightly LREE enriched rare earth element patterns also indicate continental margin magmatism. Clearly, the volcanic rocks of the Powell Creek Group and the clasts of the coeval volcanogenic conglomerates are derived from the same subduction related magmatic system. The Powell Creek Group was apparently deposited along the eastern side of a Late Cretaceous volcanic arc system built along the eastern edge of the Insular superterrane. Emplacement of the arc system was coeval with regional northeast-vergent contraction, as evidenced by syngenetic folding, thrust faulting and development of localized wedge-top basins receiving abundant volcanogenic debris.

Similarities in lithology, age, stratigraphic and structural setting, and geochemical signatures strongly argue that volcanogenic rocks on the western edge of the Intermontane superterrane were derived from volcanic edifices of the Powell Creek Group along the eastern edge of the Insular superterrane. This correlation leads to two mutually contradictory interpretations: 1) linkage between the Powell Creek Group and volcanogenic conglomerates to the east suggests only minor displacement between the Insular and Intermontane superterranes after 90 Ma; or 2) the volcanogenic conglomerates east of the main outcrop belt of the Powell Creek Group do not in fact unconformably overlie rocks of the Intermontane superterrane, but are instead associated with the Insular superterrane. If this is the case, then the Intermontane/Insular superterrane boundary lies northeast of the Churn Creek area, within rocks of the Cache Creek terrane. The second interpretation requires reevaluation of the tectonic affinity of rocks in the southern end of the Chilcotin Plateau currently assigned to either Stikinia or Quesnellia.

Physical modelling of fault propagation in roll-over structures associated with extensional (growth) faults

John M. Dixon, Simone Garneau and Julia Blackburn, Experimental Tectonics Laboratory, Department of Geological Sciences, Queen's University, Kingston, Ontario K7L 3N6

Compressional structures developed in fold-thrust belts such as the Canadian Rocky Mountains reflect the mechanical architecture of the passive margin. Primary extensional faults within the stratified cover sequence constitute significant local mechanical heterogeneities that can influence the location, timing and kinematic evolution of compressional structures. Such faults can have a variety of orientations (strike, dip and dip direction) relative to the direction of fold-thrust shortening.

We employ scaled physical models to study how primary extensional faults affect the evolution of superimposed fold-thrust structures. The models are constructed of interlayered plasticine and silicone putty, at a linear scale ratio of 10^{-6} (1mm=1km), and deformed in a centrifuge at 4000 ***g***. Tectonic compression is applied to one end of the layered stratigraphic sequence by the collapse and lateral spreading of a passive wedge of plasticine. The configuration and dimensions of the models are shown in Figure 1a.

Previous experiments have shown that a primary normal fault can readily be reactivated as a thrust, and that this process can result in an anomalously large structure which both forms early ("out-of-sequence") relative to the normal sequence of foreland-propagating fold-thrust structures. It is a prospective exploration target because of its large size and because it may develop early enough to retain an early hydrocarbon charge.

Here, we study how a roll-over structure in the hanging wall of a primary normal (growth) fault affects the evolution of superimposed fold-thrust structures. Each model was constructed with a single primary fault disrupting the stratigraphic sequence (see Figure 1). The fault dipped either towards the hinterland (Figs. 1b and 1e) or towards the foreland (Figs. 1c, 1d and 1f) of the superimposed fold-thrust belt. In some models the fault represented syn-depositional extension (i.e., it was a growth fault; Figs. 1b-1d), and in others it disrupts strata of uniform thickness (Figs. 1e-1f). All models were constructed with a subtle roll-over structure in the hanging wall of the primary fault.

The roll-over structure influenced the location of superimposed structures. When the primary fault dips towards the hinterland, the subtle dip of the roll-over is sufficient to nucleate a major foreland-verging thrust through a process of fault-propagation folding. The thrust is located within the hanging wall of the primary normal fault, rather than coincident with it. When the primary normal fault dips towards the foreland, the roll-over structure nucleates a minor back-thrust but the dominant superimposed structure is a foreland-verging thrust that ramps from the footwall to the hanging wall of the primary fault.

The models suggest that exploration for hydrocarbons in fold-thrust traps associated with primary normal faults should take into account the possibility that the normal fault had a roll-over structure in its hanging wall. This circumstance creates the possibility that major fold-thrust structures will be associated with, but displaced from, the primary normal fault in a systematic way.

Acknowledgements: This work was carried out as part of the Foothills Research Project (FRP), a collaboration between principal investigators D.C. Lawton and D.A. Spratt of the University of Calgary and J.M. Dixon of Queen=s University. Financial support from FRP sponsor firms in the petroleum industry and NSERC is acknowledged with thanks.

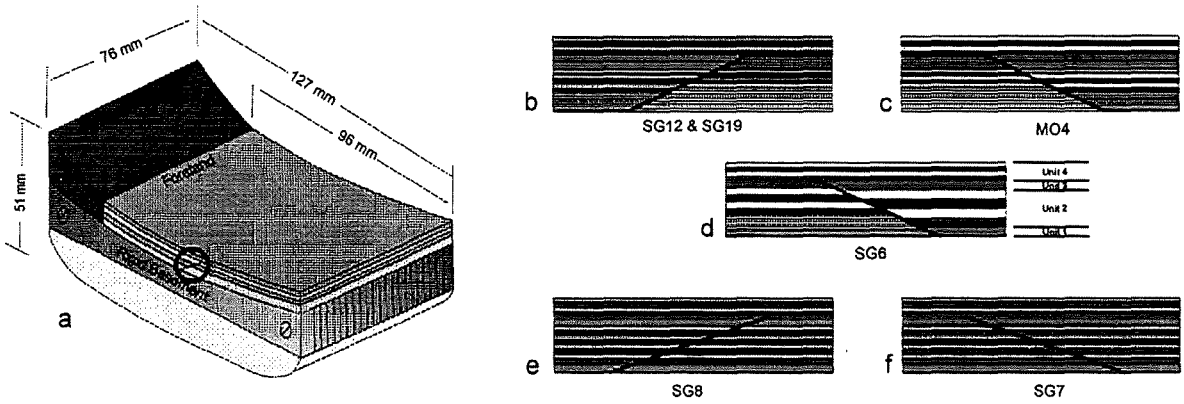

Figure 1. Dimensions and initial configurations of four types of physical model described in the present paper. (a) General geometry and dimensions. Circled area encloses the primary normal fault. (b)-(f) Enlarged schematic sections of the primary normal fault. Four stratigraphic units (1-4 from bottom to top) overlie a rigid base. Units 1 and 3 have low competency and consist of interlayered silicone putty and plasticine (1:1 ratio). Units 2 and 4 are high competency and consist of coloured laminae of plasticine. Unit 4 represents post-rift strata. In all cases the shortening is directed from left to right. (b) and (c) Models with growth geometry across the normal fault. (d) Model with growth strata but increased thickness of competent unit 2. (e) and (f) Models without growth strata geometry. All models had subtle roll-over structure in the hanging wall of the primary fault (not shown in the schematic diagrams).

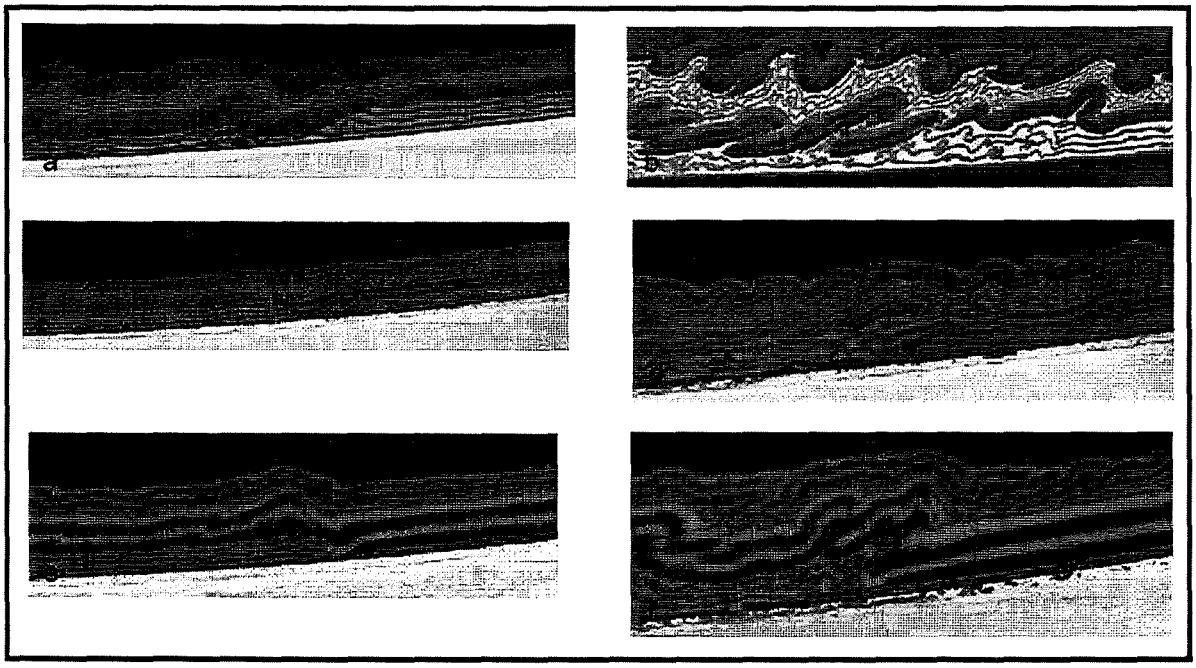

Figure 2. Transverse sections through deformed models showing how folds and thrusts are influenced by pre-existing normal faults with roll-over structures in the hanging wall. (a) and (b) Two stages of shortening of a model with initial configuration shown in Fig. 1b. (c) and (d) Two stages of shortening of a model with initial configuration shown in Fig. 1c. (e) and (f) Two stages of shortening of a model with initial configuration shown in Fig. 1d.

The Big Flush - Paleomagnetic signature of a 70 Ma regional hydrothermal event in displaced rocks of the northern Canadian Cordillera

Randolph J. Enkin, P. Jane Wynne, Judith Baker,
Geological Survey of Canada - Pacific, Box 6000, Sidney, BC, V8L 4B2, Canada
Stephen T. Johnston,
Department of Geology, University of Durban-Westville, Private Bag X54001, Durban 4000, South Africa
and Craig J. R. Hart
Yukon Geology Program, Whitehorse, YT, Y1A 2C6, Canada

The 70 Ma Carmacks Group, a subaerial volcanic succession which once covered much of central southwest Yukon, has a paleomagnetic remanent direction which passes the fold test and the reversal test. A new collection of 13 sites, combined with 13 sites collected by Marquis and Globerman (1988), renders a pole (088.6 E 78.4 N, A95=7.8) which is far-sided with respect to the pole for cratonic North America and implies a displacement from the south of 1900±700 km. Late Triassic Mandanna Member red beds and Early Jurassic Nordenskiöld Member tuffs, deformed in the Late Jurassic, fail the fold test and conglomerate test but pass a contact test with Eocene dykes. The postdeformational remanent direction is identical to that isolated from the Carmacks Group. The magnetic signature contained in these older formations is probably an overprint produced by an extensive hydrothermal system active during Carmacks extrusion. Geological work indicates that the Carmacks Group is plume-related. Given its paleomagnetic latitude and geological nature, we hypothesize that the Carmacks Group is a displaced segment of the Yellowstone hotspot track, and the hydrothermal system which remagnetized the older rocks was established by mantle upwelling below the region.

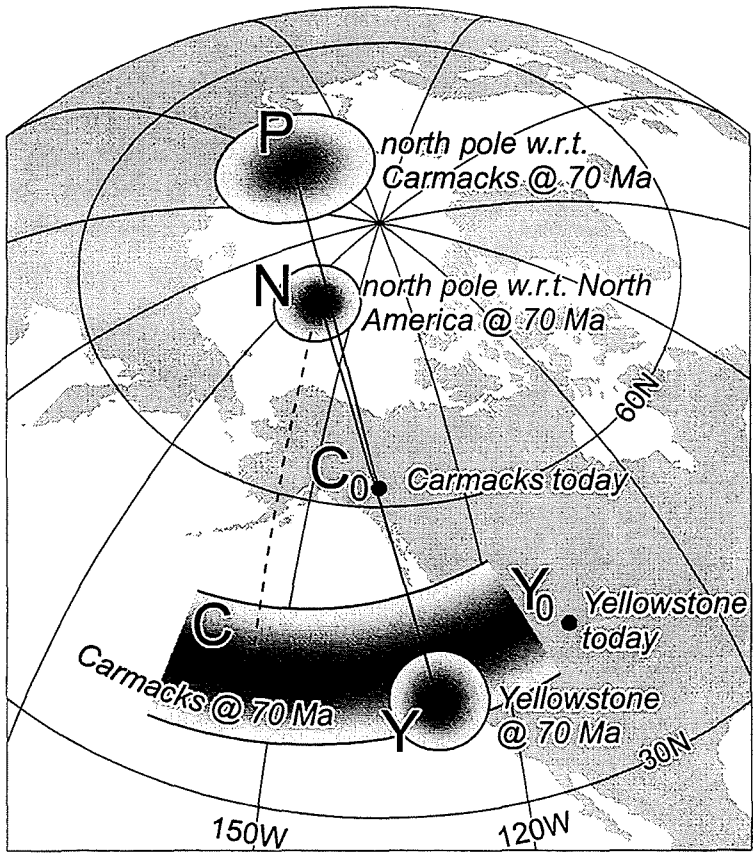

Figure Caption: Paleogeographic interpretation of the Carmacks Group paleomagnetism. The paleomagnetic poles (with their 95% confidence intervals) of North America, N, and the Carmacks Group, P, were aligned along the geographic pole at 70 Ma. This implies that central southwest Yukon was displaced to a position within swath C at the time of Carmacks extrusion. The Yellowstone hotspot was at point Y at 70 Ma, which we argue was the source of the Carmacks volcanics and the associated hydrothermal event which remagnetized underlying formations.

MIDDLE AND LATE TRIASSIC ARC VOLCANIC ROCKS AND ASSOCIATED INTRUSIONS IN SOUTHERN AND CENTRAL BRITISH COLUMBIA: EVIDENCE FOR CORRELATION OF STIKINE, CADWALLADER AND METHOW TERRANES

Friedman, R. M.[1], **Schiarizza, P.** [2], **Mustard, P.** [3], **van der Heyden, P., Mortensen, J.K.** [1], **Thompson, J.F.H.** [1] and **Deyell, C.** [1] , [1]Department of Earth and Ocean Sciences, University of British Columbia; [2]British Columbia Geological Survey Branch, Ministry of Employment and Investment; [3]Department of Geological Sciences, Simon Fraser University

Late Triassic arc magmatism, represented mainly by volcanic rocks of the Stuhini and Lewes groups and associated intrusions, has been well documented in northern Stikinia. Although it has long been postulated that this arc extends farther to the south, evidence has been scanty. Geological mapping and U-Pb and paleontologic dating studies during the past several years along the Coast Belt/Intermontane Belt boundary in southern and central British Columbia (Cadwallader-Methow terrane and Stikinia, sensu stricto, respectively) indicate the presence of Middle and Late Triassic plutonic and volcanic rocks that may be correlative with Stuhini/Lewes River arc rocks to the north.

In southern British Columbia, four plutonic bodies (8 U-Pb samples) were dated from the Chilcotin and Niut ranges of the southeastern Coast Belt, southwest of the Yalakom fault. The plutons occur in adjacent structural panels separated by Late Cretaceous to early Tertiary thrust and dextral strike-slip faults. The dioritic to tonalitic Mt. Skinner plutonic complex (227- ca. 235 Ma; n=3) is nonconformably overlain by Upper Triassic clastics correlated with Cadwallader terrane, which in turn are overlain by Lower to Middle Jurassic clastic and volcaniclastic rocks of Methow terrane. The Crazy Creek pluton (217-220 Ma; n=2) is thrust-imbricated with, and locally nonconformably overlain by, Upper Jurassic conglomerate and finer-grained clastic sedimentary rocks of the Tyaughton-Methow basin overlap sequence. The Niut pluton (212, 219 Ma; n=2) and earliest Jurassic Sapeye Creek pluton (207 Ma; n=1) intrude Ladinian to early Norian mafic to intermediate volcanic rocks that have been correlated with volcanics of Cadwallader terrane (Pioneer formation) or Stikine(?) terrane (Mt. Moore formation). One unnamed granitoid (212 Ma) dated in central British Columbia lies in the western Intermontane Belt (Stikine terrane) adjacent to the Limonite Creek prospect, some 50 km southwest of Smithers. This body intrudes volcanic rocks which were previously correlated with Lower Jurassic Hazelton Group but can now reasonably be considered as possible Upper Triassic equivalents of the Stuhini and Lewes River groups. All of the above U-Pb ages are based on concordant zircon/titanite analyses, and all of the southern rocks also appear to contain a minor inherited zircon component.

The ages and contact relationships of the plutonic rocks in the southeastern Coast Belt contribute to a growing body of data suggesting that Cadwallader and Methow terranes are part of a single Middle Triassic to Middle Jurassic arc-basin complex that developed east of the coeval Bridge River accretion-subduction complex. Similarities to the Triassic Stuhini/Lewes River and Jurassic Hazelton magmatic arcs support previous correlations between Stikine and Cadwallader terranes; the Cadwallader-Methow arc complex might be a southern continuation or a faulted fragment of Mesozoic Stikinia.

Digital Geologic Map of Yukon

S.P. Gordey, A. Makepeace and S. Talwar
Geological Survey of Canada, 101-605 Robson Street, Vancouver, B.C., V6B 5J3
(email: sgordey@gsc.nrcan.gc.ca)

The Yukon Digital Map Project will produce a digital compilation at 1:500,000 scale of Yukon bedrock geology available on CD-ROM, and a wall-map of Yukon bedrock geology at 1:1,000,000 scale by the fall of 1998. Funding for the project originates from the Yukon Government, Indian and Northern Affairs Canada, and the Geological Survey of Canada. The CD-ROM will provide a regional synthesis and up-to-date compilation of Yukon bedrock geology in a single source. The data will be made available in multiple formats whereby features of interest can be directly imported into the user's illustration, CAD, or GIS programs. Digital bedrock geology can be more easily manipulated than traditional paper overlays and when combined with cultural, topographic, geophysical and other data forms the basis of resource assessment, exploration, and land use decisions. The wall map, a derivative of the digital data set, will be a valuable educational resource and useful in regional scientific and exploration program planning.

DATA STRUCTURE

The Yukon digital geologic map will encompass a large amount of geological and topographical data. To be accessible in manageable-sized pieces, the data is organized both by geographic area and information type. The Yukon is divided into 45 tiles corresponding to the 1:250 000 scale National Topographic System, within which different types of information comprise separate themes. With this organization, single or multiple types of information can be easily extracted for a given area and used without having to manipulate the entire data set.

The digital data is compiled using ARCINFO software by ESRI Inc., a high-end geographic information system used extensively at the Geological Survey of Canada. Other software packages utilized include ARCVIEW, AUTOCAD, DBASE and QUATTRO PRO.

DATA SETS AND METHODS

Compilation of bedrock geology is the largest component of the project. Data is obtained from various, mostly non-digital sources. An ink-on-mylar overlay is compiled for each 1:250,000 map-area, which is then scanned to produce an image (TIF format). The image is imported into ARCINFO, and a conversion to vector format done automatically. The quality of linework produced is excellent, more precise than that capable by hand digitizing, and is accomplished much faster. Many subsequent steps are required to attribute the lines (ie to classify them as defined, approximate, assumed, thrust fault, normal fault, etc), make and label polygons (ie rock units), and input geological names. Several other databases are compiled concurrently, including a list of data sources, original rock unit legends, a compilation legend, as well as tectonic assemblage and terrane descriptions. Information in these related tables can be extracted, displayed or queried for each polygon on the map.

Mineral (Yukon Minfile) and fossil occurrences (Geol. Surv. Can.) as well as isotopic age data (U.B.C.) will be added as point data, without revision from the original sources. Information in the related data tables can be extracted, displayed or queried for each point on the map.

Topographic data (Digital Chart of the World, 1:1,000,000 scale) are obtained in ARCINFO digital format. Using the ARCINFO software the data are being re-organized into various categories and divided into the tiles as appropriate for the Yukon. This topographic data set is the only one available in a consistent format across the territory. It can also be re-released without royalty.

PERFORMING QUERIES

The linework and related databases are structured for analysis in a geographic information system, with which spatial and related data of different themes can be queried separately or together. With the appropriate software (eg. ARCVIEW, MAPINFO), one could extract a map of all of the granitic rocks in the Yukon, or a map of only those granitic rocks which have associated gold or tungsten occurrences for a portion of the territory. The bedrock geology will be able to be queried on geologic unit, rock type, age, source(s) of information, named geological features, tectonic assemblage and terrane.

Preliminary Interpretations of Wavenumber Filtered Potential Field Data from Northwestern Canada

Kevin W. Hall, Frederick A. Cook, Elissa Lynn

Department of Geology and Geophysics
University of Calgary, Calgary AB T2N 1N4

Application of filtering techniques to potential field data from the SNORCLE transect area provides an opportunity to analyse anomaly map patterns in relation to their tectonic setting. Here, we present regional gravity data filtered according to wavelength and correlated to SNORCLE reflection line 1 to assist in the interpretation of the crustal and lithospheric structure in northwestern Canada.

New code for applying elliptical filters in the wavenumber domain (highpass, lowpass, bandpass and directional filters) has been ported to ER Mapper for simple application to gridded potential field maps. Applications include: 1) correlation of filtered map areas to outcrops (e.g., Cook et al., 1995); 2) tracking anomalies with one strike across anomalies with a different strike, as, for example, following anomalies associated with Canadian shield rocks that are obscured by the Cordilleran Bouguer low (e.g., Geiger and Cook, 1996); and, 3) numerical modeling of filtered data sets in which high wavenumber anomalies have been removed for the purposes of modelling lower crustal and mantle features (e.g., Cook et al., 1995). In this presentation we analyze lowpass filtered versions of the isostatic gravity anomalies of northwestern Canada.

The isostatic gravity of northwestern Canda exhibits the following regional characteristics:

1. The western Slave province is characterized by isostatically low values and is therefore overcompensated at depth (SL; Figure 1).

2. The Fort Simpson structure is characterized by a linear isostatic high that is parallel to the Mackenzie Mountains front, and is separated from it by a linear north-south trending low (FSH, MMH; Figures 1 and 2).

3. The Mackenzie Mountains exhibit one of the largest and most regionally extensive isostatic highs in all of North America (MMH; Figures 1 and 3). The elevated Mackenzie Mountains are therefore not compensated at depth.

Subsurface information bearing on the deep structure of the crust and lithosphere of this region is provided by SNORCLE reflection line 1, a continuous profile from the eastern front of the Cordillera to a point about 70 km east of Yellowknife (Cook et al., 1997; this volume). For example, in the western Slave province the crust is about 33-35 km thick, roughly the same crustal thickness as observed along the transition to isostatically high values to the west, and appears to thin eastward into the Slave isostatic low (Cook et al. 1998). Thus, the Slave low is not likely due to downward deflection of the crust during the last ice age.

The Fort Simpson isostatic high coincides with the juxtaposition of the Fort Simpson terrane and the Wopmay orogen, and is likely caused by density variations within the crust and upper mantle associated with this transition. The crust thins westward from near 35-40 km at Fort Simpson to about 30 km at the western end of SNORCLE line 1 (Cook et al., 1998). The shallow Moho is situated beneath nearly 20 km of layering that is most easily

interpreted as Proterozoic sedimentary basin rocks (Fort Simpson basin). The Fort Simpson basin coincides with the isostatic low between Fort Simpson and the Mackenzie Mountains, and is almost certainly associated with low density rocks within the crust that are not accounted for in calculation of the isostatic anomaly (e. g., Cook and van der Velden, 1993).

The Mackenzie Mountains regional isostatic high (MMH; Figure 1) is located east of the Teslin tectonic zone and west of the mountain front. Its arcuate shape is convex northeastward with anomaly values typically in the +30 to +50 mGal range, and up to +75 mGal in the Wernecke and Ogilvie mountains. The cause(s) of the high isostatic values are problematic, as detailed subsurface information on crustal structure in this area is not yet available. Nevertheless, the reflection geometry seen on the west side of SNORCLE line 1 (thin crust and thick basin sediment), coupled with regional geology provides some clues. The Mackenzie Mountains east of the Tintina fault are primarily composed of deformed miogeoclinal Paleozoic and Proterozoic sediments. Accordingly, they are likely stratigraphically equivalent to the layers that appear as reflections within the Fort Simpson basin. If the Moho remains thin (ca 30 km) throughout the eastern Mackenzie Mountains at the same time as basin sediment layers are thickened by deformation, then the isostatic correction would not account for thin crust underlying the elevated topography, and the isostatic anomaly would be positive. In this scenario, the elevated topography of the Mackenzie Mountains is supported dynamically, rather that isostatically.

In Figure 2, anomalies with wavelengths greater than 250 km are displayed (lowpass filter with wavelength cut-offs = 250.0-176.78 km, where 1/250 = 0.004 1/km is full-on and 1/176.78 = 0.005657 1/km is full-off, over a half cosine bell taper). Assuming depth to source equals about 1/4 wavelength, these anomalies are primarily due to sources at depths greater than 44-63 km. The Fort Simpson high (FSH; Figure 2) crosses the west end of SNORCLE line 1 at about 120°W. The middle third of the seismic profile borders an isostatic low in the western Slave province. The arcuate Mackenzie isostatic high is clearly visible (MMH; Figure 2).

Anomalies with wavelengths greater than 750 km (Figure 3; lowpass filter with wavelength cutoffs = 750.0-530.33 km) can primarily be attributed to sources at depths greater than 133-188 km (or shallower sources with greater regional extent). Here we observe: 1) the Fort Simpson high is no longer visible, 2) a broad regional high is still apparent in the Mackenzie mountains area; 3) a regional low is still visible in the Slave province; 4) the transition between the Slave province low and the Mackenzie mountains high occurs along the western part of SNORCLE line 1; and 5) a northeast-southwest "saddle" is visible along the trend of the Great Slave Lake shear zone.

The long wavelength transition from the Mackenzie high to the Slave low may be due to subducted Fort Simpson terrane lithosphere (e.g., Cook et al., 1998). Mantle reflections observed north of Scotland that have a similar geometry to SNORCLE line 1 coincide with a regional gravity low that is also interpreted to be the result of subducted lithosphere (Warner et al., 1996). If the northeast-southwest trending isostatic low south of the Mackenzie high is in fact due to the Great Slave Lake shear zone, it is likely that the Great Slave Lake shear zone is present in the lithosphere from the Canadian Shield to the Pacific coast. Because geochemical evidence from young volcanic rocks has been interpreted to imply that different lithosphere exists on either side of the Tintina fault north of 60°N in the Yukon (Francis et al., 1997), and the Tintina fault projects southward across the isostatically low "saddle" to at least 54°N (TF; Figure 3), the Tintina fault may rise into the crust and project above (as opposed to offset) the Great Slave Lake shear zone (e.g., Geiger and Cook, 1996).

References

Cook, F.A., and van der Velden, A., 1993, Proterozoic crustal transition beneath the Western Canadian sedimentary basin: Geology, v. 21, p. 785-788.

Cook, F.A., Varsek, J.L., and Thurston, J.B., 1995, Tectonic significance of gravity and magnetic variations along the Lithoprobe southern Canadian Cordillera transect: Canadian Journal of Earth Sciences, v. 32, p. 1584-1610.

Cook, F.A., van der Velden, A., Hall, K.W., and Roberts, B.R., 1997, Lithoprobe SNORLCE-ing beneath the northwestern Canadian shield: deep lithospheric reflection profiles from the Cordillera the the archean Slave province: Lithoprobe report 56, SNORCLE and Cordilleran Tectonics Workshop, p 48-57.

Cook, F.A., van der Velden, A., Hall, K.W., and Roberts, B.R., 1998, Frozen subduction in Canada's Northwest Territories, LITHOPROBE deep lithospheric reflection profiling of the western Canadian shield: Tectonics (submitted).

Francis D., Shi, L., Abrahams, A.C., Peslier, A., Schmidberger, S., Carignan, J. Ludden, L. and Polve, M., 1997, Mantle xenolith and alkaline basalt mapping of the lithospheric mantle beneath northwestern Canada: : Lithoprobe report 56, SNORCLE and Cordilleran Tectonics Workshop, p 128.

Geiger, H., and Cook, F.A., 1996, Directional filtering of 3D gravity models: Lower crustal features revealed: Lithoprobe report 50, SNORCLE and Cordilleran Tectonics Workshop, p 191-197.

Warner, M.R., Morgan, J., Barton, P., Morgan, P., Price, C., and Jones, K., 1996, Seismic reflections from the mantle represent relict subduction zones within the continental lithosphere: Geology, v. 24, p. 39-42.

Figure Captions

Figure 1. Isostatic gravity anomaly map of northwestern Canada. Note the regional low in the Slave Province (SL), the linear high associated with the Fort Simpson structure (FSH), the parallel low associated with the Fort Simpson basin to the west, the regional high in the Mackenzie mountains region (MMH), and the linear anomalies associated with the Tintina fault (TF) and the Great Slave Lake shear zone (GSLsz). SNORCLE reflection line 1 is shown as a white line.

Figure 2. Wavelength filtered isostatic gravity map (low pass; shows anomalies with wavelengths greater than about 250 km). Note that the Fort Simpson high (FSH) is still visible, as are the Slave low (SL) and the arcuate Mackenzie Mountains high (MMH).

Figure 3. Wavelength filtered isostatic gravity map (low pass; shows anomalies with wavelengths greater than about 750 km). Note that the Fort Simpson high (FSH) is no longer visible, but that there is a dramatic transition from the Mackenzie Mountains high (MMH) to the Slave low (SL). The transition occurs along SNORCLE reflection line 1, and is likely associated with subducted Fort Simpson terrane lithosphere (Proterozoic). Note also the low that coincides with the Great Slave Lake shear zone (GSLsz) east of the TF, and continues across the Cordillera to the Pacific coast.

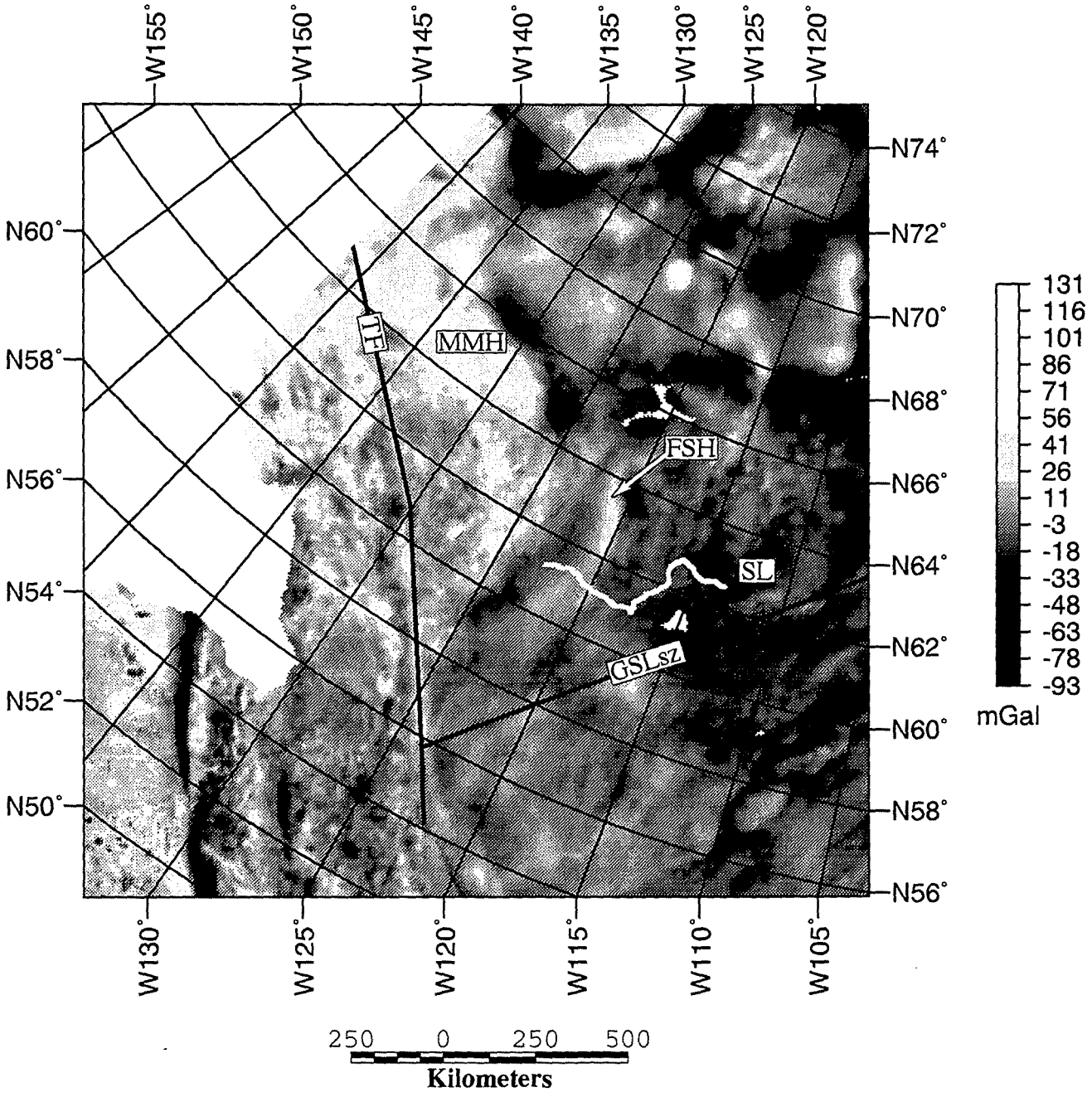

Figure 1: Unfiltered isostatic gravity map

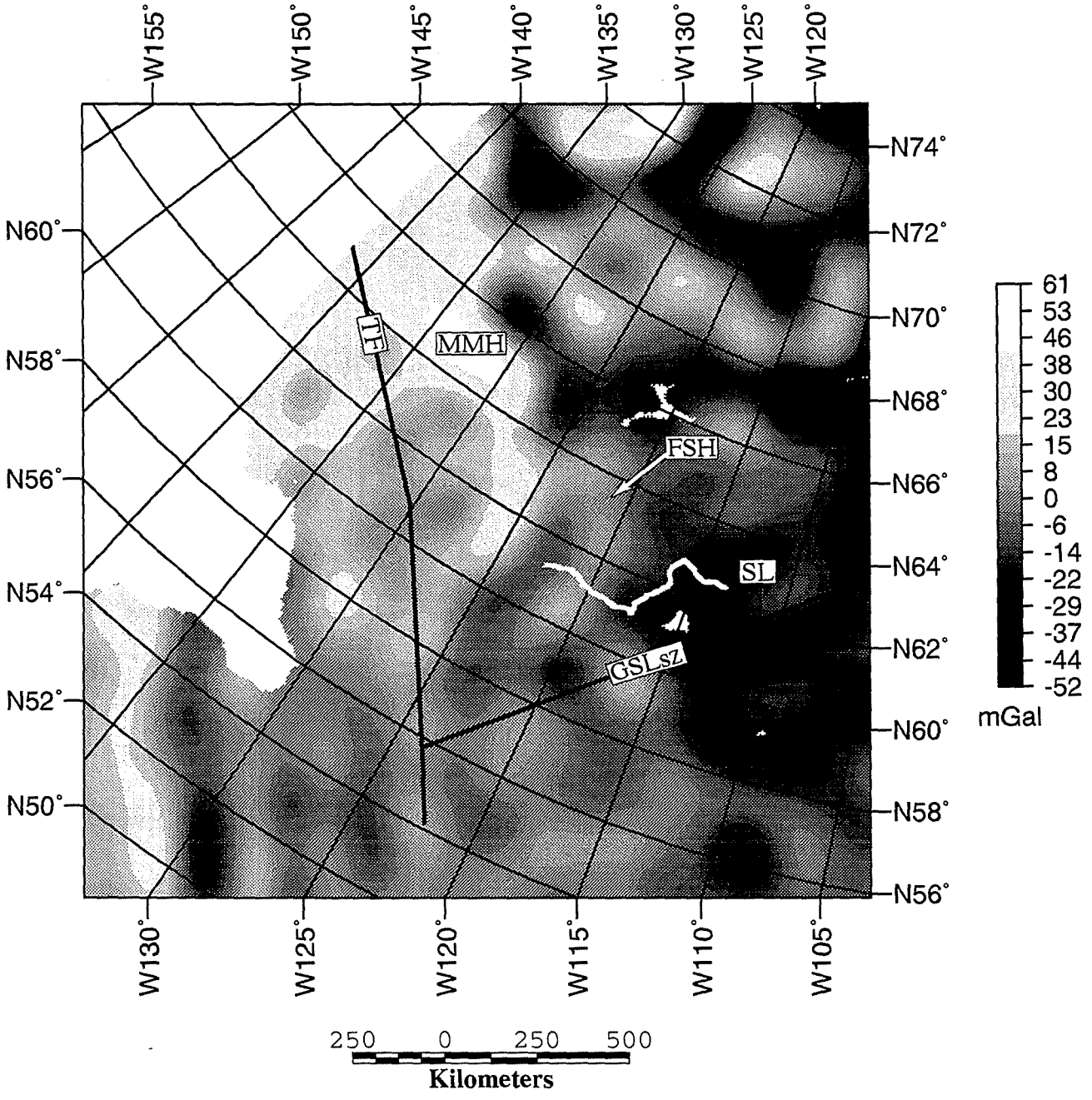

Figure 2: Lowpass filtered (250+ km wavelengths) isostatic gravity map

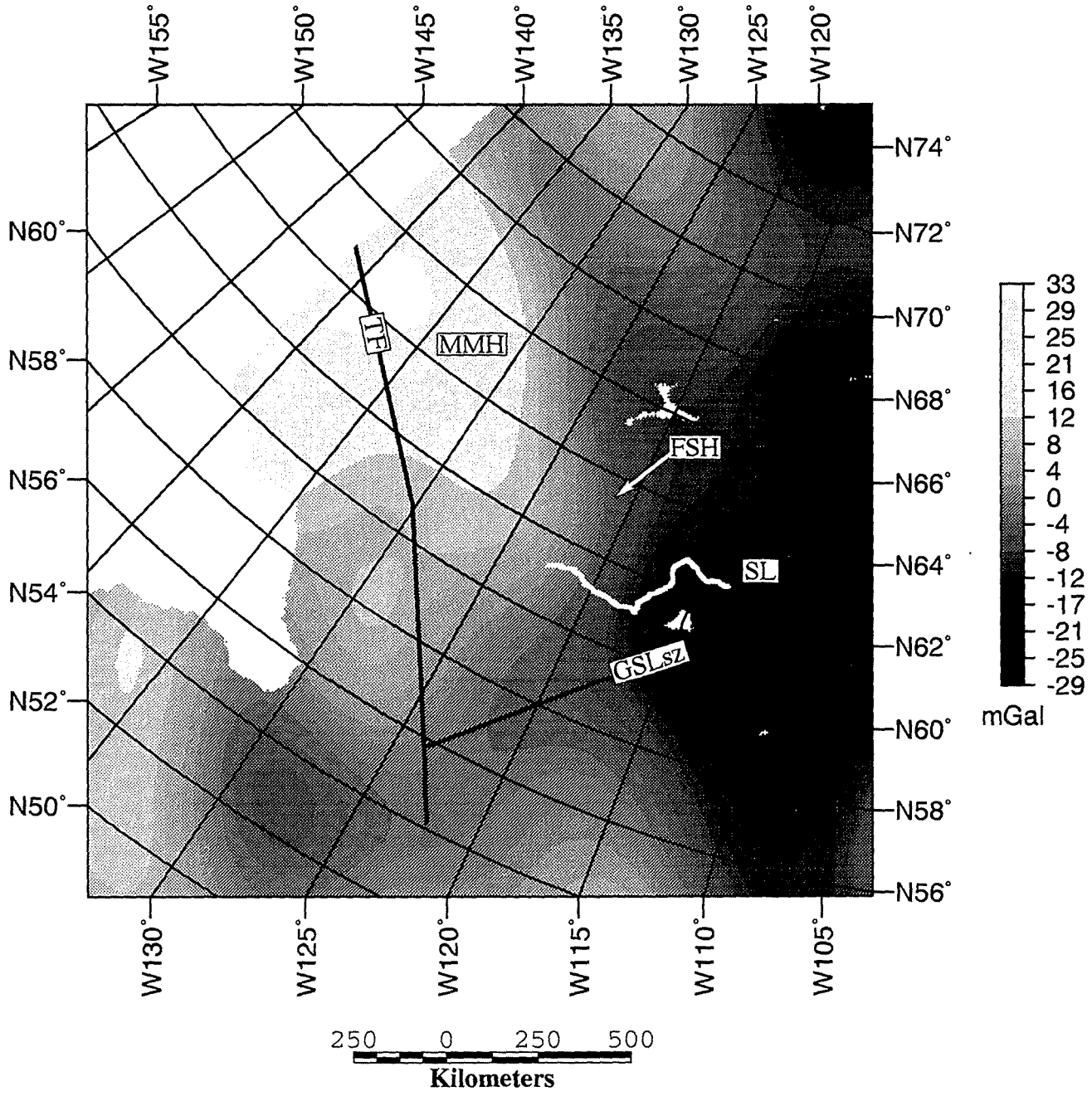

Figure 3: Lowpass filtered (750+ km wavelengths) isostatic gravity map

ACCRETE Crustal Velocity Structure Across the Coast Plutonic Complex / Stikinia Transition

Philip T.C. Hammer, Ron M. Clowes and Bob M. Ellis
Depatment of Earth and Ocean Sciences, University of British Columbia, Vancouver, BC, V6T 1Z4, hammer@eos.ubc.ca

The Coast orogen of British Columbia and southeast Alaska contains the suture resulting from the mid-Cretaceous collision between the exotic Insular superterrane (Alexander and Wrangellia terranes) and the previously accreted Intermontane superterrane (Stikine, Taku and Yukon terranes). This geotectonic environment has been targeted by ACCRETE to address fundamental questions concerning continental evolution and dynamics during terrane accretion. One focus of the project is the Coast Plutonic Complex and its eastern transition to the Skeena Fold and Thrust Belt of the Stikine terrane. Understanding the development of the Skeena belt is one of the keys to unraveling the tectonic history of the region.

The ACCRETE refraction/reflection experiment (Figure 1) was conducted along Portland Canal, a 200 km-long fjord that penetrates deeply into the Coast orogen. The seismic source was a 132 *l* airgun array towed by the R/V Maurice Ewing. In addition to near-vertical incidence data collected by the Ewing hydrophone streamer, wide-angle data were acquired with a land-based array of 60 IRIS/PASSCAL Reftek 3-component seismographs. Seventeen of these instruments were deployed inline with the shiptrack, extending 105 km northeast from the head of the fjord through the Coast Plutonic Complex and into Stikinia. In addition, the ACCRETE dataset is supplemented by data acquired during the overlapping SNORCLE Refraction Experiment that was carried out in August/ September, 1997.

The resulting wide-angle dataset provides a densely sampled, inline profile across the transition zone. The high-quality, multiphase data were used to model P- and S-velocity structure. These models indicate that velocities beneath the Skeena Fold and Thrust Belt are significantly slower than velocities beneath the Coast Plutonic Complex (CPC). In addition, a mid-lower crustal reflector is consistently observed. This impedance contrast may either be associated with the proposed detachment beneath Stikinia [Evenchick, 1991] or may be related to Miocene extension as proposed by Hollister et al. [1997]. Further geophysical constraints to tectonic interpretations of the region will be added by the SNORCLE multichannel reflection and MT experiments. The combination of the ACCRETE and SNORCLE transects will yield a near-continuous multi-disciplinary transect reaching from the Archean Slave Province across the Phanerozoic Cordilleran orogen to the Pacific Plate.

REFERENCES

Diebold, J., T. Das, L. Hollister, and K. Rohr, 1996. Seismic reflection interpretations along the fjords of the ACCRETE transect, southeast Alaska and northern British Columbia, Conference Abstract: 7th Deep Seismic Profiling of the Continents Symposium, Asilomar, CA, p. 59.

Evenchick, C.A., 1991. Geometry, evolution and tectonic framework of the Skeena Fold Belt, North Central British Columbia, *Tectonics*, 10:537-546.

Hammer, P.T.C., R.M. Clowes and R.M. Ellis, 1997. ACCRETE crustal velocity structure across the transition between the Coast Plutonic Complex and Stikinia, In *SNORCLE Transect Workshop, Lithoprobe Report No. 56*, p. 160-168.

Hollister, L.S., T. Das, J. Diebold, I.B. Morozov, and S.B. Smithson, 1997. Evidence for late (Miocene?) extension across the Coast Mountains, In *SNORCLE Transect Workshop, Lithoprobe Report No. 56.*

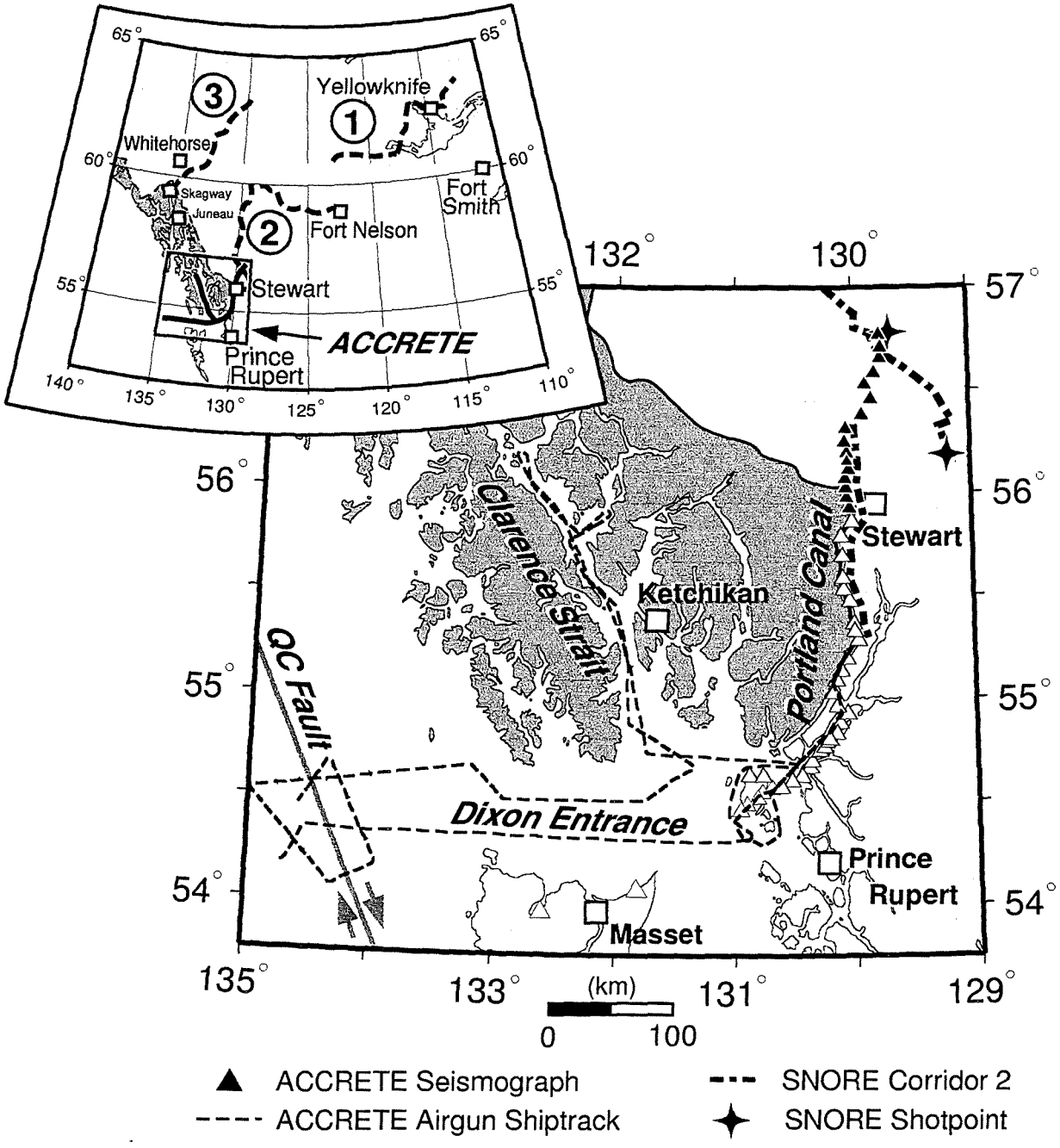

Figure 1. ACCRETE seismic experiment. Velocity structure models across the Coast Plutonic Complex/Stikinia transition are based on data recorded by the northern seismograph array (black triangles). Additional coverage is provided by the overlapping SNORCLE refraction experiment (SNORE, heavy dashed line). Inset illustrates location of the ACCRETE transect relative to the SNORCLE transect corridors.

Geophysical Data Analysis and Regional Gravity Modelling in the Southern Slave Province

Karen A.B. Hendry [1,2], Walter R. Roest [2], Wouter Bleeker [2] and Keith Benn [1]

[1] Ottawa-Carleton Geoscience Centre and Department of Geology, University of Ottawa, Ottawa, Ontario, K1N 6N5

[2] Geological Survey of Canada, 615 Booth St., Ottawa, Ontario, K1A 0E9

Regional gravity and magnetic data in the southern Slave Province are compiled and complemented with target gravity data, collected for the purpose of this study. In addition to 2½D gravity modelling, possibly expanded to 3D modelling in the future, a digital technique is being employed to reconstruct large-scale tectonic deformation. The technique allows reconstruction of horizontal motion along discrete faults as well as distributed, ductile deformation. The goal of this study is to increase knowledge of regional Archean tectonics and to better understand the Archean tectonic processes in relation to Phanerozoic plate tectonics.

Regional Geophysical Data Compilation

Compilation of the regional magnetic and gravity data covering the southern Slave Province to produce high quality maps and other derived products has been completed. A Digital Terrain Elevation Model was constructed using public domain data available from USGS, complemented with GSC data and corrected for data errors. This work will aid continued field mapping in the area and will be used also to reconstruct the tectonic history of specific tectonic features discussed below.

Detailed Gravity Profiles

Target gravity data collection in the southern Slave structural province is sponsored by the Geological Survey of Canada and Geomatics Canada. Data from two field seasons are currently being analysed and modelled. The purpose of this work is to provide first order constraints on the third dimension along the SNORCLE corridor. The first profile along which gravity data has been collected is corridor 1 of the SNORCLE transect (700 stations). This data set has been finalized and modelling is in progress, utilizing the interpretation of the seismic reflection data (Cook et al., submitted) to constrain the gravity modelling. Regional data will be used to extrapolate this knowledge away from the seismic line.

In addition to this profile, a detailed study of various plutons from the Prosperous and Defeat Suites and the Morose Granites in the Sleepy Dragon Complex is underway. During the last summer, three detailed gravity profiles were collected throughout the area, and linked to Transect 1 (see Figure 1). Final data processing will be completed in early 1998, after which these data will be analysed and modelled to constrain the depth extent and shape of the plutons. This information will aid in the development of tectonic interpretations in terms of crustal structure and regional deformation. An examination of the magnetic fabric of the area is in progress (Ham et al., this volume) and will complement this study. Once 2½D modelling is completed, expansion to a 3D model will commence.

Tectonic Reconstructions

Using the technique developed by Roest and Pilkington (1994), regional magnetic and gravity data will be used in reconstructions of regional strain. The first target is the well studied Great Slave Lake Shear Zone (GSLSZ), which forms the southern border of the Slave structural province, and is a prime example of a regional-scale structure resulting from tectonic events (e.g., Hoffman, 1987; Hanmer, 1988; Henderson et al., 1990; Ross et al., 1991). Active at ca. 2.0 Ga, it is approximately 25 km wide and consists of four major units. The amount of dextral transcurrent movement along the shear zone has been estimated to be up to 700 km (Hoffman, 1987) and due to the large amount of shearing, the geologic units to the north and south of the GSLSZ are not easily correlated. Regional magnetic patterns have been combined with knowledge of the geology of units displaced by the GSLSZ to reconstruct the shear zone (cf. Henderson et al, 1990; Ross et al., 1991; see figure 2). The main geological units to the north and south of the GSLSZ were digitized and the coordinate system rotated so that the shear zone became east-west. Then, the contacts between the units were aligned via digital means to give a simplified representation of the geology prior to movement along the shear zone. This work will help us obtain a better understanding of the regional geology before shearing. It may also increase our understanding of how such a large amount of displacement was accommodated in the area of the Thelon magmatic zone.

A similar reconstruction will be employed to determine the geometry of interfering fault patterns that offset parts of the Central Slave Basement Complex (Bleeker and Ketchum, in press.).

Acknowledgements

Roy Cooper and Mike Berrigan (Geomatics Canada) collected the target gravity data.

References

Bleeker and Ketchum, in press. Current Research.

Bleeker, Cooper, Berrigan, Roest, and Hendry, in press. Current Research.

Cook, Van der Velden, Hall, and Roberts, submitted. Tectonics.

Hanmer, 1988. Tectonophysics.

Henderson, McGrath, Theriault, and van Breemen, 1990. Can. J. Earth Sci..

Hoffman, 1987. Geology.

Roest and Pilkington, 1994. Geophys. Res. Lett..

Ross, Parrish, Villeneuve, and Bowring, 1991. Can. J. Earth Sci..

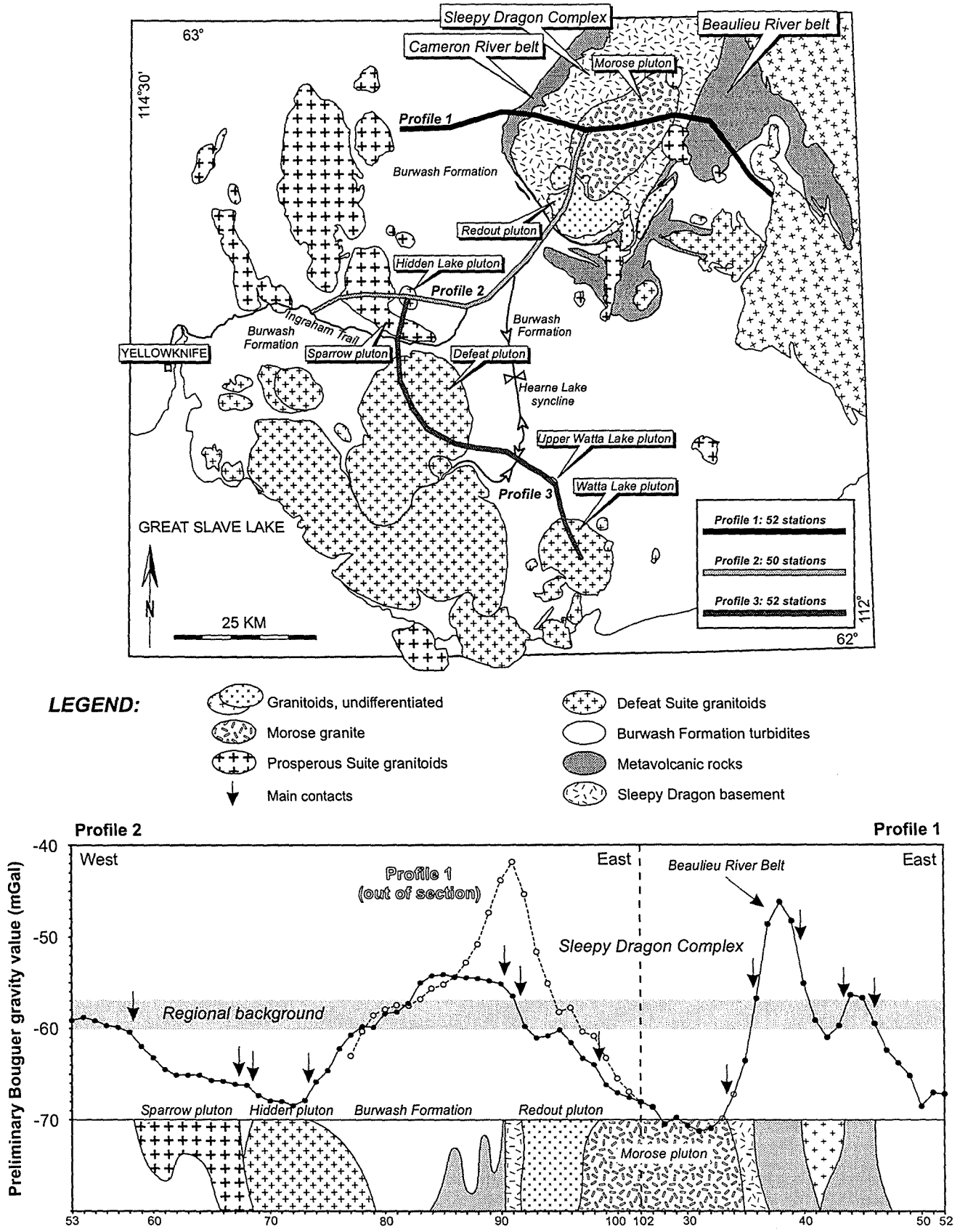

Figure 1 -- a) Location map of the study area in the Southern Slave Province. Indicated are the major geological units, including plutons from the Defeat and Prosperous Suites, as well as the locations of the three gravity transects collected in the summer of 1997. b) Bouguer gravity profile along profiles 1 (eastern panel) and 2 (western panel), demonstrating first order correlation with geology. The cross-section is schematic only. (After Bleeker et al., in press)

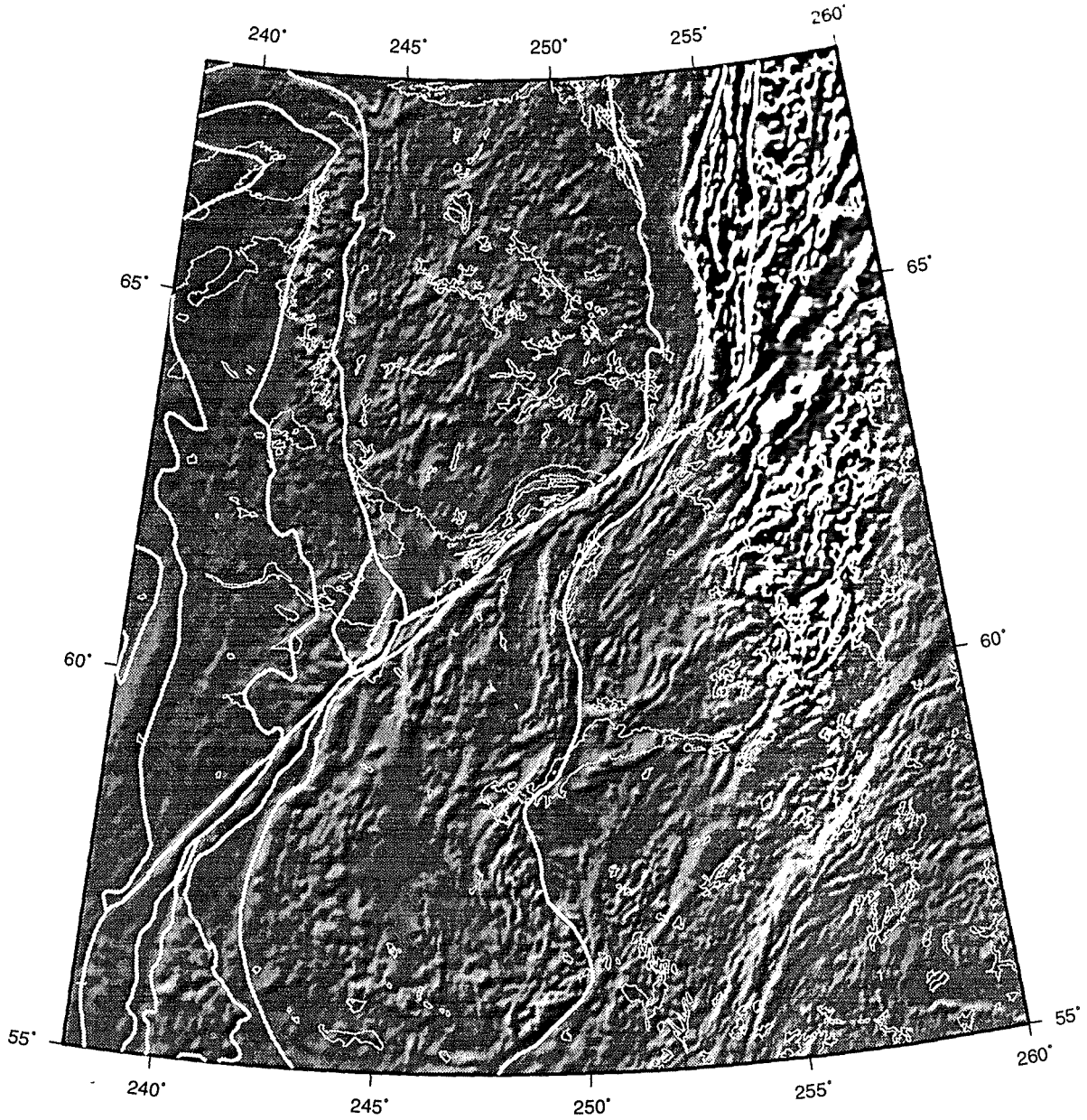

Figure 2 -- Regional magnetic data over the Great Slave Shear Zone with simplified tectonic boundaries, for use in the digital reconstruction of the fault geometry in plan view.

A regional seismic line across the Liard Depression: Possible indications of Proterozoic strata involvement in Mackenzie Mountain foreland deformation.

Hodder, Denise N., Department of Geology and Geophysics, University of Calgary

(hodder@geo.ucalgary.ca)

Currie, Lisel D., Geological Survey of Canada, Calgary

(lcurrie@gsc.NRcan.gc.ca)

A regional seismic line in the southern Mackenzie Mountains provides an excellent opportunity to examine the subsurface geology and structural relationships within an east-west section of the Paleozoic Liard Depression. Seismic data were acquired in the summer of 1995 by BFR Geophysical Consultants Ltd., who have generously made these data available to the authors for interpretation. Our interpretation incorporates surface geology and well log data from three nearby wells.

Devonian to Cretaceous age rocks are exposed at the surface. Rocks as old as the Middle Devonian Nahanni Formation have been identified on well logs, but due to shallow well penetration, little is known about the correlation of reflectors below the Nahanni Formation. However, a group of strong reflectors separating coherent reflectors above from the non-coherent reflectors below is interpreted to represent the Proterozoic-Paleozoic unconformity. The strong reflectors dip to the west in the eastern portion of the seismic line, where they are interpreted to represent an original change in slope in a westward deepening basin. Farther west, these reflectors dip to the east. This change in orientation is interpreted to be structurally controlled, with minor pull-up beneath the anticlines.

In general, stratigraphic units maintain relatively constant thicknesses across the section, albeit with some thickening in the cores of anticlines. The upper Devonian to Mississippian Besa River Formation also appears to thicken west of the Kotaneelee Anticline, where clinoforms that show west-directed sediment transportation are imaged.

Three anticlines with contrasting vergence are exposed at the surface and imaged by the seismic data; from east to west they are the Liard, Kotaneelee and the La Biche anticlines. In the eastern portion of the seismic line, east of and below the Liard Anticline, an easterly directed triangle zone is carried on a thrust that appears to root in the Proterozoic-Paleozoic unconformity, just west of the inferred shelf/slope

break. On the west flank of the Liard anticline, and structurally above the triangle zone, there is an east verging fault with small displacement that terminates near the core of the Liard Anticline. In contrast, the Kotaneelee Anticline verges toward the west. In the core of the Kotaneelee Anticline, structural thickening is apparent in both the Besa River Formation, and in the interval between the Nahanni reflector and the Proterozoic-Paleozoic unconformity. The La Biche Anticline contains both east and west verging structures. East verging faults with minor offset reach the surface on the west flank, and in the core of this anticline. Beneath the anticline, the Nahanni reflector is duplicated by a west verging fault. West of the La Biche Anticline stratigraphic units are relatively flat lying.

The easterly dip of the inferred Paleozoic-Proterozoic boundary between the La Biche and Kotaneelee anticlines is thought to involve post-Early Cretaceous uplift of Proterozoic strata because the clinoforms in the overlying Besa River Formation are presumed to have been deposited on a shallow west-dipping slope, and because mid-Cretaceous strata are involved in the deformation. Future work will be directed toward determining the nature of deformation below the Paleozoic-Proterozoic unconformity, and the cause of the change from dominantly easterly vergence in the east to primarily westerly vergence in the west.

Crustal Structure Along The ACCRETE Corridor

Hollister, L.S. (1) , Morozov, I. (2), Smithson, S. (2), Das, T. (1), Diebold, J. (3), Andronicos, C.(1), and Chardon, D. (1). linc@geo.princeton.edu

(1) Department of Geosciences, Princeton University, Princeton, NJ 08544
(2) Department of Geology, University of Wyoming, Laramie, Wyoming 82071
(3) Lamont-Doherty Earth Observatory, Columbia University, Palisades, NY 10964

We present the crustal structure of the entire 260 km long ACCRETE corridor along the border between SE Alaska and British Columbia. Multichannel seismic reflection profiles, acquired in Dixon Entrance and Portland Canal by R/V EWING in 1994, imaged crustal reflectors and Moho across the fundamental structures separating the Alexander terrane and Stikinia. We also imaged P-wave velocity structure and reflectivity using travel-time tomography, forward ray tracing and mid-point stacking of the wide-angle reflection/refraction seismic dataset. The seismic data sets are integrated with surface geology providing constraints on crustal structure from the surface to the Moho.

The stacked Moho reflector correlates well with the ray tracing model and multi-channel seismic section. The eastern margin of the Alexander terrane features strong crustal reflectors, mostly dipping gently WSW. Moho reflections within this zone are stronger and more continuous than those seen in the terranes to the east. West of the Coast shear zone (CSZ; it is one of the fundamental structures separating terranes), Moho is about 25 km in depth. NE of the CSZ, within a lateral distance of 30 km or less, the Moho deepens from about 25 km to 32 km. It shallows gently between 40 km to 70 km further NE of the CSZ, after which it deepens gradually, reaching a depth of about 36 km under the Skeena fold and thrust belt.

Several reflectors, which dip about 30-40 degrees NE, are imaged within the crust west of the CSZ. One of these reflectors is reliably traced from the near surface to the Moho under the surface exposure of the CSZ. These reflectors probably correspond to the west verging mid-Cretaceous thrust system. In the upper crust of the Coast Plutonic Complex (CPC), several reflectors dipping at about 20-25 degrees NE may correspond to a deformation fabric related to 50-53 Ma extension of the CPC. The termination of a number of prominent mid- and lower crustal reflections within the CPC reveals a discontinuity of the reflectivity in the vicinity of the CSZ. These reflectors may correspond to mafic to intermediate composition, shallow north dipping sills mapped at the surface that project to the line of seismic section

The Eocene Kasiks sill complex, consisting of a minimum 7 km thickness of shallow dipping sills, produced ~1/5 the total thickness of the present continental crust in the CPC. Detailed structural data show that the sills intruded during subvertical shortening partitioned into two directions of extensional shearing. Two kinematic domains record this partitioning. The first, along the eastern edge of the sills, records top to the northeast normal shearing. A second domain dominates the central and western parts of the complex and records top to the north-northwest normal shearing. This domain projects to the zone of lower crustal reflectors and relatively high P-wave velocities seen in the line of seismic section. Northeast directed greenschist facies shear zones overprint magmatic structures

suggesting northeast directed shearing outlasted north-northwest directed shearing. Pb/U ages (Andronicos et al, 1997) fix the sill emplacement and exhumation to between 50 and 53 Ma. The geochronologic data combined with the localization of extensional strain during decreasing temperatures suggests intrusion of the sills was synchronous with and may have triggered exhumation of the high-grade root of the CPC. Intrusion of these syn-kinematic sills suggests magmatic accretion during extension was a significant process for crustal formation of the CPC.

We conclude from the combined geologic and seismic datasets that the crust of the CPC was thickened between 53 and 50 Ma by magmatic inflation of the lower crust; the thickening was accompanied by substantial removal of the upper crust by tectonic exhumation.

Reference:

Andronicos, C.L., Chardon, D., Hollister, L.S., Gehrels, G., and Isachsen, C., 1997, Formation of Continental Crust by Magmatic Accretion During Late Orogenic Extension. EOS, v. 78, no. 46, p. F629.

BLUESCHIST METAMORPHISM WITHIN THE BRIDGE RIVER COMPLEX, GOLDBRIDGE, B.C.

Hozjan, David J., & Ghent, Edward D., *Department of Geology and Geophysics, University of Calgary, Calgary, Alberta, T2N 1N4*

The Bridge River Terrane, within the Coast Belt of the Canadian Cordillera near Goldbridge, British Columbia (51° 52'N, 122° 50'W), is the host to lenses of blueschist facies rocks. Studies by Garver et al. (1989) and Schiarizza et al. (1989, 1993) have documented five distinctive fault-bounded blocks of blueschists in the area, ranging in size from 0.2 - 1.5 km^2 and occurring in a discontinuous belt approximately 14 km in length. The characteristic lithology being a dark blue, fine-grained, foliated and commonly crenulated phyllitic to schistose rock with glaucophane, lawsonite and quartz. Also present in the blocks is the Bridge River greenstone, a massive to foliated unit displaying relict igneous minerals and textures yet commonly containing lenses and foliae of blueschist minerals (Schiarizza et al., 1995). $^{40}Ar/^{39}Ar$ dating of white mica in the blueschists by Archibald et al. (1991) indicate that the blueschist metamorphic event in the area ended at approximately 230 Ma. Recent petrographic analysis of the blueschist facies rocks demonstrates a variation in metamorphic grade among the blocks. The western blueschist blocks, found in the area around North Cinnabar Creek have a mineral assemblage consisting of glaucophane + epidote + garnet + muscovite. Blueschists further to the east, in the Tyaughton Creek area, have a mineral assemblage consisting of glaucophane + lawsonite + jadeite + quartz + stilpnomelane. The garnet + epidote bearing rocks could indicate higher metamorphic and/or lower P_{H2O} conditions compared to those blueschists lacking these minerals.

U-PB GEOCHRONOLOGIC DATA FROM THE WEST FLANK OF THOR–ODIN DOME, MONASHEE COMPLEX, B.C.

Johnston, D.H. [1], Crowley, J.L. [2], Williams, P.F. [1], Carr, S.D. [2], and Brown, R.L. [2]

[1]Department of Geology, University of New Brunswick, Fredericton, NB E3B 5A3;

[2]Ottawa-Carleton Geoscience Centre and Department of Earth Sciences, Carleton University, Ottawa, ON K1S 5B6

U-Pb isotopic data from rocks in Thor–Odin dome, a major antiformal culmination of high-grade metamorphic rocks in the Monashee complex of southeast British Columbia, constrain the timing of metamorphism and deformation in three different structural levels. A 3 km thick panel of rock, in which the regional transposition foliation (S_2) consistently dips to the west, defines the west flank of the dome. In the upper part of this panel lies the 1.5–2.0 km thick Greenbush Lake shear band zone (GLSBZ) that contains top-to-west D_5 extensional shear bands and an S_2 foliation that was reactivated and modified during D_5 extension. West of the GLSBZ lies the inferred boundary between the Monashee complex and the structurally overlying Selkirk allochthon. F_3 folds in the complex verge NE and D_3 fabrics are top-to-NE, whereas in the allochthon F_3 folds verge SW.

Ten samples were collected from lower structural levels of Thor–Odin dome (below the GLSBZ, at Blanket Mountain), from higher levels of the dome (within the GLSBZ, at Grizzly Flats), and in the overlying Selkirk allochthon (at Joss Mountain). The location of these samples is shown in Figure 1. A major conclusion made from our U-Pb data is that the metamorphic thermal peak in the allochthon predates the thermal peak in the dome by ~30 Ma. Single-grain monazite analyses from a migmatitic pelitic schist from Joss Mountain yield concordant U-Pb dates of 90-84 Ma, whereas monazite analyses from two migmatitic schists from Blanket Mountain are concordant at 57-55 Ma. These dates are interpreted as ages of metamorphic monazite growth, which is assumed to have occurred during the thermal peak. A pegmatite from Blanket Mountain that occurs in the neck of a boudin that formed on the limb of a large F_1/F_2 fold also yields U-Pb dates of ~55 Ma. These grains are interpreted as having an igneous origin based on their high U concentration and euhedral shape. An intrusion age of ~55 Ma requires that S_2 development was in progress at ~55 Ma and F_3/D_3, F_4, and most of D_5 occurred between then and ~52-50 Ma, the age of three undeformed pegmatite/aplite dykes from Blanket Mountain and Grizzly Flats. The ages of the dykes were interpreted from monazites with igneous characteristics (e.g., high U concentration and euhedral shape). We recognize that this interpreted timing is problematic because it requires rapid deformation events. Additional dating of syn-F_1/F_2 intrusives is needed to test our interpretation.

Zircon and titanite were dated from a hornblende orthogneiss from Grizzly Flats; the orthogneiss has a foliation that parallels the locally reactivated S_2 and lies within the GLSBZ. One single-grain zircon analysis is concordant at 56.5 Ma and five other analyses are discordant. Regression of the discordant analyses through 56.5 Ma yields upper intercept ages that are coeval with Proterozoic zircons dated elsewhere in southeast B.C.. Two multigrain titanite fractions overlap in age with the 56.5 Ma zircon. The tectonic significance of these data hinges on whether the zircons and titanites are igneous or metamorphic. If the grains are igneous, as is suggested by the prismatic and elongate shape of the zircons, then the protolith of the orthogneiss intruded at 56.5 Ma and significant deformation is younger. In this interpretation the discordant zircons contain inherited Proterozoic material. If the grains are metamorphic, then the protolith is probably Proterozoic and an episode of metamorphic zircon and titanite growth occurred at 56.5

Ma. Our preliminary petrographic analysis indicates that titanite and zircon were transposed into the dominant foliation. Thus, regardless of the origin of these grains, we propose that development of the regional foliation and recrystallization occurred, at least in part, after 56.5 Ma. Additional work, such as backscattered electron imaging, will be carried out to test whether the grains were transposed or simply grew after the deformation along a preexisting foliation.

These data from the west flank Thor–Odin dome are consistent with the pattern of structurally downward younging thermal peak ages that was previously documented in the Selkirk allochthon and northern Monashee complex. Our data demonstrate that a significant time gap in the thermal peak ages occurs over a narrow structural thickness, in the poorly exposed terrain between Joss Mountain and the GLSBZ at Grizzly Flats (Fig. 1). We suggest that this ~30 Ma age break is due to an omission of section that may have resulted from ductile extensional deformation in the GLSBZ and from normal-sense displacement on the brittle fault between Joss Mountain and Grizzly Flats (Joss Pass fault).

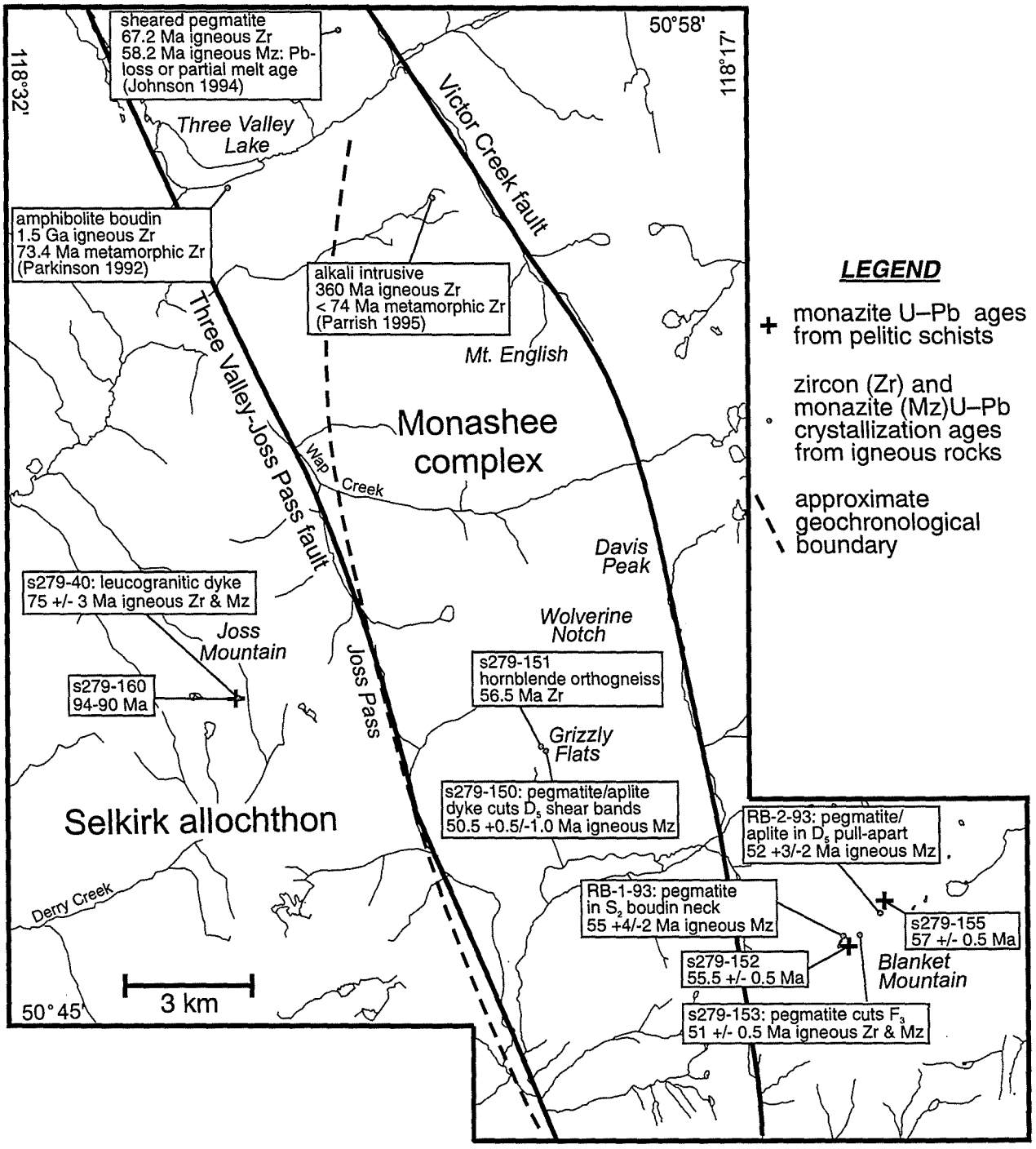

Figure 1. Map of the study area showing interpreted U–Pb ages from this study and previous studies. Note that relatively young igneous cystallization ages and young monazite ages from pelitic schists occur east of Joss Pass and Three Valley Lake (dashed line).

References:

Johnson, B.J. 1994. Structure and tectonic setting of the Okanagan Valley fault system in the Shuswap Lake area, southern British Columbia. Ph.D. thesis, Carleton University, Ottawa, Ont.

Parkinson, D.L. 1992. Age and tectonic evolution of the southern Monashee complex, southeastern British Columbia: a window into the deep crust. Ph.D. thesis, University of California, Santa Barbara, California.

Parrish, R.R. 1995. Thermal evolution of the southeastern Canadian Cordillera. Canadian Journal of Earth Sciences, 32: 1618-1642.

MICROSTRUCTURAL, PETROLOGICAL AND GEOCHRONOLOGICAL STUDIES ON THE THOR-ODIN DOME, MONASHEE COMPLEX, SOUTHERN CANADIAN CORDILLERA; PROPOSED PH.D. RESEARCH.

Kuiper, Yvette D.
Department of Geology, University of New Brunswick, Fredericton, N.B., E3B 5A3 and Department of Earth Sciences, Carleton University, Ottawa, Ontario, K1S 5B6.

The basement-cored Monashee Complex of the southern Omineca Belt comprises two structural culminations; Frenchman Cap in the north and Thor-Odin in the south. The Selkirk Allochthon, which structurally overlies the Monashee Complex has been interpreted as having been emplaced onto the Monashee Complex by NE-directed transport on the Monashee Décollement (Brown et al., 1986, 1992).

The location and the character of the décollement are based on lithologic, metamorphic, structural, geochronologic and regional arguments from a number of segments studied on the flanks of both Frenchman Cap and Thor-Odin domes (Journeay, 1986; Brown et al., 1986, 1992, and references therein; McNicoll and Brown, 1995, and references therein). However, recent work by Williams, Spark, and Johnston on the western flank of Thor-Odin has failed to reveal the décollement. Instead, a zone of uniform transposition extending throughout the exposed depth of the complex is observed. Transposition was followed by younger folds, E-W boudinage and regional extension (Johnston et al., 1996; Johnston, 1997; Spark, 1997).

U-Pb data indicate a younging of structures and thermal peak of metamorphism with decreasing structural level in the Selkirk Allochthon and Monashee Complex (Parrish, 1995, and references therein; Crowley, 1997; Gibson, 1997; Carr, 1992). Data from western Thor-Odin show the same pattern (Johnston, 1997; Johnston et al., this volume). Ages are 94-90 Ma in the Selkirk Allochthon west of the Joss Pass brittle fault and are ~58-50 Ma in the Monashee Complex east of the Joss Pass fault. The apparent downward younging pattern may have resulted from either 1) downward heat conduction from an overthrusted hot crustal slab with or without hot intrusions, 2) the juxtaposition of rocks with different metamorphic grades and ages by thrusting, normal faulting, or folding, or 3) a combination. On the western flank of Thor-Odin, more data are required to establish the variation of metamorphic grade and age with structural depth, to test whether there is a gradient or whether there are two age domains present, and to prove or disprove whether or not there is an inverted metamorphic sequence in this part of the complex.

Detailed metamorphic and U-Pb geochronology studies will be conducted on the northwest and west flanks of Thor-Odin in order to characterize the protolith age of rocks as well as the conditions and timing of deformation, high-temperature metamorphism and cooling history at all structural levels and on both sides of identified structures. This may: 1) allow Selkirk Allochthon and Monashee Complex rocks to be distinguished, 2) establish the presence or absence of the Monashee Décollement as a syn- or post-F_1 structure, 3) deduce the thermal history throughout the structural profile, 4) place some constraints on the magnitude of

displacement of structural discontinuities, 5) test ideas as to whether or not Frenchman Cap and Thor-Odin are at the same structural level, and 6) test existing tectonic models for the area (cf. Johnston et al., this volume; Parrish 1995, etc.). Research will be carried out under the supervision of P.F. Williams and S.D. Carr. This project will elucidate the structural relationships between the Monashee Complex and the Selkirk Allochthon, between the Frenchman Cap and Thor-Odin culminations, and distinguish between compressional and extensional fault systems.

References

Brown, R.L., Journeay, J.M., Lane, L.S., Murphy, D.C., and Rees, C.J. 1986. Obduction, backfolding and piggyback thrusting in the metamorphic hinterland of the southeastern Canadian Cordillera. Journal of Structural Geology, 8: 255-268.

Brown, R.L., Carr, S.D., Johnson, B.J., Coleman, V.J., Cook, F.A., and Varsek, J.L. 1992. The Monashee Décollement of the southern Canadian Cordillera: a crustal-scale shear zone linking the Rocky Mountain Foreland Belt to lower crust beneath accreted terranes. In Thrust Tectonics. Edited by K.R. McClay. Chapman & Hall Ltd., London, pp. 357-364.

Carr, S.D. 1992. Tectonic setting and U-Pb geochronology of the early Tertiary Ladybird leucogranite suite, Thor-Odin - Pinnacles area, southern Omineca Belt, British Columbia. Tectonics, 11: 258-278.

Crowley, J.L. 1997. U-Pb geochronology in Frenchman Cap dome of the Monashee complex, southern Canadian Cordillera: early Tertiary tectonic overprint of a Proterozoic history. Ph.D. thesis, Carleton University, Ottawa, Ontario, 219 p.

Gibson, H.D. 1997. Thermotectonic evolution of the northern Monashee Complex, southern Omineca Belt, southeastern British Columbia. M.Sc. thesis, Carleton University, Ottawa, Ontario, 111 p.

Johnston, D.H., Williams, P.F., and Spark, R.N. 1996. Comments on the Monashee Décollement, Thor Odin culmination of the Monashee Complex, southern Omineca Belt, southeastern B.C. LITHOPROBE report No. 50. 1996 SNORCLE and Cordilleran Tectonics Workshop, Calgary, AB, 159.

Johnston, D.H. 1997. Structural and thermal evolution of northwest Thor-Odin Dome, Monashee Complex, southeast British Columbia. Ph.D. thesis, University of New Brunswick, Fredericton, New Brunswick, 317 p.

Johnston, D.H., Crowley, J.L., Williams, P.F., Carr, S.D., and Brown, R.L. 1998 (this volume). U-Pb geochronologic data from the west flank of Thor-Odin dome, Monashee Complex, B.C. LITHOPROBE report, in press. 1998 SNORCLE and Cordilleran Tectonics Workshop, Vancouver, B.C.

Journeay, J.M. 1986. Stratigraphy, internal strain and thermo-tectonic evolution of northern Frenchman Cap dome: an exhumed duplex structure, Omineca hinterland, S.E. Canadian Cordillera. Ph.D. thesis, Queen's University, Kingston, Ontario, 401 p.

McNicoll, V.J., and Brown, R.L. 1995. The Monashee décollement at Cariboo Alp, southern flank of the Monashee complex, southern British Columbia, Canada. Journal of Structural Geology 17: 17-30.

Parrish, R.R. 1995. Thermal evolution of the southern Canadian Cordillera. Canadian Journal of Earth Sciences, 32: 1618-1642.

Spark, R.N. 1997. Crustal thickening and tectonic denudation within the Thor-Odin culmination, Monashee Complex, southern Canadian Cordillera. Ph.D. thesis, University of New Brunswick, Fredericton, New Brunswick, 407 p.

Magnetic constraints on Tertiary deformation in central British Columbia.

C. Lowe, R.J. Enkin, J. Dubois, L.Struik, J. Baker and R.G. Anderson
GSC-Pacific, P.O. Box 6000, 9860 West Saanich Road, Sidney, B.C. V8L 4B2

Abstract

It has been proposed that the Nechako Plateau NATMAP project area in central British Columbia records a significant history of Tertiary transtensional deformation. Here we examine the magnetic signature and paleomagnetic record of rocks in a 1300 km^2 area encompassing the Endako molybdenite deposit for evidence of this deformation. Magnetic anomaly and rock property data indicate subtle age differences among exposures of the Eocene Ootsa Lake Group. In addition they provide valuable information on mineralogical differences within lithologically similar units of the Jura-Cretaceous Francois Lake Plutonic Suite which hosts the Endako orebody.

Mapped faults, in and adjacent to the mine, predominantly trend northeast and northwest and typically correspond to linear zones of high magnetic gradient. Based on this, we interpret other prominent northeast- and northwest-trending magnetic lineaments to be shallow faults as well, which divide the region into fault-bounded blocks. Several of these interpreted faults cut units of the Eocene Ootsa Lake Group, as well as, the Eocene-Oligocene Endako Group.

Within the Endako Mine, paleomagnetically-determined tilts on Eocene dykes are aligned with ore-bearing veins, indicating Tertiary deformation. We recognize a kilometre-scale anticline within the pit (Fig. 1). Outside the mine area and to the east of the Casey magnetic lineament, similar down to the southeast tilts are recorded. To the west of the Casey magnetic lineament, tilts are somewhat more random but generally indicate tilting in both directions about a northwest strike.

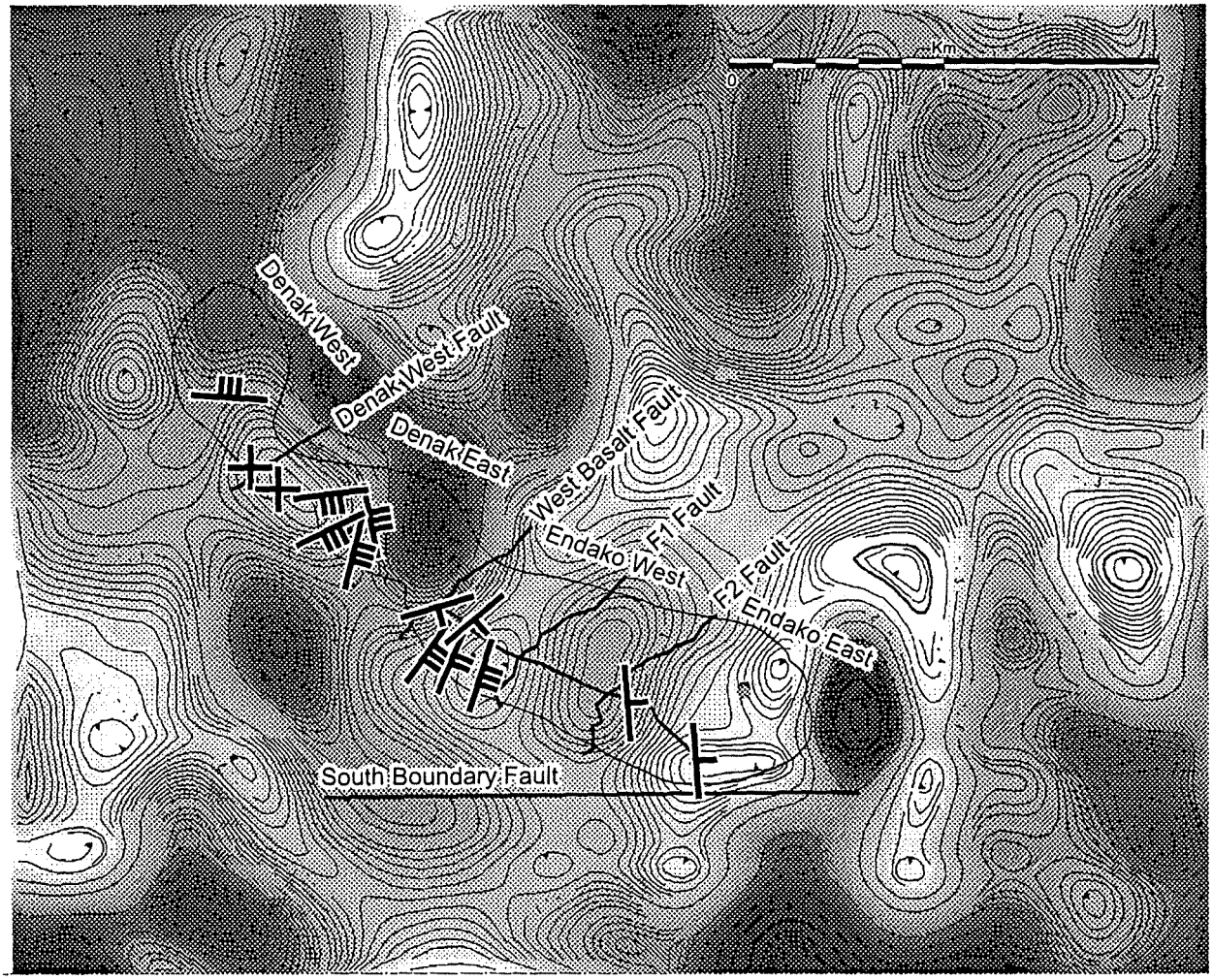

Fig. 1: *Vertical derivative aeromagnetic data and paleomagnetically-determined tilts around the Endako Mine in central British Columbia. The extent of the mine is indicated by a thin black line and the faults which separate it into four distinct pits (Denak West, Denak East, Endako West and Endako East) are indicated by thick black lines. Note that each of the four fault-bounded pits in the mine is roughly a rigid body. The observed rotation of tilts follows the orientation of ore-bearing veins, suggesting that the Jurassic veins were initially emplaced parallel, and were rotated during or after the Eocene.*

Late Cretaceous to Early Tertiary Tectonics, Magmatism and Mineral Deposits, Central British Columbia

D.G. MACINTYRE AND L.J. DIAKOW

B.C. Geological Survey Branch, Victoria, B.C.

Late Cretaceous and Eocene plutons, comagmatic volcanic rocks and associated porphyry copper deposits occur in a broad north to northeast trending belt that transects the Stikine Terrane in central B.C. This belt, here named the Skeena porphyry belt (SPB), roughly parallels the Skeena Arch and is bounded to the northwest by the Jura-Cretaceous Bowser Basin and to the southeast by volcanic cover of the Eocene and younger Chilcotin extension complex. The SPB contains a number of distinct plutonic suites and associated volcanic rocks all of which are calc-alkaline in composition.

The SPB represents the remains of a broad, north trending magmatic arc that was built on folded and uplifted Stikine terrane and its Late Jurassic to Mid Cretaceous sedimentary cover. Remnants of this arc include the Late Cretaceous volcanics of the Kasalka Group and the Eocene Newman volcanics. The plutonic roots of this arc are represented by the Late Cretaceous Bulkley intrusions and the Eocene Babine, Nanika, and Kastberg intrusions. Important porphyry copper deposits including Huckleberry, Berg, Glacier Gulch, Granisle, Bell and Morrison are associated with these intrusions. Southeast of this arc, and in part overlapping it, are rhyolitic and basaltic volcanics and high level intrusions of the Eocene Ootsa Lake and Endako Groups. Important epithermal vein systems are associated with these rocks. Further to the southeast, into the Interior Plateau, Eocene and older rocks are covered by extensive plateau basalts of the Miocene Chilcotin Group.

The Late Cretaceous and Eocene igneous rocks are similar in composition and lithology and are interpreted to represent the remains of a long-lived Andean type calc-alkaline magmatic arc that formed above a west dipping subduction zone. Isotopic age dating indicates that the arc had a long magmatic history beginning around 95 Ma and extending to around 50 Ma. This age range in part overlaps that of the Laramide porphyry belt in the U.S. Cordillera which has plutonic ages ranging from 75 to 45 Ma. During this period magmatic arcs developed at various times throughout the length of the Cordillera from Alaska to Mexico. In the SPB, as in other parts of the Cordillera, magmatism was episodic and emplacement of plutons and construction of volcanic cones occurred at different times and locations within the belt. Clusters of plutons are common and appear to be related to the development of volcanic pull apart basins. Both Late Cretaceous and Eocene plutons can occur in the same geographic area and emplacement may have been controlled by the same deep crustal fault systems. Southeast of the arc, broad volcanic fields characterized by biotite-hornblende phyric rhyodacite, andesite and basalt flows and related pyroclastic rocks of the Eocene Ootsa Lake and Endako Groups were formed. Recent geochronologic studies conducted as part of the Nechako NATMAP project indicate these rocks may be a few million years younger than the youngest porphyritic andesite members associated with the SPB. The locus of magmatism continued to migrate southeastward culminating with extrusion of extensive sheets of Miocene plateau basalts of the Chilcotin Group which now cover much of the southern Interior Plateau..

The occurrence of thick piles of porphyritic andesite within rectilinear, north trending grabens, suggest the grabens have a volcanic origin and may be the remains of cauldron subsidence complexes or volcanic basins. This is supported by the occurrence of rhyolite and diorite dikes that typically parallel the area of subsidence. Locally, high level, porphyryitic stocks intrude volcanic fill within the basins. The basins are interpreted to be pull-apart structures developed along north trending dextral strike-slip faults. These faults formed during a period of shallow, northeast directed, oblique subduction of oceanic crust beneath the North American plate. Extension of the crust resulted in emplacement of magma to progressively higher crustal levels.

The SPB and the Interior Plateau to the southeast have been subjected to Eocene or younger crustal extension. This extension is manifested by southeast tilting, subsidence and rotation of fault blocks containing rocks as young as Eocene. The areas of maximum extension are believed to be bounded by parallel dextral strike slip faults although these faults are almost always covered. In one area of extension south of Vanderhoof, a metamorphic core complex evolved between 55 and 45 Ma.

GEOCHRONOLOGICAL AND GEOCHEMICAL STUDIES OF THE COATES LAKE DIATREME, SOUTHERN MACKENZIE MOUNTAINS, WESTERN N.W.T.

James K. Mortensen (Earth & Ocean Sciences, UBC, Vancouver, B.C., V6T 1Z4, jmortens@eos.ubc.ca) and **Maurice Colpron** (GNWT, Box 1320, Yellowknife, N.W.T., X1A 2L9, maurice_colpron@gov.nt.ca)

The Coates Lake diatreme is a small (~10 m diameter) body that intrudes strata of the Neoproterozoic Redstone River Formation at the southern end of Coppercap Mountain in the southern Mackenzie Mountains. The diatreme is unique in this area because it contains a wide variety of xenoliths, including (in order of decreasing abundance) medium-grained granitoids, quartzite, limestone, actinolite-chlorite-calcite rock, greenstone, metadiorite and metagabbro. Narrow mafic dykes that locally contain smaller crystalline xenoliths occur near the diatreme and in several localities elsewhere on Coppercap Mountain, and are apparently comagmatic with the diatreme. The igneous and meta-igneous xenoliths in the Coates Lake diatreme are interpreted to have been derived from local basement and as such represent the only physical sample that exists of the crystalline basement underlying this region (Nahanni terrane). A U-Pb zircon age of ~1140 Ma was previously determined by Jefferson and Parrish (1989) for a granitoid xenolith from the diatreme, raising the possibility that at least part of the basement of the Nahanni terrane is broadly Grenvillian in age.

The goals of the present study are, 1) to conduct detailed U-Pb geochronology and geochemistry of a number of crystalline xenoliths in the diatreme to better constrain the nature and age of the underlying basement in this area, and 2) to attempt to geochemically characterize the magmatic component of the diatreme ande associated dykes in order to facilitate comparison and correlation with other mafic dykes and diatremes elsewhere in the Mackenzie Mountains. Initial U-Pb dating results for zircons from two granitoid xenoliths from the diatreme give an age of 1128.7 +3.9/-3.5 Ma, confirming the presence of Grenvillian-age rocks in the Nahanni terrane basement.

THE SOUTHEASTERN DORSEY TERRANE: CHARACTERISTICS AND CORRELATIONS

By JoAnne Nelson, B.C. Geological Survey, Tekla Harms, Department of Geology, Amherst College, and James Mortensen, Department of Earth and Ocean Sciences, University of British Columbia

INTRODUCTION

This paper reports on the results of field mapping and radiometric dating in an area along the southeastern margin of the Dorsey Terrane, near the Cottonwood River in Jennings River map area (104O). Comparisons are drawn between one of the assemblages within it and other allochthonous assemblages of far northern B.C. and southern Yukon that contain high-grade metamorphic rocks and Devono-Mississippian and Permian intrusions.

The Dorsey Terrane has been divided into several assemblages (Harms and Stevens, 1996). The lower Dorsey Terrane in the southern Yukon comprises the Ram Creek and Dorsey assemblages. The structurally lowest Ram Creek assemblage is a suite of mafic and intermediate to felsic metavolcanic rocks with lesser quartzite, marble and metaplutonic bodies. The overlying Dorsey Assemblage (Figure 1) consists of quartzose, pelitic, mafic (to possibly felsic, muscovite-quartzite?) metavolcanic and intermediate metaplutonic rocks, which underwent high-temperature, high-pressure metamorphism (609-732°C, 7.7-14.1 kilobars) prior to emplacement of the mid-Permian Ram Stock (Stevens, 1996). The Dorsey assemblage shares a number of common elements with the Yukon Tanana Terrane, including its general pericratonic character and the presence of mid-Permian and Early Jurassic(?) intrusions (Stevens, 1996). The Dorsey assemblage is overlain structurally by the Klinkit and Swift River assemblages, which show lower metamorphic grades and less penetrative deformation (Stevens and Harms, 1995, Harms and Stevens, 1996). Fossil ages in these upper assemblages of the Dorsey Terrane range from late Mississippian to Triassic (Harms and Stevens 1996). Limestones at different structural levels contain Pennsylvanian conodonts (Abbott, 1981): this may indicate fault and/or fold repetition.

On the eastern side of the Dorsey Terrane, the Klinkit and Swift River assemblages lie structurally above the Dorsey Assemblage in a southwesterly dipping structural stack (Stevens and Harms, 1995; Stevens, 1996). There is regional dip reversal within the Klinkit Assemblage, such that northeast-dipping low-grade chert, quartz sand-stone, slate and tuff in its western extent lie structurally above metamorphic rocks of the Big Salmon Complex (Gabrielse, 1969; Abbott, 1981; Mihalynuk *et al.*, 1998). It consists of a sequence of stratified rocks cut by a highly deformed pluton, the Hazel orthogneiss (Mihalynuk *et al.*, 1998). All of the units, including the Hazel orthogneiss, have been metamorphosed at grades ranging from greenschist to amphibolite, and all have undergone several episodes of folding. The Big Salmon Complex was assigned to the Slide Mountain Terrane by Wheeler *et al.* (1991); Harms and Stevens (1996) termed it the Hazel assemblage and suggested a correlation with the Yukon-Tanana Terrane, with which it lies directly along strike. Mihalynuk *et al.* (1998) document this correlation. Although no age is yet available for the Hazel orthogneiss, it may be equivalent to Early Mississippian tonalites that intrude the Yukon Tanana Terrane (Kootenay Terrane) in Teslin map-area (Gordey and Stevens, 1994).

LOCAL GEOLOGY

In the central Jennings River map area, the structurally lower part of the Dorsey Terrane is represented by four distinct lithologic packages in two or more separate thrust panels. They rest structurally on metamorphosed basinal strata that resemble rocks of the Kechika Trough and are assumed to represent the outer fringes of the Cassiar Terrane, the western edge of the North American passive continental margin. Near the headwaters of the Cottonwood River the basal contact of the allochthons over presumed continental margin strata is a dramatic juxtaposition of green rocks above black rocks, exposed in cirque walls and mountainsides over tens of kilometres.

Field mapping in 1997 identified three separate units in the lower Dorsey Terrane (Figure 2). From structurally lowest to highest they are the following:

1. "Greenstone-intrusive unit": Greenschist-grade intermediate to mafic metatuff, pyritic felsic metatuff, and tonalite/quartz diorite

2. "Metasediment-amphibolite unit": This unit consists of a lower, amphibolite-dominated part (2L on Figure 3) and an upper metasedimentary part (2U on Figure 3). The contact between the two, albeit tectonised, appears to be gradational. The lower part consists of amphibolite and garnet amphibolite, interlayered (interbedded?) with metatuffs, fine grained quartzite, biotite-muscovite±graphite schist, and quartzofeldspathic schist (metamorphosed chert, argillite and orthoquartzite, respectively), and marble. The upper part consists of thinly layered impure quartzite with biotite-muscovite partings (meta-argillite), thin bedded limestone, dark grey meta-chert; and interlayered chlorite±muscovite±garnet schist and quartz-muscovite schist that probably represent intermediate to felsic tuff protoliths. Both the upper and lower parts of this unit are intruded by pods of deformed tonalite, diorite and gabbro. Ultramafic pods are restricted to the lower, amphibolite-dominated unit.

3. "Phyllitic metasedimentary unit": Phyllitic argillite, metaquartzite, limestone, metatuff, and diorite.

North American marginal strata

Dark grey to black slate to argillite are exposed extensively in the mountains north of the headwaters of the Cottonwood River (Figure 3). These rocks form a homoclinally southwest-dipping succession. At the base, a thick section of blocky to slabby-weathering slate and silty slate contains sparse beds of buff quartzite and white limestone. The siliciclastic rocks in this sequence are dark grey to black. They form rugged cliff outcrops and slabby to platey talus. Dark iron stains coat weathered surfaces. Muscovite is present on some bedding planes. In a few localities, large-scale current ripples are preserved on the bedding surfaces of thick-bedded silty slates. These features suggest correlation with the upper Proterozoic-Cambrian basinal rocks of the central Kechika Trough (for description see Ferri *et al.*, 1996). This unit is overlain by a few metres of black calcareous argillite, and then by a thick, monotonous unit of black, rusty-weathering, platey, carbonaceous, siliceous slatey argillite, black porcellanite, and at one locality, siltstone with graded beds. These two upper units closely resemble, respectively, the Ordovician-Lower Devonian Road River Group and the Devono-Mississippian Earn Group of the central Kechika Trough. More locally, they are probably correlative with exposures of siliceous, pyritic black argillite, pyritic and baritic chert, and limestone on the COT claims 15 kilometres to the south (Nelson, 1997).

A strongly foliated and lineated, highly heterogeneous pluton intrudes the base of the sequence, roughly following bedding and cleavage. It ranges from diorite to tourmaline-bearing granitic pegmatite. Fairly homogeneous granodiorite with plagioclase and/or orthoclase phenocrysts is interspersed with areas of gneissic, compositionally banded intrusive. The margins of the pluton are extensive sill complexes.

Structurally, the metasedimentary sequence is characterised by a ubiquitous, moderately southwest-dipping cleavage. Bedding parallels this cleavage, as shown in their general parallel attitudes in outcrop and in Figure 5, and microscopically by the limbs of isoclinal folds. An earlier crinkled cleavage, not parallel to the dominant cleavage, is seen only in thin section, preserved in the cores of andalusite porphyroblasts. Minor to mesoscopic, northeasterly-verging folds (F2) fold earlier tight to isoclinal folds in a few outcrops. These folds and also crenulations parallel the west-northwesterly regional strike (Figure 3). The youngest (F3) chevron-style folds, which refold F2 at a few localities, have southwesterly plunging axes with northwesterly vergence. Perhaps related to these, top-to-the-northwest shear, determined from C and S fabrics and asymmetrical pressure shadows around relict plagioclase phenocrysts, was noted at in granite at one locality along the margin of the pluton. Sills and dikes related to the pluton are involved in F2 and F3 folds, and foliation in the pluton is parallel to that in the surrounding rocks (Figure 3), indicating that it had been emplaced prior to much of the deformation.

Metamorphic andalusite and cordierite are widespread throughout the metasedimentary sequence. Their distribution bears no spatial relationship to the pluton. In some cases elongate andalusite porphyroblasts up to several centimetres in length show very little or no preferred orientiation. Andalusite cores, however, contain a crinkled cleavage that is not parallel to the dominant rock fabric. Their later growth follows crenulations, and the crenulations themselves are deflected around the porphyroblasts. These textural relationships indicate that andalusite growth occurred throughout a sequence of progressive deformation, and even outlasted it in some localities.

"Greenstone-intrusive unit"

The "greenstone-intrusive unit" forms the lowest of the allochthons in the Cottonwood River area (Unit 1 on Figure 2), resting directly above inferred Earn Group-equivalent strata on a surface that is very gently dipping over tens of square kilometres and truncates steeper cleavage and bedding in the autochthonous rocks below. It consists

of two lithologic suites: a supracrustal, metavolcanic suite, and a suite of heterogeneous intrusions. The metavolcanic suite consists primarily of metatuffs, mostly mafic to intermediate but with pyritic quartz-sericite schist (meta-rhyolite tuff) in places. Some of the felsic metatuffs contain recognizable primary quartz and/or plagioclase phenocrysts. Quartz-sericite schist localities are shown on Figure 2 by stars. Sedimentary components of the "greenstone-intrusive unit" include volumetrically minor grey argillite and grey to sea-green chert. The metavolcanic-metasedimentary suite is intruded by deformed plutonic bodies. They range from gabbro and diorite to tonalite and quartz diorite. Foliation in them is variably developed. It ranges from weak to protomylonitic, particularily near the base of the allochthon.

The "greenstone-intrusive unit" resembles the quartz-sericite schist-intermediate metatuff-limestone-chert sequence mapped near the headwaters of the Little Rancheria River (Nelson 1997). They are correlated on Figure 2, although the Little Rancheria sequence is isolated by Quaternary cover and Mesozoic plutons, and may be separated from the Cottonwood River allochthons by a major normal(?) fault. Similarities include: predominance of metatuffs and cogenetic high-level pre-tectonic intrusions, presence of pyritic quartz-sericite schist with plagioclase and less abundant quartz phenocrysts, and greenschist grade metamorphism with widespread biotite, chlorite, epidote and sericite. The Little Rancheria sequence contains an early Mississippian limestone (Nelson, 1997).

"Metasediment-amphibolite unit"

This unit overlies the "greenstone-intrusive unit" above a sharp, nearly flat contact (Figure 2), and is distinguished from it by strong contrasts in metamorphic grade and lithologic components. The "metasediment-amphibolite unit" is divided into a lower part and an upper part (Units 2L and 2U on Figure 2). The lower part contains thick, dark green tabular amphibolite bodies and small pods of ultramafic rock, both of which are absent in the upper part. Both upper and lower parts contain very siliceous metasedimentary rocks and marble interbeds. Chlorite phyllite (metamorphosed inter-mediate tuff?) and quartz-sericite schist (felsic metatuff?) commly occur together in the upper part. The contact between the upper and lower parts is gradational, and is mapped at the top of the highest amphibolite body.

Thick bands of amphibolite and garnet amphibolite form prominent cliffside and knob exposures in the lower part of the unit (unit 2L). In petrographic section, the amphibolites consist of lepidoblastic aggregates of forest green hornblende with interstitial albite and in some cases large splotchy garnet poikiloblasts; trains of rutile and ilmenite-magnetite are heavily overgrown by retrograde sphene. The amphibolites are interlayered with quartz-rich to pelitic metasediments, some of which display protolith textures that identify them as meta-argillites, metacherts, and quartz sandstones. Small amounts of thin-bedded marble are also present, interlayered with either meta-argillite or mafic (tuffaceous) rocks. A few thin units of quartz-muscovite schist within the amphibolite are may be meta-rhyolite tuffs, although there are no relict primary textures to support this assertion. Pods and slivers of ultramafic rock occur in the lower part of unit 2. Except for one fairly intact serpentinized harzburgite tectonite near its base, these have been metamorphosed along with their enclosing rocks. Original textures are generally obliterated and they appear as coarse aggregates of actinolite/tremolite and talc.

The relatively high metamorphic grade of the lower part of the unit is indicated by hornblende (±garnet±epidote)-plagioclase-quartz-rutile in meta-basites, and assemblages of coarse biotite-muscovite-quartz-feldspar in pelitic rocks. In thin sections of the mafic rocks, trains of rutile and (?)ilmenite of the peak metamorphic assemblage are heavily mantled by retrograde sphene.

The upper part of the "metasedimentary-amphibolite unit" overlies the amphibolite-bearing lower part along a lithologically gradational contact that is also a zone of comparatively strong deformation. This may be due to remobilization of an original depositional contact. Above the contact, siliceous schists are the most abundant rock type, and amphibolite and ultramafites are rare. Three rock types dominate the upper part of the unit: siliceous, platey-layered semipelites, which are probably meta-argillites and metacherts; thin-bedded limestone; and chlorite schist with quartz-sericite schist, which reflect a metamorphosed intermediate to felsic tuffaceous protolith. These components repeat across strike, probably because of fold and/or fault repetition; however without "way up" indicators and spotty exposure the exact mechanism of the thickening is not clear.

The metamorphic grade in the upper part of the unit is somewhat lower than in the lower part: chlorite-biotite±garnet±actinolite assemblages pre-dominate in metamorphosed intermediate tuffs, although this appears to be in part due to strong retrograde metamorphism in which garnet and biotite have partly to wholly reverted to chlorite.

The base of unit 2 exhibits widespread crystalloblastic textures and fabrics typical of metamorphic rocks, including coarse-grained, schistose, mica-rich rocks; compositionally banded orthogneiss; and foliated and lineated

amphibolite. The rest of the unit, including rocks of both the lower amphibolite-rich and the upper siliceous parts, is characterized by very fine grain size and a fabric of paper-thin, laterally continuous compositional bands and rodding typical of a zone of high shear strain.

Large, mountainside-scale recumbent folds occur within this unit, particularily in cliff exposures of the lower part, where compositional layering in amphibolite bodies outlines the noses of recumbent isoclines. Mesoscopic northeasterly-verging chevron folds with gently northwest-plunging axes also occur (Figure 3). On Figure 3, the axes of small-scale isoclinal, intrafolial folds and also mineral lineations form a diffuse girdle ranging from gently northwest-plunging to steeply southwest-plunging.

Paleozoic intrusions in the "metasediment-amphibolite unit"

Both the upper and lower parts of the unit are intruded by small mafic to tonalitic pods and sills, typically coarse grained diorites, gabbros, and white leucotonalite and granite (leucosome?), which themselves are strongly foliated, folded and refolded. A highly foliated and deformed tonalite to diorite pluton, mapped in 1996 (Nelson, 1997), intrudes rocks that are considered to be within the lower part of the unit (Figure 3). This body returned a U/Pb zircon age of 349.9 $\pm$ 4.2 Ma (Nelson *et al.* 1998). A small pegmatite body with a well-developed penetrative fabric is about 266 Ma by U/Pb zircon dating (results not fully final at time of writing). The presence of these Early Mississippian and Permian intrusions, in addition to the high metamorphic grade of this unit, suggests that it is a southerly continuation of the Dorsey Assemblage near the Seagull Batholith.

"Phyllitic metasedimentary unit"

This structurally highest unit overlies the upper part of the "metasediment-amphibolite unit" across a covered contact. In the northern part of the mapped area, where the two units are seen in closest proximity, bedding attitudes above and below the contact show some angular discordance: possibly they lie in faulted contact. The base of the "phyllitic metasedimentary unit" there (subunit "3a" on Figure 2) consists of medium to thick bedded buff-coloured micaceous orthoquartzites with interbedded grey slate and silty slate, a section typical of Early Cambrian siliciclastics of the miogeocline. A minor but notable feature of this section is one dismembered bed, 0.5 to 1 metre thick, of coarse quartz-feldspar grit that forms slump blocks in impure carbonate. Towards the southwest in continuous ridge exposure, the quartzite-pelite section passes gradationally upward into finer metasedimentary strata including grey phyllite and chert (subunit "b" on Figure 2).

The main exposures of the "phyllitic meta-sedimentary unit" are southwest of Parallel Creek. There, the unit is dominated by grey, black and light green phyllitic argillite with subordinate buff, dark grey, or white quartz grit and sandstone, and thin-bedded pale green to grey chert. A few prominent bands of recrystallized limestone are present. In one continuous layer, meta-diorite grades into amphibolite and metatuff.

The "phyllitic metasedimentary unit" shows less development of metamorphic minerals and textures than the underlying "metasediment-amphibolite unit". Garnet is not seen, except in the lowermost exposures of unit 3a northeast of Parallel Creek. The structural style of this upper unit reflects deformation at a higher crustal level than the lower units. Outcrop-scale concentric folds with axial planar cleavage are common, and multiple tiny crenulations typify the phyllitic argillites.

Structural style of the allochthonous units

Prevailing dips of bedding, compositional layering, cleavage and schistosity throughout the allochthonous units are moderately to the southwest (Figure 3). Ridge- and outcrop-scale isoclinal folds, common within the "metasediment-amphibolite unit", suggest that this uniformity results, at least in part, from isoclinal folding and accompanying axial planar fabric development. Axes of outcrop-scale isoclinal, intrafolial F1 folds and mineral elongation lineations throughout all of the allochthonous units have dominantly shallow west-northwest plunges but are variably dispersed about that trend within the plane of foliation (Figure 3). This pattern is consistent with the observed isoclinal folding. More open to chevron-type, in many cases northeasterly-verging minor folds refold the earlier cleavage and mineral lineations: they are designated F2. Their axes, which plunge gently to the northwest, do not coincide with the second-phase, northeasterly vergent minor folds in the North American sequence, which plunge gently to the southeast (Figure 3). On the other hand, the consistency of orientation of fabric elements throughout the allochthons in the study area suggests that all of them underwent a uniform orientation, if not degree, of deformation.

Correlations with units of the Dorsey Terrane in the southern Yukon

The "greenstone-intrusive unit", the lowest of the allochthons in central Jennings River area, occupies an equivalent structural position to the Ram Creek assemblage, which lies immediately above the Earn Group along the Swift River in southern Yukon (Stevens and Harms, 1995; Harms and Stevens, 1996). They are lithologically similar as well: both are dominated by mafic to intermediate metatuffs and intrusive rocks. Quartz-sericite schist, exposed a few metres west of the Lucy prospect on the Swift River property of Birch Mountain Resources, may be a metamorphosed felsic tuff like those in the "greenstone-intrusive unit".

The "metasediment-amphibolite unit" resembles the Dorsey assemblage in metamorphic grade. They share a lithologic suite of pelitic schist, quartzite and metaplutonic rocks, amphibolites and garnet amphibolite. The gross distribution of rock types in this unit, with mafic protoliths more abundant in its lower part, is a further point of similarity with the Dorsey assemblage (Stevens and Harms, 1995). Stevens (1996) reports high temperatures and pressures for pre-Permian metamorphism of the Dorsey assemblage in the southern Yukon. The highly deformed Early Mississippian, and syntectonic Permian intrusions in the "metasediment-amphibolite unit" are also suggestive of shared tectonic history with the Dorsey assemblage.

The "phyllitic metasedimentary unit" west of Parallel Creek, correlates in lithologies and style and degree of deformation and metamorphism with the Swift River Assemblage as defined by Harms and Stevens (1996).

The correlation of the "greenstone-intrusive unit" with the Ram Creek assemblage, the structurally overlying "metasediment-amphibolite unit" with the Dorsey assemblage, and the highest "phyllitic metasedimentary unit" with the Swift River assemblage suggests that the assemblages and stacking orders recognized in the eastern Dorsey Terrane in southern Yukon persist southwards into the Cottonwood River area.

Correlation with other allochthonous assemblages in southern Yukon and northern British Columbia

Garnet-bearing amphibolites texturally and mineralogically very similar to those in the lower part of the "metasediment-amphibolite unit" occur within the "Anvil allochthon" of the St. Cyr klippe (Fallas, 1997) and within the Rapid River Tectonite in the Sylvester Allochthon (Figure 1; Nelson, 1997). These allochthons, along with the Dorsey Terrane, are highlighted on Figure 1. They form a discontinuous belt of terranes that lies inboard of the Big Salmon Complex/Kootenay Terrane/Teslin Tectonic Zone, which has been expressly correlated with the Yukon Tanana Terrane of the Finlayson Lake belt.

The Rapid River Tectonite lies structurally above the Slide Mountain Terrane (Figure 1); north of the Dease River it is in fault contact with unmetamorphosed late Paleozoic arc rocks of Harper Ranch subterrane affinity (Nelson and Bradford 1993). It is a complex suite of metamorphosed supracrustal rocks, including siliciclastic strata, metabasite, mafic to felsic tuff, chert and limestone; along with slivers of amphibolite and ultramafite (Gabrielse and Harms, 1989; Harms 1993; Gabrielse 1994; unit IIIvs of Nelson and Bradford, 1993). It is intruded by late synkinematic Early Mississippian and post-kinematic Early to mid-Permian plutons (Gabrielse *et al.* 1993, Harms, 1990). Recent mapping by Nelson (1997) of the Rapid River Tectonite near Cry Lake revealed extensive exposures of garnet amphibolite within a thrust sheet of metaplutonic rocks lying above interlayered amphibolite (±epidote), metamorphosed argillite, chert, limestone, and a unit of either granite conglomerate or mylonitized pre-tectonic granite that contains metamorphic garnet and aluminosilicate, and is cut by deformed granitic sills (Figure 4).

Textures in the Cry Lake garnet amphibolites are remarkably similar to those from the Cottonwood River. In both, garnet forms large synkinematic porphyroblasts, surrounded by a foliated matrix of green subidioblastic hornblende. Trains of peak-metamorphic rutile and ilmenite, heavily mantled with retrograde sphene, wrap around the garnets.

The granite conglomerate/granite mylonite has yielded an Early Devonian zircon age of 390±4 Ma. This is the oldest protolith age so far established in the Rapid River Tectonite. If it was a conglomerate, then the metabasite-limestone-meta-argillite sequence of which it is part is also Early Devonian. If it is a mylonitized intrusive body, then its age provides a minimum for the supracrustal protolith. In either case, given the high degree of deformation and metamorphism of this body, the early Devonian age gives a reasonable oldest age for the tectonic event. Peak metamorphism and strong ductile deformation in the Rapid River Tectonite are therefore constrained to be mid-Devonian to early Mississippian, post-390 Ma and pre-340 to 360 Ma, based on ages of late synkinematic plutons and K/Ar hornblende ages from amphibolites (Gabrielse *et al.* 1993).

Summary

Allochthonous assemblages of the southeastern Dorsey Terrane are correlated with those in the southern Yukon near the Seagull batholith. We highlight here the "metasediment-amphibolite unit", which in terms of stacking order, lithologic makeup, metamorphic grade, and the presence of Early Mississippian and Permian intrusions, correlates with the Dorsey assemblage. We further suggest a correlation with the Rapid River Tectonite. Both of these suites underwent late Paleozoic deformation, although that in the Rapid Rvier Tectonite is Devono-Mississippian, apparently older than the deformation in the Dorsey Terrane which affected the mid-Permian Ram Stock (Stevens and Harms 1995).

Does the deformation history in this belt of terranes, which lies between North America and the Yukon Tanana Terrane proper, bear a relationship to the Early Mississippian eclogites of the Simpson Range and Stewart Lake area described by Erdmer *et al.* (1997)? Does it aid in outlining a zone of Devono-Mississippian crustal compression, perhaps even collision?

REFERENCES

Abbott, J.G. (1981): Geology of the Seagull Tin District; *in* Yukon Geology and Exploration 1979-1980, *Indian and Northern Affairs Canada*, pp. 32-44.

Fallas, K.M. (1997): Preliminary Constraints on the Structural and Metamorphic Evolution of the St. Cyr Klippe, South-Central Yukon; Slave-Northern Cordillera Lithospheric Evolution (SNORCLE) and Cordilleran Tectonics Workshop, Report of the 1997 Combined Meeting, pages 90-95.

Ferri, F., Rees, C., and Nelson, J.L. (1996): Geology and Mineralization of the Gataga River Area, Northern Rocky Mountains (94L/10, 11, 14 and 15); *in* Geological Fieldwork 1995, B. Grant and J. Newell, editors, *B. C. Ministry of Energy, Mines and Petroleum Resources;* Paper 1996-1, pp. 137-154.

Gabrielse, H. (1963): McDame Map Area, Cassiar District, British Columbia; *Geological Survey of Canada,* Memoir 319.

Gabrielse, H. (1969): Geology of Jennings River Map Area, British Columbia (104/O); *Geological Survey of Canada,* Paper 68-55.

Gabrielse, H. (1994): Geology of Cry Lake (104I) and Dease Lake (104J/E) Map Areas, North Central British Columbia; *Geological Survey of Canada;* Open File Map 2779.

Gabrielse, H. and Harms, T.A. (1989): Permian and Devonian Plutonic Rocks in the Sylvester Allochthon, Cry Lake and McDame map areas, Northern British Columbia; *in* Current Research, Part E. *Geological Survey of Canada* Paper 89-1E, pages 1-4.

Gabrielse, H., Mortensen, J.K., Parrish, R.R., Harms, T.A., Nelson, J.L., and van der Heyden, P. (1993): Late Paleozoic Plutons in the Sylvester Allochthon, Northern British Columbia; *in* Radiogenic Age and Isotopic Studies, Report 7, *Geological Survey of Canada,* Paper 93-1, pages 107-118.

Gordey, S.P. and Stevens, R.A. (1994): Tectonic Framework of the Teslin Region, southern Yukon Territory; in Current Research, *Geological Survey of Canada* Paper 1994A, pp. 11-18.

Harms, T.A. (1990): Complex Tectonite Suites in the Sylvester Allochthon; *Geological Association of Canada,* Program with Abstracts, Volume 15, page A54.

Harms, T.A. (1993): Devonian Tectonism, Metamorphism and Sialic Plutonism Preserved in the Oceanic Sylvester Allochthon; *Geological Association of Canada,* Program with Abstracts, Annual Meeting 1993, p A-40.

Harms, T.A. and Stevens, R.A. (1996): Assemblage Analysis of the Dorsey Terrane; Slave-Northern Cordillera Lithospheric Evolution (SNORCLE) and Cordilleran Tectonics Workshop, Report of the 1996 Combined Meeting; pages 199-201

Mihalynuk, M. Nelson, J.L. and Friedman, R.M. (1998): Regional Geology and Mineralization of the Big Salmon Complex (104N NE and 104O NW), *in* Geological Fieldwork 1997, *B.C. Ministry of Employment and Investment,* Geological Survey Branch, Paper 1998-1.

Mortensen, J.K. (1992): Pre-Mid-Mesozoic Tectonic Evolution of the Yukon-Tanana Terrane, Yukon and Alaska; *Tectonics,* Volume 11, pp.836-853.

Mortensen, J.K. and Jilson, G.A. (1985): Evolution of the Yukon Tanana Terrane: Evidence from Southeastern Yukon Territory; *Geology,* Volume 13, pages 806-810.

Nelson, J.L. (1997): Last Seen Heading South: Extensions of the Yukon-Tanana Terrane into Northern British Columbia; *in* Geological Fieldwork 1996, D.V. Lefebure, W.J. McMillan and J.G. McArthur, editors, *B.C. Ministry of Employment and Investment,* Geological Survey Branch, Paper 1997-1 pp. 145-156.

Nelson, J.L. and Bradford, J. (1993): Geology of the Midway-Cassiar Area, Northern British Columbia; *B. C. Ministry of Energy, Mines and Petroleum Resources* Bulletin 87.

Nelson, J.L., Harms, T.A. and Mortensen, J. (1998): Extensions and Affiliates of the Yukon-Tanana Terrane into Northern British Columbia; *in* Geological Fieldwork 1997, *B.C. Ministry of Employment and Investment,* Geological Survey Branch, Paper 1998-1 pp. 7-1 - 7-12

Stevens, R.A. (1996): Dorsey Assemblage: Pre-Mid-Permian High Temperature and Pressure Metamorphic Rocks in the Dorsey Range, Southern Yukon Territory; Slave-Northern Cordillera Lithospheric Evolution (SNORCLE) and Cordilleran Tectonics Workshop, Report of the 1996 Combined Meeting, pages 70-75.

Stevens, R.A. and Harms, T.A. (1995): Investigations in the Dorsey Terrane, Part I: Stratigraphy, Structure and Metamorphism in the Dorsey Range, Southern Yukon Territory and Northern British Columbia; *in* Current Research, *Geological Survey of Canada* Paper 1995A, pages 117-127.

Wheeler, J.O., Brookfield, A.J., Gabrielse, H., Monger, J.W.H., Tipper, H.W. nd Woodsworth, G.J. (1991): Terrane Map of the Canadian Cordillera; *Geological Survey of Canada* Map 1713A, Scale 1:2,000,000.

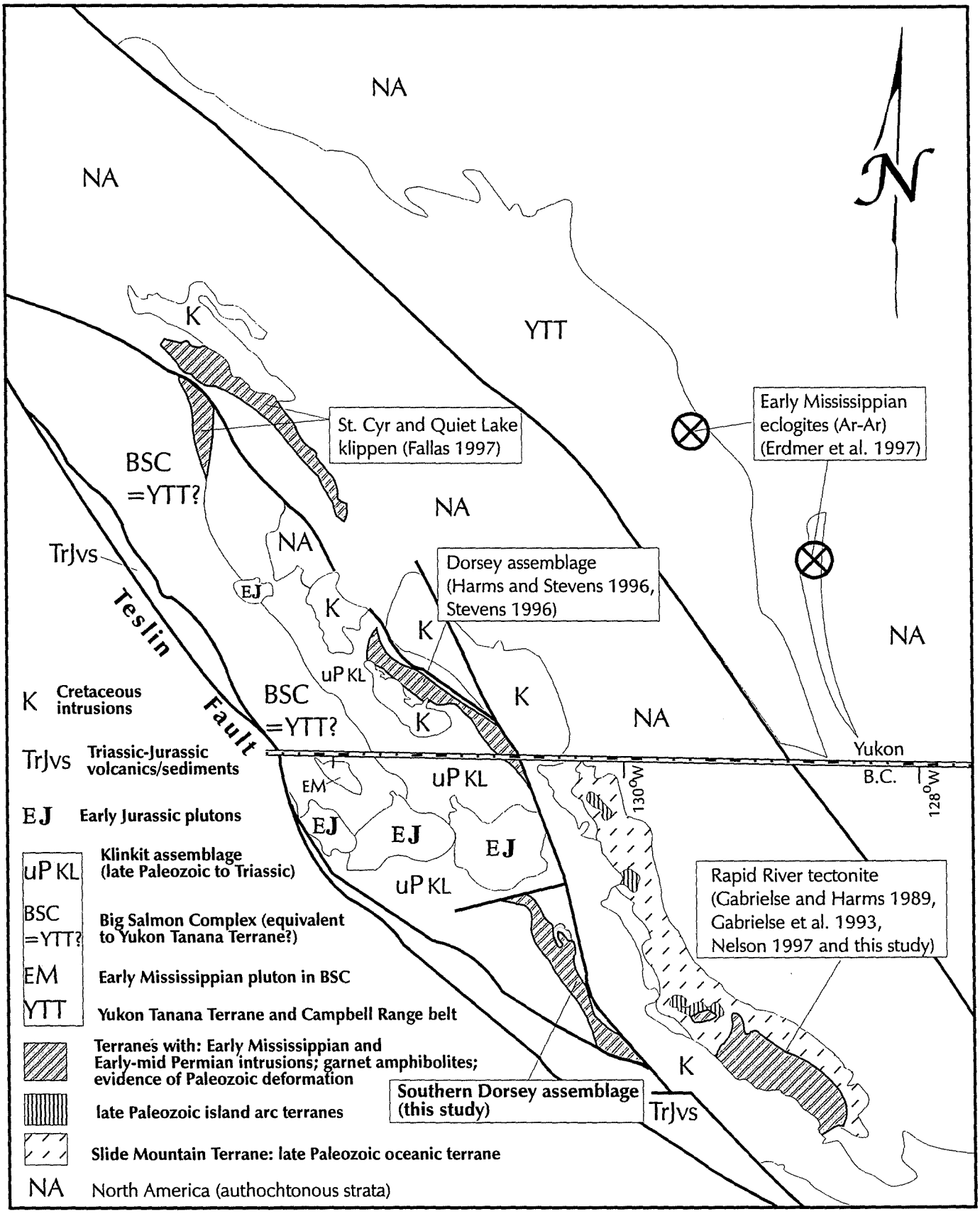

Figure 1. Sketch tectonic map showing relationship of southern Dorsey assemblage, Rapid River tectonite and possibly related tectonic elements near the inner limit of accreted terranes.

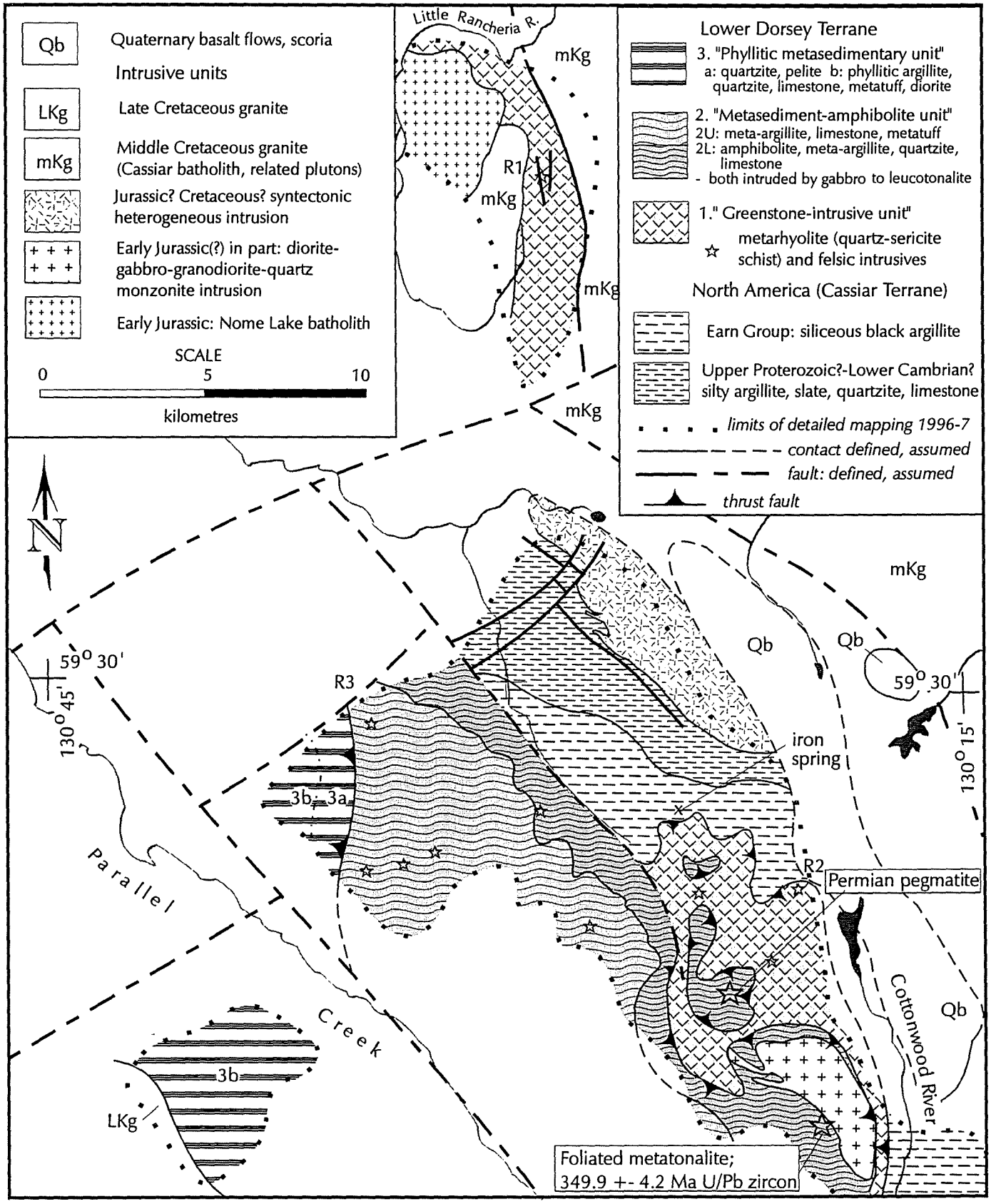

Figure 2. Geology of the area between headwaters of the Cottonwood River and Parallel Creek. Based on 1997 mapping by T. Harms, J. Nelson and M. Mihalynuk, 1996 mapping by J. Nelson and regional mapping by Gabrielse (1969)

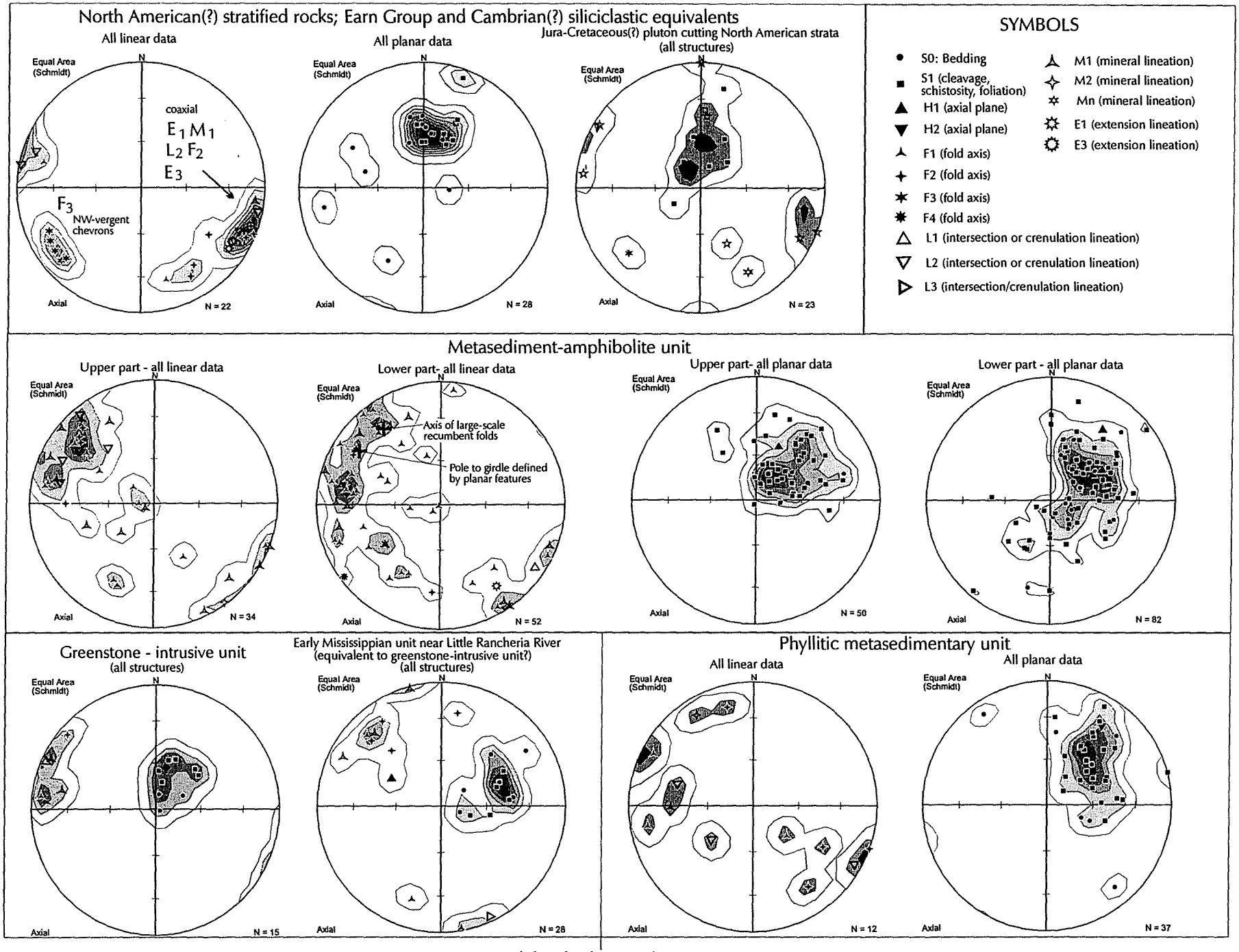

Figure 3. Structural data for the area shown on Figure 2.

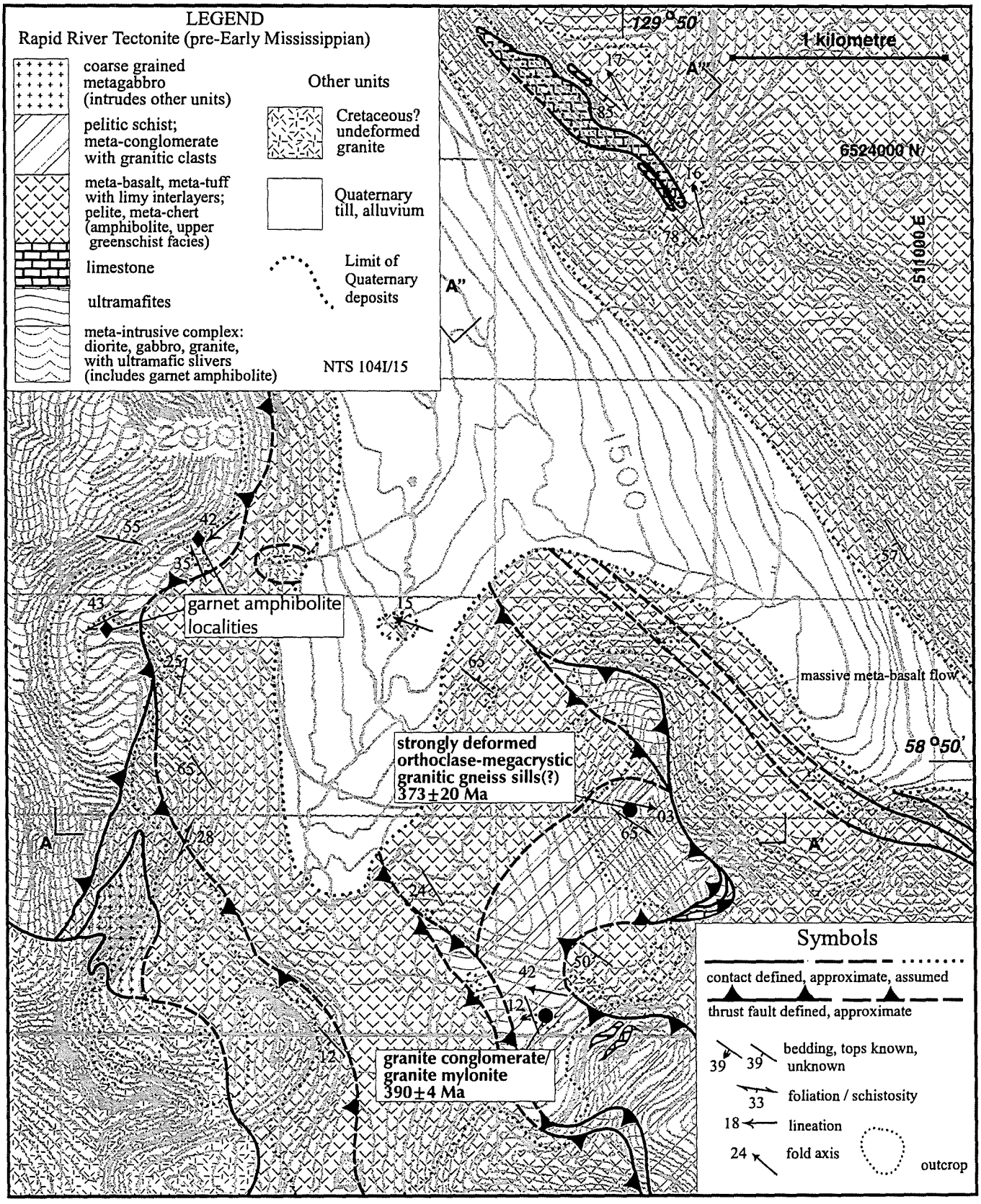

Figure 4. Rapid River Tectonite near Cry Lake; mapping by J. Nelson 1996

Volcanic Studies in Northern British Columbia

J. Nicholls and M.Z. Stout, Department of Geology & Geophysics, University of Calgary, Calgary, AB T2N 1N4

Introduction

A large number of volcanic centres scatter across northern British Columbia and The Yukon Territory (Fig. 1). Wide variations in rock type exist between and within volcanic complexes. Four centres or complexes (Fig. 2) were selected for study because they contain nearly all the varied rock types in the region. These centres are The Nisga'a lava flows, The Thumb, Mount Edziza, and Llangorse Mountain in the Atlin Area. The rock types range between basanite-nephelinite and peralkaline rhyolite. The only rock types in the area that are not included in the study are phonolites which are found in the Hoodoo Mountain complex.

Nisga'a Lava Flows

The Nisga'a flows (Fig. 3) north of Terrace, British Columbia are Fe-rich basalts with $^{87}Sr/^{86}Sr$ values equal 0.7032±0.00015 and $\delta^{18}O$ equal to 6.2, suggesting a mantle source. Rock analyses are listed in Table 1. Although homogeneous in many respects, there are pronounced variations in modal mineral amounts and minor textural variations from the vent to toe of the flows. The volume ratio of magnetite to ilmenite varies from 9% magnetite to 0.02% ilmenite to nearly equal amounts of each, 1.7% magnetite to 2% ilmenite. Modal amounts of titanaugite are higher when the ratio of magnetite to ilmenite is low. Variations in K_2O reflect variations in modal amounts of feldspar. The rocks are almost wholly crystalline with groundmass crystals ranging in size from 1-2 μm to 25 μm in different samples. Although a few phenocrysts of olivine and plagioclase are as large as 1 mm, there are sporadic pyroxene and plagioclase megacrysts up to 10 mm throughout the flow but the megacrysts more commonly occur near the cone. Olivine compositions from samples at the cones and from near the toe are more Mg-rich than those from the central part of the flows (Fo_{60} cones and toe, Fo_{52} middle). The Or content of the feldspars is higher in samples from the cones and toe (Or_{23}) than from the central part of the flow (Or_3)

The Nisga'a lava flows have been dated from accounts by native peoples, radiocarbon dates (1700 AD, Sutherland Brown 1969; 1700 and 1325 AD, Wuorinen 1978), and paleomagnetic dates (1650 AD, Symons 1975). Wuorinen (1978) postulates at least two eruptions, separated by 375 years, because of the different radiocarbon dates. The morphology of the cones, one inside the other, and the chemical variations are consistent with the possibility of more than one eruptive event.

A thermodynamic model of a crystallization path for a melt with the composition of a sample from the Nisga'a flow was constructed with the Melts data base (Ghiorso and Sack 1995). At 0.3 GPa the model predicts saturation with olivine ($Fo_{68.3}$) at 1155°C. If a fractional crystallization path was followed, olivine should be joined by plagioclase ($An_{52.5}$) at 1135°C. Olivine and plagioclase fractionate together and change composition as temperature falls. The mineral compositions in the rock, determined by electron microprobe routine analyses, are similar to the predicted mineral compositions.

To further test the thermodynamic model, measured amounts of compositional ranges in the phenocrysts can be compared with amounts predicted by the model. (Nicholls, *et al.* 1997). Comparison of relative cumulative frequency curves of the measured and predicted compositions reveals significant differences between predicted and observed zoning patterns in olivine and plagioclase. Although the chemical variations within the flows are small (Table 1), the zoning patterns in olivine and plagioclase indicate a complex differentiation process at depths of approximately 10 km.

The Thumb

The Thumb is a remnant of a larger body that was probably a valley or cirque fill rather than a volcanic neck (Lord 1948; Souther 1990). Three unconnected outcrops of basaltic lava flow suggest the original body was at least 3 km across and 60 metres thick. Two disconnected outcrops of hyaloclastite breccia are within a km of the Thumb. The outcrops are approximately 10 m across and about a metre thick. At the Thumb, the basalt rests on the Upper Cretaceous to Mid-Tertiary Sustut Group. The Sustut rocks in the vicinity of the Thumb are quartz sandstones.

The basaltic rocks contain scattered glomerocrysts and megacrysts. Glomerocrysts consist of partly digested pyroxene and olivine. Megacrysts of plagioclase, clinopyroxene and black spinel are set in a groundmass of plagioclase, olivine, clinopyroxene and Fe-Ti oxides. Clinopyroxene and plagioclase are both more abundant than olivine. Two rock analyses are listed in Table 1.

The only xenoliths found in the basalts are sandstone fragments. The hyaloclastite breccia consists of a matrix of fresh and altered glass and basaltic minerals enclosing fragments of sandstone and a few crustal xenoliths, including a fragment from a layered gabbro. The latter consists of olivine, plagioclase, orthopyroxene, and clinopyroxene. The plagioclase varies An_{46} to An_{68}; the orthopyroxene is near En_{88} with a 2V of approximately 90°.

Mount Edziza

Mt. Edziza is a late Cenozoic Volcanic Complex (Souther, 1992) that was active from at least 7.5 Ma to less than 2000 BP. The Complex is the largest volcanic structure in northern British Columbia and is one of many volcanic centres in the Canadian Cordillera (Fig. 2). Our study concerns the latest basaltic lava flows and older peralkaline rhyolites.

Basaltic Centres

The basaltic rocks come from the three youngest basaltic lava fields in the Complex: Mess Lake Lava Field, Snowshoe Lava Field, and Desolation Lava Field (Fig. 4). Each lava field consists of cinder cones, lava flows, and scoria blankets. With few exceptions, samples are from lava flows because flows are the least altered by cooling processes at the surface. The youngest basaltic lava flows were sampled first because they have the potential to provide the most information about conditions in the earth's mantle beneath Mt. Edziza. The volume of lava flows, number of cones and extent of eruptive products differs between the fields. This is illustrated on Figures 5 and 6. The locations of samples with respect to the cinder cones in the lava fields are shown on Figure 6.

The basaltic rocks from the young lava fields of Mt. Edziza are plagioclase phyric. Olivine and clinopyroxene phenocrysts are usually subordinate to plagioclase.

In a few samples, olivine is more abundant than plagioclase in the phenocryst assemblages. Clinopyroxene is always the least abundant phenocryst.

Peralkaline Centres

The peralkaline rhyolites are found in volcanic centres that form the Spectrum and Pyramid Formations (Souther 1992). These rocks formed from strongly differentiated melts under conditions and along crystallization paths that contrast with conditions and crystallization paths that led to the formation of the rocks from the younger basaltic centres. Figure 7 shows the locations of the peralkaline rhyolite centres in the complex.

Rocks from the peralkaline centres contain less than 5% microphenocrysts in a groundmass that can consist of glass, vapor phase minerals, and crystalline mixtures in any combination. The microphenocrysts are anorthoclase, fayalitic olivine (Fa_{99}), sodic amphibole, sodic pyroxene, minor quartz and aenigmatite. The feldspars in the rocks are triclinic anorthoclase ($Ab_{65}Or_{34}$ to $Ab_{40}Or_{59}$) not sanidine. Mineral analyses are listed in Table 2.

Llangorse Mountain

Geologic Setting

Ultramafic xenoliths occur at two Late Tertiary volcanic centres in the Atlin area: Ruby Mountain and Llangorse Mountain. The xenoliths are carried in basanite lava flows. The basanites from the two localities are different; Ruby Mountain xenoliths are from a basanite with approximately 9% MgO and 47.5% SiO_2. Llangorse Mountain xenoliths are from basanites with approximately 11.5% MgO and 45% SiO_2 (Table 1, LL1 and LL5).

The basanites at Llangorse Mountain is either part of a volcanic neck or a cirque fill. On the eastern and western edges, basanite is chilled against and overlies sands and gravels formed from the older granitic country rock. Inside the chilled margin, the rock body is coarser and has a different mineral assemblage than the chilled margin. Ultramafic xenoliths are found only in the chilled margin and in the sands and gravels.

Ruby Mountain is a stratovolcano with a volume of approximately 1 km^3 (Edwards, et al. 1996). The edifice consists of interlayered tephra and lava flows. The rare xenoliths occur in a basanite lava flow on the northeast side of the volcano.

The xenolith minerals show chemical variations; spinel has pronounced differences in composition amongst the 6 xenoliths suggesting the presence of two distinct groups, Cr-poor and Cr-rich. Cr_2O_3 contents in the Cr-poor group (A1, A2, LL1 and LL5-1) range from approximately 9 wt% to 15 wt% with a concommitant range in Al_2O_3 from approximately 53 wt% to 58 wt%. Cr_2O_3 contents in the Cr-rich xenoliths (LL5-3, LL5-4) range from approximately 38 wt% to 43 wt% and Al_2O_3 varies from approximately 27 wt% to 32 wt%. Compositions of the other minerals, olivine and pyroxene, show smaller variations and suggest that LL5-1 is most similar to the Cr-rich pair, LL5-3 and LL5-4. Olivine composition is the most uniform amongst all the xenoliths ranging only from Fo_{90}, in A1, A2 and LL1, to Fo_{91}-Fo_{92}, in LL5-1, LL5-3, LL5-4. Clinopyroxene in A1, A2 and LL1 has MgO contents from 15.0 wt% to just less than 15.5 wt% but ranges from 16 to 18.5 wt% in LL5-1, LL5-3 LL5-4. Orthopyroxene shows a similar MgO pattern, ranging from approximately 32 wt% to 33.7 wt% in A1, A2 and LL1 but from 35 wt% to 36 wt% in LL5-1, LL5-3 LL5-4.

The modes of the xenoliths are dominated by olivine. The proportions of the phases vary from xenolith to xenolith, in part perhaps, because sections through the xenoliths are not large enough to provide representative samples.

The pronounced differences in amounts of Cr_2O_3 and Al_2O_3 in the spinel illustrates a difference in the bulk compositions of these xenoliths and therefore infers a heterogeneous mantle source. The implied mantle heterogeneity may be lateral or vertical in space. If lateral, the close surface occurrence of the Cr-poor (LL1 and LL5-1) and Cr-rich xenoliths (LL5-3 and LL5-4) at contact edges of one flow less than 1 kilometer across at Llangorse Mountain suggests this basanite has directly tapped the 'intersection' of two different source regions. The compositional similarities of olivine and pyroxene minerals in LL5-1 with LL5-3 and LL5-4 rather than with A1, A2 and LL1, like the spinel compositions, may suggest a gradational source change over a wider area.

The coarse grained basanite, LL4, Table 1, is compositionally distinct from the basanites at the chilled margins (LL1 and LL5, Table 1). The coarse grained variety lacks xenoliths and contains less olivine and pyroxene than the chilled margins.

Acknowledgements

Carmen Neufeld performed the x-ray identifications of the phenocryst minerals in the peralkaline rhyolites.

References Cites

Edwards, B. R., Hamilton, T. S., Nicholls, J., Stout, M. Z., Russell, J. K., and Simpson, K. 1996. Late Tertiary to Quaternary volcanism in the Atlin area, northwestern British Columbia. Geological Survey of Canada Current Research, 1996-A: 29-36.

Ghiorso, M. S., and Sack, R. O. 1995. Chemical mass transfer in magmatic processes IV. A revised and internally consistent thermodynamic model for the interpolation and extrapolation of liquid-solid equilibria in magmatic systems at elevated temperatures and pressures. Contributions to Mineralogy and Petrology, 119: 197-212.

Hickson, C. J. 1990. Canadian Cordillera: Volcano Vent Map and Table. In Volcanoes of North America. Edited by C. A. Wood and J. Kienle. Cambridge University Press, New York, pp. 116-117.

Lord, C. S. 1948. McConnell Creek map-area, Cassiar District, British Columbia. Geological Survey of Canada Memoir, 251: 1,72.

Nicholls, J., Stout, M. Z., Machacek, J., and Michael, P. 1997. Volume-composition relations in concentrically zoned crystals: Application to thermodynamic modeling of igneous processes. Canadian Mineralogist, 35: .

Souther, J. G. 1990. The Thumb. In Volcanoes of North America, United States and Canada. Edited by C. A. Wood and J. Kienle. Cambridge University Press, Cambridge, England, pp. 129-130.

Souther, J. G. 1992. The Late Cenozoic Mount Edziza Volcanic Complex, British Columbia. Geological Survey of Canada Memoir, 420: 1-320.

Sutherland-Brown, A. 1969. Aiyansh lava flow, British Columbia. Canadian Journal of Earth Sciences, 6: 1460-1468.

Symons, D. T. A. 1975. Age and flow direction from magnetic measurements on the historic Aiyansh flow, British Columbia. Journal of Geophysical Research, 80: 2622-2626.

Wuorinen, V. 1978. Age of Aiyansh Volcano, British Columbia. Canadian Journal of Earth Sciences, 15: 1037-1038.

Table 1: Analyses of rocks from the Nisga'a lava flows, The Thumb, and Llangorse Mountain.

Oxide	NR1	NR2	NR2B	NR3B	NR4	NR5	NR6	NR11(1)	NR11(2)	NR12A(1)	NR12A(2)
SiO_2	46.8	47.3	46.97	46.49	46.40	46.53	47.12	47.1	47.2	47.2	47.11
TiO_2	3.53	3.51	3.60	3.66	3.68	3.72	3.66	3.55	3.55	3.55	3.55
Al_2O_3	14.7	14.8	14.43	14.30	14.41	14.40	14.56	14.8	14.8	14.7	14.7
Fe_2O_3			2.57	2.20	2.76	2.27	2.50				
FeO	14.4	14.3	12.47	12.63	12.28	12.76	12.32	14.5	14.4	14.5	14.5
MnO	0.22	0.22	0.22	0.35	0.23	0.29	0.22	0.22	0.22	0.22	0.22
MgO	4.37	4.24	4.78	4.50	4.54	4.52	4.52	4.44	4.43	4.34	4.43
CaO	7.55	7.63	7.29	7.58	7.52	7.53	7.56	7.64	7.63	7.62	7.61
Na_2O	4.08	4.09	4.08	4.24	4.45	4.12	4.14	4.06	4.07	4.10	4.05
K_2O	1.84	1.88	1.82	1.92	1.66	1.87	1.82	1.83	1.83	1.83	1.85
P_2O_5	1.28	1.31	1.16	1.08	1.17	1.15	1.15	1.26	1.26	1.28	1.28
H_2O+			0.20	0.23	0.18	0.16	0.12				
H_2O-			0.03	0.07	0.08	0.07	0.06				
Total	98.8	99.4	99.62	99.25	99.36	99.39	99.75	99.3	99.4	99.3	99.2

Table 1, Cont.: Analyses of rocks from the Nisga'a lava flows, The Thumb, and Llangorse Mountain.

Oxide	NR13	TT1	TT2	LL1(1)	LL1(2)	LL4(1)	LL4(2)	LL5
SiO_2	47.1	45.0	45.0	45.3	45.4	46.4	46.3	44.8
TiO_2	3.53	2.63	2.62	2.20	2.20	3.02	3.01	2.13
Al_2O_3	14.7	14.5	14.5	13.1	13.1	16.0	16.0	12.9
Fe_2O_3								
FeO	14.4	12.3	12.4	12.1	12.1	10.8	10.8	11.7
MnO	0.22	0.19	0.19	0.18	0.18	0.16	0.16	0.17
MgO	4.32	8.60	8.54	11.6	11.6	4.47	4.49	11.7
CaO	7.61	9.28	9.28	9.90	9.92	10.2	10.2	10.1
Na_2O	4.18	3.13	3.20	2.96	3.01	4.31	4.28	1.91
K_2O	1.86	1.69	1.66	1.19	1.20	1.65	1.65	1.09
P_2O_5	1.28	0.68	0.68	0.53	0.54	0.65	0.65	0.51
H_2O+								
H_2O-								
Total	99.3	98.0	98.0	99.0	99.3	97.6	97.5	97.1

Table 2: Analyses of microphenocrysts in peralkaline rhyolites from Mt. Edziza

Oxide	Cpx	Oxide	Amph	Oxide	Fsp	Fsp
SiO_2	50.99	SiO_2	48.87	SiO_2	66.11	62.69
TiO_2	2.91	TiO_2	0.09			
Al_2O_3	0.37	Al_2O_3	0.29	Al_2O_3	18.13	17.45
Fe_2O_3	31.65			Fe_2O_3	1.36	1.27
		FeO	36.48			
CaO	0.37	CaO	0.54	CaO	0.02	0.02
Na_2O	13.43	Na_2O	8.79	Na_2O	7.27	4.48
		K_2O	1.19	K_2O	5.68	9.90
		F	3.64			
Total	99.72		99.89		98.57	95.81

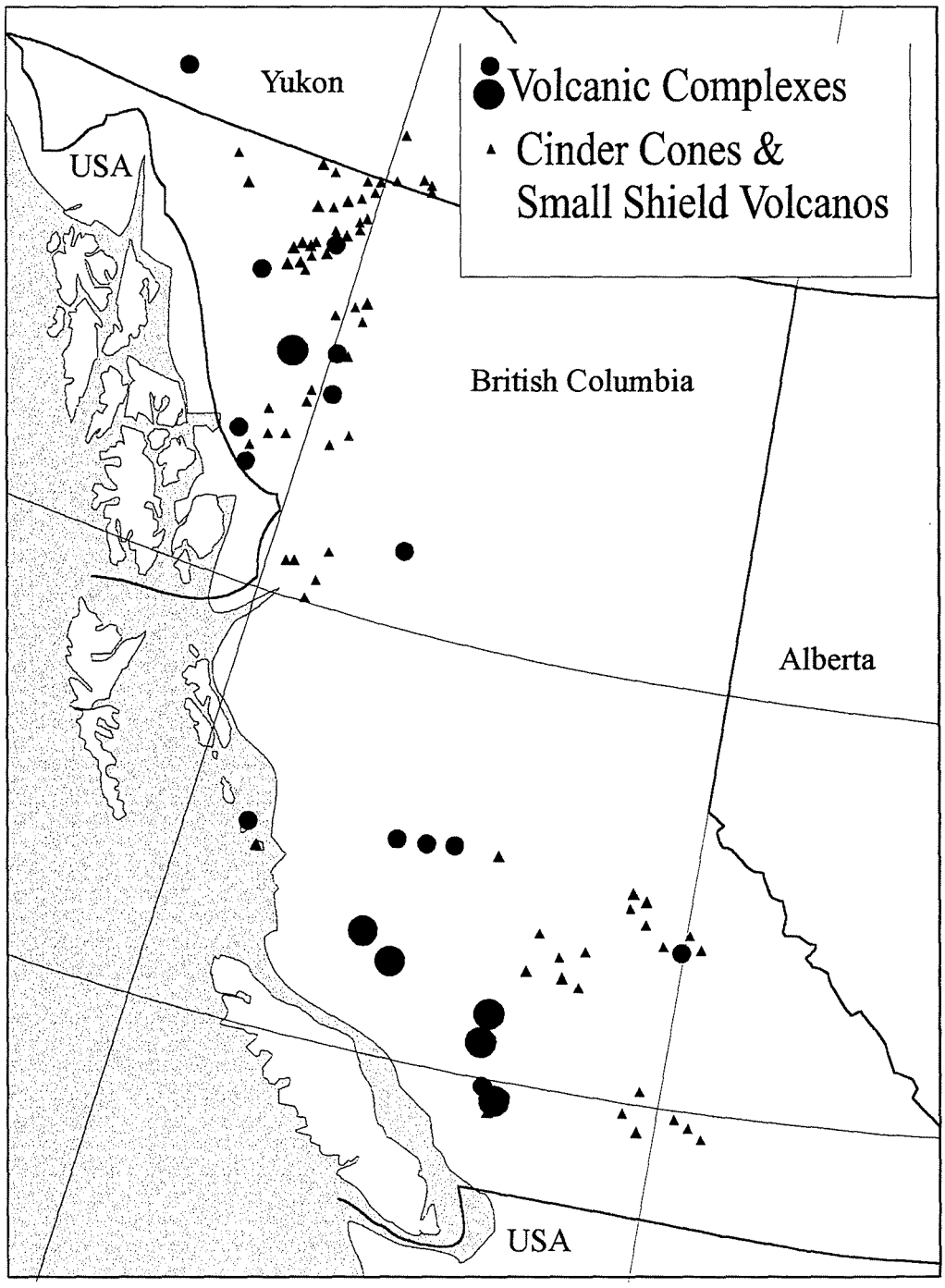

Figure 1: Distribution of volcanic centres in the Canadian Cordillera (after Hickson 1990).

Figure 2: Location of the volcanic centres being studied for the Lithoprobe project.

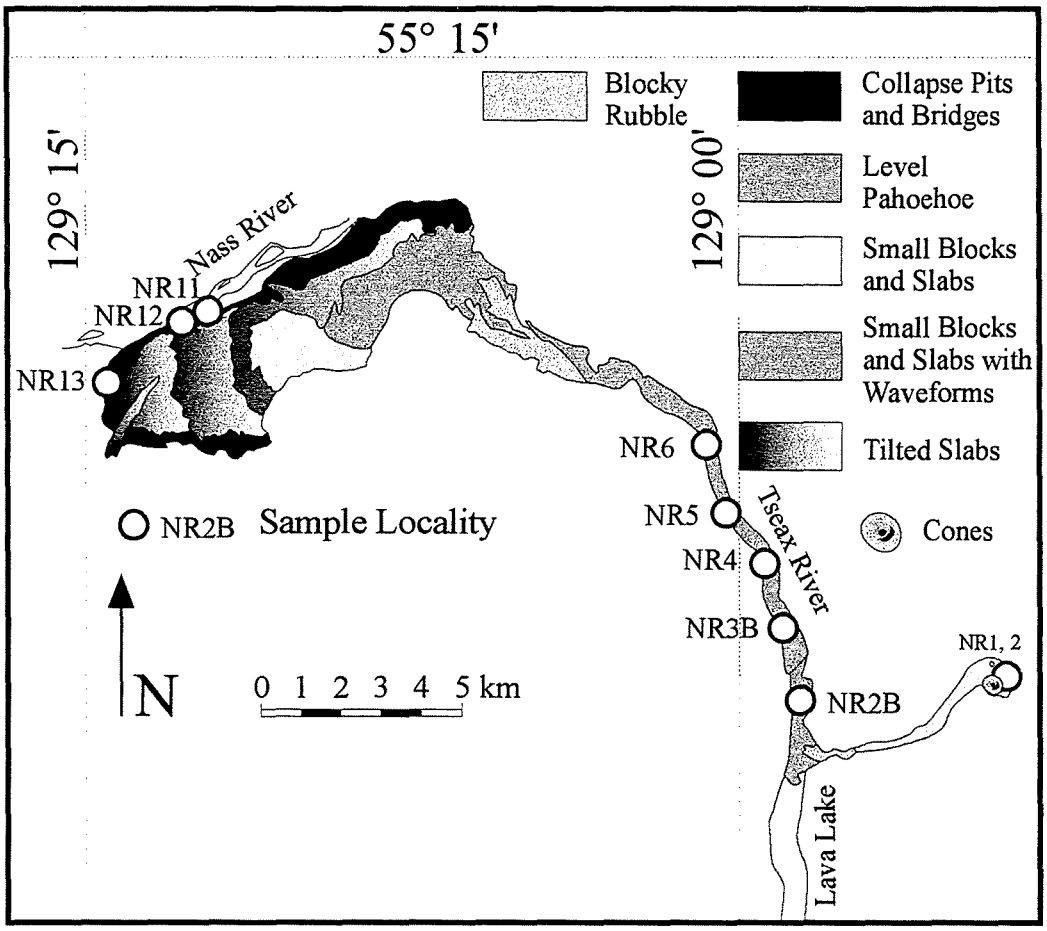

Figure 3: Map of Nisga'a lava flows showing surface form units and sample locations. After Sutherland Brown (1969).

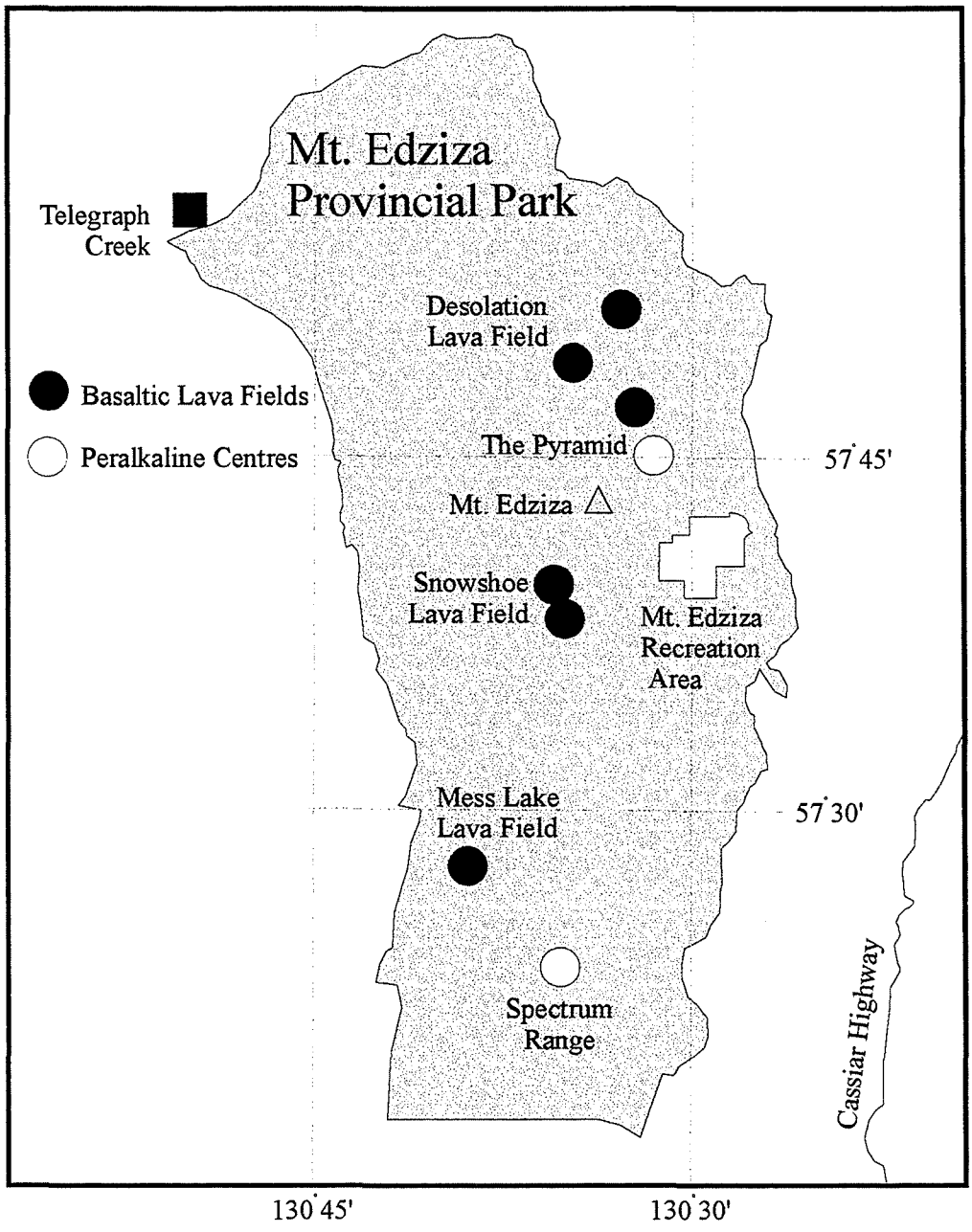

Figure 4: Location the youngest basaltic lava fields and peralkaline centres in the Mt. Edziza Volcanic Complex.

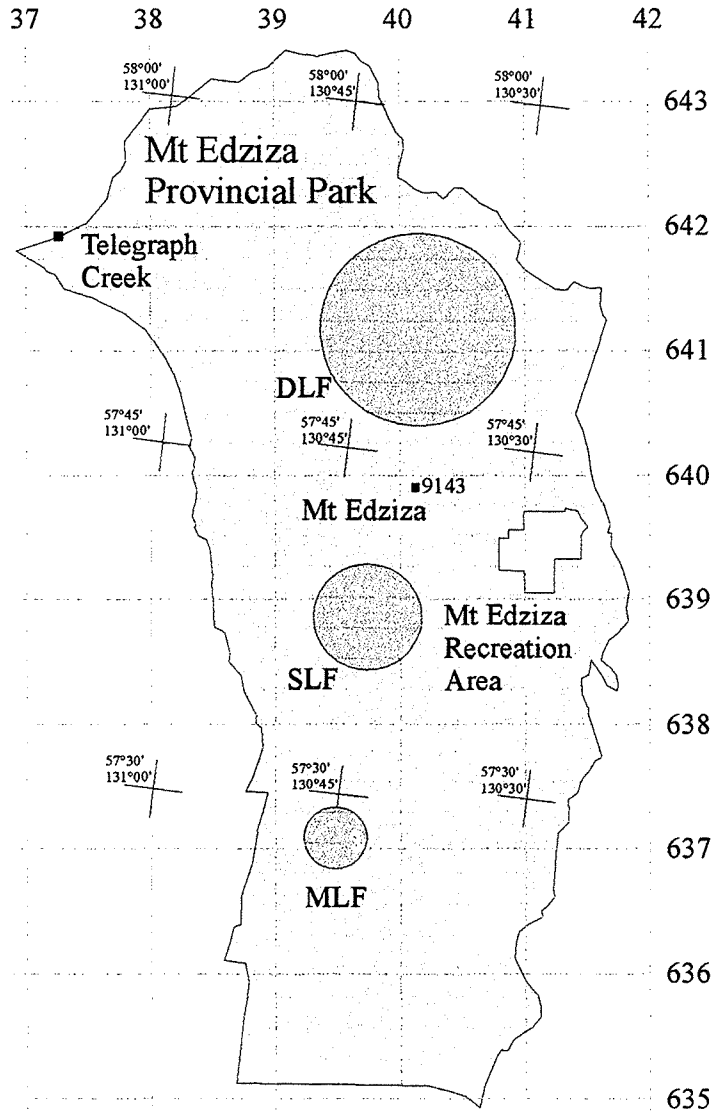

10,000 metre Universal Transverse Mercator Grid, Zone 9. MLF: Mess Lake Lava Field, SLF: Snowshoe Lava Field, DLF: Desolation Lava Field.

Figure 5: Location and approximate relative size of the youngest basaltic lava fields in the Mt. Edziza Volcanic Complex.

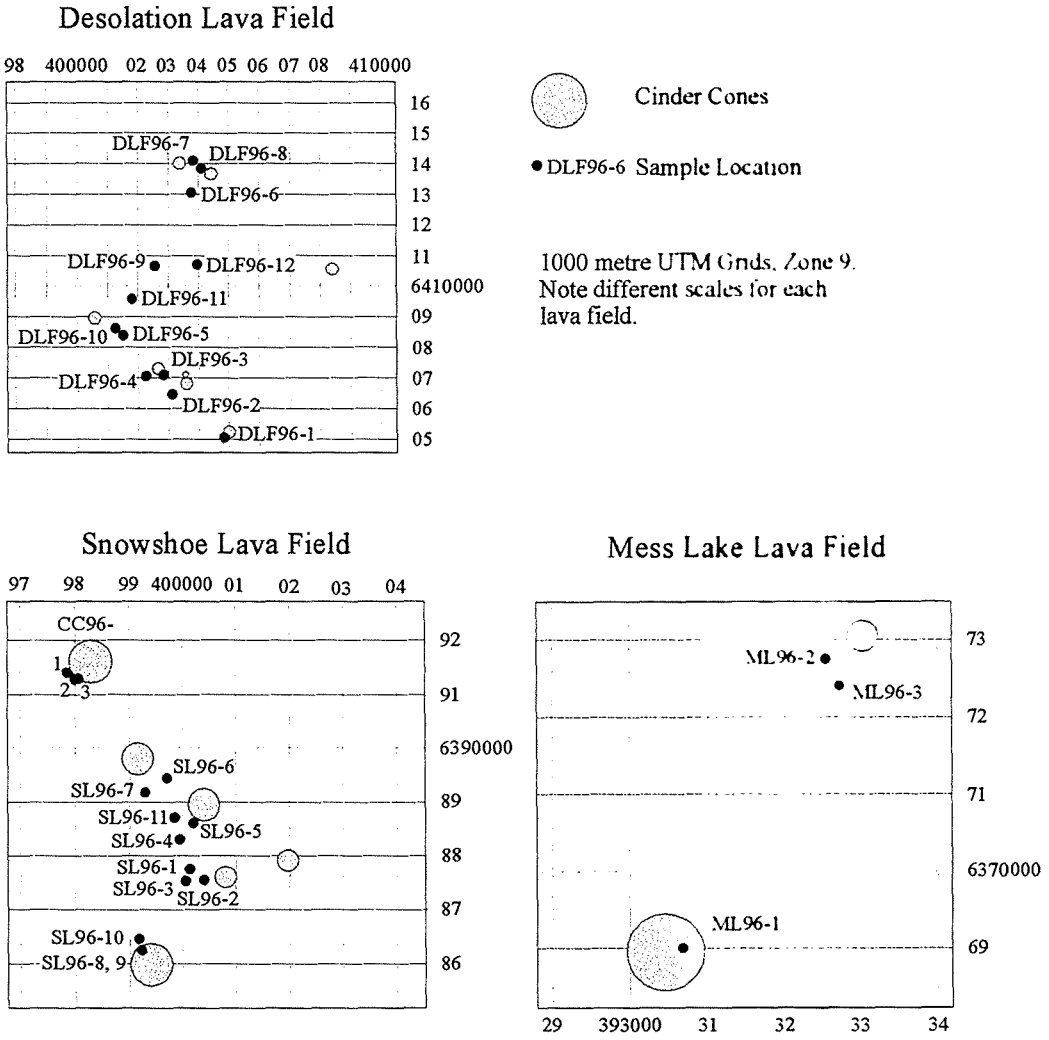

Figure 6: Maps of sample localities in the three youngest lava fields.

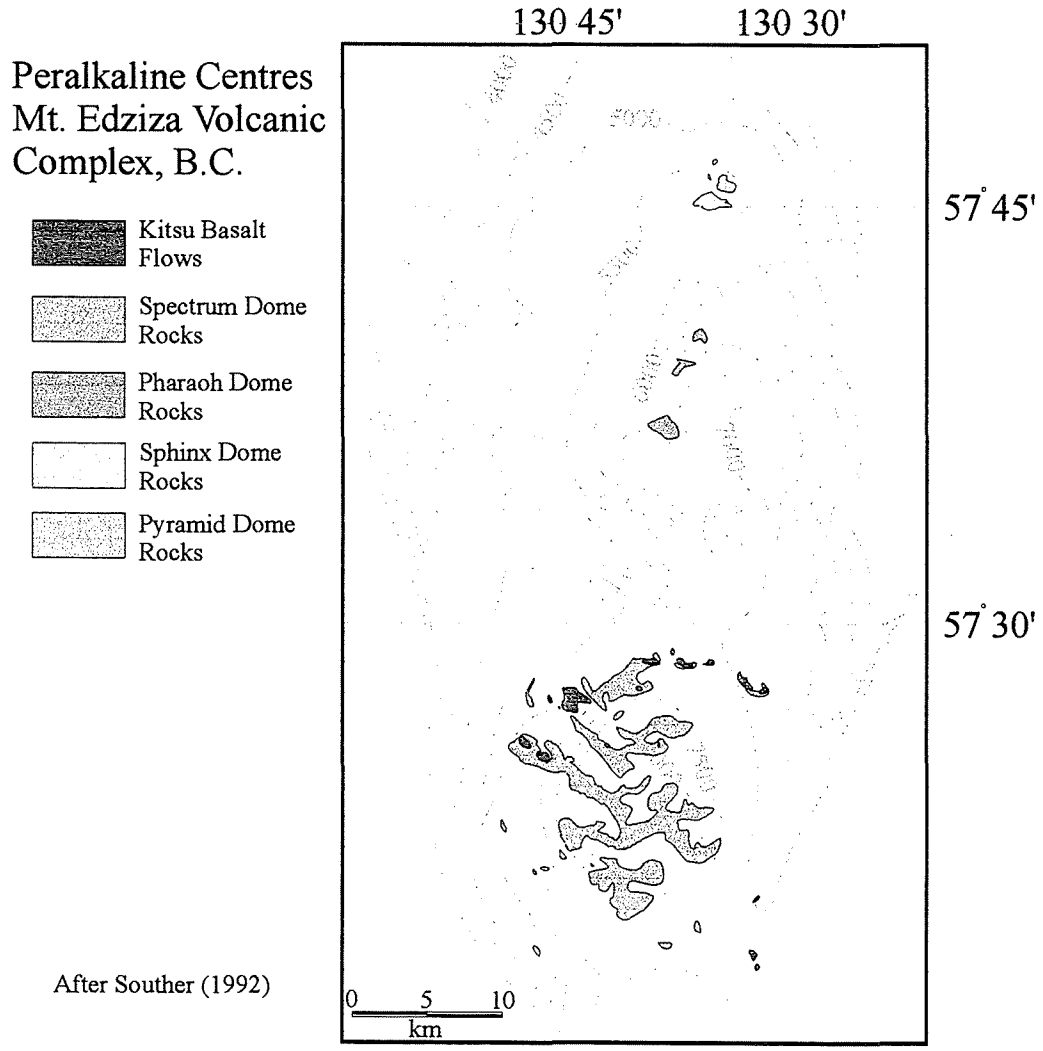

Figure 7: Outcrop map of peralkaline rhyolite centres in the Mt. Edziza Volcanic Complex.

SYSTEM OF TRANSFER FAULT ZONES ACROSS THE PACIFIC CONTINENTAL MARGIN OF WESTERN CANADA*

MAKS M. POSAVEC, DEMOFRAC GSI - Geologic Remote Sensing
809 - 25 Avenue N.W. Calgary, Alberta T2M 2B4 Canada

It has been known for decades that interaction of the oceanic and continental crust margins along the subduction zone causes the evolution of two major fault systems (FS) and their conjugates. The first is a system of **transcurrent** fault zones (FZ), which is subparallel to the trench. The other is a system of **transverse** FZ that cuts across and interacts with the transcurrent FZ or terminates against them. Within their intersection areas, subsurface intrusive activities usually develop followed by the extrusive **volcanic activities** and **mineralization** of host rocks. The result is development of volcano-magmatic (island) arc(s) with volcanic **centers** and narrow **pull-apart troughs.** The present Sumatran island arc is one of the best known and studied examples and is used as a **model** for **correlation** for the Western Canada-Pacific Continental Margin Structure.

For a more specific terminology, the transverse FZ in the oceanic crust are called **transforms**, while their equivalents across the Continental margin were named **transfer** FZ. The name 'transfer' was chosen during a discussion which the author had with Dr. Tuzo Wilson over two decades ago, because these FZ transfer **significant tectonic movements** from the oceanic transform FZ **across** the trench and **cut** across the Continental **margin**. They also transfer the molten and subducted material into the continental crust thus causing development and mineralization along the volcano-magmatic arc(s).

The existence of transfer (transverse) FZ across the Pacific Ocean continental margin have been **reported** and presented by this author using satellite imagery mosaic at previous **Lithoprobe meetings** in Edmonton and Calgary. The subsequent marine seismic survey by ECRETE along the Portland Inlet **confirmed** the existence of such a fault zone along its extension (Lithoprobe Report #59, p. 185-7). **Following** this confirmation, there is no doubt that similar transverse FZ will be **rediscovered** by new surveys along most of the straights and major channels on the west coast of Canada. They can **be seen** from the satellite imagery since they form the most striking linear **geomorphological** features extending far inland from the coast.

It is essential to **realize** that major transfer FZ have been **offset** by the regional transcurrent FZ (some misnamed as transform FZ). The Engebretson diagram for the continental **drift of** North America over the hot spots (1982 and subsequent papers) should be used to **properly** identify the **changes** of their **lateral** offsets. While the **older** offsets (during Jurassic-Cretaceous times) were in a **left lateral** sense (as along the Fraser-Mid-Tintina-Kaltag FS), the **latest** (Tertiary) offsets have the predominant **right lateral** characteristics.

The Tintina-Rocky Mountains FS is the best example of the latter (misnamed as trenches). The consequence of **extensive** strike-slip displacements along these FS was the development of thrust-fold belts and extensional basins along their margins. **Transpressional under-thrusting** of the Precambrian shield semi-plate beneath the Cordilleran/amalgamated semi-plate caused the Cordilleran tectonic structure to become even more **complex** and perplexing (Posavec, ERIM-1997).

The existence of volcanic chains along the Western USA and Canada (such as the Garibaldi chain) can best be interpreted by the above-described tectonic inter-relationships between the Cordilleran/amalgamated semi-plate and Pacific Ocean trench. The obvious conclusion is that all these structures have been initiated and **controlled** by the major Continental fault systems of **crustal extensions**.

* Presented at SNORCLE-Lithoprobe Transect and Cordilleran Tectonic Workshop, Vancouver, B.C. Canada, March 6-8, 1998.

Poster presentation - SNORCLE transect meeting, March 6-8, 1998.

An improved seismic image below Yellowknife? - Reprocessing results from line 1.

Brian Roberts
Geological Survey of Canada
1 Observatory Cres.
Ottawa, Ontario
roberts@cg.NRCan.gc.ca

ABSTRACT

The incredibly high quality seismic data from corridor 1 of the SNORCLE transect has one glaring section which is poorly imaged. This is the region immediately surrounding Yellowknife where a combination of very high cultural noise (traffic, mine noise, etc.) and less than optimal geometry has yielded a 10 km wide section of transparent seismic data. This contrasts sharply with the strong, coherent reflectivity in the Yellowknife Domain to the east and the strong, but more complex reflectivity in the Anton Domain to the west. It may be that the problems encountered recording this data cannot be overcome by processing, perhaps there is just not enough signal. However, an improved image in the Yellowknife area could help tie structures that are observed on either side of this zone, and add depth control to the well-studied geological formations in this area.

To see if an improved section is possible, we will test the effects of suppressing the various types of noise on the data, as well as severely limiting what data goes into the stack by killing undesirable traces. Different type of CDP binning strategies will be looked at to see if we can focus what small reflectivity there is and generate a better stack section.

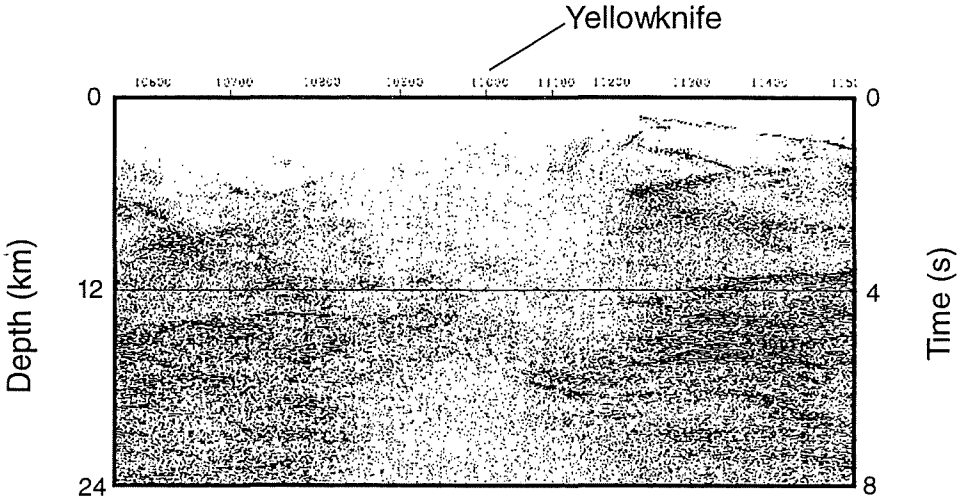

Figure 1. Portion of SNORCLE line 1 near Yellowknife with original processing

Recent Alkaline Basalt Evidence for Discontinuous Changes in the Lithospheric Mantle beneath the Northern Canadian Cordillera.

Abraham A-C., Francis D., Earth & Planetary Science, McGill Un., Montréal, **Polvé M.,** Laboratoire de Géochimie, Toulouse, France, **Ludden, J.N.,** CRPG-CRNS, Nancy, France.

Recent alkaline basalts have erupted in most of the accreted terranes of the Northern Canadian Cordillera and provide a unique systematic sampling with which to identify transitions in the lithospheric mantle between the different tectonic terranes of the Cordillera. A comparison of over 25 localities across the northern Cordillera indicates that the major element systematics of these recent alkaline magmas is independent of the terrane in which they erupt. There are, however, 3 important regional changes in the isotopic and trace element signatures of the alkaline lavas across the Cordillera.

The first change occurs across the Tintina Fault, a major transcurrent fault separating the assembled terranes of the Cordillera from the North America Craton. Lavas on the east side of the fault are characterized by significant higher Ca, Zr, but lower heavy rare-earth elements concentrations than their equivalents erupted on the west side of the fault. Isotopic data indicate a significant decrease in $^{87}Sr/^{86}Sr$ (from 0.704 to 0.7035) and increase in $^{143}Nd/^{144}Nd$ (from 0.5128 to 0.513) from west to east across the Tintina fault, which are not correlated, however, with any significant change in their Pb isotopic ratios. These results suggest that the Tintina Fault is a high angle feature that penetrates the crust and separates 2 distinct lithospheric mantle roots.

The second change occurs between the Cassiar and Teslin Faults, in the western portion of the Omineca Belt (OMI). Samples erupted to the east of the Cassiar Fault have higher Rb, Pb, Th, $^{87}Sr/^{86}Sr$, and Pb isotopic ratios, but lower $^{143}Nd/^{144}Nd$ than their equivalents in the westernmost OMI and the Intermontane Belt (IMB). In order to evaluate the possible effects of upper crust contamination, the chemical and isotopic compositions of selected granitoids from the Cassiar (OMI) and Parallel Creek Batholiths (IMB) have also been analyzed. Model calculation suggest that the Pb isotopic signatures and high Rb, Pb, Th of the OMI basalts could be explained by a maximum of 10% contamination by the Cassiar granite. The $^{87}Sr/^{86}Sr$ and $^{143}Nd/^{144}Nd$ signatures, however, can not be reproduced by any reasonable amounts of crustal contamination. These results indicate that the lithospheric mantle beneath the OMI is isotopically distinct from that beneath the IMB. Interestingly, the alkaline basalt data indicate that the mantle transition occurs between the Cassiar and Teslin Faults, about 30 km to the east of the commonly accepted crustal boundary between the IMB and OMI terranes, along the Teslin Fault.

The third change occurs between the alkaline basalts of the IMB and those from the Coast Plutonic Belt (CPB). The IMB alkaline lavas have distinctly lower $^{87}Sr/^{86}Sr$, Nb/Zr, and Rb/Zr ratios than basalts erupted within either the CPB to the west (Alligator Lake) or OMI to the east. The alkaline basalts of the CPB, however, do not share the high $^{207}Pb/^{204}Pb$ and $^{208}Pb/^{204}Pb$ ratios of the alkaline basalts of OMI.

In general, there is a striking correlation between the variation in $^{87}Sr/^{86}Sr$ in the recent alkaline basalts and the "Sr line" defined by Armstrong on the basis of Mesozoic and Tertiary granitoids. As the variations in $^{87}Sr/^{86}Sr$ and $^{143}Nd/^{144}Nd$ signatures of the basalts do not appear to be explainable in terms of crustal contamination, the results of this study indicate that blocks of distinct lithospheric mantle have been juxtaposed beneath the accreted terranes of the northern Canadian Cordillera.

Seismic Properties of the Upper Mantle beneath the Canadian Cordillera - A Study of Mantle Xenoliths

Kazuko Saruwatari & Shaocheng Ji

Département de Géologie, Université de Montréal,
C. P. 6128, Centre-Ville, Montréal, Québec, Canada H3C 3J7

Matthew H. Salisbury

Atlantic Geoscience Centre, Geological Survey of Canada, Bedford Institute of Oceanography,
Dartmouth, Nova Scotia, Canada B2Y 4A2

Introduction

The Canadian Cordillera is one of the major mantle-xenolith-bearing provinces in Canada, and has been the main target for LITHOPROBE seismic reflection and SKS splitting studies. According to Bostock & Cassidy (1995), polarization directions of the fast split SKS phases in the southern Cordillera are nearly orthogonal to the regional tectonic trend, in contrast with the northern Cordillera (Figure 1). In order to investigate the possible tectonic implications of this difference, we studied the seismic properties of the ultramafic xenoliths from alkaline volcanic complexes of British Columbia (Summit Lake, Jacques Lake, West Kettle River, Alligator Lake and Castle Rock).

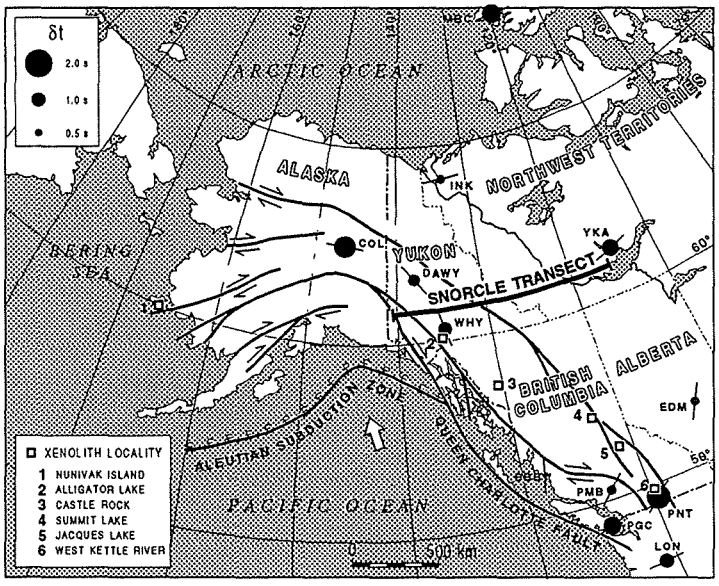

Figure 1. Simplified tectonic map of northwest America and locations of the studied ultramafic xenolith samples. Shear-wave splitting parameters (ϕ and δt) have been measured at stations *COL* and *LON* by Silver and Chan (1991) and at other stations by Bostock and Cassidy (1995).

Microstructures

Modal composition analysis shows that the mantle xenoliths are spinel-lherzolite, harzburgite, dunite, wehrlite and pyroxenite. Microstructures of the xenoliths can be classified into four types: protogranular, porphyroclastic, equigranular and poikiloblastic textures. However, protogranular texture is dominant.

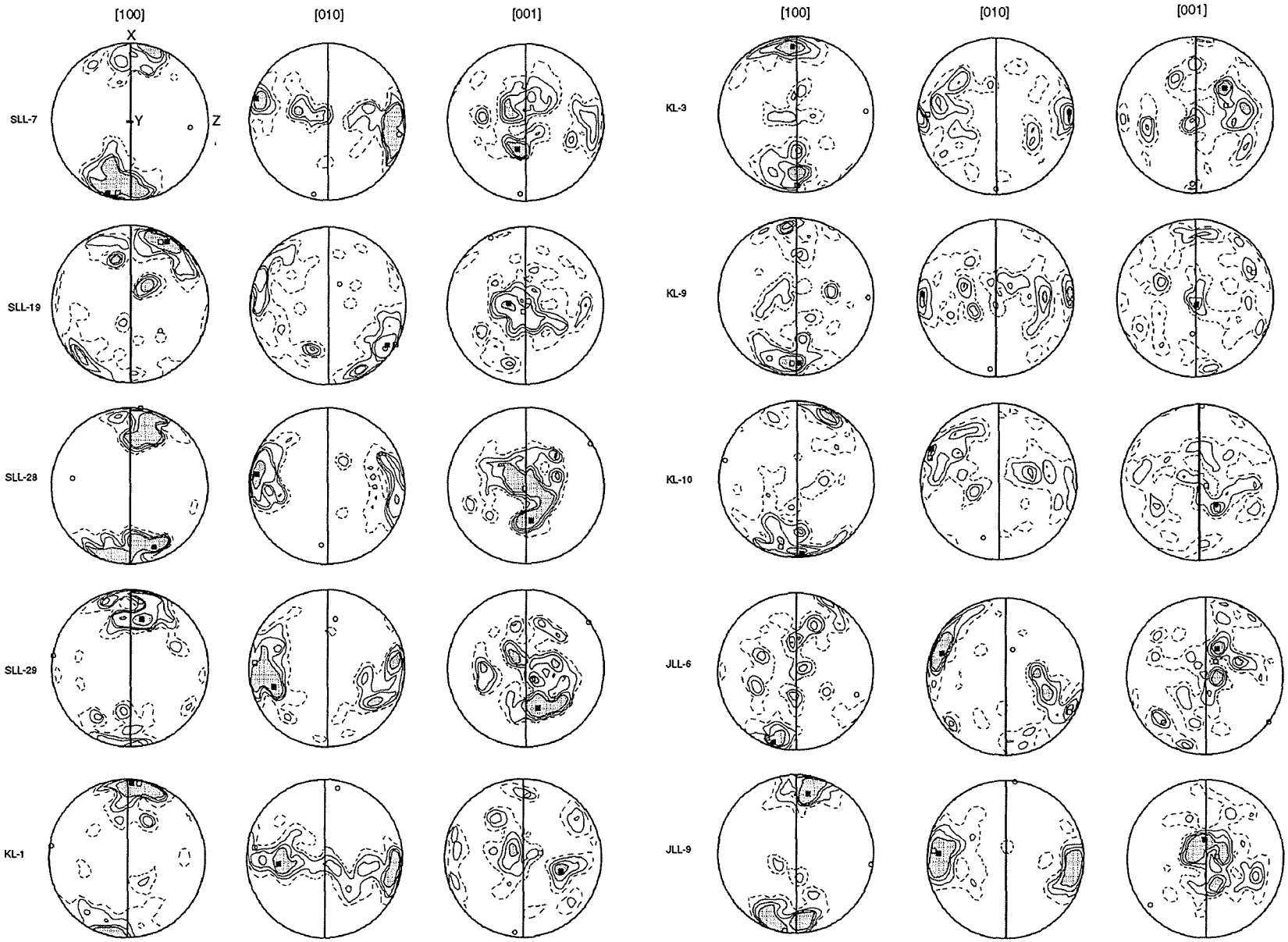

Figure 2. Lattice preferred orientations of olivine [100], [010] and [001] directions in samples from Summit Lake (SLL), West Kettle River (KL) and Jacque Lake (JLL). The contours are 1, 2, 3 and 4% of the number of measurements per 1% of the hemispherical area. The solid line is the foliation (XY plane), and the lineation (X direction) is parallel to the solid line.

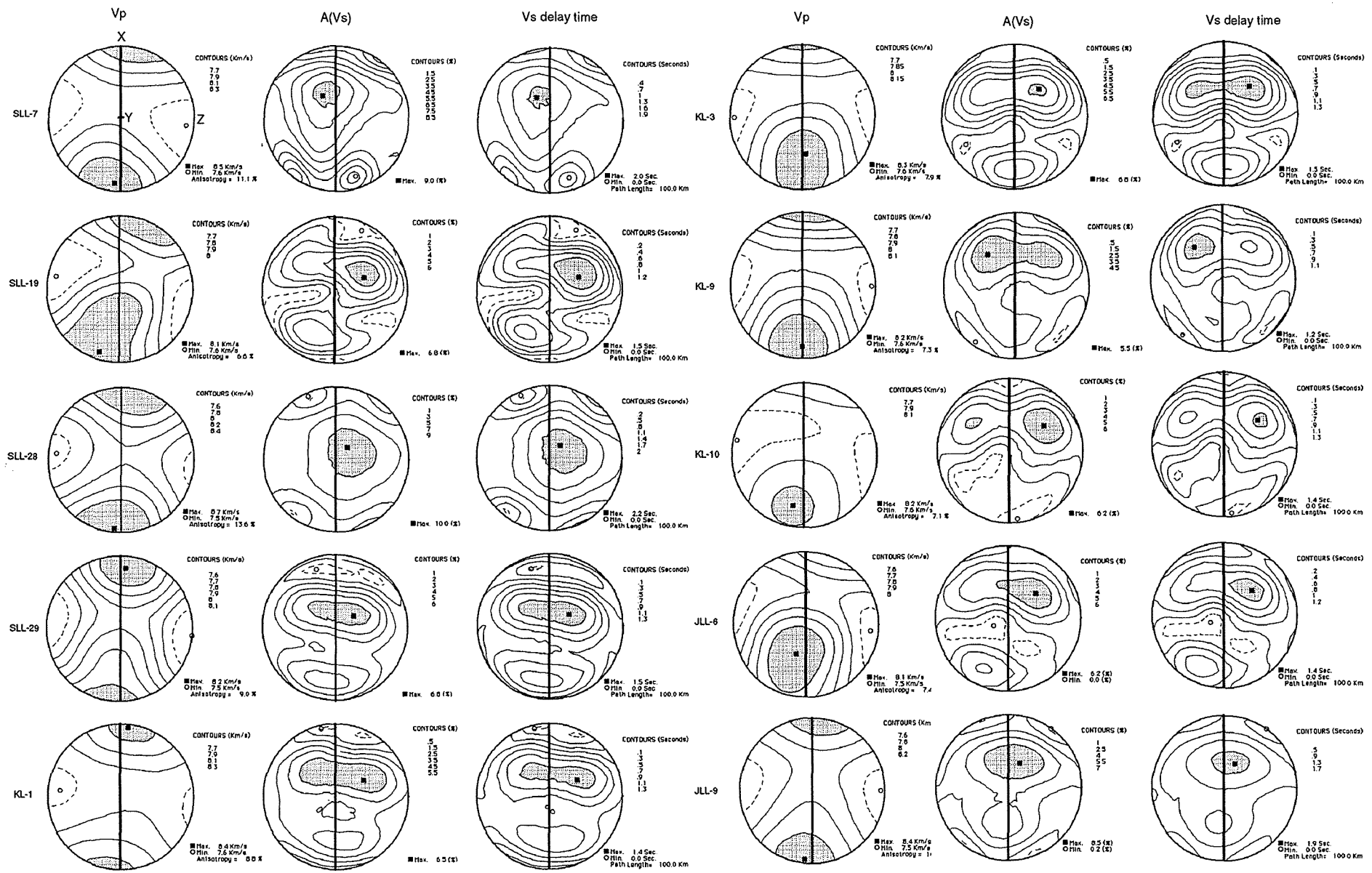

Figure 3. Seismic properties of each xenolith sample at 1000 °C and 1.4 GPa (corresponding to about 50 km depth). The Vs delay time was calculated for a path length of 100 km.

Conclusions

(1) Two olivine LPO patterns are recognized: one formed by (010)[100] slip, the other by {0kl}[100] slip.

(2) Both Vp and Vs anisotropies increase with the volume fraction of olivine, and decrease with the volume fraction of pyroxenes and spinel.

(3) Different slip systems result in different anisotropic patterns in the mantle rocks. When the high-temperature slip system (010)[100] prevails, $Vp(X)>Vp(Y)>Vp(Z)$. When the low temperature slip system {0kl}[100] prevails, however, $Vp(X)>>Vp(Y)\approx Vp(Z)$.

(4) According to our preliminary calculations, boundaries between fertile lherzolite and relatively depleted harzburgite, or between spinel-peridotite and garnet-peridotite can hardly be seismically reflective (Bostock, 1997). Thus, the observed dipping or subhorizontal seismic reflections in the upper mantle are likely caused by anastomosing metasomatism zones.

(5) The relationship between seismic properties (Vp, Vs anisotropy and splitting) and tectonic framework (i.e., foliation and lineation) for mantle xenoliths from the southern Cordillera are similar to those from the northern Cordillera (Alligator Lake and Castle Rock) and Alaska (Nunivak Island). The only reasonable explanation of the difference in the SKS splitting between the northern and southern Cordilleras (Bostock & Cassidy, 1995) is a difference in the orientation of the tectonic frameworks. In other words, the upper-mantle deformation is dominated by strike-slip shear (i.e., mantle roots of Tintina fault and Denali fault) beneath the northern Cordillera, whereas the upper-mantle deformation beneath the southern Cordillera is dominated by the subduction of the Pacific plate beneath the North America continent.

References

Bostock (1997) Nature, 390, 392-395.
Bostock and Cassidy (1995) Geophys. Res. Lett., 22, 5-8.
Ji et al. (1994) Tectonophysics, 239, 1-27.
Silver and Chan (1991) J. Geophys. Res., 96, 16429-16454.

Tertiary crustal extension in central British Columbia

L.C. Struik[1], D.G. MacIntyre[2], R.G. Anderson[1], S. Wetherup[3], M. Villeneuve[4], R. Enkin[5], M. Haskin[6], L. Snyder[6] and N. Grainger[3]

Abstract

Dextral transform faults in the Tertiary and Quaternary of the Canadian Cordillera form extensional complexes in their transfer zones. Through the Tertiary, three distinct episodes of extension and translation are interpreted. The transform systems are oblique to each other and the older systems are cross-cut by the younger ones. The early Eocene event is the most pervasive and is interpreted to have driven the formation of the Chilcotin Plateau, volcanic assemblages and locally developed core complexes like the Vanderhoof Metamorphic Complex.

The Vanderhoof Metamorphic Complex, Babine Lake metamorphic suite and Tertiary structures affecting Eocene volcanic and sedimentary sequences are interpreted to represent components of a zone of Eocene crustal extension in central British Columbia. The Tertiary metamorphism and crustal extension are superimposed on late Paleozoic and early Mesozoic oceanic and island arc assemblages of the Cache Creek and Stikine terranes and their late Mesozoic overlap assemblages of mainly granitic rocks.

Vanderhoof Metamorphic Complex consists of a biotite quartzo-feldspathic and marble/amphibolite paragneiss sequence intruded mainly by biotite granite and granodiorite orthogneisses. Paragneisses of the complex have fine-grained siliciclastic rock, limestone marl and possibly basalt protoliths. Orthogneisses of the complex form abundant sills and dykes, and some large plutonic masses. Metamorphic grade of the complex is of the amphibolite facies. At the upper contact of the metamorphic complex the orthogneisses are deformed into ductile augen mylonite and the overlying Cache Creek Group ultramafic rocks form two to four metre thick gouge zones.

Biotite cooling age from Vanderhoof Metamorphic Complex paragneiss at Sinkut Ridge. Information and diagram from Mike Villeneuve. Mylonitization along the Nulki and Sinkut detachments occurred either during or after emplacement of the 55Ma Frank Lake pluton. The effusive volcanism of the Ootsa Lake and Endako Groups occurred during the interval of mylonitization and uplift of the Vanderhoof complex, as dated by Ar-Ar ages of metamorphic hornblende of the Vanderhoof Complex, and whole rock and biotite determinations of the volcanic rocks. The metamorphic complex and the Cache Creek Group rocks are intruded and overlain by the Tertiary felsic to intermediate volcanic and intrusive rocks. The mylonite of the Sinkut fault forms a low-angle detachment that has down to the southeast motion in the central part of the exposed complex.

Vanderhoof Metamorphic Complex appears to represent one of a number of extension generated windows into the mid crust in south-central British Columbia. These windows may be separated from each other by a thin carapace of upper plate rocks, primarily of Mesozoic and Tertiary age that overlies variously uplifted metamorphic crustal blocks. That carapace in the Fort Fraser map area consists of moderately southeast and northwest dipping fault blocks.

For example the distribution of Eocene Ootsa Lake and Endako Group volcanics in the Endako map area (NTS 93K/3, see figure) defines a northeasterly trending graben flanked by Mesozoic plutons of Endako Batholith. Northwest and northeasterly trending faults offset the Eocene volcanics and therefore must be Eocene or younger. The northeasterly trending faults in the northcentral part of the map area bound small rotated blocks. These are interpreted as formed by northwesterly directed extension. The north to northwest trending Casey Fault, confined to the plutons, has dextral strike-slip shear fabrics. Northwesterly trending faults in the west part of the Endako (93K/3) map area have disrupted Eocene andesite of the Ootsa Lake Group.

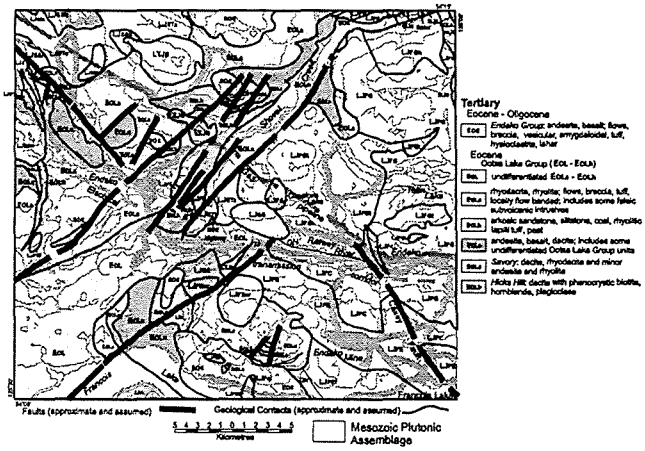

It is suspected that crustal extension-generated fault-blocks have redistributed Eocene and older mineralization in the northern end of the Nechako and Chilcotin plateaux and been responsible for the generation of new precious and base metal mineralization. For example at the Endako Molybdenum mine the mineralized plutons are disrupted in Tertiary fault blocks rotated about horizontal axes. The rotational angles of up to 40^{o} were determined by paleomagnetic measurements on Eocene dykes. Geometrically pre-Eocene sequences should be detached from underlying metamorphic sequences like the Vanderhoof Metamorphic Complex. These detachments may dip shallowly to the northwest and underlie a large part of the Skeena Arch.

References

Lowe, C., Enkin, R.J. and Dubois, J. 1998: Magnetic and paleomagnetic constraints on Tertiary deformation in the Endako region, central British Columbia; in Current Research 1998-A; Geological Survey of Canada, p. 125-134.

Struik, L.C. 1993: Intersecting intracontinental Tertiary transform fault systems in the North American Cordillera; Canadian Journal of Earth Sciences, v. 30, p. 1262-1274.

Struik, L.C. and MacIntyre, D.G., 1998: Nechako NATMAP Project Overview, central British Columbia, year three; in Current Research 1998-A; Geological Survey of Canada, p. 79-88.

Whalen, J.B., Struik, L.C., and Hrudey, M.G., 1998: Bedrock geology of the Endako map area, central British Columbia; in Current Research 1998-A; Geological Survey of Canada, p. 113-124

Wetherup, S., 1997: Geology of the Nulki Hills and surrounding area (NTS 93F/9 and F/16), central British Columbia; in Current Research 1997-A; Geological Survey of Canada, p. 125-132

Wetherup, S. and Struik, L.C. 1996: Vanderhoof Metamorphic Complex and surrounding rocks, central British Columbia; in Current Research 1996-A; Geological Survey of Canada, p. 63-70.

1. Geological Survey of Canada, 101-605 Robson Street, Vancouver, B.C. Canada V6B 5J3
2. British Columbia Geological Survey, 1810 Blanshard Street, Victoria, B.C., Canada V8V1X4
3. Department of Earth and Atmospheric Sciences, University of Alberta, Edmonton, Alta, Canada T6G 2E3
4. Geological Survey of Canada, 601 Booth Street, Ottawa, Ont., Canada K1A 0E6
5. Geological Survey of Canada, P.O. Box 4000, Sidney, B.C., Canada V
6. Department of , University of Wisconsin at Eau Claire, Eau Claire, Wisconsin, U.S.A.

L.C. Struik: bstruik@airwolf.gsc.emr.ca
R.G. Anderson: banderson@gsc.nrcan.gc.ca
D.G. MacIntyre: Don.MacIntyre@gems1.gov.bc.ca
S. Wetherup: wetherup@gpu.srv.ualberta.ca
M.M. Villeneuve: villeneuve@gsc.nrcan.gc.ca
R. Enkin: enkin@pgc.nrcan.gc.ca
M. Haskin: c/o L. Snyder
L. Snyder:snyderld@uwec.edu
N. Grainger: ng3@gpu.srv.ualberta.ca

Comparative Images of Proterozoic and Cenozoic Subduction Complexes

Arie J. van der Velden and Frederick A Cook
Department of Geology and Geophysics
University of Calgary, Calgary, Alberta T2N 1N4

The discovery of mantle reflections that are interpreted as a relict subduction zone along the LITHOPROBE SNORCLE Transect provides an opportunity to analyze geometric features of the data by comparing them to modern convergent margins. This approach provides a basis for interpreting the deep reflection profile where it is difficult to trace individual features to outcrop, as well as for determining the nature of ancient (ca. 1.9 Ga) tectonic processes in relation to processes observed today.

In this article, a comparison is made between Proterozoic subduction preserved at depth in the Fort Simpson area, as imaged on SNORCLE line 1 (Figure 1), and the modern subduction zone imaged beneath and offshore Vancouver Island (Figure 2). Many reflections observed on these images are similar in geometry, character and scale, and can thus be interpreted in a similar manner.

For example, reflections TW on the SNORCLE data (Figure 1) outline an eastward-tapering wedge that is located at the transition from the Fort Simpson Terrane (ca. 1.845 Ga) to the Wopmay orogen (ca. 2.1-1.85 Ga Hottah terrane and Coronation margin). Reflections within this wedge steepen upward and are truncated against steeply dipping reflections JH on the west. This geometry is identical to that of thrust structures in accretionary prisms thoughout the world (Karig and Sharman, 1975). Here, we compare this geometry to that of Vancouver Island line 85-01, where sedimentary layers steepen eastward and upward as sediments scraped off the downgoing Juan de Fuca plate were added from the west (Figure 2). The geometry of the wedge and its position within a convergent zone are consistent with the interpretation that reflections TW outline a trench wedge that includes rocks that were scraped off of subducted crust. In both profiles, the maximum (time) thickness of the wedge is about 5 s, and the width of the wedge along its base is 60-80 km.

Reflections Su1 and Su2 are two subparallel bands of reflections that are located beneath the accretionary wedge (Figure 1) They are similar to the C and E reflections of Vancouver Island line 1 (Figure 2), which have been interpreted to delineate a slice of material that was accreted to the North American plate by underplating (Clowes et al., 1987). On the SNORCLE data, these

reflections are interpreted as a subducting slab that was attached to the bottom of the Slave-Hottah plate.

East of wedge TW, reflection H4 is a prominent, irregular event that has the earmarks of an unconformable surface. Its position, east and structurally above the accretionary wedge, is appropriate for a forearc basin such as the Tofino Basin on line 85-01 (Figure 2). Near the east side of the Tofino Basin, reflections FT may represent a fossil trench that projects from the base of the basin to the lower crust. An analogous event H6 is present on the SNORCLE profile. A difference between the SNORCLE line and line 85-01 is that the Tofino Basin shows layered reflections from sediments within it, whereas the zone above reflection H4 is remarkably non-reflective.

Below reflection H4, the mid to lower crust shows diffuse east-dipping reflections and lacks a well-defined Moho. This reflection pattern is similar to that of SBC line 16 of the Southern Cordillera Transect, where a ramp has been interpreted in the lower crust that juxtaposes the Cenozoic subduction complex with the Insular superterrane (Varsek et al., 1993). On the SNORCLE line, this reflection pattern can be similarly interpreted as part of a Fort Simpson subduction complex.

The similarity of the reflection geometry and the scale of structures between the Fort Simpson - Wopmay transition and the modern accretionary complex near Vancouver Island is remarkable. Even though reflections cannot be tied to surface geologic data, the interpretation of the SNORCLE data is aided by comparison to modern analogs. The processes of accretion at a subduction zone during the Proterozoic appear to have been essentially identical to the development of accretionary complexes today.

References

Clowes, R.M., M.T. Brandon, A.G. Green, C.J. Yorath, A. Sutherland Brown, E.R. Kanasewich and C.R. Spencer, 1987, LITHOPROBE - southern Vancouver Island: Cenozoic subduction complex imaged by deep seismic reflections: Can. J. Earth Sci, V. 24, pp. 31-51.

Karig, D.E. and G.F. Sharman, 1975, Subduction and accretion in trenches: Bull. Geol. Soc. America, V. 86, pp. 377-389.

Varsek, J.L., F.A. Cook, R.M. Clowes, J.M. Journeay, R.R. Parrish, E.R. Kanasewich and C.R. Spencer, 1993, LITHOPROBE crustal reflection survey of the southern Canadian Cordillera II: Coast Mountains Transect: Tectonics, V. 12, pp. 334-360.

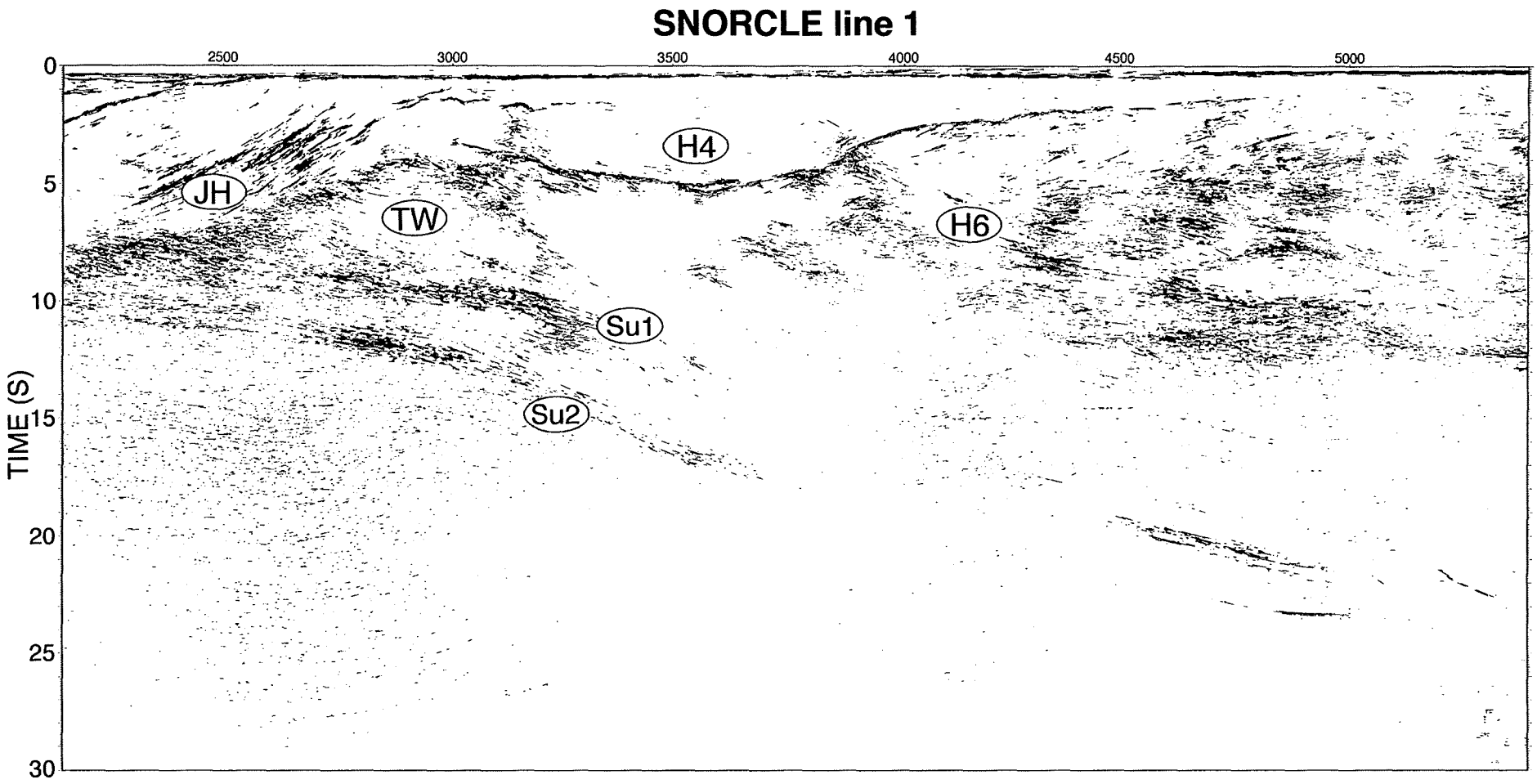

Figure 1. LITHOPROBE SNORCLE line 1 in the vicinity of the Fort Simpson-Hottah transition. TW - accretionary wedge, Su1 and Su2 - subducted slab, JH - Johnny Hoe suture.

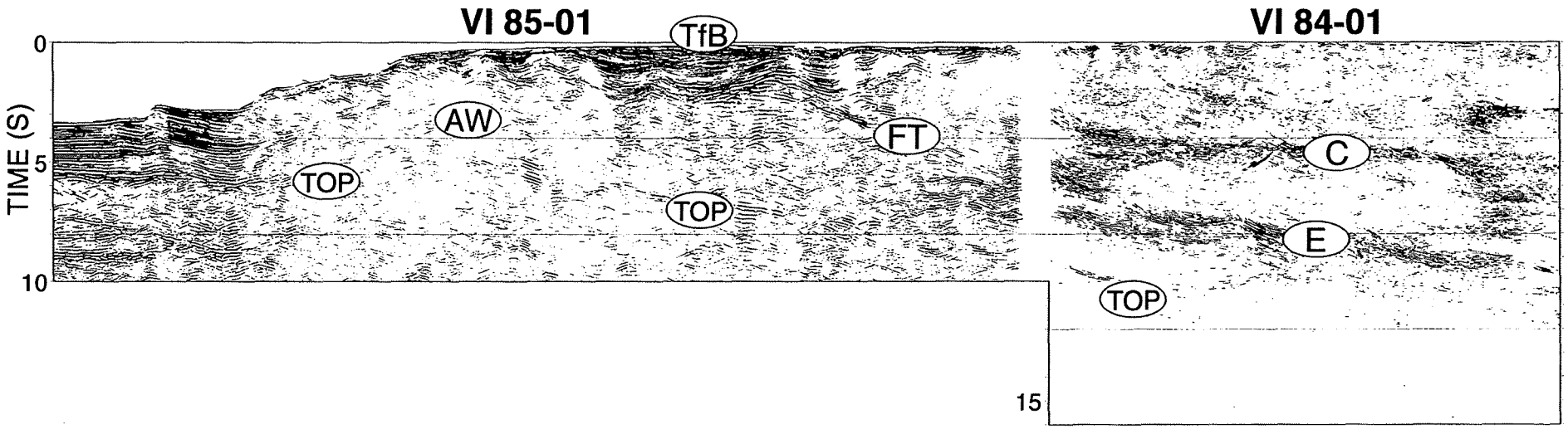

Figure 2. LITHOPROBE lines 85-01 (offshore) and 84-01 (onshore) Vancouver Island. AW - accretionary wedge, TfB - Tofino Basin, FT - possible fossil trench, TOP - top of oceanic plate.

HYDROGEN-ENHANCED ELECTRIC CONDUCTIVITY OF DIOPSIDE CRYSTALS: IMPLICATIONS FOR CONDUCTING BEHAVIOR OF THE UPPER MANTLE WEDGE ABOVE THE SUBDUCTING SLAB

Zichao Wang and Shaocheng Ji

Department of Geology, University of Montreal, C.P. 6128, Succursale "Centre-Ville", Montreal. Québec, Canada

Georg Dresen and Quan Bai

GeoForschungsZentrym Potsdam, Telegrafenberg A 26, D-14473 Potsdam, Germany

Introduction

It has been proposed that hydrogen (H) incorporated into nominally anhydrous minerals as a charged species may significantly increase their electrical conductivity (EC) if the H solubility and mobility are large enough (Karato, 1990). This hypothesis is of significant impact on electrical-conduction property of silicate minerals, origin of LVZ and electrical structure of the Earth interior. However, little progress has been made in testing this hypothesis since large part of EC measurements were performed at atmosphere pressure and unconstrained conditions only (Duba and Heard, 1980; Kingery et al., 1976; Jones, 1992). In these experiments, controlling hydrogen concentration (C_H) in crystals is extremely difficulty. In a recent experimental study on the solubility and stability of H in diopsides from Indian (In-), Sri-Lanka (Sri-) and Russian (Ru-), Bai et al. (1994) found that kinetics of H diffusion in diopsides depends critically on crystal impurity chemistry at high temperature. They observed a very fast kinetics of H diffusion in the In-diopside. In the Sri-diopside, however, hydrothermal annealing did not change C_H within experimental time scale (t>72 h), suggesting a very slow kinetics of the H diffusion. For Ru-diopside, the C_H changes continuously with annealing time indicating an intermediate kinetics of the H diffusion. This observation gives an important hint that we can obtain diopsides with different C_H so that direct experimental test on the enhancement of H in EC can be performed on these diopside crystals. In this paper, we will report the results of EC measurements on the In-, Sri- and Ru-diopsides and provide the first experimental evidence for the H-enhanced EC in diopsides with a brief discussion on possible physical mechanism.

Experimental Procedure and Results

Characterization of diopside single crystals

Diopside single crystals used in this study were from Sri-Lanka (Sri-), Russian (Ru-) and Indian (In-) with chemical composition of $(Ca_{0.985}Mg_{0.979}Me_{0.03})(Si_2O_6)$, $(Ca_{0.970}Mg_{0.973}Me_{0.05})(Si_2O_6)$ and $(Ca_{0.967}Mg_{0.961}Me_{0.07})(Si_2O_6)$ respectively. In the

chemical formula, Me stands for Fe, Cr, Mn and Ni. The ICP analysis indicated Fe as the major impurity, which ranged from 0.5 wt.% (Sri-diopside), 1.3 wt.% (Ru-diopside) to 2.3 wt.% (In-diopside).

Previous studies demonstrated isotropic behaviors of H diffusion and EC for diopside crystals (Ingrin et al., 1995; Huebner and Voigt, 1988), thus the results from one particular orientation should be representative. We chose [010] orientation in this study. Samples were thin plates with uniform dimension of 4x4x1 mm^3. The large face was parallel to (010) plane with two orthogonal sides sub-parallel to [100] and [001] crystallographic directions. Samples were first hydrothermally annealed (wet-annealing) under conditions of T=1273 °C and P=300 MPa with $Mg(OH)_2$ as water supply. The purpose of hydrothermal annealing was to obtain samples with maximum C_H at given conditions. Dehydration experiment was then performed on the wet annealed samples under the conditions of T=900-1200 °C, P=0.1 MPa and $fO_2=10^{-18}$-10^{-5} MPa in a CO-CO_2 mixture for 2 to 200 h. The purpose of dehydration experiments was to monitor the variation of C_H with time. All samples after hydrothermal and dehydration experiments were examined by FTIR spectroscopy under microscope. The C_H was calculated from obtained absorbance in the wavenumber of 3 micron using the calibration of Paterson (1982).

Electric conductivity measurement

EC measurements were performed at a 0.1 MPa, high-T apparatus with the setting similar to that described by Duba et al. (1990) and Bai et al. (1995 and in press). To determine the dependence of EC on H, we first increased temperature to desired value in a short period (<3 h), and measured the EC as function of time in the first 72 h when dehydration process concurrently occurred. To determine the dependence of EC on T, measurements were made after the first 72 h when equilibrium of C_H in crystals was reached. EC data were collected following paths of both increasing and decreasing T.

Experimental results

Variation of C_H with time: C_H was calculated from FTIR spectra as a function of time. The results were summarized as follows: (1) In-diopside crystal yields an amount of H of ~1000 H/10^6 Si after "wet-annealing". The dry annealing (at 1100 °C) removed more than 90% H within the first two hours (C_H reduced to ~100 H/10^6 Si). Very low C_H (~50 H/10^6 Si) was detected after 72 h dehydration. (2) FTIR measurements showed fairly high C_H (~1000 H/10^6 Si) in Sri-diopside. Both hydrothermal and dry anneals did not change this initial C_H in a time period up to t=120 h. The C_H remains relative constant during the whole EC measurement (~900-1000 H/10^6 Si). (3) Hydrothermal annealing leads to an increase of C_H to ~1000 H/10^6 Si in Ru-diopside. An afterwards dry annealing removed ~70-90% of the total H in 72 h. The re-equilibrium in C_H was reached after t=72 h with C_H=~100 H/10^6 Si.

The above observations demonstrate the lowest C_H (~50 H/10^6 Si) and the highest (~1000 H/10^6 Si) in In-diopside and Sri-diopside respectively, which could be kept relative constant during EC measurement for a time period up to 120 hours at T=1273 °C

(Table 1). The C_H in Ru-diopside varied with time from ~1000 to ~100 H/10^6 Si within the first 72 h.

Table 1. Summary of samples, experimental conditions and results

Diopside	Impurities		Condition			log (σ_0)	Q (kJ/mol)
	C_H (H/10^6 Si)	C_{Fe} (%wt.)	T (°C)	f_{O2} (MPa)	time (h)		
Indian [010]	50±25	2.3	1000 - 1220	10^{-12}	>72	-0.374±0.005	129±4
Russian [010]	100±50	1.3	1000- 1220	10^{-12}	>72	1.191±0.012	171±6
Sri-Lanka [010]	900±100	0.5	1000- 1220	10^{-12}	>72	0.399±0.004	132±3

Electric conductivity: EC of all three crystals was measured as a function of time at conditions of T=900-1273 °C and $f_{O_2}=10^{-9}$ MPa. Fig. 1 showed one set of results obtained at T=1000 °C. Both Sri- and Ru- diopsides showed a clear drop in EC within the first 10 h. The EC of Sri-diopside became relative constant at t>10 h. The EC of Ru-diopside decreased continuously up to t=72 h. The EC, measured at t=72 h ($\sigma_{Sri}=1.58\times10^{-5}$ S/m and $\sigma_{Ru}=1.86\times10^{-6}$ S/m), are about factors of 1.4 and 9 lower than that measured at t=2 h ($\sigma_{Sri}=2.19\times10^{-5}$ S/m and $\sigma_{Ru}=1.66\times10^{-5}$ S/m) for the Sri- and Ru-diopsides. No clear change in EC was observed for In-diopside ($\sigma_{In}=3.8\times10^{-5}$ S/m).

The dependence of EC on temperature was evaluated from the data acquired at identical time intervals (t>72 h) for each sample. The C_H values of samples were estimated as 50±25H/10^6 Si, 100±50 H/10^6 Si and 900±100 H/10^6 Si for In-, Ru- and Sri-diopside crystals respectively when the EC measurements were made. Data of all three diopsides lie on straight lines on a semi-log plot of σ vs. 1/T over the range T=900-1273 °C (Fig. 2), suggesting that a single conduction mechanism dominated under these conditions. The least square fits of the EC data to

$$\sigma = \sigma_0 \exp(-\frac{Q}{RT}) \qquad (1)$$

give activation energies of Q=132 kJ/mol for Sri-diopside, Q=171 kJ/mol for Ru-diopside and 129 kJ/mol for In-diopside. In Eq. (1) σ_0 is pre-exponential parameter and RT has the usual meaning.

Summary: (1) Different EC-time relationships were observed among these three diopsides: EC of In-diopside was time-independent at all given conditions; Sri-diopside underwent a substantial drop in EC (about a factor of 1.4) within the first 10 h, measured EC was more or less constant afterwards. The most pronounced variation of EC with time was observed in Ru-diopside, EC dropped about a factor of 9 during 72 h (from 1.66×10^{-5}

at t=2 h to 1.86×10^{-6} S/m at t=72 h, T=1000 °C). (2) In general, we observed $\sigma_{Sri} > \sigma_{In} > \sigma_{Ru}$ at T<1173 °C and $\sigma_{Sri} > \sigma_{In} \approx \sigma_{Ru}$ at T≥1173 °C (t>72 h). The Sri-diopside shows the greatest conductivity among the three diopsides at comparable conditions, which is about one order higher than that of the others. (3) Measured activation energies are similar for Sri- and Ru-diopsides, which are smaller than that of In-diopside.

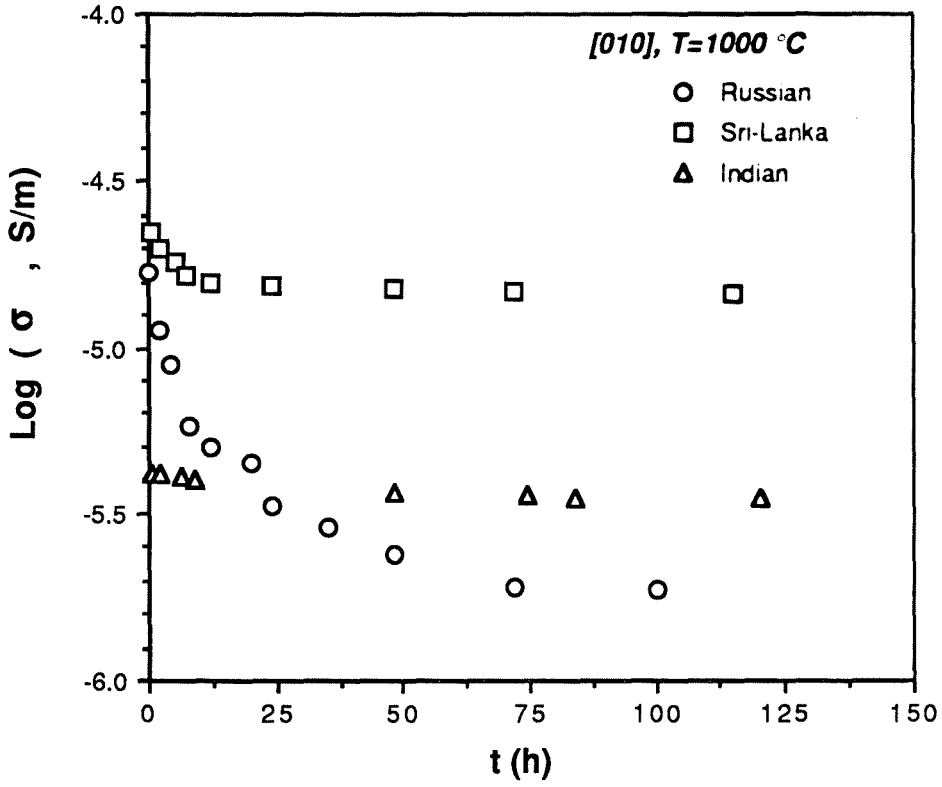

Figure 1. EC as a function of time for three diopside crystals. Notice that a longer equilibrium time (t>72 h) was required for the Ru-diopside ($f_{O2} = 10^{-9}$ MPa).

Discussion

The most important observation in this work is the difference in electric conductive behavior among the three diopsides at high temperature, which we attributed to the influence from H incorporated into diopside crystals based on the following evidences: (1) Three diopside crystals showed difference only in C_H and C_{Fe}, otherwise they are similar in either bulk or impurity chemistry. (2) One would expect a greater EC in the In- and Ru-diopside because of higher C_{Fe}, which has been associated with increased EC in orthopyroxene, synthetic olivine and diopsides (Huebner and Voigt, 1988; Duba and Nicholls, 1973; Duba et al., 1973; Hinze et al., 1981). However, the Sri-diopside, which has the lowest C_{Fe}, but the highest C_H, showed a surprisingly great conductivity comparing to the other two diopsides. We also noticed that the In-diopside,

which contains the lowest C_H, showed the lowest EC at t<10 h. It caught up with that of Ru-diopside at t>25 h, when both crystals showed comparable C_H. The EC of In-diopside was higher than that of Ru-diopside after t>72 h (Fig. 1), we assume this due to higher C_{Fe} in In-diopside. (3) A decrease in EC of the Ru-diopside with time was clearly observed, which was parallel to the process of dehydration. In contrast, the EC of both In- and Sri-diopsides equilibrated rapidly and achieved steady-state values within a few hours. The rapid equilibrium in EC can be attributed to constant C_H values, which results from the fastest (for In-diopside) and the slowest (for Sri-diopside) kinetics of hydrogen diffusion. (4) The off-sets (about 0.9 log unit) in EC (at t>72 h) between the Sri- and the In-/Ru-diopsides are much larger than that between the In-diopside and the Ru-diopsides (<0.2 log units at maximum), which is correlated to the difference in C_H among them.

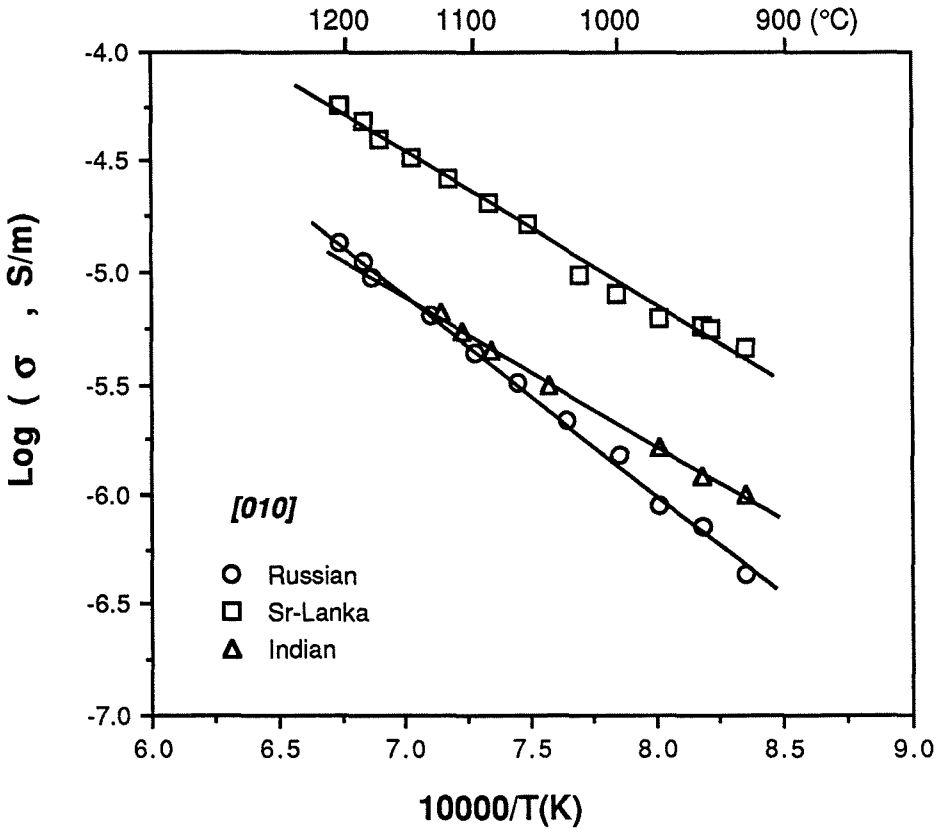

Figure 2. Plot of EC against temperature for three diopside crystals. Data were collected under the conditions of t>72 h and $f_{O2} = 10^{-9}$ MPa.

To understand the conducting behavior of diopsides, we divided observed EC (σ_T) into two components, one (σ_{CH}) for the contribution from H (by assuming H as effective charge carriers contributing separately to the total EC) and the other (σ_0) for the contributions from all other charge carriers (Kingery et al., 1976)

$$\sigma_T = \sigma_0 + \sigma_{CH} \quad (2)$$

Contribution from each charged, mobile species to EC of a solid is given by the Nernst-Einstein relation (Mott and Gurney, 1948)

$$\sigma = fDcq^2 / kT \quad (3)$$

in which f is a numerical (correlation) factor approximately equal to unit, D is the diffusivity, c is the concentration of charged species, q is the electrical charge of the charged species and k is the Boltzmann constant. We assumed that σ_{CH} is proportional to the product of C_H and mobility of hydrogen, which can be estimated through the diffusivity of H from Ingrin et al (1995) and the C_H from this study with a charge q=+e (hydrogen-related charge carriers). Fig. 3 shows the results after removing the contributions from σ_{CH}. It can be seen that the EC of diopsides now shows the order of $\sigma_{In}>\sigma_{Ru}>\sigma_{Sri}$, which follows the order of C_{Fe}. Differences in EC among diopsides are also reduced within 0.3 in log unit reflecting the contribution from C_{Fe}.

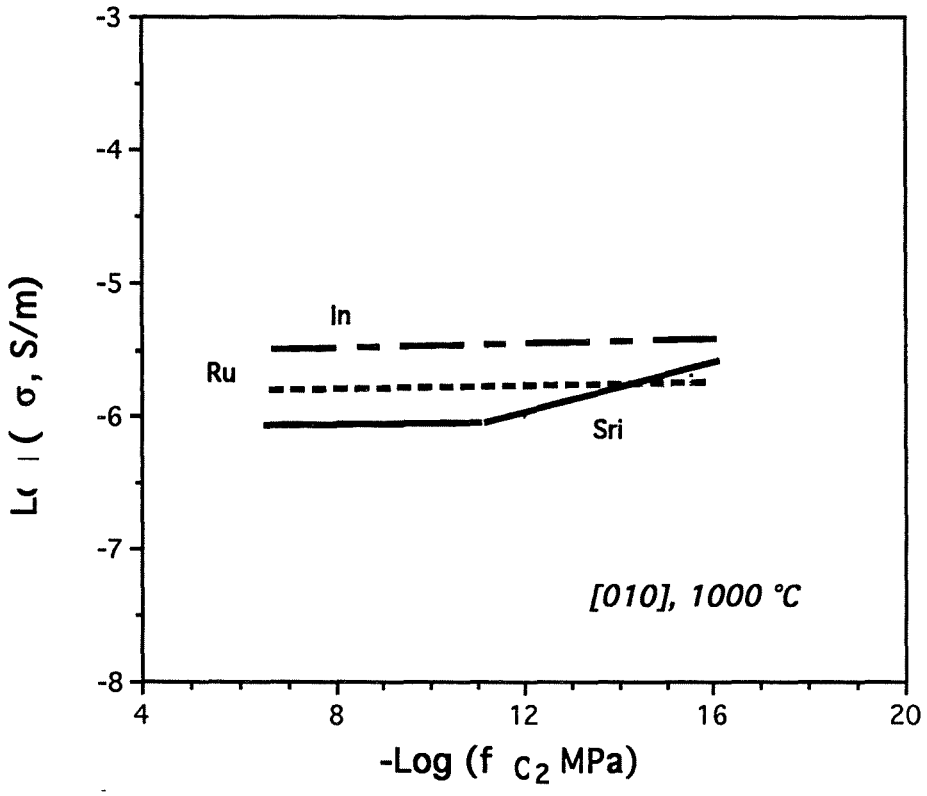

Figure 3. Simplified diagram showing the EC of diopside crystals as a function of oxygen fugacity after removing the contribution from σ_{CH}.

In previous study, oxygen vacancy was suggested as the intrinsic defect controlling EC of a pure diopside, increased EC in diopside with high C_{Fe} was associated with the thermal ionization of Fe^{2+} to form Fe^{3+} plus electrons in the conducting band (Huebner and Voigt, 1988). To interpret the H-enhanced EC, we consider two

mechanisms:

(1) The predominant charge carriers in the Sri-diopside are protons, as assumed in olivine by Karato (1990). Thus observed enhancement of EC in Sri-diopside can be a result from diffusion of H. The conducting behavior is controlled by the flux of protons being coupled with a counterflux of electron holes. This argument consists with the theory that the faster charge carrier dominates for electrical conduction, and it is supported by two observations: (A) The diffusivity of H in diopside is about two orders higher than that of oxygen vacancies (Ingrin et al., 1995; Huebner and Voigt, 1988; Farver, 1989). (B) Activation energy of Sri-diopside (132 kJ/mol) is very close to that for H diffusion (136 kJ/mol) obtained in a dehydration experiment (Ingrin et al., 1995).

(2) The alternative mechanism is that the dissolution of hydrogen increases the concentration and/or mobility of the charged intrinsic defects (for example, oxygen vacancy in diopside). This H-dissolution related increasing in intrinsic defect concentration/mobility can result in an substantial enhancement in EC, if these defects control the EC. The correlation between C_H and intrinsic point defects was experimentally studied for a number of silicate minerals including olivine and diopside (Bai et al., 1994; Ingrin et al., 1995; Huebner and Voigt, 19884), however, more works are definitely needed to understand the physics.

As a conclusion, we suggest that the presence of H can significantly increase the EC of diopsides. Enhanced EC could result from the faster diffusion of H (acting as a charged mobile species) and/or the increase of intrinsic charged defect concentration/mobility due to the incorporation of H. The upper mantle wedge above the subducting slab is an environment of high temperature and high fluid pressure. Thus observed high conducting zone inside the upper mantle wedge above the subducting slab may be originally correlated with high solubility of hydrogen in mantle minerals such as olivine and pyroxenes, which is proved by our experimental results.

Acknowledgment

We thank David Kohlstedt for their helps in providing diopside crystals and equipment for EC measurements. M. Andrew and S. Mei are appreciated for analyzing FTIR spectra and re-calculating the hydrogen concentration. This study was supported by the Lithoprobe (SNORCLE) grant.

References

Bai, Q., Z-C. Wang, G., Dresen, S., Mei, and D.L., Kohlstedt, 1994. Solubility and stability of hydrogen in diopside single crystals, in *Trans. Am. Geophys. Union, Fall Meeting Suppl.* **75**: 652.

Bai, Q., Z-C., Wang and D.L., Kohlstedt. 1995. Manganese olivine I: electrical conductivity. *Phys. Chem. Minerals*, 22: 489-503.

Bai, Q., Z-C., Wang and D.L., Kohlstedt. 1997. Manganese olivine II: Point defects relaxation. *Phys. Chem. Minerals* (in press).

Duba, A.G. and H.C., Heard, 1980. Effect of hydrogen on the electrical conductivity of olivine. *EOS* **61**: 404.

Duba, A. and I.A., Nicholls, 1973. The influence of oxidation state on the electrical conductivity of olivine. *Earth. Planet. Sci. Lett.* **18**: 59-64.

Duba, A., J.N., Boland and A.E., Ringwood, 1973. The electrical conductivity of pyroxene. *J. Geol.* **81**: 727-734.

Duba, A., R.N., Shock, E.L., Arnold and T.J. Shankland, 1990. An apparatus for measurement of electrical conductivity to 1500 °C at know oxygen fugacity. In: The Brittle-Ductile Transformation in Rocks, editors. A.G., Duba W.B, Durham, J.W., Handin, H.F., Wang, *Geophys Monogr 56*, Am. Geophys. Union, Washington, DC, 207-210.

Farver, J.R., 1989. Oxygen self-diffusion in diopside with application to cooling rate determinations. *Earth. Planet. Sci. Lett.*, **92**: 386-396.

Hinze,E., W., Will, and L., Cemic, 1981. Electrical conductivity measurements on synthetic olivines and on olivine, enstatite and diopside from Dreiser Weiher, Eifer (Germany) under defined thermodynamic activities as a function of temperature and pressure. *Phys. Earth. Planet. Int.*, **25**: 245-254.

Huebner, J S. and D.E., Voigt, 1988, Electrical conductivity of diopside: evidence for oxygen vacancies. *Am. Mineral.* **73**: 1235-1254.

Ingrin, J., S. Hercule and T. Charton. 1995. Diffusion of hydrogen in diopside: results of dehydration experiments. *J. Geophys. Res.* **100**: 15489-15499.

Jones, A G., 1992. Electrical conductivity of the continental lower crust. in: Continental Lower Crust, editors: D.M., Fountain, R., Arculus and R.W., Kay, 81-143. Elsevier, Amsterdam-London-New York-Tokyo.

Karato, S., 1990. The role of hydrogen in the electrical conductivity of the upper mantle. *Nature* **34**: 272-273.

Kingery, W.D., H.K., Bowen, and D.R., Uhlmann, 1976. Introduction to Ceramics, 2nd edition, (Ch. 18). Wiley, New York, 852-911.

Kröger, F.A. and Vink, H.J., 1956. Relation between the concentration of imperfections in crystalline solids. in Solid State Physics, 3, editors F. Seizte and D. Turnbull, Academic, New York.

Mott, N.F and R.W., Gurney, 1948. Electrical Processes in Ionic Crystals. Ch. 2, Oxford University Press.

Paterson, M S. 1982, The determination of hydroxyl by infrared absorption in quartz, silicate glass and similar materials. *Bull. Mineral*, **105**: 20-29.

Kinematics and Fault Zone Processes, Denali Fault System, SW Yukon

Joseph Clancy White
Department of Geology, University of New Brunswick
Fredericton, NB E3B 5A3

The initial objectives of the this project, proposed as part of a multi-year project, were three-fold:
(1) Evaluation of the of kinematic and displacement records along the Denali fault system.
(2) Examination of fault rock textures and fabrics to establish mechanical and chemical processes characteristic of upper crustal deformation.
(3) Comparison of deformation processes and P/T constraints with geophysical data (particularly seismic records) in the context of the rocks being records exhumed from a still-active seismogenic zone.

Re-evaluation of objectives at the end of each field season has led to an increased emphasis on neotectonic activity and the inter-relationships of physiography, seismicity and bedrock geology. The 1996 field season encompassed a regional survey of rocks along the Denali fault system from White River, Yukon (140° 35'W, 62°00'N) to Mansfield Creek, B.C. (136° 40'W, 59°52'N). The best exposures identified lay immediately west of Kluane Lake, particularly around its south end which were the focus of detailed field studies in 1997.

The first-order exercise to examine bedrock exposures as close to the fault trace as identified relevant exposures within Pennsylvanian through Cretaceous rocks of Wrangellia (Campbell & Dodds 1982a,b,c, 1983). Initial emphasis was placed on identifying the youngest deformation possible within these rocks in order to avoid Jura-Cretaceous deformation (Eisbacher 1976) that may not relate directly to the current behaviour of the Denali fault system. The latter approach involved specific care in identifying and collecting fault gouges that are often ignored in bedrock mapping. Examination of thin sections, as well as scanning and transmission electron microscopy has revealed an intensity of deformation often not evident during field mapping and brings in to question some earlier interpretations of limited deformation in many of these rocks.

Structural Geology, Fault Geometry and Earthquake Distribution

Deformation of Wrangellia rocks between the Denali (Shakwak and Dalton faults) and Duke River faults is very heterogeneous, and generally more intense than implied by previous work. Whereas basalts of the Triassic Nicolai greenstones can appear virtually untouched except for steepening of the beds, carbonates within them can be intensely deformed Foliation in the upper Paleozoic/lower Mesozoic sedimentary and volcanic units is commonly penetrative, producing a transposed compositional layering to which the regional lithostratigraphic contacts form enveloping surfaces and where observed, are zones of intense tectonism. The penetrative nature of these fabrics is difficult to observe in the field because of the fine-grained nature of many of the intermediate-silicic volcanic rocks. As a rule of thumb, if the rock looks nondescript, it is highly deformed, whereas relatively undeformed material exhibits primary textures. I believe this has led to an emphasis on low strains, in that when you see a recognizable feature, it tends to be primary.

Samples retrieved from exactly along the mapped trace of the Denali Fault in Dalton Creek (137°16'W, 60°20'N) from Permo-Triassic volcanic rocks (e.g. Nicolai Fm.) at the contact with Jura-Cretaceous arc-related sedimentary rocks (Dezdeash Fm.) exhibit minimal deformation with preservation of primary ophitic texture. Previous mapping (Eisbacher 1976, Campbell & Dodds 1982c) indicates an apparent truncation of large-scale fold structures in the Dezdeash Fm. There

appears to be an up to 5 km wide zone of transposition adjacent to the Denali Fault, with preferential accommodation of deformation in the Dezdeash units. Re-interpretation of bedding and cleavage data (Campbell & Dodds 1982c) shows re-orientation of folded bedding with NW-fold axes, as well as folding of cleavage, about a sub-horizontal NE axis i.e. an apparent transition from sinistral to dextral asymmetry relative to the fault zone boundaries. These geometries have been discussed by Eisbacher (1976), with recent extension of the ideas by Evenchick (1996), and correspond to predicted changes in Kula plate displacement.

Near the south end of Kluane Lake, the dominant foliation is steep and northwest-striking. Synoptic orientation diagrams of the foliations have an asymmetry that is consistent with dextral displacement along the Denali Fault. As one approaches the fault trace, the foliation patterns become symmetrical with respect to it, consistent with more intense transposition by higher strains near the fault. Along the Denali front, northwest of the Duke River (139°05'W, 61°25'N), fabrics are more shallowly south to southwest-dipping. Theses northern rocks show no obvious relationship with inferred transcurrent movement along the Denali Fault, but instead contain transposed layering, faults, shear zones and lineations that suggest north or northeast thrusting, for which there is supported evidence reported from the Quill Creek area (T. Bremner, pers. comm.). A few good stretching lineations are observed north of Duke River sub-parallel to the Denali Fault trend, but the relationship of these to local geometries could not be ascertained. The paucity of lineations and macroscopic kinematic indicators requires extensive kinematic study of oriented thin sections.

The regional foliation is cut by both normal and reverse faults, though in general, normal faulting is youngest. Thrust faults do not in general show consistent patterns of orientation or sense of displacement, although one candidate for a significant thrust consistent with exhumation along a transpressional zone was mapped along the Denali fault front this past summer. As with many of the faults there is difficulty extracting a slip vector and sense in the field; hence, samples along and adjacent to this fault are being prepared for thin section examination, but the nature of the rocks makes this a tedious and delicate process. It is particularly important to clarify these matters because of continuing controversy over the nature of the main fault front (Mezger 1997). The most obvious normal faults trend sub-parallel to the Denali Fault trace. These can vary from discrete brittle features with fine calcite veining to metre-thick gouge zones i.e. there is a complete range from young to mature faults.

Seismic records (Canadian National Earthquake Database) in the earthquake catalogue from 1980 to present have been collated for the St. Elias region of SW Yukon and plotted in 5-d space - *latitude-longitude-depth-magnitude and relative age*- and overlaid with the surface geology. The most striking feature is the close relationship between mapped structure and seismic activity irrespective of the age of the rocks; in other words, the "old" geology looks much like the "active" geology. This is now considered not to be fortuitous reactivation of old structures, but rather exhumation of fault rocks representative of deeper crustal levels that are tectonically active. The following interpretations are base based on this compilation:

(1) There is a very abrupt cut-off in seismicity at about 18-20 km characteristic of classic brittle-ductile transitions. Exceptions occur along the Insular superterrane - Coast Complex boundary (Denali Fault) and the Alexander-Chugach terrane boundary (Border Ranges Fault) where deeper earthquakes indicate these to be major lithospheric breaks, consistent with a 2000 km long lineament.

(2) There is a general younging of seismic events from depth towards the surface, suggesting rupture initiation in the vicinity of the brittle-ductile transition where maximum brittle strength

is typically realized, with subsequent accommodation of these displacements in the near surface.
(3) A feature that repeatedly appears in reviewing the earthquake records is a SE-trending lineament extending from the junction of the Totschunda-Duke River faults to the Fairweather Fault. Various arguments have been made for and against an extension of the Totschunda Fault through the Icefield Ranges (e.g. Lanphere 1978; Lahr & Plafker 1980; Power 1988), but the observed correlations of faults with seismicity in other areas would argue strongly for the existence of an Icefield Ranges seismic zone that could be interpreted as a young propagating transfer zone representing the continued outboard migration of displacement in the northern Cordillera.
(4) Composite serial sections of the seismicity were constructed across the Denali and Duke River faults, progressing from SE to NW (Kluane Lake to Alaska). These show transfer of earthquake activity from the Denali Fault trace to the Duke River trace, with a concentration of earthquakes around their point of diversion (a knot of activity). DRF and Denali faults appear to root into each other at depth along a SW-dipping surface. As this transfer occurs, there is a concurrent change from steeply dipping to inclined rupture planes to inclined planes that match surface observations from the adjacent area (north of Duke River). This is best shown by the concentration of seismicity beneath the Wrangell lavas (Cement Ck. area) which images in 3-d as inclined arrays of epicentres. The broad distribution of foci observed on maps simply reflects the projection of these rupture points in to plan view. These inferred rupture surfaces are consistent with transfer of displacement parallel the Denali Fault trace into reverse and strike-slip components along the Duke River Fault, as has been interpreted from with microseismic studies (Power 1988). Thrusting would be kinematically anticipated given the strong bend in the Totschunda-Duke River fault system away from the main predicted transcurrent displacement direction. The mapped deformation fabrics independently suggest N-NE trending thrusts, arguing for a close relationship between the surface geology and the current tectonic framework and correlates with the observed change in fabrics across the intersection of the Duke River with the Denali Fault front.
(5) The absence of evidence for extensive deformation along the Dalton Creek segment of the Denali Fault corresponds to partitioning of deformation in to the weaker Dezdeash Fm. rocks, as suggested by fold axis truncation and the widely disseminated seismicity.

Fault Rocks

Fault rocks vary from discrete polished slip planes, through thin micro-brecciated zones to thick, mature fault zones. Metamorphic minerals are indicative of zeolite-grade metamorphism i.e. faulting is cold. The most unifying aspect of the fault rocks, and the deformation as a whole, is the involvement of vein-introduced carbonate, most-commonly calcite, that is interpreted to reflect fault zone hydrology.

The regional foliation, particularly in the Pennsylvanian-Permian volcanic units, is largely defined by transposed calcite-quartz veins and can be overprinted by a more cleavage parallel to the Denali Fault trace e.g. a steep, northwest-trending cleavage. This is observed in the field, but is most clearly seen in thin section. Veins closest to the Denali Fault trace show excellent twin boundary migration and recrystallization. The latter is somewhat paradoxical, as zeolite-facies metamorphic grade was not anticipated to favour such features. Again, the parallelism of these vein fabrics with relict, transposed primary textures is believed to explain the interpretation of these rocks as moderately deformed. In intensely deformed zones, quartz/calcite mylonites defining the earlier foliation (often derived from syntectonic veining) are commonly overprinted by younger cataclastic deformation,

indicative of protracted deformation relevant to the fault zone.

The most intense deformation/fault zones, are associated with extensive carbonate veining and/or are localized within carbonate horizons. Mylonites, ultracataclasites and gouges equally show evidence of cyclic carbonate injection and deformation. The extremely high twin densities observed in calcite reflect high differential stress typical of upper crustal deformation. Gouges are most common near the Denali Frault front or parallel topographic breaks interpreted as normal faults. Cataclasites and mylonites are developed along orogen parallel zones, including at the major lithostratigraphic boundaries; for example at the base of the Nicloai greenstones. Of specific interest is the degree of crystal-plasticity and dynamic recrystallization exhibited by calcite at the inferred low temperatures. In many instances, grain size reduction is clearly not a brittle process and contradicts the commonly accepted behaviour of calcite at these temperatures. Likewise, submicrometre-grain-size calcite with superb flow textures contains quartz clasts with intense, but plastically-induced substructures. The primary calcite grains around the fault zones are much coarser and have a well-developed crystallographic shape fabric. This suggests discrete localization of instabilities during plastic deformation i.e. mylonite to cataclasite, during effectively the same movement episode. This potentially provides textural evidence of the transition from aseismic to seismic slip.

The best developed sections of distinct fault rocks occur along the Duke River Fault near where it diverges from parallelism with the Denali Fault. Along the eroded cliffs of Bullion Creek (138° 40'W, 60°59'N), a 100m wide zone of gouge and cataclasite is exposed. This areas is of particular interest because of the relatively high seismicity in this area (Horner 1983), including a M5.2 earthquake in June 1995 sited at 138°24'W, 60°59'N. The fault zone comprises metre-scale compositional layer typical of large, mature fault zones. These layers are themselves cut by vertically-emplaced carbonate veins, which are seen in various degrees of dismemberment. Phyllite-like gouge on the southwest edge of the fault zone consists of 1- 10 μm grain size quartz, calcite and minor sericite. The fault rocks grade into progressively more carbonate-rich material to the northeast until a unit mapped as McCarthy Fm. is reached. In thin section, this limestone is a highly strained mylonitic rock, itself cut by carbonate veins. In general, the extreme fine-grained nature of these rocks and high refractive index of calcite requires ultra-thin sections for any useful light microscopy study.

Neotectonics

The correspondence of surface geology with earthquake distribution begs comparison of the exposed fault rocks with the current tectonism. In particular, the Duke River Fault segment from from southern Kluane Lake to Alaska exhibits a concentration of seismicity at the expense of the main Denali Fault trace, apparent (?) occurrences of hot springs (pers. comm., Kluane Park staff) and intense development of a mature fault rocks that suggest this zone is a loci for current displacements.

The Duke River Fault serves as the boundary between the Alexander terrane and Wrangellia and has been interpreted to have originally been an east verging thrust (Wheeler and McFeely 1991), but the abundance of vertical hydraulic fractures and steep dip indicate that is now either a strike-slip or normal fault with the carbonate veins defining the σ_1-σ_2 plane. Where examined, these rocks showed a weak sub-horizontal lineation, favouring a strike-slip displacement. The abundant evidence for suprahydrostatic fluid paleopressures in the form of vein arrays is of note because it may mirror the current hydrologic environment in the seismogenic zone. An optimally oriented fault can be estimated to have a strength defined by $\sigma_1=4\bullet\sigma_3$ (Sibson 1990). Assuming vertical stress, σ_v, equals

σ_2 and $\sigma_2=\sigma_3$ for strike-slip, then the differential stress at failure, $\sigma_1-\sigma_3 = 3 \bullet \sigma_v$ The effect of fluid pressure is introduced as $\sigma_v' = \sigma_v(1-\lambda)$, where $\lambda \equiv$ fluid pressure/overburden pressure. At 5 km depth, typical of the June 1985 earthquake, overburden pressure corresponds to approximately 125 MPa, giving a strength of 375 MPa for dry failure . This is very high given that a differential stress of 100 MPa corresponds to the high range of observed stress drops in earthquakes and paleopiezometry measurements in mylonites. Using 100 MPa as an estimate of the upper limit of differential stress, a $\lambda \approx 0.73$ can be back-calculated. For the cut-off in seismicity at 18-20 km, comparable values of $\lambda \approx 0.8$ are calculated. Lower strength would require larger fluid pressures. Hence, it appears reasonable to anticipate that these exhumed faults are analogues to the active faults at depth to which we have no direct access and that fluids have and continue to play a significant role in the deformation.

Major topographic breaks oblique to the main orogen beg the question of whether there are additional structural controls than those related to faulting parallel to the Denali front. A NNW trend of fractures parallel to arms of Kluane Lake, and several of the young rivers (Donjek, White) have been identified. These apparent lineaments cross the Denali front and do not appear to offset major units. However, geology is rarely identical from one side to the other of these breaks, raising the possibility that there are normal fault displacement that die off to the SE (i.e. scissor faults). These breaks would in essence act as release surfaces during uplift of the front and could accommodate effective extension to the NW i.e. Kluane Lake as a small basin.

Direct evidence for recent, oblique faulting exists as gouge zones that occur parallel to the topographic lineament at the south end of Kluane Lake , parallel to the Slims. These gouge zones occur within normal faults that effectively define the faces of major slopes. Because they occur sub-parallel to active slope faces, their probability of survival in the record after exhumation is deemed to be low. The relationships between these oblique breaks and the main faults have several features in common with well-described neotectonic faults such as the Wasatch Fault, Utah (J. Evans, R. Bruhn pers. comm.) - these include the concentration of seismicity (Slims River, Cement Ck.) and the localization of hot springs (Grizzly Ck.) at the intersection of these features. Also, the Wasatch Fault is characterized by microseismic activity that has moved away from the current trace, much as current activity around Kluane is concentrated along the Duke River Fault, not the Denali Fault.

REFERENCES

Campbell, R.D. & Dodds, C.J. 1982a. Geol. Surv. Can Open File 829.

Campbell, R.D. & Dodds, C.J. 1982b. Geol. Surv. Can Open File 830.

Campbell, R.D. & Dodds, C.J. 1982c. Geol. Surv. Can Open File 831.

Eisbacher, G.H. 1976. Can. J. Earth Sci. 13, 1459-1513.

Evenchick, C.A. 1996. In Lithoprobe Report No. 50, 190.

Horner, R.B. 1983. Bull. Seismol. Soc. Am. 73, 1117-1137.

Lahr, J.C. & Plafker, G. 1980. Geology 8, 483-486.

Lanphere, M.A. 1978. Can. J. Earth Sci. 15, 817-822.

Mezger, J.E. 1997. Unpub. Ph.D. Thesis, Dept. of Earth and Atmospheric Sci., U. Alberta, 306pp.

Power, M.A. 1988. Unpub. M.Sc. Thesis, Dept. of Physics, U. Alberta, 125 pp.

Sibson, R.H. 1990. Min. Assoc. Can. Short Course vol. 18., 93-132.

Wheeler, J.O. & McFeely, P. (comp.) 1991. Tectonic Assemblage Map of the Canadian Cordillera. Geol. Surv. Can. Map 1712A, Scale 1:2 000 000.